AAPS Advances in the Pharmaceutical Sciences Series 23

Donald E. Mager
Holly H.C. Kimko *Editors*

Systems Pharmacology and Pharmaco-dynamics

aapspress

EXTRAS ONLINE

Springer

AAPS Advances in the Pharmaceutical Sciences Series

Volume 23

The AAPS Advances in the Pharmaceutical Sciences Series, published in partnership with the American Association of Pharmaceutical Scientists, is designed to deliver volumes authored by opinion leaders and authorities from around the globe, addressing innovations in drug research and development, and best practice for scientists and industry professionals in the pharma and biotech industries.

More information about this series at http://www.springer.com/series/8825

Donald E. Mager · Holly H.C. Kimko
Editors

Systems Pharmacology and Pharmacodynamics

Springer

Editors
Donald E. Mager
Department of Pharmaceutical Sciences
University at Buffalo, SUNY
Buffalo, NY
USA

Holly H.C. Kimko
Global Clinical Pharmacology
Janssen Research & Development, LLC,
Spring House, PA
USA

ISSN 2210-7371 ISSN 2210-738X (electronic)
AAPS Advances in the Pharmaceutical Sciences Series
ISBN 978-3-319-44532-8 ISBN 978-3-319-44534-2 (eBook)
DOI 10.1007/978-3-319-44534-2

Library of Congress Control Number: 2016948099

Printed on acid-free paper

This Springer imprint is published by Springer Nature
The registered company is Springer International Publishing AG
The registered company address is: Gewerbestrasse 11, 6330 Cham, Switzerland

Preface

Systems pharmacology, a relatively new discipline, is the interface between systems biology and pharmacodynamics. It is a response to the growing awareness that pharmaceutical companies should reduce the high attrition in the pipeline due to insufficient efficacy or toxicity found in proof-of-concept and/or Phase 2 studies. Systems pharmacology provides a framework for integrating information obtained from understanding physiological/pathological pathways (normal body function system vs. perturbed system due to disease) and pharmacological targets in order to predict clinical efficacy and adverse events through iterations between mathematical modeling and experimentation.

Two workshops on quantitative and systems pharmacology (QSP) were held at the NIH to discuss whether a merger of systems biology and pharmacology could advance the discovery, development, and clinical use of therapeutic drugs; the experts from academia, industry, and regulatory agencies have identified a need to integrate concepts and methods. Systems biology and pharmacodynamics have evolved in parallel, although there are significant interrelationships that can enhance drug discovery and enable optimized therapy for each patient. Currently, no singlebook exists that covers the expertise from both systems biology and pharmacodynamics researchers.

To that end, the intent of this book is to foster such dialogue by introducing systems modeling concepts to pharmacometricians and pharmaceutical scientists (Part I), introducing PK/PD principles to engineers and systems scientists (Part II), and providing detailed examples of systems pharmacology models from academia and the pharmaceutical industry that may be useful for developing drugs to treat various diseases (Part III). In addition, a perspective on the role of systems pharmacology modeling in regulatory drug approval is presented in Chap. 2, followed by the application of systems pharmacology in drug discovery and development from an industrial perspective (Chap. 3). This book will facilitate collaboration among industry, clinical, academic, and regulatory scientists so that systems pharmacology and pharmacodynamics may be developed and refined further to show practical applications in drug development.

We hope that this book is informative and relevant to any researcher or practitioner who wants to use systems pharmacology and pharmacodynamics in the design, analysis, or regulatory decisions concerning drug discovery, as well as nonclinical and clinical drug development. This book does not embrace all aspects of systems pharmacology and pharmacodynamics, nor is it intended as a technical recipe for how to apply them. Rather, it is a source of information that enables the reader to gain a better understanding of the essential background and knowledge of the fields of systems pharmacology and pharmacodynamics.

This book would not exist without the help and encouragement of many people. We are grateful to all the authors who contributed to the chapters. We also would like to thank our publisher, AAPS/Springer, for this opportunity to contribute to the fields of systems pharmacology and pharmacodynamics.

Buffalo, NY, USA Donald E. Mager
Spring House, PA, USA Holly H.C. Kimko

Contents

Part I Systems Modeling

1 Systems Pharmacology and Pharmacodynamics: An Introduction 3
Donald E. Mager and Holly H.C. Kimko

2 Role of Systems Modeling in Regulatory Drug Approval 15
Vikram Sinha, Shiew-Mei Huang, Darrell R. Abernethy, Yaning Wang, Ping Zhao and Issam Zineh

3 Quantitative Systems Pharmacology: Applications and Adoption in Drug Development 27
Saroja Ramanujan, Kapil Gadkar and Ananth Kadambi

4 Systems Pharmacology: An Overview 53
Marc R. Birtwistle, Jens Hansen, James M. Gallo, Sreeharish Muppirisetty, Peter Man-Un Ung, Ravi Iyengar and Avner Schlessinger

5 Discrete Dynamic Modeling: A Network Approach for Systems Pharmacology 81
Steven Nathaniel Steinway, Rui-Sheng Wang and Reka Albert

6 Kinetic Models of Biochemical Signaling Networks 105
Mehdi Bouhaddou and Marc R. Birtwistle

7 Mechanistic Models of Physiological Control Systems 137
Michael C.K. Khoo, Wen-Hsin Hu and Patjanaporn Chalacheva

Part II Pharmacodynamics

8 Foundations of Pharmacodynamic Systems Analysis 161
William J. Jusko

9 Direct, Indirect, and Signal Transduction Response Modeling 177
Wojciech Krzyzanski

10 Irreversible Pharmacodynamics 211
Alberto Russu and Italo Poggesi

11 Feedback Control Indirect Response Models 229
Yaping Zhang and David Z. D'Argenio

12 Nonlinear Mixed Effects Modeling in Systems Pharmacology 255
Peter L. Bonate, Amit Desai, Ahsan Rizwan, Zheng Lu and Stacey Tannenbaum

13 Detecting Pharmacokinetic and Pharmacodynamic Covariates from High-Dimensional Data 277
Jonathan Knights and Murali Ramanathan

Part III Multi-scale Models of Drug Action

14 Multi-scale Modeling of Drug Action in the Nervous System..... 305
Hugo Geerts, Patrick Roberts, Athan Spiros and Robert Carr

15 Mechanistic Modeling of Inflammation 325
Jeremy D. Scheff, Kubra Kamisoglu and Ioannis P. Androulakis

16 Systems Pharmacology of Tyrosine Kinase Inhibitor-Associated Toxicities 353
Yoshiaki Kariya, Masashi Honma and Hiroshi Suzuki

17 Translational Modeling of Antibacterial Agents 371
Gauri G. Rao, Neang S. Ly, Brian T. Tsuji, Jürgen B. Bulitta and Alan Forrest

18 Viral Dynamic Modeling of Hepatitis C Virus Infection: Past Successes and Future Challenges 403
Eric L. Haseltine and Holly H.C. Kimko

19 Using Systems Pharmacology to Advance Oncology Drug Development 421
Daniel C. Kirouac

20 Systems Pharmacology Modeling in Type 2 Diabetes Mellitus..... 465
James R. Bosley, Tristan S. Maurer and Cynthia J. Musante

Index 509

Editors and Contributors

About the Editors

Donald E. Mager is a Professor of Pharmaceutical Sciences at the University at Buffalo, State University of New York. He also served as a Visiting Professor at the University Paris Descartes in January from 2007–2013 and 2016. He currently serves on the Clinical Pharmacology Advisory Committee to the FDA and the Editorial Advisory Boards of several journals. Dr. Mager also serves as an Associate or Consulting Editor at CPT:Pharmacometrics & Systems Pharmacology (CPT:PSP), Journal of Pharmacology & Experimental Therapeutics (JPET), and Pharmacology, Research & Perspectives (PRP). He is a former President of the International Society of Pharmacometrics and is a Fellow and member of the Board of Regents of the American College of Clinical Pharmacology. In addition, he is an expert member of the Board of Pharmaceutical Sciences at FIP and serves on the Scientific Advisory Board to Simcyp. His research focuses on identifying molecular and physiological factors that control the pharmacological properties of various drugs, with a focus on anti-cancer and immunomodulatory agents. He has contributed to 120+ peer-reviewed publications.

Holly H.C. Kimko is a senior pharmacometrician in the Global Clinical Pharmacology department at Janssen Research & Development, LLC, Spring House, PA, and Adjunct Associate Professor in the Pharmacy School of Rutgers University, New Jersey. Dr. Kimko is a Janssen Research Fellow and American Association of Pharmaceutical Scientists Fellow. She championed the use of modeling and simulations in drug development at the Center for Drug Development Science at Georgetown University Medical School, Washington, DC in 1995–2002. Trained in biochemistry and pharmacy, Dr. Kimko earned her Ph.D. degree in pharmaceutical sciences from the University at Buffalo, State University of New York. She has published key papers on physiologically-based indirect response modeling and applications of clinical trial simulations and has edited two books on

clinical trial simulations. Her research interests include strategic application of modeling and simulation tools in all aspects of drug development and post-approval life cycle management. Among her scientific endeavors is a specialty in pediatric drug development.

Contributors

Darrell R. Abernethy Division of Applied Regulatory Science, Drug Safety Group, Center for Drug Evaluation and Research, Food and Drug Administration, Silver Spring, MD, USA

Reka Albert Department of Physics, Pennsylvania State University, University Park, PA, USA

Ioannis P. Androulakis Biomedical Engineering Department, Rutgers University, New Brunswick, NJ, USA; Chemical and Biochemical Engineering Department, Rutgers University, New Brunswick, NJ, USA

Marc R. Birtwistle Department of Pharmacology and Systems Therapeutics, Systems Biology Center New York, Icahn School of Medicine at Mount Sinai, New York, NY, USA

Peter L. Bonate Astellas Pharma, Northbrook, IL, USA

James R. Bosley Clermont Bosley, LLC, Kennett Square, PA, USA

Mehdi Bouhaddou Department of Pharmacology and Systems Therapeutics, Icahn School of Medicine at Mount Sinai, New York, NY, USA

Jürgen B. Bulitta Department of Pharmaceutics, College of Pharmacy, University of Florida, Orlando, FL, USA

Robert Carr In Silico Biosciences, Lexington, MA, USA

Patjanaporn Chalacheva Department of Biomedical Engineering, University of Southern California, Los Angeles, CA, USA

Amit Desai Astellas Pharma, Northbrook, IL, USA

David Z. D'Argenio Department of Biomedical Engineering, Biomedical Simulations Resource, University of Southern California, Los Angeles, CA, USA

Alan Forrest Eshelman School of Pharmacy, University of North Carolina, Chapel Hill, NC, USA

Kapil Gadkar Genentech Inc., South San Francisco, CA, USA

James M. Gallo Department of Pharmacology and Systems Therapeutics, Systems Biology Center New York, Icahn School of Medicine at Mount Sinai, New York, NY, USA

Hugo Geerts In Silico Biosciences, Lexington, MA, USA; Perelman School of Medicine, University of Pennsylvania, Berwin, PA, USA

Jens Hansen Department of Pharmacology and Systems Therapeutics, Systems Biology Center New York, Icahn School of Medicine at Mount Sinai, New York, NY, USA

Eric L. Haseltine Vertex Pharmaceuticals Incorporated, Boston, MA, USA

Masashi Honma Department of Pharmacy, Faculty of Medicine, The University of Tokyo Hospital, University of Tokyo, Tokyo, Japan; Laboratory of Pharmacology and Pharmacokinetics, Faculty of Medicine, The University of Tokyo Hospital, Tokyo, Japan

Wen-Hsin Hu Department of Biomedical Engineering, University of Southern California, Los Angeles, CA, USA

Shiew-Mei Huang Office of Clinical Pharmacology, Center for Drug Evaluation and Research, Food and Drug Administration, Silver Spring, MD, USA

Ravi Iyengar Department of Pharmacology and Systems Therapeutics, Systems Biology Center New York, Icahn School of Medicine at Mount Sinai, New York, NY, USA

William J. Jusko Department of Pharmaceutical Sciences, University at Buffalo, Buffalo, NY, USA

Ananth Kadambi Rosa & Co. LLC, San Carlos, CA, USA

Kubra Kamisoglu Chemical and Biochemical Engineering Department, Rutgers University, New Brunswick, NJ, USA

Yoshiaki Kariya Department of Pharmacy, The University of Tokyo Hospital, Faculty of Medicine, University of Tokyo, Tokyo, Japan

Michael C.K. Khoo Department of Biomedical Engineering, University of Southern California, Los Angeles, CA, USA

Holly H.C. Kimko Janssen Research & Development, LLC, Spring House, PA, USA

Daniel C. Kirouac Merrimack Pharmaceuticals Inc., Cambridge, MA, USA; Genentech Research & Early Development, South San Francisco, CA, USA

Jonathan Knights Department of Pharmaceutical Sciences, State University of New York, Buffalo, NY, USA

Wojciech Krzyzanski Department of Pharmaceutical Sciences, University at Buffalo, Buffalo, NY, USA

Zheng Lu Astellas Pharma, Northbrook, IL, USA

Neang S. Ly School of Pharmacy and Pharmaceutical Sciences, The New York State Center of Excellence in Bioinformatics and Life Sciences, University at Buffalo, SUNY, Buffalo, NY, USA; Clinical Pharmacology and DMPK, MedImmune LLC, Mountain View, CA, USA

Donald E. Mager Department of Pharmaceutical Sciences, University at Buffalo, SUNY, Buffalo, NY, USA

Tristan S. Maurer Pfizer Inc., Cambridge, MA, USA

Sreeharish Muppirisetty Department of Pharmacology and Systems Therapeutics, Systems Biology Center New York, Icahn School of Medicine at Mount Sinai, New York, NY, USA

Cynthia J. Musante Pfizer Inc., Cambridge, MA, USA

Italo Poggesi Clinical Pharmacology and Pharmacometrics, Janssen Research & Development, Beerse, Belgium

Murali Ramanathan Department of Pharmaceutical Sciences, State University of New York, Buffalo, NY, USA

Saroja Ramanujan Genentech Inc., South San Francisco, CA, USA

Gauri G. Rao School of Pharmacy and Pharmaceutical Sciences, The New York State Center of Excellence in Bioinformatics and Life Sciences, University at Buffalo, SUNY, Buffalo, NY, USA

Ahsan Rizwan Nektar Therapeutics, San Francisco, CA, USA

Patrick Roberts In Silico Biosciences, Lexington, MA, USA; Oregon Health and Science University, Portland, OR, USA

Alberto Russu Clinical Pharmacology and Pharmacometrics, Janssen Research & Development, Beerse, Belgium

Jeremy D. Scheff Biomedical Engineering Department, Rutgers University, New Brunswick, NJ, USA

Avner Schlessinger Department of Pharmacology and Systems Therapeutics, Systems Biology Center New York, Icahn School of Medicine at Mount Sinai, New York, NY, USA

Vikram Sinha Division of Pharmacometrics, Center for Drug Evaluation and Research, Food and Drug Administration, Silver Spring, MD, USA

Athan Spiros In Silico Biosciences, Lexington, MA, USA

Steven Nathaniel Steinway Penn State Hershey Cancer Institute, Penn State University College of Medicine, Hershey, PA, USA

Hiroshi Suzuki Department of Pharmacy, Faculty of Medicine, The University of Tokyo Hospital, University of Tokyo, Tokyo, Japan

Stacey Tannenbaum Astellas Pharma, Northbrook, IL, USA

Brian T. Tsuji School of Pharmacy and Pharmaceutical Sciences, The New York State Center of Excellence in Bioinformatics and Life Sciences, University at Buffalo, SUNY, Buffalo, NY, USA

Peter Man-Un Ung Department of Pharmacology and Systems Therapeutics, Systems Biology Center New York, Icahn School of Medicine at Mount Sinai, New York, NY, USA

Rui-Sheng Wang Department of Physics, Pennsylvania State University, University Park, PA, USA

Yaning Wang Division of Pharmacometrics, Center for Drug Evaluation and Research, Food and Drug Administration, Silver Spring, MD, USA

Yaping Zhang Department of Biomedical Engineering, Biomedical Simulations Resource, University of Southern California, Los Angeles, CA, USA

Ping Zhao Center for Drug Evaluation and Research, Food and Drug Administration, Silver Spring, MD, USA

Issam Zineh Office of Clinical Pharmacology, Center for Drug Evaluation and Research, Food and Drug Administration, Silver Spring, MD, USA

Part I
Systems Modeling

Chapter 1
Systems Pharmacology and Pharmacodynamics: An Introduction

Donald E. Mager and Holly H.C. Kimko

Abstract Systems pharmacology represents a hybrid, multi-scale modeling approach that seeks to combine systems or network-based structures with basic principles of pharmacokinetics and pharmacodynamics (PK/PD). Systems biology encompasses a broad spectrum of computational methods for vertically capturing molecular, cellular, and tissue level interactions that regulate biological systems. In contrast, PK/PD models are often minimal compartmental constructs (conceptual models) with parameters that integrate PK, drug-target interactions, and rate-limiting turnover processes. Both disciplines have shown value in various stages of drug development and utilization; however, there is growing interest in applying integrated systems pharmacology models, in a complimentary manner, for informing critical decisions in drug development and pharmacotherapy. Here we provide a rationale for the construction and evaluation of complex models of drug action that may serve to guide the development of new compounds and combinatorial regimens, explain sources of inter-subject variability in drug exposure and response, identify sources and influences of disease progression, and predict and understand drug efficacy and safety.

Keywords Systems model · Systems pharmacology · Systems physiology · Systems biology · Multiscale modeling · Pharmacokinetics/Pharmacodynamics

1.1 Introduction

The discovery, development, and utilization of drugs to treat disease, along with their regulation, are complicated by the multitude of factors that can influence individual patient responses. It is therefore not surprising that many scientists have

D.E. Mager
Department of Pharmaceutical Sciences, University at Buffalo, SUNY, Buffalo, NY, USA

H.H.C. Kimko (✉)
Janssen Research & Development, LLC, Spring House, PA, USA
e-mail: hkimko@its.jnj.com

D.E. Mager and H.H.C. Kimko (eds.), *Systems Pharmacology and Pharmacodynamics*,
AAPS Advances in the Pharmaceutical Sciences Series 23,
DOI 10.1007/978-3-319-44534-2_1

turned to mathematical modeling to help identify and integrate major determinants of drug action and inform key decisions within each of these endeavors. A diverse spectrum of models and computational approaches are available, ranging from comprehensive biochemical models at the molecular and cellular levels to empirical and conceptual models of clinical outcomes for individuals and patient populations. The former model type emerges from engineering principles applied to biochemistry and physiological systems, whereas the latter form often reflects compartmental structures that couple pharmacokinetics (PK) and pharmacodynamics (PD) or the time-course of response with respect to the extent of drug exposure.

Systems pharmacology seeks to combine information across such organizational scales, and a good working definition is, "an approach to translational medicine that combines computational and experimental methods to elucidate, validate, and apply new pharmacological concepts to the development and use of small molecule and biologic drugs" (Sorger et al. 2011). Accordingly, systems pharmacology models represent hybrid, multi-scale structures, focusing on the dynamic interplay among the constituents of the system that manifests as emergent properties. Systems pharmacology models will not replace current population-based PK/PD (pharmacometrics) or chemoinformatic and systems biology approaches, but instead will provide complimentary support and "create the knowledge needed to change complex cellular networks in a specified way with mono or combination therapy, alter the pathophysiology of disease so as to maximize therapeutic benefit and minimize toxicity, and implement a 'precision medicine' approach to improving the health of individual patients" (Sorger et al. 2011). Thus, systems pharmacology is interdisciplinary and its successful implementation requires effective communication and collaborations among clinicians and basic scientists.

This chapter provides a brief overview of systems pharmacology and pharmacodynamics. Chapters 2 and 3 provide perspectives on the role of systems pharmacology modeling in regulatory drug approval and the application of systems pharmacology in drug discovery and development from an industrial perspective. The subsequent chapters introduce systems modeling to PK/PD scientists, PK/PD principles to engineers and systems scientists, and provide detailed examples of systems pharmacology models that may be useful for developing drugs to treat various diseases.

1.2 Systems Theory in Biology and Pharmacokinetics

The concept of systems science is not new. Ludwig von Bertalanffy was one pioneer in general system theory (von Bertalanffy 1950), who in his classic text stated, "If someone were to analyze current notions and fashionable catchwords, he would find 'systems' high on the list. The concept has pervaded all fields of science and penetrated into popular thinking, jargon and mass media" (von Bertalanffy 1969). In his chapter on, *Some Aspects of System Theory in Biology*, he covered then-current theories of open systems, feedback models and Cannon's homeostasis, allometric scaling, and organismal growth models.

Indeed, many of the approaches in systems pharmacology have their roots in engineering and systems physiology. For example, consider the text, *Systems Theory and Biology*, which chronicles the proceedings of the 3rd systems symposium held at Case Western Reserve University (then Case Institute of Technology) (Mesarović 1968). Building off the pioneering work of Yates and Urquhart 1962, a comprehensive and continuous model of adrenocortical function is featured that includes 9 independent inputs and 34 independent parameters (Yates et al. 1968). In questioning the utility of the model, the authors "recognize that models of physiological systems usually consume far more useful published papers than they produce [, however,] the existence of the model will shape the strategy of the research, hopefully in a more rational manner than human intuition, unaided by explicit models, can do when it is confronted with great complexity." In the very next chapter, Gann et al. (1968) describe a finite state, Boolean mathematical model of the same biological system. Interestingly, the Boolean model made several predictions of intermediate variables and new system outputs, which were used to guide subsequent experimental research. This modeling approach is also often attributed to Kauffman (1969). These are just two examples of the early recognition that more comprehensive models and alternative mathematical formalisms would be needed to understand how unit processes interact to give rise to unique system properties that could not be predicted from studying individual components.

Fundamental approaches to systems modeling in biology were also becoming established. Some key initial considerations and choices in developing such models include (Yates et al. 1968):

1. Choice of the species in which to study the system
2. Specification of the describing or state variables
3. Selection of measurement techniques and estimates of the errors of measurement
4. Selection of the relevant time domain for system activity
5. Choice of sampling rates appropriate to the chosen time domain
6. Choice of stimuli, input signals or forcing functions to perturb the system

Additional decisions to be made include specifying major components of the system, how to define the connections between components, and the form of mathematics to be used in the model. In terms of the modeling process itself, Yates later listed key steps that involve (Yates 1973):

1. Development of a model that incorporates the unit process of components to stimulate selected system performance characteristics
2. Test of the model
3. Experimental tests of predictions by performance of the analogous experiments on the real system
4. Modifications of the model—further predictions and modifications within the same general structure
5. Development of a new kind of structure for the model and fresh kinds of predictions and experiments

Although analytical and computational methods have advanced considerably over the last few decades, these guiding principles are just as relevant today in systems pharmacology.

The time-course of drug concentrations at the site of action, or biophase, is considered to be the driving force for subsequent pharmacological or toxicological effects. Therefore, studies of the variability in drug action should first consider factors influencing variability in drug exposure in relevant biophases. Pharmacokinetics is a well-established field involving the mathematical characterization of drug- and system-specific properties that regulate the time-course of drug exposure following single and multiple dose regimens. Although early PK had often been associated with simple compartmental models, Teorell published a landmark paper to introduce this discipline (although the term pharmacokinetics was not used) using a systems framework (Teorell 1937). The model included physiological structures, such as tissue volumes and rate constants of distribution and elimination mechanisms, and represents an early example of so-called physiologically-based PK (PBPK) models. However, the role of blood circulation was not considered, and in 1965, Jacquez and colleagues reported the first modern mathematical PBPK model (Jacquez et al. 1960). Shortly thereafter, Bischoff and colleagues popularized computational PBPK models for compounds like thiopental and methotrexate (Bischoff and Dedrick 1968; Bischoff et al. 1971). Dedrick noted, "Physiologic modeling enables us to examine the joint effect of a number of complex inter-related processes and assess the relative significance of each" (Dedrick 1973), which is a succinct account of the role of systems analysis in PK.

PBPK modeling is arguably the best platform for studying and integrating intrinsic and extrinsic factors controlling drug absorption and disposition in drug development and regulatory science (Rowland et al. 2011). Of particular importance to pharmacodynamic systems analysis, PBPK modeling has been identified as a good tool to show a disconnect between changes in plasma drug kinetics that are not reflected in the tissue of interest and vice versa (Rose et al. 2014). PBPK concepts have also been extended to describe the PK of biological therapeutics and antibody-based drugs, which include processes unique to such compounds, such as convectional tissue uptake, FcRn-mediated salvage, tissue catabolism, and the role of lymphatic circulation (Baxter et al. 1994; Garg and Balthasar 2007).

1.2.1 Network-Based Pharmacology and Physiological Control Systems

After decades of reductionism, accompanied by major advances in analytical assays for measuring molecular species (-omics and imaging techniques), computational hardware and software, and robust computational algorithms, the field of systems biology re-emerged as a major discipline in the early 2000s (Kitano 2002a, b). The major challenge was (and continues to be) making biological sense out of the extremely large data sets from multiple experimental platforms. Other challenges

for systems biology models include: model complexity, experimental and biological noise, redundant pathways (robustness), multiple spatial and temporal scales, and inter-species differences in biological processes. Although the data and tools have changed, the overall modeling process follows the well-appreciated steps established early on, representing an iterative approach of theory and computation, model testing and analysis, and wet-lab experimentation.

One of the major goals of systems biology was to improve the discovery and development of therapeutics. As Kitano noted, "The most feasible application of systems biology research is to create a detailed model of cell regulation, focused on particular signal-transduction cascades and molecules to provide system-level insights into mechanism-based drug discovery" (Kitano 2002b). Over the last decade, systems biology techniques have been used to explore and identify new drug targets and potential biomarkers of disease and drug response. However, the overall success of this endeavor is debatable, and there is a growing consensus that systems biology approaches should be merged with general principles of PK/PD and clinical pharmacology in order to gain further confidence in drug targets, biomarkers, and the role of new chemical entities to become promising drugs to treat disease (Sorger et al. 2011; Vicini and van der Graaf 2013).

Systems pharmacology modeling is a merger of systems biology and PK/PD principles, and represents therefore by definition, a hybrid, multi-scale modeling approach. It is beyond the scope of this chapter (and this book) to review the many statistical, informatic, and model-based methods that fall under the umbrella of systems biology. Instead, we have included some of the major modeling techniques from systems biology that have shown particular promise in systems pharmacology.

One clear concept that has become well appreciated is that of signaling and physiological networks—the idea that the temporal effects of diseases and drugs on homeostasis occur from altering information flow in interconnected biochemical networks (Bhalla and Iyengar 1999; Weng et al. 1999). In Chap. 4, Birtwistle and colleagues provide an overview of systems pharmacology, from a network-based perspective, highlighting general properties and approaches to systems models. In many cases, concentrations of major network components and the quantitative interactions among these elements are unknown, and often connections are known in only qualitative terms. For these systems, discrete and continuous logic-based models can be used to emulate biochemical systems (Kauffman 1969; Wang et al. 2012), and Steinway and colleagues provide a summary of such methodology, along with a case study for mimicking a mechanistic biochemical model of signal transduction (Chap. 5). Most modelers would argue that when detailed information and data are available, mechanistic models are preferred over empirical approaches. Therefore, Birtwistle and colleagues describe the rationale and approaches to developing kinetic models of biochemical signaling networks in Chap. 6. In rounding off Part I, Khoo and colleagues describe modeling approaches to physiological control systems, which provide a scaffold and context for considering molecular mechanisms of disease and drug action (Chap. 7).

1.3 Pharmacodynamics

The field of PK/PD modeling aims to develop conceptual models that link the time-course of drug exposure, in plasma or sites of action (biophase), to the time-course and intensity of pharmacological and/or toxicological effects. Levy was the first to develop a simple mathematical expression, connecting the PK and pharmacological properties of a drug, to explain the apparent zero-order rate of decline of in vivo drug effects (E), despite an exponential decrease in drug concentrations (Levy 1966):

$$E = E_0 - k \cdot m \cdot t \tag{1.1}$$

with E_0 as the effect value at the start of the decrease in E, k is a first-order elimination rate constant of the drug, m represents the linear positive slope of a concentration-effect plot when the effect is between 20 and 80 % maximal (abscissa = natural log of drug concentration and ordinate = effect on a linear scale), and t is time. This expression identifies the $k \cdot m$ product as the determinant of the linear decrease in drug effects for simple, rapid direct effects (i.e., reversible agonists or antagonists for which turnover processes are not rate-limiting). This discovery marked the beginning of identifying factors that regulate the in vivo time-course of drug effects in a quantitative manner.

Shortly thereafter, Wagner suggested the use of the Hill equation to describe the temporal profile of direct and rapidly acting agents, which was based on a derivation starting with drug-receptor binding (Hill 1910; Wagner 1968):

$$E = E_{max} \cdot C(t)/(EC_{50} + C(t)) \tag{1.2}$$

with $C(t)$ representing the plasma drug concentration, E_{max} is the maximal drug effect, and EC_{50} is the drug concentration producing 50 % of E_{max}. The use of the full Hill equation (or E_{max} model) avoided the restriction of the 20 to 80 % maximal effect as required for Eq. 1.1. However, the E_{max} model assumes that the time to peak drug effect coincides with the time to peak drug concentration, although most drugs exhibit a temporal delay between these events (so called hysteresis in the concentration-effect plot). Sheiner popularized the use of a simple delay compartment, initially developed by Segre, to accommodate the time for drug to equilibrate with concentrations in a hypothetical effect compartment or biophase (Segre 1968; Sheiner et al. 1979). The pharmacological effect is still defined by Eq. 1.2, but driven by concentrations in the effect compartment rather than plasma concentration. This was the first simultaneous PK/PD model to describe a relatively short delay in drug action owing to drug distribution to a biophase and assumes such distribution does not influence the PK of the drug.

Many drugs can show much longer delays, not due to distribution to a biophase, but because drug-target interactions can act indirectly to stimulate or inhibit the production (K_{in}) or loss (k_{out}) of a biomarker (R) (Ariens 1954). Levy and colleagues published the first model to capture an indirect effect (Nagashima et al.

1969), and Jusko and colleagues introduced a mathematical formalism for a family of four basic indirect response models (Dayneka et al. 1993; Jusko and Ko 1994). A general expression for these models is:

$$dR/dt = K_{in} \cdot (1 \pm H_1(C)) - k_{out} \cdot (1 \pm H_2(C)) \cdot R; \quad R(0) = R_0 \tag{1.3}$$

with H_1 and H_2 representing E_{max} functions (Eq. 1.2), and R_0 is the initial condition for the biomarker. Interestingly, the time to peak (or nadir) of drug effects is independent of dose for the biophase model, whereas this property will shift to the right with increasing dose levels for the indirect effect models, owing to the longer duration of time drug concentrations remain above its EC_{50}. Although the biophase and indirect effect models can describe delays between peak concentration and peak response, neither will describe a case in which there is a long delay in the onset of effect, when the biomarker does not change despite high drug concentrations. For such systems, the use of simple transit compartments can be used to emulate the time required for signal transduction delays with a minimal number of identifiable parameters (Mager and Jusko 2001). From these basic structural models, one can add a plethora of additional complexities and arrive at a diverse array of PK/PD models for describing many animal and clinical drug effects.

Starting the PD section of this book (Part II; Chap. 8), Jusko outlines the general fundamentals of pharmacodynamic systems analysis with a spectrum of essential models. Krzyzanski provides a detailed account of the mathematical properties of direct and indirect response models, along with modeling approaches for signal transduction processes (Chap. 9). Another major class of models is irreversibly acting systems, in which a drug can permanently inactivate a target. Such models typically combine turnover (indirect or time-dependent transduction) with second-order loss terms, and Russu and Pogessi describe a series of drug-induced irreversible models along with a rationale for transitioning toward systems pharmacology models (Chap. 10). Finally, in Chap. 11, Zhang and D'Argenio introduce mechanisms of feedback regulatory processes into indirect response models, which carry major translational implications for properly interpreting temporal profiles and drug potency under such conditions.

1.3.1 Population-Based Pharmacology

The introduction of nonlinear mixed effects modeling by Sheiner and Beal had a transformative effect on the field of PK/PD modeling (Sheiner et al. 1972, 1977; Sheiner and Beal 1980, 1981; Beal and Sheiner 1982). Population-based modeling is the standard for estimating parameters of exposure-response models in a population (of in vitro profiles, animals, and humans). In brief, population algorithms allow estimation of typical mean model parameters (θ) along with the magnitude of various sources of variability (inter-subject variability in parameters η_i, residual error ε_{ij}, inter-occasion variability, etc.). Of importance is the recognition of variability as an important feature to be identified and measured during drug

development or evaluation in order to explain that variability by identifying demographic, pathophysiological, environmental, or drug-related factors (covariates a_i) that may influence PK/PD properties of a drug. One can write a general expression for this approach:

$$Y_{ij} = f\left(x_{ij}, g(a_i, \theta, \eta_i)\right) + \varepsilon_{ij} \tag{1.4}$$

in which Y represents a PK or PD outcome variable for the ith individual at the jth time point, f is the overall structural mathematical model, x represents model inputs (such as dose), and the function g is an expression describing individual subject parameters based on the covariate relationships, population mean values, and unexplained inter-individual variability. In this case η_i and ε_{ij} are *random* effects centered at zero and typically assigned a parametric distribution, and the relationships between a_i and θ are *fixed* effects (thus nonlinear *mixed* effects modeling).

In Chap. 12, Bonate and colleagues provide an overview of nonlinear mixed effects modeling and case studies of applications in systems models. A major challenge in developing population-based models is the identification of the relationships between patient covariates and model parameters, and the best method for testing such relationships and their inclusion in the final model is controversial. Furthermore, traditional covariate search strategies can be difficult to impossible to implement in the face of large multi-dimensional data sets that are common with genomic and proteomic testing. Therefore, new strategies are needed in identifying potential patient covariates under such conditions, and Knights and Ramanathan describe a novel approach (Chap. 13) using an informational theoretic method based on Shannon's entropy (Shannon and Weaver 1948).

1.4 Systems Pharmacology Models

Parts I and II of this book feature essential elements of systems and PK/PD modeling. These concepts can be combined, and Part III contains examples of integrating components to construct systems pharmacology models for specific systems, including: drugs acting in the central nervous system (Chap. 14; Geerts et al.), mechanisms of inflammation (Chap. 15; Scheff et al.), tyrosine kinase inhibitor associated toxicities (Chap. 16; Kariya et al.), antimicrobial agents (Chap. 17; Rao et al.), hepatitis C (Chap. 18; Haseltine and Kimko), oncology (Chap. 19; Kirouac), and type 2 diabetes mellitus (Chap. 20; Bosley et al.). Although systems pharmacology is still in its infancy, more examples are appearing in the literature, along with accounts of how such modeling was used to support the clinical development of drugs (Milligan et al. 2013). In addition, the FDA has been a supporter of systems pharmacology modeling, particularly PBPK (Huang et al. 2013) and safety science (Abernethy et al. 2011). Notably, FDA reviewers invoked a systems pharmacology model of bone homeostasis (Peterson and Riggs 2010) to explore dosing regimens for a recombinant human parathyroid compound submitted for consideration to the Endocrine and Metabolic Drugs Advisory

Committee September 12, 2014 and recommended that "the dose regimen should be further optimized to address the safety concerns for hypercalciuria" (Peterson and Riggs 2015). (http://www.fda.gov/downloads/AdvisoryCommittees/CommitteesMeetingMaterials/Drugs/EndocrinologicandMetabolicDrugsAdvisory-Committee/UCM413617.pdf)

The potential of using systems pharmacology models to inform the discovery and development of new compounds is great, and further research collaborations will be needed to fully realize that potential. Strategic interdisciplinary teams will be needed to ensure models are fit-for-purpose and conditions for model qualification are clearly defined in order for systems models to be adopted and used to inform critical decision-making steps.

1.5 Prospectus

As systems modeling in pharmacology matures as a discipline, there may be an opportunity to better predict individual patient responses. Once a structural model is defined, sources of genomic and proteomic variability could be integrated into the model (so called enhanced pharmacodynamic models) to simulate complex clinical phenotypes (Iyengar et al. 2012). Insights into the determinants of inter-individual PK and PD variability could prove useful in identifying patient subpopulations likely to benefit from the drug or experience adverse drug reactions, help monitor therapy over time, identify mechanisms of innate or acquired drug resistance, and help identify novel drug combinations with superior benefit/risk ratios as compared to single agent regimens. For example, one promising study combined absolute quantification of two BCL2 proteins in patient colorectal tumor cells with a systems model, and together these were used to calculate an apparent "dosing" number that was associated with patient outcomes (disease-free survival) (Lindner et al. 2013).

Some considerations for advancing the science of systems pharmacology modeling include:

1. Networks: Require more complete, unbiased, curated and readily available interactomes, along with analytical advances in proteomics, unbiased computational approaches for network reduction, and formation of hybrid, multi-scale architectures
2. Enhanced PD models: Require effective collaborations among interdisciplinary industry, clinical, academic, and regulatory scientists for (a) generating high-quality clinical and pre-clinical data, (b) expanding models to include multiple scales and systems, and (c) developing standards and best practices
3. Software: Needs to be inter-operable and capable of integrating multiple data types
4. Strategies: New approaches are needed to develop integrated workflows with pharmacometrics and statistics

Solutions to these considerations are within reach, and the future of systems pharmacology and pharmacodynamics is very bright. Systems models present the

best platform for effectively integrating innovative data and methods to inform and improve drug discovery and development, thereby helping to bring new, more effective drugs with minimal safety concerns to patients.

References

Abernethy DR, Woodcock J, Lesko LJ (2011) Pharmacological mechanism-based drug safety assessment and prediction. Clin Pharmacol Ther 89:793–797

Ariens EJ (1954) Affinity and intrinsic activity in the theory of competitive inhibition. I. Problems and theory. Arch Int Pharmacodyn Ther 99:32–49

Baxter LT, Zhu H, Mackensen DG, Jain RK (1994) Physiologically based pharmacokinetic model for specific and nonspecific monoclonal antibodies and fragments in normal tissues and human tumor xenografts in nude mice. Cancer Res 54:1517–1528

Beal SL, Sheiner LB (1982) Estimating population kinetics. Crit Rev Biomed Eng 8:195–222

Bhalla US, Iyengar R (1999) Emergent properties of networks of biological signaling pathways. Science 283:381–387

Bischoff KB, Dedrick RL (1968) Thiopental pharmacokinetics. J Pharm Sci 57:1346–1351

Bischoff KB, Dedrick RL, Zaharko DS, Longstreth JA (1971) Methotrexate pharmacokinetics. J Pharm Sci 60:1128–1133

Dayneka NL, Garg V, Jusko WJ (1993) Comparison of four basic models of indirect pharmacodynamic responses. J Pharmacokinet Biopharm 21:457–478

Dedrick RL (1973) Animal scale-up. J Pharmacokinet Biopharm 1:435–461

Gann D, Schoeffler JD, Ostrander L (1968) A finite state model for the control of adrenal corticosteroid secretion. In: Mesarović MD (ed) Systems theory and biology. Springer, New York, pp 185–200

Garg A, Balthasar JP (2007) Physiologically-based pharmacokinetic (PBPK) model to predict IgG tissue kinetics in wild-type and FcRn-knockout mice. J Pharmacokinet Pharmacodyn 34:687–709

Hill AV (1910) The possible effects of the aggregation of the molecules of haemoglobin on its dissociation curves. J Physiol 40:4–7

Huang SM, Abernethy DR, Wang Y, Zhao P, Zineh I (2013) The utility of modeling and simulation in drug development and regulatory review. J Pharm Sci 102:2912–2923

Iyengar R, Zhao S, Chung SW, Mager DE, Gallo JM (2012) Merging systems biology with pharmacodynamics. Sci Trans Med 4:126–127

Jacquez JA, Bellman R, Kalaba R (1960) Some mathematical aspects of chemotherapy-II: The distribution of a drug in the body. Bull Math Biophys 22:309–322

Jusko WJ, Ko HC (1994) Physiologic indirect response models characterize diverse types of pharmacodynamic effects. Clin Pharmacol Ther 56:406–419

Kauffman SA (1969) Metabolic stability and epigenesis in randomly constructed genetic nets. J Theoret Biol 22:437–467

Kitano H (2002a) Computational systems biology. Nature 420:206–210

Kitano H (2002b) Systems biology: a brief overview. Science 295:1662–1664

Levy G (1966) Kinetics of pharmacologic effects. Clin Pharmacol Ther 7:362–372

Lindner AU, Concannon CG, Boukes GJ, Cannon MD, Llambi F, Ryan D, Boland K, Kehoe J, McNamara DA, Murray F, Kay EW, Hector S, Green DR, Huber HJ, Prehn JH (2013) Systems analysis of BCL2 protein family interactions establishes a model to predict responses to chemotherapy. Cancer Res 73:519–528

Mager DE, Jusko WJ (2001) Pharmacodynamic modeling of time-dependent transduction systems. Clin Pharmacol Ther 70:210–216

Mesarović MD (1968) Systems theory and biology. Springer, New York

Milligan PA, Brown MJ, Marchant B, Martin SW, van der Graaf PH, Benson N, Nucci G, Nichols DJ, Boyd RA, Mandema JW, Krishnaswami S, Zwillich S, Gruben D, Anziano RJ, Stock TC, Lalonde RL (2013) Model-based drug development: a rational approach to efficiently accelerate drug development. Clin Pharmacol Ther 93:502–514

Nagashima R, O'Reilly RA, Levy G (1969) Kinetics of pharmacologic effects in man: the anticoagulant action of warfarin. Clin Pharmacol Ther 10:22–35

Peterson MC, Riggs MM (2010) A physiologically based mathematical model of integrated calcium homeostasis and bone remodeling. Bone 46:49–63

Peterson MC, Riggs MM (2015) FDA advisory meeting clinical pharmacology review utilizes a quantitative systems pharmacology (QSP) model: a watershed moment? CPT: Pharmacomet Syst Pharmacol 4:e00020

Rose RH, Neuhoff S, Abduljalil K, Chetty M, Rostami-Hodjegan A, Jamei M (2014) Application of a physiologically based pharmacokinetic model to predict OATP1B1-related variability in pharmacodynamics of rosuvastatin. CPT: Pharmacomet Syst Pharmacol 3:e124

Rowland M, Peck C, Tucker G (2011) Physiologically-based pharmacokinetics in drug development and regulatory science. Ann Rev Pharmacol Toxicol 51:45–73

Segre G (1968) Kinetics of interaction between drugs and biological systems. Farmaco Sci 23:907–918

Shannon CE, Weaver W (1948) A mathematical theory of communication. American Telephone and Telegraph Company

Sheiner LB, Beal SL (1980) Evaluation of methods for estimating population pharmacokinetics parameters. I. Michaelis-Menten model: routine clinical pharmacokinetic data. J Pharmacokinet Biopharm 8:553–571

Sheiner LB, Beal SL (1981) Evaluation of methods for estimating population pharmacokinetic parameters. II. Biexponential model and experimental pharmacokinetic data. J Pharmacokinet Biopharm 9:635–651

Sheiner LB, Rosenberg B, Melmon KL (1972) Modelling of individual pharmacokinetics for computer-aided drug dosage. Comput Biomed Res 5:411–459

Sheiner LB, Rosenberg B, Marathe VV (1977) Estimation of population characteristics of pharmacokinetic parameters from routine clinical data. J Pharmacokinet Biopharm 5:445–479

Sheiner LB, Stanski DR, Vozeh S, Miller RD, Ham J (1979) Simultaneous modeling of pharmacokinetics and pharmacodynamics: application to d-tubocurarine. Clin Pharmacol Ther 25:358–371

Sorger PK, Allerheiligen SRB, Abernethy DR, Altman RB, Brouwer KLR, Califano A, D'Argenio DZ, Iyenger R, Jusko WJ, Lalonde R, Lauffenburger DA, Shoichet B, Stevens JL, Subramaniam S, Van der Graaf P, Vicini P (2011) Quantitative and systems pharmacology in the postgenomic era: new approaches to discovering and understanding therapeutic drugs and mechanisms. An NIH White Paper from the QSP Workshop Group, in, http://www.nigms.nih.gov/Training/Documents/SystemsPharmaWPSorger2011.pdf

Teorell T (1937) Kinetics of distribution of substances administered to the body. Arch Int Pharmacodyn 57:205–225

Vicini P, van der Graaf PH (2013) Systems pharmacology for drug discovery and development: paradigm shift or flash in the pan? Clin Pharmacol Ther 93:379–381

von Bertalanffy L (1950) An outline of general system theory. Br J Phil Sci 1:134–165

von Bertalanffy L (1969) General system theory. George Braziller Inc, New York

Wagner JG (1968) Kinetics of pharmacologic response. I. Proposed relationships between response and drug concentration in the intact animal and man. J Theoret Biol 20:173–201

Wang RS, Saadatpour A, Albert R (2012) Boolean modeling in systems biology: an overview of methodology and applications. Phys Biol 9:055001

Weng G, Bhalla US, Iyengar R (1999) Complexity in biological signaling systems. Science 284:92–96

Yates FE (1973) Systems biology as a concept. In: Brown JHU, Gann DS (eds) Engineering principles in physiology. Academic Press, New York, pp 141–184

Yates FE, Urquhart J (1962) Control of plasma concentrations of adrenocortical hormones. Physiol Rev 42:359–433

Yates FE, Brennan RD, Urquhart J, Li CC, Halpern W (1968) A continuous system model of adrenocortical function. In: Mesarović MD (ed) Systems theory and biology. Springer, New York, pp 141–184

Chapter 2
Role of Systems Modeling in Regulatory Drug Approval

Vikram Sinha, Shiew-Mei Huang, Darrell R. Abernethy, Yaning Wang, Ping Zhao and Issam Zineh

Abstract The science of quantitative clinical pharmacology continues to advance at a rapid pace such that regulators must constantly evaluate the most appropriate applications of modeling, simulation, and other innovations in the public health context. FDA continues to target improvements in regulatory science, including the development of scientific tools that can bridge the gap between cutting-edge discoveries and real-world diagnostics and therapeutics and to this end has identified innovation through modeling and simulation as a major scientific priority area. Physiological based pharmacokinetic (PBPK) models, which utilize system- and drug-specific information, are being increasingly used during drug discovery and development and informing regulatory review including drug labeling. A multi-step approach may be appropriate when planning to use PBPK to determine the likely effects of drug and/or gene interactions on drug pharmacokinetics and subsequent need for dedicated studies. Published FDA guidance documents related to drug interactions and early phase pharmacogenomic evaluation have included recommendations for the use of PBPK where appropriate. As pharmacology and clinical pharmacology move forward from reductionist approaches toward integrative systems approaches to address problems, efforts are ongoing to leverage the new

V. Sinha (✉) · Y. Wang
Division of Pharmacometrics, Center for Drug Evaluation and Research, Food and Drug Administration, White Oak Campus, Building 51, Rm 3198, 10903 New Hampshire Avenue, Silver Spring, MD 20993, USA
e-mail: Vikram.Sinha@fda.hhs.gov

S.-M. Huang · I. Zineh
Office of Clinical Pharmacology, Center for Drug Evaluation and Research, Food and Drug Administration, Silver Spring, MD 20993, USA

D.R. Abernethy
Drug Safety Group, Division of Applied Regulatory Science, Center for Drug Evaluation and Research, Food and Drug Administration, Silver Spring, MD 20993, USA

P. Zhao
Center for Drug Evaluation and Research, Food and Drug Administration, White Oak Campus, Building 51, Rm 3198, 10903 New Hampshire Avenue, Silver Spring, MD 20993, USA

D.E. Mager and H.H.C. Kimko (eds.), *Systems Pharmacology and Pharmacodynamics*, AAPS Advances in the Pharmaceutical Sciences Series 23,
DOI 10.1007/978-3-319-44534-2_2

science that is evolving in systems pharmacology. This is focused on the prediction of adverse drug events using the tools of cheminformatics, bioinformatics, and systems biology. Systems pharmacology will need to be put into the larger translational science context to reach full potential in regulatory decision-making.

Keywords Physiological based pharmacokinetic (PBPK) models · Cheminformatics · Bioinformatics · Drug-drug interactions (DDI) · Gene-drug interactions (GDI) · Ontology · Cardiotoxicity · Hepatotoxicity · Pre-competitive data

2.1 Introduction

In its recent efforts to foster efficient and informative drug development, the FDA has prioritized the promotion of biomedical innovation, early communication with drug developers, and administrative and scientific flexibility.[1] The FDA approved 27 new molecular entities in 2013. Approvals included groundbreaking treatments for a variety of unmet medical needs. Additionally, many of these therapies were developed, evaluated by FDA, and/or approved via expedited mechanisms (Buckman et al. 2007; Woodcock and Woosley 2008; Barratt et al. 2012).[2]

The science of quantitative clinical pharmacology continues to advance at a rapid pace such that regulators must constantly evaluate the most appropriate applications of modeling, simulation, and other innovations in the public health context.[3] FDA continues to target improvements in regulatory science, including the development of scientific tools that can bridge the gap between cutting-edge discoveries and real-world diagnostics and therapeutics. FDA has identified innovation in clinical evaluations (e.g., through modeling and simulation) as a major scientific priority area. The FDA Office of Clinical Pharmacology (OCP) has used modeling and simulation strategies to address a variety of drug development, regulatory, and therapeutic questions over the past decade (Huang et al. 2013a; Rowland et al. 2011; Lalonde et al. 2007).

In this chapter, we discuss recent efforts by the FDA's OCP in the development and application of regulatory science focusing on systems pharmacology. Detailed descriptions and case studies discussing the impact of pharmacometric analyses on the premarket approval and labeling of new drugs and the application of accumulated regulatory experience to the review of investigational new drugs (INDs)

[1]FDA innovative drug approvals http://www.fda.gov/AboutFDA/ReportsManualsForms/Reports/ucm276385.htm.

[2]FDA Safety and Innovation Act (FDASIA) http://www.fda.gov/RegulatoryInformation/Legislation/FederalFoodDrugandCosmeticActFDCAct/SignificantAmendmentstotheFDCAct/FDASIA/ucm20027187.htm.

[3]Advancing regulatory science for public health—a framework for FDA's regulatory science initiative, October 2010 http://www.fda.gov/downloads/ScienceResearch/SpecialTopics/RegulatoryScience/UCM228444.pdf.

have been described previously (Huang et al. 2013b). This chapter focuses on the use of systems pharmacology approaches in drug evaluation and other research initiatives.

2.2 Physiologically-Based Pharmacokinetic (PBPK) Modeling

Ethical and practical issues may limit the numbers of studies one can conduct to test all clinically relevant scenarios, which has resulted in the need for innovation in drug development and evaluation to address these knowledge gaps and construct recommendations for safe and effective drug use. One such area of active development is physiologically-based pharmacokinetic (PBPK) modeling. PBPK models, which utilize system- and drug-specific information, are being increasingly used during drug discovery and development and informing regulatory review including drug labeling (Table 2.1) (Peck and Temple 1993; Zhao et al. 2011; Wagner et al. 2015; Shepherd et al. 2015; Jones et al. 2015).[4] In 2013–2014, the yearly number of submissions either requesting scientific advice or as part of approval filings using a PBPK approach was approximately 50. This is a reflection of significant advances in utilization of in vitro data, greater understanding of human physiology, and advancement in database and software development. Experience to date suggests that PBPK may be useful in:

1. Planning and assessment of conventional and population PK trial designs
2. Predicting the pharmacokinetics as a result of intrinsic/extrinsic factors and assessing the impact of sources of variability for untested clinical scenarios
3. Assessment or confirmation of dosing recommendations in specific populations.

2.2.1 Drug-Drug and Gene-Drug Interactions

Drugs that are susceptible to pharmacokinetic drug-drug interactions (DDIs) are often likewise susceptible to high inter-individual variability due to genetic differences in the population such as in drug metabolizing enzyme genes (Conrado et al. 2013). Arguably, DDIs and gene-drug interactions (GDIs) are two of the major sources of variability in drug disposition, and may often coexist in a given patient. The evaluation of an investigational drug's potential for CYP-mediated

[4]Federal Register: FDA Public Workshop "Application of Physiologically—Based Pharmacokinetic Modeling to Support Dose Selection". https://www.federalregister.gov/articles/2014/02/11/2014-02883/application-of-physiologically-based-pharmacokinetic-modeling-to-support-dose-selection-notice-of. 2014.

Table 2.1 Application of physiologically based pharmacokinetic models

Scenario	Application	FDA perspective	Industry perspective
Drug-drug interactions	Drug as enzyme substrate	• Substrate/inhibitor models verified with key clinical data may be used to simulate untested scenarios and support labeling (especially for CYP3A and CYP2D6 substrates) • Predictive performance for predicting the effect of enzyme inducer on investigational drug has not been established	• Challenges in predicting non-CYP pathways; expression levels and scaling factors unclear
	Drug as enzyme perpetrator	• Use to determine the lack of enzyme inhibition • Additional evidence needed to demonstrate predictive performance for positive interactions by comparing observed interaction magnitude and prospectively simulated magnitude from multiple examples	• Challenges in predicting combined time-dependent inhibition and induction • Challenges in predicting intestinal CYP metabolism
	Transporter-mediated interactions	• In vitro-in vivo extrapolation not mature due to inadequate body of information • Complicated by transporter-enzyme interplay • Predictive performance yet to be adequately demonstrated	• Challenges in predicting intracellular concentrations • Scaling factors poorly understood
Specific patient populations	Hepatic and renal impairment	• Predictive performance yet to be adequately demonstrated, particularly in severe impairment subjects • System component(s) needs additional research	

(continued)

Table 2.1 (continued)

Scenario	Application	FDA perspective	Industry perspective
	Pediatrics	• Allometry is reasonable for PK down to age 2 years old • Less than 2 years old, ontogeny and maturation need to be considered	
Additional specific populations and situations	Pregnancy, ethnicity, geriatrics, obesity, disease states, food, formulation, and pH effects, and tissue concentration	• Limited experience to draw conclusions	• For drug absorption, there is high confidence in predicting the effects for BCS[a] Class I drugs; for BCS Class II drugs, additional work in scaling of solubility, dissolution and precipitation data is needed (Roles of BCS Classes III and IV were not discussed)

DDIs in various clinical scenarios is an area in which we currently have the most experience. Our experience with transporter-mediated DDIs is modest, primarily due to uncertainty in system parameters pertinent to our understanding of transporters. Factors influencing the in vitro-in vivo extrapolation of transporter experimental data, such as the expression level of transporters in different tissues, are being studied (Giacomini and Huang 2013). To the extent that the functional consequences of genetic polymorphisms in drug-metabolizing enzymes and their frequencies across various ethnic groups are well documented, this information has been used to evaluate their impact on drug exposure through the use of simulations that allow stochastic modeling of virtual populations (Huang and Woodcock 2010).

In some situations, a multi-step approach may be appropriate when planning to use PBPK to determine the likely effects of DDIs and/or GDIs on drug pharmacokinetics and subsequent need for dedicated studies. For example, such an approach has been described for four drugs that are eliminated by both CYP3A and CYP2D6 (Vieira 2014). Specifically, a PBPK model can be developed based on in vitro metabolism and initial human pharmacokinetic data (Wagner et al. 2014; Rostami- Hodjegan 2012). The approach starts from using basic models, moving to static mechanistic models, followed by dynamic mechanistic models. Simulation exercises can then be performed and refined with additional data as needed. Labeling, management strategies, and need for additional studies could then be driven by the magnitude and clinical relevance of the simulated results, contextualized within the robustness of the model to changing assumptions. These exercises can be superimposed on key drug development milestones and regulator interfaces ranging from the end of phase 1 to the end of phase 2 junctures.

2.2.2 Specific Populations

PBPK modeling can be an attractive complement to the conduct and interpretation of studies in patients with organ impairment (e.g., hepatic or renal), which are logistically and clinically challenging populations to study. There is an under-developed body of information on the impact of organ impairment on important model parameters. We have notably found that the predictive performance of PBPK models of hepatic impairment has not been sufficiently developed.

PBPK modeling may also have utility in predicting pharmacokinetic differences in pediatric patients relative to adults. PBPK may be particularly useful in pediatric populations for which allometric scaling or other standard modeling methods are not sufficiently informative. We have found that standard modeling approaches (e.g., allometry) generally work well in patients older than 2 years of age, and that PBPK may have greater utility in younger patients when key differences in maturation of multiple physiological processes need to be accounted.

2.3 Mechanism-Based Drug Safety Evaluation Using Systems Pharmacology

As pharmacology and clinical pharmacology move forward from reductionist approaches toward integrative systems approaches to address problems, efforts are ongoing to leverage the new science that is evolving in systems pharmacology.[5] This is focused on the prediction of adverse drug events using the tools of chem-informatics, bioinformatics, and systems biology (Abernethy et al. 2011; Bai and Abernethy 2013). To move regulatory science forward in this area, the approach and the tools that still require development have been defined.[6]

2.3.1 Ontology of Adverse Events

The initial activities are both within the FDA and in collaboration with partners in the pharmaceutical industry and academia. The framework for a predictive drug safety systems model is being structured as a series of ontologies at different levels of biological organization (Zhichkin et al. 2012). These were developed to organize the massive amount of pertinent information that will populate this framework. This

[5] www.nigms.nih.gov/nr/rdonlyres/…/systemspharmawpsorger2011.pdf.

[6] Quantitative and systems pharmacology at the post-genome era; new approaches to discovering drugs and understanding therapeutic mechanisms—an NIH white paper by the QSP workshop group. October 2011. http://isp.hms.harvard.edu/wordpress/wp-content/uploads/2011/10/NIH-Systems-Pharma-Whitepaper-Sorger-et-al-2011.pdf.

includes an "ontology of adverse events" that is building on the ontology of adverse events developed for characterization of vaccine related adverse events (Sarntivijai et al. 2012). All of these ontologies are developed in the format consistent with recommendations from the National Centers for Biomedical Ontology to make use of standardized elements in existing ontologies at various levels of biological organization (e.g., gene ontology, cell line ontology, systematized nomenclature of medicine clinical terms).[7] As this evolves, it will constitute the systems pharmacology network that defines a drug-mediated adverse event from observed changes in gene expression up through organelle function, cellular expression, and organ level toxicity that ultimately maps to the MedDRA terms.

2.3.2 *Databases-Leveraging "Precompetitive" Data*

An important element of the program is the collection and organization of drug toxicity data. Published data are relatively easy to obtain and organize, and a number of public and proprietary efforts are creating such databases. These are useful for different forms of data-mining and establishing associations between drug toxicities, the data supporting the mechanism of such toxicity, and in some instances the prediction of toxicity from similar chemical structures (Lounkine et al. 2012). In other instances, based on the biological pathways that are involved, the prediction of clinical toxicities for drugs that have similar targets has been used. More challenging to obtain are the data contained in drug development programs, either those that were successful, or equally important, those that were not successful due to drug toxicity or for other reasons. An effort is underway to encourage pharmaceutical companies to define what of these data can be viewed as "pre-competitive" and can be shared to build more complete drug toxicity databases that are publicly available. All of these data will be placed in a common platform that allows easy integration across different data formats.

2.3.3 *Initial Test Cases: Cardiotoxicity and Hepatotoxicity*

The extent of the systems network needed to effectively predict particular drug toxicities is likely to be variable depending on the target(s), both desired and not desired, for the drug or series of related drugs to be evaluated. An initial "use" case is being developed to study the non-QT cardiotoxicity of tyrosine kinase inhibitor drugs. The clinical reports of depressed left ventricular cardiac function with exposure to select tyrosine kinase inhibitors have certainly raised a potential safety signal (Perakslis et al. 2010). However, the extent or reversibility of this

[7] http://bioportal.bioontology.org.

cardiotoxicity is not clear, and it is also unclear if this is a class effect or only tyrosine kinase inhibitors that target specific kinases are implicated.

A systems network for the prediction of drug-induced hepatotoxicity is being developed at The Hamner Institute in collaboration with a number of pharmaceutical companies and with the FDA interacting and contributing when appropriate. This is a very highly specified model that utilizes a systems network. The utility of this approach, from in vitro-in vivo extrapolation and across species hepatotoxic effects for methapyrilene and acetaminophen, was demonstrated (Athey et al. 2012; Howell et al. 2012). As experience accumulates, the comparative utility of these approaches, or a synthesis of them, will become more evident. At this time, the extent of the overall system and how well characterized the relations between nodes and edges of the system are necessary for a particular predictive drug toxicity problem requires further exploration and testing.

Applications of this program to regulatory decision making has, to date, been focused on the use of data-mining to establish relationships between common biological pathways across drugs and targets and expected or observed clinical safety signals. In addition, the tools of cheminformatics have been incorporated to predict toxicities based on molecular structural elements of the drug or compound class in association with the biological pathways affected. This latter activity is a further evolution of the quantitative structure activity relationship (QSAR) effort that has been ongoing at the FDA for some years (Kligfield et al. 2010; Kruhlak et al. 2012). The outcomes in some cases have led to the incorporation of added safety information in labeling, providing a basis to not include certain risks in other cases, and signal strengthening and (in some cases) signal weakening based on pharmacological mechanistic rationale for potential safety signals noted in post market adverse event monitoring.

2.4 Conclusion and Future Directions

The FDA has been proactive in the development of regulatory science in order to address an array of public health challenges. Modeling and simulation have been important scientific investment areas for the FDA OCP and will continue to be a major area of growth. Systems pharmacology will need to be put into the larger translational science context to reach full potential. The use of systems pharmacology in regulatory decision making has been limited and has largely been in the area of PBPK and one application of a calcium homeostasis model (Huang et al. 2013b) (http://www.fda.gov/downloads/AdvisoryCommittees/CommitteesMeetingMaterials/Drugs/EndocrinologicandMetabolicDrugsAdvisory-Committee/UCM413617.pdf). Key issues that will need to be addressed in order to see enhanced uptake of systems pharmacology approaches in drug regulation include (Force and Kolaja 2011; Ghosh et al. 2011):

- Better understanding of the mechanisms of drug action, including off target effects and maximal elucidation of the disposition pathways of drug molecules

- "Vertical integration": synergistic assimilation of the bottom up (cellular level) and the top-down (organism level) models in order to scale from molecular interactions to organismal physiology
- Targeted training and education of regulatory and non-regulatory scientists
- Sharing of pre-competitive data (preclinical and clinical datasets); efficient use of the private-public partnership models to foster academia-industry-government interactions
- Development of best practices in the development of models fit for regulatory use
- Development of mechanisms that allow for timely evaluation (and re-evaluation) of models in view of rapidly evolving methodologies and science

Despite these challenges, improved understanding of molecular mechanisms is enabling the FDA to employ modeling and simulation in evaluation of "subset" effects (based on subtype of diseases, age, sex, race, genetics, organ dysfunctions, concomitant medications, etc.). For example, published FDA guidance documents related to drug interactions and early phase pharmacogenomic evaluation have included recommendations for the use of PBPK where appropriate. Best practices are needed to appropriately utilize PBPK modeling to forecast altered pharmacokinetics in situations that have not been clinically evaluated (e.g., complex drug interactions and multiple extant co-morbidities). Whereas the FDA review experience is steadily increasing and the challenges in using PBPK remain great, it is expected that applications of PBPK will continue to show utility during drug development and regulatory review (Zhao et al. 2012).

There are several FDA and ICH guidelines that discuss the relevance of modeling in several aspects of drug development.[8,9,10,11,12] Meaningful, pragmatic advice to drug developers will need to be science- and experience-based. As such, the knowledge gained from predict-learn-confirm exercises will contribute to regulatory decision-making, and collaboration among stakeholders—industry, global regulatory agencies, academia, and others- will be important (Woosley 2012).

[8]FDA CDER guidance for industry, population pharmacokinetics. http://www.fda.gov/Drugs/GuidanceComplianceRegulatoryInformation/Guidances/ucm064982.htm.

[9]CDER Guidance for industry. Drug interaction studies—study design, data analysis, implications for dosing, and labeling recommendations. http://www.fda.gov/Drugs/GuidanceComplianceRegulatoryInformation/Guidances/ucm064982.htm.

[10]CDER Guidance for industry. Clinical pharmacogenomics: premarket evaluation in early-phase clinical studies and recommendations for labeling. http://www.fda.gov/Drugs/GuidanceComplianceRegulatoryInformation/Guidances/ucm064982.htm.

[11]FDA CDER clinical pharmacology guidance page. http://www.fda.gov/Drugs/GuidanceComplianceRegulatoryInformation/Guidances/ucm064982.htm.

[12]FDA CDER guidance page: International conference on Harmonisation-Efficacy. http://www.fda.gov/Drugs/GuidanceComplianceRegulatoryInformation/Guidances/ucm065004.htm.

References

Abernethy DR, Woodcock J, Lesko LJ (2011) Pharmacological mechanism-based drug safety assessment and prediction. Clin Pharmacol Ther 89:793–796

Athey BD, Cavalcoli JD, Jagadish HV, Omenn GS, Mirel B, Kretzler M, Burant C, Isokpehi RD, DeLisi C (2012) The NIH National Center for Integrative Biomedical Informatics (NCIBI). J Am Med Inf Assoc 19:166–170

Bai JP, Abernethy DR (2013) Systems pharmacology to predict drug toxicity: integration across levels of biological organization. Ann Rev Pharmacol Toxicol 53:22.1–22.23

Barratt RA, Bowens SL, McCune SK, Johannessen JN, Buckman SY (2012) The critical path initiative: leveraging collaborations to enhance regulatory science. Clin Pharmacol Ther 91 (3):380–383

Buckman S, Huang S-M, Murphy S (2007) Medical product development and regulatory science for the 21st century: the critical path vision and its impact on health care. Clin Pharmacol Ther 81:141–144

Conrado DJ, Rogers HL, Zineh I, Pacanowski MA (2013) Consistency of drug-drug and gene-drug interaction information in US FDA-approved drug labels. Pharmacogenomics 14 (2):215–223

Force T, Kolaja KL (2011) Cardiotoxicity of kinase inhibitors: the prediction and translation of preclinical models to clinical outcomes. Nat Rev Drug Discov 10:111–126

Ghosh S, Matsuoka Y, Asai Y, Hsin KY, Kitano H (2011) Software for systems biology: from tools to integrated platforms. Nat Rev Genet 12:821–832

Giacomini KM, Huang SM (2013) Transporters in drug development and clinical pharmacology. Clin Pharmacol Ther 94(1):3–9

Howell BA, Yang Y, Kumar R, Woodhead JL, Harrill AH, Clewell HJ III, Andersen ME, Siler SQ, Watkins PB (2012) In vitro to in vivo extrapolation and species response comparisons for drug-induced liver injury (DILI) using DILIsym: a mechanistic, mathematical model of DILI. J Pharmacokinet Pharmacodyn 39:527–541

Huang S-M, Woodcock J (2010) Commentary on ITC membrane transporters in drug development; report from the FDA critical path initiative sponsored workshop. Nat Rev Drug Disc 9:175–176

Huang S-M, Bhattaram A, Mehrotra N, Wang Y (2013a) Is this the dose for you? The role of modeling. Clin Pharmacol Ther 93(2):159–162

Huang SM, Abernethy DR, Wang Y, Zhao P, Zineh I (2013b) The utility of modeling and simulation in drug development and regulatory review. J Pharm Sci 102(9):2912–2923

Jones H et al (2015) Physiologically based pharmacokinetic modeling in drug discovery and development: a pharmaceutical industry perspective. Clin Pharmacol Ther 97:247–262

Kligfield P, Green CL, Mortara J, Sager P, Stockbridge N, Li M, Zhang J, George S, Rodriguez I, Bloomfield D, Krucoff MW (2010) The cardiac safety research consortium electrocardiogram warehouse: thorough QT database specifications and principles of use for algorithm development and testing. Am Heart J 160:1023–1028

Kruhlak NL, Benz RD, Zhou H, Colatsky TJ (2012) (Q)SAR modeling and safety assessment in regulatory review. Clin Pharmacol Ther 91:529–534

Lalonde RL, Kowalski KG, Hutmaher MM et al (2007) Model-based drug development. Clin Pharmacol Ther 82:21–32

Lounkine E, Keiser MJ, Whitebreat S, Mikhailov D, Hamon J, Jenkins JL, Lavan P, Weber E, Doad AK, Cote S, Shoichet BK, Urban L (2012) Large-scale prediction and testing of drug activity on side-effect targets. Nature 486(7403):361–367

Peck CC, Temple R, Collins JM (1993) Understanding consequences of concurrent therapies. JAMA 269(12):1550–1552

Perakslis ED, Van Dam S, Szalma S (2010) How informatics can potentiate precompetitive open-source collaboration to jump-start drug discovery and development. Clin Pharmacol Ther 87:614–616

Rostami-Hodjegan A (2012) Physiologically based pharmacokinetics joined with in vitro-in vivo extrapolation of ADME: a marriage under the arch of systems pharmacology. Clin Pharmacol Ther 92(1):50–61

Rowland M, Peck C, Tucker G (2011) Physiologically-based pharmacokinetics in drug development and regulatory science. Annu Rev Pharmacol Toxicol 51:45–73

Sarntivijai S, Xiang Z, Shedden KA, Markel H, Omenn GS, Athey BD, He Y (2012) Ontology-based combinatorial comparative analysis of adverse events associated with killed and live influenza vaccines. PLoS One 7(11):e49941. doi:10.1371/journal.pone.0049941

Shepard T, Scott G, Cole S, Nordmark A, Bouzom F (2015) Physiologically based models in regulatory submissions: output from the ABPI/MHRA forum on physiologically based modelling and simulation. CPT Pharmacomet Syst Pharmacol 4:221–225

Vieira M (2014) PBPK model describes the effects of co-medication and genetic polymorphism on systemic exposure of drugs that undergo multiple clearance pathways. Clin Pharmacol Ther 95 (5):550–557

Wagner C, Pan Y, Hsu V, Grillo JA, Zhang L, Reynolds KS et al (2014) Predicting the effect of cytochrome P450 inhibitors on substrate drugs: analysis of physiologically based pharmacokinetic modeling submissions to the US Food and Drug Administration. Clin Pharmacokinet 54(1):117–127

Wagner C et al (2015) Application of physiologically-based pharmacokinetic (PBPK) modeling to support dose selection—report of a FDA public workshop on PBPK. CPT Pharmacomet Syst Pharmacol 4:226–230

Woodcock J, Woosley R (2008) The FDA critical path initiative and its influence on new drug development. Annu Rev Med 59:1–12

Woosley RL (2012) Is it possible for FDA regulatory scientists and industry scientists to work together? Clin Pharmacol Ther 91:390–392

Zhao P, Zhang L, Grillo JA, Liu Q, Bullock JM, Moon YJ et al (2011) Applications of physiologically based pharmacokinetic (PBPK) modeling and simulation during regulatory review. Clin Pharmacol Ther 89(2):259–267

Zhao P, Rowland M, Huang SM (2012) Best practice in the use of physiologically based pharmacokinetic modeling and simulation to address clinical pharmacology regulatory questions. Clin Pharmacol Ther 92(1):17–20

Zhichkin PE, Athey BD, Avigan MI, Abernethy DR (2012) Needs for an expanded ontology-based classification of adverse drug reactions and related mechanisms. Clin Pharmacol Ther 91:963–965

Chapter 3
Quantitative Systems Pharmacology: Applications and Adoption in Drug Development

Saroja Ramanujan, Kapil Gadkar and Ananth Kadambi

Abstract Biopharmaceutical companies have increasingly been exploring Quantitative Systems Pharmacology (QSP) as a potential avenue to address current challenges in drug development. The ability to integrate diverse data into a unified framework provides a promising approach for a systematic, quantitative evaluation and prediction of the complex interaction between potential therapeutics and biological pathways of disease, with application across the research and development pipeline. In this chapter, we discuss the potential for QSP to help address pressing needs in drug development, and present numerous examples of past applications to problems ranging from target identification to in vivo experimental design through clinical trial simulation, patient stratification, and regulatory evaluation. These examples also illustrate the diversity of QSP modeling approaches. Moving forward, the adoption and success of QSP will require a clearly articulated record of impact on drug development decisions, alongside the development of approaches to address current challenges in the implementation and technical evaluation of such efforts.

Keywords Quantitative systems pharmacology (QSP) · Bone remodeling · Rheumatoid arthritis · Modeling and simulation · Drug development · Clinical · Preclinical

S. Ramanujan (✉) · K. Gadkar
Genentech Inc., 1 DNA Way, South San Francisco, CA 94080, USA
e-mail: ramanujan.saroja@gene.com

A. Kadambi
Rosa & Co. LLC, 751 Laurel St., Ste. 127, San Carlos, CA 94070, USA

D.E. Mager and H.H.C. Kimko (eds.), *Systems Pharmacology and Pharmacodynamics*,
AAPS Advances in the Pharmaceutical Sciences Series 23,
DOI 10.1007/978-3-319-44534-2_3

3.1 Introduction

3.1.1 Industry Status and Needs

Pharmaceutical drug development is a statistically low success, high cost operation. The time required to bring a single new molecular entity (NME) from bench to bedside is 10–15 years, and the eventual approval regulatory rate for new molecules entering Phase I of clinical development is as low as 5 % (Arrowsmith 2012), a result of the very high attrition rate. Furthermore, the total research and development (R&D) cost to a company for a single drug has been estimated to be greater than $1B USD (Kocher and Roberts 2014).

These high costs and long developmental cycles persist despite substantial merger and acquisition-based triaging of corporate pipeline portfolios and are more troublesome in light of a general trend towards an increasing size of development pipelines within the industry. A closer look at the attrition data suggests that approximately 75 % of failures can be attributed to either lack of efficacy or to drug-induced safety issues. These data also suggest that the proportion of efficacy and safety-related failures in pivotal trials have been increasing since the start of the new millennium (Arrowsmith and Miller 2013).

The low approval rates for new drugs can be partly explained by several common challenges that impair the ability to make the most informed decisions related to advancement or termination of drug programs, especially early in development. First, drug development suffers from a "data overload". There is, in general, a lack of quantitative integration of diverse data drawn from disparate sources (e.g., genomic and proteomic studies, in vitro assays, preclinical animal models, and early or prior human trials). In many cases, confounding or conflicting evidence in the data are difficult to reconcile, leading to suboptimal selection of follow-up experiments and clinical trial design, difficulty evaluating and testing hypotheses, and challenges to communication of decision rationale. Second, data suggest that the greatest attrition (18 % success rate in 2008–2009) occurs in Phase II proof of concept trials (Arrowsmith 2011), with roughly 50 % of failures due to lack of efficacy and another 20 % due to safety issues. Furthermore, an analysis of post-Phase II go/no-go decisions at Pfizer Inc. from 2005 to 2009 revealed that for nearly half the trials that failed due to lack of efficacy, mechanisms of action (MoA) were not investigated in the trial thoroughly enough to enable a confident decision to progress to Phase III (Morgan et al. 2012). A key stumbling block in evaluating MoA is translation of evidence from preclinical and animal models into the human setting. Although most non-clinical studies are conducted in mammalian species, physiological and pathophysiological differences between these species and humans are inadequately addressed by historically-utilized methods. Third, in many therapeutic areas (TAs), the development of new drugs is impeded by a inadequate understanding of disease pathophysiology and hence, of novel target validity, in part due to the lack of appropriate biomarkers.

Pharmaceutical companies are also facing challenges with the development of companion diagnostics. Such tools facilitate the individualization, or personalization, of therapies by identifying sub-populations of patients who are most likely to respond or who may be at risk for an adverse event following treatment. Companion diagnostics also provide value from a regulatory perspective, as patient stratification may improve the precision of the indications on a drug label and may make new drugs available to the population most likely to benefit. Regulatory agencies are already encouraging the joint development of companion diagnostics, alongside new drugs, to facilitate their safe and effective use (CDRH guidance for in vitro diagnostics, 2014: http://www.fda.gov/downloads/MedicalDevices/DeviceRegulationandGuidance/GuidanceDocuments/UCM262327.pdf). However, development of companion diagnostics significantly complicates and prolongs drug development due to the need for clinical exploration and validation of the diagnostic markers. Earlier identification or prioritization of markers could help reduce the extent of exploratory efforts in the clinic and increase the likelihood of drug development success by guiding more efficient companion diagnostic development.

The above discussion highlights a critical need for methodologies that can be applied industry-wide to improve decision-making during pharmaceutical drug and companion diagnostic development (Box 1). Application of such methodologies ultimately would be expected to reduce the time and cost hurdles that typically impede pharmaceutical R&D.

Box 1. Examples of Areas Where Methodologies to Improve Industry Decisions may Reduce Time and Costs Associated with Drug Development

- Improved understanding of target and drug mechanisms and biological context based on all available data
- Design of optimal experiments to support mechanistic understanding, target validation, compound selection, and translational confidence
- Support for go/no-go decision making and risk evaluation
- Clinical trial design and optimization, including patient selection, dose/regimen, biomarker selection and sampling, and trial duration

3.1.2 Quantitative Systems Pharmacology in the Drug Development Context

Modeling and simulation (M&S)-based approaches have been used extensively by the pharmaceutical industry since the 1990s to inform both drug development decisions and discussions with regulatory agencies. These approaches have informed dose and regimen selection for clinical trials and aided interpretation of

clinical trial data (van der Graaf and Benson 2011). Examples of cornerstones of pharmaceutical modeling are pharmacometric approaches including preclinical and translational pharmacokinetic-pharmacodynamic (PK/PD) models, population-based statistical PK/PD models, and data-driven statistical disease progression and outcomes models. Whereas these methods have proven invaluable, their utility in translating biological effects between species, a critical element of decision making during drug development, is limited (van der Graaf and Benson 2011). In addition, it is difficult to use these methods to rigorously assess MoA of new drugs, an important consideration as discussed above.

To increase drug development success rates, pharmaceutical researchers are increasingly exploring modeling approaches broadly referred to as Quantitative Systems Pharmacology (QSP) that include greater biological and physiological detail (Leil and Bertz 2014). One definition describes QSP as the "quantitative analysis of the dynamic interactions between drug(s) and a biological system that aims to understand the behavior of the system as a whole, as opposed to the behavior of its individual constituents" (van der Graaf and Benson 2011). The representation of interactions between a drug and the underlying biological processes or mechanisms affected by the drug, including commonalities and differences between species, and enables quantitative biology-based translation and clinical development, including rigorous evaluation of drug MoA. QSP approaches typically share several attributes which, taken together, help distinguish them from other modeling approaches (Box 2).

Box 2. Common Distinguishing Features of QSP Approaches

- A coherent mathematical representation of the key biological connections underlying the system of interest, consistent with the current state of knowledge
- A general prioritization of necessary biological detail over parsimony,[1] potentially including detail at the genetic, protein, cellular, tissue, organ, and whole-body-levels[2]
- Consideration of complex systems dynamics such as biological feedbacks, cross-talk, and redundancies
- Integration of diverse data and biological knowledge or hypotheses
- A representation of the pharmacology of therapeutic interventions[3]
- The ability to perform quantitative hypothesis exploration and testing via biology-based simulation in virtual humans, animals, and cells

[1]van der Graaf, personal communication

[2]Kohl et al. (2010) and Berg et al. (2010)

[3]Cohen (2008)

As the aim of QSP is to quantitatively represent the often complex behaviors of biological systems that cannot be fully characterized in any one data set, the

approach relies heavily on consideration of diverse biological data and understanding. These disparate data are integrated into a coherent mathematical framework, enabling quantitative predictions of the impact of drug-induced target modulation, often prior to the availability of clinical data on the target or drug of interest. The schematic in Fig. 3.1 highlights some of the key information types frequently integrated in QSP modeling efforts.

Several types of models are commonly classified as QSP. These most commonly include mechanistic models that represent complex biological pathways in healthy and disease physiology, and downstream PD effects (Peterson and Riggs 2010; Demin et al. 2013; Chen et al. 2009). Other pharmacometric or systems biology related M&S approaches that include quantitative biological or biophysical detail have also been described as QSP, including physiologically-based pharmacokinetic (PBPK) models that focus on compound PK and distribution (Rowland et al. 2011; Rostami-Hodjegan 2012), statistical systems models used to describe population

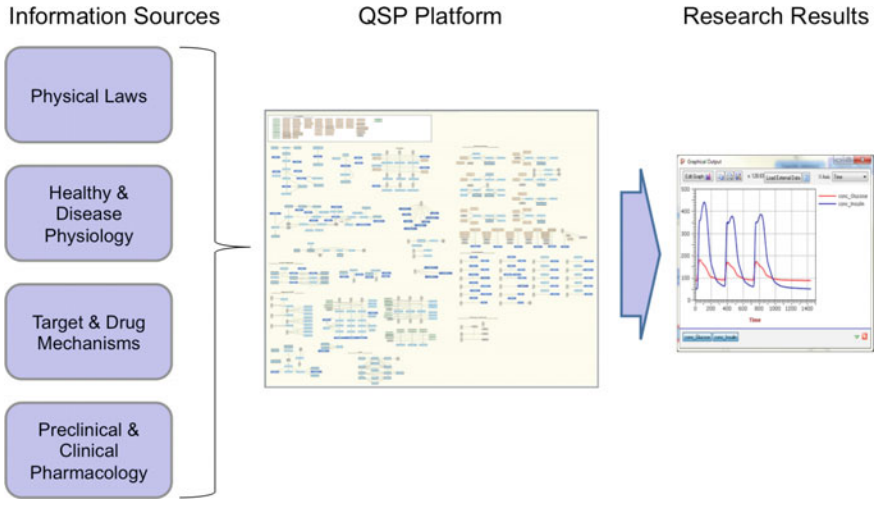

Fig. 3.1 Schematic depicting data sources frequently integrated during the development of a QSP model, in this case a PhysioPD™ Research Platform for type 2 diabetes (Reprinted with permission of Rosa & Co. LLC, © 2016). Information or data from four general classes are typically used in this process (*left*): (1) *physical laws* e.g., conservation of mass or reaction kinetic laws, (2) *physiology* e.g., organ function, (3) *mechanisms* e.g., cellular and molecular pathways, (4) *pharmacology* e.g., drug binding constants and half-lives. These information sources include in vitro, in vivo, or clinical patient data. Information from these disparate sources are incorporated in the construction of a qualitative mechanistic map (center, Rosa & Co. PhysioMap®) that describes the biological mechanisms underlying healthy and diseased physiology and subsequent implementation as a quantitative model using mathematical equations. Solution of these equations under different conditions (e.g., meal administration) yields predictions for changes in key system outputs over time (*right*), allowing research to be conducted for different scenarios of interest (e.g., drug treatment regimens). Alternate parameterizations of these models, representing virtual pathways, cells, or subjects can be used to explore the impact of alternate underlying biological hypotheses or inter-subject variability on the system behaviors

data on biological pathways or disease processes (van Herick et al. 2012), and some quantitative systems-biology approaches reliant on genomic or proteomic data (Hansen and Iyengar 2013; Zhao et al. 2013; Xing et al. 2011). Thus, the boundary between more traditional pharmacometric approaches and QSP is not well-defined, and these methods may be better viewed as coexisting along a continuum from mechanistic PK/PD to PBPK and "enhanced" mechanistic PK/PD to QSP to systems biology (Iyengar et al. 2012). The different strengths and focus of these varied approaches could be applied synergistically within the context of drug development to provide biology-driven insights that inform necessary decisions. Most obviously,

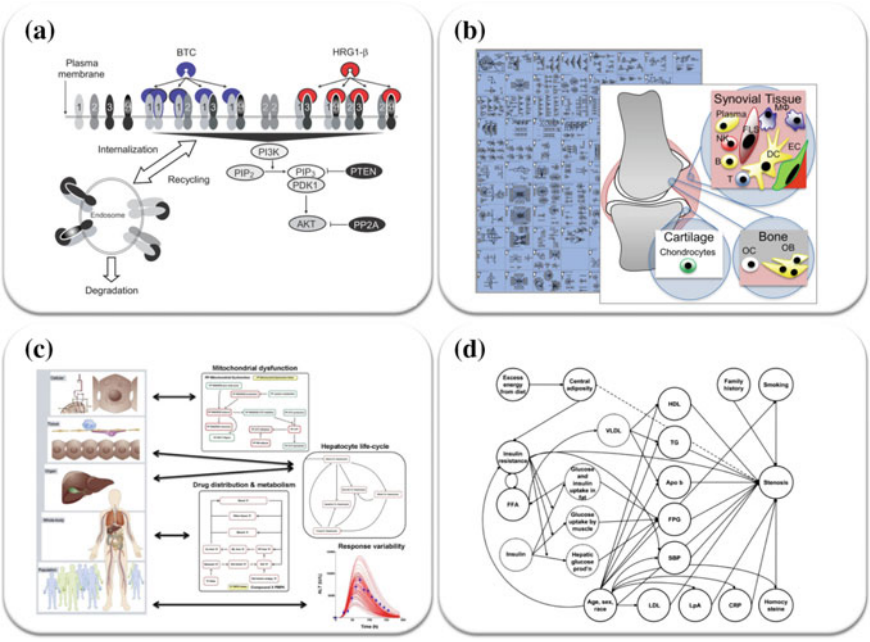

Fig. 3.2 Illustrations of some common types of QSP models. **a** Biological PD pathway models are focused on a specific biological interactions and pathways relevant to the targets, compounds, and PD biomarkers under consideration (image reproduced from Schoeberl et al. (2009) with permission of *Science Signaling,* © 2009). **b** Disease platforms, such as the Rheumatoid Arthritis PhysioLab® platform (model diagram image reproduced with permission of Entelos Inc.; *inset image* reproduced from (Schmidt et al. 2013) in accordance with terms of Creative Commons, http://creativecommons.org/licenses/by/2.0/) are broader representations of physiological and pathophysiological states which may include numerous potential targets, compounds, or patient types. **c** Toxicology and safety model platforms, such as the DILIsym® model of drug induced liver toxicity support in silico evaluation of common areas of drug toxicity (image reproduced from Bhattacharya et al. (2012) and Kuepfer (2010), with permission in accordance with terms of Creative Commons, http://creativecommons.org/licenses/by/3.0/); **d** statistical systems models such as the Archimedes model, of which a subset relevant to coronary artery disease is shown here [(Eddy et al. 2009), image reproduced with permission from *Diabetes Care,* © 2009] are statistically-based systems models for prediction of population biomarker and outcomes predictions

traditional pharmacometric models may provide critical inputs to QSP models, and QSP model-derived predictions of biomarker behavior can serve as inputs into statistical disease outcome models.

This chapter presents potential roles of QSP throughout the drug development process, with selected illustrative examples from the biopharmaceutical industry that illustrate synergies with existing approaches. Examples of QSP efforts discussed in this chapter illustrate not only a range of applications and TAs, but also a variety of model types (Fig. 3.2). These examples also use a range of mathematical techniques, including ordinary differential equations (ODEs), logic-based approaches, statistical regression models, and finite element methods (FEM).

In this chapter, we focus on biology-based QSP models that include a representation of key pathways and PD biomarkers downstream of one or more compounds or targets, and do not present efforts centered on PK and drug distribution or systems biology. Furthermore, we have emphasized published work to allow follow-up on technical details based on the reader's interests. Finally, we also discuss challenges and needs for advancement of QSP in industry, including the integration of QSP approaches into the existing pharmaceutical development process and possible means of increasing industry and regulatory adoption (van der Graaf and Benson 2011).

3.2 Application of QSP Across the R&D Pipeline

Frequently, the preclinical space from research to human translation, and especially target evaluation, has been highlighted as a "sweet spot" for the application of QSP in drug discovery and development (Agoram and Demin 2011; Vicini and van der Graaf 2013; van der Graaf and Benson 2011). This idea is consistent with the previously described need to better understand and test drug MoA in early stages. The greater focus on biology in QSP relative to traditional pharmacometric approaches enables its use early in the pipeline where decision-making is heavily predicated on an understanding of how targets and drugs relate to the broader biological or disease system of interest. Further, as discussed previously, there is a pressing practical need for pharmaceutical companies to evaluate MoA early and thoroughly as part of a "fail early" paradigm to reduce later, expensive clinical failures. Finally, initiation of QSP efforts early in drug development can allow companies more time to develop capabilities to address multiple targets or compounds in a given TA at different development stages, incorporating new data as they become available.

The relevance of QSP to early stages of pharmaceutical development by no means limits its application at later stages. QSP can provide a means of integrating prior or emerging clinical data with mechanistic and preclinical information to address relevant clinical development considerations, such as patient stratification, biomarker interpretation, combination therapy, and competitive evaluation and differentiation. It can also synergize with pharmacometrics in the optimization of

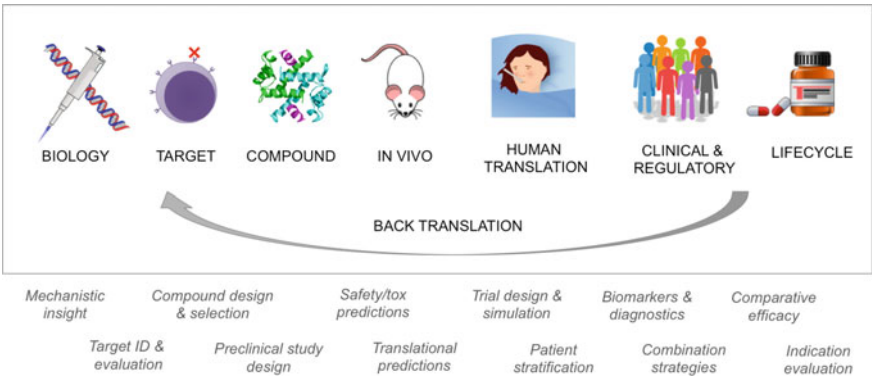

Fig. 3.3 Potential applications of QSP throughout the drug development pipeline

dose and regimen. Figure 3.3 highlights potential applications of QSP across the pharmaceutical development pipeline.

Here we describe how industry can and has employed QSP approaches in different applications, using a few illustrative examples for each stage in the pipeline (Table 3.1).

3.2.1 Research and Preclinical Applications

Early drug development is dependent on in vitro and in vivo studies to help identify, prioritize, and help validate potential drug targets. However, although valuable, these systems are imperfect models of human physiology and pathophysiology, and thus additional approaches that de-risk decision making at this stage are of great value. With its emphasis on quantitative integration of diverse data, including preclinical and clinical information, QSP offers one such approach, and there are multiple examples of its application in target identification, evaluation, characterization, and prioritization.

One such example is a detailed model of the kinetics of EGF receptor family mediated activation of the PI3K/Akt pathway in response to representative ligands (Schoeberl et al. 2009). Developed using rich in vitro signaling dynamic data, model analysis highlighted a central role of the HER3 receptor in combinatorial ligand-induced pathway activation. To validate this finding and explore the therapeutic potential of HER3 modulation, Merrimack Pharmaceuticals developed MM-121, a fully human anti-HER3 monoclonal antibody and verified their findings with in vitro cell culture, spheroid growth, and in vivo tumor growth studies. The molecule is currently in Phase II trials in breast, ovarian, and lung cancer, and clinical results to date indicate that inhibition of HER3 by MM-121 improves progression-free survival (PFS) in patients with high levels of the HER3 ligand

Table 3.1 Summary of examples presented

Pipeline stage in example	Primary application in example	Biological or therapeutic area focus	Reference
Research and preclinical	Target identification	Oncology	Schoeberl et al. (2009)
	Target identification	Pain	Benson et al. (2013)
	Combination Rx and in vivo validation	Oncology	Kirouac et al. (2013)
	Regimen optimization and combination efficacy	Oncology	Orrell and Fernandez (2010)
Translation	Immunogenicity prediction	Immunology	Chen et al. (2014a, b)
	Combination Rx evaluation	CNS	Geerts et al. (2013a)
Clinical	Combination Rx and subpopulation responses	Cardiovascular	Gadkar et al. (2014)
	Exploratory endpoint biomarker	Osteoporosis	Visser et al. (2014)
	Efficacy and safety	Cardiovascular	Dziuba et al. (2014 and Peskin et al. (2011)
Safety	Pre-clinical screening	Cardiac arrhythmia	Davies et al. (2012)
	Clinical toxicity prediction	Liver toxicity	Howell et al. (2014), Shoda et al. (2014) and Leil and Bertz (2014)
Back-translation	Mechanistic understanding and target/compound evaluation	Cardiovascular	Gadkar et al. (2016b) and Lu et al. (2014)
Cross-pipeline Disease Platforms	Target prioritization; clinical biomarker identification; mechanistic hypothesis generation	Rheumatoid arthritis	Meeuwisse et al. (2011), Rullmann et al. (2005), Schmidt et al. (2013) and Kadambi et al. (2011)
	Efficacy versus safety dose and regimen evaluation	Bone remodeling	Peterson and Riggs (2010, 2012), Riggs et al. (2012), Peterson and Riggs (2015), FDA briefing document[a]

[a]http://www.fda.gov/downloads/AdvisoryCommittees/CommitteesMeetingMaterials/Drugs/EndocrinologicandMetabolicDrugsAdvisoryCommittee/UCM413617.pdf

heregulin (MacBeath and Adiwijaya 2014). This effort shows the impact of QSP-supported target identification and subsequent in vivo and emerging clinical validation of the target.

Practical pharmacological considerations, such as druggability and PK feasibility, are also critical to successful modulation of a proposed target. These considerations are harder to address using in vitro studies or in the absence of tool compounds. Integration of prototypical PK models in QSP models of pathway biology may provide one avenue to help handle these challenges. For example, sensitivity analysis in a systems model of the nerve growth factor (NGF) pathway identified

tropomyosin receptor kinase A (TrkA), along with NGF itself, as druggable targets predicted to strongly regulate downstream PD (Benson et al. 2013). To address pharmacological considerations, administration of a virtual anti-NGF antibody and of a hypothetical small molecule (i.e., a TrkA inhibitor) were simulated using representative human PK and target binding/inhibition parameters to help evaluate the relationships between drug properties, dose, and the extent of PD inhibition, and to confirm pharmacological feasibility of the target.

The next step following identification of a viable therapeutic target is to develop compounds and test them in vitro and in vivo. The NGF target identification example illustrates how QSP can be used to understand the relationships among compound characteristics (binding and inhibitory parameters), dose, and modulation of downstream biology. QSP can also be valuable in guiding and interpreting in vitro studies and leveraging such results to plan in vivo experiments. Preclinical development faces continuous pressure to prioritize and reduce the number of experiments, especially in vivo studies, for both financial and ethical reasons. Achieving these goals can be especially challenging when exploring the combinatorics of compounds, doses, and regimens. QSP approaches have been used in this area to prioritize regimens for in vivo testing of monotherapy and combination therapies.

Kirouac et al. (2013) used QSP modeling to support the preclinical investigation of a bispecific antibody targeting HER2 and HER3 in cancer. Using in vitro data, they developed a multi-scale systems model of ErbB signaling through the MEK/ERK and PI3K/AKT pathways that included immediate signaling, translational compensatory feedbacks, and downstream effects on tumor cell growth. Of note, this effort integrated numerous modeling formalisms, including ordinary differential equations for description of PK and tumor growth dynamics, steady-state algebraic solutions for rapid signaling, and logic-based formulation of cell fate decisions. Simulation results suggested that addition of the bispecific to established drugs targeting the other EGF receptors would improve growth inhibition in HER2+ tumors and would be superior to the combination of prototypical small molecule AKT and MEK inhibitors. These findings were validated with additional in vitro and in vivo studies that verified the predicted combination therapy efficacy, thereby increasing confidence in the molecule and in the combination strategy.

Another model intended for broader use in preclinical oncology is the Virtual Tumour Preclinical platform, an in silico representation of a growing tumor that integrates available PK and cell cycle PD measurements for chemotherapeutic and targeted cancer treatment agents into a model of cell cycle and xenograft tumor growth (Chassagnole et al. 2006). The Virtual Tumour is intended for simulation and optimization of in vivo dosing regimens (e.g., for the aurora kinase inhibitor SNS-314, Sunesis), and has also predicted the non-intuitive effect of drug scheduling on growth in combination protocols, such as SNS-314 and docetaxel combination therapy (Orrell and Fernandez 2010). This model was recently expanded to support translation into the clinical setting by replacing murine xenograft-specific parameter values with values describing clinical tumor growth

rates and human cell cycle differences. Thus, the Virtual Tumour model is being applied to inform both preclinical and translational evaluation of single-agent and combination therapy dose and regimen (Visser et al. 2014).

3.2.2 *Translational Application*

Translation of preclinical to clinical findings is an area of high risk in drug development due to differences between preclinical models and human disease and an incomplete understanding of the latter particularly. Translation has proved especially challenging in certain poorly understood therapeutic areas, including Central Nervous System (CNS) disorders. However, QSP modeling approaches that represent conserved and differential biology to explain both preclinical data and any relevant human data or hypotheses should be well suited to support translation. Geerts et al. (2013b) have developed a QSP-based approach that integrates preclinical neurophysiological data with clinical and imaging data of the disease pathology. Their QSP model of the cortical network involved in the maintenance of cognitive working memory tasks (Geerts et al. 2013a) was validated by its ability to predict the opposing responses of two antipsychotic GABA modulators. Based on preclinical data, the model was then used to simulate the effects of a combination therapy in treatment-resistant schizophrenia with the antipsychotics clozapine (which binds neurotransmitter and GABA receptors) and risperidone (a dopamine antagonist with additional antagonist activities). Results indicate that specific anti-cognitive effects of the combination would outweigh the pro-cognitive effects, consistent with prior clinical results showing no improvement in symptoms and a worsening of cognitive outcomes (Honer et al. 2006). These validation results suggest that QSP approaches could help use preclinical data to predict the clinical impact of CNS-related therapies based on preclinical understanding.

QSP models of the biological response to drugs might also support translation of PK itself by modeling biological pathways that influence PK but that cannot be addressed by traditional allometric scaling, more mechanistic target-mediated drug distribution (TMDD) approaches, or even PBPK models. One concern that complicates human translation for biologic drugs in particular is difficulty in predicting drug-elicited clinical immunogenic response. Anti-drug antibodies (ADAs) can significantly impact the PK of biologics and hamper drug efficacy by interfering with target binding. Chen et al. (2014a, b) developed a first-generation mechanism-based immunogenicity model for therapeutic proteins, including details of antigen presentation, activation, proliferation and differentiation of immune cells, secretion of ADAs, as well as in vivo disposition of ADAs and therapeutic proteins. The model was validated with mouse studies, and clinical predictions for the anti-TNFα molecule adalimumab yielded appropriate trends for ADA- and time-dependent drug exposure. The model represents a significant first step in the development of a translational predictive model of immunogenicity, but first needs rigorous validation and refinement as outlined by the authors.

3.2.3 Clinical Application

In clinical development, QSP has been used to provide insights to inform a range of critical decisions, from dosing regimens and biomarker strategies to patient stratigication QSP can also allow predictions and supporting interim analyse of clinical endpoints prior to full data integration from long and costly clinical trials. In this context, QSP methods have offered insight and guidance to complement information provided by pharmacometric approaches.

As an example, Gadkar et al. (2014) developed a QSP model to support clinical development of an anti-PCSK9 antibody, to be administered as monotherapy or in combination with statins, for treatment of hyperlipidemia and cardiovascular (CV) disease. The mechanism-based model was developed using preclinical and limited Phase I clinical data. The model included a TMDD model of the anti-PCSK9 PK. This integration of the TMDD model with downstream mechanisms enabled prediction of the impact of statin-induced feedback on drug PK, and ultimately PD, as measured by LDL cholesterol lowering. The model showed that while statin background therapy would influence PK and PD, the differences would be minimal and not necessitate special consideration. The QSP effort also led to the appropriate selection between two population PK/PD models that equally well described the Phase I data but yielded different Phase II predictions; the selected population PK/PD model was then used moving forward, along with the QSP model itself, to anticipate results for dose regimens in ongoing Phase II efficacy studies and allow accelerated preparation for Phase III. The QSP model was also used to predict response to anti-PCSK9 treatment in familial hypercholesterolemia (FH) patients, for whom minimal PCSK9-related data were available, and thus informed clinical program planning. The model was also used to evaluate the predictive value of previously proposed biomarkers of response to anti-PCSK9. Many of these predictions (e.g., impact of statin background, familial heterogeneity, and dose/regimen) have since been confirmed in subsequent clinical trials and publications.

Because evaluation of clinical endpoints often requires long trials, measurements of exploratory biomarkers that allow earlier or interim evaluation of response are of great interest. However, linking exploratory biomarkers to functional or clinical outcomes typically requires rich prior clinical data. QSP models could potentially inform this connection through representation of biological or biophysical mechanisms. In one such case, a finite element method (FEM) based quantitative model was constructed to use data from clinical 2-dimensional images, obtained with high resolution peripheral quantitative computed tomography, to recreate the 3-dimensional bone structure related to fracture risk. This approach enabled the use of model-based analysis to serve as a noninvasive surrogate marker of bone strength and associated fracture risk (Visser et al. 2014). The model was used to support differentiation of odacatanib, a selective CatK inhibitor used for the treatment of postmenopausal osteoporosis, from standard of care, thus providing insight into the clinical viability of the program. Furthermore, successful validation of the model in

a non-human primate study led to the inclusion of the imaging-informed model-based assessment of bone structure as an exploratory endpoint to support a potential go/no go decision in an interim analysis of a two year Phase III clinical trial. Thus, in addition to clinical utility, this effort also demonstrates how investment in QSP during preclinical development can subsequently enable application in clinical decision-making.

In addition to bridging biomarkers with downstream functions or outcomes, QSP can also bridge mechanistic and statistical approaches to modeling those outcomes, using statistical representations of complex networks of the underlying biological connections. One example is the Archimedes model, a human physiology-based, statistical disease progression model designed to simulate the effect of established and/or novel treatments for cardiometabolic diseases. The model is calibrated and validated against a wide range of existing databases and clinical trials. It also captures the impact of treatments on clinical outcomes, including endpoints like CV risk that typically requires 3–5 year trials with large numbers of patients (Peskin et al. 2011). In one application, Dziuba et al. used the Archimedes model to predict that the SGLT-2 inhibitor dapagliflozin, when added to SoC medication for type 2 diabetes mellitus (T2DM), would not increase CV risk but actually lead to improvement in long term risk and microvascular outcomes (Dziuba et al. 2014). Subsequent trial results and meta-analysis of cardiovascular effects were consistent with these predictions (Sonesson et al. 2016).

3.3 Understanding and Back-Translation of Clinical Findings

Given the high cost and high risk in drug development, pharmaceutical researchers are extremely interested in how to best leverage past clinical experience with drugs aimed at specific targets, pathways, or diseases relevant to the development of a new drug. This back-translation often involves dissecting the biological or pharmacological basis of past success or failure to guide new efforts. For example, initial pivotal trials of cholesterol ester transfer protein inhibitors (CETPi) aimed at increasing HDL cholesterol (HDLc) were terminated due to lack of efficacy or safety, raising concerns about the validity of targets and compounds aimed at increasing total HDLc. Lu et al. (2014) developed a lipoprotein metabolism and kinetics model using available clinical and preclinical data to evaluate the impact of CETPi on reverse cholesterol transport (RCT), a primary mechanism for removing cholesterol from atherosclerotic vessels. Results from this work suggest that RCT flux does not improve and may actually decrease with CETP inhibition, contrary to expectation. This work provided a plausible mechanistic explanation for the failure of recent CETPi trials and suggested that other compounds with similar effects on HDL alone may not be viable drugs. The model was later expanded to predict the

effect of other targets and compounds in clinical development (Gadkar et al. 2016b). RCT improvements were predicted for these other HDL-related compounds, and results were qualitatively validated based on agreement with prior and subsequent imaging data on atherosclerotic plaque load. QSP results thus provided a quantitatively and biologically plausible explanation of past trial failures while predicting a potential therapeutic value of drugs affecting alternate targets on the same pathway.

3.4 Safety and Toxicity Predictions and Understanding

Safety and toxicity are critical areas of consideration in drug development. Pharmacometric approaches are frequently used to understand exposure/safety relationships and to define therapeutic windows. However, QSP based evaluations can also identify potential translational risks or aid drug screening during preclinical development. Two areas in which QSP models have been used extensively to address safety considerations include cardiac electrophysiology related safety and drug-induced liver injury (DILI), major classes of toxicity that are closely monitored in preclinical and clinical stages as part of standard drug development.

Preclinical modeling and simulation-based prediction of the potential for a compound to induce altered cardiac action potential (AP) and cardiac arrhythmia has been the focus of multiple QSP efforts (Mirams et al. 2012). One such effort adapted previously published work (Benson et al. 2008; Hund and Rudy 2004) to develop an in silico model to predict the effect of novel compounds on cardiac AP duration and QT-interval prolongation (Davies et al. 2012). Across 53 compounds, model predictions based on only in vitro ion channel screens were more than 80 % accurate at identifying compounds that would change AP duration, with 68 % accuracy at predicting the direction (prolonging or shortening) of effect. Models such as these can serve as high-throughput in silico screens to augment existing screening tools to support compound evaluation and reduce the number of costly animal experiments.

With respect to DILI, both American and European institutions are actively developing QSP platforms to enable investigation and prediction of drug-induced liver toxicity. One example is the DILIsym® modeling platform, developed by the non-profit Hamner Institutes of Health Sciences. This mechanistic QSP platform integrates PBPK, metabolism models for a compound of interest, and compound interactions with hepatocyte biology relevant to modulation of hepatic mass and function. It is intended to provide information on experimental or clinical design that could identify a risk of liver toxicity, as well as a mechanistic rationale for the underlying biochemical events that would cause such toxicity. Shoda et al. have discussed several applications of the DILIsym model during the drug development process (Shoda et al. 2014). In one example, the DILIsym model was used to study hepatocyte loss with entolimod, a toll-like receptor 5 agonist developed as a

countermeasure against total body irradiation (Howell et al. 2014). The simulations from DILIsym predicted that despite elevated levels of serum aminotransferases observed in a safety study of the drug, the hepatocyte loss would not be sufficient to pose significant health risks in entolimod-treated human subjects; entolimod is still under development. In another application, research with in the DILIsym platform was used to propose mechanisms explaining the differential hepatotoxicity of different bile salt export pump (BSEP) inhibitors (Woodhead et al. 2014). Results also highlighted specific cases where the preclinical safety findings would not be predicted to translate to clinical concerns. These examples illustrate how a platform model can be used to predict, translate, and dissect the effects of drugs on liver toxicities.

3.5 Mechanistic Disease Platforms

The development of disease platforms that capture details of underlying biology and ideally integrate preclinical and clinical data on different phenotypes, treatments, and clinical measures, cannot be only scientifically challenging but also more resource-intensive than traditional pharmacometric approaches. However, there is also a strong rationale to justify investment in a platform with broad applicability throughout the drug development process and across numerous disease pathways, targets, drugs, biomarkers, and outcomes. Some of the examples discussed above featured the use of platforms intended for broad application, such as the Virtual Tumour, the DILIsym model, and the CNS model of Geerts et al (2013b). We now present two examples where published literature illustrates how QSP disease/pathophysiology platforms have seen repeated use with cross-pipeline, cross-industry, and even regulatory impact.

3.5.1 Rheumatoid Arthritis

The Rheumatoid Arthritis PhysioLab platform (Fig. 3.2b), a large-scale mechanistic disease platform describing the inflammatory and erosive processes in afflicted joints in rheumatoid arthritis (RA) patients, has been used to explore a variety of questions at different stages of drug development. The model includes rich dynamics of numerous immune and stromal cells in the bone, cartilage, and synovial tissue compartments and their cross-regulation by soluble and contact mediated signals, along with resulting inflammatory, cartilage, and bone damage readouts, as well as numerous therapeutic interventions. In its first published application, the pharmaceutical company sponsoring its development (Organon Inc., since acquired by Merck & Co.), used the platform to rank 31 diverse immunological and inflammatory molecular targets based on the predicted effects of target modulation on disease

severity scores and cartilage degradation (Rullmann et al. 2005). In addition to providing insights into MoA of the different putative targets, the effort provided a systematic and quantitative rationale for selecting the most promising targets for Organon to move forward in the developmental pipeline.

Subsequently, the platform was used to identify potential serological markers of the severity of progressive joint destruction in RA. Measurement of damage progression currently requires longitudinal radiographic imaging over multiple years and meticulous scoring by trained individuals. Serological markers could not only enable biomarker-based tracking of difficult-to-measure long-term endpoints in trials and stratification of response based on initial severity of damage progression, but also improve clinical practice where joint damage is infrequently measured. The researchers in this case analyzed the simulated cytokine concentrations and joint damage progression rates across a cohort of numerous RA virtual patients with different underlying mechanistic parameterizations and a range of disease severities. CXCL13 was identified as a potential marker of severity of damage progression; clinical data from a cohort of 155 patients was then analyzed and found to validate the finding. In subsequent clinical publications, other groups have also reported CXCL13 as a serum biomarker of destructive severity in RA (e.g. Bugatti et al. 2014; Greisen et al. 2014), further confirming the initial model-based finding.

With respect to diagnostic biomarkers predictive of treatment response, an expanded version of the model was used with an unspecified pharmaceutical company to propose patient stratification biomarkers for blockade of a novel target (Kadambi et al. 2011). Simulated pre-treatment concentrations of 69 soluble proteins were assessed to identify combinations of 4–5 analytes that predicted clinical response to simulated blockade of a novel target in three virtual patient populations: disease modifying therapy naïve patients, methotrexate inadequate responders, and anti-TNF inadequate responders. Recommendations were provided for clinical exploration of the proposed diagnostic marker panels, although no follow-up has yet been publicly reported. Notwithstanding, this case illustrates the potential of QSP to support diagnostic biomarker identification or evaluation.

The platform was also used to explore mechanistic underpinnings of differences in response to the B-cell depleting agent rituximab (Schmidt et al. 2013). The authors created virtual patient populations to identify mechanisms associated with rituximab response. Their results highlighted a potential role of interferon beta effects on synovial fibroblasts and macrophages, consistent with a clinically observed relationship between rituximab response and a type I interferon signature (Raterman et al. 2012). Pharmaceutical companies that have licensed this RA model platform continue to use it to support their drug development efforts, for example to explore combination therapy strategies (Thalhauser et al. 2015).

3.5.2 Bone Remodeling

QSP approaches have been widely applied in the study of bone structure, strength, and remodeling. In one notable effort, three published mechanistic models (Raposo et al. 2002; Lemaire et al. 2004; Bellido et al. 2003) were integrated and modified to create a comprehensive multi-scale platform of bone remodeling (Peterson and Riggs 2010) that was subsequently adapted to support development of various drugs in different therapeutic indications. The integrated model encompassed mechanistic details of key processes in bone catabolism and metabolism, including complex interactions of osteoblast and osteoclast cells, cytokines and growth factors, and parathyroid hormone (PTH) in different tissue compartments, as well as pathways related to calcium dynamics and its regulation by the kidney. These features enabled an accurate reproduction of healthy, disease, and therapeutic conditions, including: RANKL inhibition, administration of PTH, primary and secondary hyperparathyroidism, and primary hypothyroidism (Peterson and Riggs 2010).

The model was further expanded to include menopause-related estrogen effects on bone physiology and integrated with a logistic regression-based analysis of the effect of GnRH agonists on endometrial pain (Peterson and Riggs 2012). Simulations for GnRH agonists predicted the target range of estradiol biomarker concentrations to achieve a balance between the desired efficacy and bone loss side effects, thus guiding dose optimization. The model was also expanded to address the effects of kidney dysfunction on bone mineral density (BMD) by linking the bone resorption pathways to BMD changes and simulating effects of hypothetical treatment strategies for chronic kidney disease-induced bone loss (Peterson and Riggs 2012).

Finally, the original model was used in the Food and Drug Administration (FDA) evaluation of the recently granted biological license application (BLA) submitted by NPS pharmaceuticals for the recombinant PTH drug Natpara for the treatment of hypocalcemia in patients with hypothyroidism. The FDA Advisory Panel briefing document describes the use of the model to evaluate the adequacy of the dosing regimen and examine alternate regimens, including sustained release or lower, more frequent dosing (http://www.fda.gov/downloads/AdvisoryCommittees/CommitteesMeetingMaterials/Drugs/EndocrinologicandMetabolicDrugsAdvisoryCommittee/UCM413617.pdf). A commentary on the history and evolution of the bone remodeling platform raised the idea that the use of this model in regulatory review might be a “watershed” moment for QSP, marking its progress towards adoption in the regulatory context (Peterson and Riggs 2015). Regardless, the repeated adaptation and use of this systems platform for different applications and in the context of regulatory evaluation highlights the potential broader impact of publicly disclosed or available QSP platforms of physiological and pathophysiological processes.

3.6 Adoption of QSP in Industry

Given the relatively new role of QSP in the biopharmaceutical industry, organizations have adopted different approaches to integrating QSP into their drug development process. At one end of the spectrum, the biotech/pharmaceutical company Merrimack Pharmaceuticals Inc. adopted a unique approach to exploiting systems modeling, embedding QSP alongside and interactively with experimental work as a core part of drug development from discovery through clinical stages (Fig. 3.4). Since its inception in 2000, the company has applied QSP efforts to development of agents across its pipeline for both protein and nanotherapeutic agents (Hendriks et al. 2012, 2013; Schoeberl et al. 2009; Kirouac et al. 2013). The company's strategy to incorporating QSP was enabled in part by the background of the founders who were trained in systems modeling (Chen et al. 2009) and the opportunity to include QSP as part of internal processes from the inception of the company. The specific molecules discussed are still in development. However the company has received their first regulatory drug approval for a liposomal irinotecan agent for treatment of metastatic pancreatic adenocarcinoma, providing initial support for their drug development approach and the embedding of modeling techniques.

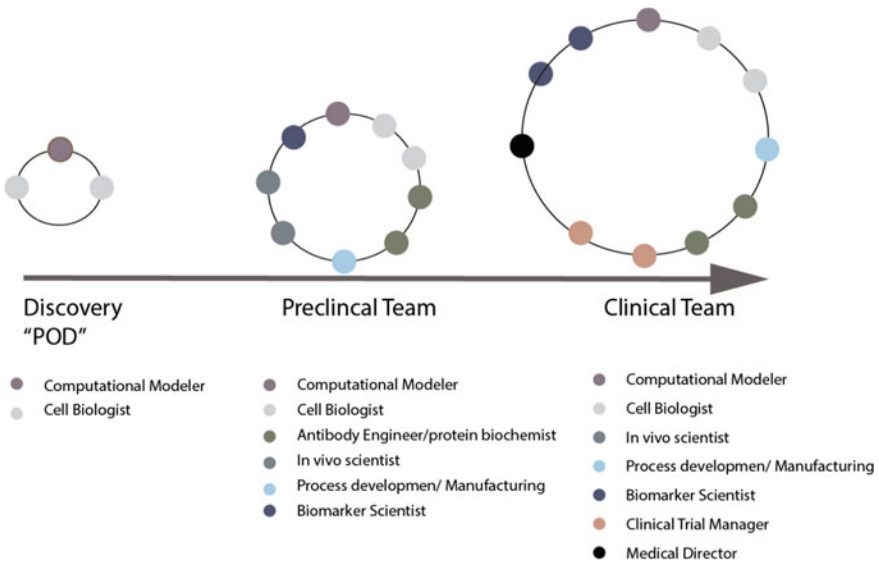

Fig. 3.4 Schematic of the team structure throughout molecule development at Merrimack Pharmaceuticals (reproduced with permission of Merrimack Pharmaceuticals Inc., © 2015) illustrating the integrated role of computational modelers throughout the drug development process, starting in early discovery

In contrast, larger pharmaceutical companies with broad pipelines and complex corporate structures are faced with the challenge of integrating QSP into pre-existing company structures and their development processes. Furthermore, given resource constraints, QSP may not be considered critical path. Researchers from Merck & Co. described how they have successfully implemented their QSP program as part of their wider efforts in quantitative pharmacometrics, with close interactions with key collaborators in different functions and a broad range of TAs (Visser et al. 2014). They have described a range of applications and modeling methodologies as well as their strategic approach to program implementation and remaining challenges. One highlighted aspect of their approach that contrasts with the Merrimack case above was the rigorous prioritization and selection of projects in which to apply QSP; this is a critical consideration in larger organizations where the number of potential projects and the demand across the pipeline outstrip QSP resource availability. Other approaches have also been adopted in the pharmaceutical industry, and implementation in different organizations has proceeded both by establishing in-house programs and collaborating with external academic researchers, nonprofit organizations, or specialized modeling and simulation consultancies and contractors. Furthermore, because of the longer-term and resource-intensive nature of some larger QSP efforts such as disease modeling, pre-competitive consortia have emerged as one approach to QSP platform development. For example, multiple drug companies are members of the DILIsym initiative, and the FDA is also involved as a collaborator. In Europe, the German government is sponsoring the development of the Virtual Liver, a public model of liver physiology and pathophysiology (Holzhutter et al. 2012).

The diversity of approaches taken to incorporate QSP reflects the diversity of company and project contexts and needs. Notably, despite the different approaches adopted in Merrimack Pharmaceuticals, Merck & Co., and DILIsym, one feature they share that is frequently cited as key to success is the central role of interdisciplinary collaboration between modelers and researchers from other functions (Leil and Bertz 2014). Though this is a feature common to many areas of drug development, it may be true to a greater extent for QSP than other modeling approaches due both to its recent introduction in industry and projects, and also to the emphasis on biological detail and mechanistic understanding that requires regular guidance, participation, and buy-in from experts in collaborating departments.

3.7 Challenges, Considerations and Future Directions for QSP in Industry

Although there is increasing interest in QSP within the biopharmaceutical industry, with a growing number of efforts and programs in multiple companies, its role in drug development is yet to be established and fully realized, and challenges remain

to be addressed before it can become a widely accepted contributor in drug development (Vicini and van der Graaf 2013). First and foremost, successful execution and publication of additional examples that clearly illustrate a direct and critical impact of QSP on decisions, efficiency, and timelines, will further support the case that QSP provides significant value in pharmaceutical R&D. Metrics that quantify the impact of QSP and communication of the value by senior industry leadership in the greater context of drug development would also be invaluable. Achieving these goals will require concise and effective messaging, which in turn requires training of QSP program leaders and the broader community in the communication of business impact rather than technical detail (Allerheiligen 2014).

Various other considerations remain for optimizing adoption and success, as summarized in Box 3. One set of pressing needs is rigorous review and guidelines around language, qualification criteria and metrics, and technical workflows and approaches that facilitate the evaluation of QSP models and results by broader audiences. The QSP community has begun to discuss the need for different qualification criteria for QSP models relative to pharmacometric models and to propose potential approaches. The qualification approaches are indeed different than those for traditional pharmacometric modeling (Agoram 2014), as illustrated in the methodology described by Friedrich (2016) (Fig. 3.5a), and thus require clear articulation and consensus on the procedure and success criteria.

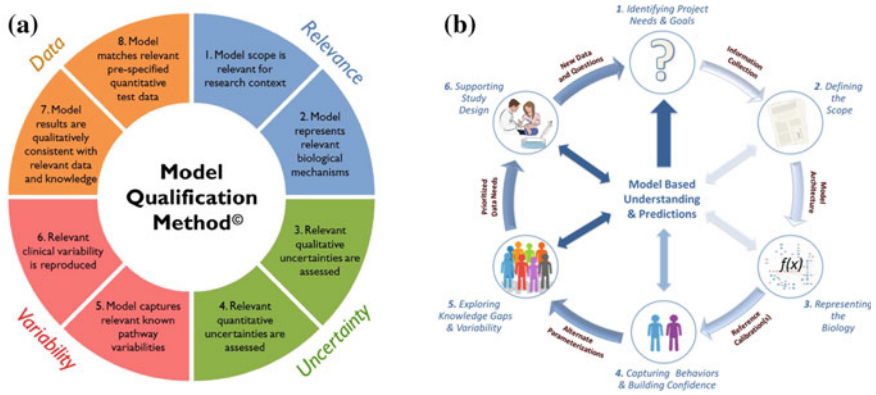

Fig. 3.5 **a** The Model Qualification Method © of Rosa & Co., LLC (Reprinted with permission by Rosa & Co. LLC., © 2016) provides an approach to determining and communicating model qualification specifications that addresses four main considerations critical to development of QSP models and confidence in their predictions. **b** A Six-Step QSP Workflow presented by Gadkar et al. (2016a) provides a systematic approach and associated technical methodologies for robust application of QSP

Box 3. Requirements to Facilitate Future QSP Adoption and Success Within the Pharmaceutical Industry

- Public disclosure of QSP examples that clearly illustrate a critical impact on drug development to industry leadership, together with easily communicable and quantifiable metrics of impact
- Standardization of language, qualification criteria, and metrics (Iyengar et al. 2012)
- More standardized and technically robust QSP workflows (Gadkar and Ramanujan 2015; Aldridge et al. 2006)
- Methods to efficiently identify and consolidate data from diverse sources (Visser et al. 2014)
- Availability of appropriate software suitable for use by researchers with diverse technical backgrounds (Ermakov et al. 2014; Ghosh et al. 2011; Ghosh et al. 2010)
- Availability of trained QSP researchers (Sorger and Allerheiligen 2011)
- Regulatory involvement, implementation, and acceptance

More technically robust and generalizable workflows, including methodologies for parameter estimation and exploration for example, are required to ensure that projects across the industry can be consistently evaluated. Again, such workflows are being proposed (Fig. 3.5b) and require greater discussion (Aldridge et al. 2006; Gadkar et al. 2016a). Common language, workflows, and evaluation criteria are especially critical in the consideration and review of QSP-based results by regulatory agencies. The pharmacometrics field provides an example of a path toward adoption and acceptance of modeling and simulation methods in regulatory filings, and currently PBPK modeling is pursuing a similar goal (Zhao et al. 2011). In addition to these strategic considerations, very practical challenges exist for project execution such as the frequently tedious task of aggregating diverse data, the availability of suitable software and tools, and the availability of researchers trained in QSP in drug development.

Despite these challenges, examples, including some described in this chapter, where QSP has meaningfully influenced decision-making already exist. As more cases emerge and are publicized, as the field addresses the above considerations, and as industry, academia, government, and nonprofit agencies continue technical innovation in the field, QSP will hopefully become a well-accepted biopharmaceutical industry approach and fulfill its promise to help improve the efficiency of the drug development process.

References

Agoram B (2014) Evaluating systems pharmacology models is different from evaluating standard pharmacokinetic-pharmacodynamic models. CPT Pharmacomet Syst Pharmacol 3:e101. doi:10.1038/psp.2013.77

Agoram BM, Demin O (2011) Integration not isolation: arguing the case for quantitative and systems pharmacology in drug discovery and development. Drug Discov Today 16(23–24):1031–1036. doi:10.1016/j.drudis.2011.10.001

Aldridge BB, Burke JM, Lauffenburger DA, Sorger PK (2006) Physicochemical modelling of cell signalling pathways. Nat Cell Biol 8(11):1195–1203. doi:10.1038/ncb1497

Allerheiligen SR (2014) Impact of modeling and simulation: myth or fact? Clin Pharmacol Ther 96 (4):413–415. doi:10.1038/clpt.2014.122

Arrowsmith J (2011) Trial watch: phase III and submission failures: 2007–2010. Nat Rev Drug Discov 10(2):87. doi:10.1038/nrd3375

Arrowsmith J (2012) A decade of change. Nat Rev Drug Discov 11(1):17–18. doi:10.1038/nrd3630

Arrowsmith J, Miller P (2013) Trial watch: phase II and phase III attrition rates 2011–2012. Nat Rev Drug Discovery 12(8):569. doi:10.1038/nrd4090

Bellido T, Ali AA, Plotkin L, Fu Q, Gubrij I, Roberson PK, Weinstein RS, O'Brien CA, Manolagas SC, Jilka RL (2003) Proteasomal degradation of Runx2 shortens parathyroid hormone-induced anti-apoptotic signaling in osteoblasts. A putative explanation for why intermittent administration is needed for bone anabolism. J Biol Chem 278(50):50259–50272. doi:10.1074/jbc.M307444200

Benson AP, Aslanidi OV, Zhang H, Holden AV (2008) The canine virtual ventricular wall: a platform for dissecting pharmacological effects on propagation and arrhythmogenesis. Prog Biophys Mol Biol 96(1–3):187–208. doi:10.1016/j.pbiomolbio.2007.08.002

Benson N, Matsuura T, Smirnov S, Demin O, Jones HM, Dua P, van der Graaf PH (2013) Systems pharmacology of the nerve growth factor pathway: use of a systems biology model for the identification of key drug targets using sensitivity analysis and the integration of physiology and pharmacology. Interface Focus 3(2):20120071. doi:10.1098/rsfs.2012.0071

Berg JM, Rogers ME et al (2010) Systems biology and pharmacology. Clin Pharmacol Ther 88(1):17–19

Bhattacharya S, Shoda LK, Zhang Q, Woods CG, Howell BA, Siler SQ, Woodhead JL, Yang Y, McMullen P, Watkins PB, Andersen ME (2012) Modeling drug- and chemical-induced hepatotoxicity with systems biology approaches. Front Physiol 3:462. doi:10.3389/fphys.2012.00462

Bugatti S, Manzo A, Vitolo B, Benaglio F, Binda E, Scarabelli M, Humby F, Caporali R, Pitzalis C, Montecucco C (2014) High expression levels of the B cell chemoattractant CXCL13 in rheumatoid synovium are a marker of severe disease. Rheumatology (Oxford) 53(10):1886–1895. doi:10.1093/rheumatology/keu163

Chassagnole C, Jackson RC, Hussain N, Bashir L, Derow C, Savin J, Fell DA (2006) Using a mammalian cell cycle simulation to interpret differential kinase inhibition in anti-tumour pharmaceutical development. Biosystems 83(2–3):91–97. doi:10.1016/j.biosystems.2005.04.007

Chen WW, Schoeberl B, Jasper PJ, Niepel M, Nielsen UB, Lauffenburger DA, Sorger PK (2009) Input-output behavior of ErbB signaling pathways as revealed by a mass action model trained against dynamic data. Mol Syst Biol 5:239. doi:10.1038/msb.2008.74

Chen X, Hickling TP, Vicini P (2014a) A mechanistic, multiscale mathematical model of immunogenicity for therapeutic proteins: part 1—theoretical model. CPT Pharmacom Syst Pharmacol 3:e133. doi:10.1038/psp.2014.30

Chen X, Hickling TP, Vicini P (2014b) A mechanistic, multiscale mathematical model of immunogenicity for therapeutic proteins: part 2—model applications. CPT Pharmacom Syst Pharmacol 3:e134. doi:10.1038/psp.2014.31

Cohen A (2008) Pharmacokinetic and pharmacodynamic data to be derived from early-phase drug development: designing informative human pharmacology studies. Clin Pharmacokinet 47 (6):373–381

Davies MR, Mistry HB, Hussein L, Pollard CE, Valentin JP, Swinton J, Abi-Gerges N (2012) An in silico canine cardiac midmyocardial action potential duration model as a tool for early drug safety assessment. Am J Physiol Heart Circ Physiol 302(7):H1466–H1480. doi:10.1152/ajpheart.00808.2011

Demin O, Karelina T, Svetlichniy D, Metelkin E, Speshilov G, Demin O Jr, Fairman D, van der Graaf PH, Agoram BM (2013) Systems pharmacology models can be used to understand complex pharmacokinetic-pharmacodynamic behavior: an example using 5-lipoxygenase inhibitors. CPT Pharmacom Syst Pharmacol 2:e74. doi:10.1038/psp.2013.49

Dziuba J, Alperin P, Racketa J, Iloeje U, Goswami D, Hardy E, Perlstein I, Grossman HL, Cohen M (2014) Modeling effects of SGLT-2 inhibitor dapagliflozin treatment versus standard diabetes therapy on cardiovascular and microvascular outcomes. Diab Obes Metab 16(7):628–635. doi:10.1111/dom.12261

Eddy D, Schlessinger L, Kahn R, Peskin B, Schiebinger R (2009) Relationship of insulin resistance and related metabolic variables to coronary artery disease: a mathematical analysis. Diabetes Care 32(2):361–366. doi:10.2337/dc08-0854

Ermakov S, Forster P, Pagidala J, Miladinov M, Wang A, Baillie R, Bartlett D, Reed M, Leil TA (2014) Virtual Systems Pharmacology (ViSP) software for simulation from mechanistic systems-level models. Front Pharmacol 5:232. doi:10.3389/fphar.2014.00232

Friedrich CM (2016) A model qualification method for mechanistic physiological QSP models to support model-informed drug development. CPT Pharmacom Syst Pharmacol 5(2):43–53. doi:10.1002/psp4.12056

Gadkar K, Budha N, Baruch A, Davis JD, Fielder P, Ramanujan S (2014) A mechanistic systems pharmacology model for prediction of LDL cholesterol lowering by PCSK9 antagonism in human dyslipidemic populations. CPT Pharmacom Syst Pharmacol 3:e149. doi:10.1038/psp.2014.47

Gadkar K, Kirouac D, Mager DE, Graaf PH, Ramanujan S (2016a) A six-stage workflow for robust application of systems pharmacology. CPT-PSP

Gadkar K, Lu J, Sahasranaman S, Davis J, Mazer NA, Ramanujan S (2016b) Evaluation of HDL-modulating interventions for cardiovascular risk reduction using a systems pharmacology approach. J Lipid Res 57(1):46–55. doi:10.1194/jlr.M057943

Gadkar K, Ramanujan S (2015) Workflow and technical methodologies for robust application of quantitative systems pharmacology approaches in model-based drug development. In: ASCPT conference

Geerts H, Roberts P, Spiros A (2013a) A quantitative system pharmacology computer model for cognitive deficits in schizophrenia. CPT Pharmacom Syst Pharmacol 2:e36. doi:10.1038/psp.2013.12

Geerts H, Spiros A, Roberts P, Carr R (2013b) Quantitative systems pharmacology as an extension of PK/PD modeling in CNS research and development. J Pharmacokinet Pharmacodyn 40 (3):257–265. doi:10.1007/s10928-013-9297-1

Ghosh S, Matsuoka Y, Asai Y, Hsin KY, Kitano H (2011) Software for systems biology: from tools to integrated platforms. Nat Rev Genet 12(12):821–832. doi:10.1038/nrg3096

Ghosh S, Matsuoka Y, Kitano H (2010) Connecting the dots: role of standardization and technology sharing in biological simulation. Drug Discov Today 15(23–24):1024–1031. doi:10.1016/j.drudis.2010.10.001

Greisen SR, Schelde KK, Rasmussen TK, Kragstrup TW, Stengaard-Pedersen K, Hetland ML, Horslev-Petersen K, Junker P, Ostergaard M, Deleuran B, Hvid M (2014) CXCL13 predicts disease activity in early rheumatoid arthritis and could be an indicator of the therapeutic 'window of opportunity'. Arthritis Res Ther 16(5):434. doi:10.1186/s13075-014-0434-z

Hansen J, Iyengar R (2013) Computation as the mechanistic bridge between precision medicine and systems therapeutics. Clin Pharmacol Ther 93(1):117–128. doi:10.1038/clpt.2012.199

Hendriks BS, Klinz SG, Reynolds JG, Espelin CW, Gaddy DF, Wickham TJ (2013) Impact of tumor HER2/ERBB2 expression level on HER2-targeted liposomal doxorubicin-mediated drug delivery: multiple low-affinity interactions lead to a threshold effect. Mol Cancer Ther 12 (9):1816–1828. doi:10.1158/1535-7163.MCT-13-0180

Hendriks BS, Reynolds JG, Klinz SG, Geretti E, Lee H, Leonard SC, Gaddy DF, Espelin CW, Nielsen UB, Wickham TJ (2012) Multiscale kinetic modeling of liposomal Doxorubicin delivery quantifies the role of tumor and drug-specific parameters in local delivery to tumors. CPT Pharmacom Syst Pharmacol 1:e15. doi:10.1038/psp.2012.16

Holzhutter HG, Drasdo D, Preusser T, Lippert J, Henney AM (2012) The virtual liver: a multidisciplinary, multilevel challenge for systems biology. Wiley Interdiscip Rev Syst Biol Med 4(3):221–235. doi:10.1002/wsbm.1158

Honer WG, Thornton AE, Chen EY, Chan RC, Wong JO, Bergmann A, Falkai P, Pomarol-Clotet E, McKenna PJ, Stip E, Williams R, MacEwan GW, Wasan K, Procyshyn R (2006) Clozapine alone versus clozapine and risperidone with refractory schizophrenia. N Engl J Med 354 (5):472–482. doi:10.1056/NEJMoa053222

Howell BA, Siler SQ, Shoda LK, Yang Y, Woodhead JL, Watkins PB (2014) A mechanistic model of drug-induced liver injury AIDS the interpretation of elevated liver transaminase levels in a phase I clinical trial. CPT Pharmacom Syst Pharmacol 3:e98. doi:10.1038/psp.2013.74

Hund TJ, Rudy Y (2004) Rate dependence and regulation of action potential and calcium transient in a canine cardiac ventricular cell model. Circulation 110(20):3168–3174. doi:10.1161/01.CIR.0000147231.69595.D3

Iyengar R, Zhao S, Chung SW, Mager DE, Gallo JM (2012) Merging systems biology with pharmacodynamics. Sci Transl Med 4(126):126ps127. doi:10.1126/scitranslmed.3003563

Kadambi K, Young D, Gadkar K (2011) Systems modeling applied to candidate biomarker identification. In: Systems biology in drug discovery and development. Wiley, New York

Kirouac DC, Du JY, Lahdenranta J, Overland R, Yarar D, Paragas V, Pace E, McDonagh CF, Nielsen UB, Onsum MD (2013) Computational modeling of ERBB2-amplified breast cancer identifies combined ErbB2/3 blockade as superior to the combination of MEK and AKT inhibitors. Sci Signal 6(288):ra68. doi:10.1126/scisignal.2004008

Kocher R, Roberts B (2014) The calculus of cures. N Engl J Med 370(16):1473–1475. doi:10.1056/NEJMp1400868

Kohl P, Crampin EJ et al (2010) Systems biology: an approach. Clin Pharmacol Ther 88(1):25–33

Kuepfer L (2010) Towards whole-body systems pharmacology. Mol Sys Biol 6(409). doi:10.1038/msb.2010.70

Leil TA, Bertz R (2014) Quantitative Systems Pharmacology can reduce attrition and improve productivity in pharmaceutical research and development. Front Pharmacol 5:247. doi:10.3389/fphar.2014.00247

Lemaire V, Tobin FL, Greller LD, Cho CR, Suva LJ (2004) Modeling the interactions between osteoblast and osteoclast activities in bone remodeling. J Theor Biol 229(3):293–309. doi:10.1016/j.jtbi.2004.03.023

Lu J, Hubner K, Nanjee MN, Brinton EA, Mazer NA (2014) An in-silico model of lipoprotein metabolism and kinetics for the evaluation of targets and biomarkers in the reverse cholesterol transport pathway. PLoS Comput Biol 10(3):e1003509. doi:10.1371/journal.pcbi.1003509

MacBeath G, Adiwijaya B (2014) A meta-analysis of biomarkers in three randomized, phase 2 studies of MM-121, a ligand-blocking anti-ErbB3 antibody, in patients with ovarian, lung, and breast cancers. In: ESMO 2014

Meeuwisse CM, van der Linden MP, Rullmann TA, Allaart CF, Nelissen R, Huizinga TW, Garritsen A, Toes RE, van Schaik R, van der Helm-van Mil AH (2011) Identification of CXCL13 as a marker for rheumatoid arthritis outcome using an in silico model of the rheumatic joint. Arthritis Rheum 63(5):1265–1273. doi:10.1002/art.30273

Mirams GR, Davies MR, Cui Y, Kohl P, Noble D (2012) Application of cardiac electrophysiology simulations to pro-arrhythmic safety testing. Br J Pharmacol 167(5):932–945. doi:10.1111/j.1476-5381.2012.02020.x

Morgan P, Van Der Graaf PH, Arrowsmith J, Feltner DE, Drummond KS, Wegner CD, Street SD (2012) Can the flow of medicines be improved? Fundamental pharmacokinetic and pharmacological principles toward improving Phase II survival. Drug Discov Today 17(9–10):419–424. doi:10.1016/j.drudis.2011.12.020

Orrell D, Fernandez E (2010) Using predictive mathematical models to optimise the scheduling of anti-cancer drugs. Biopharma

Peskin BR, Shcheprov AV, Boye KS, Bruce S, Maggs DG, Gaebler JA (2011) Cardiovascular outcomes associated with a new once-weekly GLP-1 receptor agonist vs. traditional therapies for type 2 diabetes: a simulation analysis. Diabetes Obes Metab 13(10):921–927. doi:10.1111/j.1463-1326.2011.01430.x

Peterson MC, Riggs MM (2010) A physiologically based mathematical model of integrated calcium homeostasis and bone remodeling. Bone 46(1):49–63. doi:10.1016/j.bone.2009.08.053

Peterson MC, Riggs MM (2012) Predicting nonlinear changes in bone mineral density over time using a multiscale systems pharmacology model. CPT Pharmacom Syst Pharmacol 1:e14. doi:10.1038/psp.2012.15

Peterson MC, Riggs MM (2015) FDA advisory meeting clinical pharmacology review utilizes a quantitative systems pharmacology (QSP) model: a watershed moment? CPT Pharmacom Syst Pharmacol 4(3):e00020. doi:10.1002/psp4.20

Raposo JF, Sobrinho LG, Ferreira HG (2002) A minimal mathematical model of calcium homeostasis. J Clin Endocrinol Metab 87(9):4330–4340. doi:10.1210/jc.2002-011870

Raterman HG, Vosslamber S, de Ridder S, Nurmohamed MT, Lems WF, Boers M, van de Wiel M, Dijkmans BA, Verweij CL, Voskuyl AE (2012) The interferon type I signature towards prediction of non-response to rituximab in rheumatoid arthritis patients. Arthritis Res Ther 14(2):R95. doi:10.1186/ar3819

Riggs MM, Peterson MC, Gastonguay MR (2012) Multiscale physiology-based modeling of mineral bone disorder in patients with impaired kidney function. J Clin Pharmacol 52(Suppl 1):45S–53S. doi:10.1177/0091270011412967

Rostami-Hodjegan A (2012) Physiologically based pharmacokinetics joined with in vitro-in vivo extrapolation of ADME: a marriage under the arch of systems pharmacology. Clin Pharmacol Ther 92(1):50–61. doi:10.1038/clpt.2012.65

Rowland M, Peck C, Tucker G (2011) Physiologically-based pharmacokinetics in drug development and regulatory science. Annu Rev Pharmacol Toxicol 51:45–73. doi:10.1146/annurev-pharmtox-010510-100540

Rullmann JA, Struemper H, Defranoux NA, Ramanujan S, Meeuwisse CM, van Elsas A (2005) Systems biology for battling rheumatoid arthritis: application of the Entelos PhysioLab platform. Syst Biol (Stevenage) 152(4):256–262

Schmidt BJ, Casey FP, Paterson T, Chan JR (2013) Alternate virtual populations elucidate the type I interferon signature predictive of the response to rituximab in rheumatoid arthritis. BMC Bioinform 14:221. doi:10.1186/1471-2105-14-221

Schoeberl B, Pace EA, Fitzgerald JB, Harms BD, Xu L, Nie L, Linggi B, Kalra A, Paragas V, Bukhalid R, Grantcharova V, Kohli N, West KA, Leszczyniecka M, Feldhaus MJ, Kudla AJ, Nielsen UB (2009) Therapeutically targeting ErbB3: a key node in ligand-induced activation of the ErbB receptor-PI3K axis. Sci Signal 2(77):ra31. doi:10.1126/scisignal.2000352

Shoda LK, Woodhead JL, Siler SQ, Watkins PB, Howell BA (2014) Linking physiology to toxicity using DILIsym(R), a mechanistic mathematical model of drug-induced liver injury. Biopharm Drug Dispos 35(1):33–49. doi:10.1002/bdd.1878

Sonesson C, Johansson PA, Johnsson E, Gause-Nilsson I (2016) Cardiovascular effects of dapagliflozin in patients with type 2 diabetes and different risk categories: a meta-analysis. Cardiovasc Diabetol 15(1):37. doi:10.1186/s12933-016-0356-y

Sorger P, Allerheiligen S (2011) Quantitative and systems pharmacology in the post-genomic era: new approaches to discovering drugs and understanding therapeutic mechanisms. An NIH White Paper by the QSP Workshop Group

Thalhauser CJ, Schmidt BJM M, Leil TA (2015) Mechanistic predictions of response to combinations of biologic agents in a quantitative systems pharmacology model of rheumatoid arthritis. J Pharmacokinet Pharmacodyn 42(1):S11–S107

van der Graaf PH, Benson N (2011) Systems pharmacology: bridging systems biology and pharmacokinetics-pharmacodynamics (PKPD) in drug discovery and development. Pharm Res 28(7):1460–1464. doi:10.1007/s11095-011-0467-9

van Herick A, Schuetz CA, Alperin P, Bullano MF, Balu S, Gandhi S (2012) The impact of initial statin treatment decisions on cardiovascular outcomes in clinical care settings: estimates using the Archimedes Model. Clinicoecon Outcomes Res 4:337–347. doi:10.2147/CEOR.S35487

Vicini P, van der Graaf PH (2013) Systems pharmacology for drug discovery and development: paradigm shift or flash in the pan? Clin Pharmacol Ther 93(5):379–381. doi:10.1038/clpt.2013.40

Visser SA, de Alwis DP, Kerbusch T, Stone JA, Allerheiligen SR (2014) Implementation of quantitative and systems pharmacology in large pharma. CPT Pharmacom Syst Pharmacol 3: e142. doi:10.1038/psp.2014.40

Woodhead JL, Yang K, Siler SQ, Watkins PB, Brouwer KL, Barton HA, Howell BA (2014) Exploring BSEP inhibition-mediated toxicity with a mechanistic model of drug-induced liver injury. Front Pharmacol 5:240. doi:10.3389/fphar.2014.00240

Xing H, McDonagh PD, Bienkowska J, Cashorali T, Runge K, Miller RE, Decaprio D, Church B, Roubenoff R, Khalil IG, Carulli J (2011) Causal modeling using network ensemble simulations of genetic and gene expression data predicts genes involved in rheumatoid arthritis. PLoS Comput Biol 7(3):e1001105. doi:10.1371/journal.pcbi.1001105

Zhao P, Zhang L, Grillo JA, Liu Q, Bullock JM, Moon YJ, Song P, Brar SS, Madabushi R, Wu TC, Booth BP, Rahman NA, Reynolds KS, Gil Berglund E, Lesko LJ, Huang SM (2011) Applications of physiologically based pharmacokinetic (PBPK) modeling and simulation during regulatory review. Clin Pharmacol Ther 89(2):259–267. doi:10.1038/clpt.2010.298

Zhao S, Nishimura T, Chen Y, Azeloglu EU, Gottesman O, Giannarelli C, Zafar MU, Benard L, Badimon JJ, Hajjar RJ, Goldfarb J, Iyengar R (2013) Systems pharmacology of adverse event mitigation by drug combinations. Sci Transl Med 5(206):206ra140. doi:10.1126/scitranslmed.3006548

Chapter 4
Systems Pharmacology: An Overview

Marc R. Birtwistle, Jens Hansen, James M. Gallo, Sreeharish Muppirisetty, Peter Man-Un Ung, Ravi Iyengar and Avner Schlessinger

Abstract Systems pharmacology has evolved from a discipline that focuses on drug action at the organ level to a discipline that combines traditional pharmacokinetic and pharmacodynamic modeling with recent systems biology approaches. The integration of high-throughput data technologies with computational data analysis and modeling offers new opportunities to overcome the one disease, one target, one drug approach. Whole genomic or transcriptomic sequencing and proteomics allow qualitative, and sometimes quantitative, snapshots of the cellular state at any given condition (e.g., during disease or after drug treatment) that can be the basis for the development of whole cell models to predict drug responses. Networks of protein–protein interactions that were confirmed by experimental and computational analysis of the structure of the interaction partners can be combined with graph theory to identify modules regulating the cellular state. Dynamic modeling and sensitivity analysis allow the identification of robust and fragile nodes within these modules to identify putative drug targets for single or combinatorial drug treatment. Traditional pharmacokinetic and pharmacodynamic modeling complements these approaches by predicting drug concentration and target perturbation at the site of drug action. Such general systems pharmacology models are a great leap forward towards the development of patient-specific drug response models as a main component of precision medicine.

Keywords Networks-based · Personalized medicine · Bioinformatics · Pharmacogenomics · Genbank · Cytochrome P450 · Protein–protein interaction (PPI) · Interactome · Druggability · Genomic variation · Nodes

M.R. Birtwistle · J. Hansen · J.M. Gallo · S. Muppirisetty · P.M.-U. Ung · R. Iyengar (✉) · A. Schlessinger
Department of Pharmacology and Systems Therapeutics, Systems Biology Center New York, Icahn School of Medicine at Mount Sinai, Box 1215 One Gustave Levy Place, New York, NY 10029, USA
e-mail: ravi.iyengar@mssm.edu

D.E. Mager and H.H.C. Kimko (eds.), *Systems Pharmacology and Pharmacodynamics*, AAPS Advances in the Pharmaceutical Sciences Series 23,
DOI 10.1007/978-3-319-44534-2_4

4.1 Introduction

Over the past two decades, as our understanding of molecular and cellular characteristics of biological organisms has grown, it has become clear that to understand how components come together to form functional units, such as the actin cytoskeleton for cell movement or the secretory machinery for hormone secretion, requires us to study biological processes in a holistic manner. By holistic, we mean that we keep track of both the components that make up the functional units and also how they interact to give rise to function (Sabathie et al. 1975; Weng et al. 1999). This field of study is called systems biology. The development of high throughput experimental technologies in genomics that allow us to sequence all the genes in a genome simultaneously (Shendure and Lieberman Aiden 2012) and measure genome-wide patterns of expression and gene modification (such as DNA methylation) provide a comprehensive basis for understanding the genetic and genomic underpinnings of cellular, tissue/organ, and organismal functions. Similarly, development of proteomics using mass spectrometry (Picotti and Aebersold 2012) has contributed to our knowledge of protein and protein state (e.g., phosphorylation) profiles within cells and tissues. The large data sets produced by these omics technologies can seldom be intuitively understood and require statistical and computational analyses for the data to be converted into knowledge. Typically a variety of statistical tools, Bayesian models, as well as network analyses based on graph theory are used to analyze large data sets. Bioinformatics is the field that studies the organization and storage of large data sets and their subsequent statistical and computational analysis. Although the pictures produced by such analyses are reasonably comprehensive, they are often qualitative snapshots in time and seldom or incompletely provide information about the dynamic or quantitative capabilities of systems. Yet, critical for drug action and pharmacology approaches is knowledge of precisely such characteristics—dose and timing. What is needed in this regard is a different class of experiments that are not yet high-throughput, as well as dynamical models based on differential equations to understand systems dynamics. Irrespective of the approaches used, it should be appreciated that systems biology uses an integrated approach wherein experiments and computational models are combined to provide insight into how the systems are organized and how this organization leads to function. The approach of integrating experiments and computation is not new in biomedical sciences. It has been used for over 50 years in biochemistry, physiology, and pharmacology. In the past, however, combinations of experiments and models dealt with functions at a single scale. Typically biochemistry focused on the atomic and molecular scale, whereas physiology and pharmacology focused on tissue/organ level functions. A distinctive characteristic of current systems biology approaches is that it is multiscale—often both in levels of organization as well as across time scales. Such analyses have the potential to help us understand how molecules and interactions can give rise to functions manifested at the cellular, tissue/organ, and organismal levels.

4.2 Systems Pharmacology: A Network-Based View of Drug Action

Traditionally, systems pharmacology has been used to describe studies of drug action at the level of organ systems (Brunton et al. 2011). A set of two workshops at the National Institutes of Health in 2008 and 2011 led to a white paper that provides an expansive view of quantitative and systems pharmacology in current times (Sorger et al. 2011). Currently, systems pharmacology in academia describes a research area that combines both high- and low-throughput experimental approaches of systems biology as well as a range of computational approaches including network analyses for drug discovery and studying drug action (Berger and Iyengar 2009; Zhao and Iyengar 2012).

The concepts from graph theory, the branch of mathematics focused on the study of networks, has been enormously useful in understanding regulatory features of cell and tissues/organs. Components of cells interact both directly and indirectly, and most components have multiple interactions. Networks capture these interactions and provide frameworks for understanding of how regulation arises from the interactions between cellular components. Feedback inhibition, which in network parlance is called a negative feedback loop, has been long known in biochemistry (Lehninger et al. 1992), but knowing how such loops can work in the context of other regulatory features provides insight into the regulatory capability of the system. The systematic description of regulatory units called network motifs (Milo et al. 2002), and the ability to identify such motifs within large regulatory networks (Wendell and Cianci 1992), provides mechanistic understanding of how the organization of systems contributes to regulatory capability. Since dysregulation is often a key feature of the pathophysiological state, understanding physiological and pathophysiological systems as networks is useful for both drug discovery and studying drug action. These studies are generally based on molecular interactions between the drug and its targets when these targets interact with and regulate other cellular components or the network biology of drug action (Zhao and Iyengar 2012). These network-based approaches have been useful in understanding the basis for cancer combination therapy (Boran and Iyengar 2010a, b), devising treatment regimens for optimal efficacy (Boran and Iyengar 2010a), origins of drug induced adverse events such as arrhythmias (Berger et al. 2010), and how multi-drug combinations can mitigate serious adverse events (Zhao et al. 2013). These successes indicate the value of network-based reasoning in the study of drug action.

Systems pharmacology is often thought of as extension of pharmacokinetics and pharmacodynamics that have been rooted in compartmental and physiologically based pharmacokinetic models and biomarker-based pharmacodynamic models. Each perspective—traditional and systems-based—serves a valuable role and represents the different facets of systems pharmacology that are schematically shown in Fig. 4.1. In this overview we briefly describe the components of systems pharmacology in the second decade of the 21st century that highlight an evolution in

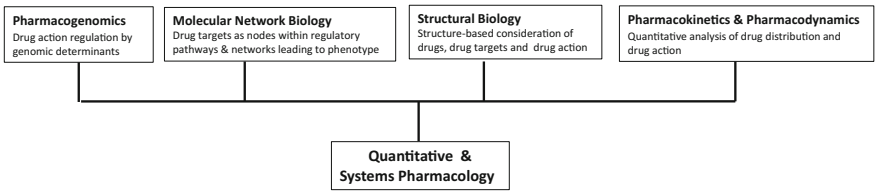

Fig. 4.1 Quantitative and systems pharmacology is a multidisciplinary field. The different areas of research that are integrated in quantitative and systems pharmacology are depicted as a flow diagram

going from structural biology-based drug discovery to a more integrated mechanistic pharmacokinetic and pharmacodynamic regime that accounts for genomic and epigenomic control of drug action. For this we start with a brief description of bioinformatics for drug discovery, drug action, and pharmacogenomics.

4.3 Systems Pharmacology: Relationships to Personalized and Precision Medicine

For some diseases, genomic determinants are useful predictors of drug efficacy as well as drug toxicity. Coding region SNPs have been very useful in identifying the ability of cytochrome P450 variants to metabolize warfarin. This relationship has allowed for the development of treatment regimens that enable the titrating of drug dosage to obtain maximal efficacy in reducing clot formation while minimizing the risk for internal bleeding (Aithal et al. 1999). The presence or absence of certain cancer mutations may determine whether a certain receptor antagonist would be an effective drug. For example, blockers of receptor tyrosine kinase activity are unlikely to be effective if there are downstream mutations in Ras that would likely change signal flux and drug efficacy. Of note, the Food and Drug Administration recommends genetic testing to ascertain that K-Ras is not mutated before the receptor tyrosine kinase inhibitor cetuximab is used for treatment of colorectal cancer (De Roock et al. 2013). Tailoring the use of medication or adjusting its dosage according to individual genetic makeup is called personalized medicine. This terminology is fairly synonymous with the term pharmacogenomics, which is described in a section below and is well known in clinical pharmacology. More recently a new term called “precision medicine” has been introduced (Toward Precision Medicine: Building a Knowledge Network for Biomedical Research and a New Taxonomy of Disease 2011) that the National Academies have defined as disease classification based on molecular characteristics. It is easy to see that the terms personalized and precision medicine are conflated to imply that genetic characteristics are the predominant characteristics to consider in disease classification and drug therapy. Whereas genetic characteristics are very important, there is

likely to be more to precision medicine in fact, to make it precise. What seems to be missing is a significant appreciation that the underlying principles of drug action are quantitative dynamic processes embodied in pharmacokinetics and pharmacodynamics. It is these disciplines that account for drug interactions—both pharmacokinetic and pharmacodynamic—and allow drug dosing schedules to be tailored to patients. In addition, depending on the extent of the models, drug toxicity can be predicted and used as a valuable guide to design therapeutic regimens. Although these dynamic processes can be analyzed semi-empirically in pharmacokinetic and pharmacodynamics studies, such analyses are not necessarily constrained by molecular details, and with the advent of systems-based approaches and its merging with pharmacokinetic/pharmacodynamic analyses, systems pharmacology has gained traction. Systems pharmacology will likely grow in importance given the interest and emphasis on precision medicine and the appeal to tailor therapy in the context of genomic and epigenomic determinants, as well as regulatory networks. Thus it is likely that systems pharmacology and precision medicine will develop in a naturally coordinated manner in the future.

4.4 Bioinformatics for Systems Pharmacology

The ability to construct large networks that can be used to understand drug action and drug discovery depends on the availability of large data sets. Among the largest and best characterized ones are those that contain gene related information, including gene variants that are related to drug action. These include the NCBI databases on various types of genomic information. Among the oldest is GenBank, which contains an annotated collection of all DNA sequences. Currently there are 19 databases under the heading DNA and RNA and another 17 databases under Genes and Expression. There may be some overlapping information, but overall these numbers provide a view of the vastness of the genomic data that is publicly available. A few databases that are directly relevant to systems pharmacology are listed in Table 4.1. In addition to genomic sequence information, there are also databases for gene and protein interactions, along with ontologies that associate genes with pathways and function. Gene Ontology is a widely used ontology database. There also exist a number of drug related databases such as Connectivity Map, DrugBank, PubChem and FAERS (Table 4.1). Each of these databases is important for systems pharmacology as these enable the construction of different types of networks to understand both drug action and to discover new drug targets for complex diseases.

Table 4.1 Representative list of databases used in systems pharmacology

Gene sequence and annotation	
NCBI gene_info	Contains gene related information such as taxonomy ids (i.e., organism), ENSEMBL gene identifiers, Human Protein Reference Database Identifiers (HPRD), official gene symbols, gene ids, gene synonym names and full gene names
NCBI gene2refseq	Contains gene related information such as taxonomy ids, gene ids, refSeq status, RNA nucleotide and protein accession identifiers and official gene symbols
NCBI homoloGene	Contains information about gene homologs between different organisms
MGI vertebrate homology	Contains information about gene homologs between mouse, human, rat and other organisms
NCBI dbSNP	Contains single nucleotide polymorphisms (SNPs), insertions and deletions, microsatellites and non-polymorphic variants
Gene or protein interactions	
TRANSFAC PWM	Associates transcription factors with their target genes
ChipX enrichment analysis (ChEA) background database	Associates transcription factors with their target genes, based on experimental results obtained from ChIP-chip and ChIP-seq studies
Stitch	Bork lab database of predicted protein-drug interactions using various approaches http://stitch.embl.de/
Kinase enrichment analysis (KEA) background database	Associates protein kinases with their protein phosphorylation targets
Ontologies: association of genes with biological processes or pathways	
Gene ontology (GO)	Probably the most extensive ontology available, categorizes its terms into three namespaces: biological process, cellular component and molecular function
Kyoto encyclopedia of genes and genomes (KEGG)	A smaller ontology with a focus on metabolic pathways. KEGG also offers metabolic pathway maps on their website
WikiPathways	Further ontologies that associate genes with biological pathways
Reactome pathway	
Online Mendelian Inheritance in Man (OMIM)	Associates human genes with genetic phenotypes
Mouse genome informatics (MGI) mammalian phenotype	A large ontology that associates genes with mammalian phenotypes
Drug related expression changes	
Connectivity map (CMPA)	Contains genome-wide transcriptional expression data from human cells that have been treated with various bioactive small molecules. It can be used to identify a small molecule that up- or down-regulated a certain gene set of interest

(continued)

Table 4.1 (continued)

Drug related databases	
Drug bank	Contains detailed drug-related information, such as an extensive list of drug target genes, drug-drug interactions, drug metabolizing enzymes and drug indication
PubChem	Database of small molecules and their activities in different biological assays that were obtained by high-throughput screening assays
ZINC	Largest dataset of purchasable small molecules for virtual screening http://zinc.docking.org/
ChEMBL	Database with small molecules and their activities against biological assays
FAERS FDA—adverse events reporting system	Contains information about adverse events documented by healthcare professionals during the treatment with a drug or drug combinations

4.4.1 Pharmacogenomics

As mentioned above, pharmacogenomics connects drug action in an individual to specific characteristics of the individual's genome. Variations in the genome are thought to account for a significant part of inter-individual variability in drug action, and genomic characteristics are used for determining dosing regimens as well as predictions for responsiveness to therapy. The best known example for prediction of dosing regimens based on genomic variations is the use of warfarin to regulate blood coagulation and thrombosis. Cytochrome P450 isoform CYP2C9 regulates the metabolism of warfarin. CYP2C9 has two polymorphisms that reduce the level of enzyme activity towards warfarin; consequently, increased warfarin concentrations in the blood result in an increased risk of bleeding. So if a patient has these CYP2C9 polymorphisms, the dosage of warfarin can be titrated to optimize therapy while reducing the risk of bleeding. Testing for warfarin metabolism has become a common approach to titrating warfarin dosage in clinical practice.

In treatment of cancers, genomic status, most often defined as presence or absence of oncogenic mutations, can be used to predict responsiveness to certain drugs. *KIT* oncogene mutations reduce the responsiveness of gastrointestinal stromal tumors to imatinib (Aithal et al. 1999); *k-RAS* oncogene mutations in colorectal cancer reduce responsiveness to cetuximab (De Roock et al. 2010); and epidermal growth factor receptor mutations in non-small-cell lung cancer alter responsiveness to gefitinib or erlotinib (Toward Precision Medicine: Building a Knowledge Network for Biomedical Research and a New Taxonomy of Disease 2011). In most of these cases, mechanisms underlying the genotype to drug response relationships are not fully understood, and one of the major goals of pharmacology is to provide mechanistic understanding of such multiscale relationships.

4.4.2 *Structural Reasoning in Systems Pharmacology*

Structural biology has long been an area in which experimental data and computational modeling have been integrated to obtain biological knowledge. Going from X-ray diffraction patterns to protein structures have always required building models, and even more so in modern structure determination via X-ray crystallography or NMR. Thus melding structural reasoning into systems pharmacology approaches for drug discovery involves integrating models to scale across multiple levels of organization. Several themes that form the basis for integrating models for multiscale understanding are described here.

4.4.2.1 Protein Structure Informs Network Biology

Since biological networks are defined by the physical interactions between their components, description of the precise molecular interactions between proteins, nucleic acids, and small molecules is a prerequisite for understanding the dynamics of lower resolution interaction networks and ultimately for designing drugs that perturb these networks. For instance, a highly connected node in a protein–protein interaction (PPI) network can be a protein that interacts with multiple partners through the same surface region at different times in different pathways, or a protein that interacts with multiple partners simultaneously using distinct surface regions (Kim et al. 2006). Currently, there are over 100,000 experimentally determined protein structures available in the Protein Data Bank (Rose et al. 2013); however, only a small fraction of these structures correspond to protein complexes within the interactome, making it difficult to map protein structure onto networks that can be easily generated with high-throughput approaches. Multiple computational approaches have been developed to predict the three-dimensional structures of protein complexes in various network types, relying on homology modeling, in which a target complex structure is based on experimentally determined structure of a related protein or protein complex (Davis et al. 2006; Sali and Blundell 1993). Mosca et al. developed Interactome3D, which is an automated homology modeling pipeline and visualization tool, to map structural information onto any PPI dataset provided by the user (Mosca et al. 2013). Homology modeling-based approaches can also be used to annotate previously unknown physical interactions. PrePPI is a Bayesian-based approach that combines protein structure information with co-expression and functional similarity data to predict protein–protein interactions (Zhang et al. 2012). PrePPI identified more protein–protein interactions in the yeast proteome than those identified with high-throughput experimental approaches and with higher accuracy, as well as covered a different fraction of the interactome (Zhang et al. 2012).

In addition, many key cellular functions are executed by large complexes or assemblies, such as the proteasome and ribosome. Experimental determination of the atomic structures of such assemblies can be technically challenging and costly,

and their modeling via homology is difficult because of limited structural coverage of their components. Integrative modeling approaches such as the integrative modeling platform (IMP), which generates three-dimensional structures or models of large complexes using restraints that are derived from various low-resolution data types (e.g., protein–protein interactions), can identify the domains and residues that are involved in specific interactions (Russel et al. 2012). The yeast nuclear pore complex structure, which includes 456 proteins, was modeled with IMP using low-resolution data from diverse sources, such as affinity purification of protein sub-complexes, sedimentation analysis, and electron microscopy (Alber et al. 2007).

4.4.2.2 Structural Considerations Guide Drug Discovery

Efficacy of a drug is strongly influenced by the extent that the target controls the phenotype and the strength of binding between the drug and target(s). The former is related to the system as a whole, and is typically analyzed by sensitivity analysis of models that link the target to phenotype (Birtwistle et al. 2007; Schoeberl et al. 2009; Zhang et al. 2014). The latter is related to target 'druggability', that is, particular structural features, such as binding pockets of suitable size, shape, and electrostatic properties to accommodate drug-like molecules with optimal bioavailability properties (e.g., the Lipinski rule-of-five (Lipinski et al. 2001)). Hopkins and Groom introduced the term "druggable genome" and estimated that about 10 % of the genes in the human genome are druggable, but only about half of these genes are both druggable and relevant to disease (Hopkins and Groom 2002). These druggable targets are primarily GPCRs, protein kinases, ion channels, and membrane transporters (Hopkins and Groom 2002).

Druggability of a putative target is typically analyzed with protein structural methods focused on physicochemical properties such as the presence of a surface hydrophobic pocket (Cheng et al. 2007; Kozakov et al. 2011; Perot et al. 2010). Recent efforts attempt to extend the druggable genome by targeting protein–protein interactions (Wells and McClendon 2007), developing covalent probes (Singh et al. 2011), as well as by targeting allosteric or cryptic binding sites that cannot always be observed in a static X-ray structure doi:10.1002/bip.22742 (Ung et al) (Ostrem et al. 2013). For example, for many years the Ras protein has been considered "undruggable". Ostrem et al. (2013) used a tethering technique to screen compounds against the cancer-associated Ras G12C variant. The X-ray structure of Ras G12C bound to a novel tethered inhibitor revealed a newly exposed pocket, thus providing a framework for developing more potent and bioavailable inhibitors.

Rational or structure-based drug discovery includes a wide range of approaches aimed at developing small organic molecules that bind druggable pockets and rely on concepts from medicinal chemistry and protein structure. This approach has been used to successfully develop at least ten marketed drugs, including the antihypertensive drug aliskiren (Rahuel et al. 2000), the antiviral telapravir (Lin et al. 2006), and the anticancer drug vemurafenib (Bollag et al. 2012). Computational

approaches are particularly useful for identifying novel chemical scaffolds and for optimizing lead molecules or known drugs against particular targets. For example, in structure-based virtual screening ('molecular docking') a large compound library is computationally screened, in which each small molecule is sampled in many configurations and scored based on its complementarity to the target structure (Shoichet 2004). This quick and inexpensive method—based on protein structure rather than the chemical structure of known small molecule ligands—is a powerful and validated tool for identifying novel chemical entities. For a protein target without an experimentally determined structure, virtual screening can be performed against homology models (Baker and Sali 2001; Jacobson and Sali 2004; Schlessinger et al. 2013). Furthermore, characterizing various conformational states of target proteins (e.g., with homology modeling or molecular dynamics simulations) enables researchers to identify conformation-specific modulators, thereby further increasing the pharmacological space (Durrant and McCammon 2013).

An emerging paradigm in modern drug discovery is one type of polypharmacology, in which a drug interacts with multiple targets with significant affinity to obtain effective therapy (Keiser et al. 2009; Roth et al. 2004; Xie et al. 2011). This is different from traditional drug discovery approaches, where a highly potent and selective drug is optimized toward a single specific biological target. Polypharmacology is observed in the treatment of various multigenic diseases such as central nervous system disorders and cancer. For example, the cancer drug sorafenib is a kinase inhibitor that binds to multiple targets such as BRAF, KDR and p38α in their inactive conformations (Fig. 4.2). Because polypharmacological modulators often have lower binding affinity to multiple targets rather than potently binding one single target (Xie et al. 2012), previously "undruggable" sites, such as those involving protein–protein interfaces, can also be targeted by such drugs. In rational polypharmacology, a drug or a cocktail of drugs is/are designed against multiple targets simultaneously, taking into account both drug and target structure. Dar et al. combined medicinal chemistry, biochemical assays, and fly genetics to systematically identify five distinct functional targets and 'anti-targets' for the treatment of Ret-MEN2B cancers (Dar et al. 2012). Anti-targets are proteins that when inhibited by drug, have undesirable effects such as increased toxicity or reduced efficacy, and thus should be avoided. They then developed two novel compounds that optimally interact with those targets/anti-targets to produce strongly efficacious compounds now in clinical trials. It can readily be seen that multiple targets could be part of a functional network, so we may in the future design single or multiple drugs that exert their effects by modulating the behavior of functional cellular networks rather than by modulating the activity of a single target. Identification of such targets and anti-targets clearly interfaces tightly with network-based thinking as described above.

Although protein structure-based approaches can be useful for rationalizing side effect and efficacy of polypharmacological drugs (Geier et al. 2013; Schlessinger et al. 2011), small molecule-based approaches are significantly more efficient in capturing unintended 'off-targets' that predict adverse drug reactions. The chemical similarity ensemble approach (SEA) relates proteins based on the chemical

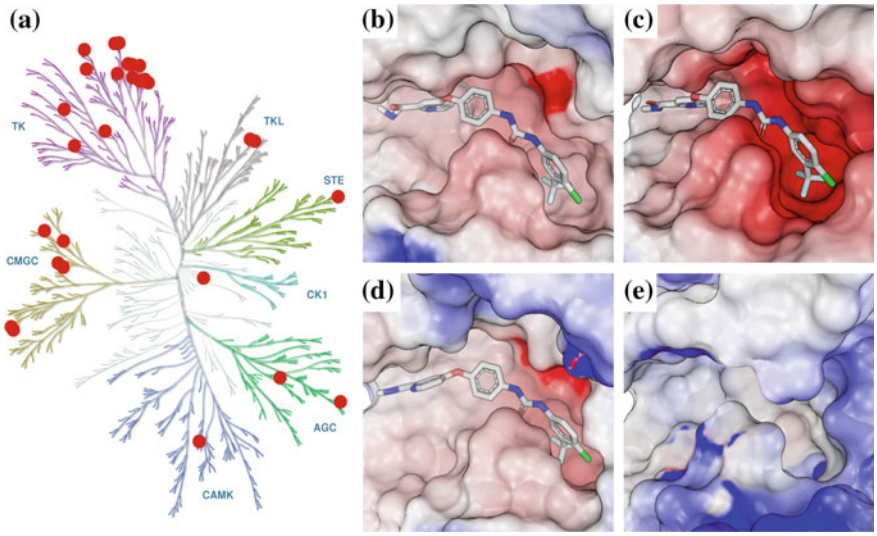

Fig. 4.2 Polypharmacology of the cancer drug sorafenib. **a** Phylogenetic tree of the human kinome (illustration reproduced courtesy of Cell Signaling Technology, Inc. (www.cellsignal.com), generated with Kinome Render (Chartier et al. 2013)), with sorafenib targets *highlighted in red circles*. The binding site structure of various protein kinases is shown in surface representation. **b** BRAF (PMID: 15035987) (Wan et al), **c** KDR (McTigue et al. 2012), and **d** p38α (Simard et al. 2009) are targets of sorafenib and their corresponding binding sites have negative electrostatic potential (*red*); **e** ERK is not a target of sorafenib and its modeled binding site exhibits lower negative electrostatic potential (*blue*) (PMID: 25420233; doi:10.1021/cb500696t) (Ung et al)

similarity among their ligands to build cross-target similarity networks that accurately identify previously unknown protein-drug interactions (Keiser et al. 2009).

4.4.2.3 Genomic Variation Imposes Constraints on Networks Through Protein and Drug Structure

Identifying which regions of a protein are responsible for different interactions is a key step toward understanding how protein function and interactions will be affected by genomic variation, including point mutations, deletions, and other mutation types. Nonsynonymous single nucleotide polymorphism (nsSNP) is a genetic variation that involves amino acid substitutions that can have a dramatic effect on stability, hydrogen-bond network, conformational dynamics, interaction, and many other physiologically important properties of proteins. Such properties can be critical for interacting with their partners including proteins, nucleic acids, and small molecule drugs (Wang and Moult 2001). For example, nsSNPs alter kinetic parameters of signaling pathways (e.g., E542K, E545K and H1047R on p110α for PI-3K catalytic activity). Protein structure reasoning can be applied to design "personalized drugs" that interact with variants associated with specific

diseases. Using X-ray crystallography and fragment-based screening, vemurafenib was specifically designed to target the BRAF V600E mutant for treating metastatic melanoma (Bollag et al. 2012).

Predicting how mutations affect protein structure, function, and druggability is therefore critical for modern drug discovery and personalized medicine. Various approaches aim at predicting mutation effect on functions such as destabilization of the native structure or interference with the binding of other proteins or small molecules (AlQuraishi et al. 2014; Kumar et al. 2009; Ramensky et al. 2002). Examples include (i) machine learning-based methods that are trained on sequence and biophysical features, such as solvent accessibility, flexibility, packing, and conservation of residues (Bromberg and Rost 2007; Kumar et al. 2009), and (ii) physics-based methods that compute the folding free energy to quantify the magnitude of a mutational effect on stability (Schymkowitz et al. 2005). Notably, deleterious point mutations can occur in binding interfaces and affect protein–protein interactions and lead to network rewiring and new targets. Interestingly, only a small fraction of the total residues in the binding interface contribute to most of the energy that is associated with binding (Wells and McClendon 2007). These interaction-stabilizing residues, which are often dubbed "hot spots", can also be predicted from structure using different approaches, such as computational alanine scanning, which computes the free energy effect of mutation to alanine for each of the binding interface residues, and other methods that consider evolutionary conservation (Kortemme and Baker 2002; Zhao et al. 2014). Analyzing the structural consequences of mutations in the context of networks and pathways can provide a mechanistic description for disease states and predict phenotypic effect. Kiel and Serrano performed a systematic analysis of 956 RASopathy and cancer mutations based on structures and energy predictions and showed that for the same gene, the type of mutation determines the diseases state (Kiel and Serrano 2014). Energy changes are higher for cancer mutations compared to RASopathy mutations, and RASopathy mutations are likely to cause only minor pathway dysregulation. These studies highlight how computational approaches allow the identification of relationships from structural variants to phenotypes to understand drug action. It is expected as such approaches get integrated into the drug discovery process, more personalized efficacious treatment for complex diseases such as type-2 diabetes, cancer, and heart failure will be forthcoming.

4.5 Network Dynamics in Systems Pharmacology

Network representations allow us to describe how molecules within the cell are connected through chemical reactions to one another. The organization within networks is often called topology, and network topology allows one to trace how a perturbation such as that evoked by a drug may be connected to important phenotypic outcomes such as cell fates or physiological responses. These networks can be analyzed to detect hubs, highly connected molecules that may be effective drug

targets. An ubiquitous network that regulates cell survival and proliferation is made up by the MAP-kinase and PI-3 kinase pathways as regulated by growth factor receptors (Fig. 4.3; von Kriegsheim et al. 2009). Such networks show topological features such as feedback and feed-forward loops. As described above, when information from network topology is combined with atomic structural information of the biological molecules within these networks, one can further identify what kinds of small molecule drugs may bind selectively to potential targets. Furthermore, at least in some cases, one can infer how this binding may depend on genomic variation that changes amino acid sequences, or understand how epigenetic information dictates connections between a perturbation and outcome in a context-dependent manner. This kind of reasoning can give tremendous insight into generating hypotheses for pharmacological targeting of disease-related networks. However there are limitations. One major limitation is the lack of consideration of quantitative and dynamic relationships between network nodes. If a certain network

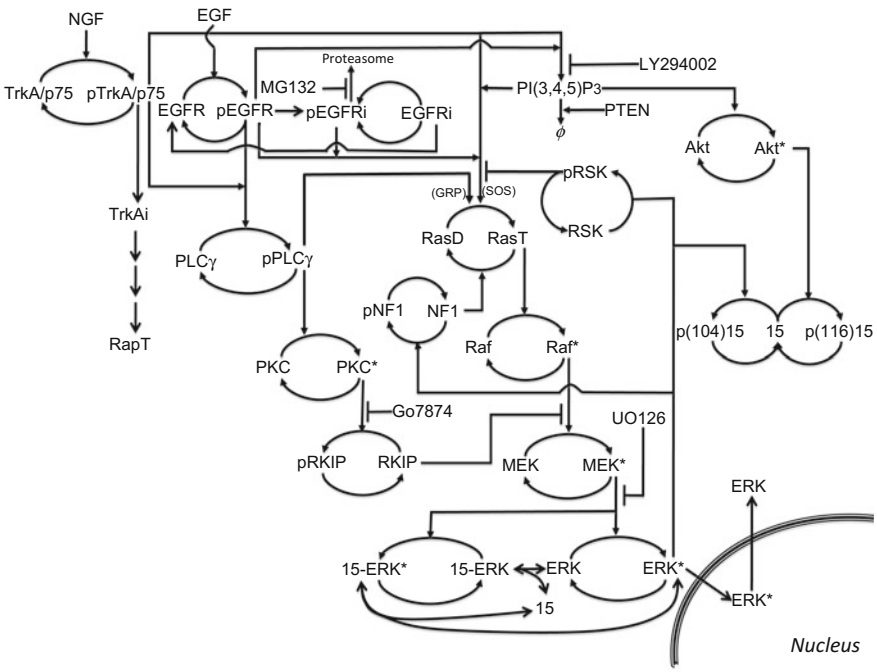

Fig. 4.3 Schematic of EGF and NGF signaling to ERK and Akt in PC-12 cells. Adapted from (von Kriegsheim et al. 2009). Epidermal growth factor (EGF) and nerve growth factor (NGF), stimulate activation of the EGF receptor (EGFR) and the TrkA receptor (NGFR), respectively, which can be internalized to different degrees (denoted by *i*). These active receptors lead to recruitment of activators and inhibitors of the Ras and PI-3K pathways, including a spatial regulator PEA-15 (denoted by 15). These pathways interact to form a complex network that regulates activity of ERK and Akt kinases, which in turn regulate multiple phenotypic outputs, depending on their temporal and spatial patterns. Multiple pharmacological compounds target nodes in this network

node is perturbed, will the perturbation be strong enough to propagate significantly to affect cell fate, or in the case of drug action, alter pathophysiological behaviors?

4.5.1 Fragile and Robust Nodes

Network and structural information give insight into a traditional definition of druggability by identifying a drug target and whether it is likely one can find a small molecule to bind this target. Although these are necessary criteria for defining drug targets, they are not sufficient. The question posed above evaluates druggability using the criterion of fragility or robustness of the target; only the former attribute is sought for a potential drug target. Fragility or robustness of a node is a systems-level feature of the biological network that defines how strong or weak a perturbation of that node affects an outcome of interest, and it is inherently quantitative. A fragile node mediates a large change in response to a small perturbation, and a robust node the opposite. We posit that an effective drug needs not only to be both structurally compatible with the target as is currently a usual focus of drug development, but also that the target must be "fragile", meaning that at therapeutic concentrations of the drug, it binds the target with adequate selectivity and avidity such that concentrations of the drug-target complex are sufficient for this perturbation to be propagated with significant strength to the functional effector of the network to evoke a therapeutic physiological response. In contrast, robust nodes would not sufficiently alter their activity upon binding the drug and hence do not induce change in response. Static, qualitative network models that are focused on topology give us a limited ability to evaluate such fragility.

4.5.2 Sensitivity Analysis to Assess Fragility

A common way to assess such systems-level druggability depends on first casting the biological network in terms of the elementary biochemical reactions that comprise it. This usually gives rise to ordinary, partial, or stochastic differential equation models that describe how these networks propagate signals and respond to drugs over space and time in a dose-dependent manner. Importantly, such models can give insight into this fragility or robustness question through a variety of systems engineering-inspired approaches including sensitivity analysis (Csete and Doyle 2002; Stelling et al. 2004; Kitano 2007). Sensitivity analysis is a collection of many methods that share the basic property of perturbing quantities in a mathematical model of a system, and then observing the change in an output(s) of interest. The magnitude of the sensitivity coefficient is related to fragility—the larger the sensitivity the more fragile the target. However, not all types of sensitivity analysis are appropriate for such biological networks. Because these networks are usually incompletely understood and non-linear, global sensitivity analyses, which

account for uncertainties in models and are not affected by non-linearities, are better suited for making such inferences of fragility (Kim et al. 2010; Zhang et al. 2014), and have even been used to make successful predictions for drug development, which surprisingly involved a kinase dead receptor ErbB3 (Schoeberl et al. 2009, 2010).

Predicting fragility of a single node is useful for understanding diseases that can be treated by a single drug or arise from defects in a single gene. However, many non-communicable diseases that are progressive are multi-factorial and would benefit from combination therapy. Additionally, an otherwise efficacious drug might have unacceptable toxicity that can be mitigated by a second drug (Zhao et al. 2013). High-throughput screening technologies can quite effectively explore responses of cells to single drugs and even dose responses of those drugs. When one is considering drug combinations; however, the number of potential experiments explodes into a number that is experimentally infeasible. Mathematical models of the system of interest can be useful to providing leads on potentially good drug combinations. Because they are based only on simulation, they are almost always quicker to evaluate than a typical high-throughput screening assay, as well as less expensive. In order for model analysis to yield useful predictions, those predictions must be precise, meaning that the variance in the prediction of drug response when model uncertainty is taken into account is relatively small. Small, here, is defined as that level which allows a robust decision to be made as to whether the drug combination is suitable for testing or not, and as such may be quite different depending on the particular scenario. Most of these models have a significant amount of uncertainty in them, both in the connections between biological molecules (network topology) and in the values of parameters that describe these interactions (e.g., binding affinities). How much experimental data does one need to build a model that makes precise and usable predictions for drug discovery as well as drug action? A gold standard would be a dataset that gives so-called full observability of the system, meaning that based on the measurements made, one can uniquely calculate the values of every unique chemical species in the model. However, one needn't know every parameter in the model precisely to make useful predictions of how model variables respond to perturbations; most if not all models of biological signaling networks exhibit a property called sloppiness in which time trajectories of key model variables are quite invariant to changes in most model parameters (Gutenkunst et al. 2007a, b). From a biological perspective this is not surprising, since this implies that key model variables are robust to most perturbations, which should be the case due to evolutionary pressures for these networks to function in the face of multiple forms of uncertainty and noise.

In any case, this understanding of sloppiness still does not answer the question of data requirements for the model. Just how well do we need to know the parameter values to make predictions of responses to single drugs and drug combinations that are of sufficient precision? To gain insight into this question, we performed simulations with a model of a mitogen activated protein kinase cascade (MAPK) (Huang and Ferrell 1996) (Fig. 4.4a) which controls many important cellular functions from yeast to mammals (Kholodenko and Birtwistle 2009) and is thus the

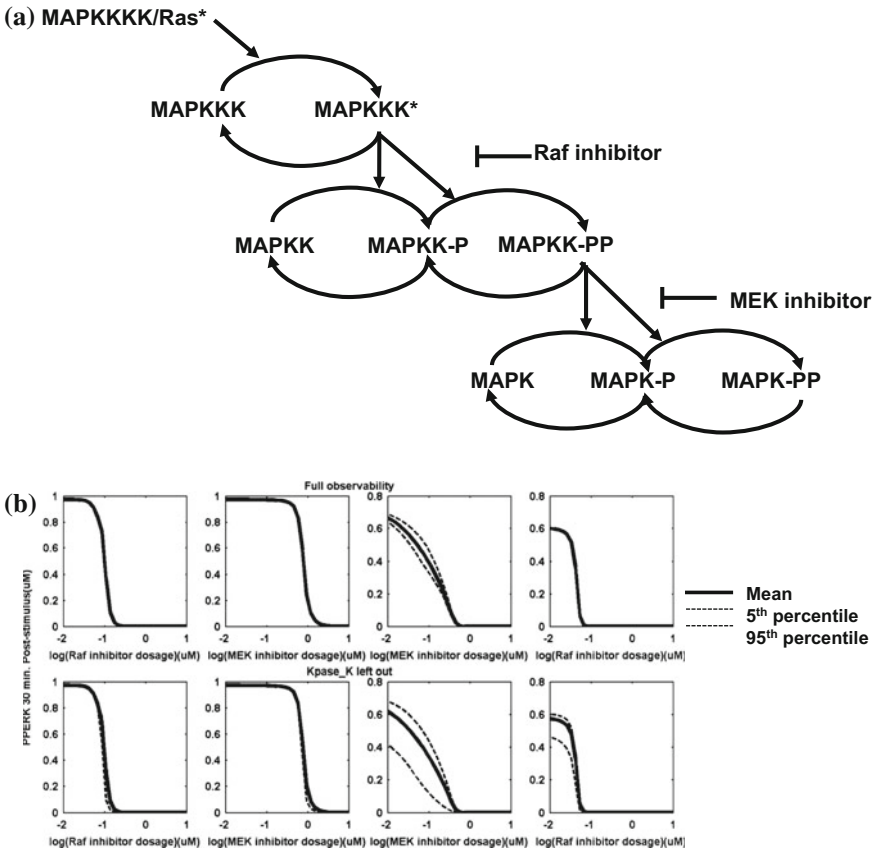

Fig. 4.4 Drug Action in the MAP—kinase pathway. Simulations with the Huang-Ferrell MAPK model using MAPKKK (Raf) and MAPKK (MEK) inhibitors. **a** Simplified model schematic. **b** Drug dosage responses computed as function of steady-state active MAPK/ERK (PPERK) concentration after drug administration for Raf, MEK, and Raf and MEK combined inhibitions. At least 25 drug dose response curves make up each plot, which correspond to different good fitting parameter sets, and are summarized by their mean, 5th and 95th percentiles. The *top panel* is simulations when the model is fit to simulated data that gives full system observability, and the *bottom panel* corresponds to when just a single observable, the MAPK-MAPK phosphatase complex, is removed from estimation. The *first two columns* are drug dosage responses for Raf and MEK inhibitors alone, and the *last two columns* correspond to drug combinations

target of many drugs, particularly anti-cancer drugs. We simulated time-course data (with added noise) from this system in response to an endogenous activation of the pathway, and ensured that the considered data were both experimentally feasible and gave full system observability. Next, different sets of kinetic parameters with the same goodness of fit were estimated based on minimizing the error between model predictions and simulated data using at least 25 different starting guesses to evaluate parametric uncertainty. These fitted parameter sets were then used to

predict MAPK (ERK) steady-state responses to a MAPKKK (Raf) drug, a MAPKK (MEK) drug, and a combination of the two that produced a range of predictions for drug responses. The gold standard dataset that allows full observability of this system (15 different quantities measured over time), not surprisingly, yielded very precise predictions of responses to single drugs and the drug combinations (Fig. 4.4b). However, if a single observable is left out during the parameter estimation, for example a somewhat non-obviously important one, such as the total level of MAPK/MAPK phosphatase complex (which actually has small sensitivity), single drug dose response predictions remain quite precise, whereas drug combination response predictions lose a significant amount of precision (Fig. 4.4b). This result holds for several such leave-one-out simulation experiments. Thus, it seems that making precise and therefore useful model-based predictions for drug combination responses requires a higher fidelity of parametric certainty, and therefore more experimental data than is often considered. More research into this important topic is needed if such models are to be useful in informing drug development and choices for potentially effective drug combinations to test further in experimental studies.

4.5.3 Sensitivity Analysis for Discovery of Targets for Combination Therapy

The previous line of thought is based on evaluating a pre-existing hypothesis for a drug combination; will the combination of two selected drugs be effective? How can we use quantitative biological network models to suggest co-fragile nodes, and therefore potential drug combinations a priori, before drugs are selected? This is an area where global sensitivity analysis is useful. While there are a variety of methods for global sensitivity analysis, we have had success in applying the method of Sobol to such differential equation models of biological pathways (Zhang et al. 2014; Sobol 2001; Saltelli 2008). One advantage of Sobol sensitivity analysis is that it allows rigorous calculation of uncertainty on the sensitivity coefficients, and each sensitivity coefficient is bounded between 0 and 1, with certain sums constrained to add to unity. Thus, the absolute value of Sobol sensitivity coefficients is directly meaningful and its statistical significance can be evaluated. Although Sobol sensitivity analysis can require a significant number of model simulations, it is a parallel problem, so utilizing high performance computing resources to implement it is quite straightforward and easily scaled. Based on Sobol sensitivity analysis, one can estimate both the impact of single parameters on an important output of interest (1st or total order terms), and the simultaneous impact that two parameters have on the output of interest (so-called 2nd order interaction terms). Single parameter sensitivity coefficients can be useful to identify drug combinations when simulations are performed with a first drug already selected and present in the model. The 2nd order parameter sensitivity coefficients that quantify interactions between

parameters give direct insight into potentially useful drug combinations without having to first consider a single drug.

Such simulations to suggest drug combinations of course do not give any insight into dosing strategies or regimens. For these purposes one must couple biological network dynamics that regulate drug action with pharmacokinetic models of the drugs.

4.6 Networks to Pharmacodynamics

Most textbooks of biochemistry contain detailed diagrams of biochemical processes; from glycolysis pathways to the TCA cycle to signaling pathways and networks. These descriptions of interconnected biochemical reactions (networks) provide a blueprint of normal physiology and also how they can be disrupted in various diseases. The level of detail and complexity is impressive and each reaction subset or single reactions that detail molecular conversions and enzyme kinetics can be further scrutinized and elaborated. Although such description of biochemical pathways and networks have existed for some time and are continually revised and expanded, they (the most part) have had little influence on drug discovery or studies of drug action. The modus operandi in drug discovery had been rational drug design for specific targets. Whether that drug design process involved protein structure and computer docking or more simply chemical modifications of lead compounds, the focus was the drug-target interaction defined by K_i and IC_{50} values. Even as drug discovery evolved into high-throughput screening techniques, the one drug-one target approach has been commonly used. It is, with few exceptions, fair to say that the worlds of detailed biochemistry of pathways and networks and the drug discovery and development were silos on different farms.

Now the drug discovery enterprise is changing; its deconstruction is not so much to do with an appreciation of the complexity of drug action but rather a realization that drug development expenditures are escalating faster than the return on investment; new blockbuster drugs are hard to find. Within this milieu of reanalysis, new strategies are being considered; from a growing emphasis on moving modeling and simulation, a standard practice in pharmaceutical companies, to more “radical” systems-based approaches (Benson and van der Graaf 2014; Milligan et al. 2013; Birtwistle et al. 2013). Such systems-based drug development is evolving from the juxtaposition of an appreciation of complex drug action and the revolution of bioinformatics heralded by the technological advances in genomics, including broad-based microarrays and next generation sequencing. The mindset that drug action is complex—not one drug-one target—is a natural evolution that also includes drug toxicity, and now, terms like “off-targets” and “repurposing” are common and have spawned new industries (Hurle et al. 2013; McCarthy et al. 2013). Informatics serves many functions from identifying prognostic risk factors such as individual genes and their variants, to gene sets or signatures as biomarkers for disease progression, to serving as a template for personalized medicine. It is the

latter use that may impact preclinical drug discovery and development with a central question, "which patients will benefit from our drug"? Superimposing complex drug action and a gene regulatory network on a single canvas paints a new picture that may be referred to as systems pharmacology. The gene network can be used to develop protein networks, or these protein networks can be developed independently using proteomic tools. A systems pharmacological view of drug action, whether for therapeutic efficacy or toxicity, can be cast as a subnetwork of drug targets within a larger regulatory network comprised of cell signaling pathways (Fig. 4.3). Pharmacodynamics (Levy 1966) predates this systems view and had more or less adopted the early view of one drug:one target where the measured response was either the direct drug target—target engagement—or a tell-tale downstream biomarker, for example phosphorylated Erk is often a measured biomarker for EGFR inhibitors (Wang et al. 2008). Not dissimilar to the black box compartmental modeling that is done in pharmacokinetics, pharmacodynamic models have also largely been a black box, the input is a drug concentration and the output of the box a measured response; mostly relative to control or pre-dose. Of course the limitation of black box pharmacodynamics is that without a mechanistic framework, patient responses may not correlate to the black box output, and even if they do, there are sufficient variations of the inner working of the black box that interpretation of the biomarker is fortuitous rather than causal. A good example is the work done by Iyengar et al. (2012) in which an EGFR biochemical network containing up to four genetic alterations (i.e., overexpression, SNP, miRNA expression, methylation status of promoter) exposed to the same degree of EGFR inhibition produced uniquely different responses based on tumor size. Measurement of a single biomarker—here tumor size or extent of EGFR inhibition—provides no insight as to why tumor size varied in these virtual patients or why the same degree of EGFR inhibition (80 % in this case) did not produce the same tumor size. The EGFR model was referred to as an enhanced pharmacodynamic model (ePD) to denote the shift from traditional pharmacodynamic models. Others have also appreciated complex drug action and put forth pharmacodynamic models that could double as a biochemical scheme. For example, a pharmacodynamic model for methotrexate depicted its multiple enzyme targets as well as interconnected metabolites (Panetta et al. 2010). The potential value of ePD models is clear. Whether a drug has only one or multiple targets, the influence of measured or predicted changes in the interconnecting proteins on signal flux and the final drug response can be determined. Thus, each patient may have a unique pharmacodynamic network or model—cast as a set of ODEs—that provides a simulation tool of their drug response (i.e., precision medicine). The individual ePD model outputs can be used directly to tailor therapy or analyzed as a population of patients to address questions like "is there a subset of patients that favorably respond to the drug and what are the biochemical characteristics"? By addressing the latter questions early in the drug development process, perhaps with a virtual population, an efficient means to decide on the future development strategy could be attained.

4.7 Systems-Based PK/PD Models

Pharmacodynamic models rarely exist as isolated entities and are linked to pharmacokinetic models to increase their usefulness by providing a total pharmacological package (Fig. 4.5). Historically, PK models were multi-compartment models that consisted of a set of black boxes to represent the various tissue regions that behaved kinetically quite similar. A link to the drug target organ via an effect compartment sufficed as a combined PK/PD model, wherein the effect compartment was often represented as the Sigmoid E_{max} model (Sheiner et al. 1979). In many cases, rather than the effect compartment formulation, the plasma drug concentration—again generated from the classic compartmental modeling approach—provided the link to the pharmacodynamic model. Even with the seminal advance of indirect response pharmacodynamic models made by Jusko and coworkers, plasma drug concentrations most often provided the link between PK and PD models (Dayneka et al. 1993). The simplicity of plasma drug concentrations was also utilized in conjunction with a VEGFR ePD model used to design novel multidrug regimens (Zhang et al. 2014). Although plasma drug concentrations have merit in

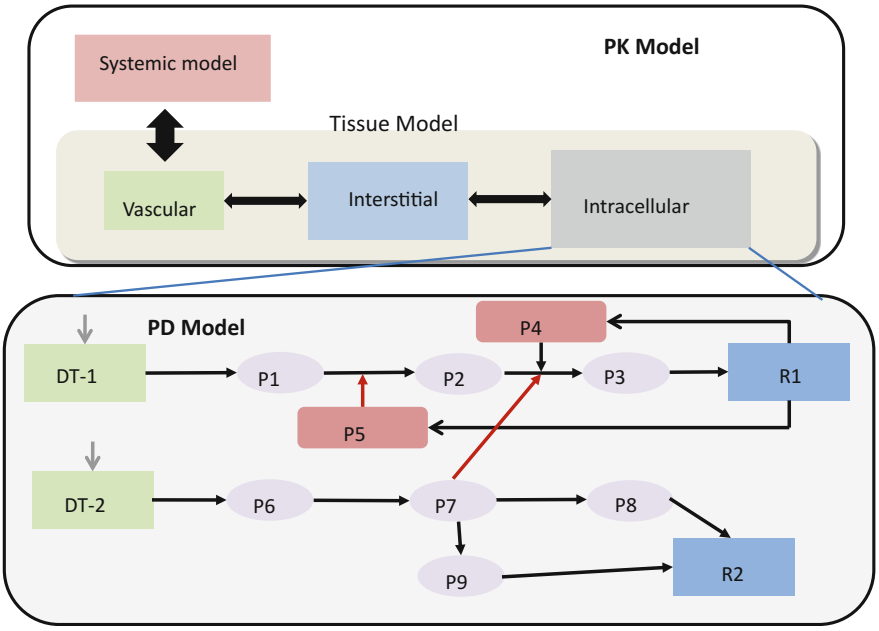

Fig. 4.5 Idealized physiologically-based pharmacokinetic/enhanced pharmacodynamic model. The ability to predict intracellular drug concentrations provides a natural link to mechanistic ePD models. *Thick black arrows* in PK model represent drug transport, DT-1 and DT-2 are 2 different drug targets, P1–P9 are different proteins with interconnecting arrows representing enzymatic reactions, R1 and R2 are two different drug responses, and *red arrows* represent negative feedback reactions

the clinical application of PK/PD models, it is known that drug concentrations at cellular receptors in tissues drive responses and may not necessarily mirror plasma drug concentrations. An alternative pharmacokinetic modeling approach—physiologically-based (PB) PK models—had been devised based on the prediction of tissue drug concentrations that was somewhat obscure until it was rediscovered during the upheaval in the drug discovery industry (Rowland et al. 2011). Since the original intent of PBPK models was to predict drug concentrations based on species- and drug-dependent parameters, it may be casted as an in silico tool to evaluate candidate drug pharmacokinetics expeditiously and without extensive data. During this same period, others appreciated the tissue-based assessment of drug disposition, its mechanistic potential, and scalability to patients (Gallo et al. 2004; Laplanche et al. 2007; Zhou et al. 2007). Now adjoining PBPK and enhanced pharmacodynamic models was a natural fit (Gallo 2013), and highlighted by an early investigation of the anticancer drug geldanamycin by the D'Argenio group (87). PBPK models can be used to estimate intracellular drug concentration (Fig. 4.5) and this capability was extended to a new paradigm referred to as cell-type specific (CTS) PBPK/ePD models (Ballesta et al. 2014). The full power of CTS PBPK/ePD models has yet to be realized; however, it provides a foundation to contrast drug efficacy and toxicity in their appropriate cell types, and further to account for heterogeneity and personalized therapy (Ballesta et al. 2014). At the same time, due to the potential size and number of model parameters in PBPK/ePD models, the same considerations of model construction and parameter estimation (sloppiness) faced by network biochemical models as mentioned above also confronts PBPK/ePD models (Gutenkunst et al. 2007a). Nonetheless, given their potential to enhance mechanistic models, drug development, and novel therapeutic strategies, it is believed that the field of system pharmacology will embrace these challenges and through innovation move the field forward.

4.8 Future of Systems Pharmacology

The majority of diseases for which we lack effective therapeutics are complex and progressive in nature. These include cardiovascular diseases such as heart failure, type-2 diabetes, and kidney disease among others. Both the progression of the disease and response to current therapy show considerable variability among patients. These differences have highlighted the need for understanding the individual patient in terms of her/his genomic and proteomic characteristics. Such understanding of disease mechanisms in individual patients has been largely focused on using genetic characteristics of the individuals. This approach has been successful in limited cases in which singular genetic (and protein) abnormalities determine drug response, such as for warfarin therapy. However, for complex diseases, we are likely to have multiple genes as well as postgenomic events regulating the disease state. Hence a systems biology-based approach that uses network topology to describe disease states is likely to be a very useful step in

developing dynamical models for disease progression. These models in turn should enable the definition of mechanism-based rules to not only understand why a drug may be effective but can further be applied to identify combinations of drug targets (Fig. 4.6, blue boxes). Some of these targets may already have drugs that bind and modulate their activity. In such cases, these drugs can be repurposed to treat other diseases distinct from the one they were originally intended to treat. In other cases, we may need to develop new drugs for particularly novel targets, but these efforts can be made more efficient when systems level models are available.

Beyond the general approach of considering disease networks in population of patients, there is an urgent need to understand variability, as disease progression differs among patients (?) and the same drugs show variable efficacy in different individuals. Here the development of disease state models that are personalized for each patient using the genomic characteristics guided by protein structure constraints, as well as dynamical features that are patient specific, can set the stage for ePD models that lead to precise individualized dosing regimens (Fig. 4.6, orange boxes). The integration of systems biology with pharmacology has given rise to the new field of systems pharmacology that provides an intellectual framework to consider complex physiology, pathophysiology, and drug action in a systematic

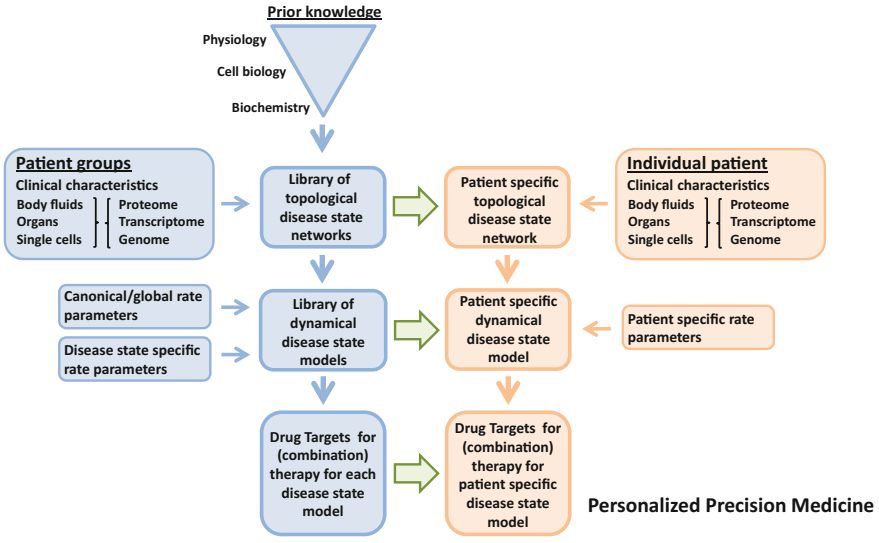

Fig. 4.6 Disease state specific models for systems pharmacology. The process diagrams for workflow in systems pharmacology for drug discovery for combination therapy and for personalized precision medicine. Typically data from groups of patients are combined to construct canonical disease state networks that can be used to construct dynamical models and ideal combinations of targets that are predicted to be efficacious. The topological disease state networks can be personalized for an individual patient using genomic, transcriptomic, or proteomic determinants. Such networks can serve as the basis of dynamical models that are personalized using patient specific parameters that can be used to predict dosing regimen and therapeutic strategies for the specific patient

manner to drive both drug discovery and therapeutics at an individual level. Thus, the impact of systems pharmacology on personalized and precision medicine is likely to be substantial.

References

Aithal GP, Day CP, Kesteven PJ, Daly AK (1999) Association of polymorphisms in the cytochrome P450 CYP2C9 with warfarin dose requirement and risk of bleeding complications. Lancet 353(9154):717–719. doi:10.1016/S0140-6736(98)04474-2

Alber F, Dokudovskaya S, Veenhoff LM, Zhang W, Kipper J, Devos D, Suprapto A, Karni-Schmidt O, Williams R, Chait BT, Sali A, Rout MP (2007) The molecular architecture of the nuclear pore complex. Nature 450(7170):695–701. doi:10.1038/nature06405

AlQuraishi M, Koytiger G, Jenney A, MacBeath G, Sorger PK (2014) A multiscale statistical mechanical framework integrates biophysical and genomic data to assemble cancer networks. Nat Genet 46(12):1363–1371. doi:10.1038/ng.3138

Baker D, Sali A (2001) Protein structure prediction and structural genomics. Science 294 (5540):93–96. doi:10.1126/science.1065659

Ballesta A., Zhou Q, Zhang X, Lv H, Gallo JM (2014) Multiscale design of cell-type-specific pharmacokinetic/pharmacodynamic models for personalized medicine: application to temozolomide in brain tumors. CPT Pharmacometrics Syst Pharmacol 3:e112

Benson N, van der Graaf PH (2014) The rise of systems pharmacology in drug discovery and development. Future Med Chem 6(16):1731–1734. doi:10.4155/fmc.14.66

Berger SI, Iyengar R (2009) Network analyses in systems pharmacology. Bioinformatics 25 (19):2466–2472. doi:10.1093/bioinformatics/btp465

Berger SI, Ma'ayan A, Iyengar R (2010) Systems pharmacology of arrhythmias. Sci Signal 3(118): ra30. doi:10.1126/scisignal.2000723

Birtwistle MR, Hatakeyama M, Yumoto N, Ogunnaike BA, Hoek JB, Kholodenko BN (2007) Ligand-dependent responses of the ErbB signaling network: experimental and modeling analyses. Mol Syst Biol 3:144. doi:10.1038/msb4100188

Birtwistle MR, Mager DE, Gallo JM (2013) Mechanistic vs. empirical networks models of drug action. CPT Pharmacometrics Syst Pharmacol 2(9):1–3

Bollag G, Tsai J, Zhang J, Zhang C, Ibrahim P, Nolop K, Hirth P (2012) Vemurafenib: the first drug approved for BRAF-mutant cancer. Nat Rev Drug Discov 11(11):873–886. doi:10.1038/nrd3847

Boran AD, Iyengar R (2010a) Systems approaches to polypharmacology and drug discovery. Curr Opin Drug Discov Devel 13(3):297–309

Boran AD, Iyengar R (2010b) Systems pharmacology. Mt Sinai J Med 77(4):333–344. doi:10.1002/msj.20191

Bromberg Y, Rost B (2007) SNAP: predict effect of non-synonymous polymorphisms on function. Nucleic Acids Res 35(11):3823–3835. doi:10.1093/nar/gkm238

Brunton L, Chabner B, Knollman B (2011) The pharmacological basis of therapeutics, 12th edn. McGrawHill Medical, London

Chartier M, Chenard T, Barker J, Najmanovich R (2013) Kinome Render: a stand-alone and web-accessible tool to annotate the human protein kinome tree. PeerJ 1:e126. doi:10.7717/peerj.126

Cheng AC, Coleman RG, Smyth KT, Cao Q, Soulard P, Caffrey DR, Salzberg AC, Huang ES (2007) Structure-based maximal affinity model predicts small-molecule druggability. Nat Biotechnol 25(1):71–75. doi:10.1038/nbt1273

Csete ME, Doyle JC (2002) Reverse engineering of biological complexity. Science 295 (5560):1664–1669. doi:10.1126/science.1069981

Dar AC, Das TK, Shokat KM, Cagan RL (2012) Chemical genetic discovery of targets and anti-targets for cancer polypharmacology. Nature 486(7401):80–84. doi:10.1038/nature11127

Davis FP, Braberg H, Shen MY, Pieper U, Sali A, Madhusudhan MS (2006) Protein complex compositions predicted by structural similarity. Nucleic Acids Res 34(10):2943–2952. doi:10.1093/nar/gkl353

Dayneka NL, Garg V, Jusko WJ (1993) Comparison of four basic models of indirect pharmacodynamic responses. J Pharmacokinet Biopharm 21(4):457–478

De Roock W, Jonker DJ, Di Nicolantonio F, Sartore-Bianchi A, Tu D, Siena S, Lamba S, Arena S, Frattini M, Piessevaux H, Van Cutsem E, O'Callaghan CJ, Khambata-Ford S, Zalcberg JR, Simes J, Karapetis CS, Bardelli A, Tejpar S (2010) Association of KRAS p.G13D mutation with outcome in patients with chemotherapy-refractory metastatic colorectal cancer treated with cetuximab. JAMA 304(16):1812–1820. doi:10.1001/jama.2010.1535

De Roock W, Jonker DJ, Di Nicolantonio F, Sartore-Bianchi A, Tu D, Siena S, Lamba S, Arena S, Frattini M, Piessevaux H, Van Cutsem E, O'Callaghan CJ, Khambata-Ford S, Zalcberg JR, Simes J, Karapetis CS, Bardelli A, Tejpar S (2013) Association of KRAS p.G13D mutation with outcome in patients with chemotherapy-refractory metastatic colorectal cancer treated with cetuximab. JAMA 304(16):1812–1820. doi:10.1001/jama.2010.1535

Durrant JD, McCammon JA (2013) Molecular dynamics simulations and drug discovery. BMC Biol 9:71. doi:10.1186/1741-7007-9-71

Gallo JM (2013) Physiologically based pharmacokinetic models of tyrosine kinase inhibitors: a systems pharmacological approach to drug disposition. Clin Pharmacol Ther 93(3):236–238. doi:10.1038/clpt.2012.244

Gallo JM, Vicini P, Orlansky A, Li S, Zhou F, Ma J, Pulfer S, Bookman MA, Guo P (2004) Pharmacokinetic model-predicted anticancer drug concentrations in human tumors. Clin Cancer Res 10(23):8048–8058. doi:10.1158/1078-0432.CCR-04-0822

Geier EG, Schlessinger A, Fan H, Gable JE, Irwin JJ, Sali A, Giacomini KM (2013) Structure-based ligand discovery for the Large-neutral Amino Acid Transporter 1, LAT-1. Proc Natl Acad Sci USA 110(14):5480–5485. doi:10.1073/pnas.1218165110

Gutenkunst RN, Waterfall JJ, Casey FP, Brown KS, Myers CR, Sethna JP (2007a) Universally sloppy parameter sensitivities in systems biology models. PLoS Comput Biol 3(10):1871–1878

Gutenkunst RN, Casey FP, Waterfall JJ, Myers CR, Sethna JP (2007b) Extracting falsifiable predictions from sloppy models. Ann NY Acad Sci 1115:203–211. doi:10.1196/annals.1407.003

Hopkins AL, Groom CR (2002) The druggable genome. Nat Rev Drug Discov 1(9):727–730. doi:10.1038/nrd892

Huang CY, Ferrell JE Jr (1996) Ultrasensitivity in the mitogen-activated protein kinase cascade. Proc Natl Acad Sci USA 93(19):10078–10083

Hurle MR, Yang L, Xie Q, Rajpal DK, Sanseau P, Agarwal P (2013) Computational drug repositioning: from data to therapeutics. Clin Pharmacol Ther 93(4):335–341. doi:10.1038/clpt.2013.1

Iyengar R, Zhao S, Chung SW, Mager DE, Gallo JM (2012) Merging systems biology with pharmacodynamics. Sci Transl Med 4(126):126ps127. doi:10.1126/scitranslmed.3003563

Jacobson M, Sali A (2004) Comparative protein structure modeling and its applications to drug discovery. Annual Reports in Medicinal Chemistry Inpharmatica Ltd., London, pp 259–276

Keiser MJ, Setola V, Irwin JJ, Laggner C, Abbas AI, Hufeisen SJ, Jensen NH, Kuijer MB, Matos RC, Tran TB, Whaley R, Glennon RA, Hert J, Thomas KL, Edwards DD, Shoichet BK, Roth BL (2009) Predicting new molecular targets for known drugs. Nature 462(7270):175–181. doi:10.1038/nature08506

Kholodenko BN, Birtwistle MR (2009) Four-dimensional dynamics of MAPK information processing systems. Wiley Interdiscip Rev Syst Biol Med 1(1):28–44. doi:10.1002/wsbm.16

Kiel C, Serrano L (2014) Structure-energy-based predictions and network modelling of RASopathy and cancer missense mutations. Mol Syst Biol 10:727

Kim PM, Lu LJ, Xia Y, Gerstein MB (2006) Relating three-dimensional structures to protein networks provides evolutionary insights. Science 314(5807):1938–1941. doi:10.1126/science.1136174

Kim KA, Spencer SL, Albeck JG, Burke JM, Sorger PK, Gaudet S, Kim do H (2010) Systematic calibration of a cell signaling network model. BMC Bioinf 11:202. doi:10.1186/1471-2105-11-202

Kitano H (2007) A robustness-based approach to systems-oriented drug design. Nat Rev Drug Discov 6(3):202–210. doi:10.1038/nrd2195

Kortemme T, Baker D (2002) A simple physical model for binding energy hot spots in protein-protein complexes. Proc Natl Acad Sci USA 99(22):14116–14121. doi:10.1073/pnas.202485799

Kozakov D, Hall DR, Chuang GY, Cencic R, Brenke R, Grove LE, Beglov D, Pelletier J, Whitty A, Vajda S (2011) Structural conservation of druggable hot spots in protein-protein interfaces. Proc Natl Acad Sci USA 108(33):13528–13533. doi:10.1073/pnas.1101835108

Kumar P, Henikoff S, Ng PC (2009) Predicting the effects of coding non-synonymous variants on protein function using the SIFT algorithm. Nat Protoc 4(7):1073–1081. doi:10.1038/nprot.2009.86

Laplanche R, Meno-Tetang GM, Kawai R (2007) Physiologically based pharmacokinetic (PBPK) modeling of everolimus (RAD001) in rats involving non-linear tissue uptake. J Pharmacokinet Pharmacodyn 34(3):373–400. doi:10.1007/s10928-007-9051-7

Lehninger A, Nelson D, Cox M (1992) Principles of biochemistry, 2nd edn. Worth Publishers Inc, New York

Levy G (1966) Kinetics of pharmacologic effects. Clin Pharmacol Ther 7(3):362–372

Lin C, Kwong AD, Perni RB (2006) Discovery and development of VX-950, a novel, covalent, and reversible inhibitor of hepatitis C virus NS3.4A serine protease. Infect Disord Drug Targets 6(1):3–16

Lipinski CA, Lombardo F, Dominy BW, Feeney PJ (2001) Experimental and computational approaches to estimate solubility and permeability in drug discovery and development settings. Adv Drug Deliv Rev 46(1–3):3–26. doi:10.1016/S0169-409X(00)00129-0

McCarthy JJ, McLeod HL, Ginsburg GS (2013) Genomic medicine: a decade of successes, challenges, and opportunities. Sci Transl Med 5(189):189sr184. doi:10.1126/scitranslmed.3005785

McTigue M, Murray BW, Chen JH, Deng YL, Solowiej J, Kania RS (2012) Molecular conformations, interactions, and properties associated with drug efficiency and clinical performance among VEGFR TK inhibitors. Proc Natl Acad Sci USA 109(45):18281–18289. doi:10.1073/pnas.1207759109

Milligan PA, Brown MJ, Marchant B, Martin SW, van der Graaf PH, Benson N, Nucci G, Nichols DJ, Boyd RA, Mandema JW, Krishnaswami S, Zwillich S, Gruben D, Anziano RJ, Stock TC, Lalonde RL (2013) Model-based drug development: a rational approach to efficiently accelerate drug development. Clin Pharmacol Ther 93(6):502–514. doi:10.1038/clpt.2013.54

Milo R, Shen-Orr S, Itzkovitz S, Kashtan N, Chklovskii D, Alon U (2002) Network motifs: simple building blocks of complex networks. Science 298(5594):824–827. doi:10.1126/science.298.5594.824

Mosca R, Ceol A, Aloy P (2013) Interactome3D: adding structural details to protein networks. Nat Methods 10(1):47–53. doi:10.1038/nmeth.2289

Ostrem JM, Peters U, Sos ML, Wells JA, Shokat KM (2013) K-Ras(G12C) inhibitors allosterically control GTP affinity and effector interactions. Nature 503(7477):548–551. doi:10.1038/nature12796

Panetta JC, Sparreboom A, Pui CH, Relling MV, Evans WE (2010) Modeling mechanisms of in vivo variability in methotrexate accumulation and folate pathway inhibition in acute lymphoblastic leukemia cells. PLoS Comput Biol 6(12):e1001019. doi:10.1371/journal.pcbi.1001019

Perot S, Sperandio O, Miteva MA, Camproux AC, Villoutreix BO (2010) Druggable pockets and binding site centric chemical space: a paradigm shift in drug discovery. Drug Discov Today 15(15–16):656–667. doi:10.1016/j.drudis.2010.05.015

Picotti P, Aebersold R (2012) Selected reaction monitoring-based proteomics: workflows, potential, pitfalls and future directions. Nat Methods 9(6):555–566. doi:10.1038/nmeth.2015

Rahuel J, Rasetti V, Maibaum J, Rueger H, Goschke R, Cohen NC, Stutz S, Cumin F, Fuhrer W, Wood JM, Grutter MG (2000) Structure-based drug design: the discovery of novel nonpeptide orally active inhibitors of human renin. Chem Biol 7(7):493–504. doi:10.1016/S1074-5521(00)00134-4

Ramensky V, Bork P, Sunyaev S (2002) Human non-synonymous SNPs: server and survey. Nucleic Acids Res 30(17):3894–3900

Rose PW, Bi C, Bluhm WF, Christie CH, Dimitropoulos D, Dutta S, Green RK, Goodsell DS, Prlic A, Quesada M, Quinn GB, Ramos AG, Westbrook JD, Young J, Zardecki C, Berman HM, Bourne PE (2013) The RCSB Protein Data Bank: new resources for research and education. Nucleic Acids Res 41(Database issue):D475–D482. doi:10.1093/nar/gks1200

Roth BL, Sheffler DJ, Kroeze WK (2004) Magic shotguns versus magic bullets: selectively non-selective drugs for mood disorders and schizophrenia. Nat Rev Drug Discov 3(4):353–359. doi:10.1038/nrd1346

Rowland M, Peck C, Tucker G (2011) Physiologically-based pharmacokinetics in drug development and regulatory science. Annu Rev Pharmacol Toxicol 51:45–73. doi:10.1146/annurev-pharmtox-010510-100540

Russel D, Lasker K, Webb B, Velazquez-Muriel J, Tjioe E, Schneidman-Duhovny D, Peterson B, Sali A (2012) Putting the pieces together: integrative modeling platform software for structure determination of macromolecular assemblies. PLoS Biol 10(1):e1001244. doi:10.1371/journal.pbio.1001244

Sabathie M, de Coninck L, Fabre P, Michel G (1975) Use of diarginine α-ketoglutarate following abdominal surgery. Apropos of 30 cases. Sem Hop Ther 51(9):457–458

Sali A, Blundell TL (1993) Comparative protein modelling by satisfaction of spatial restraints. J Mol Biol 234(3):779–815. doi:10.1006/jmbi.1993.1626

Saltelli A (2008) Global sensitivity analysis: the primer. Wiley, Chichester

Schlessinger A, Geier E, Fan H, Irwin JJ, Shoichet BK, Giacomini KM, Sali A (2011) Structure-based discovery of prescription drugs that interact with the norepinephrine transporter, NET. Proc Natl Acad Sci USA 108(38):15810–15815. doi:10.1073/pnas.1106030108

Schlessinger A, Khuri N, Giacomini KM, Sali A (2013) Molecular modeling and ligand docking for solute carrier (SLC) transporters. Curr Top Med Chem 13(7):843–856. doi:10.1016/CTMC-EPUB-20130411-7

Schoeberl B, Pace EA, Fitzgerald JB, Harms BD, Xu L, Nie L, Linggi B, Kalra A, Paragas V, Bukhalid R, Grantcharova V, Kohli N, West KA, Leszczyniecka M, Feldhaus MJ, Kudla AJ, Nielsen UB (2009) Therapeutically targeting ErbB3: a key node in ligand-induced activation of the ErbB receptor-PI3K axis. Sci Signal 2(77):ra31. doi:10.1126/scisignal.2000352

Schoeberl B, Faber AC, Li D, Liang MC, Crosby K, Onsum M, Burenkova O, Pace E, Walton Z, Nie L, Fulgham A, Song Y, Nielsen UB, Engelman JA, Wong KK (2010) An ErbB3 antibody, MM-121, is active in cancers with ligand-dependent activation. Cancer Res 70(6):2485–2494. doi:10.1158/0008-5472.CAN-09-3145

Schymkowitz J, Borg J, Stricher F, Nys R, Rousseau F, Serrano L (2005) The FoldX web server: an online force field. Nucleic Acids Res 33(Web Server Issue):W382–W388. doi:10.1093/nar/gki387

Sheiner LB, Stanski DR, Vozeh S, Miller RD, Ham J (1979) Simultaneous modeling of pharmacokinetics and pharmacodynamics: application to d-tubocurarine. Clin Pharmacol Ther 25(3):358–371

Shendure J, Lieberman Aiden E (2012) The expanding scope of DNA sequencing. Nat Biotechnol 30(11):1084–1094. doi:10.1038/nbt.2421

Shoichet BK (2004) Virtual screening of chemical libraries. Nature 432(7019):862–865. doi:10.1038/nature03197

Simard JR, Getlik M, Grutter C, Pawar V, Wulfert S, Rabiller M, Rauh D (2009) Development of a fluorescent-tagged kinase assay system for the detection and characterization of allosteric kinase inhibitors. J Am Chem Soc 131(37):13286–13296. doi:10.1021/ja902010p

Singh J, Petter RC, Baillie TA, Whitty A (2011) The resurgence of covalent drugs. Nat Rev Drug Discov 10(4):307–317. doi:10.1038/nrd3410

Sobol IM (2001) Global sensitivity indices for nonlinear mathematical models and their Monte Carlo estimates. Math Comput Simulat 55(1–3):271–280. doi:10.1016/S0378-4754(00)00270-6

Sorger PK, Allerheiligen SRB, Abernethy DR, Altman RB, Brouwer KLR, Califano A, D'Argenio DZ, Iyengar R, Jusko WJ, Lalonde R, Lauffenburger DA, Shoichet B, Stevens JL, Subramaniam S, Van der Graaf P, Vicini P (2011) Quantitative and systems pharmacology in the post-genomic era: new approaches to discovering drugs and understanding therapeutic mechanisms. Paper presented at the QSP Workshop Group

Stelling J, Sauer U, Szallasi Z, Doyle FJ III, Doyle J (2004) Robustness of cellular functions. Cell 118(6):675–685. doi:10.1016/j.cell.2004.09.008

Toward Precision Medicine: Building a Knowledge Network for Biomedical Research and a New Taxonomy of Disease (2011) Committee on a framework for development a new taxonomy of disease, board on life sciences. Division on Earth and Life Studies, National Research Council

von Kriegsheim A, Baiocchi D, Birtwistle M, Sumpton D, Bienvenut W, Morrice N, Yamada K, Lamond A, Kalna G, Orton R, Gilbert D, Kolch W (2009) Cell fate decisions are specified by the dynamic ERK interactome. Nat Cell Biol 11(12):1458–1464. doi:10.1038/ncb1994

Wang Z, Moult J (2001) SNPs, protein structure, and disease. Hum Mutat 17(4):263–270. doi:10.1002/humu.22

Wang S, Guo P, Wang X, Zhou Q, Gallo JM (2008) Preclinical pharmacokinetic /pharmacodynamic models of gefitinib and the design of equivalent dosing regimens in EGFR wild-type and mutant tumor models. Mol Cancer Ther 7(2):407–417. doi:10.1158/1535-7163.MCT-07-2070

Wells JA, McClendon CL (2007) Reaching for high-hanging fruit in drug discovery at protein-protein interfaces. Nature 450(7172):1001–1009. doi:10.1038/nature06526

Wendell A, Cianci JP (1992) Factors affecting distribution of catheter-injected local anesthetic. Anesthesiology 77(1):211–212 (author reply 213)

Weng G, Bhalla US, Iyengar R (1999) Complexity in biological signaling systems. Science 284 (5411):92–96

Xie L, Evangelidis T, Bourne PE (2011) Drug discovery using chemical systems biology: weak inhibition of multiple kinases may contribute to the anti-cancer effect of nelfinavir. PLoS Comput Biol 7(4):e1002037. doi:10.1371/journal.pcbi.1002037

Xie L, Kinnings SL, Bourne PE (2012) Novel computational approaches to polypharmacology as a means to define responses to individual drugs. Annu Rev Pharmacol Toxicol 52:361–379. doi:10.1146/annurev-pharmtox-010611-134630

Zhang QC, Petrey D, Deng L, Qiang L, Shi Y, Thu CA, Bisikirska B, Lefebvre C, Accili D, Hunter T, Maniatis T, Califano A, Honig B (2012) Structure-based prediction of protein-protein interactions on a genome-wide scale. Nature 490(7421):556–560. doi:10.1038/nature11503

Zhang XY, Birtwistle MR, Gallo JM (2014) A general network pharmacodynamic model-based design pipeline for customized cancer therapy applied to the VEGFR pathway. CPT Pharmacometrics Syst Pharmacol 3:e92. doi:10.1038/psp.2013.65

Zhao S, Iyengar R (2012) Systems pharmacology: network analysis to identify multiscale mechanisms of drug action. Annu Rev Pharmacol Toxicol 52:505–521. doi:10.1146/annurev-pharmtox-010611-134520

Zhao S, Nishimura T, Chen Y, Azeloglu EU, Gottesman O, Giannarelli C, Zafar MU, Benard L, Badimon JJ, Hajjar RJ, Goldfarb J, Iyengar R (2013) Systems pharmacology of adverse event mitigation by drug combinations. Sci Transl Med 5:206ra140. doi:10.1126/scitranslmed.3006548

Zhao N, Han JG, Shyu CR, Korkin D (2014) Determining effects of non-synonymous SNPs on protein-protein interactions using supervised and semi-supervised learning. PLoS Comput Biol 10(5):e1003592. doi:10.1371/journal.pcbi.1003592

Zhou Q, Guo P, Kruh GD, Vicini P, Wang X, Gallo JM (2007) Predicting human tumor drug concentrations from a preclinical pharmacokinetic model of temozolomide brain disposition. Clin Cancer Res 13(14):4271–4279. doi:10.1158/1078-0432.CCR-07-0658

Chapter 5
Discrete Dynamic Modeling: A Network Approach for Systems Pharmacology

Steven Nathaniel Steinway, Rui-Sheng Wang and Reka Albert

Abstract Systems pharmacology is an interdisciplinary field that aims to apply the theoretical and experimental tools of systems biology to drug development. The goal is to go beyond the interaction between a drug and the target to which it binds to explore drug effects on the cellular networks affected by disease. Over the years, vast amounts of information about the regulatory relationships among genes, proteins, and small molecules have been acquired. Similarly, there is much known about the deregulation of these systems during disease. However, many knowledge gaps still exist. There is an abundance of qualitative or relative information related to the activation of signaling pathways, but a paucity of kinetic and temporal information. Discrete dynamic modeling provides a means to create predictive models of signal transduction pathways by integrating fragmentary and qualitative interaction information. Using discrete dynamic modeling, a structural (static) network of biological regulatory relationships can be translated into a mathematical model without the use of kinetic parameters. This model can describe the dynamics of a biological system over time, both in normal and in perturbation scenarios. In this chapter, we discuss the fundamentals of discrete dynamic modeling as it pertains to systems pharmacology. As an example, we apply this methodology to a previously constructed pharmacodynamic model of epidermal derived growth factor receptor (EGFR) signaling. We (1) translate this model into two types of discrete models, a Boolean model and a three-state model, (2) show how the effects of an EGFR inhibitor (such as gefitinib) can suppress tumor growth, and (3) model how genomic variants can augment the effect of EGFR inhibition in tumor growth. We argue that discrete dynamic models can be used to facilitate many of the goals of systems pharmacology. These include understanding how individual differences contribute to variability in drug response and determining which drugs would be best depending on individual genetic differences.

S.N. Steinway (✉)
Penn State Hershey Cancer Institute, Penn State University College of Medicine,
6 University Manor East, Hershey, PA 17033, USA
e-mail: ssteinway@hmc.psu.edu

R.-S. Wang · R. Albert
Department of Physics, Pennsylvania State University, University Park, PA, USA

D.E. Mager and H.H.C. Kimko (eds.), *Systems Pharmacology and Pharmacodynamics*,
AAPS Advances in the Pharmaceutical Sciences Series 23,
DOI 10.1007/978-3-319-44534-2_5

Keywords Epidermal derived growth factor receptor (EGFR) · Boolean functions · State transition · Synchronous · Deterministic · Asynchronous · Biological homeostasis · Perturbations · Multi-state discrete models · MAPK signaling · Rasgap state

5.1 Introduction

Systems biology involves the reconstruction of a system from individual biological interactions. Small scale and high throughput experiments over a long period amass to systems-level information. Collecting this information into holistic models is a fundamental goal of systems biology, because it allows the study of biological processes at a systems level, realizing emergent properties that are critical to the biological process and that may not be recognized from traditional reductionist views. Systems biology relies on a combination of experimental and computational techniques. Experimental techniques include the acquisition of "omics" level analysis of DNA, mRNA, proteins, and metabolites related to specific biological processes and disease states. Computational techniques are required to analyze and interpret these massive amounts of data.

Systems pharmacology is an emerging interdisciplinary field that aims to use the tools of systems biology to improve the development of drugs and to understand drug effects on the body. Traditional drug discovery has largely focused on the drug-target interaction. It is apparent now that this is insufficient, as it is recognized that diseases and drug targets are connected to networks of proteins that regulate drug response. As a result, it has become quite difficult for traditional pharmacological approaches to yield promising drug candidates (Sorger et al. 2011). Understanding how drug effects propagate from the site of action through the signaling network it regulates is a critical aspect of pharmacological development.

One aspect of systems biology is network modeling, which is a formalism that can be used to represent signaling networks. In a network, nodes represent the components of the network (e.g., proteins, genes, and small molecules) and the edges are the interactions between nodes. Edges can be directed (indicating the direction of information flow, for example from a regulator to a target) and can be positive (activating) or negative (inhibitory). Construction of a network allows for topological analysis, based on measures related to the structure of the network. Many measures have been developed to describe the features of networks based on their structure. For example, centrality measures have been used to identify the relative importance of a node within a network (Telesford et al. 2011).

An additional layer of modeling is the dynamic model, which characterizes each network node with a state variable and describes how these states change in time due to the interactions among nodes. Both quantitative and qualitative models exist to describe the dynamics of systems. Quantitative dynamic models generally use systems of differential equations to describe the continuous change of the system over time. These models can be highly accurate, but the limited kinetic and

temporal information about individual nodes in the network limits their feasibility and widespread use, especially for large-scale systems (Wang et al. 2012).

Discrete dynamic modeling represents a class of qualitative dynamic models used to study signal transduction processes because of its computational feasibility and capacity to be constructed with qualitative biological data (Albert and Wang 2009). The simplest kind of discrete models are Boolean models. In these models, nodes can have two qualitative states, ON (above an activity threshold) or OFF (below an activity threshold). The biological relationships defined by the structure of the network can be translated into mathematical equations using Boolean operators (Saadatpour and Albert 2012). Network-based discrete dynamic models can be used to generate testable hypotheses and are particularly useful in poorly characterized biological systems (Gross 2006). Boolean network models have led to new insight into signal transduction and gene regulatory networks in numerous organisms (Thakar et al. 2007; Walsh et al. 2011; Zhang et al. 2008; Albert and Othmer 2003).

In this chapter, we introduce discrete dynamic modeling in the context of systems pharmacology. We first describe how to reconstruct a network from available experimental information, which is often disparate and incomplete. We then describe how we can translate this network framework into a dynamic model that can predict the behavior of a biological system in response to some kind of signal (e.g., a drug) and in the presence of model perturbations (e.g., genomic or epigenomic alterations). We explain in detail how to construct Boolean dynamic models, including synchronous and asynchronous updating schemes and model reduction techniques. We further discuss how to analyze the dynamics of a system, including attractors, initial conditions, basins of attraction, and the network's state space. Based on these models, predictive and testable hypotheses can be obtained. As an example, we have constructed a Boolean and a multi-state discrete model of EGFR signaling and of the effect of an EGFR inhibitor on tumor growth in the context of different tumor mutations. We demonstrate that this model is consistent with existing knowledge and that it can be used to predict tumor response to drug treatment in the context of different mutations.

5.2 Methodology in Discrete Dynamic Modeling

5.2.1 Constructing the Network

In order to develop a dynamic Boolean model, a network must be first constructed, which represents the players to be modeled and their interactions or regulatory relationships. Importantly, networks provide a unifying representation of heterogeneous biological information. This allows diverse regulatory relationships from protein-protein interactions, post-translational modifications, to mRNA transcriptional changes and/or sub-cellular localization to be modeled in a unified language.

Networks are commonly constructed from pre-existing literature. Primary literature and review papers provide a valuable resource for identifying (1) the components that regulate a cellular process and (2) the qualitative regulatory relationships among these components. For example, a putative component might be added to a network if a known node in the network of interest alters the activity or expression of the putative network component. This information may be gleaned experimentally by studying the effects of activating mutations or over-expression of a network component. Specifically, if over-expressing the known network component leads to up-regulation or increased activity of the putative network component, it suggests that an activating relationship exists between the two nodes. However, if over-expressing the known node produces down-regulation or decreased activity of the component, then this suggests that an inhibitory relationship exists between the two nodes.

Determining the response of a gene or molecular entity after mutating or over-expressing a regulator of that gene provides genetic evidence for the involvement of the regulator in a signal transduction event. Over-expression vectors, the use of dominant negatives, RNA interference, and genome editing are common genetic manipulations to produce this kind of evidence. Chemical inhibitors may be used to provide pharmacological evidence about the relationship between two nodes. It is important to note that most chemical inhibitors block a specific interaction, whereas many genetic techniques (e.g., over-expression or knockdown) are producing node effects. It should also be noted that chemical inhibitors frequently have off-target effects, possibly affecting other network components, so these inhibitors should be used cautiously when trying to understand their effect on a network. Other evidence that may be used when constructing networks includes enzymatic activity, protein-protein interactions, post-translational modifications (Walhout and Vidal 2001), transcription factor binding (Buck and Lieb 2004), and mRNA transcriptional changes (Wu and Chan 2012). In addition to primary literature, curated databases of signaling pathways may also be of use in building networks (Kanehisa 2013). Software packages exist to aid in the rapid acquisition of model-producing information from databases like Pubmed (de Jong 2002; Chiang and Yu 2003). One such software package, Chilibot, mines Pubmed for causal and parallel relationships between two or more gene or protein names (Chen and Sharp 2004; Margolin et al. 2006). Furthermore, methods have been developed to reverse engineer networks from high throughput expression-type datasets (Margolin et al. 2006; Basso et al. 2005).

Genetic, pharmacological, and biochemical evidence can be represented as component-to-component relationships such as “I activates A” (denoted as I ➞ A) or “B inhibits O” (denoted by B—|O), which correspond to directed edges from an upstream regulator to a downstream target in a graph representing a signaling network (Fig. 5.1a, b). In some situations, experimental evidence leads to double causal inferences such as “X activates the process through which Y activates Z”. In some cases these inferences can be logically broken down to two separate component-to-component relationships. Some experimental evidence however, represents indirect casual relationships that are not easy to interpret. A method has

(a)

Nodes	Causal Relationship
I	I activates A I activates B
A	A activates B A activates O
B	B activates A B activates O
O	

(b)

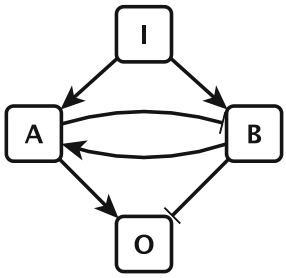

(c)

Nodes	Boolean rule
I	
A	A* = I OR B
B	B* = I AND NOT A
O	O* = A AND NOT B

(d)

Node A		
I*	B*	A*
1	1	1
1	0	1
0	1	1
0	0	0

Node B		
I*	A*	B*
1	1	0
1	0	1
0	1	0
0	0	0

Node O		
A*	B*	O*
1	1	0
1	0	1
0	1	0
0	0	0

Fig. 5.1 A simple signaling network and its Boolean representations. **a** The relationships among the nodes in this hypothetical network. **b** The graphical representation of the network. *Nodes* are in boxes and *edges* connect pairs of nodes. Activating relationships are denoted by *arrows* (➞) and inhibitory edges by *blunt ends* (—|). **c** The Boolean rules representing the network. **d** Truth table representation of the Boolean relationships. *Asterisk* marking a node's name indicates the future state of the node

been developed that uses techniques from combinatorial optimization to find the sparsest network consistent with all experimental observations (Albert et al. 2007). This method was implemented in the software NET-SYNTHESIS (http://www.cs.uic.edu/~dasgupta/network-synthesis). The input to NET-SYNTHESIS is a text file of positive or negative relationships among nodes in the biological network. The software produces a simplified network representation and a text file with the edges of the inferred signaling network (Kachalo et al. 2008).

5.2.2 *Determining the Boolean Functions*

The network representation of a signal transduction process is static, while biological processes happen over time. In order to understand the dynamic behavior of a system, each node needs to be characterized by a state variable that can change in time. Specifically, each node's state variable is determined by the state variable of the nodes that regulate it. This dependency is expressed through a node-specific

Boolean function. This function aggregates the effect of upstream nodes (activation or inhibition) on a regulated node as well as the relationships among the regulators for a given node. A popular way of representing Boolean functions is through the Boolean operators NOT, AND, and OR. The is used to specify inhibitory effects; AND and OR are used to define the relationships among regulators. If node Y has a single activator X, represented by X ➞ Y and rooted in experimental evidence that X leads to activation or up-regulation of Y after a period of time, the state of node Y can be represented by the Boolean function Y* = X. In this representation, the state of the nodes is represented by the node labels and Y* denotes the state of node Y at a future time point. The rule indicates that the future state of node Y will be equal to the current state of node X. Biologically, this means that a high level or activity of X will lead to high level or activity of Y. Nodes can be inhibited by upstream nodes (e.g., X —| Y), indicating that the activation of the target node Y requires a low level or activity of the inhibitory node X. The effect of a single negative regulation is thus represented by the Boolean rule Y* = NOT X. Here the NOT represents logical negation, where NOT ON = OFF and NOT OFF = ON.

Cases of combinatorial regulation can be explored using the hypothetical Boolean relationships in Fig. 5.1c. The Boolean function for the state of node A:

$$A^* = I \text{ OR } B,$$

uses the OR operator to represent that node A can be independently activated by node I or by node B. In general, an OR relationship represents the convergence of two independent and individually effective pathways on a target node. The AND operator is used to represent situations where the synergistic activity of multiple regulators is required to activate the target node. For example, in Fig. 5.1:

$$B^* = I \text{ AND NOT } A$$

indicates that node B will be active (ON) if there is a high level (ON state) of I and low level (OFF state) of A in the cell. Similarly to B, the output O of the hypothetical network is regulated by an activating node A and an inhibitory node B:

$$O^* = A \text{ AND NOT } B$$

O is activated under the condition that A is ON and B is OFF. Under circumstances where more than two regulators exist for a node, the Boolean function can be comprised of a combination of AND, OR, and NOT operators, depending on the biological regulation involved.

Each Boolean function can also be represented by a truth table, which lists all possible future states of a node resulting from all possible states of its regulators. Each row in the truth table lists a combination of values of the Boolean variables of the node's regulators and the associated output value (i.e. future state of the regulated node). "1" represents a node being ON and "0" represents a node being OFF. The truth table of a Boolean function with x regulators has 2^x rows and x + 1

columns. Figure 5.1d shows the truth tables corresponding to the Boolean functions of the four nodes in the network.

Boolean functions are usually determined based on known relationships in the published literature. If a node's Boolean function cannot be unequivocally determined from the literature, then multiple Boolean functions can be created and tested against known biological outcomes. The equation that best recapitulates known network outcomes can then be used. Boolean rule construction could thus yield information about regulatory relationships that were not previously known. For example, if an AND rule between two regulators best recapitulates the known responses for a network, this suggests a putative biological synergy between the two regulators. Lastly, approaches have been developed to produce Boolean networks and functions from high throughput expression data (Chueh and Lu 2012; Laubenbacher and Stigler 2004; Mehra et al. 2004).

5.2.3 *Selecting Time Implementation for State Transitions*

Boolean models and discrete dynamic models in general focus on state transitions instead of following the system in continuous time. Thus, time is an implicit variable in these models. After constructing the static signal transduction network and translating it into a system of Boolean functions, the next step is to choose an algorithm for the time implementation. Time implementation refers to the timing of transitions from one network state to the next. Synchronous models are the simplest update method: all nodes are updated at multiples of a common time step based on the previous state of the system:

$$X_i(t+1) = F_i(X_1(t), X_2(t), \ldots, X_N(t)).$$

Here X_i (t) represents the state of node i at timestep t of a network with N nodes, given by $i = 1, 2, \ldots, N$. The state of node i at a future timestep, X_i $(t + 1)$, is a function of the previous states of the nodes that regulate it. The synchronous model is deterministic in that the sequence of state transitions is definite for identical initial conditions of a model (Dubrova and Teslenko 2011). This update method is valid if the time scales of all signal transduction processes represented as edges of the model are quite similar.

The kinetics of biological reactions and processes has been shown to vary substantially. For example, post-translational modifications like phosphorylation events can occur in thousandths of a second, whereas transcriptional events may take hundreds of seconds (Papin et al. 2005). Thus updating algorithms that account for differences in process timing must be used. In asynchronous models, the nodes are updated individually, depending on the timing information, or lack thereof, of individual biological events. In this section we discuss three asynchronous updating models: the random order asynchronous, general asynchronous, and deterministic asynchronous models.

In a random order asynchronous model, at each time step every node is updated in a random order chosen from all possible node orders with equal probability (Chaves et al. 2005). In this model, the state of node i at the next time step, $t + 1$, is obtained from the most recently updated states of its input nodes:

$$X_i(t+1) = F_i(X_1(\tau_{i1}), \ldots, X_N(\tau_{iN})$$

where $\tau_{ij} \in \{t, t + 1\}$, for any node i and j, where $j = 1, 2, \ldots, N$. If node j is before node i in the randomly chosen update order, then $\tau_{ij} = t + 1$, otherwise, $\tau_{ij} = t$. With this update method each node is updated once in each round of updating.

In the general asynchronous model (Chaves et al. 2005), a single node is randomly updated at each time step. Under this approach, it is possible that a node chosen in the current time step will be chosen in a future time step. The unit of time in the general asynchronous model is $(1/N)$ of the time unit of the random order asynchronous model.

Both random order and general asynchronous models are stochastic, reflecting the variability in the timing of signal transduction events at the population level. If there is a priori knowledge about the relative timescales over which biological processes in the signaling network of interest occur, it can be incorporated as a constraint of the updating scheme. This may also be accomplished through a deterministic asynchronous model. In this model each node i is associated with an intrinsic time unit γ_i and is updated at multiples of that unit, $t_i = k\gamma_i$ (Chaves et al. 2006). At a time $t + 1$, the node i whose $t_i = t + 1$ is updated and all other nodes remain in the same state:

$$X_i(t+1) = \begin{cases} F_i(X_1(t), \ldots, X_N(t)) & \text{if } t+1 = k\gamma_i \quad k = 1, 2, \ldots \\ X_i(t) & \text{otherwise} \end{cases}$$

In the deterministic asynchronous model, nodes with longer time units will have less updates than nodes with shorter time units. This update mode is best suited for cases when the relative frequency or rate of biological events is known or can be estimated from biological knowledge. As this is a deterministic model, there is a guaranteed trajectory for state transitions.

5.2.4 *Evaluating the Dynamics and Steady-States of the System*

Choosing a time implementation for a Boolean model allows one to explore the dynamics of the system; that is, how it changes over time. Initial conditions can be set to represent the initial biological phenotype of the system and any signals or environmental conditions that may cause the system to change over time. By varying the initial conditions, the effect of different initial conditions on an output can be modeled.

Initial conditions for a model can be set based on a priori biological knowledge. For example, in the hypothetical signal transduction network of Fig. 5.1, if we are curious about the effect of the input (signal) I on the output, O, and we know that prior to receiving the signal node A is ON and node B is OFF, we can use the initial conditions I = ON, A = ON, B = OFF, O = OFF, to study the predicted effects by the model. It is also good to compare this system to the case where the signal, I = OFF, to determine the state of O when no signal is present. If the information is not sufficiently specific, multiple initial conditions can be used as starting points of replicate simulations. The percentage of replicate simulations where a node (e.g. the network's output node) is ON can be calculated for each time step, representing the probability that a node will be activated or an outcome will occur given a stimulus. Additionally, patterns for initial conditions that lead to O = ON versus O = OFF can be explored, to determine the conditions that allow the signal to induce the output.

Starting from a plausible initial condition and updating the nodes' states according to the Boolean rules in the model, the system's state will change over time until it reaches a stable outcome called an attractor. An attractor can be a fixed point (steady-state) or a set of states that repeat indefinitely (a complex attractor). The basin of attraction refers to the initial conditions that lead the system to a specific attractor.

There are several software applications to simulate the trajectory of the system from the initial condition to the attractor(s). BooleanNet (http://code.google.com/p/booleannet/) is a Python library that facilitates Boolean simulations of biological regulatory networks. This software requires a text file containing Boolean rules as input, and users can choose from various updating schemes for their models (Albert et al. 2008). BoolNet, SimBoolnet, and ChemChains are other software tools for Boolean modeling (Mussel et al. 2010; Helikar and Rogers 2009; Zheng et al. 2010).

Under the hypothetical circumstance that nothing is known about the initial conditions of the signal transduction network in Fig. 5.1, and that we are curious about the effect an input I on the output node, O, we can set I to ON, randomly set nodes A, and B, and have node O OFF in the initial conditions. Using BooleanNet, we can simulate this using a random order asynchronous model (Albert et al. 2008) and determine the fraction of O = ON in 100 replicate simulations as shown in Fig. 5.2.

Analysis of attractors is important in signaling networks because they represent the long term effect of a signal on an output. The attractors of gene regulatory networks that do not have external signals represent different cell fates. We can analytically find all possible fixed points of a network by recalling that in the fixed point the future state of any node equals its current state. Thus the Boolean update functions become equations. The solutions of these equations are the fixed points of the system. If the system of equations does not have a solution, the model does not have fixed points, just one or several complex attractors. For the four node signaling network illustrated in Fig. 5.1, if we assume I = 0, then the Boolean equations simplify to A = 0 OR B = B, B = 0 AND NOT A = 0, O = A AND NOT B.

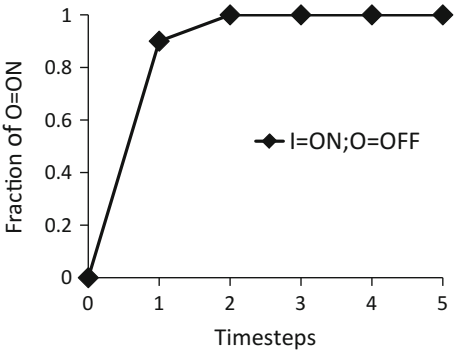

Fig. 5.2 Fraction of simulations where O = ON as a function of time, given I = ON and nodes A and B are randomly set to ON or OFF in the initial condition for the Boolean model given in Fig. 5.1 (100 replicates; random order asynchronous update)

Substituting B = 0 in the first and third equation we find the solution I, A, B, O = 0000. If we substitute this state back into the set of equations, we see the same result; thus 0000 is a fixed point of the system. If we assume I = 1, then A = 1 OR B = 1, B = 1 AND NOT A = NOT A = NOT 1 = 0, and O = 1 AND NOT 0 = 1, thus we get the result 1101. Thus, there are two fixed points, one for each value of the signal. The state of the output node O equals the state of the input node I in each fixed point, which is representative of a response to a signal.

For a Boolean network with N nodes, there are 2^N possible states. In the absence of specific information, each of these states can be considered as an initial state, and the trajectory of the system, starting from this state and ending in one of the attractors, can be determined. A compact representation of all possible trajectories is given by the state transition network. The nodes of this network are the 2^N states of the system, and a directed edge is drawn from state S_1 to state S_2 if applying the Boolean rules to state S_1 transforms it into state S_2 (i.e. there is a state transition from S_1 to S_2). Figure 5.3 illustrates the state transition network for the Boolean network of Fig. 5.1 using synchronous update. The state transition network indicates the two previously found steady-states as nodes that do not have edges that point toward other nodes. It also indicates that all states in which the signal is OFF converge into the 0000 state and all states in which the signal is ON converge into the 1101 state.

Synchronous and asynchronous Boolean models have the same fixed points, because fixed points are independent of the implementation of time. However, the basins of attraction that lead to the fixed points may differ between synchronous and asynchronous models. Synchronous and deterministic asynchronous models have a definite trajectory between states, whereas stochastic asynchronous models may have multiple trajectories depending on the specific update sequence chosen. Specifically, each state can have up to N successors when following a general asynchronous update, as any of the nodes of the system could be updated. In random order update, each state can have up to $N!$ successors. Thus, initial conditions that lead to a single attractor in deterministic models may enter multiple attractors in asynchronous models. Lastly, certain complex attractors may disappear when switching from synchronous to stochastic asynchronous models. This is

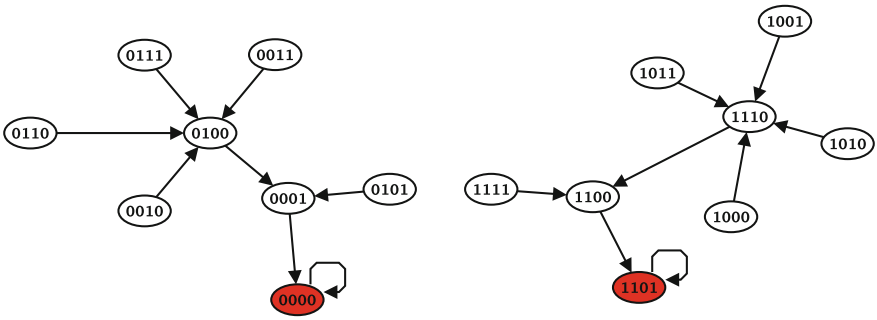

Fig. 5.3 The state transition network of the four node network given in Fig. 5.1 obtained using the synchronous update method. *Each symbol* represents a network state. The binary sequence in each symbol, from *left* to *right*, represents the state of node I, A, B, and O in the network. There are two attractors, both of which are fixed points: 0000 and 1101. Both states only have incoming edges and a self-loop. Fixed points 0000 and 1101 both have seven states in their basins of attraction

because those attractors (called limit cycles) depend on multiple nodes changing states at the same time (Harvey and Bossomaier 1997).

As an illustration, Fig. 5.4 indicates the random order asynchronous state transition network of the system in Fig. 5.1. As expected, the fixed points of the system are the same as in Fig. 5.3. In this case the basins of attraction of the steady-states remain the same as well, because they are determined by the state of the input node.

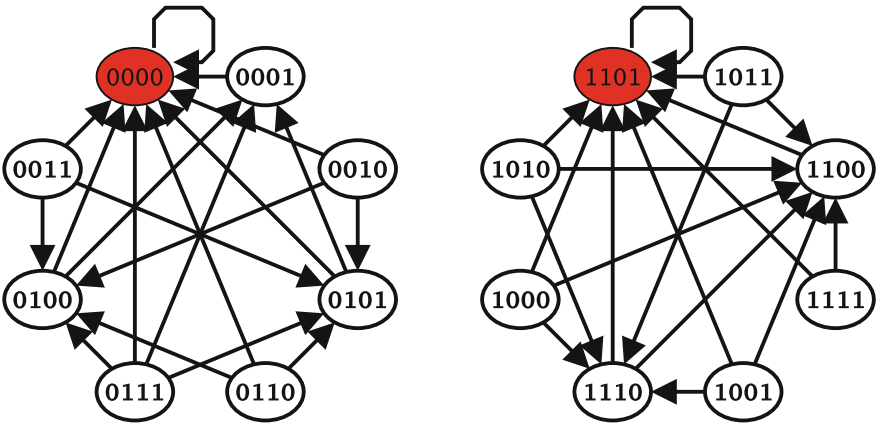

Fig. 5.4 The state transition network of the four node network given in Fig. 5.1 obtained using a random order asynchronous updating scheme. Each symbol represents a network state. The binary sequence in *each symbol*, from *left* to *right*, represents the state of node I, A, B, and O in the network. The two fixed points (steady-states) produced using the synchronous updating algorithm are conserved in the asynchronous model. Their basins of attraction are the same as well; however, many of the states have multiple trajectories to the corresponding steady-state (e.g., 1011 has four trajectories to 1101)

Multiple trajectories from a single initial condition may exist in Fig. 5.4, as this updating scheme is non-deterministic. State transition networks for both updating schemes are implemented in BooleanNet (Albert et al. 2008).

5.2.5 Network Reduction Techniques

In large Boolean networks, it is computationally unfeasible to map the network's state space (Zhao 2005). Methods have been developed to reduce the size of networks to make them easier to handle algorithmically, while maintaining the attractor repertoire of the larger network. Two methods have been developed that search for "frozen nodes," which are nodes that stay constant regardless of the initial condition. Because these nodes do not change, they are irrelevant for differentiating attractors and thus can be removed from attractor and state space analyses (Bilke and Sjunnesson 2002; Richardson 2005). Two other computational methods iteratively remove non-auto-regulatory components (i.e. nodes without a self-loop). These methods have been proven to conserve fixed points but may produce complex attractors that do not exist in the larger network (Naldi et al. 2011; Veliz-Cuba 2011). Another reduction method involves a two-step process, which identifies nodes which stabilize due to the presence of a sustained signal, followed by removing simple mediators (nodes with a single incoming and outgoing edge) (Saadatpour et al. 2010). Lastly, a network reduction approach has been developed that identifies (possibly nested) feedback loops that have a defined steady-state associated with them, then uses this steady-state to simplify the network as in Saadatpour et al. (Zanudo and Albert 2013).

5.2.6 Testing the Validity of the Dynamic Model

Discrete dynamic models are constructed to understand the dynamics of biological systems, or how a biological system might change or respond to a stimulus or signal. In order to explore unknown features of biological systems, it is first important to assess whether the model reproduces known features of the system being studied. In order to do this, one needs to study the long-term behaviors (e.g., steady-states) of the system, as well as the intermediate states leading to them. If there is a baseline, unstimulated, or signal-free state in the system, it is important to determine whether that state exists in the dynamic model as a steady-state. If the baseline condition does not exist, or is transient, the cause is probably an error in the Boolean logic (for example the use of OR instead of AND) or the incompleteness of the model.

Once a baseline condition is reproduced, it is important to check whether the model recapitulates a known relative order of events after a stimulus. If it does not, the erroneous state changes can be traced back and errors in the Boolean logic or

incompleteness of the model may be discovered. It is also important to determine whether a biologically realistic steady-state exists. If in addition to a biologically realistic steady-state the model also indicates another steady-state that has never been realized biologically before, the new steady-state should not necessarily be discounted. It is possible that this steady-state could represent a previously undiscovered biological outcome for the system. In these circumstances, the initial conditions and intermediate states that lead to this novel steady-state can be explored and their biological feasibility can be determined.

5.2.7 Introducing Model Perturbations

Discrete dynamic models allow for the exploration of the effect of network perturbations on the dynamics of the biological system. Perturbations are the network equivalent of a deviation from biological homeostasis. Essentially all diseases are a deviation from a homeostatic or "normal" state. These perturbations may be the direct result of single or multiple mutations (e.g., cancer or genetic diseases). Other causes of biological perturbations include environmental influences like pharmacological use and abuse or traumatic injury. Certain environmental cues may cause genetic aberrations, so these modes of biological perturbations are not mutually exclusive. Discrete dynamic models can also be used to model the effect of pharmacological interventions, in the presence of no, single or multiple genomic abnormalities, and how these effects percolate through a network to produce a biological phenotype.

There are several ways to study the effect of perturbations on biological networks. Biological over-expression or over-activity of a node can be modeled by keeping its state as ON irrespective of its regulators. Biological knockouts or down-regulation of a node can be modeled by keeping the state of a node as OFF, irrespective of the state of its regulators. The effect of these perturbations can be determined by performing simulations or state space analysis in their presence, and comparing perturbed outcomes to their normal states. Drug or growth factor treatments can be simulated by inhibiting or activating certain nodes transiently (setting the node state and allowing it to update based on its biological regulation) or permanently (over-riding the existing rules). BooleanNet has built-in functions to facilitate network perturbations in Boolean models (Albert et al. 2008).

Perturbations to discrete dynamic models can facilitate the efforts of systems pharmacology by facilitating the development of personalized networks representing individuals in disease. We can model the effect of drugs in the presence of individual network differences (i.e. individual genetic differences) and can predict the effect of pharmacological intervention in specific individuals. Discrete dynamic models can be used in these ways to choose pharmacological interventions that will work for specific patients and to avoid treatments that would have no benefit.

5.2.8 *Non-boolean Discrete Dynamic Modeling (Multi-state Discrete Models)*

Until this point we have discussed the simplest kind of discrete dynamic model, the Boolean model. Multi-state discrete dynamic models can also be constructed to analyze biological systems and in certain cases may be more appropriate than Boolean models. As with Boolean models, truth tables can be constructed to represent the regulatory relationships among nodes. For example, in a three-state model, nodes can be assigned three states (e.g., −1, 0, 1 or 0, 1, 2) to represent under-activity (down-regulation), normal activity, and over-activity (up-regulation). The value of a regulated node will depend on the logical constraints designated by the modeler in the truth tables.

There are alternative mathematical formalisms for a more compact representation of multi-state discrete models: logical models (Thomas 1991), implemented in the software GINsim (Naldi et al. 2009) and polynomial dynamical systems (Veliz-Cuba et al. 2010) implemented in the software ADAM (Hinkelmann et al. 2011). The logical functions used in the logical model framework specify the conditions for which the regulated node's state is different from the baseline (Thomas 1991). Polynomial dynamical systems represent each truth table by a polynomial function. Polynomial algebra can then be used to identify the steady states of the model. One disadvantage of this method is that the polynomial representation (even for Boolean models) is less intuitive than other forms, e.g., logical models (Veliz-Cuba et al. 2010).

5.3 A Discrete Dynamic Model of Tumor Response to an EGFR Inhibitor

Previously an enhanced pharmacodynamic (ePD) model was constructed by Iyengar et al. to model the effects of an EGFR inhibitor (e.g., gefitinib) on $EGFR^{+}$ tumor growth (Iyengar et al. 2012). This model was novel because it merged traditional PK/PD models, which focus on the site of drug action (EGFR protein) with ordinary differential equation models of signaling events downstream. This is important, essentially encapsulating the goals of systems pharmacology, because many factors beyond the direct effect of the drug on the receptor contribute to the effect of a drug in treating disease. As with other differential equation based models, the EGFR model used a large number of parameters, whose value was estimated based on experiments reported in the literature. The model demonstrated that three genes (*RASAL1*, *PEBP1*, and *miR221*), all of which are downstream of the site of drug action (EGFR), affect whether a tumor responds to gefitinib treatment. The model also quantified how sensitive a tumor is to gefitinib; whether the tumor was resistant, went into a partial remission, or complete remission (Iyengar et al. 2012). As an illustration, we translate this ePD model of EGFR inhibition into two types of

discrete dynamic models: (1) a Boolean model and (2) a three-state discrete model. Furthermore, we demonstrate the efficacy of discrete models at reproducing the results obtained from the ePD model.

5.3.1 A Boolean Model of EGFR Inhibition on Tumor Growth

The ePD model represents the EGFR signaling pathway as a linear pathway augmented with a feed-forward motif from EGFR to Raf1 (Fig. 5.5a). Active EGFR signaling leads to the induction of proliferation (output node). Tumor cell proliferation regulates tumor growth and thus tumor size. Since we have the network structure, we can move on to creating Boolean rules for each node in the network. Most rules are simple to determine: nodes with a single input (regulator) can be represented as Node* = Regulator. For example, from Fig. 5.5a, the rule for Pkc is the following: Pkc* = Plcγ. There are three nodes with multiple regulators, Kras, Raf1, and Cdk4/6. As discussed in Sect. 5.2.2, most biological regulators act independently of one another and can be combined by an OR rule; however, it is important to understand the biology behind the network and to determine if synergistic relationships exist between regulators of the same node (AND rule). In the case of the well-studied EGFR signaling network, the only evidence of biological synergy occurs for the Cdk4/6 node, indicating that p27kip binds to CyclinD and prevents its interaction with Cdk4, inhibiting cell proliferation (Polyak et al. 1994). Thus, Cdk4/6* = CyclinD AND NOT P27kip (Fig. 5.5a).

Using the reduction of simple mediator nodes as described in Sect. 5.2.5 and previously (Saadatpour et al. 2010), we reduced this network to an equivalent 7 node and 7 edge network by collapsing nodes with an in-degree and out-degree of 1 (Fig. 5.5b). For example, EGFR ➡ Plcy ➡ Pkc —|Rkip was collapsed to EGFR —|Rkip. We subsequently substituted upstream regulators into rules for downstream nodes. For example, Rkip* = NOT EGFR would be produced from collapsing the previously described rules. Using these methods, we constructed a set of Boolean equations for the reduced EGFR network (Table 5.1).

In the ePD model of an EGFR inhibitor, perturbations in three different gene products were the focus. RasGAP and miR221 were assumed to have three states: over-active, normal, and under-active. Rkip was assumed to have two states: normal and over-active (see Table 5.2). In the ePD model, combinations of these mutations were integrated with the effect of an EGFR inhibitor to explore individual patient response to treatment. As examples, R−, K0, M+ patients were predicted to have EGFR inhibitor resistant tumors, R0, K+, M− led to tumors that are EGFR inhibitor sensitive (full remission), and R0, K0, M0 tumors were predicted to lead to a partial remission phenotype.

In order to test the fidelity of our Boolean model at reproducing these results, we have to make some assumptions and simplifications. The ePD model had three possible states for Rasgap and miR221 (e.g., R−, R0, and R+ for Rasgap) and also

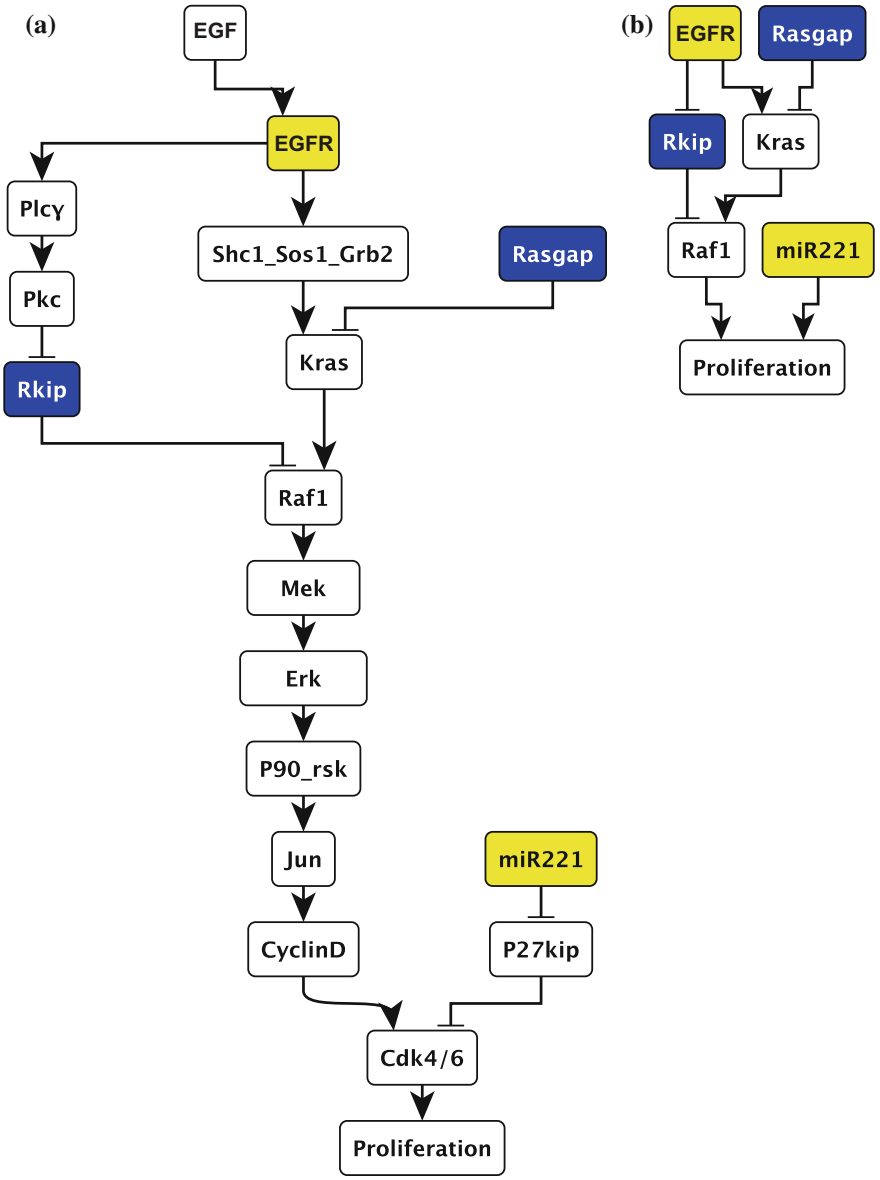

Fig. 5.5 The EGFR signaling network used to model EGFR inhibitor therapeutics. **a** This model contains 18 nodes including three source (unregulated) nodes, and 18 edges. Nodes with mutational changes to be modeled are *colored*. Nodes that under normal circumstances inhibit EGFR signaling and proliferation have a dark background and nodes that induce EGFR signaling and cell proliferation have a light background. **b** A reduced network was produced by collapsing simple mediator nodes (nodes with one upstream regulator and one downstream target, see Sect. 5.2.5). This led to a network with 7 nodes and 7 edges

Table 5.1 Boolean rules for the reduced (7 node) EGFR network

Rkip* = NOT EGFR
Kras* = EGFR OR NOT Rasgap
Raf1* = Kras OR NOT Rkip
Proliferation* = Raf1 AND miR221

Table 5.2 Genes and perturbations modeled in the EGFR ePD model

Gene	Symbol: perturbation	Normal function	Effect on tumor growth (proliferation)
RASAL1 (Rasgap)	R−: hypermethylation	Suppresses Ras signaling (catalyzes Ras-GTP to Ras-GDP)	Suppresses tumor growth by inhibiting MAPK signaling (Ras)
	R0: normal		
	R+: hypomethylation		
PEBP1 (Rkip)	K0: responsive to PKC	Rkip inhibits Raf (MAPK signaling). Pkc inhibits Rkip	Suppresses tumor growth by inhibiting MAPK signaling (Raf)
	K+: non-responsive to PKC		
miR221	M−: decreased miR221	*miR221* suppresses p27. p27 suppresses CDK4	*miR221* induces tumor growth
	M0: normal miR221		
	M+: increased miR221		

three possible model outputs: resistant, partial remission, and full remission; however, Boolean models can only handle two states. Let us first make the assumption that there are two model outputs: proliferation and no proliferation, which correspond to resistance to EGFR inhibitor treatment and remission (response to EGFR inhibitor treatment), respectively. Now we have to determine how to handle the Rkip and Rasgap states. In order for the model to reproduce tumor cell proliferation when EGFR signaling is active (EGFR = ON) in the absence of EGFR inhibitor and no mutations, normal miR221 needs to correspond to the ON state, and thus decreased miR221 is the OFF state. The increased miR221 level cannot be distinguished from the normal level in a Boolean model so M0 = M+ = ON. If we assume that the normal Rasgap state (R0) is closer to the R+ state; that is, that under normal circumstances, Rasgap suppresses EGFR signaling and tumor cell proliferation, then we can say R0 = R+ = ON.

Using the above assumptions for converting node perturbations for Rasgap (R0 = R+ = ON) and miR221 (M0 = M+ = ON), we can determine the steady-state of the Proliferation node for a Boolean model for each tumor genotype by substituting these values into the Boolean equations or by using BooleanNet. We can then compare with the results of the ePD model by making a correspondence between proliferation and a resistant tumor, and between the absence of proliferation and full remission (Table 5.3).

The agreement between the ePD and Boolean model of an EGFR inhibitor is quite strong. We see that 100 % (4 out of 4) of the tumors that are resistant in the

ePD model undergo proliferation in the Boolean model and that 67 % (4 out of 6) of tumors that achieve full remission in the ePD model undergo no proliferation in the Boolean model. Interestingly, even though there is no partial remission category in the Boolean model, it seems that the Boolean model stratifies into proliferation versus no proliferation groups right in the middle of the partial remission category. Assuming that the Boolean model is correct if it attains the proliferation outcome to the left of this mark and the no proliferation outcome to the right of this mark, then the model correctly predicts the ePD outcomes in 83 % of the cases.

5.3.2 *A Multi-state Discrete Model of EGFR Inhibition on Tumor Growth*

The ePD model of EGFR inhibition has some non-Boolean discrete properties:

1. The model output was classified into three discrete categories: resistant, partial remission, or complete remission, depending on the tumor size (Table 5.3).
2. Rasgap and Rkip have three states: under-active, normal, and over-active (Table 5.2).

Therefore, a multi-state discrete model may better reproduce the results of this model. Because the model output was assigned three categories: resistant, partial remission, or complete remission, we can assign the "Proliferation" node the same three states: −1 (remission), 0 (partial remission), and 1 (resistant). Similarly, the states of Rasgap and miR221 could be assigned three states depending on activity: −1 (under-active), 0 (normal), and 1 (over-active). The states of EGFR and Rkip can remain as Boolean (two-state) variables.

We configure the truth tables so that they preserve or refine the Boolean relationships indicated on Table 5.1. For example, the Boolean rule for Kras indicates that the presence of EGFR or the absence (OFF state) of Rasgap can lead to the activation of Kras. The refined truth table will have three states for Rasgap and Kras. We assume that the presence of EGFR combined with a low or intermediate state of Rasgap leads to a high activity (state 1) of Kras, as does the under-activity (state −1) or Rasgap. We assume that the absence of EGFR combined with over-activity of Rasgap leads to low activity (state −1) of Kras. The remaining two conditions are assumed to lead to an intermediate Kras activity (see Fig. 5.6). The resulting model recapitulates all but two findings of the ePD model, or almost 89 % of ePD model findings (Table 5.3). In fact, the R0, K+, M+ case is on the border between the partial and complete remission categories and would be consistent if a slight change were made in the tumor mass threshold between these two categories. Furthermore, we can stratify our results into three categorical outcomes instead of just two in the Boolean model, which is substantially more informative. Lack of intermediate categories like "partial remission" is one of the major limitations of Boolean models. Using multi-state models, intermediate states can be recapitulated.

Table 5.3 Comparison of the outcomes of the ePD model and of the Boolean model for the effect of an EGFR inhibitor on tumors with specific genome profiles

ePD model outcomes (tumor size)	Resistant (2–4.5 g)				Partial remission (0.1–2 g)						Full remission (<0.1 g)							
Tumor genotypes	R−	R−	R−	R0	R−	R−	R0	R−	R0	R0	R0	R0	R+	R+	R+	R+	R+	R+
	K0	K0	K+	K0	K+	K0	K0	K+	K0	K+	K+	K+	K0	K0	K0	K+	K+	K+
	M+	M0	M+	M+	M0	M−	M0	M−	M−	M+	M0	M−	M+	M0	M−	M+	M0	M−
Proliferation status in the Boolean model	1	1	1	1	1	**0**	1	0	0	0	0	0	**1**	**1**	0	0	0	0
Proliferation status in the three-state model	1	**0**	1	1	0	0	0	0	0	**−1**	−1	−1	−1	−1	−1	−1	−1	−1

Cells with bold values indicate disagreement with ePD model

EGFR	Rkip*
0	1
1	0

EGFR	Rasgap	Kras*
0	-1	0
0	0	1
0	1	1
1	-1	-1
1	0	0
1	1	1

EGFR	Rasgap	Kras*
0	-1	1
0	0	0
0	1	-1
0	1	-1
1	-1	1
1	0	1
1	1	0

Raf1	*miR221*	Proliferation*
-1	-1	-1
-1	0	-1
-1	1	-1
0	-1	-1
0	0	-1
0	1	-1
1	-1	0
1	0	0
1	1	1

Fig. 5.6 Truth tables for the multi-state discrete model of EGFR inhibition on tumor growth. The EGFR and Rkip nodes have two states. Rasgap, Kras, Raf1, miR221, and Proliferation have three states. *Asterisk* marking a node's name indicates the future state of the node

5.4 Conclusions

Very frequently the kinetic details of biological processes are not known because they are very difficult to measure experimentally. Discrete dynamic modeling is formidable in the absence of such details. As an example of how discrete dynamic modeling can be used in systems pharmacology, we translated a pre-existing ePD model of an EGFR inhibitor and its effect on tumor growth in the context of various tumor mutations. The results demonstrated that even in the absence of the rigorous experimental detail (e.g., kinetics and concentration information) that was required to create the ePD model, our discrete dynamic model was able to recapitulate almost 90 % of the ePD model results. This is a testament to not only the utility of discrete models but the importance of the structure of a biological network over the kinetic details of the individual processes in determining network function.

In the post-genomic era, we have largely realized that there are major genomic differences among humans, and that these individual differences are likely very important contributors to disease and disease susceptibility. The major issue now is how we use this information to make smarter decisions about who we treat and how we treat them. Systems pharmacology offers a framework to approach these issues. Discrete dynamic modeling is a critical means to understand the network effects of a drug, how and why it might work in the context of differences in individual networks, and which drugs might work best in different individuals. The era of personalized medicine is upon us. Discrete dynamic modeling is and will continue to be a powerful tool to systems pharmacology and personalized medicine in this new age of pharmaceutical intervention.

Acknowledgments This work was partially supported by grants NIH Ruth L. Kirschstein National Research Service Award (F30 DK093234) and NSF PHY-1205840.

References

Albert I, Thakar J, Li S, Zhang R, Albert R (2008) Boolean network simulations for life scientists. Source Code Biol Med 3:16. doi:10.1186/1751-0473-3-16

Albert R, DasGupta B, Dondi R, Kachalo S, Sontag E, Zelikovsky A, Westbrooks K (2007) A novel method for signal transduction network inference from indirect experimental evidence. J Comput Biol 14(7):927–949. doi:10.1089/cmb.2007.0015

Albert R, Othmer HG (2003) The topology of the regulatory interactions predicts the expression pattern of the segment polarity genes in Drosophila melanogaster. J Theor Biol 223(1):1–18. doi:10.1016/S0022-5193(03)00035-3

Albert R, Wang RS (2009) Discrete dynamic modeling of cellular signaling networks. Meth Enzymol 467:281–306. doi:10.1016/S0076-6879(09)67011-7

Basso K, Margolin AA, Stolovitzky G, Klein U, Dalla-Favera R, Califano A (2005) Reverse engineering of regulatory networks in human B cells. Nat Genet 37(4):382–390. doi:10.1038/ng1532

Bilke S, Sjunnesson F (2002) Stability of the Kauffman model. Phys Rev E Stat Nonlinear Soft Matter Phys 65(1 Pt 2):016129

Buck MJ, Lieb JD (2004) ChIP-chip: considerations for the design, analysis, and application of genome-wide chromatin immunoprecipitation experiments. Genomics 83(3):349–360

Chaves M, Albert R, Sontag ED (2005) Robustness and fragility of Boolean models for genetic regulatory networks. J Theor Biol 235(3):431–449. doi:10.1016/j.jtbi.2005.01.023

Chaves M, Sontag ED, Albert R (2006) Methods of robustness analysis for Boolean models of gene control networks. Syst Biol (Stevenage) 153(4):154–167

Chen H, Sharp BM (2004) Content-rich biological network constructed by mining PubMed abstracts. BMC Bioinform 5:147. doi:10.1186/1471-2105-5-147

Chiang JH, Yu HC (2003) MeKE: discovering the functions of gene products from biomedical literature via sentence alignment. Bioinformatics 19(11):1417–1422

Chueh TH, Lu HH (2012) Inference of biological pathway from gene expression profiles by time delay boolean networks. PLoS ONE 7(8):e42095. doi:10.1371/journal.pone.0042095

de Jong H (2002) Modeling and simulation of genetic regulatory systems: a literature review. J Comput Biol 9(1):67–103. doi:10.1089/10665270252833208

Dubrova E, Teslenko M (2011) A SAT-based algorithm for finding attractors in synchronous Boolean networks. IEEE/ACM Trans Comput Biol Bioinf/IEEE ACM 8(5):1393–1399. doi:10.1109/TCBB.2010.20

Gross L (2006) When evidence is scant, mathematical modeling offers a roadmap for discovery. PLoS Biol 4(10):e323. doi:10.1371/journal.pbio.0040323

Harvey I, Bossomaier T (1997) Time out of joint: attractors in asynchronous random Boolean networks. Paper presented at the Proceedings of the fourth European conference on artificial life (ECAL97)

Helikar T, Rogers JA (2009) ChemChains: a platform for simulation and analysis of biochemical networks aimed to laboratory scientists. BMC Syst Biol 3:58. doi:10.1186/1752-0509-3-58

Hinkelmann F, Brandon M, Guang B, McNeill R, Blekherman G, Veliz-Cuba A, Laubenbacher R (2011) ADAM: analysis of discrete models of biological systems using computer algebra. BMC Bioinform 12:295. doi:10.1186/1471-2105-12-295

Iyengar R, Zhao S, Chung SW, Mager DE, Gallo JM (2012) Merging systems biology with pharmacodynamics. Sci Transl Med 4(126):126–127. doi:10.1126/scitranslmed.3003563

Kachalo S, Zhang R, Sontag E, Albert R, DasGupta B (2008) NET-SYNTHESIS: a software for synthesis, inference and simplification of signal transduction networks. Bioinformatics 24 (2):293–295. doi:10.1093/bioinformatics/btm571

Kanehisa M (2013) Molecular network analysis of diseases and drugs in KEGG. Meth Mol Biol 939:263–275. doi:10.1007/978-1-62703-107-3_17

Laubenbacher R, Stigler B (2004) A computational algebra approach to the reverse engineering of gene regulatory networks. J Theor Biol 229(4):523–537. doi:10.1016/j.jtbi.2004.04.037

Margolin AA, Wang K, Lim WK, Kustagi M, Nemenman I, Califano A (2006) Reverse engineering cellular networks. Nat Protoc 1(2):662–671. doi:10.1038/nprot.2006.106

Mehra S, Hu WS, Karypis G (2004) A Boolean algorithm for reconstructing the structure of regulatory networks. Metab Eng 6(4):326–339. doi:10.1016/j.ymben.2004.05.002

Mussel C, Hopfensitz M, Kestler HA (2010) BoolNet–an R package for generation, reconstruction and analysis of Boolean networks. Bioinformatics 26(10):1378–1380. doi:10.1093/bioinformatics/btq124

Naldi A, Berenguier D, Faure A, Lopez F, Thieffry D, Chaouiya C (2009) Logical modelling of regulatory networks with GINsim 2.3. Bio Syst 97(2):134–139. doi:10.1016/j.biosystems.2009.04.008

Naldi A, Remy E, Thieffry D, Chaouiya C (2011) Dynamically consistent reduction of logical regulatory graphs. Theoret Comput Sci 412:2207–2218

Papin JA, Hunter T, Palsson BO, Subramaniam S (2005) Reconstruction of cellular signalling networks and analysis of their properties. Nat Rev Mol Cell Biol 6(2):99–111. doi:10.1038/nrm1570

Polyak K, Lee MH, Erdjument-Bromage H, Koff A, Roberts JM, Tempst P, Massague J (1994) Cloning of p27Kip1, a cyclin-dependent kinase inhibitor and a potential mediator of extracellular antimitogenic signals. Cell 78(1):59–66

Richardson KA (2005) Simplifying Boolean networks. Adv Complex Syst 8(4):365–381

Saadatpour A, Albert I, Albert R (2010) Attractor analysis of asynchronous Boolean models of signal transduction networks. J Theor Biol 266(4):641–656. doi:10.1016/j.jtbi.2010.07.022

Saadatpour A, Albert R (2012) Boolean modeling of biological regulatory networks: a methodology tutorial. Methods. doi:10.1016/j.ymeth.2012.10.012

Sorger PK, Allerheiligen S, Abernethy DR, Altman RB, Brouwer KR, Califano A, D'Argenio DZ, Iyengar R, Jusko WJ, Lalonde R, Lauffenburger DA, Shoichet B, Stevens JL, Subramaniam S, Van der Graaf P, Vicini P (2011) Quantitative and systems pharmacology in the post-genomic era: new approaches to discovering drugs and understanding therapeutic mechanisms. An NIH white paper by the QSP Workshop Group

Telesford QK, Simpson SL, Burdette JH, Hayasaka S, Laurienti PJ (2011) The brain as a complex system: using network science as a tool for understanding the brain. Brain Connectivity 1 (4):295–308. doi:10.1089/brain.2011.0055

Thakar J, Pilione M, Kirimanjeswara G, Harvill ET, Albert R (2007) Modeling systems-level regulation of host immune responses. PLoS Comput Biol 3(6):e109. doi:10.1371/journal.pcbi.0030109

Thomas R (1991) Regulatory networks seen as asynchronous automata: a logical description. J Theor Biol 153(1):1–23. doi:10.1016/S0022-5193(05)80350-9

Veliz-Cuba A (2011) Reduction of Boolean network models. J Theor Biol 289:167–172. doi:10.1016/j.jtbi.2011.08.042

Veliz-Cuba A, Jarrah AS, Laubenbacher R (2010) Polynomial algebra of discrete models in systems biology. Bioinformatics 26(13):1637–1643. doi:10.1093/bioinformatics/btq240

Walhout AJ, Vidal M (2001) High-throughput yeast two-hybrid assays for large-scale protein interaction mapping. Methods 24(3):297–306. doi:10.1006/meth.2001.1190

Walsh ER, Thakar J, Stokes K, Huang F, Albert R, August A (2011) Computational and experimental analysis reveals a requirement for eosinophil-derived IL-13 for the development of allergic airway responses in C57BL/6 mice. J Immunol 186(5):2936–2949. doi:10.4049/jimmunol.1001148

Wang RS, Saadatpour A, Albert R (2012) Boolean modeling in systems biology: an overview of methodology and applications. Phys Biol 9(5):055001. doi:10.1088/1478-3975/9/5/055001

Wu M, Chan C (2012) Learning transcriptional regulation on a genome scale: a theoretical analysis based on gene expression data. Brief Bioinform 13(2):150–161. doi:10.1093/bib/bbr029

Zanudo JG, Albert R (2013) An effective network reduction approach to find the dynamical repertoire of discrete dynamic networks. Chaos 23(2):025111. doi:10.1063/1.4809777

Zhang R, Shah MV, Yang J, Nyland SB, Liu X, Yun JK, Albert R, Loughran TP Jr (2008) Network model of survival signaling in large granular lymphocyte leukemia. Proc Natl Acad Sci USA 105(42):16308–16313. doi:10.1073/pnas.0806447105

Zhao Q (2005) A remark on "scalar equations for synchronous Boolean networks with biological applications" by C. Farrow, J. Heidel, J. Maloney, and J. Rogers. IEEE Trans Neural Netw 16 (6):1715–1716. doi:10.1109/TNN.2005.857944

Zheng J, Zhang D, Przytycki PF, Zielinski R, Capala J, Przytycka TM (2010) SimBoolNet—a Cytoscape plugin for dynamic simulation of signaling networks. Bioinformatics 26(1):141–142. doi:10.1093/bioinformatics/btp617

Chapter 6
Kinetic Models of Biochemical Signaling Networks

Mehdi Bouhaddou and Marc R. Birtwistle

Abstract Kinetic models of biochemical signaling networks are a mechanistic description of pharmacodynamics, and thus are potentially well-poised to fill gaps in the drug development pipeline by: (i) allowing putative drugs to be tested via simulations for efficacy and safety before expensive experiments and failed clinical trials; (ii) providing a framework for personalized and precision medicine that incorporates genomic information into a prediction of drug action in an individual; and (iii) interfacing with traditional pharmacokinetic models to yield computable yet mechanistic simulations that can inform drug dosing and frequency. However, biochemical signaling networks are currently incompletely understood on a basic level and are extremely complex compared to traditional applications of kinetic modeling. Herein, we describe current methods used to build such models and highlight strengths and weaknesses of the various approaches, as well as identify areas that need more research to drive the field towards influencing these important potential applications.

Keywords Crosstalk · Input signal · Feedforward · Feedback · Perturbations · Enhanced pharmacodynamic (ePD) models · Occam's razor · Reaction rate laws · Michaelis-Menten equations · Microdomains · Parameter values · Ordinary differential equation (ODE) · Stoichiometries

Electronic supplementary material The online version of this article (doi:10.1007/978-3-319-44534-2_6) contains supplementary material, which is available to authorized users.

M. Bouhaddou · M.R. Birtwistle (✉)
Department of Pharmacology and Systems Therapeutics, Icahn School of Medicine at Mount Sinai, One Gustave L. Levy Place, Box 1603, New York, NY 10029, USA
e-mail: marc.birtwistle@mssm.edu

D.E. Mager and H.H.C. Kimko (eds.), *Systems Pharmacology and Pharmacodynamics*, AAPS Advances in the Pharmaceutical Sciences Series 23,
DOI 10.1007/978-3-319-44534-2_6

6.1 Introduction

Kinetic models are those that represent the dynamics of a system in response to perturbation, and are almost ubiquitously quantitative. This chapter focuses on how one builds a quantitative kinetic model to describe the coupled chemical reactions that together dictate how cells respond dynamically to a perturbation, such as treatment with a drug. These collections of coupled chemical reactions are often called biochemical signaling networks, or signal transduction networks. The word network should be stressed, because although the historic notion of linear signaling pathways has allowed us to understand basic routes of biochemical signaling, it is becoming clear that signaling pathways in cells rarely operate linearly in isolation, but rather are highly interconnected with feedforward and feedback loops and exhibit significant crosstalk (Kholodenko et al. 2010).

Why should one care about kinetic models of biochemical signaling networks? They are useful, if not essential tools in understanding and predicting how perturbations to biochemical signaling networks influence cell behavior. The validity of this assertion is not clear if one still views signaling in terms of linear pathways without feedforward and feedback loops or crosstalk. However, when one embraces these ubiquitous features of signaling systems, the importance of kinetic models as a tool to predict quantitative signaling behavior becomes lucent. As a simple example, consider the simple biochemical network shown in Fig. 6.1, where an input signal S is controllable and activation of D leads to a cell fate. In this simple yet common "incoherent feedforward loop" network, the input signal S leads to activation of A and C, but A activates D while C represses D. What will the cell fate be if S is increased? If the levels of C were high, then increasing S would decrease D, and if they were low, the opposite. Further compounding this seemingly simple question are the spatiotemporal dynamics of A and C activation. If A is localized with D but C is not, then D would go up, but if C is localized with D and A is not, the opposite. Moreover, if C affects D more quickly than does A, D would go down then up, and if C affects D more slowly than does A, vice versa. Thus, even in this idealized example, *quantitative knowledge of network spatiotemporal dynamics is needed to predict cell fate*. Qualitative knowledge for maps such as those in Fig. 6.1 is currently abundant, but the quantitative knowledge needed to predict behavior in response to perturbations is scarce. This quantitative predictability problem is amplified by the overwhelming complexity of real biochemical networks, in which a large number of species are interconnected by a multitude of feedforward and feedback regulatory motifs. Kinetic models of biochemical signaling networks have properties that are suitable for dealing with these types of problems.

This kind of quantitative understanding of signaling dynamics is at the heart of much current signal transduction research. If one understands the relationship between biochemical network behavior and cell fate, it becomes possible to answer a related but critically important question: how can one manipulate a biochemical network to control cell fate? The ability to answer this second question has seemingly countless potential applications. For instance, understanding how to

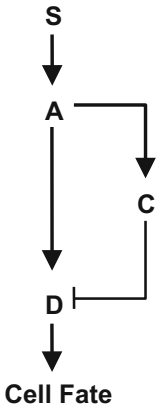

Fig. 6.1 A simple incoherent feedforward motif

make stem cells migrate, differentiate, and proliferate as needed could potentially lead to cures for several hitherto untreatable diseases, and understanding how to perturb deregulated signaling networks in cancer cells such that they cease proliferation and migration could lead to novel cancer treatments. Improving the efficiency of the drug development pipeline is critical as the cost of drug development rises while success rates fall (Birtwistle et al. 2013; Returns on R&D investments continue to fall 2014), and the ability of kinetic models to predict the effects of putative new drugs or drug combinations, both for efficacy and toxicity, can place a meaningful computational layer into the pharmaceutical drug development pipeline that can help prevent costly failed clinical trials (Schoeberl et al. 2009). Moreover, if the model is grounded in biochemical mechanisms, as we advocate for in this chapter, then adapting the model to different patients based on their particular genomic characteristics may be straightforward. In this regard, kinetic models of biochemical signaling networks have been referred to as enhanced pharmacodynamic (ePD) models (Iyengar et al. 2012). The ability of ePD models to cleanly interface with traditional pharmacokinetic models can also help inform drug dosing and scheduling (Zhang et al. 2014). These potential applications poise kinetic modeling of biochemical signaling pathways to have significant impact in the developing disciplines of systems and personalized pharmacology.

6.2 Building Kinetic Models of Biochemical Signaling Networks

Figure 6.2 illustrates the general process that one would follow to develop a kinetic model of a biochemical signaling network. It begins with a question or problem-of-interest, and ends with a validated model that describes the relevant system

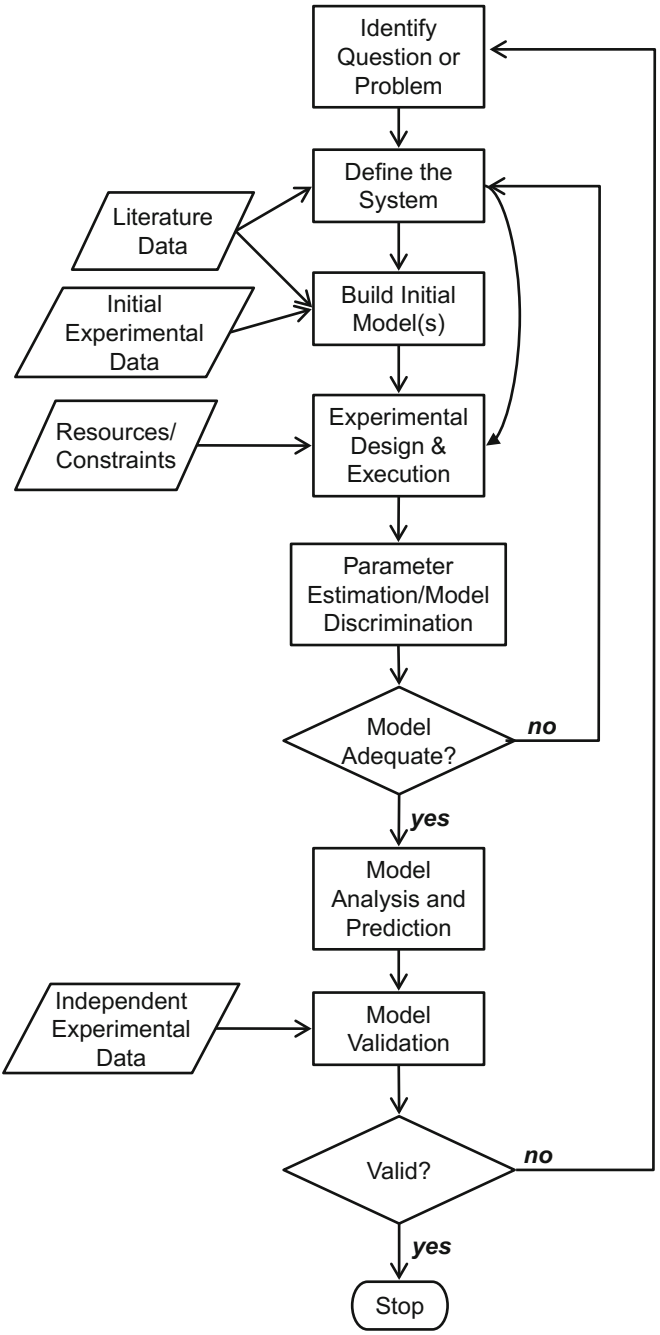

Fig. 6.2 An overall workflow for building kinetic models of biochemical signaling networks. The various aspects of the process are described throughout this chapter in sequence. *Box*—process to be carried out, *trapezoid*—input information or data, *diamond*—decision to be made

behavior and answers the initial question in a meaningful way. This process is not unique to the models we consider in this chapter but is instead rather general to many types of modeling. Notably, it depicts an ideal situation; in practice typically many of these steps are either not performed or do not follow rigorous protocols. Models that are not developed via this ideal process nevertheless are often quite useful and have had impact in systems biology research. Yet, applying all the steps of this pipeline would certainly improve the final developed model and would help to standardize the currently widely-varying protocols employed to develop these models. Such protocol standardization would help to boost confidence in the fidelity of this class of models, as well as increase model sharing and reuse. This is of particular importance if the goal of one's modeling efforts is to inform preclinical or clinical pharmaceutical development in an industrial or clinical setting.

In what follows, we expand on each step of this process, surveying current methods and approaches as well as illustrating with real examples when possible. Also, although we give an inherent bias towards mammalian systems and methods, as the focus of this chapter is pharmacology, many of the presented methods are general and can be applied to a multitude of biological systems.

6.2.1 Identify the Question or Problem

The process begins by identifying the question or problem-of-interest. This step is absolutely critical to embarking on a well-posed modeling exercise that is likely to yield meaningful research results, and is analogous to starting a research project with a well-founded and experimentally-testable hypothesis. The question should (i) rely on or be enhanced by kinetic modeling for providing an answer and (ii) provide focus for the scope and granularity of the model when choosing from among the many alternatives to be discussed below.

Throughout this Chapter, we will illustrate some (but not all) of the methods with a case study focused on the role of Kinase Suppressor of Ras 2 (KSR2) in extracellularly-regulated kinase 1 (ERK1) and ERK2 signaling mediated by the B-isoform of rapidly accelerated fibrosarcoma (B-Raf) (Brennan et al. 2011). The ERK1/2 signaling pathway plays a central role in a variety of cellular processes, including migration, differentiation, and death (Yoon and Seger 2006). B-Raf is commonly mutated in a variety of human cancers. A well-documented B-Raf mutation is V600E, which is frequent in melanoma and constitutively activates the kinase activity of B-Raf, leading to inappropriate ERK1/2 activation and cell proliferation, survival, and migration (Dankort et al. 2009). A targeted small molecule inhibitor of only B-Raf V600E, but not wild-type B-Raf or C-Raf (vemurafenib) was recently developed with structure-based approaches, and has

showed a remarkable 80 % response rate in melanoma patients with the V600E mutation (although the tumor regression only lasted 2–18 months presumably due to adaptive resistance) (Sondergaard et al. 2010; Das Thakur et al. 2013; Bollag et al. 2010). However, not all Raf inhibitor drugs have worked out so well. Pan small molecule inhibitors of Raf family proteins, such as GDC-0879 and PLX4720 that target mutated and non-mutated B-Raf as well as the C-Raf isoform, have been developed but have seen relatively limited clinical success (Hatzivassiliou et al. 2010; Poulikakos et al. 2010). This may be due to the fact that, in some cases, these inhibitors can actually have paradoxical activating effects on Raf-family proteins by inducing their dimerization (Poulikakos et al. 2010) and depend on the mutational status of the upstream Ras family proteins (Hatzivassiliou et al. 2010). A new and potentially critical mechanism has been shown for how the scaffold protein KSR2 operates in the context of mediating B-Raf activation and signaling to ERK1/2 (Brennan et al. 2011), and it may be feasible to design drugs that disrupt KSR2's ability to activate B-Raf-mediated ERK1/2 signaling. What oncogenic mutations might make a particular tumor sensitive and/or resistant to such a KSR2 drug? What other drugs, such as Raf inhibitors, may synergize with a KSR2 drug? What affinity must a KSR2 drug have to exert ERK1/2 pathway inhibition, and what are the most effective mechanisms to target? A kinetic model of the ERK1/2 signaling pathway incorporating these new KSR2 mechanisms may help answer such questions.

6.2.2 Define the System

Defining the system forms the foundation for the entire modeling process, yet it is very difficult to systematize and embodies what many refer to as "the art of modeling". Many choices and assumptions must be made that are based more on intuition rather than rigor and mathematics. Yet, one guiding principal that almost universally holds true is that of Occam's Razor, which suggests that when confronted with many possibilities, one should choose the simplest that describes all desired features. Thus, we prefer to start simple with relatively restrictive models, and only expand the model to be more complex when warranted by inability to describe experimental data relevant to the question-of-interest. At this stage it is prudent to consider the experimental system as well (e.g., cell lines vs. animal models; which lines or animals, etc.), although this could also be considered at the experimental design phase.

6.2.2.1 Inputs and Outputs

The question-of-interest should inform a clear choice for the input(s) and output(s) of the model. The input should be experimentally perturbable, the output should be

experimentally observable, and ideally vice versa. For our example, we choose Ras as the input and ERK1/2 as the output. Ras is a small G-protein that sits at the top of the B-Raf-ERK1/2 signaling cascade. Activation of Ras leads to B-Raf and ERK1/2 activation. ERK1/2 activation is a key regulator of proliferation, and its aberrant activation in cancer is often a driver of unregulated growth.

6.2.2.2 Connecting the Inputs and Outputs with a Kinetic Scheme

The kinetic scheme is a precise pictorial representation of the chemical transformations that are assumed to occur between the model inputs and outputs. It is the foundation and a central part of the model. There have been some formalisms proposed to depict kinetic schemes, such as those suggested by CellDesigner (Kitano et al. 2005), but they have yet to be widely adopted. Nevertheless, there are a few basic features that are widely understood (see Fig. 6.3 for examples): (i) binding of one species to another to form a complex is depicted by two arrows smoothly coming together into one arrow, and dissociation as the reverse; (ii) enzymatic transformation is depicted by a curved unidirectional arrow from substrate to product, with a straight unidirectional arrow from the enzyme to the nadir of the curved arrow; (iii) degradation is depicted by chemical transformation to the empty set $\varnothing$; (iv) synthesis is depicted by chemical transformation from nothing. Of course, there are many variations on this theme, but these generalities will help one to understand many kinetic schemes.

Deciding on reactions to connect the inputs and outputs is again part of the art of modeling. Moving backwards from the output to the input is usually a reasonable method. How does my output get produced? What biochemical entities are needed to do that? How does this mechanism move me one step closer to my input? By repeatedly answering these questions, one can arrive at a list of species and reactions that are likely important to connect the model inputs and outputs. It will also suggest when "dead-ends" are present and thus suggest species and reactions that may be culled.

We opt to build "mechanistic" models when possible, meaning that if an elementary reaction mechanism is known, then we prefer to include it in the model explicitly. This is desirable as the model is grounded by its clear connection to real biochemical entities and mechanisms, and as such is usually easier to compare to experimental data than a model that is not mechanistic. Most importantly, a mechanistic model can be quite adaptable to different cell systems or contexts (Bouhaddou and Birtwistle 2014) because its parameters and species have explicit biochemical meaning and can be changed by measurements in the new system. This is in contrast to empirical models that may be very good at describing the behavior of a particular system, but are not easily adaptable to other systems because the parameters do not have biochemical meaning. Yet, more often than not in biochemical signaling networks, uncertainty is abundant, and mechanisms are not known. This necessitates semi-mechanistic or empirical approaches, at least for connecting those species where mechanisms are not known. Approaches based on

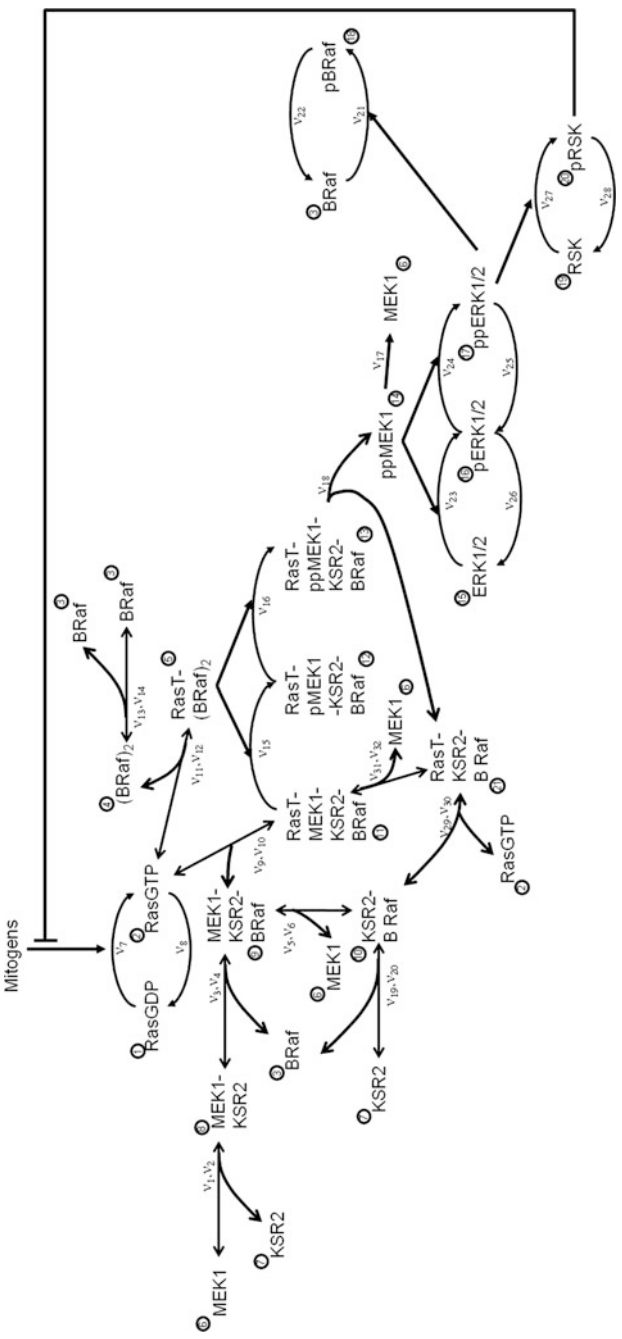

Fig. 6.3 Kinetic scheme for our B-Raf/KSR2 model example. Reactions are chosen as described throughout the text, and the equations underlying this model are given in the supplementary material in the MATLAB code. *Circled numbers* correspond to species indices, and reaction rates are *labeled* next to their *arrows*

fuzzy logic, Bayesian inference, and quantitative logic gates have had success in such endeavors (Morris et al. 2011; Kirouac and Onsum 2013; Sachs et al. 2005), as well as those based on modular response analysis (Klinger et al. 2013) or similar perturbation-centric methods (Molinelli et al. 2013). Moreover, the mechanistic links between signaling kinetics and cell fate, such as apoptosis, are sometimes not clear; in such cases regression based methods, such as partial least squares regression, have been shown to work well (Miller-Jensen et al. 2007; Janes et al. 2005). Useful models will likely be a mix of mechanistic with empirical functions when necessary.

Sometimes, explicitly modeling all known biochemical mechanisms is overly burdensome or not relevant to the question of interest. For example, often times in models of kinase signaling pathways, ATP is not explicitly modeled. Of course, ATP is important for kinase signaling; yet, its concentration almost never changes in the cell and its binding to enzyme is typically very fast and does not appreciably influence the overall reaction kinetics. Thus, one must exercise some restraint to balance the costs vs. the benefits of incorporating mechanistic detail. Without this restraint, one ends up with an extremely large model that becomes computationally impractical to apply the downstream modeling process steps. Thus, we strongly prefer parsimony as a first assumption over complexity.

The initial kinetic scheme we have chosen to depict our KSR2/B-Raf model is shown in Fig. 6.3. Note that we have also indicated reaction rate numbers and species indices; this greatly facilitates model development and its understanding by others. As stated above, we describe scheme development starting with the output and work upstream. ERK1 and ERK2 are doubly phosphorylated and activated by active MEK1 or MEK2; however, only MEK1 has been sufficiently studied to be included in the model (Brennan et al. 2011). MEK1 is activated by double phosphorylation as well, and it is claimed that only MEK1, which is bound to the KSR2-B-Raf complex, can be doubly phosphorylated by a different B-Raf molecule (Brennan et al. 2011). We assume that active GTP-bound Ras serves to recruit these MEK1-KSR2-B-Raf complexes (presumably through the Ras binding domain of B-Raf) and catalytically active B-Raf dimers to the plasma membrane so that the B-Raf dimers can phosphorylate and activate MEK1. We assume that KSR2, MEK1, and B-Raf can bind in any order to one another, but that B-Raf is needed for binding to RasGTP. As mentioned above, we choose Ras as our model input, which can be in two states, the inactive GDP or active GTP bound state. The conversion of RasGDP to RasGTP is mediated by guanine exchange factors, whose activity are typically regulated by external factors such as mitogens. It is well established that active, doubly phosphorylated ERK1/2 (ppERK1/2) enacts strong negative feedback upstream by directly phosphorylating and inactivating C-Raf, and possibly to a lesser extent B-Raf (Sturm et al. 2010; Fritsche-Guenther et al. 2011; Pratilas et al. 2009). Another well-established mechanism of ERK1/2-mediated feedback, which is thought to travel through p90 ribosomal S6 kinase (RSK), is dampening of Ras

activation by inhibiting the GEFs (von Kriegsheim et al. 2009). Negative feedback is important for dictating input/output responses and drug sensitivity/resistance, and therefore we include them since one of the modeling goals is to investigate drug sensitivity/resistance.

Inspection of all the various association and dissociation reactions presented in Fig. 6.3 highlights that it is often difficult to allow for all combinations of biochemical transformations in a rigorous manner (i.e., it is easy to leave some out by mistake). Furthermore, consider how difficult it would be to incorporate C-Raf into this model, which can heterodimerize with B-Raf and can also bind many of the same targets as B-Raf. Yet, incorporating C-Raf would likely be important to our question-of-interest, since it is the target of many current Raf drugs and influences their effectiveness (Sullivan and Flaherty 2013; Heidorn et al. 2010). This "combinatorial complexity" arises when model species have multiple sites that can each be in many states, and arises not only from complex binding scenarios (as described here), but more commonly from multisite modification such as phosphorylation. For example, the epidermal growth factor receptor has approximately 10 tyrosines that can each be unphosphorylated, phosphorylated, or bound to various downstream adaptor proteins; accounting for all these combinations yields 3^{10} possible species. This is clearly infeasible to draw on a kinetic scheme (and code) (Birtwistle 2014). An innovative solution to building models that account for such combinatorial complexity is "rule-based modeling" (Chylek et al. 2013; Sorokina et al. 2013). BioNetGen and its derivatives, such as NFsim, are the more commonly used variants (Sneddon et al. 2011). Instead of specifying a detailed kinetic scheme of all unique chemical species, one only lists the domains and states of each molecule and a handful of reaction rules that describe interactions between these domains and states, which the software then iterates over to generate all potential chemical species. Although attractive-in-principle, rule-based approaches tend to generate extremely large models (sometimes even of infinite size if there are ring-forming or polymerization reactions), which practically limits their applicability and sometimes necessitates assumptions to reduce model size so that they are computationally feasible. As computational power grows and rule-based algorithms improve, such approaches will become more attractive. Nevertheless, whether the kinetic scheme is depicted with the traditional enumeration of unique chemical species or by reaction rules, the modeling steps illustrated in Fig. 6.2 and discussed below still generally apply.

6.2.2.3 System Properties

Whereas the kinetic scheme is a quite comprehensive summary of all the biochemical species and reactions being considered, there are still several key

properties of the system to specify beyond that. Below we list these properties and describe rationale for their selection:

1. Single Cell or Cell Population Average: Are the experimental data to be gathered on a single cell level, or from millions of cells combined into a single measurement? Are the questions-of-interest relevant to behavior of individual cells or a population of cells?
2. Spatial or Compartmental: Do possible diffusional effects or spatial gradients of biochemical species play a role? Can various subcellular compartments be viewed as effectively well-mixed? How many cellular compartments are needed?
3. Stochastic or Deterministic: Are any molecular species present in low copy number (~ 100), making stochastic effects potentially important? Is one interested in cell heterogeneity? Does gene expression noise affect the question-of-interest?
4. Dynamic or Steady-State: Are cellular dynamics important for your question-of-interest? Will the experimental data consist of time courses?

Determining these properties gives well-defined tasks and methods for later in the model development process.

For our example, we choose (1) cell population average, as drug sensitivity and resistance are typically evaluated in cell populations, (2) compartmental with one whole cell compartment, as the kinetic scheme does not involve any transport or subcellular organelles, (3) deterministic, as these components are not very lowly expressed (see below Build Initial Model section), and we do not wish to explain any cellular heterogeneity (although drug response heterogeneity may be interesting), and (4) dynamic, because often ERK1/2 and/or drug dynamics can be important for mediating biological effects, and there are dynamic data available to help constrain the model behavior.

Unfortunately, there is not enough space in this chapter to describe how to build spatial models of biochemical signaling networks; however, there are a number of excellent reviews on the topic (Kholodenko 2006; Neves and Iyengar 2002), and many pieces of the model building process do not depend on whether the model is spatial or compartmental.

6.2.3 Build Initial Model(s)

Once the system is defined and the kinetic scheme is in hand, one can specify the model equations and then simulate and adjust the model, if needed, based on literature or pre-existing experimental data.

6.2.3.1 Choosing Reaction Rate Laws

Each reaction in the kinetic scheme has a corresponding rate law, which describes the rate at which that reaction proceeds in units of concentration per time. The type of reaction will drive the choices for the mathematical form of the rate law. These rate laws can be used directly for deterministic simulations, and with minimal effort for stochastic simulations (by converting units to reaction propensities and molecule numbers).

Association and dissociation reactions are often assumed to follow mass-action kinetics, in which the reaction rate is proportional to the concentration of the reactants. For example, v_1 is an association reaction between MEK1 and KSR2 and we assume the rate law to be $v_1 = k_1$[MEK1][KSR2], where k_1 is a rate constant (1/time/concentration) and [] denotes concentration. The corresponding dissociation reaction is $v_2 = k_2$[MEK1-KSR2], where k_2 is a rate constant (1/time). For simplicity and organizational purposes, we prefer to match rate constant subscript indices with those of the reaction.

Enzymatic reactions can be broken down into elementary steps of association, catalysis, and dissociation, or a lumped rate law can be assumed. Michaelis-Menten lumped rate laws are common and capture the saturating nature of enzymatic reactions even though the basic assumptions that go into such rate laws may not firmly hold in some scenarios to which they are applied (such assumptions are often difficult to validate in vivo) (Chen et al. 2010). If competition or sequestration is thought to be important, then full elementary reactions should be used, in which the binding of enzyme and substrate are considered explicitly.

Many times we further reduce the Michaelis-Menten equations to effective linear rate laws that on their surface look like mass action laws. This requires assumptions of Michaelis constants being much greater than the substrate concentration, giving an effective first-order rate constant of k_{cat}/K_m, where k_{cat} is the enzyme catalytic constant and K_m is the Michaelis constant. However, often due to parameter identifiability issues (see below), one usually cannot determine whether such assumptions are valid or not, and therefore we opt to use Occam's Razor and go with the simpler linear rate laws unless there is experimental evidence that they are too simplistic.

Other potential rate laws are many, depending on specific assumptions the researcher would like to make about each reaction. They include, for example, Hill-type equations for multi-step or unknown mechanisms, and also for transcriptional regulation. Our choices for all the rate laws in our example cannot be described here due to space constraints, but can be found in the MATLAB code for the model contained in the Supplementary Material (SimulateKSRv1.m and SimulateKSRv2.m).

One important consideration is that all of these reaction rate laws are predicated upon the hypothesis that cellular compartments are "well-mixed", meaning that the species are uniformly distributed throughout a compartment. Clearly, in many biological situations such an assumption is suspect. For example, the plasma membrane is not a homogeneous compartment but rather contains microdomains

where receptors are located and downstream signaling occurs. Yet, models based on this well-mixed assumption over the past 40 years, from metabolism to signaling, have been very successful at describing the biological behaviors of interest and providing insight into their mechanisms and function. Nevertheless, one must be aware of this underlying assumption of traditional reaction kinetics approaches, and if there is reason to believe it is causing model-experiment mismatch, one can use more complex agent-based or spatial kinetic Monte Carlo approaches (Collins et al. 2010; Costa et al. 2009). Alternatively, one can instead opt to use empirical approaches in such situations, as described above.

6.2.3.2 Initial Parameter Value Choices

Although parameter estimation is an explicit and significant step later in the modeling process, much can be done here at the initial model development stage to determine parameter values. There is a rich literature describing in vitro studies on enzyme kinetics for many enzymes of interest, as well as affinities of protein–protein interactions. These should serve as initial parameter value estimates. Even if a particular protein–protein interaction or enzyme was not explicitly studied, one can infer a feasible range for the parameter based on experimental studies of homologs or similar processes. Such primary experimental studies should be a first resource for determining initial parameter values. However, it should be noted that there is no guarantee that parameter values measured in an in vitro setting correspond to a live cell situation; thus, caution must be taken to remember that these values are only initial estimates, and may need to be refined.

Another source of parameter values is previously developed kinetic models. These are not as trustworthy as values that have been directly determined experimentally, because parametric identifiability of these types of models is largely not guaranteed (see Parameter Estimation section below). Nevertheless, such values are reasonable starting points when no other information is available.

Because many of the reactions are founded in mechanism, reasonable lower and upper bounds can be posited based on thermodynamic and physical principles, such as detailed balance and diffusion limit. Detailed balance specifies that the product of equilibrium constants for a circular cycle of binding reactions that do not produce or consume energy must equal one, and the diffusion limit specifies that no association reaction can proceed faster than the two reactants can find each other. If one assumes that a particular protein–protein association has the same equilibrium constant no matter what the states of the proteins (e.g., bound to other proteins, phosphorylated, etc.), then detailed balance will be satisfied. There is some spread in the literature as to what the diffusion limit is, perhaps because of uncertainty in how diffusion proceeds in the complex cellular environment as compared to a pure solution, but it is typical to limit on rate constants at approximately 0.1 s^{-1} nM^{-1}. In our experience, association rate values are well described by values a few orders of magnitude less than this ($\sim$0.001 s^{-1} nM^{-1}). One will often find values of dissociation constants or affinities in the literature; we prefer to hold the association

constant at 0.001 s^{-1} nM^{-1} and then calculate the off rate constant, based on the reasoning that affinity will more likely affect the lifetime of the complex (k_{off}), rather than the association rate constant (often determined by encounter rate set by diffusion). If one finds that the association rate constant must be increased far past the diffusion limit to describe the data well, a likely explanation is that the two components are co-localized in a volume smaller than the compartment being considered. For example, the association of two signaling proteins recruited to the plasma membrane will have a much higher apparent rate constant due to their co-localization. Thus, such constraint-violating situations can be resolved with new mechanistic hypotheses, and then the rate law can be adjusted by assuming a volume of this new subcompartment and scaling the two reactant concentrations accordingly.

Another major class of parameters to determine is initial species concentrations. Cellular protein concentrations range from about 0.1 nM ($\sim$100 molecules/cell) on the low end to about 1 μM ($\sim 10^6$ molecules/cell) at the high end (based on a 2000 μm^3 cell—8.3×10^{-4} nM × cell/molecules). A recent study has obtained absolute quantification of many cellular protein concentrations (Schwanhausser et al. 2011), and we routinely use this resource to obtain species concentration estimates. We also used this resource to estimate the overall levels of the species in Fig. 6.3 (see Supplementary Material), but KSR2 levels were not available so this is something we must estimate by analyzing its effects on model behavior. However, it is important to note that these estimates should be refined later by parameter estimation or through direct experimentation, as protein concentrations vary widely across cell types.

6.2.3.3 Deriving the Differential Equations

For a deterministic model, each species will have its own ordinary differential equation (ODE) (or a partial differential equation if a spatial model is being considered; stochastic models do not have differential equations but rather reactions are fired probabilistically using rate laws derived from the deterministic case). A large majority of kinetic models of biochemical signaling networks are based on ODEs. Thus we describe in detail here the derivation of the ODEs (there are numerous excellent reviews on these other topics for interested readers).

The ODE for each species is simply the sum over all reactions that produce or consume that species, with all reactions multiplied by the stoichiometry of the species in that reaction. Consuming stoichiometries are negative, whereas producing stoichiometries are positive. The entire system of ODEs is succinctly represented in matrix-vector notation using the stoichiometric matrix **S**

$$\frac{d\mathbf{x}}{dt} = \mathbf{S}\mathbf{v} \tag{6.1}$$

here, **x** is an n-by-1 vector of species concentrations, $\boldsymbol{v}$ is an m-by-1 vector of reaction rates, and **S** is an n-by-m matrix containing the stoichiometric coefficients, with species corresponding to rows and reactions corresponding to columns. In principal, one does not need to specify the stoichiometric matrix to derive the differential equations, and can instead write out sums of the reaction rates for each species. However, we strongly prefer to use this stoichiometric matrix approach to deriving the differential equations for several reasons: (i) reaction stoichiometries are stored in one place and it is much easier to ensure their correctness; (ii) calculating the differential equations requires only one line of code (with linear algebra libraries); (iii) any errors will be confined to the stoichiometric matrix itself, which is straightforward to troubleshoot, rather than possibly being contained in hard coded sums of reaction rates in multiple places; (iv) there are a host of analyses that provide model information based on analysis of the stoichiometric matrix alone (e.g., conserved moieties (Vallabhajosyula et al. 2006)); (v) providing a stoichiometric matrix facilities combining, modifying, and sharing models. An example stoichiometric matrix for our model is provided in the Supplementary Material (KSRModelv2Stoich.csv).

When reactions transport species across compartments, or when two reactants are localized to a compartment but the reactant concentrations are defined with respect to different volumes, special care must be taken to ensure the ODEs are correct. In the case of transport, the product stoichiometry should be the volume ratio between the compartments. For example, if a species A is transported from the cytoplasm to the nucleus, with rate $v = k_t[A]_{cyt}$, then the stoichiometric matrix entry for this reaction for cytoplasmic A is -1, but the entry for nuclear A is the volume ratio V_{cyt}/V_{nuc}, with the subscripts cyt and nuc referring to the cytoplasm and nucleus. Alternatively, one can multiply the vector of reaction rate laws by their respective volumes, to obtain a left-hand side that is in terms of molecules (or moles) per time, rather than concentration. In the case of species localization, both species concentrations must be rescaled to the volume of the reaction compartment. A typical example is ligand-receptor binding. Ligand-receptor association occurs in the extracellular space, but ligand concentration is defined in the extracellular compartment and receptor concentration in the cellular compartment. In this case, the receptor concentration in the ligand-receptor association rate law should be multiplied by the factor V_c/V_{ec}, with the subscripts ec and c denoting extracellular and cellular compartments. This rescales the receptor concentration to the extracellular compartment for this particular reaction (but not in the entire model).

6.2.3.4 Simulating the Model-Deterministic

At this point one will have an ODE model that describes the mechanistic relationships between the chosen inputs and outputs. To simulate this model, one first needs to specify the initial conditions. In most scenarios this is a two-step process. First, one sets all of the unmodified, unbound species equal to the total concentrations determined above, and all other concentrations to zero. Then, with the input

level set to that corresponding to the system prior to experimental perturbation, the model is integrated to its natural steady-state. This step is called "equilibration." Integration should be done with an algorithm designed for stiff systems, such as `ode15s` in MATLAB. The values for all states after equilibration become the initial conditions for a relevant simulation in response to a perturbation. Then, the response of a system to the perturbation is simulated by integrating over the desired time interval, starting from the equilibrated initial conditions.

Simulations with the initial model should be used to verify that the model does not have errors and that it displays expected behavior. No species should have negative concentrations and moiety conservation should be confirmed. It is typical to do a preliminary study of the dynamics and dose response of the system, and compare it to what might be expected. Almost always the model must be altered. We did this for our KSR2 model with the following characteristics in mind: (i) ERK1/2 activation in response to mitogens usually occurs over $\sim$5 min., and in the presence of strong negative feedback with decline by $\sim$30 min.; (ii) there should be a smooth dose response of RasGTP, active B-Raf (RasGTP bound), ppMEK1, and ppERK1/2 to mitogen levels 60 min. post mitogen stimulus; (iii) most MEK1 and ERK1/2 should be in the doubly phosphorylated form at high mitogen doses; (iv) there should be an optimal KSR2 concentration for causing maximal ERK1/2 activation 60 min post mitogen stimulus; (v) increasing negative feedback strength should smoothen the dose response to make ppMEK1 and ppERK1/2 (at 60 min.) increase more gradually in response to increased mitogen levels. Unfortunately, we cannot expand in detail how we made specific modifications to meet these criteria here, but the model code with comments before (file name with suffix '*v*1') and after ('*v*2') modification is given in the Supplementary Material (SimulateKSRv1.m and SimulateKSRv2.m). Interested readers are encouraged to analyze the differences between the two, and contact us with questions.

6.2.3.5 Simulating the Model-Stochastic

If the model is stochastic, then there are no ODEs to integrate, and reactions are fired through random sampling approaches. If one is unsure whether the molecule numbers of various species are low enough to warrant stochastic simulation, it is prudent to compare deterministic to stochastic simulation results and analyze if there are significant differences. Common stochastic simulation methods reviewed (Golightly and Gillespie 2013) are predominantly based on the Gillespie algorithm or variants thereof. A preferred exact algorithm is that of Gibson and Bruck (2000), but this is usually computationally intensive and cannot be widely applied to larger models, particularly for stiff systems as is common for biochemical signaling networks. The implicit tau-leaping algorithm (Cao et al. 2007) is the numerical equivalent to ODE integrators for stiff systems, and although it is not exact, it usually gives acceptable results by time-averaging the behavior of fast reactions. There are also hybrid methods that divide the model into stochastic and deterministic portions (Salis et al. 2006). Many software packages make many such

algorithms readily available in standard code libraries or with graphical user interfaces, such as StochKit and Cain.

Sometimes, even though system behavior on the single cell level is stochastic, all the molecule numbers are large resulting in little variability in reaction rates with traditional stochastic simulations. Such noise may be largely due to cell-to-cell protein expression variability, which arises from the stochastic nature of gene expression. One can take such noise into account without direct stochastic simulations, or rather by sampling total protein concentrations from known distributions, and then integrating the ODE model for many sets of these initial conditions (~ 1000) (Birtwistle et al. 2012a; Gaudet et al. 2012). Although some have used the log-normal distribution for such sampling, it predicts a scaling behavior between mean protein concentrations and the variance of protein concentrations that is not consistent with experimental observations (Birtwistle et al. 2012b). The gamma distribution is a more appropriate choice that captures cell-to-cell variability in protein expression over a wider range of conditions (Birtwistle et al. 2012b; Shahrezaei and Swain 2008). Alternatively, knowledge of the transcription and translation rates, as well as mRNA and protein degradation rates for each species in a model, permits the simulation of burst-like transcription and translation events de novo using algorithms that simulate stochastic processes such as the Gillespie algorithm.

6.2.3.6 Annotating the Model

For others to understand and reuse the model, it is essential to provide carefully documented code, record the assumptions and parameter values that were used, and then upload them to model-sharing resources such as BioModels or convert them into a universal format such as SBML as well as provide source code (e.g., MATLAB or C++ code) (Waltemath et al. 2011). There is much literature devoted to these topics and we do not discuss them in detail, but it is nevertheless important to emphasize this step. We mention it here, rather than at the end, because it is typically easier to annotate while the model is being initially developed, rather than at the end when many versions of the model have been created, and many of the assumptions were made long ago (sometimes several years).

6.3 Experimental Design and Execution of Experiments

It can often take months, if not longer, to gather reliable experimental data for the initial development of a kinetic model. Thus, one should aim to plan such experiments at a very early stage in the model development process, perhaps as early as the kinetic scheme is produced (see curved arrow in Fig. 6.2). Although some experimental design methods depend on an initial model, some experiments can be planned and completed prior to completion of an initial model.

Table 6.1 Selected experimental methods and their properties relevant to kinetic modeling

Method	What it measures	Single cell or population measure	Live, fixed, or lysed cells	Ability to multiplex	Ability to generate time-course data	Absolute or relative quantification
qRT-PCR	RNA	Both	Lysed	Medium	Medium	Relative
RNA-seq	RNA	Both	Lysed	High	Low	Absolute or relative
FISH	RNA or DNA	Single cell	Live or fixed	Medium	Low	Relative
Protein tagging	Protein	Both	Live or fixed	Low	High	Relative
FRET	Protein interactions	Single cell	Live or fixed	Low	High	Relative
Western blot	Protein	Population	Lysed	Low-medium	Medium	Absolute or relative
Flow cytometry	Protein	Both	Live or fixed	Low-medium	Medium	Relative
Luminex	Protein	Population	Lysed	Medium	Medium	Relative
Mass spectrometry	Protein	Population	Lysed	High	Low	Absolute or relative
Mass cytometry (CyTOF)	Protein	Both	Fixed	High	Low	Relative

Experimental design for kinetic models of biochemical signaling networks consists of answering two questions. What types of perturbations should I apply? What should I measure, and when should I measure it for each perturbation? If a biological system has not yet been chosen, this also needs to be addressed here based on the question-of-interest and system definition above. Are cell lines sufficient or do we need animal models? What lines are appropriate? We focus on cell lines. Here, we briefly describe the types of perturbation and measurement methods that are commonly used, with the goal of providing enough information for readers to make an informed choice, although it is impossible to comprehensively list all methods here. As an aid, we provide a summary in Table 6.1.

We note that although it is seldom done, we strongly advocate for directly measuring the total absolute abundances of all model proteins in the experimental system of interest. Without these measurements to constrain the magnitude of the various species in the model and the initial conditions, it is generally difficult to make relevant predictions of the system behavior.

6.3.1 Types of Perturbations

The most straightforward way to perturb the system is to apply a defined and time-invariant concentration (dose) of a compound. Such compounds can be pharmacological (e.g., a small molecule kinase inhibitor), or biological (e.g., a growth factor). While biological compounds are usually applied at the moment defined as time point 0, pharmacological inhibitors are often applied to the system prior to biological compound treatment, to ensure its uniform distribution in cells. Standard pipette-based approaches are limited to simple perturbation time courses, such as the time 0 step response or a pulse-chase where the original dose is washed out and then replaced with a new dose. However, sophisticated pump-based perfusion chamber or microfluidics methods (Mettetal et al. 2008) and optogenetic-based methods (Toettcher et al. 2011, 2013) can allow for complex time-dependent perturbations, such as sine waves or increasing ramps.

The system can also be perturbed at the transcript level. One can transfect (liposome-based methods) or infect (virus-based methods) genetic material into cells. The genetic material (usually a DNA plasmid) can express a gene ectopically, overexpress an endogenous gene, or downregulate a gene via RNA interference (e.g., shRNA) in a transient setting. A negative selection mechanism is needed to obtain cells that permanently exhibit the alteration. To do this, the plasmid also usually encodes resistance to a particular drug, such as puromycin. However, genome-editing methods, such as those involving CRISPR and TALEN (Ran et al. 2013; Reyon et al. 2012), are becoming more realistic.

Once a gene has been permanently integrated, it can be controlled using drugs such as tetracycline (or more commonly its higher affinity analog doxycycline) so long as the gene is engineered to be Tet responsive. Expression can be modulated in a dose-dependent manner, permitting a level of control similar to that describable by a kinetic model. Aside from such transcription rate control, one can use the small molecule Shield1 to increase the half-life of proteins that contain a DD domain (Banaszynski et al. 2006).

6.3.2 Types of Measurements-Transcripts

To obtain a quantitative measure of the mRNA expression levels, one can perform a qRT-PCR, or quantitative reverse-transcription polymerase chain reaction. This technique is useful if one is interested in a few transcripts in a cell population setting, but sometimes is done on single cells (although it can be technically challenging). The alternative to enumerating individual transcripts a priori is to measure transcripts globally, using a technique such as RNA-seq. RNA-seq data can provide absolute mRNA copy number information as long as internal controls are included in the analysis. Although RNA-seq is most commonly performed on cell populations, the ability to perform RNA-seq in single-cells is rapidly emerging

(Islam et al. 2013). If one is unable obtain RNA-seq data, microarray is a comparable methodology though it possesses several drawbacks such as high background noise and the limitation of having to define target sequences of interest a priori (Xu et al. 2013). Fluorescence in situ hybridization (FISH) is a technique one can use to visualize a particular mRNA transcript via a fluorescently labeled nucleic acid probe. FISH can lend insight into differences in gene expression across a population of cells and has been used to study stochastic gene expression in mammalian cells with success (Raj et al. 2006). Generally, one fixes and permeabilizes the cells prior to FISH, thus killing them; however, it is possible to perform FISH in live cells with minimal perturbation (Simon et al. 2010). Highly multiplexed FISH methods are also becoming available (Lubeck and Cai 2012).

6.3.3 Types of Measurements-Proteins

One way to measure the levels (and/or spatial location) of a protein over time is to "tag" it with a fluorescent protein, by cloning them together such that they are transcribed as a fusion protein. This method could serve to monitor protein expression levels in response to a stimulus, such as cFos levels following growth factor-mediated ERK activation. Importantly, protein tagging can be used to measure protein levels and/or localization in live cells over time. Another live-cell technique involves genetically encoded probes based on Forster Resonance Energy Transfer (FRET) (Miyawaki 2011). Such probes allow one to measure the spatio-temporal dynamics of biochemical signaling activities. For example, the EKAR-EV FRET probe responds to ERK1/2 activity by changing its FRET (Komatsu et al. 2011), and the past decade has provided a wealth of these probes for various biochemical activities one may be interested in.

To measure protein levels in a cell population, the western blot is the gold standard. In this technique, an antibody is used to bind to and measure the amount of a protein or protein state in whole cell lysate that has been separated by molecular weight. As an example, one could measure the level of a phosphorylated protein in response to increasing mitogen dose. Further, the technique can be combined with immunoprecipitation to quantify levels of protein–protein interactions. Although enhanced chemiluminescence is often used to quantify western blot signals, there can be non-linearity in such measurements; therefore for quantitative kinetic models, systems such as LI-COR are preferred which provide a linear signal-response. Absolute quantification is seldom done but possible by including known protein concentrations as internal controls. It should be noted that the western blot has been miniaturized into a so-called "microwestern" which is potentially useful for kinetic modeling applications, since it allows probing with many antibodies over many perturbation conditions (dose/time points). A Luminex assay allows multiplexing to a similar extent as microwesterns (Ciaccio et al. 2010).

Flow cytometry allows one to measure the relative level of proteins in a large number of single cells at a single time point, capturing the distribution of protein

levels found in a population of cells using fluorescently labeled antibodies. In principal, modern flow cytometers can quantify up to 16 analytes, but in practice this is quite difficult and 3–4 color imaging is more typical. A flow cytometer coupled to a mass spec (CyTOF) potentially allows quantification of ~40 analytes in single cells (Bendall et al. 2011), but requires specialized equipment and antibodies.

As previously stated, one must determine initial protein concentrations in order to construct a kinetic model that is biologically meaningful. One way to gather initial protein concentrations in the cells of interest is via a proteomics approach using mass spectrometry (MS), which can globally quantify protein levels in a population of cells. Advances in mass spectrometry have enabled the quantification of proteins in terms of absolute copy numbers, easily convertible to units of molecules/cell (Schwanhausser et al. 2011).

6.3.4 Formal Statistical Design of Experiments

With an initial model that is based on and reproduces to an acceptable level available literature or preliminary experimental data, it is possible to implement a formal statistical design of experiments (DoE) tailored to the goal of the modeling exercise. DoE is a mature field, and many have demonstrated how it might be applied to the types of biochemical signaling models we describe here (Bandara and Meyer 2012; Banga and Balsa-Canto 2008). The specific approaches that have been described depend on whether the goal is parameter estimation for one model, or discrimination between many candidate models. Although such established DoE methods have historically been successful in other fields, their original development is largely grounded in application to relatively low dimensional linear models, with only a handful of states and experimental decision variables. Kinetic models of biochemical signaling networks, however, have many properties that in our opinion preclude meaningful application of such approaches with current computational technology:

1. They are almost ubiquitously highly non-linear. Thus, local linear approximations of the model are used to apply these traditional DoE methods, the validity of which is often unclear.
2. They are typically high-dimensional (>10 states). Thus, the potential number of states to measure that the DoE algorithm must choose from is often overwhelmingly large.
3. There are many potential experimental perturbations. This causes a combinatorial explosion of possibilities for these DoE methods that optimize over the experimental decision variable space.
4. It is generally not yet known how to guarantee parametric identifiability (see Parameter Estimation below). Thus, it is unlikely that these DoE methods would produce a design that significantly enhances our ability to identify model

parameters or discriminate between two models, as compared to a more pragmatic approach.
5. The validity of the initial model structure and parameter values is unknown at this point. Thus, it makes little practical sense to spend a significant amount of experimental resources to implement an optimal experimental design based on an initial model that is likely inadequate.

These major reasons are most likely why in practice, formal DoE methods are typically not employed to develop kinetic models of biochemical signaling networks. This is not to say that such methods lack importance, but rather that much research is needed to develop new DoE methods that are suited to the properties of this class of models and fill the current void in the model development process.

6.3.5 *Practical Design of Experiments*

The more pragmatic yet common approach to experimental design is to use the insight of expert biologists to answer the two basic questions needed for experimental design. This can often be done only with a kinetic scheme and thus can be done before the initial model is completed. At this initial stage of model development, a broad experimental design that perturbs the system using the model inputs and measures across "important" states is preferred. Typically, perturbations consist of applying extracellular agonists or antagonists (e.g., a growth factor) to cells that have been serum-starved overnight (to minimize confounding variables), in the presence or absence of pharmacological or small molecule inhibitors of "key pathways" in the model. What states are "important" and what pathways are "key" is best informed by expert opinion or initial experimental data. Dose responses for the extracellular agonists or antagonists give important information to constrain model behavior and should be done if the resources are available. Logarithmic dose spacing (e.g., base 10) between saturating and limit of detection levels is often most informative. Which species to measure is also best informed by an experimental biologist with expertise in that system, and of course is limited by available technologies and resources. The time point selection should also be informed by expert opinion, and depends on how one defined the system, the question(s) of interest, the limits of the chosen technology, and available resources.

Biochemical signaling models have been termed "sloppy" (Gutenkunst et al. 2007), which refers to the fact that many key system outputs are quite robust to variations in many model parameters (discussed more in Parameter Estimation below). This property may be why such a pragmatic approach to experimental design often results in a successful modeling exercise, because sloppiness dictates that many of the choices simply do not matter for the behavior of key system outputs.

6.3.6 *Comparison of Experimental Data to Model Simulations*

In general an experimental measurement does not directly correspond to a particular model species. For example, if one is measuring a kinase activity in live cells by FRET, the resulting FRET measurement cannot be directly related to the kinase activity in the model, because there is not a linear relationship between the two (Birtwistle et al. 2011). As another example, if one measures the total amount of cellular RasGTP by pull down and western blot, this would correspond to a sum over several model states in Fig. 6.3. Moreover, the way in which the western blot data are normalized can have a significant impact on the quality of the normalized data (Degasperi et al. 2014). Thus, great care should be taken to ensure that the best comparison between experimental data and model simulations is being employed, and often requires mapping the model variables onto so-called "observable" variables with defined functions. This requires a thorough understanding of both the computational model and the experimental data; thus close collaboration and effective communication between wet and dry lab researchers is essential.

6.4 Parameter Estimation

With an initial model and experimental data in hand, the next task is to determine whether the model is capable of describing the experimental data, and what range of parameter values give good fit. This exercise is called parameter estimation or "training." Parameters include total protein abundances (if not directly measured) and kinetic rate parameters in each rate equation. Although one will have reasonable initial values for all these quantities, it is highly unlikely that the model will be able to reproduce the new experimental data without modifying the parameter values. This is expected since many of the initial parameter values will have come from in vitro studies or from data collected in a different biological system.

Parameter estimation for kinetic models of biochemical signaling pathways is an extremely challenging exercise for two main reasons. First, the model is high-dimensional and nonlinear. Thus it is computationally expensive to explore the parameter space extensively when searching for good-fitting parameter sets. Second, it is not understood how to guarantee parametric identifiability for these models, and even this general class of nonlinear chemical kinetic models. An identifiable parameter is one whose value is well-constrained by the experimental data, such that it is known with acceptable precision. A typical kinetic model of a biochemical signaling pathway will not have identifiable parameters. This is quite shocking and perhaps even disturbing to modelers from other disciplines, such as pharmacokinetics and pharmacodynamics described in other chapters in this book. Despite this ubiquitous parametric uncertainty, an emerging theme in this type of modeling is that key temporal outputs are typically robust to large changes in most

parameter values. This property seems to be general for this class of systems biology models and is referred to as "sloppiness" (Gutenkunst et al. 2007). From a biological and evolutionary perspective, this makes sense, because key dynamic behavior should not be affected by common noise sources. From a modeling perspective, this to some extent mitigates the problem that unidentifiable parameters cause, with respect to reproducing biologically relevant behavior. However, one should still strive to ensure all rate constants and concentrations are within biophysically feasible ranges, such as not exceeding the diffusion limit, and are justified to do so because model parameters typically have a biophysical interpretation. Nonetheless, we are still left with the problem that we cannot be certain that unidentifiable parameters do not affect our conclusion. That is why downstream model analyses must account for how parametric uncertainty affects predictions, such as global sensitivity analysis methods (see Model Analysis).

The first step in parameter estimation is to define lower and upper bounds for the unknown parameter values. As described above, these can typically be set through hard biophysical or thermodynamic limits. Next, one must define an objective function that represents goodness-of-fit. There are many options, including log-likelihood and sum-of-squared errors between simulations and data, and the particular choice depends on assumptions for the expected errors in the experimental data (Raue et al. 2013). Regardless, it is essential to scale each quantity such that error does not depend on units (variance scaling is common and often statistically valid). Then, one must choose an algorithm that will vary the parameters over the bounds to optimize the objective function. Local, deterministic gradient-based optimization is inappropriate for this class of models as they are nonlinear and of high dimension. Global optimization methods are a necessary component of any choice. One simple global method is to repeatedly employ local methods but from different initial parameter values judiciously chosen from across the parameter space (e.g., with latin hypercube sampling), and in fact such methods may be both accurate and efficient (Raue et al. 2013). However, the majority of studies have had success using either the genetic algorithm (Nakakuki et al. 2010; Schoeberl et al. 2002) or simulated annealing (Wang et al. 2009). Bayesian methods have been applied in a few cases with success (Vyshemirsky and Girolami 2008; Eydgahi et al. 2013), and such methods are very attractive since they rigorously account for multi-dimensional parametric uncertainty, although at much higher computational cost than other global methods. Lastly, the chosen algorithm should be run many times over, due to the inherent sloppiness of these models and therefore parameter uncertainty. This allows one to estimate the range of parameter values that give rise to models with "acceptable" fit. We suggest obtaining at least 10 good fitting parameter sets; $\sim$100 would give a much better indicator of parametric uncertainty but even 10 is sometimes difficult to obtain due to the computational burden.

Most of these parameter estimation algorithms are well-suited to parallelization and should be implemented on high performance computing resources. One potentially promising new technology is graphical processing unit (GPU)-based computation. A single GPU card can contain $\sim$3000 processors that run the same

program (i.e., model) given different input values (i.e., parameter sets), which is ideal for this parameter estimation task. A desktop workstation can house up to 4 such cards, giving ~12,000 GPU processors in a single machine. However, robust ODE solvers that operate in the specialized GPU environment (e.g., NVIDIA CUDA language) must first be developed for such an approach to be implemented. Some attempts exist, such as `cudasim` which can take an SBML model input and use the GPU to simulate it both stochastically or deterministically (Zhou et al. 2011), or code libraries such as `odeint`. Any GPU-based solver must be able to implement implicit solver methods that can tackle the stiffness that is present in these types of models.

After parameter estimation, one must decide whether the model has acceptable fit or not. This is commonly done by simply plotting the model simulations against the experimental data, and looking for close match between the two. In addition, one can analyze the distribution of residual errors (differences between simulations and data) for evidence of bias (non-zero mean). If there is bias, then that suggests that the model structure and/or parameter bounds must be changed. A clear indicator that parameter bounds should be changed is if estimated parameter values are constantly on or near the bound. It is desired to first try to expand parameter bounds if it is likely to improve fits, before altering the model structure. How to alter the model structure is highly dependent on the nature of the model-experiment mismatch and needs to be analyzed on a case-by-case basis. Regardless, if the structure needs refinement, one must return to defining the system to come up with new hypotheses.

6.5 Model Discrimination

Model discrimination refers to determining which model among a set is most appropriate given experimental observations. Usually, parameter estimation must be done before model discrimination. Some have investigated model discrimination in a formal way, using Bayesian methods to compute Bayes factors for each model (Xu et al. 2010). More straightforward and computationally inexpensive methods are simply considering the sum of squared residual errors for each model and weighting it by the number of free parameters with the Akaike or Bayesian Information Criterion. As mentioned briefly above, there are some statistical design of experiments methods that are focused on model discrimination, but largely any experiments that are tailored to determining which model among many is most appropriate are designed in a pragmatic manner.

6.6 Model Analysis and Prediction

After successfully completing parameter estimation, one is ready to analyze the model to provide potential answers for the question-of-interest in the form of experimentally testable hypotheses. The type of model analysis will differ depending on the question-of-interest. For example, if nonlinear dynamical phenomena such as bistability or oscillations are of interest (e.g., cell cycle or circadian clock), then traditional bifurcation analysis techniques can be applied (Chickarmane et al. 2005), although this can be difficult with the high dimensional models typical of biochemical signaling pathways and need expert knowledge to reduce the number of parameters one is considering.

One general type of model analysis that is almost universally useful is parameter sensitivity analysis. This consists of varying parameter values and observing the effect on outputs-of-interest. Sensitivity analysis, like parameter estimation methods, can be local or global. Local methods consider only a particular region of parameter space, and are typically inappropriate because (i) the models are nonlinear and (ii) parameters are not identifiable and therefore their values are not known precisely. Unfortunately, local methods include metabolic control analysis which has been widely applied to understand steady-state phenomena in metabolic networks (Kholodenko et al. 1994). Global methods consider an entire multi-dimensional region of parameter space, and therefore can account for the inherent parametric uncertainty present in these models. There are many global sensitivity analysis methods available (reviewed in (Saltelli 2008)), and it is not yet clear which may be best for these types of models. We have previously used a rigorous yet straightforward global method called Sobol sensitivity analysis, which quantitatively decomposes the total variance in outputs-of-interest into the contributions by individual parameters and the interactions between parameters (Sobol 2001). A larger variance indicates a more important parameter and therefore important mechanism. The method functions by evaluating model outputs for a large number of different parameter sets, and, importantly, is capable of providing error estimates on the sensitivity coefficients. Although a very large number of model evaluations are needed to produce statistically significant results, the algorithm is easily parallelizable. We were able to perform Sobol sensitivity analysis on a model of the VEGFR pathway containing 77 parameters with relative computational ease (Zhang et al. 2014).

6.7 Model Validation

The model analysis stage will produce many predictions, and these predictions must be sorted into those that can be experimentally tested and those that cannot, which, like experimental design, requires close contact between the wet and dry labs. Among those predictions that can be experimentally tested, typically the

counter-intuitive or unexpected ones are the best to explore experimentally, in addition of course to those that directly address the question-of-interest. Only a small subset of all predictions can be experimentally addressed, so it is important to carefully select those to further consider. Importantly, any experiments for model validation must be independent from those used to develop and train the model.

After the new experiments are performed (or mined from the literature), one must compare simulation predictions to the new data, and then interpret what it means for the question-of-interest. Currently, a model is considered valid if it is able to reproduce independent experimental data outside the scope of the original training data set. If the model is not valid, typically it can still yield insight into the question-of-interest, and may still be valuable in that regard. Such disagreement prompts a new hypothesis and iteration back to the first step of the modeling process. Yet, even if a model is validated in this way, it is not certainly universally valid, and assuming that the model can predict many other quantities outside of its training set would be grossly premature. Much more research must be done to elucidate how a more unbiased approach to model validation can be designed, so that confidence in model predictions can be quantified in a rigorous manner.

6.8 Conclusions

Building a kinetic model of a biochemical signaling network is a significant investment of time and effort, and therefore one should have very clear goals and expectations for what the eventual model will accomplish for the research question-of-interest. Such kinetic models have many properties that can potentially fill a significant gap in the drug development pipeline and inform personalized medicine approaches. However, to reach this potential, much theoretical work must be done to improve and standardize each step of the model building process shown in Fig. 6.2. Any new methods must take special care to accommodate the properties of biochemical signaling networks that hamper current methods, namely, the complexity of these networks, their large scale, and inherent uncertainty.

Acknowledgments We thank Arvin Dar for helpful discussions about the KSR2/B-Raf example. We gratefully acknowledge funding from the Icahn School of Medicine at Mount Sinai, an IBM Faculty Award, and the NIH Grants P50 GM071558 (Systems Biology Center New York), R01GM104184, and U54HG008098 (LINCS Center). MB is supported by a NIGMS-funded Integrated Pharmacological Sciences Training Program grant (T32 GM062754). We regret not being able to cite many good papers in the literature on these diverse topics due to space constraints.

References

Banaszynski LA, Chen LC, Maynard-Smith LA, Ooi AG, Wandless TJ (2006) A rapid, reversible, and tunable method to regulate protein function in living cells using synthetic small molecules. Cell 126(5):995–1004

Bandara S, Meyer T (2012) Design of experiments to investigate dynamic cell signaling models. Methods Mol Biol 880:109–118

Banga JR, Balsa-Canto E (2008) Parameter estimation and optimal experimental design. Essays Biochem 45:195–209

Bendall SC, Simonds EF, Qiu P, el Amir AD, Krutzik PO, Finck R, Bruggner RV, Melamed R, Trejo A, Ornatsky OI, Balderas RS, Plevritis SK, Sachs K, Pe'er D, Tanner SD, Nolan GP (2011) Single-cell mass cytometry of differential immune and drug responses across a human hematopoietic continuum. Science 332(6030):687–696

Birtwistle MR (2014) Analytical reduction of combinatorial complexity arising from multiple protein modification sites. J R Soc Interface 12(103)

Birtwistle MR, von Kriegsheim A, Kida K, Schwarz JP, Anderson KI, Kolch W (2011) Linear approaches to intramolecular Forster resonance energy transfer probe measurements for quantitative modeling. PLoS ONE 6(11):e27823

Birtwistle MR, Rauch J, Kiyatkin A, Aksamitiene E, Dobrzynski M, Hoek JB, Kolch W, Ogunnaike BA, Kholodenko BN (2012a) Emergence of bimodal cell population responses from the interplay between analog single-cell signaling and protein expression noise. BMC Syst Biol 6:109

Birtwistle MR, von Kriegsheim A, Dobrzynski M, Kholodenko BN, Kolch W (2012b) Mammalian protein expression noise: scaling principles and the implications for knockdown experiments. Mol BioSyst 8(11):3068–3076

Birtwistle MR, Mager DE, Gallo JM (2013) Mechanistic vs. empirical network models of drug action. CPT Pharmacomet Syst Pharmacol 2:e72

Bollag G, Hirth P, Tsai J, Zhang J, Ibrahim PN, Cho H, Spevak W, Zhang C, Zhang Y, Habets G, Burton EA, Wong B, Tsang G, West BL, Powell B, Shellooe R, Marimuthu A, Nguyen H, Zhang KY, Artis DR, Schlessinger J, Su F, Higgins B, Iyer R, D'Andrea K, Koehler A, Stumm M, Lin PS, Lee RJ, Grippo J, Puzanov I, Kim KB, Ribas A, McArthur GA, Sosman JA, Chapman PB, Flaherty KT, Xu X, Nathanson KL, Nolop K (2010) Clinical efficacy of a RAF inhibitor needs broad target blockade in BRAF-mutant melanoma. Nature 467(7315):596–599

Bouhaddou M, Birtwistle MR (2014) Dimerization-based control of cooperativity. Mol Bio Syst 10:1824–1832

Brennan DF, Dar AC, Hertz NT, Chao WC, Burlingame AL, Shokat KM, Barford D (2011) A Raf-induced allosteric transition of KSR stimulates phosphorylation of MEK. Nature 472 (7343):366–369

Cao Y, Gillespie DT, Petzold LR (2007) Adaptive explicit-implicit tau-leaping method with automated tau selection. J Chem Phys 126

Chen WW, Niepel M, Sorger PK (2010) Classic and contemporary approaches to modeling biochemical reactions. Genes Dev 24:1861–1875

Chickarmane V, Paladugu SR, Bergmann F, Sauro HM (2005) Bifurcation discovery tool. Bioinformatics 21(18):3688–3690

Chylek LA, Harris LA, Tung CS, Faeder JR, Lopez CF, Hlavacek WS (2013) Rule-based modeling: a computational approach for studying biomolecular site dynamics in cell signaling systems. Wiley Interdiscip Rev Syst Biol Med

Ciaccio MF, Wagner JP, Chuu CP, Lauffenburger DA, Jones RB (2010) Systems analysis of EGF receptor signaling dynamics with microwestern arrays. Nat Methods 7(2):148–155

Collins S, Stamatakis M, Vlachos DG (2010) Adaptive coarse-grained Monte Carlo simulation of reaction and diffusion dynamics in heterogeneous plasma membranes. BMC Bioinform 11:218

Costa MN, Radhakrishnan K, Wilson BS, Vlachos DG, Edwards JS (2009) Coupled stochastic spatial and non-spatial simulations of ErbB1 signaling pathways demonstrate the importance of spatial organization in signal transduction. PLoS ONE 4(7):e6316

Dankort D, Curley DP, Cartlidge RA, Nelson B, Karnezis AN, Damsky WE Jr, You MJ, DePinho RA, McMahon M, Bosenberg M (2009) Braf(V600E) cooperates with Pten loss to induce metastatic melanoma. Nat Genet 41(5):544–552

Das Thakur M, Salangsang F, Landman AS, Sellers WR, Pryer NK, Levesque MP, Dummer R, McMahon M, Stuart DD (2013) Modelling vemurafenib resistance in melanoma reveals a strategy to forestall drug resistance. Nature 494(7436):251–255

Degasperi AB, MR; Volinsky, N; Rauch, J; Kolch, W; Kholodenko, BN (2014) Evaluating strategies to normalise biological replicates of Western Blot Data. PLoS One (in press)

Eydgahi H, Chen WW, Muhlich JL, Vitkup D, Tsitsiklis JN, Sorger PK (2013) Properties of cell death models calibrated and compared using Bayesian approaches. Mol Syst Biol 9:644

Fritsche-Guenther R, Witzel F, Sieber A, Herr R, Schmidt N, Braun S, Brummer T, Sers C, Bluthgen N (2011) Strong negative feedback from Erk to Raf confers robustness to MAPK signalling. Mol Syst Biol 7:489

Gaudet S, Spencer SL, Chen WW, Sorger PK (2012) Exploring the contextual sensitivity of factors that determine cell-to-cell variability in receptor-mediated apoptosis. PLoS Comput Biol 8(4): e1002482

Gibson MA, Bruck J (2000) Efficient exact stochastic simulation of chemical systems with many species and many channels. J Phys Chem 104(9)

Golightly A, Gillespie CS (2013) Simulation of stochastic kinetic models. Methods Mol Biol 1021:169–187

Gutenkunst RN, Waterfall JJ, Casey FP, Brown KS, Myers CR, Sethna JP (2007) Universally sloppy parameter sensitivities in systems biology models. PLoS Comput Biol 3(10):1871–1878

Hatzivassiliou G, Song K, Yen I, Brandhuber BJ, Anderson DJ, Alvarado R, Ludlam MJ, Stokoe D, Gloor SL, Vigers G, Morales T, Aliagas I, Liu B, Sideris S, Hoeflich KP, Jaiswal BS, Seshagiri S, Koeppen H, Belvin M, Friedman LS, Malek S (2010) RAF inhibitors prime wild-type RAF to activate the MAPK pathway and enhance growth. Nature 464 (7287):431–435

Heidorn SJ, Milagre C, Whittaker S, Nourry A, Niculescu-Duvas I, Dhomen N, Hussain J, Reis-Filho JS, Springer CJ, Pritchard C, Marais R (2010) Kinase-dead BRAF and oncogenic RAS cooperate to drive tumor progression through CRAF. Cell 140(2):209–221

Islam S, Zeisel A, Joost S, La Manno G, Zajac P, Kasper M, Lonnerberg P, Linnarsson S (2013) Quantitative single-cell RNA-seq with unique molecular identifiers. Nat Methods

Iyengar R, Zhao S, Chung SW, Mager DE, Gallo JM (2012) Merging systems biology with pharmacodynamics. Sci Transl Med 4(126):126–127

Janes KA, Albeck JG, Gaudet S, Sorger PK, Lauffenburger DA, Yaffe MB (2005) A systems model of signaling identifies a molecular basis set for cytokine-induced apoptosis. Science 310 (5754):1646–1653

Kholodenko BN (2006) Cell-signalling dynamics in time and space. Nat Rev Mol Cell Biol 7 (3):165–176

Kholodenko BN, Sauro HM, Westerhoff HV (1994) Control by enzymes, coenzymes and conserved moieties. A generalisation of the connectivity theorem of metabolic control analysis. Eur J Biochem 225(1):179–186

Kholodenko BN, Hancock JF, Kolch W (2010) Signalling ballet in space and time. Nat Rev Mol Cell Biol 11(6):414–426

Kirouac DC, Onsum MD (2013) Using network biology to bridge pharmacokinetics and pharmacodynamics in oncology. CPT Pharmacomet Syst Pharmacol 2:e71

Kitano H, Funahashi A, Matsuoka Y, Oda K (2005) Using process diagrams for the graphical representation of biological networks. Nat Biotechnol 23(8):961–966

Klinger B, Sieber A, Fritsche-Guenther R, Witzel F, Berry L, Schumacher D, Yan Y, Durek P, Merchant M, Schafer R, Sers C, Bluthgen N (2013) Network quantification of EGFR signaling unveils potential for targeted combination therapy. Mol Syst Biol 9:673

Komatsu N, Aoki K, Yamada M, Yukinaga H, Fujita Y, Kamioka Y, Matsuda M (2011) Development of an optimized backbone of FRET biosensors for kinases and GTPases. Mol Biol Cell 22(23):4647–4656

Lubeck E, Cai L (2012) Single-cell systems biology by super-resolution imaging and combinatorial labeling. Nat Methods 9(7):743–748

Mettetal JT, Muzzey D, Gomez-Uribe C, van Oudenaarden A (2008) The frequency dependence of osmo-adaptation in Saccharomyces cerevisiae. Science 319(5862):482–484

Miller-Jensen K, Janes KA, Brugge JS, Lauffenburger DA (2007) Common effector processing mediates cell-specific responses to stimuli. Nature 448(7153):604–608

Miyawaki A (2011) Development of probes for cellular functions using fluorescent proteins and fluorescence resonance energy transfer. Annu Rev Biochem 80:357–373

Molinelli EJ, Korkut A, Wang W, Miller ML, Gauthier NP, Jing X, Kaushik P, He Q, Mills G, Solit DB, Pratilas CA, Weigt M, Braunstein A, Pagnani A, Zecchina R, Sander C (2013) Perturbation biology: inferring signaling networks in cellular systems. PLoS Comput Biol 9 (12):e1003290

Morris MK, Saez-Rodriguez J, Clarke DC, Sorger PK, Lauffenburger DA (2011) Training signaling pathway maps to biochemical data with constrained fuzzy logic: quantitative analysis of liver cell responses to inflammatory stimuli. PLoS Comput Biol 7(3):e1001099

Nakakuki T, Birtwistle MR, Saeki Y, Yumoto N, Ide K, Nagashima T, Brusch L, Ogunnaike BA, Okada-Hatakeyama M, Kholodenko BN (2010) Ligand-specific c-Fos expression emerges from the spatiotemporal control of ErbB network dynamics. Cell 141(5):884–896

Neves SR, Iyengar R (2002) Modeling of signaling networks. BioEssays 24(12):1110–1117

Poulikakos PI, Zhang C, Bollag G, Shokat KM, Rosen N (2010) RAF inhibitors transactivate RAF dimers and ERK signalling in cells with wild-type BRAF. Nature 464(7287):427–430

Pratilas CA, Taylor BS, Ye Q, Viale A, Sander C, Solit DB, Rosen N (2009) (V600E)BRAF is associated with disabled feedback inhibition of RAF-MEK signaling and elevated transcriptional output of the pathway. Proc Natl Acad Sci USA 106(11):4519–4524

Raj A, Peskin CS, Tranchina D, Vargas DY, Tyagi S (2006) Stochastic mRNA synthesis in mammalian cells. PLoS Biol 4(10):e309

Ran FA, Hsu PD, Wright J, Agarwala V, Scott DA, Zhang F (2013) Genome engineering using the CRISPR-Cas9 system. Nat Protoc 8(11):2281–2308

Raue A, Schilling M, Bachmann J, Matteson A, Schelke M, Kaschek D, Hug S, Kreutz C, Harms BD, Theis FJ, Klingmuller U, Timmer J (2013) Lessons learned from quantitative dynamical modeling in systems biology. PLoS ONE 8(9):e74335

Returns on R&D investments continue to fall (2014). Nat Rev Drug Discov 13 (1):9 doi:10.1038/nrd4224

Reyon D, Tsai SQ, Khayter C, Foden JA, Sander JD, Joung JK (2012) FLASH assembly of TALENs for high-throughput genome editing. Nat Biotechnol 30(5):460–465

Sachs K, Perez O, Pe'er D, Lauffenburger DA, Nolan GP (2005) Causal protein-signaling networks derived from multiparameter single-cell data. Science 308(5721):523–529

Salis H, Sotiropoulos V, Kaznessis YN (2006) Multiscale Hy3S: hybrid stochastic simulation for supercomputers. BMC Bioinform 7:93

Saltelli A (2008) Global sensitivity analysis: the primer. Wiley, Chichester

Schoeberl B, Eichler-Jonsson C, Gilles ED, Muller G (2002) Computational modeling of the dynamics of the MAP kinase cascade activated by surface and internalized EGF receptors. Nat Biotechnol 20(4):370–375

Schoeberl B, Pace EA, Fitzgerald JB, Harms BD, Xu L, Nie L, Linggi B, Kalra A, Paragas V, Bukhalid R, Grantcharova V, Kohli N, West KA, Leszczyniecka M, Feldhaus MJ, Kudla AJ, Nielsen UB (2009) Therapeutically targeting ErbB3: a key node in ligand-induced activation of the ErbB receptor-PI3K axis. Sci Signal 2(77):ra31

Schwanhausser B, Busse D, Li N, Dittmar G, Schuchhardt J, Wolf J, Chen W, Selbach M (2011) Global quantification of mammalian gene expression control. Nature 473(7347):337–342

Shahrezaei V, Swain PS (2008) Analytical distributions for stochastic gene expression. Proc Natl Acad Sci USA 105(45):17256–17261

Simon B, Sandhu M, Myhr KL (2010) Live FISH: imaging mRNA in living neurons. J Neurosci Res 88(1):55–63

Sneddon MW, Faeder JR, Emonet T (2011) Efficient modeling, simulation and coarse-graining of biological complexity with NFsim. Nat Methods 8(2):177–183

Sobol IM (2001) Global sensitivity indices for nonlinear mathematical models and their Monte Carlo estimates. Math Comput Simulat 55(1–3):271–280

Sondergaard JN, Nazarian R, Wang Q, Guo D, Hsueh T, Mok S, Sazegar H, MacConaill LE, Barretina JG, Kehoe SM, Attar N, von Euw E, Zuckerman JE, Chmielowski B, Comin-Anduix B, Koya RC, Mischel PS, Lo RS, Ribas A (2010) Differential sensitivity of melanoma cell lines with BRAFV600E mutation to the specific Raf inhibitor PLX4032. J Transl Med 8:39

Sorokina O, Sorokin A, Douglas Armstrong J, Danos V (2013) A simulator for spatially extended kappa models. Bioinformatics 29(23):3105–3106

Sturm OE, Orton R, Grindlay J, Birtwistle M, Vyshemirsky V, Gilbert D, Calder M, Pitt A, Kholodenko B, Kolch W (2010) The mammalian MAPK/ERK pathway exhibits properties of a negative feedback amplifier. Sci Signal 3(153):ra90

Sullivan RJ, Flaherty K (2013) MAP kinase signaling and inhibition in melanoma. Oncogene 32 (19):2373–2379

Toettcher JE, Gong D, Lim WA, Weiner OD (2011) Light-based feedback for controlling intracellular signaling dynamics. Nat Meth 8(10):837–839

Toettcher JE, Weiner OD, Lim WA (2013) Using optogenetics to interrogate the dynamic control of signal transmission by the ras/erk module. Cell 155(6):1422–1434

Vallabhajosyula RR, Chickarmane V, Sauro HM (2006) Conservation analysis of large biochemical networks. Bioinformatics 22(3):346–353

von Kriegsheim A, Baiocchi D, Birtwistle M, Sumpton D, Bienvenut W, Morrice N, Yamada K, Lamond A, Kalna G, Orton R, Gilbert D, Kolch W (2009) Cell fate decisions are specified by the dynamic ERK interactome. Nat Cell Biol 11(12):1458–1464

Vyshemirsky V, Girolami M (2008) BioBayes: a software package for Bayesian inference in systems biology. Bioinformatics 24(17):1933–1934

Waltemath D, Adams R, Beard DA, Bergmann FT, Bhalla US, Britten R, Chelliah V, Cooling MT, Cooper J, Crampin EJ, Garny A, Hoops S, Hucka M, Hunter P, Klipp E, Laibe C, Miller AK, Moraru I, Nickerson D, Nielsen P, Nikolski M, Sahle S, Sauro HM, Schmidt H, Snoep JL, Tolle D, Wolkenhauer O, Le Novere N (2011) Minimum information about a simulation experiment (MIASE). PLoS Comput Biol 7(4):e1001122

Wang CC, Cirit M, Haugh JM (2009) PI3K-dependent cross-talk interactions converge with Ras as quantifiable inputs integrated by Erk. Mol Syst Biol 5:246

Xu TR, Vyshemirsky V, Gormand A, von Kriegsheim A, Girolami M, Baillie GS, Ketley D, Dunlop AJ, Milligan G, Houslay MD, Kolch W (2010) Inferring signaling pathway topologies from multiple perturbation measurements of specific biochemical species. Sci Signal 3(134):ra20

Xu X, Zhang Y, Williams J, Antoniou E, McCombie WR, Wu S, Zhu W, Davidson NO, Denoya P, Li E (2013) Parallel comparison of Illumina RNA-Seq and Affymetrix microarray platforms on transcriptomic profiles generated from 5-aza-deoxy-cytidine treated HT-29 colon cancer cells and simulated datasets. BMC Bioinf 14(Suppl 9):S1

Yoon S, Seger R (2006) The extracellular signal-regulated kinase: multiple substrates regulate diverse cellular functions. Growth Factors 24(1):21–44

Zhang XY, Birtwistle MR, Gallo JM (2014) A general network pharmacodynamic model-based design pipeline for customized cancer therapy applied to the VEGFR pathway. CPT Pharmacomet Syst Pharmacol 3:e92

Zhou Y, Liepe J, Sheng X, Stumpf MP, Barnes C (2011) GPU accelerated biochemical network simulation. Bioinformatics 27(6):874–876

Chapter 7
Mechanistic Models of Physiological Control Systems

Michael C.K. Khoo, Wen-Hsin Hu and Patjanaporn Chalacheva

Abstract Dynamic modeling has played an important role in advancing and integrating the fields of pharmacokinetics and pharmacodynamics. However, the vast majority of models in the literature do not take into account the fact that pharmacological responses are frequently affected by the homeostatic mechanisms inherent in physiological control systems. This article provides a short tutorial presenting examples that illustrate the basic properties of closed-loop control and how these can influence model predictions of drug responses in both the steady-state and under dynamic conditions. Physiological control systems can be modeled using two basic approaches: (a) "minimal modeling", in which all model parameters for individuals can be estimated from experiment; and (b) "structured modeling", in which the model parameters are isomorphic to key physiological entities, but not all can be identified from the measurements. A discussion of these two approaches is presented, along with a case study of how minimal modeling can be applied to extend a larger structured model. Finally, the importance of modeling functional linkages and interactions across organ systems and across scales is highlighted through a brief exposition of a recently developed structured model of cardiorespiratory, sleep-wake state and metabolic control.

Keywords Minimal modeling · Structured modeling · Sleep-wake state · Metabolic control · Homeostasis · Open-loop system · Closed-loop system · Total peripheral resistance (TPR) · Central sleep apnea (CSA) · PNEUMA · Cardiovascular control · Hypothermia · Windkessel model · Baroreflex components · Mechanical effect of respiration (MER) · Mean arterial pressure (MAP)

M.C.K. Khoo (✉) · W.-H. Hu · P. Chalacheva
Department of Biomedical Engineering, University of Southern California,
Los Angeles, CA, USA
e-mail: khoo@usc.edu

D.E. Mager and H.H.C. Kimko (eds.), *Systems Pharmacology and Pharmacodynamics*,
AAPS Advances in the Pharmaceutical Sciences Series 23,
DOI 10.1007/978-3-319-44534-2_7

7.1 Introduction

Fundamental to all living systems is the phenomenon of homeostasis, in which the key physiological variables are regulated so that internal conditions remain relatively stable and operate within narrow bounds, even when the system in question is perturbed by changes in the external environment. Homeostasis is generally maintained through the interplay of multiple factors, some of which act to oppose the changes induced by the external disturbance whereas others act to reinforce these changes. The longstanding practice in physiology has been to identify each of the many associated factors and to develop a conceptual model of how they interact with one another to produce homeostasis in the variable in question. However, although the end result established in homeostasis is a relatively bounded condition, the physiological processes that produce this state are highly dynamic. Moreover, the dynamics of regulation for a physiological variable can span multiple time scales, ranging from seconds to years. For example, arterial blood pressure fluctuates between diastolic and systolic levels within each cardiac cycle, while diastolic and systolic pressures fluctuate within a breathing cycle. Over longer time scales, there are also fluctuations that result from dynamic changes in cardiac output and vascular resistance. And over even more extended time scales, blood pressure fluctuates as a byproduct of the dynamic processes at play in renal autoregulation and thermoregulation. The complex dynamics that emerge from the interaction of the multiple underlying mechanisms make it difficult to distinguish cause from effect. As such, a conceptual model quickly becomes inadequate as a tool for analysis, and it is necessary to turn to the rigorous framework inherent in a mathematical model to help extricate the influences of the various interacting physiological mechanisms from one another. Since feedback regulation is involved in virtually all these processes, a basic understanding of control theory is also important in providing insight into how unexpected behavior of the integrated system can emerge from the network of components that individually might have very different dynamics.

Dynamic modeling has played an important role in advancing and integrating the fields of pharmacokinetics (PK) and pharmacodynamics (PD) over the past several decades; comprehensive summaries of these efforts from various perspectives may be found in a number of excellent reviews (Derendorf and Meibohm 1999; Mager et al. 2003; Csajka and Verotta 2006; Danhof et al. 2007). However, the vast majority of models in the PK/PD literature do not take into account the effects of physiological feedback, even though some studies have suggested that homeostatic mechanisms constitute the basis for a variety of observations that traditional PD models are not able to account for. These include counter-regulatory effects in the development of tolerance to chronic treatment (Francheteau et al. 1993; Bauer and Fung 1994; Mandema and Wada 1995), dependency of physiological responses on the time-course of drug infusion (Kleinboesem et al. 1987), and the development of oscillatory dynamics in body temperature following administration of 5-HT_{1A} agonist (Zuideveld et al. 2001). The purpose of this article is to highlight the

importance and utility of incorporating considerations of closed-loop control in the underlying physiology when PK/PD models are developed for situations in which therapeutic interventions may interact with a potent autoregulatory system.

7.2 Open-Loop Versus Closed-Loop Systems

As a simple illustration of how the intrinsic regulatory mechanism of a physiological system can mask the true pharmacodynamic effects of a drug, consider the specific example displayed in Fig. 7.1. Here, we examine, in simplistic fashion, the efficacy with which a calcium channel blocker drug, such as nifedipine, produces vasodilation, thereby reducing total peripheral resistance (TPR). Following infusion of the drug into the bloodstream, the plasma concentration (C_p) of the drug assumes a certain time-course, consistent with the underlying pharmacokinetics. C_p decreases TPR by an amount ΔTPR through an assumed effect compartment. However, since the product of TPR and cardiac output (CO) yields the mean arterial pressure (MAP), the reduced TPR leads to a reduction in MAP. The decreased MAP unloads the baroreceptors located in the carotid sinuses, leading subsequently to an increase in heart rate and thus CO. The decreased MAP also leads to a reflex peripheral vasoconstriction, increasing TPR, which along with the increase in CO, restores MAP back towards its baseline level. The overall result is that TPR is not reduced as much as one would have predicted based on the known vasodilatory effects of the drug. This is a classic example of "closed-loop control" with negative feedback. In contrast, an example of "open-loop control" would be one in which the baroreceptors have been denervated. In this case, the final steady-state level of TPR

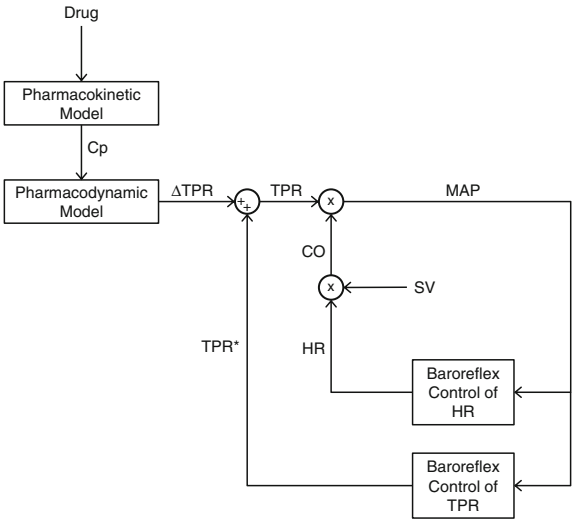

Fig. 7.1 Schematic representation of PK/PD model for characterizing the mean arterial pressure (MAP) and total peripheral resistance (TPR) response to a vasodilator drug. C_p plasma concentration of drug; ΔTPR expected decrease in TPR induced by drug at concentration level C_p; *HR* heart rate; *SV* stroke volume; *CO* cardiac output

would be the original baseline level of TPR minus the change ΔTPR induced by the drug.

Under resting conditions, the controlled variables (e.g., arterial blood pressure, body temperature) in physiological control systems generally operate within a relatively narrow range—this is Walter Cannon's "homeostatic principle" (Cannon 1939) at work. How are these "equilibrium" or "steady-state" conditions determined? Essentially, negative feedback couples the different components of a closed-loop system together, constraining the mode of operation in each of these components. This is best illustrated in terms of the simplistic example of control of blood pressure displayed in Fig. 7.2. The straight lines, labelled CM_1, CM_2 and CM_3, represent the basic property of vascular resistance in circulatory mechanics: for a given TPR, increasing MAP would increase CO. The slope of each of these lines is inversely proportional to TPR. Thus, CM_1 has the highest TPR and CM_2 the lowest. The reverse sigmoid curve represents the baroreflex component of this system—as MAP increases, the baroreceptors act to decrease HR and thus CO (since CO = HR × stroke volume, assuming stroke volume remains constant). Changes in MAP elicit changes (in the opposite direction) of HR—this is the source of negative feedback in this closed-loop system. Assuming that CM_1 represents circulatory mechanics under normal resting conditions, "E1", at which the baroreflex function curve and CM_1 intersect one another, represents the point at which the factors that act to increase or decrease MAP balance out. If MAP falls below its value at E1, the baroreflex component would increase HR and CO, which in turn would elevate MAP (through the circulatory mechanics component), thereby restoring MAP towards E1.

Consider what happens during constant rate intravenous infusion of the vasodilator drug. The resulting decrease in TPR is represented by an increase in slope of the circulatory mechanics line (broken line labelled CM_2 in Fig. 7.2). If the baroreflexes were absent and there is no corresponding compensation in CO, the MAP would drop from ~90 mmHg (E1) to ~65 mmHg (E2*). However, with baroreflex feedback, the lowered MAP triggers an increase in HR, and the

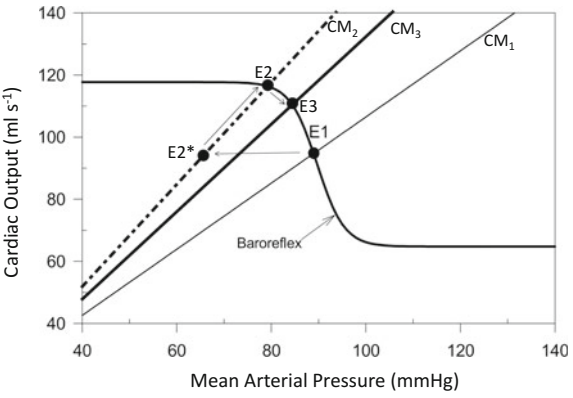

Fig. 7.2 Graphical analysis showing how the equilibrium levels of TPR and MAP are changed from baseline (E1) when there is no feedback from the baroreflexes (E2*), when the baroreflex control of heart rate is operative (E2), and when both baroreflex control of heart rate and TPR are operative (E3). See text for details

consequent increase in CO raises MAP to ~80 mmHg, establishing the new equilibrium point E2, which lies at the intersection of the baroreflex function curve and CM_2.

The solution represented by equilibrium point E2 is incomplete, since the calculations took into account the baroreflex control of HR but not the baroreflex of TPR. In the latter case, the reduced MAP would stimulate the baroreceptors to produce a reflex vasoconstriction that offsets the drug-induced vasodilation. As such, the final equilibrium value of TPR would be a compromise between the drug-induced decrease and the reflex-induced increase in TPR. The final TPR (associated with equilibrium point E3) would be lower than its pre-infusion level (E1) but higher than that in E2.

7.3 Open-Loop Versus Closed-Loop Dynamics

The aforementioned graphical analysis method is useful in providing intuitive insight into how the equilibrium or steady-state levels in closed-loop systems are established. But the utility of this approach is limited to relatively simple examples that involve only two or three control variables. Moreover, the conclusions are strictly correct only under static conditions. To overcome these limitations, we turn to the dynamic model below, which closely follows the formulation proposed by Francheteau et al. (1993).

The structure of the model is schematized in Fig. 7.1. The dynamics associated with circulatory mechanics are assumed to be much faster than the dynamics associated with the baroreflexes or pharmacokinetics of the drug, and thus, blood pressure can be considered to be instantaneously related to blood flow. Thus, the following equation represents the relationship linking MAP, TPR and HR:

$$MAP(t) = SV \cdot HR(t) \cdot TPR(t) \tag{7.1}$$

In Eq. 7.1, SV is assumed constant and equal to 0.097 L.

The equations that follow represent the dynamics associated with the dependencies of HR and TPR on baroreceptor feedback, as well as the dynamics of baroreceptor transduction:

$$\tau_1 \frac{d(HR)}{dt} + HR = HR_{eq}(1 - \alpha U) \tag{7.2}$$

$$\tau_2 \frac{d(TPR^*)}{dt} + TPR^* = TPR_{eq}(1 - \beta U) \tag{7.3}$$

$$\tau \frac{dU}{dt} + U = S_p\left(MAP - MAP_{eq}\right) + S_r \frac{dMAP}{dt} \tag{7.4}$$

with S_p and S_r as the baroreceptor sensitivities to changes in MAP and the rate of changes in MAP. α and β represent the relative gains with which the baroreceptors affect HR and TPR control. τ, τ_1, and τ_2 are the time constants associated with baroreflex dynamics. MAP_{eq}, HR_{eq}, and TPR_{eq} are the pre-infusion equilibrium values of *MAP*, *HR*, and *TPR*. In the simulation examples presented here, α and β are both assigned values of 1, and the time constants τ, τ_1, and τ_2 are each given the value of 0.01 h. MAP_{eq}, HR_{eq}, and TPR_{eq} are assumed to be 90 mmHg, 70 beats min^{-1}, and 12.5 RU (resistance units).

For simplicity, we assume the pharmacodynamic effect of the drug to be proportional (through a gain factor *m*) to the plasma concentration, $C_p(t)$, at any given time t:

$$\Delta TPR(t) = m \cdot C_p(t) \tag{7.5}$$

and

$$TPR(t) = TPR^*(t) + \Delta TPR(t) \tag{7.6}$$

The pharmacokinetic model is a single compartment model with first-order elimination, as given below:

$$C_p(t) = \frac{C_0}{\gamma T}\left(1 - e^{-\gamma t}\right) \quad \text{for } 0 \le t \le T \tag{7.6a}$$

$$C_p(t) = \frac{C_0}{\gamma T}\left(1 - e^{-\gamma T}\right).e^{-\gamma(t-T)} \quad \text{for } t > T \tag{7.6b}$$

We assume a constant rate infusion of the drug over a period T. γ is the elimination rate constant. C_0 is the initial (fictive) drug plasma concentration that would be obtained after a bolus of the same dose, and is equal to the (constant) rate of infusion multiplied by T and divided by the volume of distribution. In the simulation examples that follow, T is 10 h, γ is 0.7 h^{-1}, and C_0 is 350 $\mu g\ L^{-1}$, based on a uniform drug infusion rate of 350 $\mu g\ h^{-1}$ and volume of distribution of 10 L. The pharmacodynamic gain factor, *m*, is assumed to be 0.09 RU L μg^{-1}.

Figure 7.3 compares model responses to a constant rate infusion of a vasodilator for 10 h ($0 < t < 10$) under open-loop (broken lines) and closed-loop (solid lines) conditions. In the open-loop situation, the baroreceptor sensitivities S_b and S_r are assumed to be zero. TPR decreases in proportion to the plasma concentration of the drug, and MAP follows the same time-course as TPR, since both HR and CO remain unchanged from equilibrium values. Under closed-loop conditions (S_b = 0.01 $mmHg^{-1}$, S_r = 0.01 h $mmHg^{-1}$), as TPR decreases, MAP falls. But this triggers the baroreflexes to increase CO by increasing HR, thus partially offsetting the reduction in TPR. As such, the resulting reductions in MAP and TPR are substantially smaller than in the open-loop case, but these occur in association with an elevated HR.

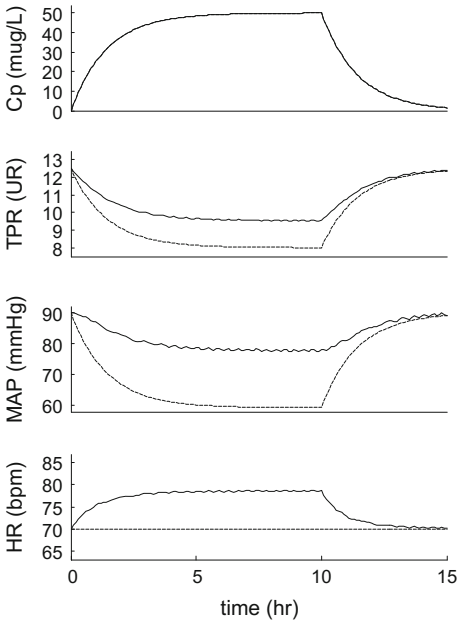

Fig. 7.3 Pharmacodynamic response of TPR, MAP, and HR in model of Fig. 7.2 to constant-rate infusion of vasodilator drug for 10 h starting at time zero, under conditions of no baroreflex regulation (*broken tracings*) and with baroreflex regulation (*solid tracings*). The *top panel* represents the time-course of the drug plasma concentration, C_p. The baroreflex sensitivity parameters are assumed to be $S_b = 0.01$ mmHg^{-1} and $S_r = 0.01$ h mmHg^{-1}

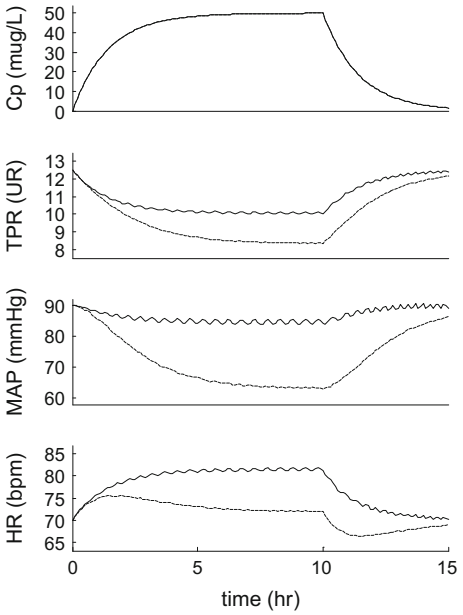

Fig. 7.4 Predicted pharmacodynamic responses in TPR, MAP, and HR for low baroreflex sensitivity ($S_b = 0.001$ mmHg^{-1}, broken tracing) and high baroreflex sensitivity ($S_b = 0.03$ mmHg^{-1}, solid tracing). The value of the baroreceptor rate sensitivity, S_r, is assumed to be 0.01 h mmHg^{-1}in both cases

In Fig. 7.4, a comparison is made between the predicted response to drug infusion of a case with low S_b (0.001 $mmHg^{-1}$, broken lines) and the response in a case with high S_b (0.03 $mmHg^{-1}$, solid lines). In the low S_b case, both TPR and MAP exhibit significant drops during drug infusion. At the same time, HR shows a small increase, which initially overshoots but subsequently settles down to a level that is only slightly higher than its prior equilibrium value. Following termination of drug administration, HR displays a brief undershoot before it returns towards its pre-infusion equilibrium level.

The model simulation examples displayed in Figs. 7.3 and 7.4 demonstrate that closed-loop systems with negative feedback are in general less vulnerable to external perturbations, and that the ability to offset the effects of external interventions increases with feedback gain. However, in systems with high feedback gain, there is a tendency for the corrective action generated by the controller to overcompensate for the effect of the initial disturbance, thereby creating an artificially induced perturbation in the opposite direction. Under the "right conditions", this cyclic chain of events can propagate around the feedback loop, giving rise to oscillatory behavior (Khoo 2000). This can be clearly seen in the response of the high-gain system displayed in Fig. 7.4.

Thus, for reasons related to the underlying homeostatic mechanism rather than pharmacological potency, vasodilator drugs are less likely to be effective, for the same dosage, in patients with strong baroreflexes compared to patients with low baroreflex gains. This basic property of closed-loop control systems may account for the differences in responses to dihydropyridine drugs between normotensive healthy subjects and patients with hypertension: normal subjects display an increase in heart rate with little drop in blood pressure, whereas hypertensive patients, blood pressure can drop substantially with little change in heart rate (Lederballe Pedersen et al. 1980; MacGregor et al. 1982). The differences in responses between the two subject groups may be explained by the observation that hypertensive patients generally have reduced baroreflex sensitivity relative to normotensives (Gribbin et al. 1971; Mussalo et al. 2002).

7.4 Structured Versus Minimal Models

The kind of model presented in Fig. 7.1 is what is known as a "structured model". "Structured" or "comprehensive" models allow our knowledge of the underlying physiology to be systematized and encapsulated concisely into an efficient library of mathematical "rules". The presence of model parameters that are isomorphic to key physiological entities greatly simplifies the problem of interpretation. Moreover, simulations and sensitivity analyses performed with the structured model can provide insight into which physiological parameters are more important in the mediation of the mechanisms under study. However, in structured models with large numbers of parameters, estimation of all the model parameters (including the parameters that characterize the pharmacokinetics and drug pharmacology) from experimental data can become problematic due to system identifiability or "noise to

signal" issues (Cobelli and DiSteffano 1980). An alternative approach is to develop and employ a "minimal model", i.e., one that is able to account for most of the dynamic features of a set of physiological responses and yet be simple enough that all its characteristic parameters can be estimated from measurements obtained in individual subjects. The cost of parsimony in the number of parameters, however, is that the model may not be able to provide insights into the detailed mechanisms of the underlying physiology. On the other hand, minimal models have demonstrated their practical utility in providing quantitative "biomarker" information that can be used to delineate normal from pathological function in various physiological applications. Examples include estimates of insulin sensitivity derived from the Bergman minimal model (Bergman et al. 1985), and respiratory-cardiac coupling gain as a measure of autonomic function under various pharmacological interventions (Mullen et al. 1997) and in patients with obstructive sleep apnea (Khoo 2008). Although structured and minimal modeling approaches are generally applied separately, it is possible to employ a combination of both in which minimal modeling is used to provide components that may be missing in a structured model, as illustrated in the following example.

7.5 Improved Model of TPR Control

The model displayed in Fig. 7.5a, which we will refer to as "Simulation Model A", incorporates a number of additional elements directly pertinent to the control of MAP, HR, and TPR that were missing in the rather simplistic model of Fig. 7.1. The extended model is based largely on previous work by deBoer et al. (1987), Madwed et al. (1989), and Saul et al. (1991). In contrast with the simpler model of

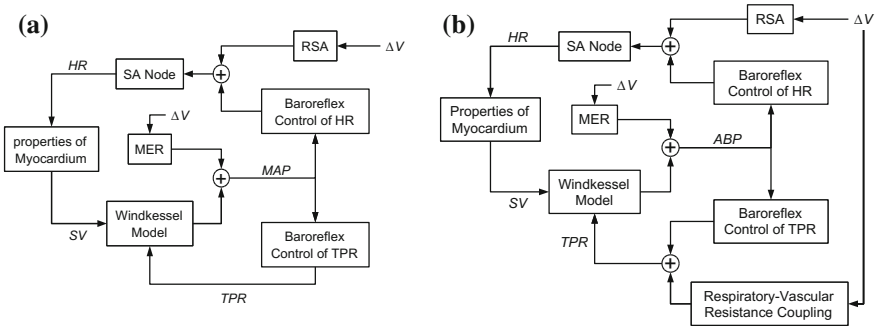

Fig. 7.5 **a** Extended structured model of the control of arterial blood pressure and heart rate, incorporating the effects of respiration and pulsatility of the heart. See text for details. **b** Further extension of Simulation Model A with the incorporation of the respiratory-peripheral vascular resistance coupling (RVC) component. The dynamic characteristics of RVC are estimated using a minimal model applied to individual measurements of peripheral arterial tonometry (surrogate measure of TPR), MAP, and respiration

Fig. 7.1, beat-to-beat changes are introduced by employing a two-element Windkessel model (representing arterial resistance and compliance) to generate a pulsatile waveform in blood pressure within each cardiac cycle. Respiration, represented as incremental changes in lung volume, ΔV, is assumed to be directly related to the autonomic inputs at the sino-atrial (SA) node through neural coupling between the respiratory and autonomic centers in the medulla, as well as through input from the pulmonary stretch receptors. This transfer relation is labelled "RSA" in Fig. 7.5a. Feedback from the baroreceptors also directly influences the autonomic inputs to the heart. Through changes in intrathoracic pressure, respiration produces mechanically-induced alterations in stroke volume which in turn lead to fluctuations in blood pressure. This mechanical effect of respiration (MER) is modeled as a derivative of ΔV multiplied by a negative gain. The time-course of arterial blood pressure, which contains these influences combined, then becomes the input to the model components that represent baroreflex control of HR and TPR.

The model components that represent baroreflex control of TPR and HR are each assumed to contain static gain functions that are inverse-sigmoidal (so that higher blood pressure produces lower HR and lower TPR) placed in series with a dynamic low-pass filter and time delay. The HR and TPR outputs of these baroreflex components are dynamically changing, depending on beat-to-beat blood pressure. The TPR output is fed into the Windkessel model, allowing the time constant of the Windkessel to change from beat to beat. Systolic and diastolic arterial pressures, and thus MAP, fluctuate from beat to beat. The dynamics of the SA node are divided into sympathetic and parasympathetic components. Both branches are modeled as low-pass filters with constant gains. In addition, a time delay is added to the sympathetic branch to mimic latency in the sympathetic response. The outputs from each branch in the SA node are combined to obtain the final HR. This HR then enters the "properties of myocardium" block, which represents the influence of the duration of pulse interval on stroke volume. A longer pulse interval would lead to an increase in the stroke volume and thus pulse pressure of the next cardiac cycle.

Although not indicated in Fig. 7.5a, white noise sequences with coefficient of variation of 8–10 % of the total variance of resulting time-series are added on a breath-to-breath basis to respiratory frequency and tidal volume, and on a beat-to-beat basis to HR, SV, and TPR. The injected noise sequences represent disparate sources of random input fluctuations (e.g., neural and mechanical) that continually perturb the system. Propagation of these random influences through the multiple feedback loops of the closed-loop system and interaction among the coupled feedback loops give rise to spontaneous fluctuations, most notably a strong oscillation near the 0.1 Hz region in HR, MAP, and TPR, as displayed in the frequency spectra of these variables (Fig. 7.6, middle column. "Model A Simulation"). This simulation result is consistent with the "low frequency" oscillation in blood pressure and heart rate widely reported in the literature (Malliani et al. 1991). For comparison, the frequency spectra of respiration and the cardiovascular variables measured in a

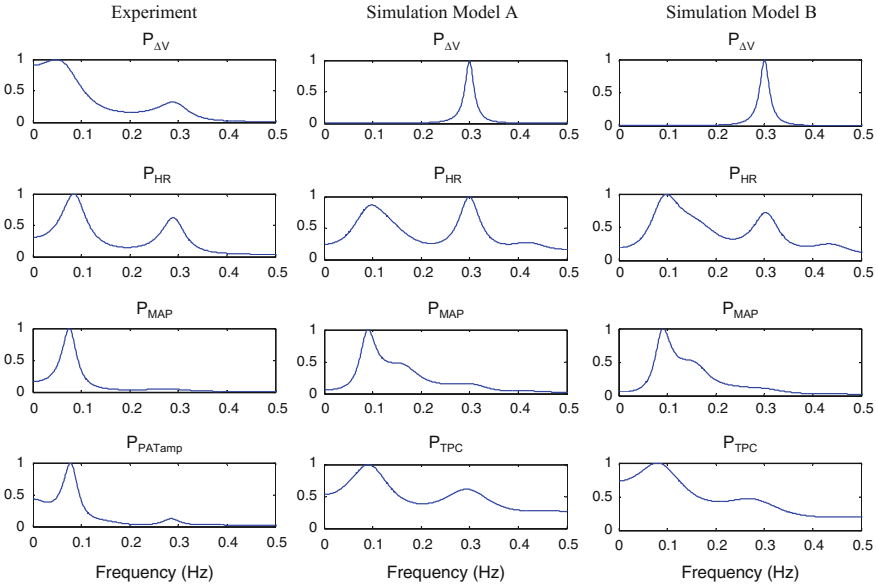

Fig. 7.6 Comparison of the frequency content of respiration, HR, MAP, and TPC time-series derived from experimental data (*left column*), Simulation Model A (*middle column*), and Simulation Model B (*right column*). All frequency spectra have been normalized to their peak values. Both simulation models show a prominent spectral peak at around 0.1 Hz, representing an oscillation with periodicity of ~10 s that has been generated through propagation of system noise around the baroreflex loops of the closed-loop control system. In the experimental data, peripheral arterial tonometry recordings were used as a surrogate measure of the total peripheral conductance, TPC (defined as the inverse of TPR)

healthy subject are displayed in Fig. 7.6 (left column, "Experiment"). Peripheral vasoconstriction is measured using peripheral arterial tonometry (Schnall et al. 1999), and the resulting beat-to-beat amplitude, PATamp, of this signal is used. However, for the sake of comparison with the model simulation results, it is more convenient to use the total peripheral conductance (TPC = 1/TPR) instead of TPR, since peripheral vasoconstriction results in both reduced PATamp and TPC.

An important feature that Simulation Model A is **not** able to reproduce correctly is the peripheral vascular response to large breaths (sighs), as displayed in Fig. 7.7 (middle column, "Model A Simulation"). During the sigh, Model A predicts a brief increase in HR. This leads to a transient increase in MAP, which subsequently lowers HR through the baroreflex. The increase in MAP also triggers a vasodilatory response through the baroreflex control of TPR. However, this prediction runs counter to observation, as peripheral vasoconstriction following deep inspiration has been well documented in humans (Bolton et al. 1936). This peripheral vasoconstriction is clearly visible in the PATamp (or TPC) measurements displayed in Fig. 7.7 (left column, "Experiment").

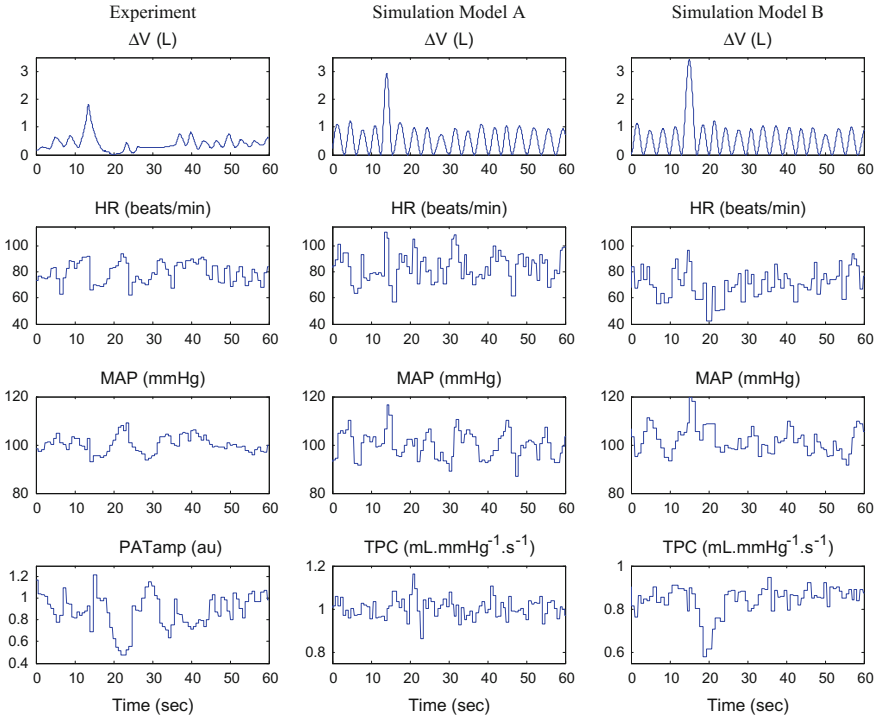

Fig. 7.7 Comparison of the responses (in the time domain) of HR, MAP, and TPC to a large hyperventilatory breath (sigh) from experimental data (*left column*), Simulation Model A (*middle column*) and Simulation Model B (*right column*). In the experimental data, PATamp (amplitude of the peripheral arterial tonometry signal) is used as a surrogate of TPC (=1/TPR). Simulation Model B reproduces the peripheral vasoconstriction response to the sigh observed in experimental data, but Simulation Model A exhibits a small vasodilatory response instead

7.6 Extending the Structured Model of TPR Control: Use of Minimal Modeling

The inability of Model A to adequately predict the occurrence of peripheral vasoconstriction following a large breath suggests that this phenomenon may be the result of not having included a relevant mechanism—in this case, a distinct reflex linking respiration to TPR—in the model. Since no existing computational model of cardiovascular regulation has taken this mechanism into account, it is possible to infer this relationship quantitatively from data by using a minimal modeling approach, and to develop the extended structured model by inserting the data-derived module into the network of components of Model A. Thus, although the minimal model linking respiration to TPR may not shed light into the physiological mechanisms underlying this coupling, including this dynamic component in the structured model allows us to incorporate an important aspect not fully

appreciated previously and to determine how it contributes to the integrated responses of the larger closed-loop system.

The minimal model presented here may be considered "kernel-based" (Marmarelis 1993), since the dynamics of its major components are explicitly characterized by their corresponding impulse responses or, if this methodology is extended to the nonlinear case, their Volterra kernels. This contrasts with the more traditional "parametric" approach in which the dynamics are more compactly described using differential equations with unknown coefficients that represent the parameters to be estimated. An advantage of the kernel-based approach is that it does not limit us to a particular model structure. Although this approach is sometimes labelled as "non-parametric", the unknown coefficients of the model impulse responses nonetheless may be considered "parameters" that need to be estimated from the data. In the particular case at hand, assuming only linear dynamics, the model is formulated as:

$$\begin{aligned} \boldsymbol{PAT}_{amp}(\boldsymbol{t}) = & \int_0^{\infty} \boldsymbol{h}_{BPR}(\boldsymbol{\tau}).\boldsymbol{MAP}(\boldsymbol{t}-\boldsymbol{\tau}-\boldsymbol{T}_{BPR})\boldsymbol{d\tau} \\ & + \int_0^{\infty} \boldsymbol{h}_{RVC}(\boldsymbol{\tau}).\boldsymbol{\Delta V}(\boldsymbol{t}-\boldsymbol{\tau}-\boldsymbol{T}_{RVC})\boldsymbol{d\tau} + \boldsymbol{\varepsilon}(\boldsymbol{t}) \end{aligned} \tag{7.7}$$

In the above equation, the unknown impulse responses, representing the dynamics of baroreflex control of TPR ($h_{BPR}(\tau)$) and the dynamics of respiratory-peripheral vascular coupling ($h_{RVC}(\tau)$), have to be estimated from the measured time-series of MAP, ΔV, and PAT_{amp}. T_{BPR} and T_{RVC} are the delays associated with the two kernels, and $\varepsilon(t)$ represents the errors between the measurements and the predictions. If Eq. 7.7 is converted to discrete-time form, all the sampled values of $h_{BPR}(\tau)$ and $h_{RVC}(\tau)$ can be determined from the data using least squares or maximum likelihood estimation. This is one of the advantages of employing this kernel-based algorithm rather than the approach that requires solution of multiple differential equations. Another important point to highlight in this technique is the fact that estimation of the model parameters is carried out in the time domain. The presence of time delays allows us to impose causality on the model—allowing us to computationally "open the loop" of the closed-loop system, thereby separating the feedforward from the feedback components. Frequency domain methods do not permit this kind of temporal delineation.

Depending on the sampling interval and the memory of the systems being estimated, the number of sampled values of $h_{BPR}(\tau)$ and $h_{RVC}(\tau)$ can be large, and thus the estimation error can be substantially high. In order to reduce the level of parameterization and thus increase estimation accuracy, the impulse responses of our model components can be expanded to be the sum of weighted Laguerre (Marmarelis 1993) or Meixner (Asyali and Juusola 2005) basis functions, $B_i(t)$. For example,

$$h_{RVC}(t) = \sum_{i=1}^{q} c_i B_i(t) \tag{7.8}$$

where $B_i(t)$ represents the ith Laguerre or Meixner basis function, each of which is a known, pre-generated time series. Thus, instead of having to estimate all the sampled values of the kernels $h_{BPR}(\tau)$ and $h_{RVC}(\tau)$, we need only estimate all q unknown weights of the q basis functions. In general, q is much smaller than the total number of sampled values of the impulse responses to be estimated. Further details of this methodology may be found in Khoo (2008) and Chaicharn et al. (2009). Whereas the model kernels considered here assume linear dynamics, they can be easily extended to incorporate nonlinear dynamics (Jo et al. 2007) or time-varying parameters (Blasi et al. 2006).

Following estimation of the respiratory-peripheral vascular coupling component, $h_{RVC}(t)$, from datasets in which large sighs are present, the corresponding transfer function can be inserted into the Model A to create the extended structured model (Fig. 7.5b). Figure 7.6 (right column, "Simulation Model B") shows the frequency spectra of the relevant cardiorespiratory variables with the model operating in closed-loop mode with the same random noise inputs as in Model A (8–10 % coefficient of variation). The behaviors of Models A and B become more distinct when the comparison is made in the time domain. As one would expect, in Model B, a large sigh is followed by a significant drop in the predicted TPC, or correspondingly, a noticeable vasoconstriction (Fig. 7.7, right column, "Simulation Model B"). Further details of the methodology employed in the development of Simulation Model B and the associated minimal modeling may be found in Chalacheva and Khoo (2013).

7.7 Integrative Models

The aforementioned examples were presented to illustrate the utility of both structured and minimal models of physiological control systems. As well, the structured modeling and minimal modeling approaches are not mutually exclusive, and minimal models of system components that are not well understood can be used to characterize those components within a larger structured model. A minimal closed-loop model can be used in conjunction with a pharmacokinetic model and a model of the drug pharmacodynamics, if the objective is to quantify the drug response of a physiological variable in individuals and to extend the integrated model to characterize population responses. On the other hand, the use of a structured model of physiological control in combination with PK/PD models may offer greater insight into which mechanisms are more affected by the therapeutic intervention. Moreover, the responses elicited by the administered drug are likely to affect other organ systems that are connected with the system under study. Thus,

there is a role for comprehensive structured models that characterize multiple organ systems to play in PK\PD modeling.

One of the earliest comprehensive structured models was that of Guyton et al. (1972), which provided a detailed quantitative characterization of the circulation, focusing particularly on the mechanisms responsible for short-term and long-term control of blood pressure. This was extended to include several other organ systems (e.g., respiratory, endocrine, and neural) in a model named "Human" by Coleman and Randall (1983). "Human" has been expanded further and now takes the form of "HumMod"—a comprehensive, multilevel modeling environment for human physiology (Hester et al. 2011). PNEUMA is a somewhat less comprehensive model, one that was developed to integrate the cardiovascular, respiratory, and sleep/wake control systems in the context of sleep-related breathing disorders (Cheng et al. 2010). A schematic representation of PNEUMA is displayed in Fig. 7.8. PNEUMA has been developed using the Simulink® (Mathworks, Inc., Natick, MA) programming environment that is platform-independent. Simulink programs take the form of interconnected graphical objects, similar to the block diagrams of classical control theory. This graphical environment allows relatively easy deciphering of the mathematical structure of each model component and how they interact with one another. This format also promotes the portability of models,

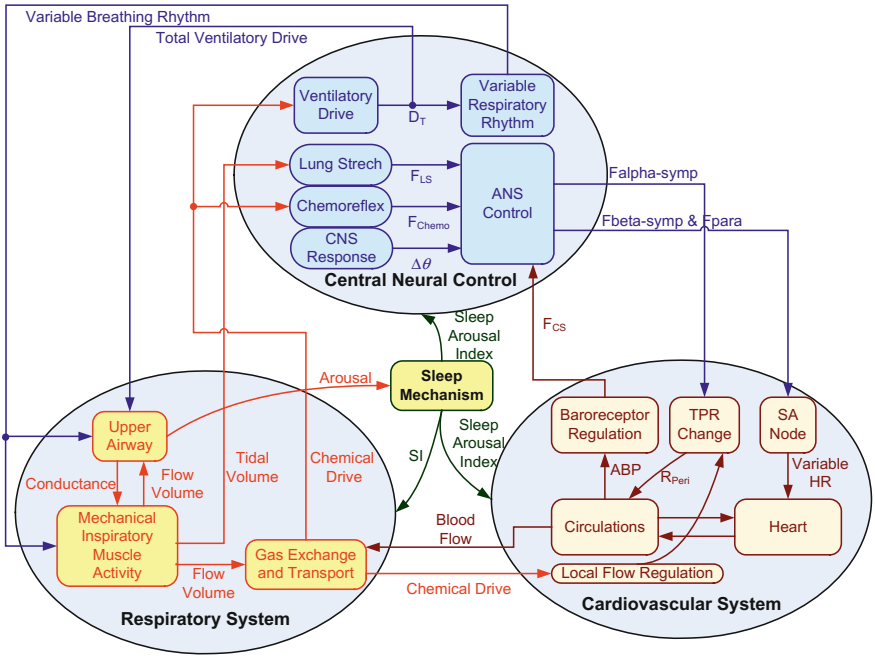

Fig. 7.8 Schematic representation of the main functional connections in PNEUMA, the comprehensive structured model of cardiorespiratory, sleep-wake, and metabolic control (reproduced with permission from Cheng et al. (2010))

thereby enhancing the free exchange of ideas and the ability to test competing models.

The programming environment of PNEUMA makes it easy to divide the large-scale model into hierarchies of nested subsystems. At the highest level in this hierarchy, the model contains three main subsystems—the respiratory, cardiovascular, and central neural control systems. Each of these main subsystems consists of a hierarchy of several levels of smaller subsystems, as illustrated in Fig. 7.9. The cardiovascular model incorporates a pulsatile cardiovascular compartment with mechanics of the heart and the systemic and pulmonary circulations. The sinoatrial node is modeled as a simple pacemaker, regulated by the parasympathetic and beta-sympathetic inputs. Heart period is generated from the SA output using an integration/saturation mechanism. The beta-sympathetic branch affects heart contractility, thus modulating the systolic period. Each atrio-ventricular compartment is characterized by a time-varying nonlinear elastance function which depends on beta-sympathetic tone. The systemic circulatory model includes a detailed arterial tree including aorta, systemic arteries, veins, capillaries, and vena cava. The pulmonary circulatory model includes pulmonary arteries, arterioles, capillaries, and veins. Total peripheral resistance incorporates vasodilation and vasoconstriction and can be affected by the alpha-sympathetic tone. The stroke volume can vary under the influence of venous return, heart period and contractility, and circulatory flow is determined by the stroke volume and vascular tone. The arterial blood pressure thus results from the interactions between the cardiac output, the peripheral resistance, and the arterial compliance.

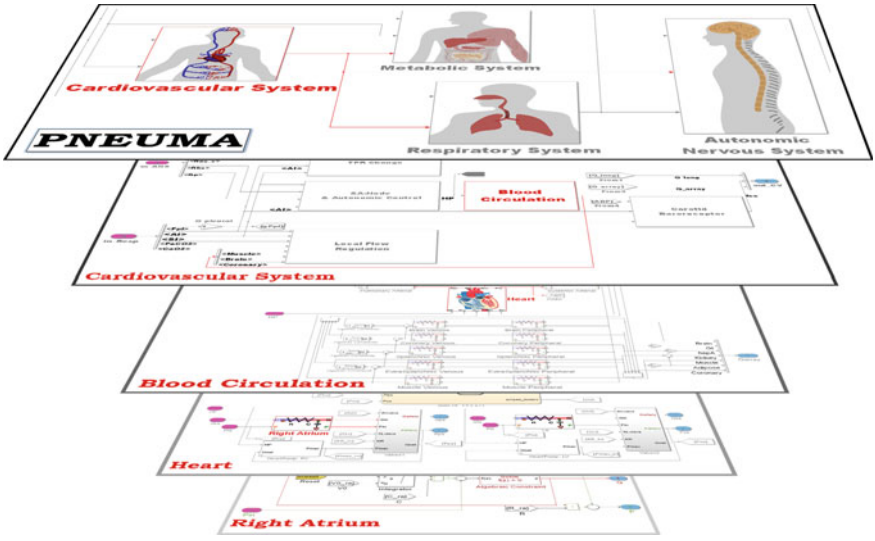

Fig. 7.9 Diagrammatic representation of the hierarchical structure of PNEUMA, a feature that is easily implemented using the Simulink® platform

The respiratory system includes both mechanical and the gas exchange mechanisms. Respiration is driven by a central neural control block and generates airflow based on the curvilinear relationship between the respiratory muscles and the lung volume, and incorporates the respiratory muscles and all necessary components for gas exchange and transport. The gas exchange and gas transport compartments model the convection and the mixing of oxygen and carbon dioxide in both the lungs and the heart, incorporating the responses to hypoxia and hypercapnia of the central and peripheral chemoreceptors.

The neural control system governs respiratory and cardiovascular activities and includes the baroreflex, chemoreflex, the pulmonary stretch reflex, respiratory sinus arrhythmia (RSA), the effect of pleural pressure on arterial blood pressure, and the influence of cardiac output on blood flow. The baroreflex is triggered by changes in arterial blood pressure, and modulate heart rate via parasympathetic and sympathetic channels. The chemoreflex includes the contribution of the central and the peripheral chemoreceptors. The lung stretch reflex increases heart rate in response to moderate lung inflation, while RSA modulates the heart rate in response to neural inspiration and expiration. Pleural pressure modulation leads to a transient decrease in blood pressure during inspiration, and blood flow determines the time delay for the gas transport to the chemoreceptor sites. The breathing period is determined by an autorhythmic generator, and, when combined with the ventilatory drive, determines the neuromuscular drive. PNEUMA also incorporates the cardiorespiratory effects of wakefulness, sleep, sleep onset, and arousal from sleep, using a sleep-wake model based on that of Borbely and Achermann (1999). Sleep is assumed to reduce heart rate and arterial blood pressure, and increase respiratory load with the concomitant decrease in ventilation.

PNEUMA has been validated by duplicating a number of important physiologic phenomena. For example, PNEUMA demonstrates spontaneous cardiovascular variability typical of normal human response, showing spectral components at 0.2–0.3 Hz and 0.05–0.15 Hz, similar to those displayed in Fig. 7.6. The sleep/wake feature of PNEUMA also enables it to simulate the complex sleep-cardiorespiratory interactions that occur during obstructive sleep apnea or Cheyne Stokes breathing (CSR). CSR, characterized by a periodic wax-wane pattern of tidal volume, occurs commonly among patients with congestive heart failure (CHF). In the more exaggerated form, CSR-CSA,, central apneas alternate with periods of hyperpnea. PNEUMA, CSR-CSA can be generated by increasing chemoreflex gain several-fold as well as reducing cardiac output, thus prolonging circulation time (Fig. 7.10, 4800–7200 s). This is compatible with published observations in CHF patients who also have CSR, that show increased chemoreflex gain and long circulation times. The cardiovascular variables, such as heart rate and arterial blood pressure, are also entrained by the waxing and waning respiratory pattern. Treatment with supplemental CO_2 ($\sim$3 % inhaled concentration) leads to a rapid and complete disappearance of the repetitive episodes of apnea, and restoration of a uniform tidal breathing pattern along with stable sleep (Fig. 7.10, 3600–4800 s). More frequently, in clinical practice, treatment is administered through O_2 supplementation. Figure 7.10 (7200–8400 s) shows that, when inhaled O_2 ($\sim$28 %) is administered,

the large fluctuations of ventilation and the cardiovascular variables are markedly attenuated. However, the periodic modulation of breath-by-breath ventilation remains. Although not displayed in Fig. 7.10, the model predicts that the periodic arousals from sleep that generally accompany the periodic pattern of ventilation disappear, even after ventilatory periodicity persists. The simulations suggest that treatment with supplemental CO_2 is more effective in eliminating CSR than

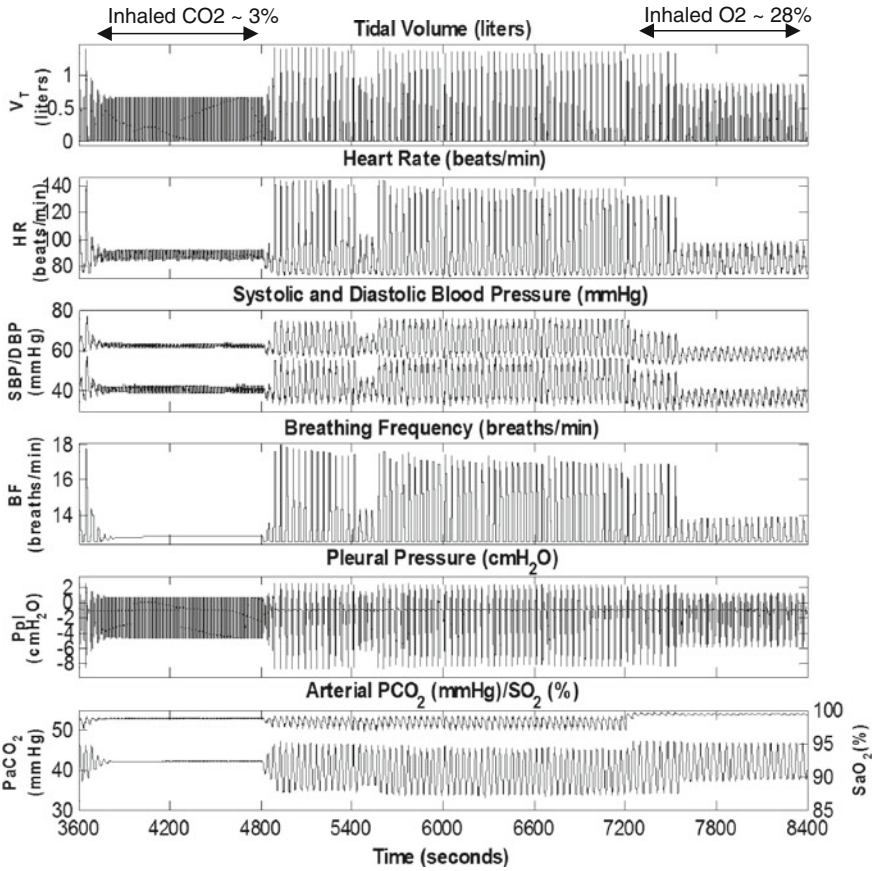

Fig. 7.10 Simulation of Cheyne-Stokes respiration with central sleep apnea (CSR-CSA) in a "subject" with congestive heart failure (4800–7200 s) using PNEUMA. Periodic waxing and waning of the respiratory pattern (VT, *top panel*) occurs with a periodicity of ~1 min. This is produced by reducing cardiac output (and thus prolonging circulation time) and increasing chemoreflex gain in the model. The periodic ventilatory pattern is accompanied by fluctuations in breathing frequency (BF) and pleural pressure (Ppl), and entrains oscillations in HR, blood pressure ("ABP"), arterial P_{CO_2}, and arterial O_2 saturation. When supplemental CO_2 (~3 % in air) is administered, the oscillations are eliminated after a couple minutes (3600–4800 s). When supplemental O_2 (~28 %) is administered, the CSR pattern is attenuated and the apneas are abolished, but an oscillatory pattern of ventilation remains (7200–8400 s)

treatment with supplemental O_2. The responses to CO_2 and O_2 administration are clearly different than what would be predicted if the regulatory or closed-loop aspects of the model were not taken into consideration.

PNEUMA has been extended to incorporate a metabolic sub-model (Cheng and Khoo 2011). The latter has been developed by combining the existing minimal model of glucose-insulin regulation by Bergman et al. (1985) with a model by Roy and Parker (2006) that includes the regulation of free fatty acid (FFA). Glucose and free fatty acid metabolism in this "extended minimal metabolic model" is also assumed to be influenced by plasma epinephrine concentrations. Inputs from the dietary intake of glucose and external interventions, such as insulin injections, have also been incorporated into the model. The primary connection between the sleep-cardiorespiratory model of PNEUMA and this extended metabolic model is the efferent sympathetic output produced by PNEUMA. Changes in sympathetic output from the cardiorespiratory portion of PNEUMA, as well as changes in sleep-wake state, lead to changes in epinephrine output, which in turn affects the metabolism of glucose, insulin, and FFA. Sympathetic activity produces higher epinephrine concentrations in the heart, muscle, and pancreas compartments. "Metabolic feedback" takes the form of changes in insulin concentration, which lead to changes in sympathetic tone through stimulation of the alpha-sympathetic receptors. Extensive testing employing sensitivity analyses has been performed to test the robustness of the model with respect to variations in the critical parameters.

Running PNEUMA to simulate physiological behavior over periods of up to 10 days leads to higher levels of blood pressure, epinephrine, FFA, and insulin, along with slightly elevated plasma glucose concentrations. Essentially, sleep apnea produces sympathetic overactivity, elevating epinephrine concentrations which stimulate glycogenolysis and gluconeogenesis, thus increasing blood glucose. This, along with the elevated epinephrine concentration, stimulates the production of insulin, which helps to attenuate the rise in blood glucose. As such, the model ends up in a hyperinsulinemic state. Although the parameters of the metabolic sub-model that collectively represent insulin sensitivity remain unchanged in the model, whole-body insulin resistance is effectively increased. The model predicts that increased severity of sleep apnea, as reflected in an increase in apnea-hypopnea index, leads to higher concentrations of fasting plasma insulin.

The extended version of PNEUMA is being used as the starting point for developing a model of disease progression linking sleep apnea and metabolic syndrome (Khoo et al. 2013). This endeavor requires the incorporation of biological and biochemical processes that occur at the cellular, and ultimately, molecular levels, thus expanding PNEUMA to become a truly multiscale model. It is anticipated that this future version of PNEUMA could be a useful tool in enhancing our understanding of the development of autonomic and metabolic dysfunction in pre-diabetic subjects. Such a comprehensive model could be used in conjunction with specific PK/PD models to investigate the efficacy of drugs that are aimed at slowing down disease progression.

7.8 Conclusion

Pharmacological responses are affected to various degrees by the homeostatic mechanisms inherent in physiological control systems. To underscore this point, in this article, we have presented examples that illustrate the basic properties of closed-loop control and how these can influence model predictions of drug responses in both the steady-state and under dynamic conditions. Physiological control systems can be modeled using two basic approaches: (a) "minimal modeling", in which all model parameters for individuals can be estimated from experiment; and (b) "structured modeling", in which the model parameters are isomorphic to key physiological entities, but not all can be identified from the measurements. These two approaches are not mutually exclusive, but can be applied in tandem and iteratively, so that one approach informs the other and vice versa. Finally, we have also highlighted the importance of modeling functional linkages and interactions across organ systems and across scales, through a brief exposition of a recently developed structured model of cardiorespiratory, sleep-wake state and metabolic control.

References

Asyali MH, Juusola M (2005) Use of meixner functions in estimation of Volterra kernels of nonlinear systems with delay. IEEE Trans Biomed Eng 52:229–237

Bauer JA, Fung HL (1994) Pharmacodynamic models of nitroglycerin-induced hemodynamic tolerance in experimental heart failure. Pharm Res 11:816–823

Bergman RN, Finegood DT, Ader M (1985) Assessment of insulin sensitivity in vivo. Endocr Rev 6:45–86

Blasi A, Jo JA, Valladares E, Juarez R, Baydur A, Khoo MC (2006) Autonomic cardiovascular control following transient arousal from sleep: a time-varying closed-loop model. IEEE Trans Biomed Eng 53:74–82

Bolton B, Carmichael EA, Sturup G (1936) Vaso-constriction following deep inspiration. J Physiol 86:83–94

Borbely AA, Achermann P (1999) Sleep homeostasis and models of sleep regulation. J Biol Rhythms 14:557–568

Cannon WB (1939) The wisdom of the body. Norton, New York

Chaicharn J, Lin Z, Chen ML, Ward SL, Keens T, Khoo MC (2009) Model-based assessment of cardiovascular autonomic control in children with obstructive sleep apnea. Sleep 32:927–938

Chalacheva P, Khoo MC (2013) An extended model of blood pressure variability: incorporating the respiratory modulation of vascular resistance. Conf Proc IEEE Eng Med Biol Soc 2013:3825–3828

Cheng L, Khoo MC (2011) Modeling the autonomic and metabolic effects of obstructive sleep apnea: a simulation study. Front Physiol 2:111

Cheng L, Ivanova O, Fan HH, Khoo MC (2010) An integrative model of respiratory and cardiovascular control in sleep-disordered breathing. Respir Physiol Neurobiol 174:4–28

Cobelli C, Distefano JJ 3rd (1980) Parameter and structural identifiability concepts and ambiguities: a critical review and analysis. Am J Physiol 239:R7–R24

Coleman TG, Randall JE (1983) HUMAN: a comprehensive physiological model. Physiologist 26:15–21

Csajka C, Verotta D (2006) Pharmacokinetic-pharmacodynamic modelling: history and perspectives. J Pharmacokinet Pharmacodyn 33:227–279

Danhof M, de Jongh J, De Lange EC, Della Pasqua O, Ploeger BA, Voskuyl RA (2007) Mechanism-based pharmacokinetic-pharmacodynamic modeling: biophase distribution, receptor theory, and dynamical systems analysis. Annu Rev Pharmacol Toxicol 47:357–400

deBoer RW, Karemaker JM, Strackee J (1987) Hemodynamic fluctuations and baroreflex sensitivity in humans: a beat-to-beat model. Am J Physiol 253:H680–H689

Derendorf H, Meibohm B (1999) Modeling of pharmacokinetic/pharmacodynamic (PK/PD) relationships: concepts and perspectives. Pharm Res 16:176–185

Francheteau P, Steimer JL, Merdjan H, Guerret M, Dubray C (1993) A mathematical model for dynamics of cardiovascular drug action: application to intravenous dihydropyridines in healthy volunteers. J Pharmacokinet Biopharm 21:489–514

Gribbin B, Pickering TG, Sleight P, Peto R (1971) Effect of age and high blood pressure on baroreflex sensitivity in man. Circ Res 29:424–431

Guyton AC, Coleman TG, Granger HJ (1972) Circulation: overall regulation. Annu Rev Physiol 34:13–46

Hester RL, Brown AJ, Husband L, Iliescu R, Pruett D, Summers R, Coleman TG (2011) Hummod: a modeling environment for the simulation of integrative human physiology. Front Physiol 2:12

Jo JA, Blasi A, Valladares EM, Juarez R, Baydur A, Khoo MC (2007) A nonlinear model of cardiac autonomic control in obstructive sleep apnea syndrome. Ann Biomed Eng 35:1425–1443

Khoo MC (2008) Modeling of autonomic control in sleep-disordered breathing. Cardiovasc Eng 8:30–41

Khoo MCK, IEEE Engineering in Medicine and Biology Society & Institute of Electrical and Electronics Engineers (2000) Physiological control systems: analysis, simulation, and estimation. IEEE Press, New York

Khoo MC, Oliveira FM, Cheng L (2013) Understanding the metabolic syndrome: a modeling perspective. IEEE Rev Biomed Eng 6:143–155

Kleinbloesem CH, van Brummelen P, Danhof M, Faber H, Urquhart J, Breimer DD (1987) Rate of increase in the plasma concentration of nifedipine as a major determinant of its hemodynamic effects in humans. Clin Pharmacol Ther 41:26–30

Lederballe Pedersen O, Christensen NJ, Ramsch KD (1980) Comparison of acute effects of nifedipine in normotensive and hypertensive man. J Cardiovasc Pharmacol 2:357–366

Macgregor GA, Rotellar C, Markandu ND, Smith SJ, Sagnella GA (1982) Contrasting effects of nifedipine, captopril, and propranolol in normotensive and hypertensive subjects. J Cardiovasc Pharmacol 4(Suppl 3):S358–S362

Madwed JB, Albrecht P, Mark RG, Cohen RJ (1989) Low-frequency oscillations in arterial pressure and heart rate: a simple computer model. Am J Physiol 256:H1573–H1579

Mager DE, Wyska E, Jusko WJ (2003) Diversity of mechanism-based pharmacodynamic models. Drug Metab Dispos 31:510–518

Malliani A, Pagani M, Lombardi F, Cerutti S (1991) Cardiovascular neural regulation explored in the frequency domain. Circulation 84:482–492

Mandema JW, Wada DR (1995) Pharmacodynamic model for acute tolerance development to the electroencephalographic effects of alfentanil in the rat. J Pharmacol Exp Ther 275:1185–1194

Marmarelis VZ (1993) Identification of nonlinear biological systems using Laguerre expansions of kernels. Ann Biomed Eng 21:573–589

Mullen TJ, Appel ML, Mukkamala R, Mathias JM, Cohen RJ (1997) System identification of closed-loop cardiovascular control: effects of posture and autonomic blockade. Am J Physiol 272:H448–H461

Mussalo H, Vanninen E, Ikaheimo R, Laitinen T, Laakso M, Lansimies E, Hartikainen J (2002) Baroreflex sensitivity in essential and secondary hypertension. Clin Auton Res 12:465–471

Roy A, Parker RS (2006) Dynamic modeling of free fatty acid, glucose, and insulin: an extended "minimal model". Diab Technol Ther 8:617–626

Saul JP, Berger RD, Albrecht P, Stein SP, Chen MH, Cohen RJ (1991) Transfer function analysis of the circulation: unique insights into cardiovascular regulation. Am J Physiol 261:H1231–H1245

Schnall RP, Shlitner A, Sheffy J, Kedar R, Lavie P (1999) Periodic, profound peripheral vasoconstriction—a new marker of obstructive sleep apnea. Sleep 22:939–946

Zuideveld KP, Maas HJ, Treijtel N, Hulshof J, van der Graaf PH, Peletier LA, Danhof M (2001) A set-point model with oscillatory behavior predicts the time course of 8-OH-DPAT-induced hypothermia. Am J Physiol Regul Integr Comp Physiol 281:R2059–R2071

Part II
Pharmacodynamics

Chapter 8
Foundations of Pharmacodynamic Systems Analysis

William J. Jusko

Abstract The pillars of pharmacodynamic modeling are the pharmacokinetics of the drug, the nature of the pharmacology that underlies drug interactions with their targets, and the physiology of the system considering molecular to whole body levels of organization and functioning. This chapter provides a general assessment of the fundamental components and some interactions of each of these pillars indicating how they serve as building blocks for systems models. Key elements of pharmacokinetics include the operation of Fick's Laws for diffusion and perfusion along with the often nonlinear mechanisms of drug distribution and elimination. Target-binding relationships in pharmacology evolve from the law of mass action producing capacity-limitation in most operative control functions. Mammalian physiology and pathophysiology feature a wide breadth of turnover rates for biological compounds, structures, and functions ranging from rapid electrical signals to lengthy human lifespans, which often determine the rate-limiting process and basic type of model to be applied. Appreciation of the diverse array, mechanisms, and interactions of individual components that comprise the pillars of pharmacodynamics can serve as the foundation for building more complex systems models.

Keywords Fick's laws · Target-binding · Drug-biological interface · Affinity · Capacity · Substrate control · Operational efficacy · Turnover · Homeostasis · Gaddum equation

8.1 Introduction

The three pillars of pharmacodynamics (PD), as depicted in Fig. 8.1, are the pharmacokinetics (PK) of the drug, the pharmacology and mechanism of the drug-biological interface, and the physiology or pathophysiology of the system

W.J. Jusko (✉)
Department of Pharmaceutical Sciences, University at Buffalo,
404 Kapoor Hall, Buffalo, NY, USA
e-mail: wjjusko@buffalo.edu

D.E. Mager and H.H.C. Kimko (eds.), *Systems Pharmacology and Pharmacodynamics*,
AAPS Advances in the Pharmaceutical Sciences Series 23,
DOI 10.1007/978-3-319-44534-2_8

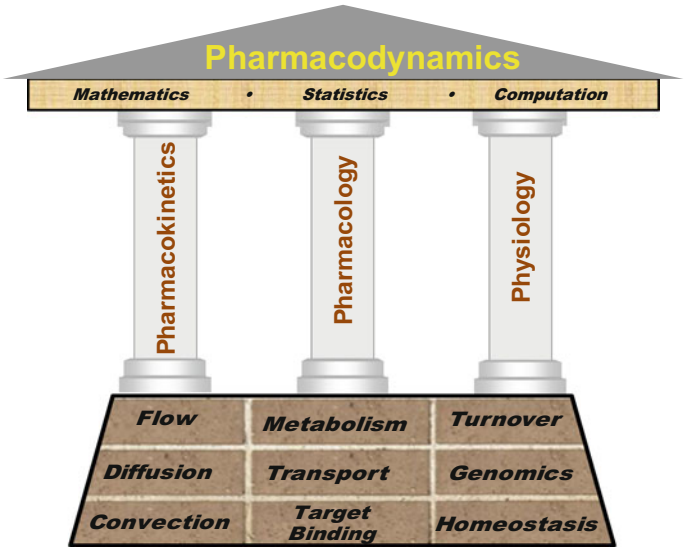

Fig. 8.1 The palace of pharmacodynamics with its foundation, structural components, and three pillars

being altered by the drug (Mager et al. 2003; Jusko 2013). Each can contribute to the extent and time-course of observed pharmacodynamic responses depending on their intrinsic properties and rate-limiting step(s). The foundations of systems analysis will be explored by delineating the basic "rules of biology" for the major components that govern each of the pillars of pharmacodynamics. Along with the determinants of PK, two general principles, namely capacity-limitation and turnover, form the basis for a variety of commonly used PK/PD and systems models. Genomics is included in Fig. 8.1 as the presence, location, and functioning of determinants of PK/PD are governed by genomics and genetics. The quantitative skills of mathematics, statistics, and computation are needed to identify relationships, integrate them into models, analyze experimental data, and perform simulations.

8.2 Pharmacokinetics

Common approaches for analyzing pharmacokinetic data utilize noncompartmental, compartmental (mammalian), and physiological concepts and methods, with ascending degrees of complexity. Physiologically-based PK (PBPK) models provide mechanistic and insightful separation of drug and systems properties as well as their interfaces and interactions. Three key relationships that underpin drug distributional processes in PBPK models are:

$$\text{Fick's Law of Diffusion:} \quad \frac{dA}{dt} = PS(C_h - C_l)$$

where the rate of drug movement (Amount/time, *dA/dt*) from higher (C_h) to lower (C_l) concentrations is governed by the permeability-surface area (*PS*) coefficient (Fick 1855). Permeability (*P*) is governed by molecular size and lipid solubility of the compound along with the nature of the biological membrane and its surface area (*S*). This equation is often invoked to describe small molecule (drug) absorption rates, movement between interstitial fluids (ISF) and cell water spaces, and has been adapted to account for biophase distribution of drugs.

$$\text{Fick's Law of Perfusion:} \quad \frac{dA}{dt} = Q(C_a - C_v)$$

where the rate of organ uptake (*dA/dt*) is governed by arterial (C_a) and venous (C_v) drug concentrations and organ blood flow (Q) (Teorell 1937). The ratio of $(C_a - C_v)/C_a$ is also termed the Extraction Ratio (*ER*). This equation is commonly used in PBPK models to describe drug distribution to various organs and tissues via blood flow.

$$\text{Convection:} \quad \frac{dA}{dt} = L(1-\sigma)\cdot C = f_L \cdot Q(1-\sigma)\cdot C$$

where organ uptake of molecules is determined by water movement equaling lymph flow (L) and the vascular reflection coefficient (σ) associated with water flux across capillary membranes into ISF (Renkin 1979). Lymph flow is usually assumed as a small fraction (f_L = 0.02–4 %) of blood flow to each organ or tissue as determined by the Starling (1896) approximation, while the reflection coefficient varies with type of organ capillaries (some 'leaky' such as liver, some 'tight' such as muscle). This equation is used in PBPK models of monoclonal antibodies (mAbs) and other large molecules to describe their limited and slow movement from plasma to ISF (Cao et al. 2013). Glomerular filtration rate is primarily a convection process as well.

The joint roles of blood flow and permeability for control of the distribution of molecules from blood to tissues is termed Distribution Clearance (CL_d) in PK and quantified as:

$$CL_d = f_d \cdot Q = Q\left(1 - e^{-PS/Q}\right)$$

where f_d is the fraction of Q accounting for organ uptake of drug, *PS* is the rate-limiting factor when Q is small, and Q is the rate-limiting factor when *PS* is large (Stec and Atkinson 1981).

The array of nonlinear protein binding, metabolism, transport, and clearance relationships commonly encountered in PK are listed in Table 8.1 (Jusko 1989).

Table 8.1 Common capacity-limited functions in pharmacokinetics

Process	Function	Equation	Capacity	Affinity	Substrate	References
Metabolism	Metabolite (M) formation rate	$\frac{dM}{dt} = \frac{V_{max} \cdot C}{K_m + C}$	V_{max}	K_m	Concentration	Michaelis and Menten (1913)
Transport	Flux	$\frac{dA_T}{dt} = \frac{V_{max} \cdot C}{K_m + C}$	V_{max}	K_m	Concentration	Shannon (1939)
Protein binding	Bound drug	$D_b = \frac{n \cdot P_t \cdot D_f}{1/K_A + D_f}$	n: No. Binding Sites P_t: Protein Conc.	K_A: Equilibrium Association constant	D_f: free drug	Goldstein, (1949)
Organ clearance	Clearance	$CL = \frac{Q \cdot CL_{\text{int}}}{Q + CL_{\text{int}}}$	Q: Blood Flow	CL_{int}: Intrinsic clearance	Concentration	Rowland et al. (1973) and Wilkinson and Shand (1975)

They all evolve from the law of mass action where the limited quantity of binding substances, metabolic enzymes, or transporters results in capacity-limited processing of drugs and other substrates. At low drug concentrations, the functions operate linearly, such as with the common relationship for intrinsic clearance, $CL_{int} = V_{max}/K_m$, pertaining to drug metabolism. Often the preferred or operative drug concentration is the free or unbound drug in either plasma or in tissues. These distributional and elimination relationships are components of full PBPK models and are presented here partly owing to their fundamental value in PK, but also because they are helpful in describing the kinetics of physiological substances or biomarkers when analyzed in PK/PD and systems models. For example, the PK/PD modeling of cortisol as an indicator of adrenal suppression and of nitrate as a biomarker of inflammation is best handled by considering their intrinsic kinetics (Krzyzanski and Jusko 2001; Sukumaran et al. 2012).

8.3 Pharmacology

The interaction of drugs (D) with their biophase targets (R) is the interface that controls the array of subsequent genomic, proteomic, biochemical, and physiological changes. These targets may be receptors, enzymes, transporters, ion channels, and/or DNA. A common feature is that the concentration or quantity of such targets is limited and can be described with the law of mass action:

$$D + R \underset{k_{off}}{\overset{k_{on}}{\rightleftharpoons}} DR$$

as described by:

$$\frac{dR}{dt} = k_{on} \cdot D \cdot R - k_{off} \cdot DR$$

where k_{on} is the association rate constant, k_{off} is the dissociation rate constant and, at equilibrium, the equilibrium dissociation constant is $K_D = k_{off}/k_{on}$. This type of interaction leads to a nonlinear relationship that the author calls "The Equation of Life":

$$Function = \frac{Capacity \cdot Substrate}{Affinity + Substrate}$$

In this fashion, *Capacity*, *Affinity*, and *Substrate* control numerous biological processes: those involved in PK as listed in Table 8.1 and those describing many pharmacological actions as listed in Table 8.2. These pharmacologic processes or

Table 8.2 Common capacity-limited functions in pharmacology

Process	Function	Equation	Capacity	Affinity	Substrate	References
Receptor binding	Bound drug	$D_b = \frac{B_{max} \cdot D_f}{K_D + D_f}$	B_{max}	K_D or $\frac{k_{off}}{k_{on}}$	D_f: free drug	Clark (1933)
PD effects	Direct effect	$E = \frac{E_{max} \cdot C^{\gamma}}{EC_{50}^{\gamma} + C^{\gamma}}$	E_{max}	EC_{50}	C or C^{γ} γ = Hill Coefficient	Hill (1910)
Transduction	Effect	$E = \frac{[AR]^n \cdot E_m}{K_E^n + [AR]^n}$	E_m	K_E: Transducer Constant	$[AR]$: Agonist-receptor concentration n: Power Coefficient	Black and Leff (1983)
Cytotoxicity	Killing rate	$-\frac{dR}{dt} = \frac{K_{max} \cdot C}{KC_{50} + C}$	K_{max}	KC_{50}	Concentration	Jusko (1971), Zhi et al. (1988)
Inhibition	Altered input or removal	Fractional Change $= 1 - \frac{I_{max} \cdot C}{IC_{50} + C}$	I_{max}	IC_{50}	Concentration	Dayneka et al. (1993), Jusko and Ko (1994)
Stimulation	Altered input or removal	Numerical change $= 1 + \frac{S_{max} \cdot C}{SC_{50} + C}$	S_{max}	SC_{50}	Concentration	Dayneka et al. (1993) and Jusko and Ko (1994)

mechanisms include receptor binding, transduction, cytotoxicity, inhibitory and stimulatory changes, as well as simple directly observed drug effects.[1]

It is important to appreciate the need for sufficiently high doses or drug concentrations to attain an observed maximum response (*Capacity*) and the occurrence of the *Affinity* constant at concentrations when responses equal one-half of *Capacity*. Such conditions facilitate operation of all PK/PD models and assist in resolution of the parameter values (Dutta et al. 1996; Krzyzanski et al. 2006). Some of the relationships include a power coefficient (n, γ) accompanying the concentration and *Affinity* terms. Although this power coefficient may not have a mechanistic basis, it sometimes adds flexibility in fitting pharmacological data. Of special note is that the *Affinity* term in the equations is of the nature that lower, rather than higher, concentration values reflect greater potency of the drug.

The simple pharmacologic relationships listed in Table 8.2 have been applied for a vast array of drugs and response measures. However, pharmacology textbooks may offer additional more complex relationships that have usually evolved from in vitro systems (Kenakin 1997). One of note is the Adair equation (1925) relevant for biphasic or hormesis drug effects:

$$E = \frac{E_{max} \cdot C}{EC_{50} + C + K_2 \cdot C^2}$$

where K_2 is a secondary binding coefficient. This equation produces a bell-shaped Effect (E) versus concentration (C) relationship. Cao et al. (2012) applied this equation to describe the effects of GLP-1 on stimulating insulin secretion for a wide range of doses examined in rats.

Another complex relationship of considerable value is the Black and Leff (1983) equation for nonlinear transduction of the effects of an agonist:

$$Effect = \frac{E_m \cdot \tau^n \cdot C^n}{(K_D + C)^n + \tau^n \cdot C^n}$$

where τ is Operational Efficacy defined as B_{max}/K_E (other symbols are defined in Table 8.2). Resolution of all parameters in this equation may require assessment of both nonlinear drug-receptor binding (B_{max}, K_D) as well as nonlinear responses (E_m, K_E) in relation to receptor occupancy. This equation is of great value as the PK and drug-receptor interactions are usually specific for individual compounds, while the subsequent events yielding an effect are controlled by the biological transduction or signaling system. One applied example is where the plasma concentrations of methylprednisolone were found to control receptor binding while the receptor

[1]The author tells his students that this equation will also predict their future success in pharmacometrics: a function of the combination of brain capacity (IQ), affinity for mathematics, statistics, and computation, and the relevant assimilated information (coursework and studies).

binding of free and liposomal-incorporated drug served as the basis for the time-course of immunosuppression for lymphocytes in the spleen of rats (Mishina and Jusko 1994).

8.4 Physiology

Nearly all mechanistic PD models are based on the concepts of turnover and homeostasis (Mager et al. 2003; Jusko 2013). Biological compounds (biomarkers), structures, and functions are continually being produced and degraded. The starting condition or baseline of most PD models is thus the steady-state that exists in the organism. Numerous physiological controls can be invoked to maintain homeostasis of the system and factor being measured.

Figure 8.2 provides a listing of many biological entities that have served as PD measures. Their time-frames for turnover range from very fast (electrical signals) to very slow (human lifetimes). The factors in the upper part of the list are often biomarkers of body processes while the lower components may require clinical measures of major organ or system functioning (e.g., arthritis or depression symptom scores). Of course, patient survival is a key endpoint in cancer chemotherapy where measurements are made in a population sense.

The turnover rate may determine which type of PK/PD model applies. For very rapid turnover processes, direct effect or biophase models are relevant as the PK of the drug will be rate-limiting in controlling observed responses. When the production (k_{in}) and loss (k_{out}) rates of the biological factors are slower and directly altered by drugs, indirect response models pertain. As systems become more complex with multiple controls, then transduction, multi-component, or systems models are needed. These time-frames also determine study designs as slow processes need lengthier monitoring of the response measures.

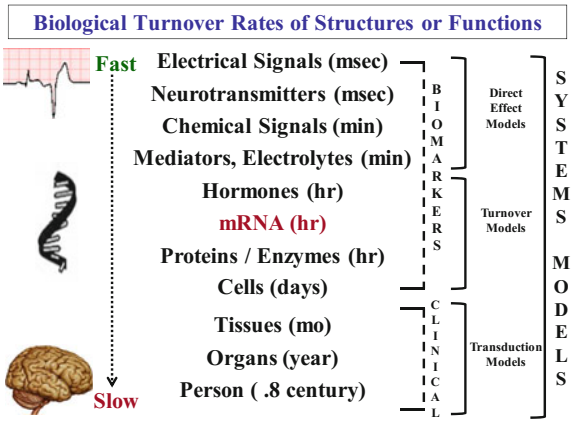

Fig. 8.2 Diversity of turnover rates and models (adapted from Mager and Jusko 2008)

Table 8.3 Basic types of turnover models or components used in pharmacodynamics

Model type	Diagram	Input function	Loss function	References
Indirect response	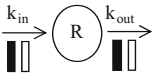	k_{in} (drug modified) Zero-order	k_{out} (drug modified) First-order	Dayneka et al. (1993), Jusko and Ko (1994)
Precursor-indirect	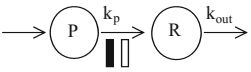	$k_p \cdot P$ (drug modified) First-order	k_{out} First-order	Sharma et al. (1998)
Cytotoxicity		k_g First-order	$k_l \cdot C$ (drug modified) Second-order	Jusko, (1971), Zhi et al. (1988)
Irreversible	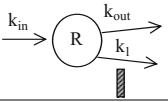	k_{in} Zero-order	$k_l \cdot C$ (drug modified) Second-order	Yamamoto et al. (1996)
Transit	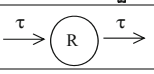	First-order $1/\tau$	First-order $1/\tau$	Sun and Jusko (1998)
Feedback–Tolerance (Tol)		k_t First-order	k_t First-order	Friberg et al. (2002)
Receptor binding Target-mediated	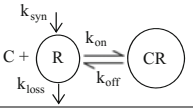	$k_{on} \cdot C \cdot R$ Second-order	$k_{off} \cdot CR$ First-order	Shimada et al. (1996), Mager and Jusko (2001)

▮ Usually nonlinear inhibition: $\left(1 - \frac{I_{max} \cdot C}{IC_{50} + C}\right)$

▯ Usually nonlinear stimulation: $\left(1 + \frac{S_{max} \cdot C}{SC_{50} + C}\right)$

▨ Drug-induced loss may be simple 2nd-order $k_l \cdot C \cdot R$ or nonlinear: $\left(\frac{K_{max} \cdot C}{KC_{50} + C}\right) \cdot R$

Turnover and homeostasis are part of most of the basic PD models or components currently known.[2] Homeostasis reflects the baseline and final steady-state condition of body systems before and after drug administration and the diverse feedback and set-point mechanisms that help maintain normal functioning. The primary PD turnover models are depicted in Table 8.3 with indication of input and loss functions, types of rate processes, and commonly associated pharmacological functions. In the receptor and target-mediated models, turnover may be viewed as drug binding and dissociating from receptors particularly when k_{on} is relatively slow (Swinney 2009). The synthesis (k_{syn}) and degradation (k_{deg}) rates of the receptors also contribute to the PD, particularly for longer studies. The Precursor model and Feedback component are often employed to account for tolerance and rebound phenomena.

[2]Here turnover is generalized to include any process where the response or control factor is affected by production and loss. Some authors consider only basic indirect response models as turnover models.

The listings in Table 8.3 provide the most basic models or components. Various complexities can be added to any model such as transit steps, feedback, additional compartments, circadian baselines (Krzyzanski et al. 2000a), disease-altered baselines (Lepist and Jusko 2004), life-span loss (Krzyzanski et al. 2000b), and/or physiological limits in responses (Yao et al. 2006).

8.5 Disease Progression

Disease progression models often reflect the time-course of disturbance of PD baselines, turnover components, or subsystems with changes in homeostasis (Mould et al. 2007; Earp et al. 2008a, b). A classic disease model for cell proliferation and tumor growth is the 'resistance to death' Gompertz function (1825) as shown in the modern convenient form:

$$N = N_{ss} \cdot e^{-\ln\frac{N_{ss}}{N_0} \cdot e^{-kg \cdot t}}$$

where k_g is a first-order growth constant, N_0 is the initial number, and N_{ss} is the steady-state number of cells, tumor size, and/or body mass. This equation accounts for early exponential growth with an ultimate attainment of a plateau value.

The simpler, preferred equation used for size measures or numbers of cells in many chemotherapy studies is the logistic function (Robertson 1923):

$$Growth\ Rate = k_g\left(1 - \frac{N_0}{N_{ss}}\right) \cdot N$$

Cell proliferation rates have also been modeled with an adaptation of the Michaelis-Menten equation (Meagher et al. 2004). All of these growth or disease models are "Equations of Life" in a somewhat different format as they are nonlinear and exhibit capacity-limitation.

8.6 Drug Interactions

The wealth of existing drug-drug interactions and quantitative methods are well-appreciated in pharmacokinetics. When two or more drugs are administered, additional interactions can occur owing to either the nature of their pharmacological mechanisms or their alteration of the same or convergent turnover process or both.

The isobolograph approach based on Loewe Additivity (1926) is often used in assessing pharmacologic interactions of two agents (Gessner 1974). However, this and most drug interaction methodology in pharmacology has involved measurement of a static endpoint and do not take into account the PK/PD time-course of

drug action. Fortunately, time-honored mechanistic equations allow the PK to be incorporated into their interaction relationships:

Gaddum (1937) Equation for Competitive Interactions:

$$E_{A+B} = \frac{E_{max_A} \cdot \frac{C_A}{EC_{50_A}} + E_{max_B} \cdot \frac{C_B}{EC_{50_B}}}{\frac{C_A}{EC_{50_A}} + \frac{C_B}{EC_{50_B}} + 1}$$

where C_A is the concentration of agonist and C_B is the concentration of a drug competing for the same target site. This equation is applicable for two agents typically having similar molecular structures and targets. The Gaddum equation simplifies for an antagonist when $E_{maxB} = 0$ as:

$$Effect = \frac{E_{maxA} \cdot C_A}{C_A + EC_{50A}\left(1 + \frac{C_B}{EC_{50B}}\right)}$$

The ability to fully resolve antagonistic drug effects requires careful assessment of the actions of the agonist to obtain its E_{maxA} and EC_{50A} values and further examining the offsetting effects of the antagonist in order to calculate EC_{50B}. It is difficult to do this in most in vivo studies, but Mandema et al. (1992) accomplished this in quantifying the agonist effects of midazolam and antagonistic action of flumazenil in studies in human subjects.

Ariens et al. (1957) provided basic equations for more complex drug interactions such as noncompetitive, uncompetitive, and irreversible drug combinations that require careful enactment for experimental data. The Kenakin (1997) book provides highly useful instructions regarding these diverse relationships.

If one of these basic mechanistic equations does not suffice in accounting for the joint effects of two agents, then an empirical drug interaction parameter (ψ) can be introduced by multiplying it times one of the EC_{50} terms. Chakraborty et al. (1999) used the inhibitory forms of the Gaddum equation and Ariens equations and demonstrated how adding the ψ term allowed assessment of possible immunosuppressive interactions between IL-10 and prednisolone for inhibiting lymphocyte proliferation. In fitting joint drug data, $\psi < 1$ reflects synergy and $\psi > 1$ reflects antagonism. Another interpretation, if ψ does not equal 1, is that a more complex mechanism may exist than accounted for by these basic interaction equations.

Turnover models often allow a mechanistic approach for discernment of natural synergy occurring for two or more drugs. Earp et al. (2004) provided equations for indirect response models and demonstrated how strong synergism can result when there is either joint inhibition of k_{in} and stimulation of k_{out} or, conversely, stimulation of k_{in} and inhibition of k_{out}. The principle that synergy or augmented drug

effects are produced by opposing drug effects on the two sides of a turnover process also applies in chemotherapy when inhibition of growth along with cytotoxicity on the loss side occur. This was nicely demonstrated for the effects of rituximab and rhApo2L on tumor xenografts in a small systems model enacted by Harrold et al. (2012).

8.7 Summary and Prospectus

This compilation of PK/PD models and components provides a 'toolbox' of kinetic processes, pharmacological functions, and turnover features of major basic models. Enhanced PK/PD or small to large systems models can often be assembled by consideration of the sequence of events leading to an observed drug effect and utilization of the appropriate mechanistic pieces that capture major rate-limiting steps. For example, Earp et al. (2008a, b) described disease progression in arthritic rats and inhibitory effects of dexamethasone on pro-inflammatory cytokines and edema with model components that included PK, receptor binding, transduction, competitive interactions, end organ Turnover (paw and bone), and inhibitory pharmacological functions. Similarly, Fang et al. (2013) assembled a small systems model to account for the diabetogenic effects of methylprednisolone in a meta-analysis of receptor, genomic, and biomarker (glucose, insulin, FFA) data from several studies in rats. The similarity that exists for numerous capacity-limited pharmacologic and disease progression functions and the fundamental nature of diverse turnover processes greatly facilitates the meshing of these components in assembling complex models.

Acknowledgments This work was supported by NIH Grants GM 24211 and GM 57980 and by the University at Buffalo Center of Excellence in Pharmacokinetics and Pharmacodynamics. Technical assistance was provided by Mrs. Suzette Mis. The author greatly appreciates the mentorship and friendship of Gerhard Levy, deemed the "Father of Pharmacodynamics", for his seminal contributions in recognizing concepts and models for simple direct drug effects (Levy 1966), indirect responses (Nagashima et al. 1969), target-mediated drug disposition (Levy 1994), and many other aspects of PK/PD.

References

Adair GS (1925) The hemoglobin system. VI. The oxygen dissociation curve of hemoglobin. J Biol Chem 63:529–545

Ariens EJ, Van Rossum JM, Simonis AM (1957) Affinity, intrinsic activity and drug interactions. Pharmacol Rev 9:218–236

Black JW, Leff P (1983) Operational models of pharmacological agonism. Proc R Soc Lond B Biol Sci 220:141–162

Cao Y, Gao W, Jusko WJ (2012) Pharmacokinetic/pharmacodynamic modeling of GLP-1 in healthy rats. Pharm Res 29:1078–1086

Cao Y, Balthasar JP, Jusko WJ (2013) Second-generation minimal physiologically-based pharmacokinetic model for monoclonal antibodies. J Pharmacokin Pharmacodyn 40:597–607
Chakraborty A, Blum RA, Cutler DL, Jusko WJ (1999) Pharmacoimmunodynamic interactions of IL-10 and prednisone in healthy volunteers. Clin Pharmacol Ther 65:304–318
Clark AJ (1933) The mode of action of drugs on cells. Edward Arnold, London
Dayneka N, Garg V, Jusko WJ (1993) Comparison of four basic models of indirect pharmacodynamic responses. J Pharmacokin Biopharm 21:457–478
Dutta A, Matsumoto Y, Ebling WF (1996) Is it possible to estimate the parameters of the sigmoid Emax model with truncated data typical of clinical studies? J Pharm Sci 85:232–239
Earp J, Krzyzanski W, Chakraborty A, Zamacona MK, Jusko WJ (2004) Assessment of drug interactions relevant to pharmacodynamic indirect response models. J Pharmacokin Pharmacodyn 31:345–380
Earp JC, DuBois DC, Molano DS, Pyszczynski NA, Keller CE, Almon RR, Jusko WJ (2008a) Modeling corticosteroid effects in a rat model of rheumatoid arthritis I: mechanistic disease progression model for the time course of collagen-induced arthritis in Lewis rats. J Pharmacol Exp Ther 326:532–545
Earp JC, DuBois DC, Molano DS, Pyszczynski NA, Almon RR, Jusko WJ (2008b) Modeling corticosteroid effects in a rat model of rheumatoid arthritis II: mechanistic pharmacodynamic model for dexamethasone effects in Lewis rats with collagen-induced arthritis. J Pharmacol Exp Ther 326:546–554
Fang J, Sukumaran S, DuBois DC, Almon RR, Jusko WJ (2013) Meta-modeling of methylprednisolone effects on glucose regulation in rats. PLoS ONE 8:e81679
Fick A (1855) On liquid diffusion. Philos Mag 10:30–39
Friberg LE, Henningsson A, Maas H, Nguyen L, Karlsson MO (2002) Model of chemotherapy-induced myelosuppression with parameter consistency across drugs. J Clin Oncol 20:4713–4721
Gaddum JH (1937) The quantitative effects of antagonistic drugs. J Physiol 89:7P–9P
Gessner PK (1974) In: Moselli PL, Garattini S, Cohen SN (eds) Drug interactions. Raven Press, New York
Goldstein A (1949) The interaction of drugs and plasma proteins. Pharmacol Rev 1:102–165
Gompertz B (1825) On the nature of the function expressive of the law of human mortality, and on a new mode of determining the value of life contingencies. Philos Trans R Soc Lond 36:513–585
Harrold JM, Straubinger RM, Mager DE (2012) Combinatorial chemotherapeutic efficacy in non-Hodgkin lymphoma can be predicted by a signaling model of CD20 pharmacodynamics. Cancer Res 72:1632–1641
Hill AV (1910) The possible effects of the aggregation of the molecules of haemoglobin on its dissociation curves. J Physiol 40:iv–vii
Jusko WJ (1971) Pharmacodynamics of chemotherapeutic effects: Dose-time–response relationships for phase-nonspecific agents. J Pharm Sci 60:892–895
Jusko WJ (1989) Pharmacokinetics of capacity-limited pharmacokinetic systems. J Clin Pharmacol 29:488–493
Jusko WJ (2013) Moving from basic toward systems pharmacodynamics models. J Pharm Sci 102:2930–2940
Jusko WJ, Ko HC (1994) Physiologic indirect response models characterize diverse types of pharmacodynamic effects. Clin Pharmacol Ther 56:406–419
Kenakin TP (1997) Pharmacologic analysis of drug-receptor interaction, 3rd edn. Raven Press, New York
Krzyzanski W, Chakraborty A, Jusko WJ (2000a) Algorithm for application of Fourier analysis for biorhythmic baselines of pharmacodynamic indirect response models. Chronobiol Internat 17:77–93
Krzyzanski W, Ramakrishnan R, Jusko WJ (2000b) Basic pharmacodynamic models for agents which alter production of natural cells. J Pharmacokin Biopharm 27:467–489

Krzyzanski W, Jusko WJ (2001) Indirect pharmacodynamic models for responses with multicompartmental distribution or polyexponential disposition. J Pharmacokin Pharmacodyn 28:57–78
Krzyzanski W, Dmochowski J, Matsushima N, Jusko WJ (2006) Assessment of dosing impact on intra-individual variability in estimation of parameters for basic indirect response models. J Pharmacokin Pharmacodyn 33:635–655
Lepist E-I, Jusko WJ (2004) Modeling and allometric scaling of s(+)ketoprofen pharmacokinetics and pharmacodynamics: a retrospective analysis. J Vet Pharmacol Ther 27:211–218
Levy G (1966) Kinetics of pharmacologic effects. Clin Pharmacol Ther 7:362–372
Levy G (1994) Pharmacologic target-mediated drug disposition. Clin Pharmacol Ther 56:248–252
Loewe S, Muischnek H (1926) Effect of combinations: mathematical basis of the problem. Arch Exp Pathol Pharmakol 114:313–326
Mager DE, Jusko WJ (2001) General pharmacokinetic model for drugs exhibiting target-mediated drug disposition. J Pharmacokin Biopharm 28:507–532
Mager DE, Jusko WJ (2008) Development of translational pharmacokinetic-pharmacodynamic models. Clin Pharmacol Ther 83:909–912
Mager DE, Wyska E, Jusko WJ (2003) Diversity of mechanism-based pharmacodynamic models. Drug Met Disp 31:510–518
Mandema JW, Tukker E, Danhof M (1992) In vivo characterization of the pharmacodynamic interaction of a benzodiazepine agonist and antagonist: midazolam and flumazenil. J Pharmacol Exp Ther 260:36–44
Meagher AK, Forrest A, Dahhoff A, Stass H, Schentag JJ (2004) Novel pharmacokinetic-pharmacodynamic model for prediction of outcomes with an extended-release formulation of ciprofloxacin. Antimicrob Agents Chemother 48:2061–2068
Michaelis L, Menten ML (1913) Die Kinetik der Invertinwirkung. Biochem Z 49:333–369
Mishina EV, Jusko WJ (1994) Inhibition of rat splenocyte proliferation with methylprednisolone: in vivo effect of liposomal formulation. Pharm Res 11:848–854
Mould DR, Denman NG, Duffull S (2007) Using disease progression models as a tool to detect drug effect. Clin Pharmacol Ther 82:81–86
Nagashima R, O'Reilly RA, Levy G (1969) Kinetics of pharmacologic effects in man: the anticoagulant action of warfarin. Clin Pharmacol Ther 10:22–35
Renkin EM (1979) Relation of capillary morphology to transport of fluid and large molecules. Acta Physiol Scand Suppl 463:81–91
Robertson TB (1923) The chemical basis of growth and senescence, Lippincott, Philidelphia
Rowland M, Benet L, Graham C (1973) Clearance concepts in pharmacokinetics. J Pharmacokin Biopharm 1:123–136
Shannon JA (1939) Renal tubular excretion. Physiol Rev 19:63–93
Sharma A, Ebling WF, Jusko WJ (1998) Precursor-dependent indirect pharmacodynamic response model for tolerance and rebound phenomena. J Pharm Sci 87:1577–1584
Shimada S, Nakajima Y, Yamamoto K, Sawada Y, Iga T (1996) Comparative pharmacodynamics of eight calcium channel blocking agents in Japanese essential hypertensive patients. Biol Pharm Bull 19:430–437
Starling EH (1896) On the absorption of fluids from connective tissue spaces. J Physiol 19:312–326
Stec GP, Atkinson AJ (1981) Analysis of the contributions of permeability and flow to intercompartmental clearance. J Pharmacokin Biopharm 9:167–180
Sukumaran S, Lepist E-I, DuBois DC, Almon RR, Jusko WJ (2012) Pharmacokinetic/pharmacodynamic modeling of methylprednisolone effects on iNOS mRNA expression and nitric oxide during LPS-induced inflammation in rats. Pharm Res 29:2060–2069
Sun Y-N, Jusko WJ (1998) Transit compartments versus gamma distribution function to model signal transduction processes in pharmacodynamics. J Pharm Sci 87:732–737
Swinney DC (2009) The role of binding kinetics in therapeutically useful drug action. Curr Opin Drug Discov Devel 12:31–39
Teorell T (1937) Kinetics of distribution of substances administered to the body. II. The intravascular modes of administration. Arch Int Pharmacodyn Ther 57:226–240

Wilkinson G, Shand D (1975) A physiologic approach to hepatic drug clearance. Clin Pharmacol Ther 18:377–390

Yamamoto K, Abe M, Katashima M, Yamada Y, Sawada Y, Iga T (1996) Pharmacodynamic analysis of antiplatelet effect of aspirin in the literature—modeling based on inhibition of cyclooxygenase in the platelet and the vessel wall endothelium. Jpn J Hosp Pharm 22:133–141

Yao Z, Krzyzanski W, Jusko WJ (2006) Assessment of basic indirect response models with physiological limits. J Pharmacokin Pharmacodyn 33:167–193

Zhi JG, Nightingale CH, Quintiliani R (1988) Microbial pharmacodynamics of piperacillin in neutropenic mice of systematic infection due to Pseudomonas aeruginosa. J Pharmacokinet Biopharm 16:355–375

Chapter 9
Direct, Indirect, and Signal Transduction Response Modeling

Wojciech Krzyzanski

Abstract Based on the paradigm of mechanistic modeling, three types of pharmacodynamic models are introduced: direct effect, indirect response, and signal transduction. The underlying pharmacological and biological assumptions about the model structures and operations are provided along with examples of their applications. A brief historical perspective is introduced for each model class. Mathematical equations defining the model are presented and explored to link model parameters with model characteristics such as the shape of the response curve. The impact of dose on the time courses of pharmacodynamic responses is evaluated for large doses and exemplified with computer simulations. A common theme is the extent of delay between drug pharmacokinetics and response. When relevant, alternative parameterizations and parameter identifiability are discussed. Only the simplest forms of models are provided with some guidelines on how to build more complex models based on a systems pharmacology approach.

Keywords Direct effect · Indirect response · Signal transduction · Receptor occupancy theory · Biophase model · Biosensor process · Biosignal flux · Power model · Link model · Alternative parameterization · Transit compartment model · Agonism · Concentration

9.1 Introduction

Receptor occupancy theory states that drug molecules exert a pharmacological effect only if bound to a receptor, and the intensity of the effect is determined by the size of the drug-receptor complex pool (Clark 1933). In majority of situations, the

W. Krzyzanski (✉)
Department of Pharmaceutical Sciences, University at Buffalo, SUNY,
370 Kapoor Hall, Buffalo, NY 14214, USA
e-mail: wk@buffalo.edu

D.E. Mager and H.H.C. Kimko (eds.), *Systems Pharmacology and Pharmacodynamics*,
AAPS Advances in the Pharmaceutical Sciences Series 23,
DOI 10.1007/978-3-319-44534-2_9

concentration of the bound receptors at the effect site is a function of drug plasma concentration that is typically quantifiable from blood samples. The drug plasma concentration is a key variable used to mathematically describe the extent and duration of pharmacological effect. Such relationships are termed *pharmacodynamic models* examples of which are the focus of this chapter.

Basic components of a pharmacokinetic/pharmacodynamic (PK/PD) model include drug disposition, biophase distribution, biosensor process, biosignal flux, transduction, and response (Jusko et al. 1995; Mager et al. 2003). Depending on the presence or absence of one or more of above mentioned components and time that elapses between introducing a drug to the system and recording the response, the relationship between drug plasma concentration and response can be *direct* or *indirect*, resulting in two fundamentally different modeling approaches: explicit algebraic functions and differential equations. The former applies when there is no delay between pharmacokinetics and pharmacodynamics, whereas the latter is commonly used if such a delay is present. Development of a relevant model should be based on understanding both the pharmacology of drug action and biology of the system the drug acts upon.

In the following sections two types of PD models are introduced that account for direct and indirect pharmacological responses. Additionally, modeling techniques describing transduction processes are discussed. Model equations are presented so the parameters can be interpreted based on their biological meaning and the role they play in controlling the response curve. Model behavior is explored by simulating response time-courses for typical PK functions. Quantitative relationships between doses and the response curve geometric characteristics are provided. When relevant, typical issues arising in fitting the model to the data are discussed.

9.2 Direct Effect Models

By definition, a direct effect takes place if the response is a function of drug concentration at the effect site. Since quite often the site of drug action is difficult to sample for assessment of drug concentrations or simply is not known, an additional assumption is made that drug plasma concentration (C) is in a rapid equilibrium with the effect site, so that the drug concentration at the effect site is proportional to C. Then a general form for the direct effect model is

$$E = f(C) \tag{9.1}$$

where E denotes the effect and f(C) is a function of C. Examples of direct effects include drugs acting on the autonomic nervous system such as adrenergic receptor agonists relaxing smooth muscles in various tissues (Frazier et al. 2006). The direct effect models are used to describe data from in vitro experiments where cell cultures are incubated in media containing the known concentration of drug and the cellular status serves as a marker of the effect (Jamal et al. 2006).

A mathematical form of the function describing the direct effect (9.1) is determined empirically based on the shape of the E versus C curve for the observed data. Therefore, such models are termed *empirical*. A multitude of empirical direct effect models have been reported in the literature: linear, power, hyperbolic, sigmoid, logarithmic, and logistic depending on an appropriate algebraic function selected for the model. Below only two direct effect models are analyzed which seem to be most often applied due to their simplicity and flexibility. For unbound effects, the power model is recommended (with the linear model as a special case), and for bound (saturable) effects, the sigmoid model is proposed.

9.2.1 Power Model

The power model of direct effect is of the following form:

$$E = S \cdot C^{\gamma} \tag{9.2}$$

where S is a scaling factor and $-\infty < \gamma < \infty$ is a dimensionless power coefficient. If $\gamma = 1$, Eq. (9.2) defines a linear model with the slope S. It should be noted that γ can be negative. For $\gamma < 0$, the power model is a decreasing function of C that approaches infinity if C becomes small. On the other hand, for $\gamma > 0$, the effect increases to infinity as C increases to large values. The typical profiles of the power model for various γ are shown in Fig. 9.1. An example of a linear model ($\gamma = 1$) is provided by Yamakage (1992) to describe the effect of halothane on smooth muscle dilatation.

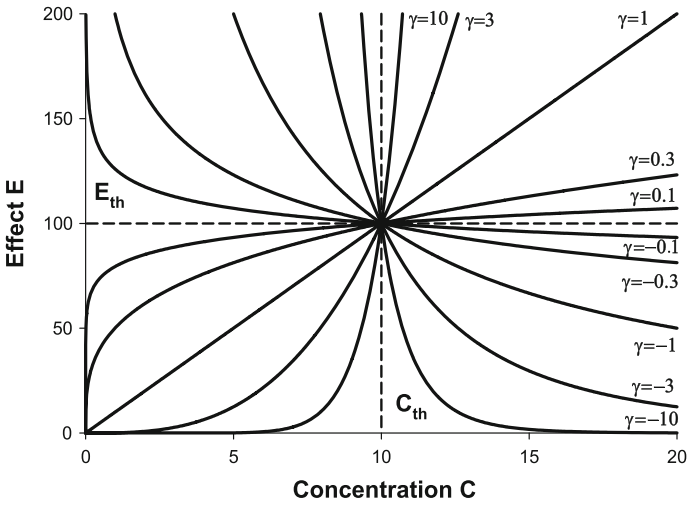

Fig. 9.1 Effect versus plasma concentration profiles for various power coefficients γ for the power model parameterized as in (9.3). The E_{th} is the only effect value that corresponds to the drug concentration C_{th} for all γ values

Alternative Parameterization

In (9.2) the power coefficient γ plays a role of a shape factor, whereas S is a scaling factor without a clear interpretation (except for $\gamma = 1$ when S is the slope of the line). Moreover the dimension of S is [Effect][Concentration]$^{-\gamma}$ which becomes problematic for rational or irrational γ. A parameterization where a reference concentration C_{th} is introduced:

$$E = E_{th}\left(\frac{C}{C_{th}}\right)^{\gamma} \tag{9.3}$$

offers an interpretation of the scaling factor E_{th} as the effect value corresponding to the concentration C_{th}. E_{th} is obtained for $C = C_{th}$ regardless of γ. The dimension of E_{th} is the dimension of the effect. Additionally, as shown in Fig. 9.1, C_{th} can be interpreted as a threshold (th) value for effects with large γ. The effect (9.3) becomes a none-or-infinity step function as $\gamma \to \infty$

$$E = \begin{cases} 0, & C < C_{th} \\ \infty, & C > C_{th} \end{cases} \tag{9.4}$$

However, it should be noted that the parameters E_{th} and C_{th} are not identifiable and one needs to be set to a known value when estimated. The property in (9.4) constitutes the basis for a "switch" mechanism in the tumor growth rate introduced by Simeoni et al. (2004) in modeling of inhibitory effects of anticancer agents.

9.2.2 *Sigmoid E_{max} Model*

The sigmoid E_{max} model is without a doubt the most commonly used direct PD model with applications reaching far beyond pharmacodynamics. It has been introduced by Hill (1910) to describe the oxygen-hemoglobin dissociation curve. Wagner (1968) used the Hill equation to describe the relationship between response and drug plasma concentration. The mathematical form is as follows:

$$E = \frac{E_{max}C^{\gamma}}{EC_{50}^{\gamma} + C^{\gamma}} \tag{9.5}$$

where E_{max} is the maximal effect, EC_{50} is the drug plasma concentration that elicits 50 % of the maximal effect, and γ is the Hill coefficient that plays the role of a shape factor. If $\gamma = 1$, then the sigmoid E_{max} model is known as the *E_{max} model*.

The fundamental property of the sigmoid model is that it bounds the effect between $0 \le E < E_{max}$. Secondly, as seen in Fig. 9.2, the effect is an increasing function of plasma concentration that approaches E_{max} as $C \to \infty$. The name "sigmoid" originates for a characteristic S-shape of the E versus C curve for $\gamma > 1$. For $\gamma = 1$, Eq. (9.5) becomes a hyperbola with a horizontal asymptote at $E = E_{max}$, and for $0 < \gamma < 1$ the model maintains the hyperbolic behavior.

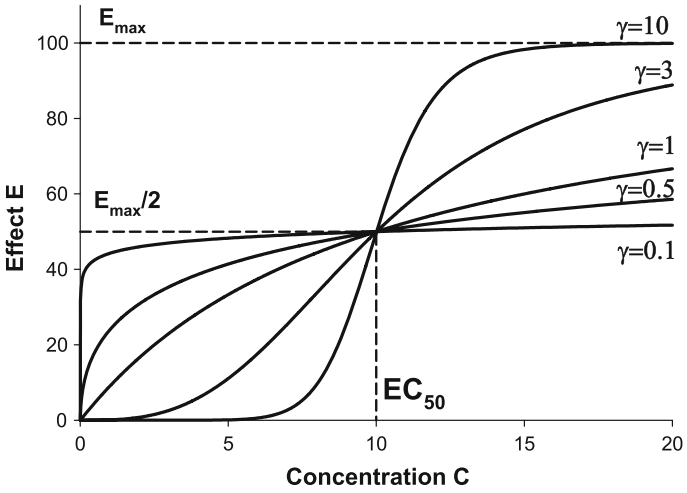

Fig. 9.2 Effect versus plasma concentration profiles for various power coefficients γ for the sigmoid E_{max} model (9.5)

Both E_{max} and EC_{50} are easily identifiable from the E versus C curve as explained in Fig. 9.2. To define γ, one needs to determine the slope of that curve at $C = EC_{50}$ (Krzyzanski and Jusko 1998):

$$\frac{dE}{dC}(EC_{50}) = \frac{\gamma E_{max}}{EC_{50}} \text{ and } \frac{dE}{d(\ln C)}(\ln(EC_{50})) = \gamma E_{max} \tag{9.6}$$

where the second term quantifies the slope of E versus lnC curve (E vs. C plot in the linear-log scale) evaluated at $\ln(EC_{50})$.

E_{max} Model in Pharmacology

Based on receptor occupancy theory, Clark (1933) postulated that the drug effect is proportional to the fraction of occupied receptors with the maximal effect corresponding to full occupancy. The drug-receptor concentration (DR) at equilibrium between receptor binding and disassociation according to receptor occupancy theory is described by the following equation:

$$DR = \frac{R_{tot}C}{K_D + C} \tag{9.7}$$

where R_{tot} is the total receptor concentration and K_D is the equilibrium disassociation constant. Then *receptor occupancy* can be calculated as DR/R_{tot} and the effect becomes

$$E = E_{max}\frac{DR}{R_{tot}} = \frac{E_{max}C}{K_D + C} \tag{9.8}$$

The proportionality coefficient must be equal to the maximum effect E_{max} to ensure that at 100 % receptor occupancy the effect is maximal. This assumption holds true only for full agonists. There are drugs that do not elicit maximal effect despite 100 % occupancy (partial agonists). This observation underlies the concept of *intrinsic activity* introduced by Ariens (1954).

Drug *potency* is the concentration required to produce a given response and drug *efficacy* is its ability to change a receptor, such that it produces a cellular response (Kenakin 2006). The dose-response curves are frequently applied in pharmacology to determine drug potency and efficacy based on a relationship between drug concentrations and a measurable response in an in vitro system. According to Eqs. (9.5) and (9.8), the E_{max} serves as a marker of drug efficacy and EC_{50} as a marker of drug potency. Moreover, drug potency is determined by its affinity to the receptor and efficacy. This interpretation has been extended to any type of concentration-response data described by the E_{max} model, and subsequently by the sigmoid E_{max} model.

Alternative Form

One can divide the numerator and denominator of Eq. (9.5) by $EC_{50}{}^{\gamma}$ arriving at the following form that is numerically favorable:

$$E = \frac{E_{max}(C/EC_{50})^{\gamma}}{1 + (C/EC_{50})^{\gamma}} \tag{9.9}$$

This implies that for $C \ll EC_{50}$ the sigmoid model behaves like the power model (9.3). Consequently, EC_{50} and E_{max} cannot be identified from PD data collected for $C \ll EC_{50}$. The identifiability of E_{max} and EC_{50} parameters is further discussed by Dutta et al. (1996). Another property of (9.9) is often exploited in modeling PD data. For large γ the sigmoid model behaves like a step function as follows:

$$E \to \begin{cases} 0, & C < EC_{50} \\ E_{max}, & C > EC_{50} \end{cases} \qquad \text{as } \gamma \to \infty \tag{9.10}$$

Due to a discontinuity, the numerical implementation of a step function becomes problematic. In practice, for $\gamma \geq 10$, the sigmoid model is a good continuous approximation of (9.10).

9.2.2.1 Sigmoid E_{max} Model with Baseline

The sigmoid model (9.5) applies only to data where there is no effect in the absence of drug. Many pharmacological effects are at nonzero baseline $E_0 > 0$ prior to drug treatment. If the drug effect is direct, one of two models with the baseline can be used:

$$S = E_0 + \frac{S_{max}C^{\gamma}}{SC_{50}^{\gamma} + C^{\gamma}} \quad \text{and} \quad I = E_0 - \frac{I_{max}C^{\gamma}}{IC_{50}^{\gamma} + C^{\gamma}} \tag{9.11}$$

where the model that adds to the baseline is considered stimulatory and one that subtracts from the baseline is called inhibitory. Changing the letter "E" in the names of variables and parameters to "S" and "I", respectively, emphasizes that behavior. For the inhibitory effect model it is assumed that $0 \leq I_{max} \leq E_0$ to ensure positiveness of I. An example of the inhibitory E_{max} model is the effect of an angiotensin-converting-enzyme (ACE) inhibitor on ACE activity (Edeki et al. 1994).

9.2.2.2 Sigmoid E_{max} Model as Function of Time

The data to which direct effect models apply consist of measurements of responses at specific concentrations, which is typical for in vitro studies but requires a special effort for achieving steady-state concentrations for in vivo experiments. In the majority of preclinical and clinical studies, PK and PD measurements are made at specified time points. The relationship (9.1) can be inferred from a PK model describing C as a function of time C(t) and the effect as a function of time:

$$R(t) = f(C(t)) \tag{9.12}$$

The importance of the time course of pharmacological effect was first recognized by Levy (1966) setting the foundation for pharmacodynamic relationships. The sigmoid E_{max} model (9.5) as a function of time is defined as follows

$$R(t) = \frac{E_{max} C(t)^{\gamma}}{EC_{50}^{\gamma} + C(t)^{\gamma}} \tag{9.13}$$

where C(t) is drug plasma concentration at time t described by a separate PK model. Figure 9.3 shows the time courses of the effect (9.13) corresponding to drug concentrations described by a monoexponential function:

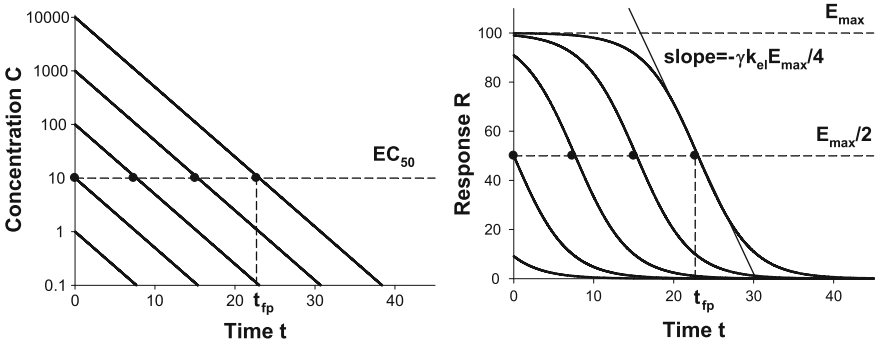

Fig. 9.3 Monoexponential drug plasma concentration time profiles (*left*) and the corresponding responses (*right*) for the sigmoid E_{max} model (9.13) with $\gamma = 1$ for escalating dose. The *symbols* indicate times of the inflection point t_{fp} on the response versus time curves. The slope of the tangent line to R(t) at $t = t_{fp}$ is given in (9.17)

$$C(t) = \frac{D}{V} e^{-k_{el}t} \tag{9.14}$$

where D denotes the dose, V is the volume of distribution, and k_{el} is the elimination rate constant.

The immediate consequence of a direct relationship (9.13) is that the peak of concentration coincides with the peak of response. The rate of the response decay is determined by the elimination rate of drug concentration. If λ_z is the terminal slope for C(t) and C_z is the back-extrapolated y-axis intercept,

$$C(t) \sim C_z e^{-\lambda_z t} \text{ as } t \to \infty \tag{9.15}$$

then the terminal slope for R(t) is $\gamma \cdot \lambda_z$:

$$R(t) \sim E_{max} \left(\frac{C_z}{EC_{50}} \right)^{\gamma} e^{-\lambda_z \gamma t} \quad \text{as } t \to \infty \tag{9.16}$$

where the symbol $g(t) \sim h(t)$ means that $g(t)/h(t) \to 1$ as $t \to \infty$. If C(t) is monoexponential (9.14) and $C(t) > EC_{50}$, then the R(t) versus t curve has an inflection point at time t_{fp} such that $C(t_{fp}) = EC_{50}$ (see Fig. 9.3) and the slope at t_{fp} is (Krzyzanski and Jusko 1998):

$$\frac{dR}{dt}(t_{fp}) = -\frac{1}{4} \gamma E_{max} k_{el} \tag{9.17}$$

9.2.3 *Biophase Model*

If the drug distribution to the site of action is not rapid, then a delay between the drug concentration at the effect site C_e and C can be present. In such a case the effect is not a function of C but C_e:

$$E = f(C_e) \tag{9.18}$$

Because of the delay, the plot of E versus C exhibits a *hysteresis*, which is a hallmark of the biophase distribution. Since drug concentrations in the effect compartment are rarely measured, C_e is inferred from the plasma concentrations by means of a *biophase model* that links the time course of C(t) with the time course of $C_e(t)$ resulting in the response versus time relationship:

$$R(t) = f(C_e(t)) \tag{9.19}$$

Responses known to have a delay related to the biophase include muscle paralysis following administration of neuromuscular blocking agents such as

pancuronium (Evans et al. 1984), cardiovascular effects caused by calcium channel blockers (e.g., verapamil) (Schwartz et al. 1989), or respiratory function affected by bronchodilators (e.g., theophylline) (Whiting et al. 1981).

9.2.3.1 Link Model

Sheiner et al. (1979) proposed a model describing the degree of paralysis caused by infusion of a muscle relaxant d-tubocurarin in healthy subjects:

$$R(t) = \frac{E_{max} C_e(t)^{\gamma}}{EC_{e50}^{\gamma} + C_e(t)^{\gamma}} = \frac{E_{max} A_e(t)^{\gamma}}{EA_{e50}^{\gamma} + A_e(t)^{\gamma}} \tag{9.20}$$

where the sigmoid model (9.13) was used with C_e replaced by the ratio of drug amount A_e in the effect compartment and its volume V_e resulting in another parameter $EA_{e50} = EC_{e50} \cdot V_e$. This representation of the response eliminated the volume of the effect compartment from the model equations. The drug distributes to the effect site according to a first-order rate constant k_{1e} and is eliminated by a first-order rate constant k_{e0}:

$$\frac{dA_e}{dt} = k_{1e} A - k_{e0} A_e \tag{9.21}$$

where $A = C \cdot V$ is the drug amount in the plasma compartment. A key assumption is that the amount of drug distributed to the effect compartment is negligible so that it does not affect the pharmacokinetics of drug in the plasma. Since the parameters EA_{e50} and k_{1e} are not typically identifiable, a new variable is introduced:

$$C_{pss} = \frac{k_{e0} A_e}{k_{1e} V} \tag{9.22}$$

This can be interpreted as the drug plasma concentration at which the effect compartment is at equilibrium. Equation (9.21) implies that the differential equation for $C_{pss}(t)$ becomes:

$$\frac{dC_{pss}}{dt} = k_{e0}\left(C - C_{pss}\right) \tag{9.23}$$

Accordingly, the response is:

$$R(t) = \frac{E_{max} C_{pss}(t)^{\gamma}}{EC_{pss50}^{\gamma} + C_{pss}(t)^{\gamma}} \tag{9.24}$$

where the parameter EC_{pss50} is defined by (9.22) with A_e replaced by A_{e50}. The final model with (9.23) and (9.24) does not require k_{1e}, and k_{e0} is a sole parameter accounting for the drug distribution to the biophase.

9.2.3.2 Biophase Model

The link model of (9.23) and (9.24) has been further modified by assuming that the clearance of the drug from plasma due to the distribution to the effect compartment is equal to the clearance of the drug from that compartment ($k_{1e}V = k_{e0}V_e$) yielding equality of $C_{pss} = C_e$. This simplifies EC_{pss50} to EC_{e50} and the link model to the following form:

$$\frac{dC_e}{dt} = k_{e0}(C - C_e) \tag{9.25}$$

and the response becomes

$$R(t) = \frac{E_{max}C_e(t)^{\gamma}}{EC_{e50}^{\gamma} + C_e(t)^{\gamma}} \tag{9.26}$$

It should be noted that the two models of (i) (9.23)–(9.24) and (ii) (9.25)–(9.26) are mathematically identical. They differ only in the interpretation of the C_{pss} versus C_e with the former being a theoretical drug plasma concentration yielding equilibrium at effect site and the latter being the drug concentration at the effect site.

Assuming there is no drug in the effect compartment at time t = 0, the concentration $C_e(t)$ can be expressed by the convolution integral:

$$C_e(t) = \int_0^t C(t - z)e^{-k_{e0}z}dz = C(t) * e^{-k_{e0}t} \tag{9.27}$$

For monoexponential PK (9.14), the integral can be calculated explicitly yielding:

$$C_e(t) = \frac{D}{V}\frac{k_{e0}}{k_{e0} - k_{el}}\left(e^{-k_{el}t} - e^{-k_{e0}t}\right) \tag{9.28}$$

The $C_e(t)$ versus t and R(t) versus t profiles corresponding to increasing doses are shown in Fig. 9.4.

Typically for direct effect models, there is no delay between $C_e(t)$ and R(t) resulting at the same peak time t_p that can be calculated for the monoexponential C (t) (9.14):

$$t_p = \frac{\ln(k_{e0}/k_{el})}{k_{e0} - k_{el}} \tag{9.29}$$

The peak time can serve as a measure of the delay between C(t) and R(t). An obvious observation is that t_p does not depend on dose. This property holds for any linear (dose proportional) C(t).

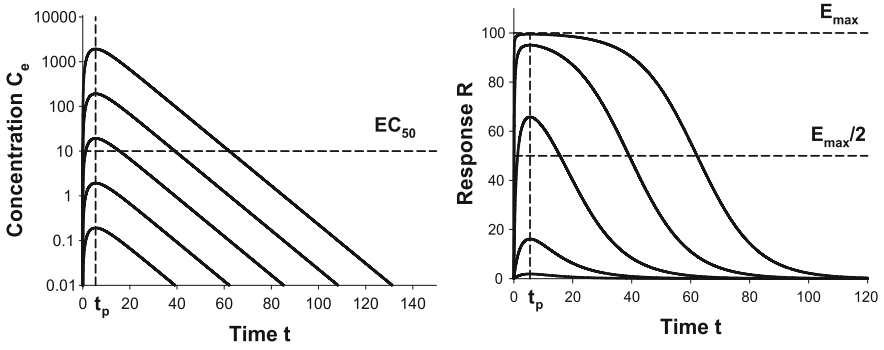

Fig. 9.4 Time-courses of the concentration of drug in the effect compartment and the response described by the biophase model of (9.25)–(9.26). The drug plasma concentrations follow monoexponential kinetics (9.14) with escalating doses. The peak time t_p is identical for both $C_e(t)$ and R(t)

9.3 Indirect Response Models

Many pharmacological targets are subjected to a continuous process of degradation compensated by a renewal to maintain the stable steady-state termed as *homeostasis*. Human gastric acid pH is maintained at the level of 1.5–3.5 by secretion of chloride and hydrogen ions from the cytoplasm of parietal cells in the stomach. The human body temperature of 37 °C is tightly controlled by the thermoregulatory center in the hypothalamus. Many hormones need to be kept in a specific concentration range to regulate functions of the body tissues and organs. Blood glucose concentration is controlled by the pancreas secreting glucagon and insulin. Hematopoietic cells are produced by the bone marrow and die as a result of senescence or random destruction so that their levels are sufficient to deliver enough oxygen to tissues, to stop bleeding, or to initiate an immune response. Mechanisms of action of a variety of drugs are based on perturbing the homeostatic baseline of target or its biomarker by affecting the process of production or elimination. In result, a temporal change in the marker value will be observed generating a *response*. If upon disappearance of the drug from the system, the response returns to the baseline, then the drug effect is *reversible*. Since the process of balancing the drug effect takes time, a delay between the drug time-course and the response time-course is apparent. The extent of the delay and the amplitude of the response are determined by the strength of the effect and the turnover rates of the pharmacological target. Such mechanisms of drug action are inherently *indirect*, meaning that the drug directly affects the turnover process that controls the response rather than the response itself. Nagashima et al. (1969) are credited for using the first indirect response model to evaluate the effect of the anticoagulant warfarin on the prothrombin complex activity.

9.3.1 Basic Indirect Response Models

Dayneka et al. (1993) introduced general mathematical models of indirect pharmacological responses. The response R is produced at a zero-order rate k_{in} and lost according to a first-order rate constant k_{out}. The drug inhibits or stimulates the production or elimination process according to one of the following models:

Model I (inhibition of k_{in}):

$$\frac{dR}{dt} = k_{in}I(C(t)) - k_{out}R \tag{9.30}$$

Model II (inhibition of k_{out}):

$$\frac{dR}{dt} = k_{in} - k_{out}I(C(t))R \tag{9.31}$$

Model III (stimulation of k_{in}):

$$\frac{dR}{dt} = k_{in}S(C(t)) - k_{out}R \tag{9.32}$$

Model IV (stimulation of k_{out}):

$$\frac{dR}{dt} = k_{in} - k_{out}S(C(t))R \tag{9.33}$$

where I and S are the inhibitory and stimulatory drug effect functions described by Eq. (9.11) with $E_0 = 1$. Prior to drug administration ($C = 0$), the response is assumed to be at the steady-state (baseline) R_0:

$$R(0) = R_0 = \frac{k_{in}}{k_{out}} \tag{9.34}$$

Examples of systems described by basic indirect response models are provided by Jusko and Ko (1994). The inhibition of trafficking of basophils from the extravascular tissues to the blood by methylprednisolone comprises Model I. The inhibition of water reabsorption from the tubules and collecting duct by a loop diuretic drug furosemide resulting in the increase of urine volume is an example of Model II. The stimulation of the production of cyclic adenosine monophosphate (cATP)-induced bronchodilation by the β-adrenergic receptor agonist terbutaline is described by Model III. The increase in cAMP activates the cellular membrane sodium-potassium pump leading to the increase of K^+ ions efflux from the plasma into cells constituting another terbutaline effect that can be described with Model IV.

The time-courses of responses described by Models I–IV are shown in Fig. 9.5. If C(t) decreases to zero as time increases, then the inhibition of the production

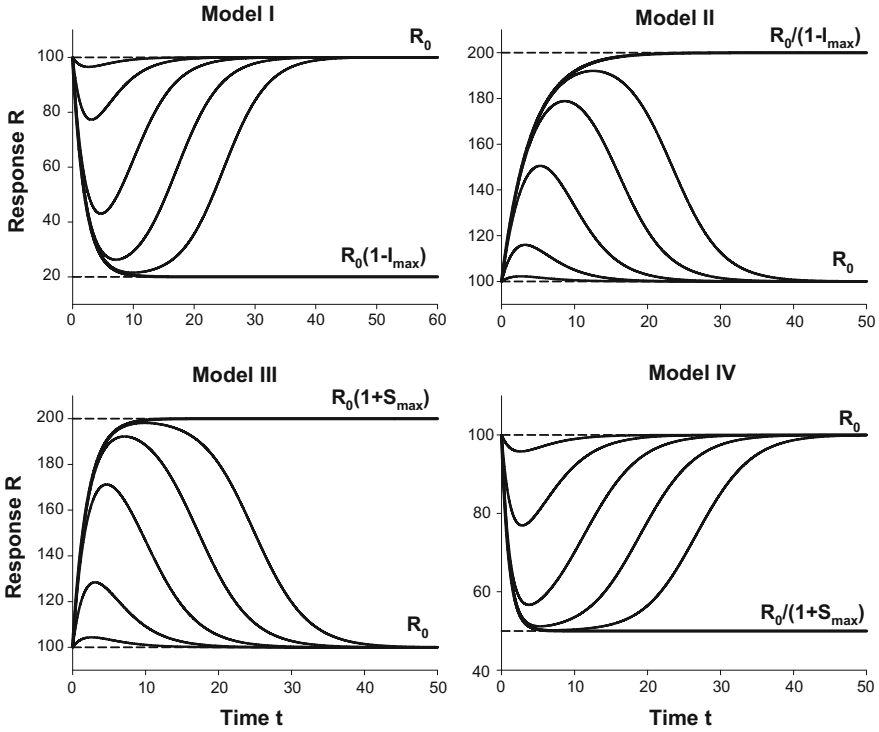

Fig. 9.5 Time courses of four basic indirect response models (9.30)–(9.33). The drug plasma concentrations follow monoexponential kinetics (9.14) with escalating doses. The *bold lines* are the limit values of the response as Dose → ∞ (9.39)–(9.43)

(Model I) causes the response to decrease below the baseline to reach a nadir and return to the baseline as drug washes out. A similar behavior can be observed for the stimulation of the response elimination (Model IV). The stimulation of the production (Model III) elevates the response above the baseline to culminate at a peak and descends to the baseline after the drug is cleared from the system. The response time-course for the inhibition of the elimination (Model II) behaves similarly.

For general PK functions, there are no explicit solutions to any of differential equations (9.30)–(9.33). However, they can be integrated to the following forms:

$$\text{Model I} \qquad R(t) = R_0 - k_{in}\int_0^t (1 - I(C(z)))e^{-k_{out}(t-z)}dz = R_0 - k_{in}(1 - I(C(t))) * e^{-k_{out}t} \tag{9.35}$$

$$\text{Model II} \qquad R(t) = R_0 + k_{in}\int_0^t (1 - I(C(z)))e^{-k_{out}\int_z^t I(s)ds}dz \tag{9.36}$$

$$\text{Model III} \qquad R(t) = R_0 + k_{in}\int_0^t (S(C(z)) - 1)e^{-k_{out}(t-z)}dz = R_0 + k_{in}(S(C(t)) - 1) * e^{-k_{out}t} \tag{9.37}$$

$$\text{Model IV} \qquad R(t) = R_0 - k_{in}\int_0^t (S(C(z)) - 1)e^{-k_{out}\int_z^t I(s)ds}dz \tag{9.38}$$

If C(t) is the monoexponential function (9.14), then the explicit solutions can be obtained by means of hypergeometric ${}_2F_1$ functions (Jordan and Gieschke 2005).

9.3.1.1 Large Dose Approximation

For increasing doses, drug plasma concentrations C(t) approach infinity, and the sigmoid effects (9.11) attain their maximal values. Under this simplifying assumption, the integrals in (9.35)–(9.38) can be evaluated resulting in the following limiting curves (see Fig. 9.5) as dose $D \to \infty$

$$\text{Model I} \qquad R(t) \to R_0(1 - I_{max}) + R_0 I_{max} e^{-k_{out}t} \tag{9.39}$$

$$\text{Model II} \qquad R(t) \to \frac{R_0}{1 - I_{max}} - \frac{R_0 I_{max}}{1 - I_{max}} e^{-k_{out}(1-I_{max})t}, \quad \text{if } I_{max} < 1 \tag{9.40}$$

$$R(t) \to R_0 + k_{in}t, \quad \text{if } I_{max} = 1 \tag{9.41}$$

$$\text{Model III} \qquad R(t) \to R_0(1 + S_{max}) - R_0 S_{max} e^{-k_{out}t} \tag{9.42}$$

$$\text{Model IV} \qquad R(t) \to \frac{R_0}{1 + S_{max}} + \frac{R_0 S_{max}}{1 + S_{max}} e^{-k_{out}(1 + S_{max})t} \tag{9.43}$$

Maximal Response Eqs. (9.39)–(9.43) imply that for all models (except Model II with $I_{max} = 1$), the response reaches the finite maximal value R_{max} as dose increases to infinity:

$$R_{max} = \begin{cases} R_0(1 - I_{max}), & \text{Model I} \\ \frac{R_0}{1 - I_{max}}, & \text{Model II} \\ R_0(1 + S_{max}), & \text{Model III} \\ \frac{R_0}{1 + S_{max}}, & \text{Model IV} \end{cases} \tag{9.44}$$

Peak Time The peak time t_p is defined as the time point at which the response attains its local maximum or minimum. The hallmark of all indirect responses is that t_p depends on dose. If C(t) decreases with time and increases to infinity with increasing doses, then for Models I–IV (Krzyzanski and Jusko 1997):

$$t_p \to \infty \quad \text{as } D \to \infty \tag{9.45}$$

For monoexponential C(t) (9.14), the dose dependence of t_p can be further quantified (Peletier et al. 2005). As $D \to \infty$:

$$\text{Model I} \qquad t_p \sim \frac{\gamma^2 k_{el}}{\gamma k_{el} + k_{out}} \ln\left(\frac{D/V}{IC_{50}}\right) \tag{9.46}$$

$$\text{Model II} \qquad t_p \sim \frac{\gamma^2 k_{el}}{\gamma k_{el} + k_{out}(1 - I_{max})} \ln\left(\frac{D/V}{IC_{50}}\right) \tag{9.47}$$

$$\text{Model III} \qquad t_p \sim \frac{\gamma^2 k_{el}}{\gamma k_{el} + k_{out}} \ln\left(\frac{D/V}{SC_{50}}\right) \tag{9.48}$$

$$\text{Model IV} \qquad t_p \sim \frac{\gamma^2 k_{el}}{\gamma k_{el} + k_{out}(1 + S_{max})} \ln\left(\frac{D/V}{IC_{50}}\right) \tag{9.49}$$

Relationships (9.46)–(9.49) in essence state that the peak time increases logarithmically with dose.

Recession Slope For large doses, the offset part of the response versus time curve becomes linear (see Fig. 9.5) similarly to the sigmoid model (9.17). The slope of this curve can characterized by the derivative of R(t) at the inflection point t_{fp} called the recession slope. It informs about the rate at which the response returns to the baseline. Contrary to (9.17), the limit value of the recession slope for large doses cannot be expressed as an explicit function of the model parameters (Krzyzanski and Jusko 1998).

9.3.1.2 Parameter Identifiability

The basic indirect response model parameters consist of *system parameters*, k_{in} and k_{out}, and drug related parameters, I_{max}, IC_{50}, γ (Models I and II) and S_{max}, SC_{50}, γ (Models III and IV). Typically the parameter identifiability is determined by *sensitivity analysis* where the response time-courses are simulated for various sets of parameter values. Results of that nature have been reported by Sharma and Jusko (1996). In the absence of the drug, the response is at the constant baseline R_0, and k_{in} and k_{out} cannot be identified from the baseline data alone. Since the inhibitory and stimulatory functions are the sigmoid models, identifiability of I_{max} and IC_{50} (or S_{max} and SC_{50}) is possible only for drug concentrations that remain above IC_{50} or SC_{50} concentrations long enough to elicit a response that is close to the maximal

response. Therefore, a necessary requirement for the identifiability of these parameters from single-dose drug administration data is a large dose resulting in a peak value near R_{max} that should be observed as a temporal plateau. As seen from the large dose approximation equations (9.44), I_{max} and S_{max} can be calculated from R_{max} and R_0. Given I_{max} or S_{max}, (9.39)–(9.43) imply that k_{out} can be determined from the onset part of the response curve. The recession slope and the peak response are informative about γ. Response data corresponding to a single large dose have been reported to be sufficient to resolve all model parameters with imprecise estimates of IC_{50} and SC_{50} (Krzyzanski et al. 2006). Therefore, two dose level response data are recommended for the accurate and precise parameter estimation.

Alternative Parameterization The baseline serves as a reference for assessing the extent of the response. Therefore, without sufficient information about the baseline R_0, the estimation of I_{max} and S_{max} and other model parameters is impossible. The presence of the placebo (control) response data is necessary for an unbiased estimation of R_0. Because of the baseline relationship (9.34), R_0 is a *secondary parameter* expressed as a ratio of k_{in} and k_{out}. This often results in a high correlation between estimates of these parameters. An alternative parameterization that expresses k_{in} as a product of R_0 and k_{out} can ameliorate this problem:

$$k_{in} = R_0 k_{out} \tag{9.50}$$

Having R_0 as a *primary parameter* is necessary in the absence of the baseline data when R_0 has to be fixed to a single pre-dose response measurement or a known value.

9.3.2 Extended Basic Indirect Response Models

The basic indirect models (9.30)–(9.33) can be modified to account for different processes from zero-order production and first-order elimination processes controlling the change of the response. The production process can vary in time, which would require k_{in} to be time-dependent (Chakraborty et al. 1999). The loss rate might be determined by the lifespan of cells, whose counts serve as a marker for the response (Krzyzanski et al. 1999). The production and loss processes can be nonlinear functions of the response to account for capacity limited processes or to keep the response within physiological limits (Yao et al. 2006).

9.3.2.1 Basic Indirect Response Models with Circadian Input

The light-dark cycle affects physiological functions of many organs causing their *circadian* (periodic 24 h) fluctuations. The master clock present in the anterior part

of the hypothalamus controls peripheral clocks in other parts of the body (Reppert and Weaver 2002). Gastric acid secretion, cardiac output, hepatic enzyme activity, and glomerular filtration are subject to circadian variability that impact pharmacokinetics of various drugs (Labrecque and Belanger 1991). Gene expression (Sukumaran et al. 2010), hormone secretion, body temperature, heart rate, and blood pressure (Sallstrom et al. 2005) are known PD responses that undergo circadian changes.

To account for time-dependent production, the zero-order rate constant k_{in} is assumed to be a continuous function of time $k_{in}(t)$ that is T-periodic (T = 24 h):

$$k_{in}(t+T) = k_{in}(t) \quad \text{for all } t \tag{9.51}$$

The basic indirect response with the inhibition of the circadian input is of the form (9.30) with k_{in} replaced with $k_{in}(t)$

$$\frac{dR}{dt} = k_{in}(t)I(C(t)) - k_{out}R \tag{9.52}$$

In the absence of drug (C(t) = 0), there exists only one T-periodic solution to (9.52) $R_b(t)$

$$\frac{dR_b}{dt} = k_{in}(t) - k_{out}R_b \tag{9.53}$$

that can be determined by the following initial condition:

$$R_b(0) = R_b(T) = \frac{1}{e^{k_{out}T} - 1}\int_0^T k_{in}(t)e^{k_{out}t}dt \tag{9.54}$$

The T-periodic function $R_b(t)$ has all attributes of a baseline for an indirect response but stationarity. If drug perturbs $R_b(t)$ by inhibiting $k_{in}(t)$ and C(t) vanishes after a long time, then R(t) approaches $R_b(t)$, in the sense that the difference $R_b(t)$-R(t) becomes 0 as $t \to \infty$. The convolution representation of the response R(t) (see (9.35)) is:

$$R(t) = R_b(t) - \int_0^t k_{in}(z)\frac{I_{max}C(z)^{\gamma}}{IC_{50}^{\gamma} + C(z)^{\gamma}}e^{-k_{out}(t-z)}dz = R_b(t) - \left[k_{in}(t)\frac{I_{max}C(t)^{\gamma}}{IC_{50}^{\gamma} + C(t)^{\gamma}}\right] * e^{-k_{out}t} \tag{9.55}$$

For the model to be complete, a specific function should be selected to describe $k_{in}(t)$. The simplest choice favored by many modelers is a trigonometric function.

Cosine Model The cosine function was first introduced by Lew et al. (1993) to model the inhibitory effect of methylpredisolone on cortisol concentrations in healthy subjects. In this model, $k_{in}(t)$ is described by the mean production rate (*mesor*) k_{inM}, amplitude k_{inA}, and peak time (*acrophase*) t_k:

$$k_{in}(t) = k_{inM} + k_{inA}\cos\left(\frac{2\pi}{T}(t - t_k)\right) \tag{9.56}$$

Then the baseline can be calculated explicitly as:

$$R_b(t) = R_{bM} + R_{bA}\cos\left(\frac{2\pi}{T}(t - t_b)\right) \tag{9.57}$$

where

$$R_{bM} = \frac{k_{inM}}{k_{out}}, \quad R_{bA} = \frac{k_{inA}}{\sqrt{k_{out}^2 + (2\pi/T)^2}}, \quad t_b = t_k + t_{shift},$$
$$t_{shift} = \frac{T}{2\pi}\operatorname{atan}\left(\frac{2\pi/T}{k_{out}}\right) \tag{9.58}$$

As seen in Fig. 9.6, the baseline $R_b(t)$ is shifted by time t_{shift} with respect to $k_{in}(t)$. As for the basic indirect models, if the drug is administered at time t = 0, then the response must be at the baseline value:

$$R(0) = R_b(0) = R_{bM} + R_{bA}\cos\left(\frac{2\pi}{T}(t_b)\right) \tag{9.59}$$

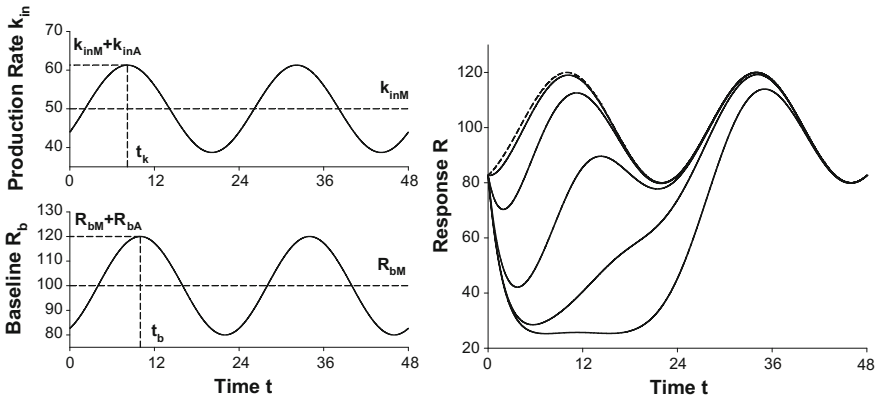

Fig. 9.6 Time courses of the production rate and the baseline (*left*), and the response profiles for escalating dose (*right*) for the cosine model (9.56)–(9.57). The drug plasma concentrations are monoexponential. The shift between the peak times of $k_{in}(t)$ and $R_b(t)$ $t_{shift} = t_b - t_k$ depends only on k_{out} and period T (9.58). The *dashed line* in the *right panel* represents the baseline $R_b(t)$

Alternative Parameterization The parameters describing the production rate k_{inM}, $k_{inA,}$ and t_k are difficult to determine from PD data. On the other hand, the baseline parameters R_{bM}, $R_{bA,}$ and t_b are readily identifiable from the baseline data. Therefore, using them as primary parameters might be more practical. Then (9.61) can serve to calculate k_{inM}, $k_{inA,}$ and t_k

$$k_{inM} = R_{bM}k_{out}, \quad k_{inA} = R_{bA}\sqrt{k_{out}^2 + (2\pi/T)^2}, \quad t_k = t_b - t_{shift} \tag{9.60}$$

Note that k_{out} is not identifiable from the baseline data alone. Equation (9.60) implies that k_{inM}, $k_{inA,}$ and t_k are also not identifiable from the baseline data.

Asymmetric Circadian Rhythms Since the cosine function is symmetric, the cosine model can be used to describe PD data with symmetric baselines. When an asymmetry is observed, asymmetric functions should be used to define $k_{in}(t)$. Various models have been reported such as exponential and linear release models (Rohatagi et al. 1996) and dual cosine and harmonic models (Chakraborty et al. 1999).

9.3.2.2 Basic Lifespan Based Indirect Response Models

The concept of lifespan controlled cell removal is based on the assumption that each cell has the same lifespan T_R. This assumption implies that the cell removal rate is the production rate $k_{in}(t)$ delayed by $T_{R,}$ $k_{in}(t\text{-}T_R)$. The rate of change in the cell number becomes:

$$\frac{dR}{dt} = k_{in}(t) - k_{in}(t - T_R) \tag{9.61}$$

If $k_{in}(t)$ has a constant baseline k_{in0}:

$$k_{in}(t) = k_{in0} \text{ for } t < 0 \text{ and } k_{in}(t) \to k_{in0} \text{ as } t \to \infty \tag{9.62}$$

then the response R(t) has the baseline R_0 (Koch and Schropp 2013):

$$R_0 = k_{in0}T_R \tag{9.63}$$

that serves as an initial condition for (9.61). The response R(t) can be calculated in terms of the integral of $k_{in}(t)$:

$$R(t) = \int_{t-T_R}^{t} k_{in}(z)dz \tag{9.64}$$

Basic Indirect Model with Lifespan Controlled Loss The lifespan concept of cell elimination was first implemented in indirect response models by Krzyzanski et al. (1999). The basic indirect response Model III was adopted to describe the stimulatory effect of hematopoietic growth factors erythropoietin, thrombopoietin, and granulocyte-colony stimulating factor on the production of reticulocytes, platelets, and neutrophils, respectively, in healthy subjects. The cell production rate under baseline conditions is assumed to be constant k_{in0}. The drug stimulation of k_{in0} is described as the basic indirect response Model III (9.32). Since the loss rate is the production rate delayed by T_R, (9.61) implies that

$$\frac{dR}{dt} = k_{in0}S(C(t)) - k_{in0}S(C(t - T_R)) \tag{9.65}$$

The initial condition for (9.65) is the baseline value (9.63)

$$R(0) = R_0 \tag{9.66}$$

The lifespan based indirect response models have been applied to hemoglobin responses to treatment with erythropoiesis stimulating agents (Budha et al. 2011), and pegylated thrombopoietin effect on platelets in healthy subjects (Samtani et al. 2009). The response time-courses for escalating doses are shown in Fig. 9.7.

The fundamental difference between the indirect response Model III and model (9.65)–(9.66) is that for drug plasma concentrations decreasing with time the peak response is dose independent and

$$t_p = T_R \tag{9.67}$$

Similarly to Model III, if dose becomes very large, $D \to \infty$, there is a limiting response curve (Krzyzanski and Perez Ruixo 2012):

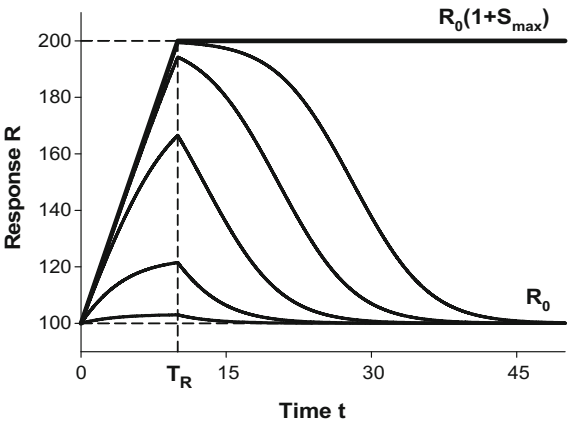

Fig. 9.7 Time-courses of the basic lifespan based indirect response model (9.65). The drug plasma concentrations follow monoexponential kinetics (9.14) with escalating doses as shown in Fig. (9.3). The *bold line* is the limit value of the response as $D \to \infty$ (9.68). The peak time for all response curves is equal to T_R

$$R(t) \rightarrow \begin{cases} R_0 + k_{in0} S_{max} t, & \text{for } 0 < t < T_R \\ R_0(1 + S_{max}), & \text{for } T_R \leq t \end{cases} \tag{9.68}$$

and the maximal response is

$$R_{max} = R_0(1 + S_{max}) \tag{9.69}$$

The lifespan concept has been implemented to model hematological toxicities (Bulitta et al. 2009) and tumor growth inhibition (Mo et al. 2014) by anticancer agents.

9.3.3 Indirect Response Models with Precursor

A *precursor* for a response R is another response P controlled by a turnover process such that the output from P is the input to R. Bone marrow hematopoietic cells are precursors for the circulating blood cells. Hormones produced and stored in glands and organs are precursors secreted to the blood where they become measurable responses. If the drug acts on the precursor, then the effect propagates on the response. Iron stored in the liver and muscle is an example of a precursor with the release to the circulation controlled by hepcidin (Detivaud et al. 2005). The dynamics of such effect differs from the drug effect with a simple zero-order production rate for the response.

Sharma et al. (1998) introduced a precursor to the basic indirect models to account for *tolerance* and *rebound phenomena* observed for drugs acting on precursors. The precursor P is produced at a zero-order rate k_0 and eliminated at a first-order rate k_p. The loss rate of the precursor is the production rate for the response R, which is eliminated according to a first-order rate constant k_{out}. The drug affects k_p according to the basic indirect model mechanisms (9.32) or (9.33).

Model V (blockage of precursor):

$$\frac{dP}{dt} = k_0 - k_p I(C(t))P \tag{9.70}$$

$$\frac{dR}{dt} = k_0 I(C(t))P - k_{out} R \tag{9.71}$$

Model VI (depletion of precursor):

$$\frac{dP}{dt} = k_0 - k_p S(C(t))P \tag{9.72}$$

$$\frac{dR}{dt} = k_p S(C(t))P - k_{out}R \tag{9.73}$$

As for the basic indirect response models, it is assumed that, prior to drug administration at time t = 0, both precursor and response are at their baseline values

$$P(0) = P_0 = \frac{k_0}{k_p} \quad \text{and} \quad R(0) = R_0 = \frac{k_0}{k_{out}} \tag{9.74}$$

Model V has been applied to describe the inhibition of T-helper cell trafficking by prednisolone (Magee et al. 2001). An example of Model VI application is the stimulation of prolactin secretion by antipsychotic drug chlorprothixene (Bagli et al. 1999).

The response versus time profiles for escalating doses from the precursor model are shown in Fig. 9.8. After a single dose of drug with decreasing PK, the response time course of Model V decreases to reach a nadir R_p followed by an increase towards the baseline, crossing to show a rebound RB_p with a subsequent asymptotic return to the baseline. For Model VI the response time-course is inversed. The response increases to reach a peak R_p followed by a decrease towards the baseline, crossing to show a rebound RB_p with a subsequent asymptotic return to the baseline.

The differential equations (9.71) and (9.73) can be integrated to the following integral representation of responses for Models V and VI

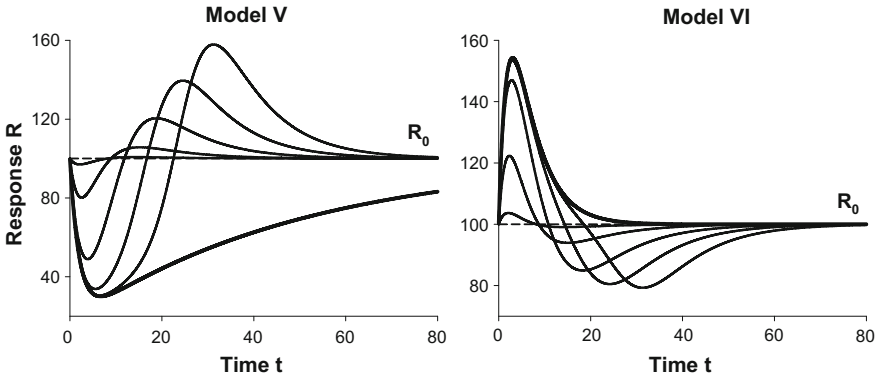

Fig. 9.8 Time courses of two indirect response models with precursor (9.70)–(9.73). The drug plasma concentrations follow monoexponential kinetics with escalating doses. The *bold lines* are the limit values of the responses as $D \to \infty$ (9.76)–(9.77)

$$R(t) = R_0 + P_0 e^{-k_{out}t} - P(t) + k_{out}\int_0^t P(z)e^{-k_{out}(t-z)}dz = R_0 + P_0 e^{-k_{out}t} - P(t) + k_{out}P(t) * e^{-k_{out}t} \tag{9.75}$$

where P(t) is given by Eqs. (9.36) (Model V) and (9.38) (Model VI), with k_{in} replaced by k_0 and k_{out} by k_p.

Large Dose Approximation If dose approaches infinity, so does C(t), and the integral in (9.75) can be evaluated, yielding (Hazra et al. 2006):

Model V

$$R(t) \to R_0 - \frac{R_0 I_{max} k_{out}}{k_{out} - k_p(1 - I_{max})}\left(e^{-k_p(1-I_{max})t} - e^{-k_{out}t}\right), \quad \text{if } k_{out} \neq k_p(1 - I_{max}) \tag{9.76}$$

Model VI

$$R(t) \to R_0 + \frac{R_0 S_{max} k_{out}}{k_{out} - k_p(1 + S_{max})}\left(e^{-k_p(1+S_{max})t} - e^{-k_{out}t}\right), \quad \text{if } k_{out} \neq k_p(1 + S_{max}) \tag{9.77}$$

The limit curves (9.76)–(9.77) after a correction for the baseline R_0 are essentially Bateman functions.

Maximal Response The peak or nadir of the limit functions (9.76)–(9.77) are the maximal responses approached by the peak or nadir response as dose increases to infinity:

$$R_{max} = \begin{cases} R_0 - R_0 I_{max}\left(\frac{k_{out}}{k_p(1-I_{max})}\right)^{\frac{k_p(1-I_{max})}{k_p(1-I_{max})-k_{out}}}, & \text{if } k_p(1 - I_{max}) \neq k_{out}, \quad 0 < I_{max} < 1, \quad \text{Model V} \\ R_0 + R_0 S_{max}\left(\frac{k_{out}}{k_p(1+S_{max})}\right)^{\frac{k_p(1+S_{max})}{k_p(1+S_{max})-k_{out}}}, & \text{if } k_p(1 + S_{max}) \neq k_{out}, \quad \text{Model VI} \end{cases} \tag{9.78}$$

Peak Time and Rebound Peak Time For doses increasing to infinity, the response peak times approach a finite time (except for Model V with $I_{max} = 1$) (Hazra et al. 2006).

Model V

$$t_p \to \frac{\ln\left(k_p(1 - I_{max})/k_{out}\right)}{k_p(1 - I_{max}) - k_{out}}, \quad \text{if } k_p(1 - I_{max}) \neq k_{out}, \; 0 < I_{max} < 1 \tag{9.79}$$

Model VI

$$t_p \to \frac{\ln\left(k_p(1 + S_{max})/k_{out}\right)}{k_p(1 + S_{max}) - k_{out}}, \quad \text{if } k_p(1 + S_{max}) \neq k_{out}, \tag{9.80}$$

The peak of the rebound t_r approaches infinity for large doses for both Model V and Model VI (Hazra et al. 2006):

$$t_r \to \infty \quad \text{as} \quad D \to \infty \tag{9.81}$$

Area Between Baseline and Response Regardless of dose, as long as the drug concentration vanishes after a long time, the area between the baseline and response part of the response curve and the area between the baseline and rebound are always equal (Sharma et al. 1998).

9.4 Signal Transduction Models

Signal transduction is a sequence of events that takes place between binding and activation of the receptor and observable effect. This sequence involves intracellular processes such as a signaling cascade that begins with activation of transmembrane proteins or enzymes, followed by activation of secondary messengers leading to up- or down-regulation of genes, their transcription to mRNA that is further translated to functional proteins, which change the cell status and can cause a cellular response. The affected cells can further propagate the signal either by trafficking and interacting directly with other cells or affecting them indirectly. The indirect interaction can involve initiating a neural signal or secreting hormones that travel with the blood stream. Such cellular responses can lead to changes in functions of tissues and organs, which can impact the behavior of the entire organism. Each step of this multi-scale transduction process might be a measured response. An example of a signal transduction is a sequence of events following binding of methylprednisolone to the glucocorticosteroid receptor that results in its translocation to the nucleus and up- or down-regulation genes causing temporal changes in mRNA for the tyrosine aminotransferase and other enzymes (Ramakrishnan et al. 2002).

By definition, every transduction process has two attributes: it transforms the original signal and can introduce a delay. If the transduction steps are rapid given the experimental scale, the delay might be negligible and the measurable response might be a function of the initial stimulus. However, if such a delay is apparent, modeling of the transduction process must involve mathematical apparatus generating delays.

9.4.1 Signal Transduction Without Delay

A central component for modeling signal transduction is the *stimulus* concept introduced by Stephenson (1956). The stimulus is the product of receptor occupancy and *efficacy,* e. The response is a nonlinear function of the stimulus:

$$E = f\left(\frac{eC}{K_D + C}\right) \tag{9.82}$$

Since efficacy can be both tissue and drug specific, Furchgott (1966) introduced an *intrinsic efficacy,* ε, such that the efficacy is the product of ε and the total receptor concentration R_{tot}

$$E = f\left(\frac{\varepsilon R_{tot} C}{K_D + C}\right) \tag{9.83}$$

9.4.1.1 Operational Model of Agonism

Black and Leff (1983) proposed an operational model of agonism where the efficacy term in the Furchgott model was ignored and the response was only a function of the occupied receptor concentration

$$E = f\left(\frac{R_{tot} C}{K_D + C}\right) \tag{9.84}$$

Moreover, the *transducer function,* f, was assumed to be sigmoidal

$$f(DR) = \frac{E_m DR^n}{K_E^n + DR^n} \tag{9.85}$$

where E_m is the maximum effect, and K_E is the concentration of bound receptors that elicits half-maximal effect. Combining (9.84) and (9.85) allows for the response to be a function of the drug plasma concentration

$$E = \frac{E_m \tau^n C^n}{(K_D + C)^n + \tau^n C^n} \tag{9.86}$$

where the *transducer ratio* $\tau = R_{tot}/K_E$ is a measure of the efficiency of transduction of occupied receptors into the pharmacological effect. The operational model (9.86) was applied to describe the effects of agonists for A_1 adenosine receptor on the heart rate in rat (Van der Graaf et al. 1997).

9.4.2 Signal Transduction with Delay

When the time scale for the transduction delay is not negligible, a delay might be observed in the response. Then the signal transduction is a dynamic process that changes the signal over time. The most common approach is the transit compartment

model that stands out for majority of applications because of its robustness and simplicity. Other possible modeling techniques involve convolution integrals or delay differential equations which are mathematically more advanced and require special software.

9.4.2.1 Transit Compartment Model

The transit compartment model consists of a sequence of transit compartments, M_i, representing non-observable steps of the transduction process by transferring the signal at the same first-order rate constant $1/\tau$, where τ denotes the mean transit time of the signal through a single compartment. The transit compartments are unidirectionally connected, so the output from M_i is the input to M_{i+1} (Fig. 9.9).

The signal enters the first compartment as a time-dependent input, Input(t):

$$\frac{dM_1}{dt} = \text{Input}(t) - \frac{1}{\tau} M_1 \tag{9.87}$$

$$\frac{dM_i}{dt} = \frac{1}{\tau}(M_{i-1} - M_i), \quad i = 2, \ldots, n \tag{9.88}$$

where n is the number of transit compartments. It is assumed that the input for negative times is at the baseline value In_0, approached by the input function after a long time:

$$\text{Input}(t) \to In_0 \quad \text{as } t \to \infty \tag{9.89}$$

Then the initial conditions for the model equations (9.87)–(9.88) are defined by the steady-state

$$M_i(0) = M_0 = In_0 \tau, \quad i = 1, \ldots, n \tag{9.90}$$

For most applications $In_0 = 0$, but the situation where $In_0 > 0$ is not uncommon. Many receptors targeted by drugs are constitutively activated by endogenous ligands (hormones or cytokines) which results in a continuous baseline signal. The integral representation of the solution to (9.87)–(9.88) is

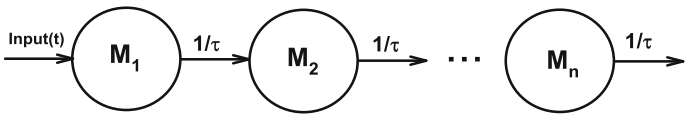

Fig. 9.9 Schematic of the transit compartment model. The first-order output from a compartment is the first-order input to the following compartment. The transit rate constants are the same for each compartment and equal to $1/\tau$, where τ is the mean transit time

$$M_i(t) = M_0 + \tau \int_0^t (In(z) - In_0)\ell_i(t-z)dz = M_0 + \tau(In(t) - In_0) * \ell_i(t),\ i = 1, \ldots, n \tag{9.91}$$

where $\ell_i(t)$ is the gamma probability distribution function (Zelen and Severo 1972)

$$\ell_i(t) = \frac{1}{\tau(n-1)!}\left(\frac{t}{\tau}\right)^{i-1} e^{-t/\tau} \tag{9.92}$$

Gamma Function For the unit impulse input, Input(t) = δ(t), where δ(t) is the Dirac delta function, $In_0 = 0$ and the convolution integral in (9.90) reduces to

$$M_n(t) = \tau\ell_n(t) \tag{9.93}$$

Equation (9.92) implies that the signal in the n-th compartment, initiated by a unit impulse, is proportional to the gamma probability distribution function. The time-courses of $M_n(t)$ corresponding to different numbers of transit compartments are shown in Fig. 9.10.

The signal propagation results in delayed peaks, lowering their heights, and increasing the dispersion with increasing n. The peak time (mode) and the corresponding peak value for $\ell_n(t)$ are

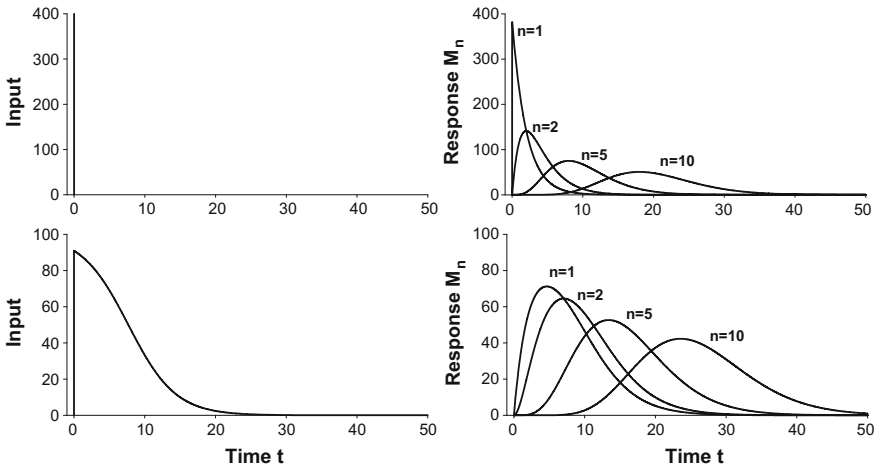

Fig. 9.10 Time courses of inputs (*left*) and responses (*right*) described by the transit compartment model for the varying number of transit compartments n. The input for the upper panel is Input (t) = ABEC·δ(t)/τ whereas the input for the lower panel is Input(t) = 1/τE(C(t)), where E(C) is the E_{max} model and ABEC is the area under the E(C(t)) versus t curve. The concentration C(t) is monoexponential (9.14)

$$t_{mode} = (n-1)\tau \quad \text{and} \quad \ell_n(t_{mode}) = \frac{1}{\tau(n-1)!}\left(\frac{n-1}{e}\right)^{n-1} \tag{9.94}$$

The standard deviation of $\ell_n(t)$ serves as a measure of signal dispersion

$$SD = \sqrt{n}\tau \tag{9.95}$$

Since the signal weakens and dissolves with increasing n, the addition of an amplification factor γ in the last transit compartment equation was suggested by Sun and Jusko (1998):

$$\frac{dM_n}{dt} = \frac{1}{\tau}\left(M_{n-1}^{\gamma} - M_n\right) \tag{9.96}$$

Transit Compartment Model with Stimulus For a transduction process with delays, the relationship between the stimulus and the response cannot be described by a function. Mager and Jusko (2001) introduced a model where the input was the stimulus introduced by Stephenson (9.83) that served as an input to the transit compartment sequence:

$$\text{Input}(t) = \frac{1}{\tau}\frac{\varepsilon R_{tot} C(t)}{K_D + C(t)} \tag{9.97}$$

where the $1/\tau$ is the first-order constant at which the initial signal is generated. In the final form, the model is as follows:

$$\frac{dM_1}{dt} = \frac{1}{\tau}\left(\frac{E_{max} C(t)}{EC_{50} + C(t)} - M_1\right) \tag{9.98}$$

$$\frac{dM_i}{dt} = \frac{1}{\tau}(M_{i-1} - M_i), \quad i = 2, \ldots, n \tag{9.99}$$

where $E_{max} = \varepsilon R_{tot}$ and $EC_{50} = K_D$. In the absence of the baseline drug effect, the initial conditions were set to zeroes

$$M_i(0) = 0, \quad i = 1, \ldots, n \tag{9.100}$$

The model (9.96)–(9.99) was applied to describe the effect of scopolamine and atropine on the parasympathomimetic activity in rats (Perlstein et al. 2002).

The time-courses of $M_n(t)$ for the increasing number of transit compartments are shown in Fig. 9.10. As for the gamma distribution function, the response peaks decrease and peak times increase with n. Also, the response dissipates with increasing n. Although some results regarding the peak time t_p as a function of n have been reported (Yates 2008), a more quantitative relationship between t_p and n for a general model is not known.

Large Dose Approximation The time-courses of the response for escalating doses are shown in Fig. 9.11. If dose becomes large, then the input in (9.97) approaches E_{max}/τ, and the convolution integral in (9.90) can be calculated explicitly:

$$M_n(t) \to E_{max} \int_0^t \ell_n(z)dz = \frac{E_{max}}{(n-1)!} g(n,t/\tau) \quad \text{as} \quad D \to \infty \tag{9.101}$$

where g(n,x) is the incomplete gamma function (Davis 1972). Note that $g(n,t/\tau)/(n-1)!$ is the explicit representation of the cumulative distribution function for the gamma distribution that approaches 1 as $t \to \infty$. Therefore, the maximal response for $M_n(t)$ is

$$M_{nmax} = E_{max} \tag{9.102}$$

Alternative Parameterization Based on the interpretation of τ as the mean transit time of the signal through a transit compartment, the mean transit time of the signal through n compartments (MTT) is the product of n and τ

$$MTT = n\tau \tag{9.103}$$

The MTT parameter characterizes the maturation time for aging cell populations (e.g., Friberg et al. 2002; Harker et al. 2000) and can be measured from in vitro or in vivo experiments contrary to the transit time τ in many cases.

Parameter Estimation A notorious problem for the transit compartment model is a selection of the number of transit compartments. A brute force approach often applied in practice is to assign n a series of integers and select the lowest one that

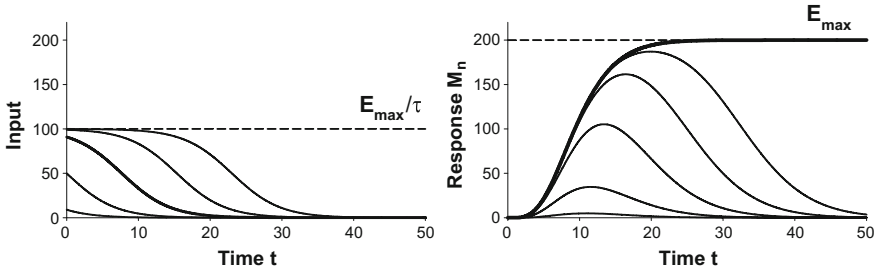

Fig. 9.11 Time-courses of the Input(t) and response $M_n(t)$ for the transit compartment model (9.93)–(9.94) for escalating doses with n = 5. Input(t) = $1/\tau E(C(t))$, where E(C) is the E_{max} model. The concentrations C(t) are monoexponential (9.14). The *bold line* is the limit values of the response as $D \to \infty$ (9.96)

does not significantly improve the goodness of fit criterion value. A more sophisticated approach that applies only to models with explicit solution to M_n (9.93) is to estimate n as a real number. This requires the factorial in (9.93) to be replaced by a continuous Euler gamma function $\Gamma(n)$ (Davis 1972) or to use Stirling's approximation (Savic et al. 2007):

$$n! \sim \sqrt{2\pi n} n^n e^{-n} \quad \text{as} \quad n \to \infty \tag{9.104}$$

9.5 Summary

In this chapter, the basic components of the major PD models (Jusko et al. 1995) have been introduced. These have encompassed direct, indirect, and transit compartment models. Ever evolving experimental technology offers new biomarkers or extends existing ones as measures of PD responses. This enables the better quantification of mechanisms of drug action resulting in an increased complexity of the mathematical models describing such biological systems. Consequently, the basic models serve as unit blocks that can be connected in a multi-scale and multi-level complex model capable of describing available data. The model complexity typically necessitates an increase in the system dimension (number of state variables), but also requires a network of interactions between the model components. Examples of such complex systems can be found among PD models describing interactions between glucagon, insulin, and glucose (Peng et al. 2014). High dimensionality and cross-talk between model variables are the key features of *systems biology* models. Merging PK/PD modeling principles with systems biology approaches sets ground for the field of *systems pharmacology* (Jusko 2013).

References

Ariens EJ (1954) Affinity and intrinsic activity in the theory of competitive inhibition. I. Problems and theory. Arch Int Pharmacodyn Ther 99:32–49

Bagli M, Süverkrüp R, Quadflieg R, Höflich G, Kasper S, Möller HJ, Langer M, Barlage U, Rao ML (1999) Pharmacokinetic-pharmacodynamic modeling of tolerance to the prolactin-secreting effect of chlorprothixene after different modes of drug administration. J Pharmacol Exp Ther 291:547–554

Black JW, Leff P (1983) Operational models of pharmacological agonism. Proc R Soc Lond B: Biol Sci 220:141–162

Budha NR, Kovar A, Meibohm B (2011) Comparative performance of cell lifespan and cell transit models for describing erythropoietic drug effects. AAPS J 13:650–661

Bulitta JB, Zhao P, Arnold RD, Kessler DR, Daifuku R, Pratt J, Luciano G, Hanauske A-R, Gelderblom H, Awada A, Jusko WJ (2009) Multiple-pool cell lifespan models for neutropenia

to assess the population pharmacodynamics of unbound paclitaxel from two formulations in cancer patients. Cancer Chemother Pharmacol 63:1035–1048

Chakraborty A, Krzyzanski W, Jusko WJ (1999) Mathematical modeling of circadian cortisol concentrations using indirect response models: comparison of several methods. J Pharmacokinet Biopharm 27:23–43

Clark AJ (1933) The mode of action of drugs on cells. Edward Arnold, London

Davis PJ (1972) Gamma function and related functions. In: Abramowitz M, Stegun I (eds) Handbook of mathematical functions with formulas, graphs, and mathematical tables. Dover Publications, New York

Detivaud L, Nemeth E, Boudjema K, Turlin B, Troadec MB, Leroyer P, Ropert M, Jacquelinet S, Courselaud B, Ganz T, Brissot P, Loreal O (2005) Hepcidin levels in humans are correlated with hepatic iron stores, hemoglobin levels, and hepatic function. Blood 106:746–748

Dayneka NL, Garg V, Jusko WJ (1993) Comparison of four basic indirect pharmacodynamic responses. J Pharmacokinet Biopharm 21:457–478

Dutta S, Matsumoto Y, Ebling WF (1996) Is it possible to estimate the parameters of the sigmoid Emax model with truncated data typical of clinical studies? J Pharm Sci 85:232–239

Edeki T, Johnston A, Li Kam Wa E, Turner P (1994) Enalapril pharmacokinetics and ACE inhibition, following single and chronic oral dosing. Int J Clin Pharmacol Ther 32:142–146

Evans MA, Shanks CA, Brown KF, Triggs EJ (1984) Pharmacokinetic and pharmacodynamic modelling with pancuronium. Eur J Clin Pharmacol 26:243–250

Frazier EP, Schneider T, Michel TM (2006) Effects of gender, age and hypertension on β-adrenergic receptor function in rat urinary bladder. Naunyn-Schmiedeberg's Arch Pharmacol 373:300–309

Friberg LE, Henningsson A, Maas H, Nguyen L, Karlsson MO (2002) Model of chemotherapy induced myelosuppression with parameter consistency across drugs. J Clin Oncol 20:4713–4721

Furchgott RF (1966) The use of β-haloalkylamines in the differentiation of receptors and in the determination of dissociation constants receptor-agonist complexes. In: Harper NJ, Simmonds AB (eds) Adavnces in drug research, vol 3. Academic Press, New York

Harker LA, Roskos LK, Marzec UM, Carter RA, Cherry JK, Sundell B, Cheung EL, Terry D, Sheridan W (2000) Effects of megakaryocyte growth and development factor on platelet production, platelet life span, and platelet function in healthy human volunteers. Blood 95:2514–2522

Hazra A, Krzyzanski, Jusko WJ (2006) Mathematical assessment of properties of precursor-dependent indirect pharmacodynamic response models. J Pharmacokin Pharmacodyn 33:683–717

Hill A (1910) The possible effects of the aggregation of the molecules of haemoglobin on its dissociation curves. J Physiol 40:IV–VIII

Jamal NM, Krzyzanski W, Cheung W, Lau CY, Messner HA (2006) Evaluation of epoetin alpha (rHuEPO) and darbepoetin alpha (DARB) on human burst-colony formation (BFU-E) in culture. J Int Med Res 34:42–51

Jordan P, Gieschke R (2005) Explicit solutions for a class of indirect pharmacodynamic response models. Comput Methods Programs Biomed 77:91–97

Jusko WJ (2013) Moving from basic toward systems pharmacodynamic models. J Pharm Sci 102:2930–2940

Jusko WJ, Ko HC (1994) Physiologic indirect response models characterize diverse types of pharmacodynamic effects. Clin Pharmacol Ther 56:406–419

Jusko WJ, Ko HC, Ebling WF (1995) Convergence of direct and indirect pharmacodynamic response models. J Pharmacokinet Biopharm 23:5–8

Kenakin TP (2006) A pharmacology primer. Theory, applications, and methods. Elsevier, Amsterdam

Koch G, Schropp J (2013) Solution and implementation of distributed lifespan models. J Pharmacokinet Pharmacodyn 40(6):639–650

Krzyzanski W, Dmochowski J, Matsushima N, Jusko WJ (2006) Assessment of dosing impact on intra-individual variability in estimation of parameters for basic indirect response models. J Pharmacokin Pharmacodyn 33:635–655

Krzyzanski W, Jusko WJ (1997) Mathematical formalism for the properties of four basic models of indirect pharmacodynamic responses. J Pharmacokin Biopharm 25:107–123

Krzyzanski W, Jusko WJ (1998) Characterization of pharmacodynamic recession slopes for direct and indirect response models. J Pharmacokin Biopharm 26:409–436

Krzyzanski W, Perez Ruixo JJ (2012) Lifespan based indirect response modelds. J Pharmacokinet Pharmacodyn 39:109–123

Krzyzanski W, Ramakrishnan R, Jusko WJ (1999) Basic models for agents that alter production of natural cells. J Pharmacokin Biopharm 27:467–489

Labrecque G, Belanger PM (1991) Biological rhythms in the absorption, distribution, metabolism and excretion of drugs. Pharmacol Ther 52:95–107

Levy G (1966) Kinetics of pharmacologic effects. Clin Pharmacol Ther 7:362–372

Lew KH, Ludwig EA, Milad MA, Donovan K, Middleton E Jr, Ferry JJ, Jusko WJ (1993) Gender-based effects on methylprednisolone pharmacokinetics and pharmacodynamics. Clin Pharmacol Ther 54:402–414

Nagashima R, O'Reilly RA, Levy G (1969) Kinetics of pharmacologic effects, in man: the anticoagulant action of warfarin. Clin Pharmacol Ther 10:22–35

Magee MH, Blum RA, Lates CD, Jusko WJ (2001) Prednisolone pharmacokinetics and pharmacodynamics in relation to sex and race. J Clin Pharmacol 41:1180–1194

Mager DE, Jusko WJ (2001) Pharmacodynamic modeling of time-dependent transduction systems. Clin Pharmacol Ther 70:210–216

Mager DE, Wyska E, Jusko WJ (2003) Diversity of mechanism-based pharmacodynamic models. Drug Met Disp 31:510–518

Mo G, Gibbons F, Schroeder P, Krzyzanski W (2014) Lifespan based pharmacokinetic-pharmacodynamic model of tumor growth inhibition by anticancer therapeutics. PLoS ONE 9(10):e109747

Peletier LA, Gabrielsson J, den Haag J (2005) A dynamical systems analysis of the indirect response model with special emphasis on time to peak response. J Pharmacokinet Pharmacodyn 32:607–654

Peng JZ, Denney WS, Musser BJ, Liu R, Tsai K, Fang L, Reitman ML, Troyer MD, Engel SS, Xu L, Stoch A, Stone JA, Kowalski KG (2014) A semi-mechanistic model for the effects of a novel glucagon receptor antagonist on glucagon and the interaction between glucose, glucagon, and insulin applied to adaptive phase II design. AAPS J 16:1259–1270

Perlstein I, Stepansky D, Krzyzanski W, Hofman A (2002) A signal transduction pharmacodynamic model of the kinetics of parasympathomimetic activity of low-dose scopolamine and atropine in rats. J Pharm Sci 91:2500–2510

Ramakrishnan R, DuBois D, Almon RA, Pyszczynski NA, Jusko WJ (2002) Fifth-generation model for corticosteroid pharmacodynamics: steady-state receptor down-regulation and enzyme induction patterns during seven-day continuous infusion of methylprednisolone in rats. J Pharmacokin Pharmacodyn 29:1–24

Reppert SM, Weaver DR (2002) Coordination of circadian timing in mammals. Nature 418:935–941

Rohatagi S, Bye A, Falcoz C, Mackie AE, Meibohm B, Mollmann H, Derendorf H (1996) Dynamic modeling of cortisol reduction after inhaled administration of fluticasone proprionate. J Clin Pharmacol 36:938–941

Sallstrom B, Visser SAG, Forsberg T, Peletier LA, Ericson AC, Gabrielsson J (2005) A pharmacodynamics turnover model capturing assymetric circadian baselines of body temperature, heart rate and blood pressure in rats: challenges in terms of tolerance and animal-handling effects. J Pharmacokinet Pharmacodyn 32:835–859

Samtani MN, Perez-Ruixo JJ, Brown K, Carneus D, Molloy C (2009) Pharmacokinetic and pharmacodynamic modeling of pegylated thrombopoietin mimetic peptide (PEG0TPOm) after single intravenous dose in healthy subjects. J Clin Pharmacol 49:336–350

Savic RM, Jonker DM, Kerbusch T, Karlsson MO (2007) Implementation of a transit compartment model for describing drug absorption in pharmacokinetic studies. J Pharmacokinet Pharmacodyn 34:711–726

Schwartz JB, Verotta D, Sheiner LB (1989) Pharmacodynamic modeling of verapamil effects under steady-state and nonsteady state conditions. J Pharmacol Exp Ther 251:1032–1038

Sharma A, Ebling WF, Jusko WJ (1998) Precursor-dependent indirect pharmacodynamic response model for tolerance and rebound phenomena. J Pharm Sci 87:1577–1584

Sharma A, Jusko WJ (1996) Characterization of four basic models of indirect pharmacodynamics responses. J Pharmacokin Biopharm 24:611–635

Sheiner LB, Stansky DR, Vozeh S, Miller RD, Ham J (1979) Simultaneous modeling of pharmacokinetics and pharmacodynamics: application to d-tubocurarine. Clin Pharmacol Ther 25:358–371

Simeoni M, Magni P, Cammia C, De Nicolao G, Croci V, Pesenti E, Germani M, Poggesi I, Rocchetti M (2004) Predictive pharmacokinetic-pharmacodynamic modeling of tumor growth kinetics in xenograft models after administration of anticancer agents. Cancer Res 64:1094–1101

Stephenson RP (1956) A modification of receptor theory. Br J Pharmacol 11:379–393

Sukumaran S, Almon RR, DuBois DC, Jusko WJ (2010) Circadian rhythms in gene expression: Relationship to physiology, disease, drug disposition and drug action. Adv Drug Deliv Rev 62:904–917

Sun YN, Jusko WJ (1998) Transit compartments versus gamma distribution function to model signal transduction processes in pharmacodynamics. J Pharm Sci 87:732–737

Van der Graaf PH, Van Schaick EA, Matho RAA, Ijzermn AP, Danhof M (1997) Mechanism-based pharmacokinetic-pharmacodynamic modeling of the effects of N^6-cyclopentyladenosine analogs on heart rate in rat: Estimation of in vivo operational affinity and efficacy at adenosine A1 receptors. J Pharmacol Exp Ther 283:809–816

Wagner JG (1968) Kinetics of pharmacologic response: I. Proposed relationship between response and drug concentration in the intact animal and man. J Theor Biol 20:173–201

Whiting B, Kelman AW, Barclay J, Addis GJ (1981) Modeling theophylline response in individual patients with chronic bronchitis. Br J Clin Pharmacol 12:481

Yamakage M (1992) Direct inhibitory mechanism of halothane on canine tracheal smooth muscle contraction. Anesthesiology 77:546–553

Yao Z, Krzyzanski W, Jusko WJ (2006) Assessment of basic indirect pharmacodynamic response models with physiological limits. J Pharmacokin Pharmacodyn 33:167–193

Yates JWT (2008) Mathematical properties and parameter estimation for transit compartment pharmacodynamic models. Eur J Pharm Sci 34:104–109

Zelen M, Severo NC (1972) Probability functions. In: Abramowitz M, Stegun IA (eds) Handbook of mathematical functions with formulas, graphs, and mathematical tables. Dover Publications, New York

Chapter 10
Irreversible Pharmacodynamics

Alberto Russu and Italo Poggesi

Abstract The assessment of pharmacodynamics (PD) and their relationship to drug exposure are of paramount importance in drug development processes. PD effects are typically initiated by the interaction of drugs with target systems (receptors, enzymes, channels, membranes, etc.). These interactions can be reversible (i.e., governed by chemical equilibria) or irreversible (as is the case of a compound forming covalent bonds with its target). Following these interactions, a cascade of events is triggered, that can again be reversible or irreversible in nature. This chapter describes some examples of drug-induced irreversible processes, focused on the mathematical models that have been used in the literature to describe them. In many cases, imperfect knowledge and limitations of experimental designs are reflected in uncertainties in the interpretation of the experimental results: different classes of models, both irreversible and reversible, may provide reasonably accurate descriptions of a certain set of data. The use of System Pharmacology approaches, which incorporate the knowledge of the interconnections between events involved in the observation of a particular drug response, will help in providing a more mechanism-based interpretation of irreversible pharmacodynamics.

Keywords Chemical equilibrium · Irreversible drug action · Concentration-effect relationship · Target · Slow dissociation · Turnover model · Direct-effect model · Mechanism of action

10.1 Introduction

Pharmacodynamic (PD) models, which describe the time-course of drug effect and their relationship to drug exposure (PK/PD), are important tools for drug development (Mager et al. 2003; Ploeger et al. 2009). Substantial portions of a drug's

A. Russu (✉) · I. Poggesi
Clinical Pharmacology and Pharmacometrics, Janssen Research and Development, Turnhoutseweg 30, 2340 Beerse, Belgium
e-mail: arussu@its.jnj.com

D.E. Mager and H.H.C. Kimko (eds.), *Systems Pharmacology and Pharmacodynamics*, AAPS Advances in the Pharmaceutical Sciences Series 23,
DOI 10.1007/978-3-319-44534-2_10

label nowadays describe these relationships to provide practitioners with indications on how to handle dose levels and dosing regimens to obtain the desired therapeutic effect. For instance, the label of gabapentine reports: "Pharmacokinetic/pharmacodynamic modeling provided confirmatory evidence of efficacy across all doses" (Gabapentine package insert 2014).

Therapeutic drug effects are related to the interaction with targets (e.g., receptors, proteins, hormones, or ion channels). These interactions develop a cascade of downstream effects that result in a clinical response (Mager et al. 2003; Danhof et al. 2005; Ploeger et al. 2009). This process is schematically represented in Fig. 10.1. It is possible that the interaction of a drug with the target happens via a chemical equilibrium (i.e., via a process that is reversible by definition). Likewise, it is possible that the same interaction occurs via an irreversible process, for instance, the so-called "suicide inhibition". There are a number of drugs acting in this way, for instance: suicide inhibitors of cytochrome P-450 (CYP) 19, such as exemestane (Miller et al. 2009), and CYP17, such as abiraterone (Bryce and Ryan 2012) are part of the therapeutic armamentarium for the treatment of breast and prostate cancer, respectively. In many cases, compounds such as these are transformed into reactive metabolites, which bind covalently to the target, thereby inactivating the target itself (Miller et al. 2009). To recover the pre-dose situation, de novo synthesis of the target is required. Other processes along the chain linking the target interaction step to the final clinical response can be irreversible in nature, for instance, killing of pathogens (e.g., bacteria, viral load) or processes implying cell kill, such as those occurring during tumor growth inhibition.

The objective of this chapter is to examine the drug-induced processes (drug target engagement, target activation, and downstream occurrence of physiological or pathophysiological responses) that may be described as irreversible processes and to provide some of the basic model building blocks that are used to describe these events, together with some key examples reported in the literature.

Due to a variety of reasons, such as imperfect knowledge, suboptimal experimental designs, lack of information related to important covariates, or relative empiricism of the available models, there is sometime a disconnect between the irreversible nature of some processes and the "reversible-like" nature of the models

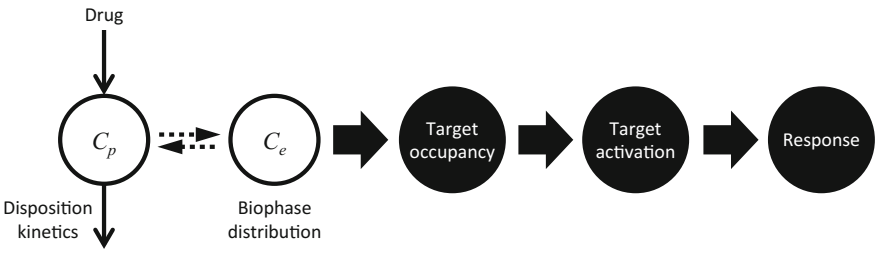

Fig. 10.1 Schematic representation of processes involved in the generation of a pharmacological response

used to describe them. The use of System Pharmacology approaches (Van Der Graaf 2012), which are grounded on detailed mechanisms, may help in providing a more mechanism-based interpretation of irreversible pharmacodynamics.

10.2 Mechanistic/Biological Principles of Irreversible Drug Action

10.2.1 Background

The interaction between a natural agonist and a target (e.g., a receptor) is typically the first event that triggers a certain biological process. A drug response is elicited when a compound interacts with a target and modifies its natural function, thus altering the downstream cascade of events, as shown in Fig. 10.1.

In the case of interactions at the receptor level, simple considerations based on the law of mass action suggest that the formation of the agonist-receptor complex can be described by a saturable function of the agonist concentration. According to classical receptor theories (e.g., Occupational Theory, Operational Model of Agonism, see Kenakin 1997 for a review), pharmacological response to an agonist drug can be related to the quantity of drug-receptor complex and, in turn, to drug concentration through a proportionality factor, e.g., the "intrinsic activity" (Ariens 1954) or the "transducer constant" (Black and Leff 1983). Therefore, the overall relationship

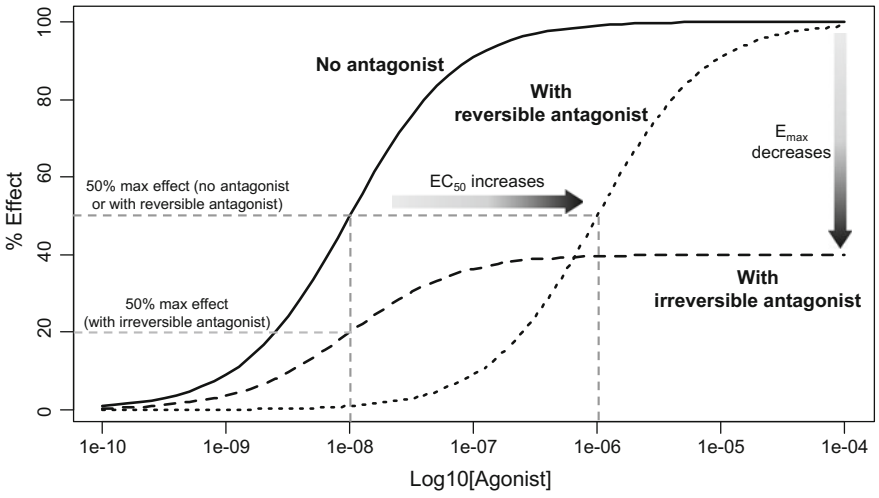

Fig. 10.2 Example of concentration-effect relationship for a hypothetical agonist, in absence and presence of a given antagonist. Two specific cases of reversible and irreversible antagonism are shown: increased EC_{50} with E_{max} unchanged, and decreased E_{max} with EC_{50} unchanged

between agonist concentration and effect may in turn be described by a saturable function, as exemplified by the "No antagonist" curve in Fig. 10.2.

On the contrary, a drug acting as an antagonist decreases the effect of a natural agonist. In this case, these drugs bind to receptors but do not act like agonists and, therefore, do not activate receptor function. These antagonists may block the ability of agonists to bind to the receptor, for example by competing for the same receptor site. In this respect, the antagonist-receptor interaction is regulated by a chemical equilibrium, which is a reversible process.

10.2.2 Irreversible Interaction with the Target

In case the antagonist forms covalent bonds with the receptor at the agonist binding site (for instance, via the formation of a reactive intermediate), a complex with the receptor is formed via an irreversible process, which effectively inactivates the receptor. The number of remaining unoccupied receptors may be too low for even high concentrations of agonist to elicit a maximal response.

Figure 10.2 provides a simple example of how the concentration-effect relationship of an agonist would change in the presence of a reversible or an irreversible antagonist, compared to a scenario with no antagonist. In presence of a reversible antagonist competing with the agonist for the same binding site, the agonist EC_{50} would increase, according to the law of mass action. In the presence of an irreversible antagonist, the EC_{50} (i.e., the agonist concentration associated to half-maximal effect) would remain unchanged with respect to a scenario with no antagonist, since the agonist undergoes no competition at antagonist-free receptors. Conversely, the E_{max} (i.e., maximum effect as percentage of the effect obtained with the agonist alone) would be decreased by the presence of the irreversible antagonist, since less free receptors would be available for agonist binding. The reader is referred to Kenakin (1997) for further details and a thorough overview of possible scenarios.

In an in vivo setting, the scenario is even more complex because of the presence of dynamic aspects. For example, the antagonist concentrations are not constant, but change with time as a consequence of the drug input (i.e., dosing regimen and absorption processes) and of the processes related to subsequent drug disposition. Also, once bound to the receptor, there is no need for an irreversible antagonist to be resent in the biophase to inhibit the effects of the agonist. Thus the duration of action of such an inhibitor is relatively independent of its rate of elimination from the body and essentially dependent on the rate of turnover of receptor molecules. Recovery of receptor takes place through re-synthesis, rather than dissociation of the drug-receptor complex (as in reversible inhibition). Similarly, in irreversible inhibition of targets such as enzymes, the time to recovery is dependent upon the synthesis of new enzyme, rather than upon the dissociation and elimination of the inhibitor.

Therefore, because of the aforementioned time-dependency aspects, the models that describe the relationships between dosing regimens and effects need to consider the dynamic nature of these processes. The static relationships exemplified in Fig. 10.2 are in general not adequate for such a task, and rather represent a special case where effect can be related to constant concentrations of agonist and antagonist (e.g., an in vitro setup). In an in vivo scenario, receptor binding and/or effect are often more suitably expressed by means of differential equations, which provide a convenient tool for modeling possible delays between pharmacokinetics (PK), receptor binding, and onset of effect.

10.2.3 Reversible Interaction with the Target Under Slow Dissociation

In many scenarios of drug-receptor interaction, the equilibrium between bound and unbound forms of the receptor is characterized by much faster kinetics than the other processes involved, such as turnover of the free receptors, or the natural degradation of the drug-receptor complex. However, there may be cases where the dissociation processes involving drug and receptor are much slower compared to the other dynamics of the system. Therefore, although the mechanism is in principle reversible, the overall interaction can be essentially considered irreversible. Consequently, re-synthesis of the receptor becomes the dominant mechanism of receptor recovery, since the drug-receptor dissociation process takes place on a much longer time scale. Moreover, slow dissociation kinetics may have implications on the duration of pharmacological and toxicological effects, as exemplified in the reviews by Tummino and Copeland (2008) and Copeland et al. (2006), where the relevance of long residence times associated with different receptor-ligand complexes is described.

10.2.4 Induction of an Irreversible Phenomenon

A pharmacodynamic effect can be considered irreversible in general if the drug induces a given irreversible phenomenon, regardless of the mechanism of interaction with the target (i.e., either reversible or irreversible). In this respect, all events dealing with organism or cell kill can be considered irreversible. Various examples of irreversible processes are:

- Bactericidal action of antibiotics (Nielsen et al. 2011);
- Reduction of viral load due to the treatment with antivirals (Snoeck et al. 2010);
- Cell death processes induced by anticancer drugs, which elicit tumor growth inhibition compared to controls in preclinical models (Simeoni et al. 2004), or which cause the tumor shrinkage with respect to the initial condition in cancer patients (Claret and Bruno 2009);

- White blood cell progenitor kill process induced by cytotoxic therapies leading to myelosuppression (Friberg et al. 2000);
- Occurrence of mutagen or teratogen effects (Jusko 1971a);
- Irreversible inhibition of enzyme turnover, as is reported for the turnover of cyclo-oxygenase-1 (COX-1) enzyme by aspirin (Hong et al. 2008) or gastric H^+, K^+-ATPase by omeprazole (Äbelö et al. 2000).

Also in this case, as for the irreversible reaction leading to a covalent drug-receptor complex, the processes can be interpreted as the extraction of a component (pathogen, cell, enzyme etc.) or the formation of a new component (mutated cell) from the system via the interaction with the xenobiotic.

10.3 Turnover Model with Irreversible Inactivation

According to classical receptor theory, receptor binding is governed by the law of mass-action and assumes reversible binding, as shown in Eq. (10.1):

$$\begin{cases} \dfrac{drC}{dt} = k_{on}\left(r_T - rC\right)C - k_{off}\,rC & rC(0) = 0 \\ \dfrac{dr}{dt} = k_{syn} - k_{deg}\,r + k_{off}\,rC - k_{on}\left(r_T - rC\right)C & r(0) = r_T \end{cases} \qquad \begin{array}{ccccc} & & k_{syn} & & \\ & & \downarrow & & \\ D & + & r & \underset{k_{off}}{\overset{k_{on}}{\rightleftharpoons}} & rD \\ & & \downarrow & & \vdots \\ & & k_{deg} & & k_{elim} \end{array} \tag{10.1}$$

where r is the concentration of free receptors (denoted as lowercase, to distinguish from response R), C is the concentration of drug D in the biophase, and rC is the concentration of drug-receptor complex (rD). The total concentration of receptors (i.e., in free and bound form) is given by $r_T = r + rC$. Synthesis and degradation of the receptor are ruled by the zero-order rate constant k_{syn} and the first-order degradation rate constant k_{deg}, respectively. Formation of the drug-receptor complex is governed by the association rate constant k_{on} and the dissociation rate constant k_{off} (the degradation of the drug-receptor complex with rate constant k_{elim} has been omitted from the equation for simplicity), as shown also graphically in the scheme at the right of the equation.

A mathematical model for irreversible receptor binding can then be readily derived from Eq. (10.1) by dropping the term $k_{off} \times rC$, as shown in Eq. (10.2):

$$\begin{cases} \frac{drC}{dt} = k_{on}(r_T - rC)C & rC(0) = 0 \\ \frac{dr}{dt} = k_{syn} - k_{deg}r - k_{on}(r_T - rC)C & r(0) = r_T \end{cases} \tag{10.2}$$

From Eq. (10.2), it is easy to observe that, because of irreversible receptor binding, the free receptors can only be restored through re-synthesis (via the formation rate constant k_{syn}). This also accounts for the time-dependent pharmacodynamic features of irreversible binding, in that the restoration of free receptors is rate-limited by the re-synthesis process, assuming that the drug half-life is relatively shorter.

A pharmacological response R, elicited from receptor binding, may be assumed proportional to rC/r_T (e.g., for agonists, so that response increases with increasing

concentrations rC), or to $(r_T - rC)/r_T$ (e.g., for antagonists, so that response decreases with increasing concentrations of rC), although other choices of the transduction function are possible, depending on the specific context (see Kenakin 1997 for a review). Assuming that response is proportional to the fraction of free receptors with a linear transduction constant equal to 1, i.e., $R = R_0 \times (r/r_T)$, Eq. (10.2) can be easily reparametrized in terms of response R, yielding:

$$\frac{dR}{dt} = k_{in} - k_{out}R - f(C)R \quad R(0) = R_0 \tag{10.3}$$

where R denotes the response variable, R_0 is its initial value, k_{in} is a zero-order production rate of the response, and k_{out} is a first-order elimination rate constant, representing the turnover rate of the response. At equilibrium and in absence of drug effect, it follows that $R_0 = k_{in}/k_{out}$. Comparing Eqs. (10.2) and (10.3), it can be observed that $k_{in} = k_{deg} \times R_0$, $k_{out} = k_{deg}$, $f(C) = k_{on} \times C$.

In general, the turnover model, which can be schematically represented as in Fig. 10.3, can be effectively used to model pharmacodynamic effects arising not only from irreversible receptor binding, but also from irreversible interaction between a drug and other targets such as endogenous enzymes or ion channels. In such cases, parameters k_{in} and k_{out} represent apparent rates of response formation and dissipation, rather than parameters related to receptor synthesis and degradation. In the general form of Eq. (10.3), drug effect is implemented as a function of the drug concentration, $f(C)$, and the elimination term $f(C) \times R$ can be interpreted as a bimolecular interaction between the drug and the target, which is irreversibly inactivated. Possible choices of $f(C)$ are a linear function, $f(C) = slope \times C$, or a sigmoid-type function, e.g. $f(C) = E_{\max} \times C^{\gamma}/(EC_{50}^{\gamma} + C^{\gamma})$. In general, the concentration C can be a plasma concentration (C_p) or the concentration in a hypothetical effect compartment (C_e). Although more complex scenarios are possible, requiring suitable models to be developed on an ad hoc basis, the turnover model has been widely used in the literature, for example in modeling the irreversible effects of omeprazole (Äbelö et al. 2000) and irreversible 5α-reductase inhibitors (Gisleskog et al. 1998; Katashima et al. 1998).

We discuss here the concepts of irreversible target inactivation with an example on exemestane, an irreversible aromatase inactivator used for the treatment of postmenopausal women with advanced breast cancer. The work by Valle et al. (2004) investigates the impact of exemestane PK on plasma estrone sulphate (E1S), using a PK/PD approach. The proposed PD model assumes that E1S plasma concentrations are determined by a zero-order synthesis rate k_s, indirectly related to aromatase activity, and a first-order elimination constant k_o. Inhibition of E1S synthesis by plasma exemestane concentration C is controlled by an IC_{50} parameter,

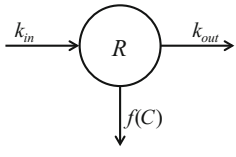

Fig. 10.3 Schematic representation of the turnover model with irreversible elimination of response

which gives rise to a standard type I indirect response model (Dayneka et al. 1993), as shown in Eq. (10.4):

$$\frac{dE1S}{dt} = k_s\left(1 - \frac{C^\gamma}{IC_{50}^\gamma + C^\gamma}\right) - k_o E1S \quad E1S(0) = E1S_0 \tag{10.4}$$

where γ is a Hill coefficient and $E1S_0$ is the baseline E1S concentration.

The delay observed between the peak plasma exemestane exposure and the peak effect on E1S was suitably modeled through a type I indirect response model, which is a reasonable modeling choice whenever such delays between PK and PD are observed, and/or when the mechanism of action is unknown. Such a simple, semi-empirical approach fitted the data well and required only four parameters (baseline E1S, k_o, IC_{50}, and γ), although in many applications the Hill coefficient is not introduced so as to obtain an even more parsimonious model. As an alternative, a type IV indirect response model was applied, with a slightly less satisfactory fitting than the type I model (Poggesi et al. 1999).

Although the PK/PD data were satisfactorily fitted using the semi-empirical, indirect-response model, a more mechanism-based approach was also developed, whereby irreversible aromatase inhibition was explicitly modeled. The mechanistic model introduces aromatase concentration, Ar, as a system variable which controls the synthesis rate of E1S. The rate of change of Ar is in turn governed by a zero-order rate constant of production, k_{se}, and a first-order rate constant of elimination, k_{oe}. Irreversible aromatase inhibition was modeled by allowing plasma exemestane concentrations to increase aromatase elimination (i.e., enzyme inactivation), by means of a second-order rate constant k_i. The mechanism-based irreversible effects model is given by Eq. (10.5a,b):

$$\begin{aligned} &\tfrac{dAr}{dt} = k_{se} - k_{oe}Ar - k_i C \cdot Ar \quad Ar(0) = Ar_0 \\ &\tfrac{dE1S}{dt} = k_s Ar - k_o E1S \qquad\qquad E1S(0) = E1S_0 \end{aligned} \tag{10.5a, b}$$

where Ar_0 is the baseline aromatase concentration. Note that model of Eq. (10.5a,b) is fully identifiable provided that Ar is observed. Otherwise, as mentioned in Sect. 10.6, a re-parametrization must be performed so as to remove the redundancy between k_{se} and k_s, thus enabling parameter identifiability.

In this specific example, the hypothesized mode of action for exemestane would have favored the adoption of such an irreversible aromatase inhibition model. Interestingly, however, the irreversible and type I indirect-response models proved reasonably equivalent in terms of goodness-of-fit and model selection criteria. Despite being semi-empirical in nature, in that it does not implement the actual exemestane mode of action, the type I indirect-response model was able to predict the drug effect in different conditions (dose levels, dosing regimens), in reasonable agreement with data not used for the PK/PD model development. Overall, this seems to suggest that, in certain circumstances, the available data may not provide

sufficient information to prefer a mechanistic model to a more empirical one, even when the mechanism of action can be explicitly modeled.

10.4 Model of Slow Reversible Drug-Receptor Binding

As indicated in Sect. 10.3, a particular case of the reversible receptor binding model (see Eq. 10.1) occurs when the dissociation process is much slower compared to the other processes. In such a case, although the molecular interaction is reversible, it is not possible to describe the system through the equilibrium equation of fast and reversible binding (i.e., $rC = r_T \times C/(K_D + C)$, where $K_D = k_{off}/k_{on}$ is the equilibrium dissociation constant). Therefore, in practice, Eq. (10.1) will have to be used as-is to fit experimental data. Parameter estimation will then enable to assess the relative magnitude of the different kinetics involved in the binding and the velocity of the dissociation process (often reported as a dissociation half-life, i.e., $t_{1/2,off} = log(2)/k_{off}$). It is interesting to note that, in principle, the same data could potentially be described also through Eq. (10.2), which is equivalent to Eq. (10.1) with the term $k_{off} \times rC$ dropped, because of the assumption of slow dissociation.

The work by Yassen et al. (2007) provides a practical example of such a scenario, whereby the respiratory depressant effects of buprenorphine is described through a mechanistic PK/PD modeling approach. A biophase equilibration model with receptor association/dissociation (Eq. 10.1), combined with a linear transduction function, was selected as the most suitable model to fit ventilatory response data. The analysis of parameter estimates confirmed that buprenorphine is characterized by relatively slow kinetics of dissociation from the μ-opiod receptor, with a dissociation half-life $t_{1/2,off} = 68$ min ($K_D = 0.089$ nM), which is consistent with results from previous in vitro studies. Moreover, the delay in onset and the prolonged duration of respiratory effect appeared to be explained not only by slow receptor binding kinetics, but also by the relatively slow effect site equilibration ($log(2)/k_{eo} = 75$ min).

10.5 Modeling the Induction of Irreversible Processes

In certain physiological systems, a response variable can be subject to growth or proliferation over time (e.g., tumor cells, pluripotent stem cells, and bacterial or viral load). This is usually modelled by assuming that the rate of change of a response variable R is governed by a growth function $g(R)$ (e.g., exponential growth, $g(R) = k_g \times R$, or logistic growth, $g(R) = k_g \times R \times (1 - R/R_{\max})$, where k_g and $R_{\max}$ represent the growth rate constant and the maximum value of response). When the response variable is represented by proliferating cells, irreversible inactivation or cell killing (e.g., by means of a chemotherapeutic agent) can be modelled as in Eq. (10.6):

$$\frac{dR}{dt} = g(R) - f(C)R \quad R(0) = R_0 \tag{10.6}$$

As described earlier, $f(C)$ is often modelled as a linear or sigmoid-type function of drug concentration either in plasma or in a biophase compartment. Under repeated dosing or infusion regimens, the system in Eq. (10.6) may converge to a steady-state equilibrium R_∞ (possibly even $R_\infty = 0$), or diverge to infinity, depending on the relative magnitude of proliferation (expressed by $g(R)$) and cell inactivation (expressed by $f(C)$).

This class of models has been originally introduced to describe phase specific or non-specific cell inactivation by chemotherapeutic drugs (Jusko 1971b, 1973). These concepts have been extended to account for possible delays between irreversible drug action on a given target and cell elimination. In the field of cytotoxic chemotherapeutic drugs, the work by Simeoni et al. (2004) assumed that drug concentration opens an elimination pathway for proliferating cells, which are then removed from the system through a chain of transit compartments expressing several steps of cell degradation. In an alternative approach by Lobo and Balthasar (2002), drug concentration is assumed to trigger a "cell destruction" signal which is propagated to the proliferating cells through a chain of delay compartments: inactivation of target cells takes place as soon as the destruction signal is delivered. Because of such "distributional" aspects, the above models were also termed "cell distribution" and "signal distribution" models (Yang et al. 2010).

A model based on similar principles of Eq. (10.6) was used by Friberg et al. to characterize the time course of leukopenia after administration of 5-fluorouracil (Friberg et al. 2000). Their semi-physiological PK/PD model assumed that replicating cells (progenitors) in the bone marrow may maturate to become non-replicating cells and, ultimately, circulating leukocytes, by means of a chain of maturation compartments. The model included a feedback loop on the progenitor production rate dependent on the amount of peripheral circulating cells. Exposure to 5-fluorouracil was then assumed to act on two compartments of replicating cells (representing two different stages of maturation) by irreversible inactivation.

Recently, the concepts of cell proliferation and inactivation by irreversible drug action have been applied to model the cell-killing effects of dulanermin (rhApo2L/TRAIL) and conatumumab, two pro-apoptotic receptor agonists (PARAs), on COLO205 tumor cells implanted in mice (Kay et al. 2012). The two drugs bind to transmembrane death receptors DR4 (dulanermin only) and DR5 (both compounds) and trigger the extrinsic cellular apoptotic pathway through a caspase-signaling cascade resulting in cell death.

Tumor size data from rodent tumor xenograft studies following administration of either compound were combined to develop an intracellular-signaling tumor regression model that includes two levels of signaling: upstream signals unique to each compound (representing initiator caspases), and a common downstream apoptosis signal (representing executioner caspases) shared by the two agents. The model is represented in Fig. 10.4 and in Eq. (10.7a,b,c):

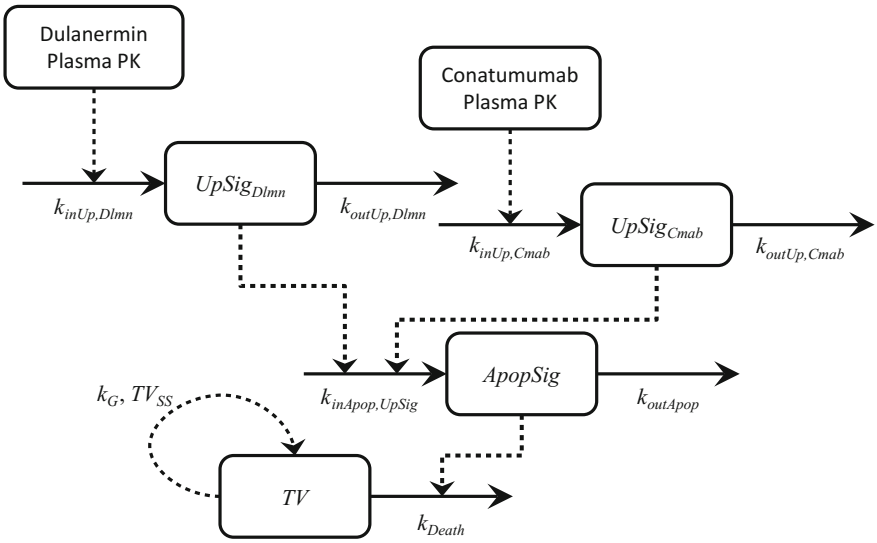

Fig. 10.4 Model scheme of PARAs pharmacodynamics (with kind permission from Springer Science + Business Media: adapted from Kay et al. 2012, p. 580, Figure 1)

$$\frac{d}{dt}UpSig = k_{in,Up} \cdot C - k_{out,Up} \cdot UpSig \qquad UpSig(0) = 0$$

$$\frac{d}{dt}ApopSig = k_{in,Apop} \cdot UpSig - k_{out,Apop} \cdot ApopSig \qquad ApopSig(0) = 0$$

$$\frac{d}{dt}TV = k_G \cdot \left(1 - \frac{TV}{TV_{SS}}\right) \cdot TV - k_{Death} \cdot ApopSig \cdot TV \qquad TV(0) = TV_0$$

(10.7a, b, c)

In the model, *UpSig* is the upstream signal (governed by a first-order formation rate constant $k_{in,Up}$ and first-order dissipation rate constant $k_{out,Up}$), *ApopSig* is the apoptosis signal (governed by a first-order formation rate constant $k_{in,Apop}$ and first-order dissipation rate constant $k_{out,Apop}$), and *TV* is the tumor volume, which is characterized by a logistic function of unperturbed growth (k_G: first-order net growth rate constant; TV_{ss}: steady-state or maximum tumor volume; TV_{ss}: baseline tumor volume) and an elimination term with second-order rate constant parameter, k_{Death}, activated by the apoptosis signal. The upstream signal is linked to the PARA plasma concentration and represents initiator caspases. Its dynamics include the delivery of PARA to the cells, PARA binding to the death receptors, PARA dissociation from its target receptors, and removal of PARA from the tumor site, each of which is likely to be different for the two PARAs. The dynamics of the Upstream Signal also include the initiator caspase activation by the death domains of the activated death receptors and the turnover of initiator caspases. That is, the

dynamics of the apoptosis signal are not drug specific and represent the activation of the executioner caspases by the initiator caspases as well as the turnover of the executioner caspases. The apoptosis signal increases the turnover rate of the tumor cells, thus leading to an additional elimination pathway via the term $k_{Death} \times ApopSig$. It is interesting to observe that, although the interaction between drug and target is reversible (i.e., is characterized by association and dissociation with the death receptors), the downstream pharmacodynamic effect is to be considered irreversible, in that it leads to cell apoptosis.

10.6 Reduction of Irreversible-Effects Mechanistic PD Models

Hutmacher et al. have proposed a framework to reduce or "collapse" mechanistic pharmacodynamic models that are not a priori identifiable (Hutmacher et al. 2005). More specifically, the concepts of turnover models and irreversible elimination are exemplified through a PK/PD modeling exercise on a selective irreversible antagonist, which is assumed to bind irreversibly to a target enzyme and essentially kill it. The above mechanisms were incorporated into a "total mechanistic" model, which postulated synthesis and degradation of enzyme and drug distribution to an effect site, as shown in Eq. (10.8a,b,c):

$$\begin{aligned} \frac{dC_e}{dt} &= k_{eo}\left(C_p - C_e\right) & C_e(0) &= 0 \\ \frac{dE}{dt} &= k_{syn} - k_{deg}(1 + f(C_e))E & E(0) &= \frac{k_{syn}}{k_{deg}} = E_0 \\ \frac{dR}{dt} &= k_{in}E - k_{out}R & R(0) &= \frac{k_{in}}{k_{out}}E_0 = R_0 \end{aligned} \qquad (10.8\text{a, b, c})$$

where E represents the enzyme concentration, C_p is the plasma concentration of the inhibitor, k_{eo} is the effect site rate constant, C_e is the effect site concentration, E is the enzyme, k_{syn} is the zero-order rate of enzyme synthesis, k_{deg} is the first-order rate constant of enzyme degradation, $f(C_e)$ is the function that mediates the clearance of the enzyme by the drug, R is the response, k_{in} is the apparent first-order conversion rate constant of enzyme to response, and k_{out} is the first-order elimination rate constant of response dissipation (substrate, S, is assumed to be in excess and thus constant, i.e., $k_{in} = k_{in,true} \times S$). The function $f(C_e)$ can be assumed as a linear, power, or sigmoid-type function of inhibitor concentration at the effect site.

In certain cases, data may fail to support fully mechanistic models, because not all physiological variables can be sampled, because the sampling scheme is too sparse to allow reliable identification, or because the fully mechanistic model is inherently over-parametrized. In these cases, alternative modeling strategies are usually pursued, such as the adoption of simpler, more empirical models, or fixing some parameter (e.g., rate constants) of a fully mechanistic model. However, if the pathway contains processes with "fast" dynamics, the clear-cut approach is to

reduce, or "collapse", the mechanistic model so as to obtain parametrically simpler classes of models that retain the mechanistic interpretation of the full one. The integrity of the total mechanistic model is retained by assuming equilibrium conditions for certain "fast" processes. For example, two possible collapsed models can be obtained depending on the relative velocity of enzyme degradation and response dissipation (i.e., the relative magnitude of rate constants k_{deg} and k_{out}).

Equation (10.9a,b) shows the case in which enzyme degradation occurs at a much faster rate than response dissipation:

$$\begin{aligned} E &= \frac{E_0}{1+f(C_e)} \\ \frac{dR}{dt} &= k_{in}\frac{E_0}{1+f(C_e)} - k_{out}R \quad R(0) = \frac{k_{in}}{k_{out}}E_0 = R_0 \end{aligned} \tag{10.9a, b}$$

where the equation for the enzyme dynamics can be solved assuming an equilibrium (with respect to the dynamics of the response), given the assumption that k_{deg} is much larger than k_{out}.

Equation (10.10a,b), on the contrary, shows the case in which response dissipation occurs at a much faster rate than enzyme degradation:

$$\begin{aligned} \frac{dE}{dt} &= k_{syn} - k_{deg}(1+f(C_e))E \quad E(0) = \frac{k_{syn}}{k_{deg}} = E_0 \\ R &= \frac{E}{E_0}R_0 \end{aligned} \tag{10.10a, b}$$

where the equation for the response dynamics can be solved assuming equilibrium (with respect to the dynamics of the enzyme), given the assumption that k_{out} is much larger than k_{deg}. Note that none of the models above is structurally identifiable if the enzyme concentration E is not measured, because it is not possible to separate k_{syn} from k_{in} (Eq. 10.8a,b,c), E_0 from k_{in} (Eq. 10.9a,b), and k_{syn} from R_0 (Eq. 10.10a,b) (see also Gisleskog et al. 1998 for a discussion). In order to ensure identifiability, a reparametrization must be performed, by removing one unnecessary parameter. Additionally, it can be shown that, if the dynamics of both the enzyme degradation and response dissipation are fast compared to the kinetics of the drug concentration, a direct-effect model is obtained.

It is interesting to observe how a model of irreversible effects, typically expressed by means of a differential equation containing a term of irreversible elimination, can take several possible mathematical forms, depending on the availability of data, the need for model simplification, or the presence of fast dynamics that can be collapsed to yield a reduced model. In this respect, the equivalence between the mechanistic model of irreversible aromatase inhibition and the indirect response model of E1S, presented in Sect. 10.3, may be interpreted in terms of collapsed models. As a matter of fact, the indirect response model in Eq. (10.4) could be regarded as a "collapsed" version of the irreversible inhibition

model of Eq. (10.5a,b) (with $\gamma = 1$), assuming that the equation of aromatase dynamics is solved at equilibrium and substituted in the E1S equation. Similarly, Eq. (10.8a,b,c), a fully mechanistic enzyme-response model, can be reduced to Eq. (10.9a,b), a type I indirect response model, after solving the enzyme equation at equilibrium.

10.7 Discussion

Understanding the pharmacodynamic effects that trigger drug response is difficult due to the complexity of physiology and the limited or partial knowledge about pharmacological mechanisms of action of drugs. Even focusing on the sub-class of irreversible pharmacological effects, the diversity of possible mechanisms, the number of molecules participating in the interaction, and the complexity of processes that trigger the response call for suitable modeling techniques to allow interpretation of the data and meaningful inference.

In this review, we have provided some examples of simple and common mechanism-based models that describe and quantify irreversible pharmacodynamic effects. However, it should be stressed that, in many instances, this is necessarily a simplification of reality. For example, in many real-life scenarios, it is not possible to classify a given drug effect, observed in a pre-clinical experiment or in a clinical trial, as either "reversible" or "irreversible" class. In this respect, from a PK/PD modeling standpoint, a given irreversible pharmacodynamic effect could potentially be described using models that do not incorporate the actual mechanism of action, such as a reversible-effect model or a semi-mechanistic, indirect-response model. Moreover, as demonstrated in the work by Hutmacher et al. (2005), indirect-effect or direct-effect models can indeed be interpreted as collapsed irreversible mechanistic models, and are suitable for use, in absence of additional data, when certain assumptions regarding relative kinetics of processes within a pathway are met. In general, the conditions for modeling irreversible events with "reversible" structural models (or vice versa) may not always be clear, or data may not always be fully informative to allow the identification of a model that incorporates the actual mechanism of action. This has been shown by the exemestane case (Valle et al. 2004; Poggesi et al. 1999), where an indirect-response model of exemestane effect could be successfully fitted to data from clinical studies, and was used to predict drug effect in studies characterized by a different design. The PK/PD model that incorporates the actual exemestane mode of action, namely aromatase inactivation, was not superior with respect to the semi-mechanistic indirect response model in terms of goodness-of-fit criteria. A similar issue can be encountered in case of the confounding between the process with slow dissociation of drug-receptor complex and the irreversible formation of a drug-receptor complex (Yassen et al. 2007). This

appears to suggest that, in absence of prior knowledge about the underlying mechanism of action, it may not be possible to select the correct mechanistic model among several candidates, as equivalencies may exist among model classes. In general, it would be interesting to formally investigate under what conditions (e.g., in terms of experimental design and values of rate constants) two model classes could be considered equivalent, at least in terms of goodness-of-fit and/or predictive performances.

It should be recognized that focusing on a single, specific target or receptor interaction and neglecting the interconnections among different processes may hamper the interpretation of the experimental results. We observed how different classes of models of irreversible and reversible effects may sometimes describe a given dataset equivalently. This may be the case when prior biological knowledge is absent, when the mechanism of action is unknown, and/or when the information content of the data is limited. In such cases, the choice of a suitable mechanistic model is difficult and may have to be guided by empirical or data-driven criteria, rather than physiological understanding. In this respect, Systems Pharmacology modeling (Van Der Graaf 2012) is a promising tool to understand biological and pharmacological phenomena to test hypotheses about mechanisms of action, and to identify a target for compound selection (Agoram and Demin 2011). The White Paper by the National Institute of Health working group on Quantitative Systems Pharmacology acknowledged that, in order to better understand therapeutic and toxic effects of a given compound, the pharmacometrics community should progressively move away from the traditional "*one-gene, one-receptor, one-mechanism*" paradigm, "*in favor of a network-centric view that relies on mathematical models to achieve the necessary integration of data and hypotheses*" (Sorger et al. 2011). Papers started adopting PK/PD models within System Pharmacology approaches, as is the case of methylprednisolone pharmacodynamics (Ramakrishnan et al. 2002) and fatty acid amide hydrolase inhibition in pain (Benson et al. 2014). Because of its network-oriented approach, Systems Pharmacology may also enable the resolution of the ambiguousness between reversible and irreversible pharmacodynamic effects, which is sometimes an obstacle to mechanistic PK/PD modeling.

In conclusion, this review presented some key elements, or "basic blocks", that can be used within more comprehensive modeling frameworks to describe complex pathways or networks of interactions among a drug and possibly multiple targets. Despite their simplicity, such models capture fundamental mechanistic concepts that reflect the rate-limiting steps of pharmacological response. With the progressive establishment of quantitative Systems Pharmacology, it is expected that the integrated application of several basic pharmacodynamic models within a comprehensive systems-based framework will become the rule rather than the exception.

References

Äbelö A, Eriksson UG, Karlsson MO et al (2000) A turnover model of irreversible inhibition of gastric acid secretion by omeprazole in the dog. J Pharmacol Exp Ther 295:662–669

Agoram B, Demin O (2011) Integration not isolation: arguing the case for quantitative and systems pharmacology in drug discovery and development. Drug Discov Today 16:1031–1036

Ariens EJ (1954) Affinity and intrinsic activity in the theory of competitive inhibition. Arch Int Pharmacodyn Ther 99:32–49

Benson N, Metelkin E, Demin O et al (2014) A systems pharmacology perspective on the clinical development of fatty acid amide hydrolase inhibitors for pain. CPT Pharmacometrics Syst Pharmacol 3:e91. doi:10.1038/psp.2013.72

Black JW, Leff P (1983) Operational models of pharmacological agonism. Proc R Soc Lond B Biol Sci 220:141–162

Bryce A, Ryan CJ (2012) Development and clinical utility of abiraterone acetate as an androgen synthesis inhibitor. Clin Pharmacol Ther 91:101–108

Claret L, Girard P, Hoff PM et al (2009) Model-based prediction of phase III overall survival in colorectal cancer on the basis of phase II tumor dynamics. J Clin Oncol 27:4103–4108

Copeland RA, Pompliano DL, Meek TD (2006) Drug-target residence time and its implications for lead optimization. Nat Rev Drug Discov 5:730–739

Danhof M, Alvan G, Dahl SG et al (2005) Mechanism-based pharmacokinetic-pharmacodynamic modeling—a new classification of biomarkers. Pharm Res 22:1432–1437

Dayneka NL, Garg V, Jusko WJ (1993) Comparison of four basic models of indirect pharmacodynamic responses. J Pharmacokinet Biopharm 21:457–478

Friberg LE, Freijs A, Sandström M, Karlsson MO (2000) Semiphysiological model for the time course of leukocytes after varying schedules of 5-fluorouracil in rats. J Pharmacol Exp Ther 295:734–740

Gabapentine package insert. http://labeling.pfizer.com/ShowLabeling.aspx?id=630. Accessed 3 Feb 2014

Gisleskog PO, Hermann D, Hammarlund-Udenaes M, Karlsson MO (1998) A model for the turnover of dihydrotestosterone in the presence of the irreversible 5α-reductase inhibitors GI198745 and finasteride. Clin Pharmacol Ther 64:636–647

Hong Y, Gengo FM, Rainka MM et al (2008) Population pharmacodynamic modelling of aspirin and ibuprofen-induced inhibition of platelet aggregation in healthy subjects. Clin Pharmacokinet 47:129–137

Hutmacher MM, Mukherjee D, Kowalski KG, Jordan DC (2005) Collapsing mechanistic models: an application to dose selection for proof of concept of a selective irreversible antagonist. J Pharmacokinet Pharmacodyn 32:501–520

Jusko WJ (1971a) Pharmacodynamic principles in chemical teratology: dose-effect relationships. J Pharmacol Exp Ther 183:469–480

Jusko WJ (1971b) Pharmacodynamics of chemotherapeutic effects: dose-time-response relationships for phase-nonspecific agents. J Pharm Sci 60:892–895

Jusko WJ (1973) A pharmacodynamic model for cell-cycle-specific chemotherapeutic agents. J Pharmacokinet Biopharm 1:175–200

Katashima M, Yamamoto K, Tokuma Y et al (1998) Pharmacokinetic and pharmacodynamic study of a new nonsteroidal 5-α-reductase inhibitor, 4-[3-[3-[bis(4-isobutylphenyl)methylamino]benzoyl]-1H-indol-1-yl]-butyric acid, in rats. J Pharmacol Exp Ther 284:914–920

Kay BP, Hsu CP, Lu JF et al (2012) Intracellular-signaling tumor-regression modeling of the pro-apoptotic receptor agonists dulanermin and conatumumab. J Pharmacokinet Pharmacodyn 39:577–590

Kenakin T (1997) Pharmacologic analysis of drug-receptor interaction, 3rd edn. Lippincott-Raven, Philadelphia

Lobo ED, Balthasar JP (2002) Pharmacodynamic modeling of chemotherapeutic effects: application of a transit compartment model to characterize methotrexate effects in vitro. AAPS PharmSci 4:212–222

Mager DE, Wyska E, Jusko WJ (2003) Diversity of mechanism-based pharmacodynamic models. Drug Metab Dispos 31:510–519

Miller WR, Bartlett J, Brodie AMH et al (2009) Aromatase inhibitors: are there differences between steroidal and nonsteroidal aromatase inhibitors and do they matter? Oncologist 13:829–837

Nielsen EI, Cars O, Friberg LE (2011) Pharmacokinetic/pharmacodynamic (PK/PD) indices of antibiotics predicted by a semimechanistic PKPD model: a step toward model-based dose optimization. Antimicrob Agents Chemother 55:4619–4630

Ploeger BA, Van Der Graaf PH, Danhof M (2009) Incorporating receptor theory in mechanism-based pharmacokinetic-pharmacodynamic (PK-PD) modeling. Drug Metab Pharmacokinet 24:3–15

Poggesi I, Jannuzzo MG, diSalle E et al (1999) Effect of food on pharmacokinetics (PK) and pharmacodynamics (PD) of exemestane (Aromasin, EXE). In: 35th annual meeting of American society of clinical oncology. Atlanta, GA May 15–18, 1999

Ramakrishnan R, DuBois DC, Almon RR et al (2002) Fifth-generation model for corticosteroid pharmacodynamics: application to steady-state receptor down-regulation and enzyme induction patterns during seven-day continuous infusion of methylprednisolone in rats. J Pharmacokinet Pharmacodyn 29:1–24

Simeoni M, Magni P, Cammia C et al (2004) Predictive pharmacokinetic-pharmacodynamic modeling of tumor growth kinetics in xenograft models after administration of anticancer agents. Cancer Res 64:1094–1101

Sorger PK, Allerheiligen SRB, Abernethy DR et al (2011) Quantitative and systems pharmacology in the post-genomic era: New approaches to discovering drugs and understanding therapeutic mechanisms. An NIH White Paper, QSP Workshop Group. http://www.nigms.nih.gov/Training/Documents/SystemsPharmaWPSorger2011.pdf. Accessed 30 Jan 2014

Snoeck E, Chanu P, Lavielle M et al (2010) A comprehensive hepatitis C viral kinetic model explaining cure. Clin Pharmacol Ther 87:706–713

Tummino PJ, Copeland RA (2008) Residence time of receptor-ligand complexes and its effect on biological function. Biochemistry 47:5481–5492

Valle M, Di Salle E, Jannuzzo MG et al (2004) A predictive model for exemestane pharmacokinetics/pharmacodynamics incorporating the effect of food and formulation. Br J Clin Pharmacol 59:355–364

Van Der Graaf PH (2012) CPT: pharmacometrics and systems pharmacology. CPT Pharmacometrics Syst Pharmacol 1:e8. doi:10.1038/psp.2012.8

Yang J, Mager DE, Straubinger RM (2010) Comparison of two pharmacodynamic transduction models for the analysis of tumor therapeutic responses in model systems. AAPS J 12:1–10

Yassen A, Olofsen E, Romberg R et al (2007) Mechanism-based PK/PD modeling of the respiratory depressant effect of buprenorphine and fentanyl in healthy volunteers. Clin Pharmacol Ther 81:50–58

Chapter 11
Feedback Control Indirect Response Models

Yaping Zhang and David Z. D'Argenio

Abstract Most physiological processes are subject to feedback regulation. We hypothesize that PK/PD models that do not appropriately incorporate known autoregulatory mechanisms are incomplete representations of the drug-response relationship, and may lead to an underestimation of a drug's potency. In this chapter, a new general framework is introduced for modeling pharmacodynamic processes that are subject to autoregulation, in which the canonical IDR models of Jusko are extended to incorporate the time-course of the difference between the pharmacodynamic response and its basal value (the error signal). Following the well-established approach of traditional engineering control theory, the proposed feedback control indirect response (FC IDR) models include linear combinations of terms proportional to the error signal itself, the integral of the error signal, and the derivative of the error signal. Model equations are derived and simulations are conducted to illustrate the characteristic behaviors of FC IDR models. It is demonstrated that ignoring the contributions of feedback control mechanisms in PD studies would lead to the underestimation of drug potency. Four examples were selected from literature to illustrate the broad application of the FC IDR framework. The similarities and differences of this proposed framework and two alternate approaches that also include feedback are further discussed. The FC IDR modeling framework allows the drug's effects to be quantified independently of the autoregulatory mechanisms that also act on the controlled variables. It addresses the difficulties long-recognized by systems physiologists in understanding the mechanisms of drug action that underlie processes subject to feedback regulation, and may provide a bridge for development of more mechanistic systems pharmacology models.

Y. Zhang · D.Z. D'Argenio (✉)
Department of Biomedical Engineering, Biomedical Simulations Resource,
University of Southern California, Los Angeles, CA 90089, USA
e-mail: dargenio@bmsr.usc.edu

D.E. Mager and H.H.C. Kimko (eds.), *Systems Pharmacology and Pharmacodynamics*,
AAPS Advances in the Pharmaceutical Sciences Series 23,
DOI 10.1007/978-3-319-44534-2_11

Keywords Feedback regulation · Indirect response model · Homeostasis · Autoregulation

11.1 Introduction

Regulation is a hallmark of living systems. The scholarship of the physiologist Adolph (1961) highlighted early concepts of physiological regulation, from Alcmaeon's notion that blending opposites secures the constancy of constitution, through Lavoisier's experiments on energy metabolism that identified regulators keeping the animal body in a state of equilibrium. But it was the codification of these ideas beginning with Bernard and especially with the work of Cannon (1929), which has led to almost a century of work by systems physiologists, joined more recently by systems biologists, aimed at uncovering the regulatory mechanisms that govern life.

Well-versed in Cannon's concept of homeostatic mechanisms and armed with the tools used for the design of automatic feedback control systems as well as other enabling technologies that resulted from World War II, a cadre of pioneering systems physiologists began to uncover the mechanism of feedback regulation underlying a number of physiological responses. One of the earliest of these is the contribution of Grodins and Gray in 1954 introducing the role of a respiratory control system in the feedback regulation of arterial CO_2. This and other applications based on engineering feedback control principles were presented in Grodins's landmark 1963 monograph on control theory in biological systems (Grodins 1963). During this same time period, Guyton et al. (1973) were using these ideas of feedback control to elucidate various levels of regulation at play in the cardiovascular system in health and disease. Several other especially influential examples during this seminal period include: the pupillary light reflex studied by Sherman and Stark (1957); Bolie's model of insulin control of glucose (Bolie 1961); feedback control of plasma adrenocortical hormones by Yates and Urquhart (1962); the role of hypothalamic control in temperature regulation by von Euler (1964); the closed loop control model for the muscle stretch reflex of Milhorn (1966). These and other contributions during the 1950s–1970s were synthesized and made available in a number of influential monographs (Milsum 1966; Stark 1968; Clynes and Milsum 1970; Jones 1973) that inspired the next generation of systems physiologists and bioengineers. For a contemporary treatment of physiological control systems, the reader is referred to the encompassing monograph of Khoo (2000).

Using the techniques of the molecular biology revolution, systems biologists have also been ably guided by concepts and techniques used in the control of engineered systems to understand, for example, how intracellular signaling networks regulate specific cell behaviors. A few examples include: the use of integral control to describe the perfect adaptation observed in bacterial chemotaxis (Yi et al. 2000); rate sensitive and persisting signaling pathways in feedback regulation of erythropoiesis (Koulnis et al. 2011); and negative feedback properties of the

MAPK/ERK signaling pathway (Sturm et al. 2010). These concepts and approaches of feedback control have also been presented as essential components of monographs and textbooks on systems biology (for example in Kitano 2001; Alon 2007; Kremling 2014).

Concepts of regulation now constitute a central tenet and integrating principle for studying living systems from the molecular, sub-cellular, cellular, multi-cellular, tissue, organ, organism, through the population levels. These ideas and their associated implementing machinery that have been used with great effect by systems physiologists and systems biologists, however, are not widely used in service to the drug discovery and development enterprise. There are some notable exceptions. First, Urquart's (2003) compelling insights on this topic, informed by the expansive arc of his first-hand experience in physiology, pharmacology, device, and drug development, are essential reading to begin understanding the challenges involved with studying and modeling drug action when the drug's response(s) is itself subject to endogenous feedback control. There have also been specific models reported in the literature that incorporate pharmacodynamic feedback elements developed for particular compounds (Woo et al. 2008), as well as some more general approaches that have been used to model such autoregulated pharmacodynamic processes (Gabrielsson and Weiner 2007; Gabrielsson and Peletier 2008). In addition, the precursor-dependent indirect response model (Sharma et al. 1998), while not explicitly incorporating feedback mechanisms, has been used to describe tolerance and rebound caused by feedback regulation.

Our purpose in the remainder of this chapter is to illustrate how some of the ideas and tools for feedback regulation used for controlling engineered systems, may provide not only a conceptual but also a general working framework for modeling pharmacodynamic processes that are subject to autoregulation. Toward this end, we (1) introduce a feedback control framework based on indirect response models, (2) provide some illustrative simulations using different feedback controllers, (3) compare the proposed feedback control indirect response model framework to other approaches, and (4) further illustrate the application of the proposed approach using several examples from the literature.

11.2 Feedback Control Indirect Response Models

In this section we present the feedback control indirect response modeling framework by: (1) introducing linear feedback control (FC) as applied to engineered systems; (2) illustrating several feedback control indirect response (FC IDR) models; (3) presenting extensions to the linear feedback control framework particularly relevant to modeling drug action; (4) relating the FC IDR framework introduced to other approaches used for modeling drug action involving autoregulated pharmacodynamic processes; and (5) highlighting the challenges of quantifying the contributions of feedback control mechanisms in PD studies.

11.2.1 Linear Feedback Control Framework

We outline below the essential elements of the classic feedback control framework that we will apply to IDR models. For a thorough and rigorous treatment of physiological control systems, the inquisitive reader is referred to the bioengineering monograph of Khoo (2000).

The block diagram in Fig. 11.1 depicts a generic feedback control system configuration in which the output of the system to be controlled $y(t)$ is fed back to the controller, which in turn constructs the input to the system $u(t)$. The design of the controller is dictated by the desired performance goals of the feedback control system (e.g., regulation, servomechanism). When the system to be controlled is linear and the performance goal is to regulate the system output at a desired reference value y_{ref} (set point) (that is, to reduce the error $e(t) = y_{ref} - y(t)$ that may result from disturbances acting on the system or changes in the system characteristics), the controller may construct the input signal using terms involving (1) the error, (2) the integral of the error, (3) the derivative of the error, or (4) linear combinations of these terms. We can then write the control input as follows:

$$u(t) = G_p e(t) + G_i \int_0^t e(\tau) d\tau + G_d \frac{de(t)}{dt} \tag{11.1}$$

The components in Eq. (11.1) are referred to, in turn, as the proportional (P), integral (I), and derivative (D) control terms and the constants G_p, G_i, G_d are their respective gains reflecting their contribution to the control input $u(t)$. Inspection of Eq. (11.1) reveals that the control input is composed of terms representing the current, past, and future state of the system output.

A commonly encountered example of such a control system is the automatic cruise control in a car that acts to maintain the car's speed at a selected value in the presence of changes in load on the engine (e.g., resulting from changes in the incline of the road). Such cruise control systems are generally composed of both the proportional and integral terms in Eq. (11.1) (PI control). Another example is the operation of an atomic force microscope in which the vertical position of the cantilever base is controlled (in contact mode AFM, the bending of the cantilever is controlled) via a piezo drive, based on a laser reflected off the cantilever as the feedback signal (again a PI control law is used). The applications of these control ideas are ubiquitous in areas such as process engineering, power transmission, aerospace and flight control, transportation, robotics, telecommunications, instrumentation, and numerous others.

In ending this briefest of introductions to linear feedback control systems, we direct the interested reader to the history informed perspective of classic feedback

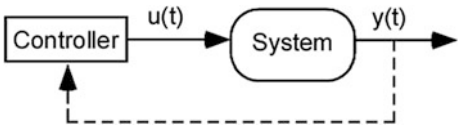

Fig. 11.1 Feedback control system

control in the encompassing 2010 monograph of Astrom and Murray (2010). We also note that numerous extensions of this basic feedback control idea have been developed and applied over the past 70 years and are the subject of ongoing research. They include contributions under the following rubrics: optimal control, adaptive control, robust control, stochastic control, fuzzy control, hierarchical control, distributed control, autonomous control, and quantum control. An extensive literature exists on the theory and practice for controlling engineered systems.

The approaches developed to handle these even more realistic and challenging engineered system control problems have also been used to guide our understanding of control and regulation in biology at the molecular, cellular, organ, organism, and population levels. Of course, in these applications one is not faced with the task of designing the controller as is the control engineering (the forward control problem), but instead with the challenge of understanding the control mechanisms established through the evolutionary pressures that direct self-organization in biological systems (the inverse control problem). We return to these ideas later in this chapter.

In what follows, we propose, illustrate, and apply an inverse control approach that can be coupled with the IDR modeling framework, to allow the characterization of drug action when the pharmacodynamic response is itself subject to endogenous feedback control.

11.2.2 Feedback Control Indirect Response Model Framework

The indirect response modeling framework introduced, developed, and applied by Jusko and his colleagues, has provided a formal, general and powerful companion to pharmacokinetic modeling approaches. Its widespread use has transformed the study of pharmacodynamics. In this section, we outline how the feedback control framework summarized above can be merged with IDR models.

We adopt the notation for indirect response models used in Dayneka et al. (1993) and consider the following four canonical IDR models:

Model I: Inhibition of k_{in}

$$\frac{dR}{dt} = k_{in}(1 - H_1(C)) - k_{out} \cdot R, \quad R(0) = R_0 \tag{11.2}$$

Model II: Inhibition of k_{out}

$$\frac{dR}{dt} = k_{in} - k_{out}(1 - H_1(C))R, \quad R(0) = R_0 \tag{11.3}$$

Model III: Stimulation of k_{in}

$$\frac{dR}{dt} = k_{in}(1 + H_2(C)) - k_{out} \cdot R, \quad R(0) = R_0 \tag{11.4}$$

Model IV: Stimulation of k_{out}

$$\frac{dR}{dt} = k_{in} - k_{out}(1 + H_2(C))R, \quad R(0) = R_0 \tag{11.5}$$

In the above equations, C is the plasma or biophase concentration of the drug, and $H_1(C)$, $H_2(C)$ are defined as follows:

$$H_1(C) = \frac{I_{\max} \cdot C}{IC_{50} + C}, \; H_2(C) = \frac{S_{\max} \cdot C}{SC_{50} + C}$$

For those applications in which the PD response is subject to endogenous regulation, the IDR model framework can be extended, as depicted in Fig. 11.2, with the addition of the feedback control introduced above in Eq. (11.1).

For the case of linear feedback control, the specific form of the function $f(R, R_0, t)$ defining the $k_{in}(t)$, can include one or more of the terms in Eq. (11.1). We explicitly note the dependence of k_{in} on t to emphasize its time dependence independent of drug concentration. In the framework shown in Fig. 11.2, the drug action corresponds to the system disturbance discussed above (e.g., change in position of the cantilever base in AFM) that invokes a control action.

We now combine IDR Model I with the different feedback control mechanisms introduced above. Simulations are also provided for each case presented to illustrate the consequences of feedback regulation on the IDR model's response. A similar exposition using IDR Models II, III and IV is not shown.

The illustrating simulations will use a one-compartment iv bolus model to describe plasma concentration ($C = 1000e^{-0.3t}$), along with the following pharmacodynamic parameter values for the IDR models: $R_0 = 50$, $k_{out} = 0.1$, $I_{\max} = 1$, $IC_{50} = 10$.

11.2.2.1 Inhibition of Kin: Proportional Feedback

The equations below define the FC IDR model for IDR Model I and proportional feedback control:

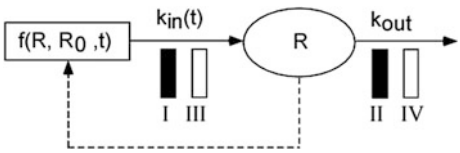

Fig. 11.2 Feedback control indirect response model

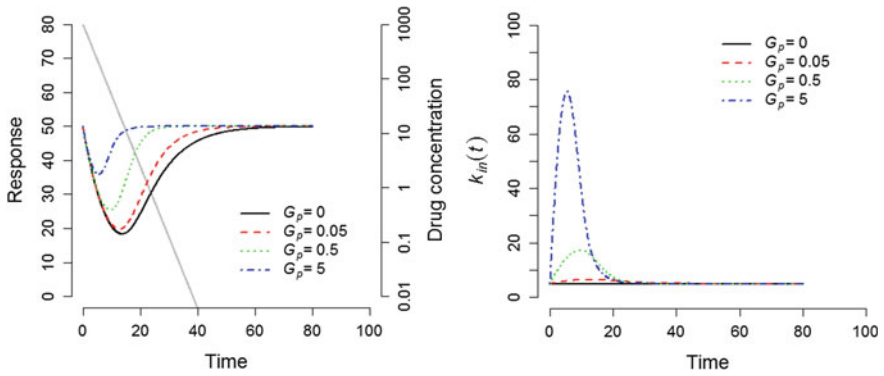

Fig. 11.3 IDR Model I with proportional feedback control. PD response (*left panel*) and $k_{in}(t)$ (*right panel*) for no feedback control ($G_p = 0$) and increasing values of the proportional feedback gain. The *light line in the left panel* (axis scale on *right*) indicates the drug concentration-time profile for reference

$$\frac{dR}{dt} = k_{in}(t)\left(1 - \frac{I_{max} \cdot C}{IC_{50} + C}\right) - k_{out} \cdot R, \quad R(0) = R_0$$
$$\text{where} \quad k_{in}(t) = k_{in0} + G_p(R_0 - R)$$

The second equation defining $k_{in}(t)$ includes a constant term k_{in0} ($k_{in0} = R_0 \cdot k_{out}$), plus a feedback term that is proportional (gain term G_p) to control error $e = R_0 - R$ (negative feedback). The effect of the feedback control is evident from the equation: it will act to increase $k_{in}(t)$ above k_{in0} when R is below its basal value (R_0) as a result of drug action. We note that the above equations assume the drug acts on the net synthesis, versus on its components [i.e., the basal synthesis k_{in0} or the feedback contribution $G_p(R_0 - R)$]. Figure 11.3 illustrates the response of this FC IDR model to different values of the feedback gain G_p.

The left panel in Fig. 11.3 illustrates the effect of increasing the contribution of the proportional feedback term in reducing the deviation of the response R from its basal value $R_0 = 50$. The right panel of Fig. 11.3 shows the results of the feedback control on the time course of $k_{in}(t)$, as the control mechanism acts to return R to its basal value due to the disturbance caused by the drug's action. For now we defer discussion of physiological constraints on $k_{in}(t)$. Finally we note that the response of the FC IDR model resulting from increasing values of G_p, shown in the left panel of Fig. 11.3, is qualitatively consistent with the predictions of IDR Model I (that is, an IDR model without feedback) generated with increasing IC_{50} (decreasing drug potency). We return to this unsettling observation below.

11.2.2.2 Inhibition of Kin: Integral Feedback

The equations below define the FC IDR model for IDR Model I and integral feedback control.

$$\frac{dR}{dt} = k_{in}(t)\left(1 - \frac{I_{max} \cdot C}{IC_{50} + C}\right) - k_{out} \cdot R, \quad R(0) = R_0$$
$$\text{where} \quad k_{in}(t) = k_{in0} + G_i \int_0^t (R_0 - R(\tau))d\tau$$

The term representing the integral of the control error in the second equation above, can be obtained by introducing a new state $x(t)$ defined by the following dynamic model:

$$\frac{dx}{dt} = (R_0 - R), \quad x(0) = 0$$

Thus the following equations define the IDR Model I and integral feedback:

$$\frac{dR}{dt} = k_{in}(t)\left(1 - \frac{I_{max} \cdot C}{IC_{50} + C}\right) - k_{out} \cdot R, \quad R(0) = R_0$$
$$\frac{dx}{dt} = (R_0 - R), \quad x(0) = 0$$
$$\text{where } k_{in}(t) = k_{in0} + G_i \cdot x$$

Figure 11.4 illustrates the response of this FC IDR model for different values of the integral feedback gain G_i. For the highest value of the gain term, the response shows a clear overshoot $R > R_0$, before a return to its basal value. We will discuss comparison of the FC IDR models to other models used to describe such phenomena (e.g., moderator state models) below.

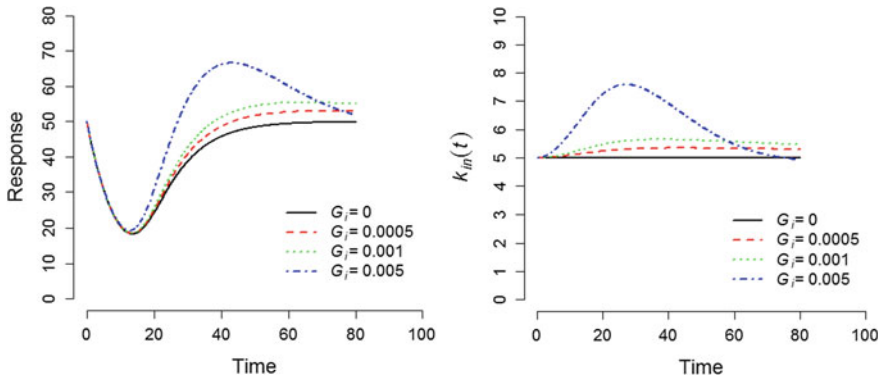

Fig. 11.4 IDR Model I with integral feedback control. PD response (*left panel*) and $k_{in}(t)$ (*right panel*) for no feedback control ($G_i = 0$) and increasing values of the integral feedback gain

11.2.2.3 Inhibition of Kin: Proportional Plus Integral Feedback

$$\frac{dR}{dt} = k_{in}(t)\left(1 - \frac{I_{max} \cdot C}{IC_{50} + C}\right) - k_{out} \cdot R, \quad R(0) = R_0$$
$$\frac{dx}{dt} = (R_0 - R), \quad x(0) = 0$$
$$\text{where} \quad k_{in}(t) = k_{in0} + G_p(R_0 - R) + G_i \cdot x$$

Figure 11.5 illustrates the response of the combined proportional plus integral feedback control model for IDR Model I, for different values of the integral feedback gain G_i with fixed proportional gain G_p (upper panels) and for different values of the proportional feedback gain G_p with fixed integral gain G_i (lower panels).

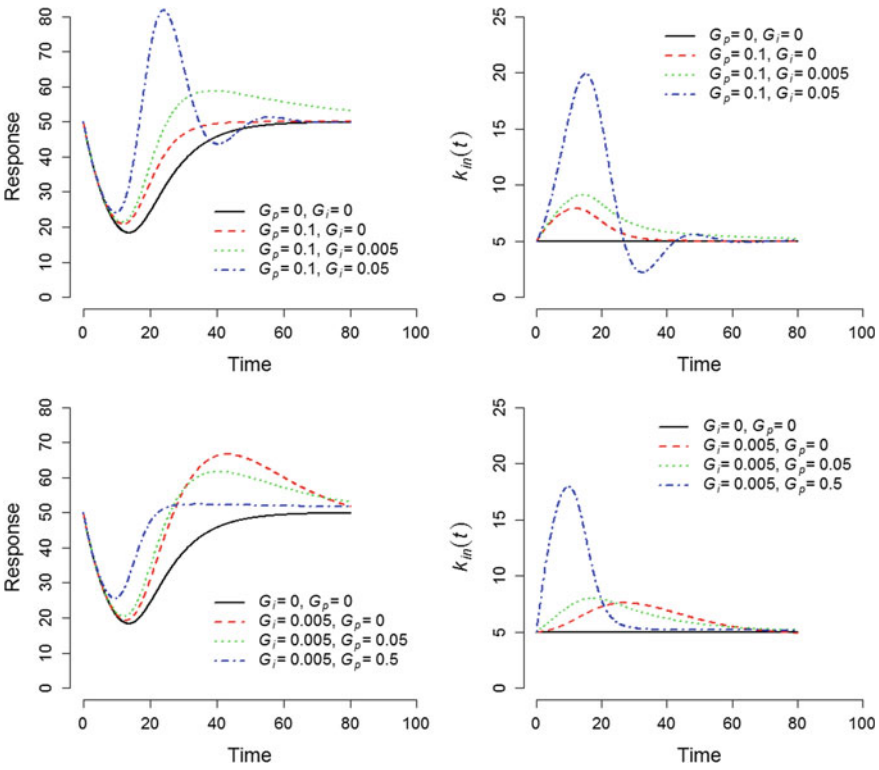

Fig. 11.5 IDR Model I with proportional plus integral feedback control. PD response (*left panels*) and $k_{in}(t)$ (*right panels*). *Upper panels* show results with G_p fixed and G_i increasing, while in the *lower panels*, G_i is fixed and G_p is increasing

11.2.2.4 Inhibition of Kin: Proportional Plus Integral Plus Derivative Feedback

We now combine all three terms, proportional, integral and derivative, in the feedback control model.

$$\frac{dR}{dt} = k_{in}(t)\left(1 - \frac{I_{max} \cdot C}{IC_{50} + C}\right) - k_{out} \cdot R, \quad R(0) = R_0$$

$$\text{where} \quad k_{in}(t) = k_{in0} + G_p(R_0 - R) + G_i \int_0^t (R_0 - R(\tau))d\tau + G_d \frac{d(R_0 - R)}{dt}$$

As before, a new state is introduced for the integral control term, while the derivative term is defined by the differential equation for R. Thus, the following equations represent the proportional plus integral plus derivative FC IRM model:

$$\frac{dR}{dt} = \frac{1}{1 + G_d \cdot \left(1 - \frac{I_{max} \cdot C}{IC_{50} + C}\right)} \left\{ \left(k_{in0} + G_p(R_0 - R) + G_i \cdot x\right)\left(1 - \frac{I_{max} \cdot C}{IC_{50} + C}\right) - k_{out} \cdot R \right\}, \quad R(0) = R_0$$

$$\frac{dx}{dt} = (R_0 - R), \quad x(0) = 0$$

Figure 11.6 illustrates the response of the combined proportional plus integral plus derivative feedback control model for IDR Model I, for different values of the derivative feedback gain G_d with fixed proportional gain G_p and integral gain G_i.

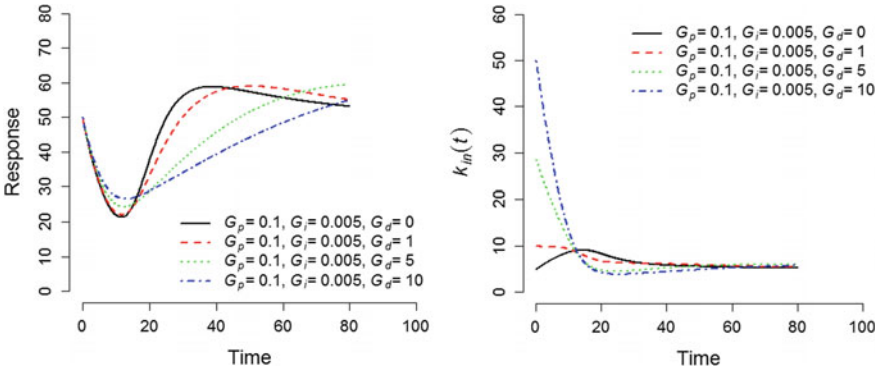

Fig. 11.6 IDR Model I with proportional plus integral plus derivative feedback control. PD response (*left panel*) and $k_{in}(t)$ (*right panel*) for no derivative feedback control ($G_d = 0$) and increasing values of the derivative feedback gain

11.2.3 Extensions of the Linear Feedback Control Framework

Important extensions to the classical linear feedback control framework have been developed and applied to the control of engineered systems (anti-windup, deadband, setpoint weighting, and others (Astrom and Murray 2010)). Of particular relevance in pharmacodynamics involves limits on the control signal itself. We illustrate this by replacing the proportional error term in Eq. (11.1) by a non-proportional term to reflect an upper limit on the control input.

For the case of IDR Model I with proportional feedback, we can incorporate an upper limit on $k_{in}(t)$ through using a non-proportional feedback as exemplified below (of course, other nonlinear terms could be used, including the use of a non-zero lower limit on the feedback control contribution to $k_{in}(t)$):

$$\frac{dR}{dt} = k_{in}(t)\left(1 - \frac{I_{max} \cdot C}{IC_{50} + C}\right) - k_{out} \cdot R, \quad R(0) = R_0$$

$$\text{where} \quad k_{in}(t) = k_{in0}\frac{R_{50}^n + R_0^n}{R_{50}^n + R^n}$$

We return to this example below.

Physiologists have long recognized the importance of the change in a physiological variable in receptor response and overall regulation (e.g., in blood pressure regulation), which can be reflected by the derivative control term in Eq. (11.1). System biologists have identified the importance of this rate sensitivity at the level of receptor-ligand interactions (e.g., G-protein coupled down regulation) and cellular signaling. Moreover, a ubiquitous element in biological control systems is unidirectional rate sensitivity, which introduces a hard nonlinearity into the overall system behavior. Urquart has discussed and emphasized this critical topic and its relevance to pharmacology and drug therapy (Urquhart 2003), and the feedback control indirect response models can be extended to incorporate this property.

11.2.4 Relation of the FC IDR Framework to Other Feedback Pharmacodynamic Modeling Approaches

A number of application and model specific approaches for incorporating feedback regulation in PK/PD models have been presented in the literature (for a summary listing of several, see Gabrielsson and Peletier 2008). Two approaches for modeling drug action involving autoregulated pharmacodyamic processes have been applied to different drugs and targets, and they are illustrated below.

In one approach, feedback is incorporated and used to modify $k_{in}(t)$ using a hyperbolic function as follows (Woo et al. 2008; Friberg et al. 2002):

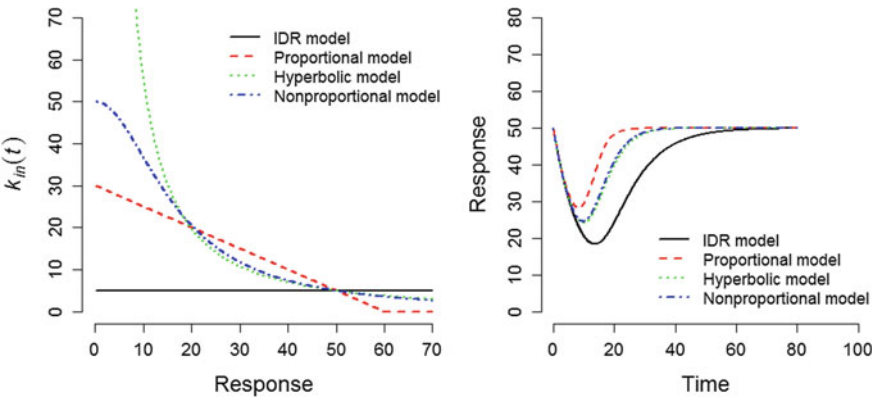

Fig. 11.7 IDR Model I with no feedback, proportional, hyperbolic, and nonproportional feedback control. The *left panel* shows $k_{in}(t)$, while the *right panel* shows the response $R(t)$ for each of the models. $G_p = 0.5$ in the proportional model, $\gamma = 1.5$ in hyperbolic model, and $R_{50} = 16.7$, $n = 2$ in the nonproportional model. Also, $R_0 = 50,\ k_{out} = 0.1,\ I_{max} = 1,\ IC_{50} = 10$

$$\frac{dR}{dt} = k_{in}(t)\left(1 - \frac{I_{max} \cdot C}{IC_{50} + C}\right) - k_{out} \cdot R, \quad R(0) = R_0$$
$$\text{where} \quad k_{in}(t) = k_{in0}\left(\frac{R_0}{R}\right)^{\gamma}$$

Negative feedback results, since $k_{in}(t)$ is inversely related to R for deviations of the response around R_0. The relationship between the FC IDR model with proportional feedback, the non-proportional feedback model given in the previous section, and the hyperbolic feedback model is shown in Fig. 11.7. The left panel shows $k_{in}(t)$ versus R, while the right panel shows the model response versus time for each of these three feedback control models. These models could yield similar results, depending on the respective values of their parameters, at least around the steady-state response R_0. Of course in the hyperbolic feedback model, $k_{in}(t)$ increases without limit as R is reduced below R_0.

Gabrielsson and colleagues have introduced and applied a pharmacodynamic feedback control model that includes an additional state ("moderator" state) that feeds back to alter the response synthesis or turnover (see Wakelkamp et al. 1996; Gabrielsson and Weiner 2007; Bundgaard et al. 2006; Gabrielsson and Peletier 2008; Ahlstrom et al. 2013). A specific application of this moderator model can be illustrated using the IDR Model I as shown below.

$$\frac{dR}{dt} = k_{in}(t)\left(1 - \frac{I_{max} \cdot C}{IC_{50} + C}\right) - k_{out} \cdot R, \quad R(0) = R_0$$
$$\frac{dM}{dt} = -k_{tol}(M - R), \quad M(0) = M_0$$
$$\text{where} \quad k_{in}(t) = k_{in0}\left(\frac{M_0}{M}\right)$$

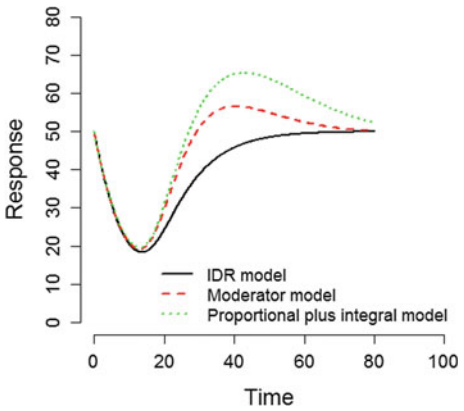

Fig. 11.8 The response of the IDR Model I with no feedback control, moderator feedback control, and proportional plus integral feedback control. $k_{tol} = 0.04$ in the moderator model, and $G_p = 0.01$, $G_i = 0.005$ in the proportional plus integral model. Also, $R_0 = 50$, $k_{out} = 0.1$, $I_{max} = 1$, $IC_{50} = 10$

In the above implementation, $k_{in0} \cdot M_0$ corresponds to k_{in} in the Gabrielsson model, which makes the correspondence to the hyperbolic feedback model shown above more evident (also, $M_0 = R_0$).

We can also compare the moderator model to the FC IDR framework and do so using proportional plus integral feedback. Shown below is the implemented form of the integral feedback term to allow for comparison to the moderator model.

$$\frac{dR}{dt} = k_{in}(t)\left(1 - \frac{I_{max} \cdot C}{IC_{50} + C}\right) - k_{out} \cdot R, \quad R(0) = R_0$$

$$\frac{dx}{dt} = (R_0 - R), \quad x(0) = 0$$

$$\text{where} \quad k_{in}(t) = k_{in0} + G_p(R_0 - R) + G_i \cdot x$$

In both cases, the complete closed loop system is a second-order system, and can produce the characteristic under damped, critically damped, or over damped response behavior, depending on the specific value of the drug independent parameters of the respective models. The moderator model, however, is nonlinear while the FC IRM is linear (reference is to the model without drug). The FC IDR model's feedback includes the integral of the difference between R_0 and the response, while the moderator model feeds back the integral of the moderator state minus the response, subject to a time constant. From a control perspective, the moderator model represents a leaky integrator of the error signal and thus will result in a steady-state error (imperfect adaptation) in the presence of drug. Figure 11.8 shows a simulation of the response for the two models, illustrating some qualitative similarities.

11.2.5 The Consequences of Ignoring Feedback Control Mechanism in Pharmacodynamic Studies

Systems physiologists have long-recognized the difficulties in understanding the mechanisms that underlie processes subject to feedback regulation. To study such systems in situ they have devised clever experimental approaches aimed at "opening the loop" in an effort to separately characterize the system and feedback processes. A few examples of such loop-opening experiments include the voltage clamp technique of Cole to study ion channel regulation of transmembrane potential in the giant squid axon (Cole 1949), and the denervated heart model of Sheppard for understanding the neural and humoral control of cardiac output in racing greyhounds (Donald et al. 1964). See Khoo (2000) for a summary of others.

Quantifying the contribution of feedback control mechanism in pharmacodynamic studies of drug action is no less challenging. From the forgoing simple illustrations, it is apparent that assessing the in vivo potency of a drug's action on a process that involves autoregulation of the observed PD response will confound a quantitative estimation of the drug's potency. The following example provides a quantitative illustration of this issue.

The simulated response values shown in Fig. 11.9 were generated using FC IDR Model I with proportional feedback with parameters of $k_{out} = 0.1$, $IC_{50} = 10$, $R_0 = 50$, and different values of G_p: 0.05 (squares), 0.5 (circles) and 5 (triangles). The results of fitting the IDR Model I (i.e., no feedback) are shown as the

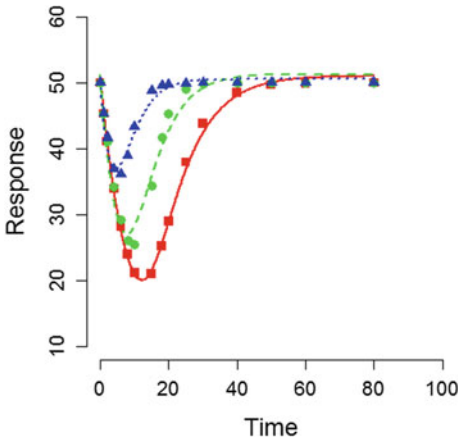

Fig. 11.9 The results of fitting IDR model to simulated data generated from an FC IDR model with proportional feedback control with different values of the feedback gain G_p. *Symbols* are simulated data using FC IDR I model with proportional feedback control with parameters of $k_{out} = 0.1$, $IC_{50} = 10$, $R_0 = 50$, and varying values of G_p: 0.05 (*squares*), 0.5 (*circles*) and 5 (*triangles*). *Lines* are the fitted curves to those data with IDR model I with following estimates of parameters: $k_{out} = 0.109$, $IC_{50} = 16.8$, $R_0 = 51.1$(*solid line*); $k_{out} = 0.152$, $IC_{50} = 107$, $R_0 = 51.3$ (*dashed line*); $k_{out} = 0.255$, $IC_{50} = 705$, $R_0 = 50.6$ (*dotted line*)

corresponding lines in Fig. 11.9. In each case the fits are excellent but the estimates of IC_{50} and k_{out} deviate from the true values. Most critically, IC_{50} is overestimated as 16.8, 107, 705 (with increasing G_p), thus leading to significant underestimation of the in vivo potency of the drug.

For discussion of the challenging issue of pharmacodynamic modeling of drug action involving autoregulated systems, the reader is referred to the extensive analysis of Urquart (2003) and the recent example of Ahlstrom et al. 2013.

11.3 Applications

In this section we present four examples illustrating the application of the FC IDR framework. The examples were selected to reflect each of the four mechanisms of drug action as represented via each of the canonical IDR models (e.g., Models I–IV in Fig. 11.2). In each example, mean or sample individual data were digitized from published figures and used in the analysis with different forms for the feedback control as introduced above.

11.3.1 Selective Serotonin Reuptake Inhibitors and Extracellular Serotonin

Gabrielsson and colleagues have extensively studied and modeled the action of selective serotonin reuptake inhibitors (SSRI) on extracellular concentrations of serotonin (5-HT) in the brain and introduced a model that includes 5-HT feedback via a moderator state. As reviewed (Pineyro and Blier 1999) and summarized in (Bundgaard et al. 2006), neuronal release of 5-HT is under autoregulation, suggesting that the action of feedback regulation may be an important component of any PD model aimed at quantifying the action of SSRIs on the 5-HT release.

To illustrate the application of the FC IDR modeling framework for this problem, a model was constructed for the PK of unbound plasma escitalopram (a SSRI) based on the average escitalopram concentration time data presented in Bundgaard et al. (2006, see Fig. 3), and then used to explore FC IDR models for 5-HT. Figure 11.10 (upper left panel) shows the mean concentration data and the resulting two-compartment model predictions for each dose (2.5, 5, and 10 mg/kg). With pharmacokinetic parameter values fixed at their estimates for each dose (results not shown), the mean 5-HT response-time data (Fig. 4 in Bundgaard et al. 2006) were then pooled and analyzed using IDR Model II, FC IDR Model II with proportional feedback and with proportional plus integral feedback as defined in the following equations:

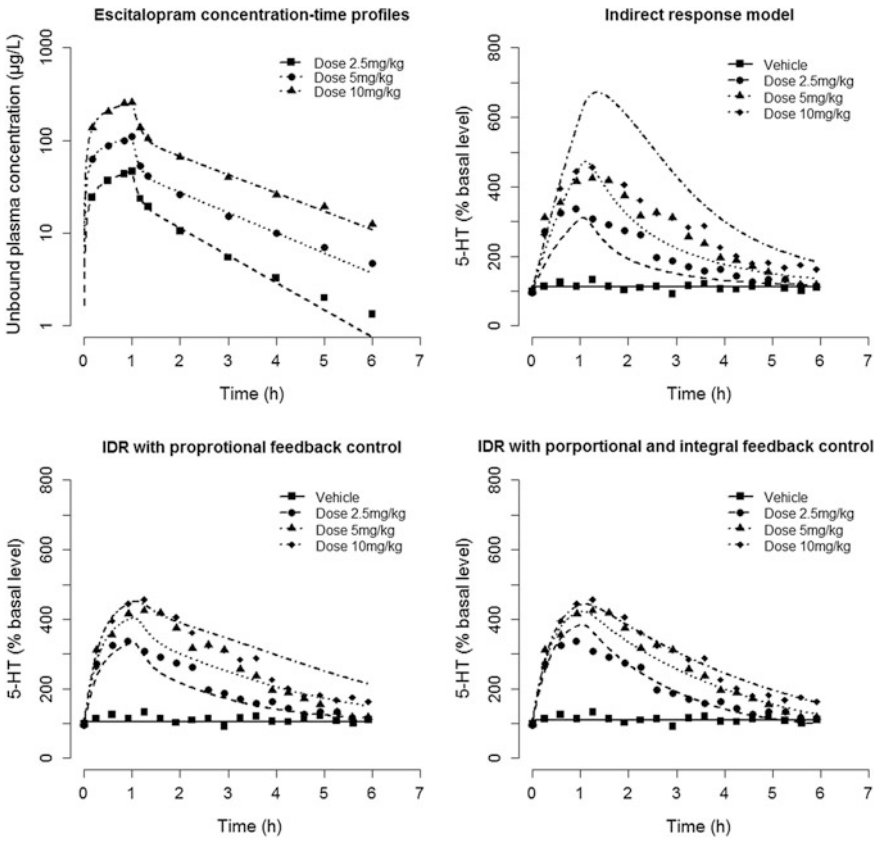

Fig. 11.10 *Upper left panel* shows the PK model predcitions and the mean unbound escitalopram concentrations for each of the three doses. Mean response-time data of 5-HT and model predictions using the IDR model (*upper right panel*), the IDR proportional feedback model (*lower left panel*), and the the IDR proportional plus integral feedback model (*lower right panel*) are also shown

IDR Model II without feedback:

$$\frac{d5HT}{dt} = k_{in} - k_{out}\left(1 - \frac{I_{max} \cdot C}{IC_{50} + C}\right)5HT, \quad 5HT(0) = 5\mathrm{HT}_0$$

IDR Model II with proportional feedback:

$$\frac{d5HT}{dt} = \left(k_{in0} + G_p(5HT_0 - 5HT)\right) - k_{out}\left(1 - \frac{I_{max}C}{IC_{50} + C}\right)5HT,$$
$$5HT(0) = 5\mathrm{HT}_0$$

Table 11.1 Pharmacodynamic parameter estimates and percent relative standard errors (%RSE) for each pharmacodynamic model

Implemented model	Parameter (units)	Estimate (%RSE)
IDR model II	k_{in} (% basal value/h)	710 (12)
	IC_{50} (μg/L)	19.8 (8.1)
	$5HT_0$ (% basal value)	112 (3.1)
FC IDR model II with proportional feedback	k_{in0} (% basal value/h)	1280 (19)
	IC_{50} (μg/L)	6.82 (13)
	G_p (h^{-1})	3.15 (24)
	$5HT_0$ (% basal value)	106 (2.4)
FC IDR model II with proportional plus integral feedback	k_{in0} (% basal value/h)	949 (9.5)
	IC_{50} (μg/L)	2.85 (15)
	G_p (h^{-1})	2.24 (11)
	G_i (h^{-2})	0.528 (11)
	$5HT_0$ (% basal value)	109 (1.6)

The corresponding values for AIC are in order: 849, 790, 723

IDR Model II with proportional plus integral feedback

$$\frac{d5HT}{dt} = \left(k_{in0} + G_p(5HT_0 - 5HT) + G_i \cdot x\right) - k_{out}\left(1 - \frac{I_{max}C}{IC_{50} + C}\right)5HT, \quad 5HT(0) = 5\mathrm{HT}_0$$

$$\frac{dx}{dt} = 5HT_0 - 5HT, \quad x(0) = 0$$

Table 11.1 lists the estimated parameters obtained using each of these three models, while the corresponding model predictions of the 5-HT concentrations versus time are shown in the upper right and lower two panels of Fig. 11.10. The inability of an IDR model without feedback to describe the 5-HT data over the dose range considered has been discussed and analyzed by Bundgaard et al. (2006). The results presented herein illustrate that an FC IDR model with both proportional plus integral feedback are consistent with the mean data analyzed, resulting in the lowest value of AIC of the models considered (see Table 11.1). We note that the FC IRM model with proportional plus integral control results in a value of IC_{50} of 2.9 μg/L.

11.3.2 Histamine H2-Receptor Antagonists and Gastric Acid

This example illustrates the feedback regulation of gastric acidity based on a study of ranitidine (a histamine H2-receptor antagonist) administration in patients in an intensive care unit setting during extended intravenous dosing, as report by Mathot and Geus (1999). It is well established that the reduction in gastric pH following

elevated production of gastric acid, results in an increase in somatostatin secretion, which in turn inhibits histamine and gastrin release, ultimately leading to the inhibition of acid secretion via negative feedback mechanism (Shulkes and Read 1991). Thus incorporating this autoregulation may be a critical component of any comprehensive PK/PD model to describe the dose response of histamine H2-receptor antagonists.

In their study, Mathot and Geus (1999) administered a single 50 mg intravenous dose of ranitidine, and twelve hours later delivered a second bolus of 50 mg followed by a continuous infusion of 0.125 mg/kg/h ranitidine. The mean ranitidine plasma concentration time data reported (Fig. 2 in Mathot and Geus 1999) were fitted by a two-compartment pharmacokinetic model and the resulting model fit and data are shown in Fig. 11.11 (upper left panel).

The resulting PK model was then used with the IDR model reported by Mathot et al. to describe the changes of pH ($pH = -\log[H^+]$) after drug administration.

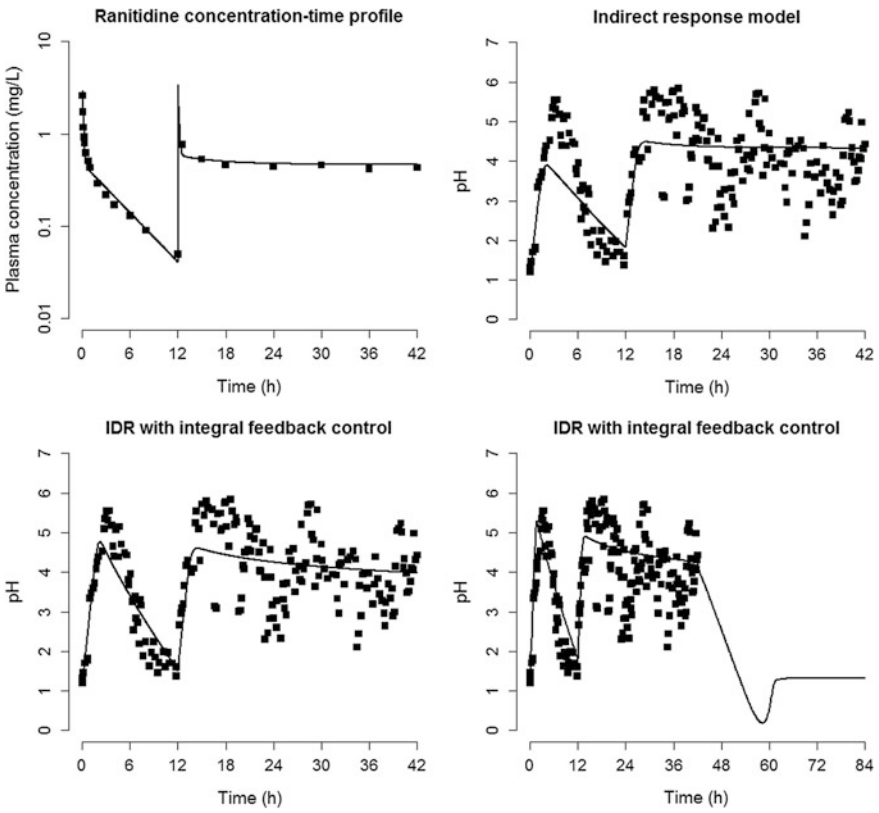

Fig. 11.11 Mean plasma concentration-time profile of ranitidine and model prediction using a two-compartment pharmacokinetic model (upper left panel). Measured response-time data of pH and model predictions from the indirect response model without feedback of Mathot et al. (*upper right panel*). Response-time data of pH and model predictions using IDR model with integral feedback control (*lower left panel*), and model predictions of pH response over 84 h with drug infusion discontinued at 42 h (*lower right panel*)

Their model includes two different steady-states, with the first representing the basal condition and the second representing the maximal drug effect achieving the maximum attainable acidity (pH of 7.4). We also investigated FC IDR models and show the results for IDR Model I with integral feedback:

IDR Model I without feedback

$$\frac{dH^+}{dt} = k_{in}\left(1 - \frac{I_{max} \cdot C^H}{IC_{50}^H + C^H}\right) - k_{out}H^+, \quad H^+(0) = H_0^+$$
$$\text{where,} \quad k_{in} = k_{out}H_0^+ \quad \text{and} \quad I_{max} = 1 - H_{phys}^+/H_0^+$$

IDR Model I with integral feedback

$$\frac{dH^+}{dt} = (k_{in0} + G_i \cdot x)\left(1 - \frac{I_{max} \cdot C^H}{IC_{50}^H + C^H}\right) - k_{out}H^+, \quad H^+(0) = H_0^+$$
$$\frac{dx}{dt} = \left(H_0^+ - H^+\right), \quad x(0) = 0$$

The resulting estimated parameters from these two models are shown in Table 11.2. The model with integral feedback control results in a smaller IC_{50} estimate compared to the IDR model used by Mathot et al. (0.026 vs. 0.0065 mg/L). The upper right panel in Fig. 11.11 shows the measured pH values over the course of the study along with the predicted values from the IDR model without feedback, while the lower left panel in Fig. 11.11 shows the predictions based on the FC IDR model. During the constant maintenance infusion of ranitidine, the feedback attempts to return pH towards its basal value (see lower left panel). After a discontinuation of drug infusion at 42 h, the FC IDR model predicts an undershoot in pH before its return to its baseline value as shown in the plot in the lower right panel of Fig. 11.11.

Table 11.2 Pharmacodynamic parameter estimates and percent relative standard errors (%RSE) for the two models

Implemented model	Parameter (units)	Estimate (%RSE)
IDR model I without feedback	k_{in} (mol/L/h)	0.286 (32)
	IC_{50} (mg/L)	0.0261 (18)
	H	2.53 (6.3)
	$pH(0)$	1.16 (24)
FC IDR model I with integral feedback	k_{in0} (mol/L/h)	0.307 (26)
	IC_{50} (mg/L)	0.00648 (66)
	H	3.00 (10)
	G_i (h^{-2})	51.2 (260)
	$pH(0)$	1.16 (21)

The corresponding values for AIC are in order: 498, 448

11.3.3 Growth Hormone Secretagogues and Circulating Growth Hormone

The mechanisms of neuroendocrine control of growth hormone (GH) release are well established and involve negative feedback regulation based on circulated concentrations of GH and IGF-1 (Muller et al. 1999). This example explores the dose-effect relationship between the growth hormone secretagogue NN703 and plasma growth hormone concentrations as observed in a study of human volunteers administered NN703 as an oral solution at doses of 6 and 12 mg/kg (see Agerso et al. 2001).

A two-compartment model with zero-order input over 1.5 h described the mean NN703 plasma concentration data for both doses, resulting in the model fit shown in the upper left panel of Fig. 11.12. With the pharmacokinetic parameters fixed,

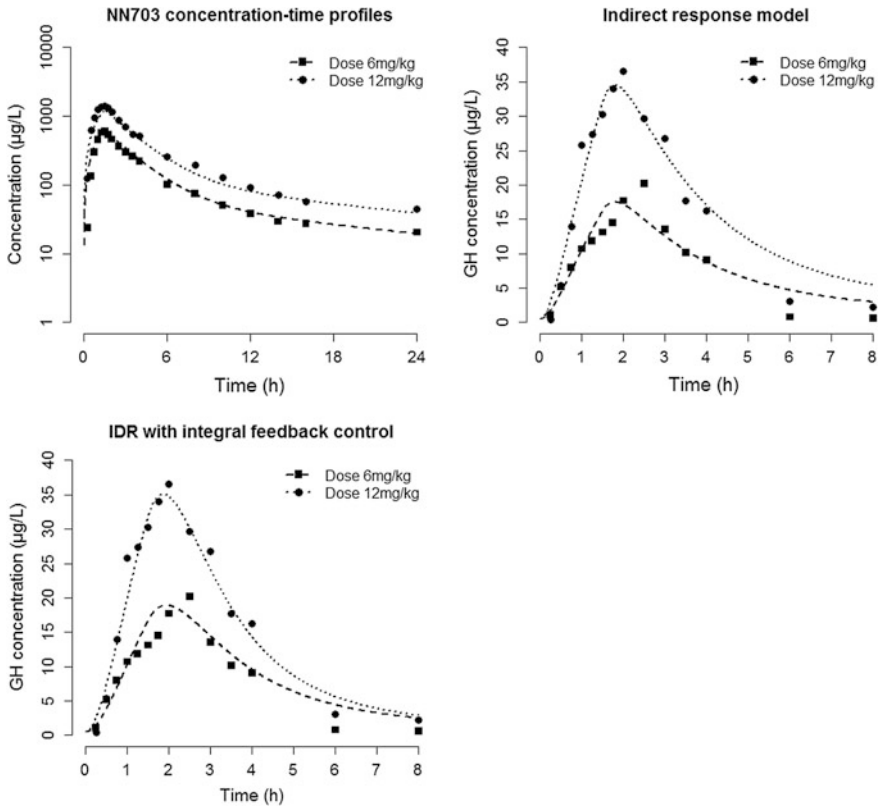

Fig. 11.12 Mean concentration-time measurements of NN703 and model predictions using a two-compartment pharmacokinetic model for each of two doses (*upper left panel*). Response-time data of growth hormone concentration and model predictions using IDR Model III (*upper right panel*). Response-time data of growth hormone concentration and model predictions using the IDR Model III with integral feedback control (*lower left panel*)

Table 11.3 Pharmacodynamic parameter estimates and percent relative standard errors (%RSE) for the two models

Implemented model	Parameter (units)	Estimate (%RSE)
IDR model III without feedback	k_{in} (μg/L/h)	1.51 (16)
	k (L/μg)	0.0620 (3.2)
	$GH(0)$ (μg/L)	0.5 (Fixed)
FC IDR model III with integral feedback	k_{in0} (μg/L/h)	0.861 (18)
	k (L/μg)	0.0794 (8.5)
	G_i (h^{-2})	0.00484 (17)
	$GH(0)$ (μg/L)	0.5 (Fixed)

The corresponding values for AIC are in order: 140, 134

the response-time data of plasma growth hormone were modeled by IDR Model III using a linear effect on the production rate of growth hormone. In addition, an FC IDR model with integral feedback control was used to describe the plasma growth hormone. The equations for both models are given below:

IDR Model III without feedback

$$\frac{dGH}{dt} = k_{in}(1 + k \cdot C_p) - k_{out} \cdot GH, \quad GH(0) = GH_0$$

FC IDR Model III with integral feedback

$$\frac{dGH}{dt} = (k_{in0} + G_i \cdot x)(1 + k \cdot C_p) - k_{out} \cdot GH, \quad GH(0) = GH_0$$
$$\frac{dx}{dt} = (GH_0 - GH), \quad x(0) = 0$$

Table 11.3 lists the parameter estimates for the two models and Fig. 11.12 shows the resulting model fits. The FC IDR model is associated with a smaller AIC value, a better prediction of the later values of plasma GH, and predicts a somewhat greater drug sensitivity as indicated by the larger drug effect (bigger k) compared to the corresponding value in the simple indirect response model (0.0794 vs. 0.0620 L/μg).

11.3.4 β_2-Selective Adrenergic Agonists and Potassium

Plasma potassium concentration is also under feedback regulation that acts by altering cellular uptake and renal excretion (Greenlee et al. 2009). In this example, the effects of the β_2-selective adrenergic agonist terbutaline on plasma potassium

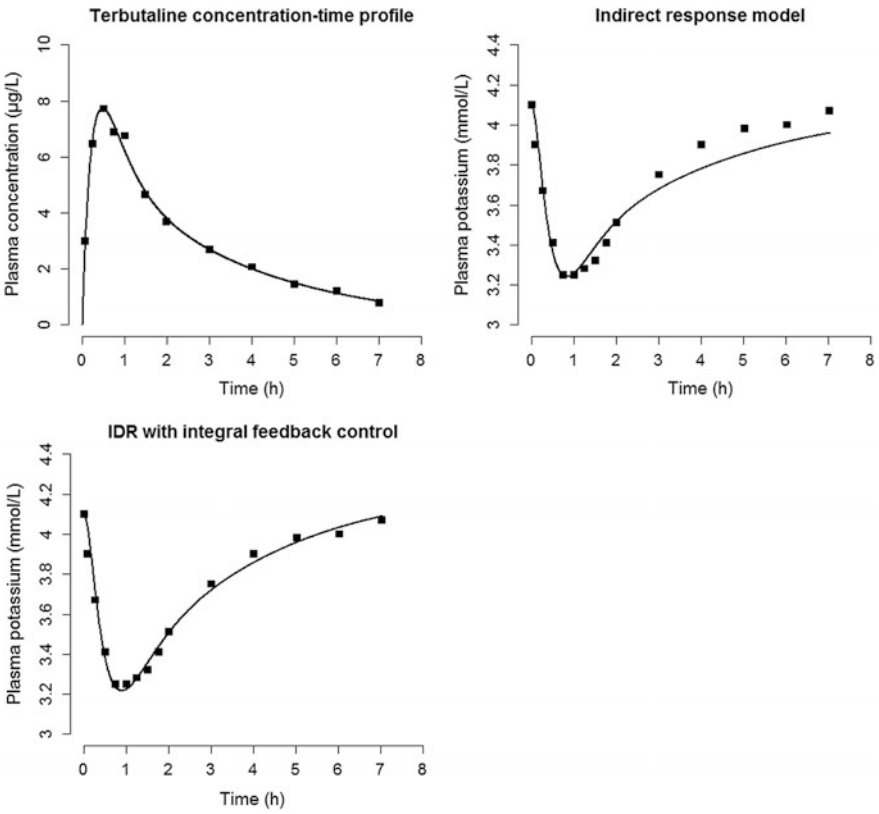

Fig. 11.13 Mean plasma concentration-time profile of terbutaline and model prediction using a two-compartment model (*upper left panel*). Mean potassium plasma concentration and model predictions using IDR Model IV (*upper right panel*) and with the IDR Model IV with integral feedback control (*lower left panel*)

are used to further illustrate feedback control indirect response models. The example is based on the results reported in the study of Jonkers et al. (1987).

In their study, six subjects were given a single subcutaneous dose of 0.5 mg terbutaline, and both plasma terbutaline and potassium concentrations were measured over seven hours. A two-compartment model with a first-order absorption rate was used to describe the mean terbutaline concentration data presented in the paper, resulting in the model fit shown in the upper left panel of Fig. 11.13. An IDR Model IV using a linear effect on the elimination of potassium and an FC IDR model with integral feedback control were then used to describe the mean plasma potassium concentration data reported in (Jonkers et al. 1987). The equations for both models are given below:

Table 11.4 Pharmacodynamic model parameter estimates and percent relative standard errors (% RSE)

Implemented model	Parameter (units)	Estimate (%RSE)
IDR model IV without feedback	k_{in} (mmol/L/h)	13.3 (16)
	k (L/μg)	0.0387 (4.2)
	K_0^+ (mmol/L)	4.1 (Fixed)
FC IDR model IV with integral feedback	k_{in0} (mmol/L/h)	10.5 (9.4)
	k (L/μg)	0.0429 (3.2)
	G_i (h^{-2})	0.161 (20)
	K_0^+ (mmol/L)	4.1 (Fixed)

The corresponding values for AIC are in order: -28.8, -41.5

IDR Model IV without feedback

$$\frac{dK^+}{dt} = k_{in} - k_{out}(1 + k \cdot C)K^+, \quad K^+(0) = K_0^+$$

IDR Model IV with integral feedback

$$\frac{dK^+}{dt} = (k_{in0} + G_i \cdot x) - k_{out}(1 + k \cdot C_p)K^+, \quad K^+(0) = K_0^+$$
$$\frac{dx}{dt} = (K_0^+ - K^+), \quad x(0) = 0$$

Figure 11.13 shows the resulting model fits and Table 11.4 lists the parameter estimates for the two models, indicating that the FC IDR model is associated with a smaller AIC value. Addition of a proportional feedback control term did not further improve the model fit. The model with integral feedback control predicts an overshoot of potassium concentration with the decrease of terbutaline concentration over a prolonged time (result not shown).

11.4 Summary

In this chapter, a feedback control method widely used in engineered systems has been applied to the indirect response modeling framework, providing a pharmacodynamic modeling formulation for studying a drug's action when its response is subject to endogenous feedback control. After briefly introducing the feedback control framework, its application was illustrated using one of the canonical IDR models, which thereby provided an outline for its general application to other IDR models. Simulations were presented to illustrate the model responses under different assumptions about the feedback control mechanisms. Several extensions to the linear control framework were presented, as were comparisons to some general modeling approaches for incorporating feedback regulation used previously in

pharmacodynamic modeling. The challenging issue of identifying the contribution and form of feedback mechanisms in PK/PD studies was also highlighted. Finally, four examples based on published studies from literature were used to illustrate the application of the proposed FC IDR framework Since the original submission of this chapter, a version of this material has been published (Zhang and D'Argenio 2016).

Acknowledgments This work was supported in part by Grant NIH/NIBIB P41-EB001978.

References

Adolph EF (1961) Early concepts of physiological regulations. Physiol Rev 41:737–770

Agerso H, Ynddal L, Sogaard B, Zdravkovic M (2001) Pharmacokinetic and pharmacodynamic modeling of NN703, a growth hormone secretagogue, after a single po dose to human volunteers. J Clin Pharmacol 41(2):163–169

Ahlstrom C, Kroon T, Peletier LA, Gabrielsson J (2013) Feedback modeling of non-esterified fatty acids in obese Zucker rats after nicotinic acid infusions. J Pharmacokinet Pharmacodyn 40 (6):623–638. doi:10.1007/s10928-013-9335-z

Alon U (2007) An introduction to systems biology. CRC Press, London

Astrom KJ, Murray RM (2010) Feedback systems. Princeton University Press, Princeton

Bolie VW (1961) Coefficients of normal blood glucose regulation. J Appl Physiol 16:783–788

Bundgaard C, Larsen F, Jorgensen M, Gabrielsson J (2006) Mechanistic model of acute autoinhibitory feedback action after administration of SSRIs in rats: application to escitalopram-induced effects on brain serotonin levels. Eur J Pharm Sci 29(5):394–404. doi:10.1016/j.ejps.2006.08.004

Cannon WB (1929) Organization for physiological homeostasis. Physiol Rev 9(3):399–431

Cole KS (1949) Dynamic electrical characteristics of the squid axon membrane. Annu Rev Physiol 3:253–258

Dayneka NL, Garg V, Jusko WJ (1993) Comparison of four basic models of indirect pharmacodynamic responses. J Pharmacokinet Biopharm 21(4):457–478

Donald DE, Milburn SE, Shepherd JT (1964) Effect of cardiac denervation on the maximal capacity for exercise in the racing greyhound. J Appl Physiol 19:849–852

Euler CV (1964) The gain of the hypothalamic temperature regulating mechanisms. Prog Brain Res 5:127–131

Friberg LE, Henningsson A, Maas H, Nguyen L, Karlsson MO (2002) Model of chemotherapy-induced myelosuppression with parameter consistency across drugs. J Clin Oncol 20(24):4713–4721

Gabrielsson J, Peletier LA (2008) A flexible nonlinear feedback system that captures diverse patterns of adaptation and rebound. AAPS J 10(1):70–83. doi:10.1208/s12248-008-9007-x

Greenlee M, Wingo CS, McDonough AA, Youn JH, Kone BC (2009) Narrative review: evolving concepts in potassium homeostasis and hypokalemia. Ann Intern Med 150(9):619–625

Grodins FS (1963) Control theory and biological systems. Columbia University Press, New York

Grodins FS, Gray JS, Schroeder KR, Norins AL, Jones RW (1954) Respiratory responses to CO2 inhalation; a theoretical study of a nonlinear biological regulator. J Appl Physiol 7(3):283–308

Guyton AC, Thomas CEJ, Coleman G (1973) Circulatory physiology: cardiac output and its regulation. W.B. Saunders Company, Philadelphia

Gabrielsson J, Weiner D (2007) Pharmacokinetic and pharmacodynamic data analysis: concepts and applications. Swedish Pharmaceutical Press, Stockholm

Jones RW (1973) Principles of biological regulation. Academic Press, New York

Jonkers R, Van Boxtel CJ, Oosterhuis B (1987) Beta-2-adrenoceptor-mediated hypokalemia and its abolishment by oxprenolol. Clin Pharmacol Ther 42(6):627–633
Khoo MCK (2000) Physiological control systems. IEEE Press, Piscataway
Kitano H (2001) Foundations of systems biology. MIT Press, Cambridge
Koulnis M, Liu Y, Hallstrom K, Socolovsky M (2011) Negative autoregulation by Fas stabilizes adult erythropoiesis and accelerates its stress response. PLoS ONE 6(7):e21192. doi:10.1371/journal.pone.0021192
Kremling A (2014) Systems biology. CRC Press, Abingdon
Clynes M, Milsum JH (1970) Biomedical engineering systems. McGraw-Hill, New York
Mathot RA, Geus WP (1999) Pharmacodynamic modeling of the acid inhibitory effect of ranitidine in patients in an intensive care unit during prolonged dosing: characterization of tolerance. Clin Pharmacol Ther 66(2):140–151. doi:10.1053/cp.1999.v66.99988
Milhorn HT (1966) Application of control theory to physiological Systems. W. B. Saunders Company, Philadelphia
Milsum JH (1966) Biological control systems analysis. McGraw-Hill, New York
Muller EE, Locatelli V, Cocchi D (1999) Neuroendocrine control of growth hormone secretion. Physiol Rev 79(2):511–607
Pineyro G, Blier P (1999) Autoregulation of serotonin neurons: role in antidepressant drug action. Pharmacol Rev 51(3):533–591
Sharma A, Ebling WF, Jusko WJ (1998) Precursor-dependent indirect pharmacodynamic response model for tolerance and rebound phenomena. J Pharm Sci 87(12):1577–1584
Sherman PM, Stark L (1957) A servoanalytic study of consensual pupil reflex to light. J Neurophysiol 20(1):17–26
Shulkes A, Read M (1991) Regulation of somatostatin secretion by gastrin- and acid-dependent mechanisms. Endocrinology 129(5):2329–2334. doi:10.1210/endo-129-5-2329
Stark L (1968) Neurological control systems. Plenum Press, New York
Sturm OE, Orton R, Grindlay J, Birtwistle M, Vyshemirsky V, Gilbert D, Calder M, Pitt A, Kholodenko B, Kolch W (2010) The mammalian MAPK/ERK pathway exhibits properties of a negative feedback amplifier. Science Signal 3(153):ra90. doi:10.1126/scisignal.2001212
Urquhart J (2003) History-informed perspectives on the modeling and simulation of therapeutic drug actions. In: Kimko HC, Duffull SB (eds). Simulation for designing clinical trials. Marcel Dekker, New York, pp 245–269
Wakelkamp M, Alvan G, Gabrielsson J, Paintaud G (1996) Pharmacodynamic modeling of furosemide tolerance after multiple intravenous administration. Clin Pharmacol Ther 60(1):75–88. doi:10.1016/S0009-9236(96)90170-8
Woo S, Krzyzanski W, Jusko WJ (2008) Pharmacodynamic model for chemotherapy-induced anemia in rats. Cancer Chemother Pharmacol 62(1):123–133. doi:10.1007/s00280-007-0582-9
Yates FE, Urquhart J (1962) Control of plasma concentrations of adrenocortical hormones. Physiol Rev 42:359–433
Yi TM, Huang Y, Simon MI, Doyle J (2000) Robust perfect adaptation in bacterial chemotaxis through integral feedback control. Proc Natl Acad Sci USA 97(9):4649–4653
Zhang Y, D'Argenio DZ (2016) Feedback control indirect response models. J Pharmacokinet Pharmacodyn 43(4):343–358

Chapter 12
Nonlinear Mixed Effects Modeling in Systems Pharmacology

Peter L. Bonate, Amit Desai, Ahsan Rizwan, Zheng Lu and Stacey Tannenbaum

Abstract Quantitative systems pharmacology (QSP) is the design and application of mathematical models to explain how drugs function at a systems level. Whereas traditional pharmacokinetic-pharmacodynamic modeling takes an empirical or mechanistic approach to modeling, QSP takes a holistic approach exploring whole biochemical and metabolic pathways and how drugs interact in those pathways. These models are often unidentifiable from any single set of data. Instead they are built using diverse datasets with many parameters fixed to mean values from different experiments resulting in models that are over-confident in their parameter values. Few models currently take into account these sources of variability in their parameter estimation. This chapter discusses nonlinear mixed effects models, a modeling approach that specifically accounts for sources of variability in a model, and their application to QSP.

Keywords Nonlinear mixed effects models (NMEMs) · Variability · Linear model · Monoexponential · Overparameterization · Covariates · Between-subject variability · Multimodal distributions · Drug potency · Myeloperoxidase (MPO) · Turnover rates

12.1 Introduction

Any experiment can be viewed as a system, a collection of objects that interact to create a unified whole. Mathematical models, whether it is a differential equation or a statistical model like simple linear regression, attempt to define the structure and behavior of the system in mathematical terms and explain how components in the

P.L. Bonate (✉) · A. Desai · A. Rizwan · Z. Lu · S. Tannenbaum
Astellas Pharma, 1 Astellas Way, Northbrook, IL 60062, USA
e-mail: peter.bonate@astellas.com

Present address:
A. Rizwan
Nektar Therapeutics, San Francisco, CA, USA

D.E. Mager and H.H.C. Kimko (eds.), *Systems Pharmacology and Pharmacodynamics*,
AAPS Advances in the Pharmaceutical Sciences Series 23,
DOI 10.1007/978-3-319-44534-2_12

system change over time or with respect to other components in the system. When an observation is made in an experiment, scientists talk about accuracy and precision. Accuracy refers to how close the observed value is to the true value, while precision refers to the variability in the observation. The precision of an observation is dependent on the sources of variability in the experiment, and there can be many. Preclinically, there can be variability in response within an animal, across animals, across cages, and across animal housing units. Within a lab, there can be variability introduced by different lab technicians with respect to how they prepare dosing solutions, how they handle animals, how they dose the animals, how they draw blood samples, and how they measure pharmacodynamic responses. Bioanalytically, there can be variability in measurement of analytes within runs, across runs, and across different assays. In all, there are many potential sources of variability, any of which can decrease the precision of an observation.

One goal of mathematical modeling is to separate the noise from the "information" or systematic component in the system; the more imprecise an observation, the greater the noise, and the harder it is to define the underlying structure of the system. Models consist of a mapping function, parameters, and variables. Variables are the inputs to the system, whereas parameters are constants that map the variables to the observations. For example, with the simple model

$$Y = 2 + 3x + \varepsilon \tag{12.1}$$

Y is an observation made about the system, x is a variable, 2 is called the intercept and is a model parameter, 3 is the slope and it too is a model parameter, and ε is the error between the mapping function 2 + 3x and the observation Y. Given a set of observations {Y, x}, the goal of modeling is to often identify the mapping function and to estimate the parameters of the model, in this case the slope and intercept. As the magnitude of ε becomes larger and larger, which means the precision of the observation Y becomes smaller and smaller (it is often assumed that x is measured perfectly without error), the ability to identify the underlying structure of the model diminishes as does the ability to accurately estimate the model parameters.

As a modeler there are two choices: ignore the variability or model the data taking into account and controlling for these sources of variability. Nonlinear mixed effects models (NMEMs) are one class of models that choose the latter approach—to model the data taking into account the sources of variability in order to obtain better parameters estimates (Davidian and Giltinan 1995). A mixed effects model consists of a model that contains both fixed and random effects. Fixed effects define the structural model (the mapping function that defines the mean response for the population) and are variables manipulated by the experimenter, like the dose of drug administered to an animal or the timing of samples for bioassay. Random effects do not contribute to the structural model but instead define the variance model; they are latent variables not controlled by the experimenter and are stochastic in nature. All the random effects in a model define the sources of variability and are referred to as the variance components. The term "nonlinear" in NMEM refers to the fact that the underlying structural model is nonlinear in nature

with respect to the model parameters. This chapter will focus on the use of NMEMs in systems pharmacology, a relatively new area of research. This chapter will further explain the sources of variability, the basics of NMEMs, why you want to use NMEMs, will present an overview of software and estimation of model parameters, and will conclude with some case studies.

12.2 Source of Variability and NMEMs

Suppose you are interested in measuring blood pressure Y after some pharmacological intervention and you wanted to know what was the population mean blood pressure after treatment μ. If you measured one time point in n different animals, a linear model of the form

$$Y_i = \mu + \varepsilon_i, \quad i = 1, 2.. \ldots, \mathrm{n}, \tag{12.2}$$

could be written, where ε is an error term that represents all sources of variability. The population estimate for μ would be the sample mean $\bar{Y}$ and would be equal to $\bar{Y} = \sum Y_i/n$. Because none of the sources of variability can be distinguished, there would be only one variance component called unexplained variability, defined as the sample variance Var(Y) = σ^2. As n → ∞, then by the Law of Large Numbers, $\bar{Y}$ should be closer and closer to μ.

Unlike the example above, most biological experiments are repeated measures experimental designs wherein observations are serially measured on a subject, which can be a mouse, rat, or human. Now suppose you measured blood pressure at three different time points 10 min apart in each subject. Each of these time points will be called an occasion. Assuming the treatment effect is a constant at each occasion, a model of the form

$$Y_{ij} = \mu + S_i + \varepsilon_{ij}, \quad i = 1, 2, \ldots, \mathrm{n}, \mathrm{j} = 1,2,3 \tag{12.3}$$

could be written, where S_i is now the individual subject effect of the ith subject. The population mean would still be the overall sample mean $\bar{Y} = \sum_{j=1}^{3} \sum_{i=1}^{n} Y_{ij}/n$. However, because repeated observations are available for each subject, each subject's mean can be written as $\bar{Y}_i = \sum_{j=1}^{3} Y_{ij}/n$. The variance of $\bar{Y}_i$ across all subjects represents between-subject variability: ω^2. Hence, under this repeated measures design, there are two variance components: ω^2 and σ^2. All of the variance components in the model are referred to as random effects. It should be noted that σ^2 in Eq. (12.2) is not the same σ^2 in Eq. (12.3): by definition, the total variance of the observations never changes, so the total variability in Eq. (12.2) has been partitioned into two components in Eq. (12.3) such that σ^2 in Eq. (12.2) equals ω^2 + σ^2 in Eq. (12.3).

Now, suppose that on each occasion, 2 measures are taken 10 s apart so that each subject now has 6 observations. A linear model of the form

$$Y_{ijk} = \mu + S_i + t + \varepsilon_{ijk}, \quad i = 1, 2, \ldots, \text{n, j = 1,2,3, k = 1,2} \tag{12.4}$$

could be written, where t_k is the effect at each occasion. Using the same concepts as with Eq. (12.3), the total variability in Y can be partitioned into between-subject variability ω^2, inter-occasion variability κ^2, and unexplained variability σ^2, such that $\text{Var(Y)} = \omega^2 + \kappa^2 + \sigma^2$. With each design, as more and more data are collected, the unexplained variability is reduced as total variability is partitioned more and more. These concepts can now be extended to a NMEM.

Suppose Y is a vector of m observations from n subjects and x is a matrix of fixed effects from n subjects. For simplicity, all subjects will be assumed to have the same number of observations m, but this does not necessarily have to be so. A general NMEM can be written as

$$Y = f(\text{x};\theta;\Omega;\Sigma) \tag{12.5}$$

where f(.) is a function that maps x to Y, θ is a vector of estimable regression parameters of size p, Ω is a matrix of variance components that define the sources of variability in the model, and Σ is a vector of residual variance components that model the unexplained variability in the data. For example, in a pharmacokinetic experiment where plasma drug concentrations are serially measured after intravenous dosing and are found to decline monoexponentially over time, a model for such an experiment might be

$$\underbrace{C_{ij} = \frac{D}{V_i}\exp\left(\frac{-CL_i}{V_i}t_{ij}\right)}_{\text{Structural Model}} \underbrace{\exp(\varepsilon_{ij})}_{\text{Variance Model}} \tag{12.6}$$

where C_{ij} is the concentration at the jth time point for the ith subject and is modeled as a function of the structural model and variance model. The fixed effects in the structural model are dose D and time t_{ij}. The random effects are V_i, the volume of distribution for the ith subject, and CL_i, the total systemic clearance for the ith subject, and the variance model is a function of the residuals ε_{ij}. This model is referred to as a 1-compartment model.

It is often assumed that the distribution of the subject-specific pharmacokinetic parameters are log-normal in distribution, that the distribution of the subject-specific random effects are normal in distribution, and that the two can be related though an exponential transformation. For example, the volume of distribution for the ith subject would be expressed as

$$V_i = \theta_1 \exp(\eta_{Vi}) \tag{12.7}$$

where θ_1 is the population mean value and η_{Vi} is the deviation of the ith subject from the mean value, which is assumed to have mean 0 and variance ω_V^2. Clearance would similarly be expressed as

$$CL_i = \theta_2 \exp(\eta_{CLi}) \tag{12.8}$$

where θ_2 is the population mean value and η_{CLi} is the deviation of the ith subject from the mean value, which is assumed to have mean 0 and variance ω_{CL}^2. Similarly, for bioanalytical data, it is assumed that ε_{ij} has mean 0 and variance σ^2. Going back to Eq. (12.5), in matrix notation θ is then the vector of estimable parameters $\{\theta_1, \theta_2\}$, Ω is the set of variance components $\{\omega_V^2, \omega_{CL}^2\}$, $\Sigma = \{\sigma^2\}$, and the NMEM now can be written as

$$\begin{aligned}
&\begin{bmatrix}\eta_{CL}\\ \eta_V\end{bmatrix} \sim N\left(\begin{bmatrix}0\\0\end{bmatrix}, \Omega\right)\\
&\varepsilon \sim N(0, \sigma^2)\\
&\Omega = \begin{bmatrix}\omega_{CL}^2 & 0\\ 0 & \omega_{CL}^2\end{bmatrix}\\
&\sum = \sigma^2\\
&C_{ij} = f(\theta; D; \mathrm{t}; \mathrm{CL}; \mathrm{V}; \Omega; \Sigma)\\
&C_{ij} = \frac{D}{\theta_1 \exp\left(\eta_{i,V}\right)} \exp\left(\frac{-\theta_2 \exp\left(\eta_{i,CL}\right)}{\theta_1 \exp\left(\eta_{i,V}\right)} t_{ij}\right) \exp\left(\varepsilon_{ij}\right)
\end{aligned} \tag{12.9}$$

This model is illustrated graphically in Fig. 12.1 (Bonate 2011), in which the concentration-time profile for 2 subjects are shown relative to the population mean. Each observation is expressed as a deviation from the population mean, which is what Eq. (12.9) expresses mathematically.

While estimates of θ are most often of primary interest, estimates of the variance components are also of interest because, conditional on the model and population estimates and then using Bayes theorem, an estimate of individual subject parameters θ_i can be obtained (Aarons 1991; Fitzmaurice et al. 2004). These individual subject parameters are referred to as empirical Bayes estimates (EBE). Availability of EBE can be used to examine groups of subpopulations that may be of interest or to look for correlations between-subject-specific characteristics (such as genotype) and the parameter of interest.

The assumptions made in Eqs. (12.7) and (12.8) with regards to the distribution of the random effects (i.e., log-normal distribution) are not predetermined; other distributions can be assumed depending on the data type. For many studies examining physiological parameters, a normal distribution is more appropriate. Also, in Eq. (12.9) the residual, unexplained error ε was assumed to be multiplicative in nature, but this does not have to always be the case. Other common residual error models include:

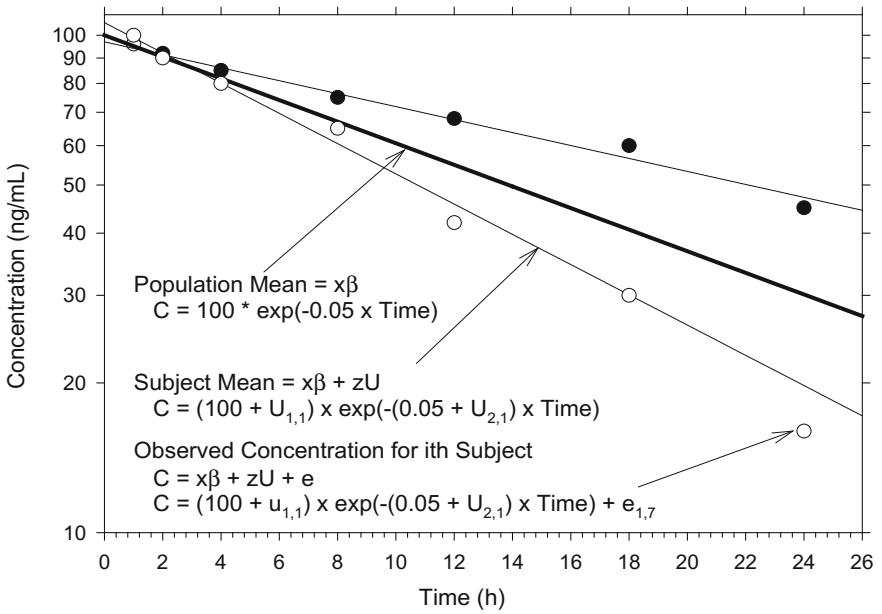

Fig. 12.1 Plot demonstrating the relationship between the population mean, subject mean, and deviation from the subject mean for 2 different subjects using a 1-compartment open model plotted on a semi-log scale. Reprinted from Bonate (2011)

- Additive error model

$$Y = f(X;\theta;\Omega) + \varepsilon \tag{12.10}$$

- Constant coefficient of variation (CV) or proportional error model

$$Y = f(X;\theta;\Omega)(1+\varepsilon) \tag{12.11}$$

- Combined additive and proportional error model

$$Y = f(X;\theta;\Omega)\exp(\varepsilon_1) + \varepsilon_2 \tag{12.12}$$

The most common residual variance model being used for pharmacokinetic data is the proportional error model, with the additive model being most commonly used for pharmacodynamic data.

Structural models in conventional pharmacokinetics-pharmacodynamics (PK/PD), like in Eq. (12.6), are generally empirical in nature. For example, a typical pharmacokinetic model, the "two compartment model", represents the body as 2 linked compartments with flows in and out of each (Gabrielsson and Weiner 2000). While often such empirical models are sufficient to represent the concentration or response as a function of time, mechanistic models used in systems

pharmacology take the underlying (patho)physiology and the mode of drug action into consideration. According to Danhof et al. (2007), "*mechanism-based PK/PD models differ from conventional PK/PD models in that they contain specific expressions to characterize, in a quantitative manner, processes on the causal path between drug administration and effect. This includes target site distribution, target binding and activation, pharmacodynamic interactions, transduction, and homeostatic feedback mechanisms*". The structural model generally defines the underlying model for the population mean data. Using a population approach, in which a statistical model is added to the structural model, may add value to a traditional systems pharmacology approach by allowing an examination of the variability between and within subjects, and between observed and model-predicted values (i.e., residual variability).

In models with a simple structure, like Eq. (12.9) and many types of compartmental pharmacokinetic models, random effects generally are included on all parameters; however, systems pharmacology models tend to have a very large number of parameters. Adding variability to each parameter may lead to model instability or structural unidentifiability due to overparameterization, not to mention run times that are inconveniently long (Chis et al. 2011). Before adding variability to the model, one may consider reducing the model to a simpler one which retains the dynamic properties of the original, as demonstrated by Schmidt et al. with bone remodeling (Schmidt et al. 2011). Once the model is reduced (if applicable), care should be taken to first model between-subject variability on parameters for which extensive variability is observed. Change in model stability and relative improvement in fit should be assessed upon adding additional variability terms.

One of the powerful things about NMEMs is that the model parameters themselves can be modeled as a function of other predictor variables. These predictor variables, called covariates, can be defined as either intrinsic (such as weight, sex, age, etc.) or extrinsic (such as smoking status, concomitant medications, conditions of the drug treatment like formulations or dose regimens, etc.) characteristics that describe a subject (United States Department of Health and Human Services et al. 1999). Returning to the model presented in Eq. (12.9), suppose it was believed that clearance was a linear function of weight, Eq. (12.8) could be rewritten as

$$CL = (\theta_2 + \theta_3 \times Weight)\exp(\eta_{CL}) \tag{12.13}$$

and Eq. (12.9) would then be modified to

$$C_{ij} = \frac{D}{\theta_1 \exp(\eta_{i,V})}\exp\left(\frac{-\{(\theta_2 + \theta_3 \times \text{weight})\exp(\eta_{i,CL})\}}{\theta_1 \exp(\eta_{i,V})}t_{ij}\right)\exp(\varepsilon_{ij}). \tag{12.14}$$

In this manner, covariates can be added to the model to further improve its predictive capabilities. For a particular systems pharmacology model, the covariates to be explored should be those of scientific or clinical interest as well as mechanistic plausibility in that disease state (Gastonguay 2011) and/or for that treatment: for

example, in bone reabsorption modeling, Post et al. (2013) suggest "baseline serum estrogen, FSH or calcium concentrations, age and age at menarche" as potential covariates.

Variability in disease status, response rate, and system dynamics can often be explained in part by covariates; addition of an appropriate covariate to a parameter may improve the model fit for individual subjects and reduce the magnitude of unexplained variability in the population. In addition, knowledge of the covariate's impact on a particular component of the model may be used to advise dose or treatment adjustment, suggest a subgroup analysis (e.g., responders vs. non-responders), or inform future study designs. As in the case of between-subject variability components, with so many parameters in a systems pharmacology model which may be affected by intrinsic or extrinsic factors, there is a danger of over-parameterizing the model. Care should be taken to select only the most influential and meaningful covariates that improve the model fit or allow the exploration of important scientific or clinical questions.

"Traditional" PK/PD data that are analyzed using a population approach tend to have only a few observations per individual (parent drug, sometimes a metabolite, and perhaps 1–2 PD measurements), generally all of which are on a similar time scale. However, systems pharmacology models often incorporate processes that occur at different time scales during the course of disease (Schmidt et al. 2011). Osteoporosis, in particular, has observations that range from seconds (receptor binding, enzymatic reactions), to hours (drug concentrations), to weeks (biochemical turnover markers such as NTx and CTx), to months (bone mineral density), and even to years (fracture risk) (Peterson and Riggs 2010); whereas "fast" observations may show a quick response to intervention and thus be useful for informing proof of mechanism or dose selection, "slower" observations may be more useful for exploring the long-term impact of intervention on disease progression or assessing drug safety. One of the advantages of NMEMs is that they are not limited to a single data type, e.g., only pharmacokinetic or only pharmacodynamic data, but can be extended to model many different data types of different scales simultaneously, although it may be necessary to mathematically reduce the model to "physiologically and therapeutically relevant time scales" and to select only the most important parameters upon which to add variability terms.

12.3 What's Wrong with Modeling the Mean?

During preclinical drug development, particularly in experiments with mice and rats, it is often not possible to collect multiple blood samples in the same animal. Usually only one blood sample per animal is available in a drug concentration analysis and certainly only one tissue or organ sample is available per animal. Therefore, in the past it was common practice to do one of two things: naïve pooling or naïve averaging. With naïve averaging, the measurements across animals at each time point are first averaged and then the averages are used for modeling.

Numerous examples of this approach can be found in the development of models for corticosteroid pharmacodynamics (Nichols et al. 1989; Ramakrishnan et al. 2002; Xu et al. 1995). With naïve pooling, all individual animals are pooled and treated as independent observations, even if there are repeated measurements per animal (Sun et al. 1998). This approach is in contrast to NMEMs in which all data from all subjects are fit simultaneously taking into account the sources of variability. A natural question is how the parameter estimates differ between the naïve pooled approach and NMEMs: it turns out the model parameter estimates of the fixed effects are often, but not always, similar between the methods and there are no real differences observed (Bonate 2011; Upton and Mould 2014; Wright 1998).

So what advantage do NMEMs have over using naïve pooling? If the goal is to obtain estimates of the fixed effects, the estimates are similar between the two approaches so there is no advantage in that regard. However, what NMEMs do offer is that in addition to fixed effect estimates, estimates of the variance components can also be obtained. This advantage though comes at a price—speed. It is much faster to model the mean using a software program like ADAPT V or SAAM II than to use a program like NONMEM. One modeling plan then could be to develop the underlying structural model using the naïve approach but then to port the model over to a NMEM software package like NONMEM and use a NMEM approach to estimate the model parameters and variance estimates using all the data.

12.4 Does Variance Scale Across Species?

As discussed previously, one of the advantages of NMEMs is that in addition to estimates of the fixed effects, estimates of the variance components are also available. In clinical studies, these variance components may include between-study, between-center, between-subject, inter-occasion, and residual or unexplained variability, while in animal studies they may include between-study, between-technician, between-cage, between-animal, inter-occasion, and residual variability. In nonclinical drug development, studies may be done in rats, mice, dogs, or other less common species. It may be necessary to bridge the model across different animal species, or scale a model developed in animals to humans, such as what might be done when predicting human pharmacokinetics based on animal pharmacokinetics. A great body of evidence suggests that many fixed effect pharmacokinetic parameters, like clearance and volume of distribution, as well as many other physiological processes like heart rate, blood flow, or organ volume, scale to body weight (Boxenbaum 1982) using a power equation of the form

$$\text{PK} = \alpha(\text{Weight})^{\beta}. \tag{12.15}$$

β is generally about 0.75 for clearance terms and 1.0 for volume terms (Holford 1996). Because of this relationship, in many instances it is possible to predict pediatric pharmacokinetics based on adult data or adult pharmacokinetics based on animal data (Mahmood 2006; Sinha et al. 2008). Equation (12.15) may also be used

to scale the pharmacokinetics in mice to rats; this may be useful when pharmacodynamic studies of efficacy are done in mice, but pharmacokinetic studies are done in rats, and it is necessary to bridge the studies across species.

Some fixed effect parameters, usually pharmacodynamic in nature, like IC_{50} and EC_{50}, do not scale with body weight across species (Mager et al. 2009). For example, Lepist and Jusko (2004) generated pharmacokinetic-pharmacodynamic models for s(+)-ketoprofen in cat, goat, calf, sheep, and horse and found no relation between model-estimated pharmacodynamic parameters and body weight. However, some pharmacodynamic parameters, while they do not scale with weight, need to be corrected using species differences. For example, Zuideveld et al. (2007) studied 2 biomarkers for 5HT-1a receptor mediated responses, hypothermia and corticosterone increase, in rats using 2 agonists: buspirone and flesinoxan. Pharmacokinetic models were developed and scaled to humans using Eq. (12.15) and mechanistic pharmacodynamic models were developed in rats. The drug-related pharmacodynamic parameters (potency, intrinsic activity, and slope) were not scaled and were treated as equal between rats and man, whereas differences in EC_{50} were accounted for based on species differences in receptor binding and potency assays (van der Graaf et al. 1997). Under these assumptions, human predictions were very close to observed experimental results. Other examples can be found in Melham (2013).

Less attention has been paid to whether variance components scale across species. Typically, variability is assumed to be similar between animals and humans despite there being no a priori justification for this to be true (Mager et al. 2009). One might in fact expect the opposite to be true since experimental animals tend to come from the same genetic strain so as to minimize between-subject variability (BSV). A few studies have used population pharmacokinetics to model the pharmacokinetics of a drug across species by modeling all data from all species simultaneously. These studies typically account for BSV across species using a modification of the power model shown in Eq. (12.15), i.e.,

$$\text{PK} = \alpha(\text{Weight})^{\beta} \exp(\eta). \tag{12.16}$$

The η term in Eq. (12.16) accounts for BSV after controlling for weight and is assumed to be normally distributed with mean 0 and variance ω^2. For example, Wu and Feng (2011) modeled the interspecies pharmacokinetics of dasatinib in mouse, rat, monkey, and dog, while Mu et al. (2004) modeled the interspecies pharmacokinetics of drug LY in rats, dogs, and monkeys. Both scaled the model to predict the pharmacokinetics in humans, assuming that the BSV across species was the same, i.e., that the variance across rats or mice or dogs was the same as the variance across humans.

Similar assumptions are made when adult pharmacokinetic data are scaled down to pediatric populations. For example, Morris et al. (2013) reported on artesunate pharmacokinetics in adults and children and Robbie et al. (2012) reported on

Table 12.1 Estimated variances for drugs in animals and humans

Drug	Parameter	BSV in rats (%)	BSV in dogs (%)	BSV in humans (%)	References
Fentanyl	CL	25		36	Freise et al. (2012)
	Vss	40	64	57	Yassen et al. (2007)
	Ka	25	24		Kaneda and Han (2005)
	Kel		5		
Amiodarone	CL			44	Vadiei et al. (1997)
	V	43		29	Campos-Moreno et al. (1997)
	K10	19			
Pregabalin	CL	25		16	Shoji et al. (2011)
	Vss	45		17	Bender et al. (2009)
	Ka			98	
Buprenorphene	CL	37		24	Jensen et al. (2007)
	Vss	81		106	Yassen et al. (2007)
	Q	43		35	
Ertapenem	CL	45		55	Boulemery et al. (2013)
	Vss			25	
	V2			51	

palvizumab pharmacokinetics in adults and children. In both studies, all pharmacokinetic parameters were modeled using Eq. (12.16), and both assumed that the variability in children was the same as the variability in adults. No study to our knowledge has ever modeled the variability in children to be different than the variability in adults or the variability in animals to be different than the variability in adults.

A PubMed literature review was conducted looking for population pharmacokinetic reports of the same drug independently done in mice, rats, dogs, or humans. Only a few drugs were found (Table 12.1), and while these results are far from definitive, the estimates of the variance components are generally similar across species. No large differences were noted. These results suggest that the use of similar variance estimates in the scaling of pharmacokinetic or pharmacodynamic models appears justified.

12.5 Estimation and Software

To analyze the longitudinal data generated from a systems pharmacology study, that is, data in the form of repeated measurements on each subject over time, there are three parameters (θ, Ω, and Σ, which have been previously introduced) that

must be estimated. Among several methods of estimation, maximum likelihood (ML) is an old and well-established method originally established by R.A. Fisher in the early 1900s that has a variety of optimal properties (Aldrich 1997). But in order to implement ML estimation, one of the basic requirements is that of assuming an underlying joint probability distribution for the data Y, which is also the likelihood function of the parameters given the data. A natural choice is to assume a normal distribution for both the random effects and unexplained variance, and the NMEM can be written as

$$Y = f(\theta; X; \eta) + g(\varepsilon) \tag{12.17}$$

where $\eta \sim N(0, \Omega)$ and $\varepsilon \sim N(0,\Sigma)$, the joint probability distribution function can be expressed as a marginal distribution.

$$\begin{aligned} p\left(Y_{ij}|\theta;\Omega;\Sigma\right) &= L_{ij}\left(\theta;\Omega;\Sigma|Y_{ij}\right) = \int p\left(Y_{ij};\eta_i|\theta;\Omega\right)\mathrm{d}\eta_i \\ &= p\left(Y_{ij}|\eta_i;\theta;\Omega\right)\mathrm{p}(\eta_i|\theta;\Omega)\mathrm{d}\eta_i \end{aligned} \tag{12.18}$$

where the random effects are integrated out (Wang 2009). The likelihood function is then $\prod L_{ij,}$ and when the likelihood function is maximized, the values of (θ, Ω, Σ) are referred to as the ML estimates.

If Eq. (12.17) is linear in the parameters, an explicit analytical solution to Eq. (12.18), which is similar in nature to the solution for a multivariate regression problem, can be obtained and the ML estimates are easily found. However, non-linearity in f(.) and g(.), particularly with g(.), makes it difficult to evaluate the integral in Eq. (12.18) explicitly. The integral must therefore be evaluated either numerically or by using some approximation. The first method to solve the integral, called the first-order (FO) approximation by Sheiner and Beal (1980, 1981, 1983), does not compute the integral but instead linearizes the model in Eq. (12.17) using a first-order Taylor series approximation, and then explicitly evaluates the marginal distribution. Although the FO-approximation method has proven adequate for many pharmacokinetic problems, one key disadvantage of this method is that when there is substantial between-subject variability or the model is highly nonlinear, like with typical models for pharmacodynamic data, the linearized model may be a poor approximation, leading to biased and imprecise estimation of the parameters. An alternative solution that takes the first-order approximation around the conditional estimates of the random effects, first-order conditional estimation (FOCE), is more accurate for nonlinear problems and is now the standard method used for most pharmacokinetic-pharmacodynamic NMEMs (Boeckmann et al. 2006). FOCE is more computationally intensive than the FO method, but with significant advances in computer technology and the introduction of parallel computing, the run times with FOCE are quite reasonable.

Another way to solve Eq. (12.18) is to numerically evaluate the integral. There are many ways to do so, each of varying accuracy. One method is Gaussian quadrature which evaluates the integral using the quadrature rule, essentially a

weighted sum over the limits of integration (SAS Institute 2009). The method, which is the gold standard for numerical estimation of the integral, is also the slowest and least computationally efficient, particularly as the number of random effects in the model increases. Therefore, for modest size problems, Gaussian quadrature is not practical. A more reasonable solution is to evaluate the integral using Monte Carlo simulation. A number of different options are available, including stochastic approximation expectation-maximization [SAEM (Kuhn and Lavielle 2005)]. The main disadvantages of the EM algorithm are the slow convergence rate and no immediate standard errors for the estimates as in the FO and FOCE method; however, many extension versions of the EM algorithm have been developed for improvements.

There are many either commercially available (MATLAB, MONOLIX, NONMEM, Pharsight Phoenix® NLME™, SAS) or free (ADAPT, R, S-ADAPT, WINBUGS) software packages that can be used to fit NMEMs. Among them, NONMEM has been regarded by many as the gold standard for PK/PD modeling in the pharmaceutical community. NONMEM was originally developed by Stuart Beal and Lewis Sheiner in the University of California at San Francisco for fitting NMEMs (Sheiner and Beal 1980, 1981, 1983). The first version of NONMEM was introduced by them in 1979; the current version 7.3 was formally released in 2013 from its licensor ICON (http://www.iconplc.com/technology/products/nonmem/). NONMEM, which stands for "NONlinear Mixed Effects Model", was designed to fit general statistical (nonlinear) regression-type models to PK/PD data. Compared with other statistical software packages (R, S-PLUS, SAS) for fitting nonlinear mixed effect models, the current version of NONMEM is much more versatile, including a variety of estimation algorithms and offers parallel computing capabilities. NONMEM also uniquely allows for complex dosing schedules which are typically included in the design of PK/PD studies through specification of dosing information in the dataset, and has extensive predefined libraries for most commonly used PK models. These useful features are acknowledged and built into recently emerging PK/PD software packages such as MONOLIX and Phoenix® NLME™.

MONOLIX (http://www.lixoft.eu/products/monolix/product-monolix-overview/) is also well accepted by the community of PK/PD for population analysis using NMEMs, and implements the SAEM algorithm for ML estimation. MONOLIX was initially developed as an open-source program in 2005 but in 2009 was changed to a commercial package; it does however remain free of charge for academics, students, and regulatory agencies. MONOLIX is implemented in the MATLAB environment, but is also available as a full-featured standalone software compiled with MATLAB libraries, and therefore does not require one to purchase MATLAB licenses. One nice feature of MONOLIX is the availability of a user-friendly graphical user interface (GUI) that links the user-defined PK/PD model and data file for the data analysis and has four sessions: data and model, initialization, algorithms, and results. Under the data and model session, NONMEM-type datasets can be uploaded, and a PK/PD model can either be chosen from the built-in library or be defined and uploaded by the MONOLIX user. In this session, models to characterize the between-subject and within-subject

variability and covariate models can be also specified. The initial estimates of the parameters of fixed effects and random effects including residual error can be specified under initialization.

12.6 Case Studies

12.6.1 Development of a Systems Pharmacology Model for Osteoporosis

An excellent example of the application of a population approach to a systems pharmacology model was reported by Post et al. (2013). In this analysis, the authors applied clinical data from post-menopausal women administered tibolone to a mechanism-based model for osteoporosis (Fig. 12.2). Plasma bone-specific biomarkers, bone mineral density (BMD) in hip and spine, and tibolone

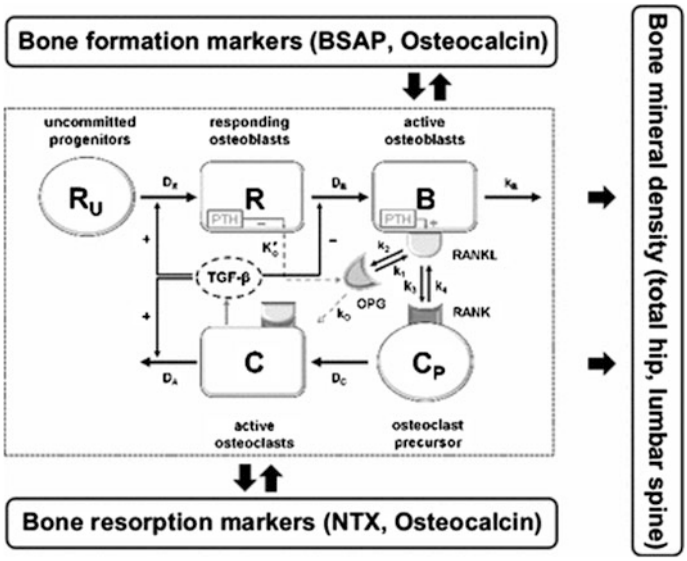

Fig. 12.2 Schematic description of the layered model structure reported by Post et al. (2013) with the bone cell interaction model at its core (*dashed box*), from which links to the corresponding biomarkers are established. Here, R_u denotes the activity of the uncommitted osteoblast progenitor, R of the responding osteoblast, B of the active osteoblast responsible for bone formation, C_p for the osteoclast progenitor, and C for the active osteoclast responsible for bone resorption. PTH stands for parathyroid hormone, TGF-β for transforming growth factor-β, OPG for osteoprotegerin, RANK for receptor activator of NF-κB, and RANKL for receptor activator of NF-κB ligand. RANKL binds to RANK and promotes osteoclast differentiation, while OPG inhibits this differentiation by binding RANKL. Figure and legend were originally adapted from Lemaire et al. (2004)

pharmacokinetics were incorporated into the model. A NMEM was used to control between-subject variability on specific model parameters, to estimate residual variability, and to characterize the distinction between responders and low-responders to tibolone treatment using mixture modeling.

Judicious application of between-subject variability to the most influential parameters was a feature of the analysis. For example, adding between-subject variability to the pharmacokinetics of tibolone did not substantially improve the model performance after controlling for variability in the biomarker pharmacodynamics. While it would be generally not advised for one to consider ignoring between-subject variability in pharmacokinetics using a traditional population approach, when faced with an already complex and highly parameterized model, the authors opted to favor the more influential pharmacodynamic variability. Even when applying between-subject variability to the biomarkers, only the most variable of the dynamic parameters for the biomarkers was initially examined: the baseline values. The authors did attempt the inclusion of additional variability parameters in a step-wise fashion, but found that adding these values resulted in model instability and/or a lack of improvement in fit.

While a covariate analysis may have served to explain the individual fluctuations in some of the bone turnover markers (as well as reduce the unexplained variability in the parameters), covariate exploration was not conducted as it was outside the scope of the analysis; the authors did note that such an analysis would be informative with respect to disease and system dynamics and would be considered for future evaluation.

While not discussed to any extent in this book chapter, mixture models may be used to describe populations with bi- or multimodal distributions. In practice, software programs like NONMEM will assign individual patients to particular subpopulation with the highest probability. Post et al. applied this methodology to the parameter for drug potency (ID_{50}) in order to identify two subpopulations which differed in terms of treatment response: responders and low-responders. NONMEM assigned 60 and 40 % of patients, respectively, to these two groups. It should be noted that clinically, it is not clear whether these two subgroups truly exist or whether the data drove the need for the mixture model. This question could also be addressed with a covariate analysis to explain the between-subject variability in treatment response in a future analysis.

In summary, by choosing to use a population analysis approach to analyze a systems pharmacology model, Post et al. were able to assess between-subject variability and to characterize individual subjects' treatment response. Use of this methodology led to improved learning and hypothesis generation compared to a traditional systems pharmacology approach.

12.6.2 *Development of a Systems Pharmacology Model for Thyroid Regulation*

Ekerot et al. (2013) describe how the development of a myeloperoxidase (MPO) inhibitor for thyroid regulation (MPO-IN1) was aided by integrating knowledge of systems pharmacology with population PK/PD concepts. This example demonstrates how systems pharmacology knowledge can be used as a tool to efficiently analyze pre-clinical data by assuming the underlying physiology between species is similar. The advantage of animal studies is that they can be exploratory in nature and several scenarios can be tested using the relatively rich data (several doses, long dosing times) before applying the model in humans. Translation to humans then becomes a matter of altering the model by substituting human turnover numbers, rate constants, affinities, etc. for animal values.

Figure 12.3 provides a schematic illustration of the hypothalamic-pituitary-thyroid (HPT) axis. Thyroid stimulating hormone (TSH) is secreted by the pituitary gland under the control of hypothalamic thyrotropin-releasing hormone (TRH) and negative feedback regulation from circulating thyroxine (T4). TSH stimulates the thyroid gland to produce and secrete T4 and T3. A fraction of T4 is also converted to T3, mostly peripheral to the thyroid gland. MPO-IN1 targets the thyroid system by inhibiting thyroperoxidase (TPO), an enzyme that frees iodine for the formation of T4 and T3. The inhibition of T4 production is therefore expected to result in the lowering of T4 and T3 levels during treatment. The reduced T4 is in turn expected to increase TRH and TSH levels through negative feedback regulation.

The first step towards model building is to understand the system well enough such that it can be described using systems parameters that can be measured or imputed (in this case: turnover rates, fraction of T4 converted to T3, plasma

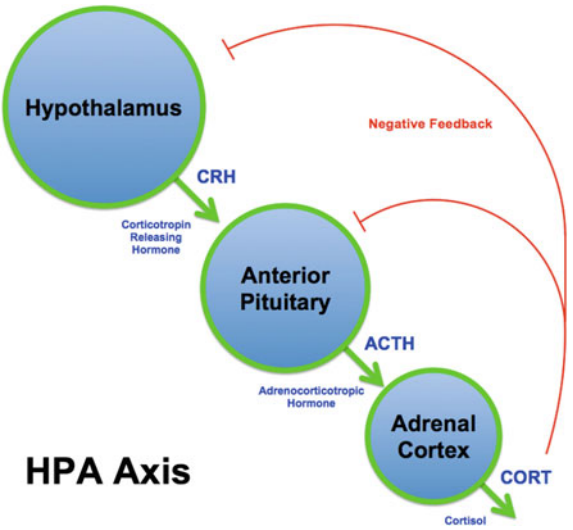

Fig. 12.3 Basic hypothalamic–pituitary–adrenal axis summary (corticotropin-releasing hormone = CRH, adrenocorticotropic hormone = ACTH). Created by Brian M Sweiss; original work from Jessica Malisch and Theodore Garland; under the Creative Commons Attribution license, https://commons.wikimedia.org/wiki/File:HPA_Axis_Diagram_(Brian_M_Sweis_2012).png#filelinks

concentrations of TSH, T4, T3, etc.) and mathematical equations that can describe the interrelationships between these parameters. Much work has already been done toward making a physiological model of the thyroid system and HPT axis. Numerous complex models that describe the thyroid system in great detail already exist (Degon et al. 2008). What Ekerot et al. did was to start exploring the next step, which was how to assess the modulation of the thyroid system by pharmacological manipulation through condensing a relatively complex systems pharmacology model into a simpler form that could be used for candidate selection in drug development.

In their study, MPO-IN1 was administered to beagle dogs once daily for 1 or 6 months. Three MPO-IN1 dose levels were tested, and serial pharmacokinetic and hormone samples were collected. Using these data and in vitro IC_{50} and I_{max} values for TPO inhibition obtained from inhibition experiments with the test compounds, the production and elimination rate constants for T4, T3, and TSH were estimated either by the model or were fixed to values reported in the literature. The architecture of the model is described by Fig. 12.4 and consisted of compartments for TSH, T4, and T3 that were linked based on physiology of thyroid hormone regulation. TSH

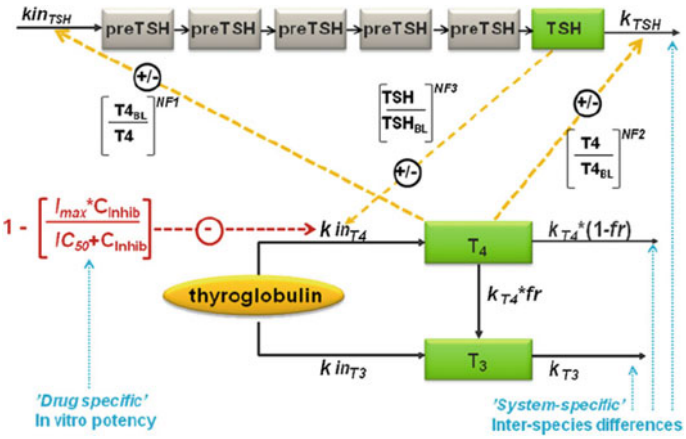

Fig. 12.4 Proposed feedback model of thyroid hormone homeostasis and drug mediated inhibition of TPO. Hormone interactions are shown with dashed lines, where ± indicate a positive or negative interaction following decreased or increased hormone concentrations. Reduced concentrations of T4 stimulate production of TSH and lower the elimination of TSH. Increased concentrations of TSH stimulate production of T4. Green-shaded compartments are those where thyroid hormone observations were available in plasma. TSH_{BL}, $T4_{BL}$, and $T3_{BL}$ are baseline (steady state plasma concentrations) of the thyroid hormones. The drug-specific parameter potency (IC_{50}) was different between compounds. The system-specific parameters such as first-order elimination rate constants of TSH, T4, and T3 (K_{TSH}, K_{T4} and K_{T3}) and the fraction of T4 that is conversed to T3 (fr) were different between species (dog and human). I_{max} is the maximal inhibition of T4. NF1 and NF2 are the slope factors of the relationship describing the influence of T4 on TSH production and elimination. NF3 is the slope factor of the relationship describing the influence of TSH on T4 production. kin_{TSH}, kin_{T4}, and kin_{T3} are the zero-order elimination rate constants of TSH, T4, and T3, Reprinted from Ekerot et al. (2013)

production was described by a transit compartment model, a technique often used in pharmacometrics (see Chap. 9). The transit model was used to describe the time delay between MPO administration and effect on the PD endpoint (i.e., TSH concentration changes in plasma). Based on evidence from the literature, a reduction in plasma T4 concentration was allowed to both stimulate the production of TSH and decrease its turnover by linking T4 concentration to kin_{TSH} (zero-order production of the precursor of TSH) and k_{TSH} (first-order rate constant of elimination of TSH). In turn, T4 and T3 production and elimination was described by their own production and elimination rate constants as well as by TSH. The model accounted for the fact that T3 is produced both from thyroglobulin and the fraction of T4 was converted to T3. Finally, the effect of drug was introduced into this systems model by introducing an I_{max} type inhibition equation in which the rate of production of T4 was dependent on the IC_{50} and steady-state concentration of the TPO-inhibitor. The concentration of T4 was also dependent upon TSH concentrations, the effect being that increased TSH resulted in increased T4 production. Finally, thyroid hormone profiles under the influence of MPO inhibitor were predicted based on the ability to inhibit TPO (shown in red in Figs. 12.3, 12.4).

The model was developed using population PK/PD methodology making use of the NONMEM program to code the equations that described the relationships between different compartments. Results were obtained in the form of the population estimates for the model parameters along with the inter-individual variability for select parameters. Overall, the model described the TSH, T4, and T3 concentration versus time profiles quite well. Figure 12.5 shows the observed data along

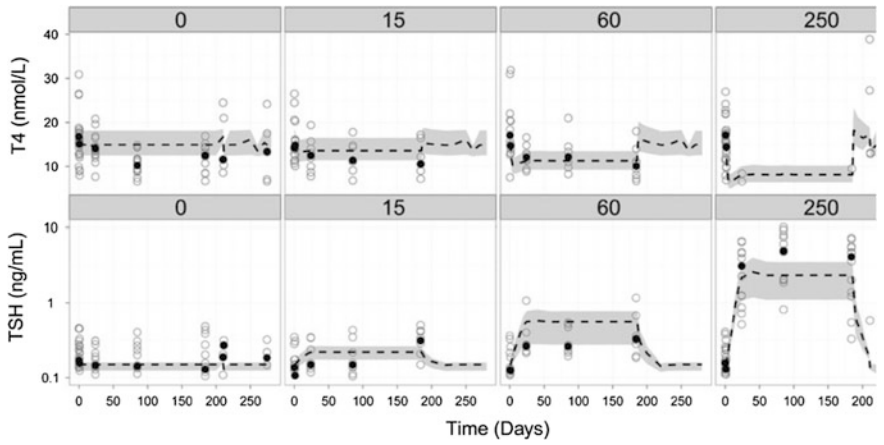

Fig. 12.5 Visual predicted check plots for T4 and TSH based on the uncertainties in population parameter estimates after 6 month oral dosing of MPO-IN1 at doses of 0, 15, 60, and 250 μmol/kg. *Dashed line* median of predictions, closed circles: median of observations, *open symbols* individual observations, *shaded area* 95 % prediction interval. *Note* the uncertainty in the inter- and intra-individual variation was excluded from the VPC predictions and values below the LLOQ were excluded in the figure. Reprinted from Ekerot et al. (2013)

with the model predictions overlaid for the 6-month study. The model was able to describe the rapid decrease in T4 as a result of TPO inhibition. Additionally, because of the incorporation of feedback effects, the model was able to capture the increase in TSH during drug administration and the rebound effect after drug administration was stopped. Inclusion of a transit compartment adequately captured the delay of about 1 day for the increase in TSH concentration following administration of the test compound.

An advantage of using systems pharmacology based models is that when data do not permit the estimation of a parameter then it can be fixed to a reliable estimate from literature to simplify or speed up the model. In this case, the elimination rate constants of T4 and T4 were fixed to known physiological values. The advantage of using the population approach was that it provided not only population estimates for TSH, T4, and T3 concentrations but also the inter-individual and intra-individual variability associated with these parameters. The data could also be analyzed to assess the significance of different covariates. Relevant in this case was the finding that T4 and TSH concentrations were estimated to be 43 % higher in males for the highest dose group.

The robustness of this model was tested by several methods. With the knowledge of differences between hormone turnover rates and IC_{50} values of MPO inhibition, this model could be used to make an informed guess of what the thyroid hormone profile is likely to be upon administration of a different MPO inhibitor and, more importantly, what the thyroid hormone profile is likely to be in a human clinical trial. The model can also be adapted for the development of candidate drugs that affect T3/T4 concentrations via other mechanisms shown in Figs. 12.3 and 12.4.

12.7 Conclusions

All experiments suffer from the curse of variability. At all turns, experimenters try to control the variability: variability between animals, variability across analytical results, variability between experiments. Variability is a nuisance that obscures the true results of an experiment and obfuscates the underlying model structure. NMEMs are an efficient method to model the underlying structure of a system and control for variability by the explicit modeling of variability in the data through the addition of random effects and residual variance models. While early systems pharmacology models were based on modeling the mean data from experiments and ignoring the variability in the data, more recent models take into account such variability to obtain more accurate estimates of the model parameters. The future of NMEMs in systems pharmacology looks bright and its use is expected to grow as more pharmacologists start to become more comfortable with models and begin the recognize the power of mathematical modeling as a tool to characterize experiments, summarize data, and to predict future outcomes.

References

Aarons L (1991) The kinetics of flurbiprofen in synovial fluid. J Pharmacokinet Biopharm 19:265–269

Aldrich JRA (1997) Fisher and the making of maximum likelihood 1912–1922. Stat Sci 12:162–176

Bender G, Gosset J, Florian J, Tan K, Field M, Marshall S, DeJongh J, Bies R, Danhof M (2009) Population pharmacokinetic model of the pregabalin-sildenafil interaction in rats: application of simulation to preclinical PK–PD study design. Pharm Res 26:2259–2269

Boeckmann AJ, Sheiner LB, Beal SL (2006) NONMEM users guide (1989–2006). ICON Development Solutions, Ellicott City

Bonate PL (2011) Pharmacokinetic–pharmacodynamic modeling and simulation. Springer, New York

Boulemery A, Marsot A, Bruguerolle B, Simon B (2013) Population pharmacokinetics of ertapenem in juvenile and old rats. Fundam Clin Pharmacol 28:144–150

Boxenbaum H (1982) Interspecies scaling, allometry, physiological time, and the ground plan of pharmacokinetics. J Pharmacokinet Biopharm 10:201–227

Campos-Moreno E, Merino-Sanjuan M, Merino V, Martin Algarra RV, Casabom VG (1997) Population modeling to describe pharmacokinetics of amiodarone in rats: relevance of plasma protein and tissue depot binding. Eur J Pharm Sci 30:190–197

Chis OT, Banga JR, Balsa-Canto E (2011) Structural identifiability of system biology models: a critical comparison of methods. PLOS One 6:e27725

Danhof M, de Jongh J, De Lange ECM, Della Pasqua OE, Ploeger BA, Voskuyl RA (2007) Mechanism-based pharmacokinetic-pharmacodynamic modeling: biophase distribution, receptor theory, and dynamical systems analysis. Annu Rev Pharmacol Toxicol 47:357–400

Davidian M, Giltinan DM (1995) Nonlinear models for repeated measures data. Chapman and Hall, New York

Degon M, Chipkin SR, Hollot CV, Zoeller RT, Chait Y (2008) A computational model of the human thyroid. Math Biosci 212:22–53

Ekerot P, Ferguson D, Glamsta EL, Nilsson LB, Andersson H, Rosqvist S, Visser SA (2013) Systems pharmacology of modeling of drug-induced modulation of thyroid hormone in dogs and translation to humans. Pharm Res 30:1513–1524

Fitzmaurice GM, Laird NM, Ware JH (2004) Applied longitudinal analysis. Wiley, New York

Freise KJ, Linton DD, Newbound DC, Tudan C, Clark TP (2012) Population pharmacokinetics of transdermal fentanyl solution following a single dose administered prior to soft tissue and orthopedic surgery in dogs. J Vet Pharmacol Ther 35(Suppl 2):65–72

Gabrielsson J, Weiner D (2000) Pharmacokinetic and pharmacodynamic data analysis: concepts and applications. Swedish Pharmaceutical Press, Stockholm

Gastonguay MR (2011) Full covariate models as an alternative to methods relying on statistical significance for inferences about covariate effects: a review of methodology and 42 case studies. Presented at the population analysis group in Europe, Greece (Abstract 2229)

Holford NHG (1996) A size standard for pharmacokinetics. Clin Pharmacokinet 30:329–332

Jensen ML, Foster DJR, Upton RN, Kresitensen K, Hansen SH, Jensen NH, Nielsen BN, Skram U, Villesen HH, Christup L (2007) Population pharmacokinetics of buprenorphine following a two-stage intravenous infusion in healthy volunteers. Eur J Clin Pharmacol 63:1153–1159

Kaneda K, Han TH (2005) Comparative pharmacokinetics of fentanyl using nonlinear mixed effects modeling: burns vs. non-burns. Burns 35:790–797

Kuhn E, Lavielle M (2005) Maximum likelihood estimation in nonlinear mixed effects models. Comput Stat Data Anal 49:1020–1038

Lemaire V, Tobin FL, Greller LD, Cho CR, Suva LJ (2004) Modeling the interaction between osteoblast and osteoclast activities in bone remodeling. J Theor Biol 7:293–309

Lepist EI, Jusko WJ (2004) Modeling and allometric scaling of s(+)-ketoprofen pharmacokinetics and pharmacodynamics: a retrospective analysis. J Pharmacol Exp Ther 27:211–218

Mager DE, Woo S, Jusko WJ (2009) Scaling pharmacodynamics from in vitro and preclinical animal studies to humans. Drug Metab Pharmacokinet 24:16–24

Mahmood I (2006) Prediction of drug clearance in children from adults: a comparison of several allometric methods. Br J Clin Pharmacol 61:545–557

Melham M (2013) Translation of CNS occupancy from animal models: application of pharmacokinetic/pharmacodynamic modeling. J Pharmacol Exp Ther 347:2–6

Morris CA, Tan B, Dupare S, Borghini-Fuhrer I, Jung D, Shin CS, Fleckstein L (2013) Effects of body size and gender on the population pharmacokinetics of artesunate and its active metabolite dihydroartesunate in pediatric malaria patients. Antimicrob Agents Chemother 57:5889–5890

Mu S, Anderson S, Mahadevan S (2004) Evaluate human PK prediction of compound LY based on elementary scaling with three species. Clin Pharmacol Ther 75:P30

Nichols AI, Boudinot FD, Jusko WJ (1989) Second generation model for prednisolone pharmacodynamics in the rat. J Pharmacokinet Biopharm 17:290–297

Peterson MC, Riggs MM (2010) A physiologically based mathematical model of integrated calcium homeostasis and bone remodeling. Bone 46:49–63

Post TM, Schmidt S, Peletier LA, de Greef R, Kerbusch T, Danhof M (2013) Application of mechanism-based disease systems modeling for osteoporosis to clinical data. J Pharmacokinet Pharmacodyn 40:143–156

Ramakrishnan R, DuBois DC, Almon RR, Pyszczynski NA, Jusko WJ (2002) Fifth-generation model for corticosteroid pharmacodynamics: application to steady-state receptor down-regulation and enzyme induction patterns during seven-day continuous infusion of methylprednisolone in rats. J Pharmacokinet Biopharm 29:1–24

Robbie GJ, Zhae L, Mondick J, Lesensky G, Roskos LK (2012) Population pharmacokinetics of palvizumab, a humanized anti-respiratory syncytial monoclonal antibody, in adults and children. Antimicrob Agents Chemother 56:4927–4936

SAS Institute (2009) SAS/STAT 9.2 user's guide. SAS Institute, Cary

Schmidt S, Post TM, Peletier LA, Beroujerdi MA, Danhof M (2011) Coping with time scales in disease systems analysis: application to bone remodeling. J Pharmacokinet Pharmacodyn 38:873–900

Sheiner LB, Beal SL (1980) Evaluation of methods for estimating population pharmacokinetics parameters. I. Michaelis-Menten model: routine clinical pharmacokinetic data. J Pharmacokinet Biopharm 8:553–571

Sheiner LB, Beal SL (1981) Evaluation of methods for estimating population pharmacokinetic parameters. II. Biexponential model and experimental pharmacokinetic data. J Pharmacokinet Biopharm 9:635–651

Sheiner LB, Beal SL (1983) Evaluation of methods for estimating population pharmacokinetic parameters. III. Monoexponential model: routine clinical pharmacokinetic data. J Pharmacokinet Biopharm 11:303–319

Shoji S, Suzuki M, Tomono Y, Brockbrader HN, Matsui S (2011) Population pharmacokinetics of pregabalin in healthy subjects and patients with postherpetic neuralgia or diabetic neuropathic pain. Br J Clin Pharmacol 72:63–76

Sinha VK, De Buck SS, Fenu LA, Smit JW, Nijsen M, Gilissen RAHJ, Van Peer A, Labrijsen K, Mackie CE (2008) Predicting oral clearance in humans: how close can we get with allometry? Clin Pharmacokinet 47:35–45

Sun YN, DuBois DC, Almon RR, Jusko WJ (1998) Fourth generation model for corticosteroid pharmacodynamics: a model for methylprednisolone effects on receptor/gene glucocorticoid receptor down regulation and tyrosine aminotransferase induction in rat liver. J Pharmacokinet Biopharm 289:317

United States Department of Health and Human Services, Food and Drug Administration, Center for Drug Evaluation and Research, and Center for Biologics Evaluation and Research (1999) Guidance for industry: population pharmacokinetics

Upton RN, Mould DR (2014) Basic concepts in population modeling, simulation, and model-based drug development: part 3, introduction to pharmacodynamic modeling methods. CPT Syst Pharmacol Pharmacomet 3:e88

Vadiei K, Troy S, Korth-Bradley J, Chiang ST, Zimmerman JJ (1997) Population pharmacokinetics of intravenous amiodarone and comparison with two-stage pharmacokinetic analysis. J Clin Pharmacol 37:610–617

van der Graaf PH, van Schaick EA, Mathot RA, Ijzerman AP, Danhof M (1997) Mechanism-based pharmacokinetic-pharmacodynamic modeling of the effects of N6-cyclopentyladenosine analogs on heart rate: estimation of in vivo operational affinity and efficacy at A1 receptors. J Pharmacol Exp Ther 283:809–816

Wang Y (2009) Derivation of various NONMEM estimation methods. J Pharmacokinet Pharmacodyn 34:575–593

Wright PMC (1998) Population based pharmacokinetic analyses: why do we need it; what is it; what has it told us about anesthetics? Br J Anaesth 80:488–501

Wu SP, Feng S (2011) Interspecies pharmacokinetic scaling of dasatinib—an application of nonlinear mixed effects modeling. Presented at the American conference on pharmacometrics, Las Vegas

Xu ZX, Sun YN, DuBois D, Almon RR, Jusko WJ (1995) Second generation model for corticosteroid pharmacodynamics: roles of the glucocorticoid receptor mRNA and tyrosine aminotransferase mRNA in rat liver. J Pharmacokinet Biopharm 23:163–181

Yassen A, Olofsen E, Kan J, Dahan A, Danhof M (2007) Pharmacokinetic-pharmacodynamic modeling of the effectiveness and safety of buprenorphine and fentanyl in rats. Pharm Res 25:183–193

Zuideveld KP, van der Graaf PH, Peletier LA, Danhof M (2007) Allometric scaling of pharmacodynamic responses: application to 5-HT1a receptor-mediated responses from rat to man. Pharm Res 24:2031–2039

Chapter 13
Detecting Pharmacokinetic and Pharmacodynamic Covariates from High-Dimensional Data

Jonathan Knights and Murali Ramanathan

Abstract With the rapid evolution of technologies capable of generating high-dimensional data sets such as those from the 'omic' platforms commonly encountered during pharmacogenetic/genomic clinical trials, there is need for computationally efficient methodologies capable of integrating that information into the drug development pipeline; however, the computational cost of identifying covariates and interactions through traditional parametric statistical approaches has impeded their utilization for these large data sets. Within the context of population pharmacokinetic/pharmacodynamic modeling, the potential for detecting interactions on such data sets is of great interest: Specifically, the applications of interactions in this context would be the creation of more comprehensive and biologically sound covariate models, leading to better prediction of individual values for PK/PD parameters of interest, and moving one step closer to the goal of personalized medicine. However, there are currently no commercially available software packages, or computational approaches, that can handle covariate interaction detection or model synthesis at a genome scale. Thus, the most immediate and tractable benefit from such interaction analyses at this scale would be the identification of the most informative subset of predictors that could be used for 'formal' covariate model synthesis. This chapter will provide a discussion on the following topics of interest in this area: A general discussion on covariates and interactions; specific challenges and opportunities that arise when large datasets are considered; search metrics that are applicable on high-dimensional data sets; and a justification for the need to distinguish between covariate detection and formal covariate model synthesis in this context.

Keywords High-dimensional data sets · Biomarkers · Individualized therapy · Regression · Akaike information criterion · Schwarz information criterion · Parsimony · Multidimensional · Automated · Informative genes

J. Knights · M. Ramanathan (✉)
Department of Pharmaceutical Sciences, State University of New York, Buffalo, NY 14214-8033, USA
e-mail: murali@buffalo.edu

D.E. Mager and H.H.C. Kimko (eds.), *Systems Pharmacology and Pharmacodynamics*, AAPS Advances in the Pharmaceutical Sciences Series 23,
DOI 10.1007/978-3-319-44534-2_13

13.1 Introduction

The fields of pharmacodynamics and systems pharmacology have developed in parallel and share the common goal of improving patient and drug outcomes. They also share many methodological challenges, which include the development of methods for identifying biomarkers and clinically informative relationships capable of individualized predictions. Whereas pharmacokinetics and pharmacodynamics (PK/PD) are relatively well established as the predominant methods for identifying and optimizing dosing regimens during drug development and clinical trials, systems pharmacology is an emerging area of research with great promise in drug target identification and in individualizing therapies.

The number of dimensions can loosely be defined as the number of independent variables that have been measured. The term high-dimensional data refers to datasets with a large number of independent predictors, commonly on the order of 10^2–10^6, but may contain on the order of up to 10^8 predictors. In high-dimensional data from clinical trials, many of the predictors in the available data represent genetic variations, proteins, biomarkers, and other environmental factors that interact with each other. Often, one of the core objectives in modeling projects is to parsimoniously describe all of the significant relationships in the underlying system, to obtain a high level of mechanistic insight and to enable prediction. For these reasons, identifying and quantifying covariates and covariate interactions concomitantly within a unified framework is useful, and arguably essential to realizing the goal of individualized predictions for treatments.

This chapter highlights the challenges and unique opportunities for knowledge gain from covariate searching and model building when analyzing high-dimensional datasets, which are becoming common in systems pharmacology and PK/PD modeling.

13.2 What Are Covariates?

Covariates are variables capable of explaining inter- and intra-individual variability of an observed outcome in a given population (see Chap. 10.1007/978-3-319-44534-2_12). The identification of effective covariates can provide the basis for personalized medicine because it can enable the selection of the best drug and dosing regimen for a given patient. In population PK/PD modeling, covariate models extend the formal description of factors leading to the observed variability in drug concentrations or effects, beyond that of the structural model. A useful covariate model describes variability in outputs arising from differences in expected values and/or differences in the variability of a PK/PD parameter between different groups.

Figure 13.1 illustrates how covariates enable the description of observed variability. The solid line in Fig. 13.1a represents the expected concentration in the study sample at a given time point; Fig. 13.1c shows the raw distribution of

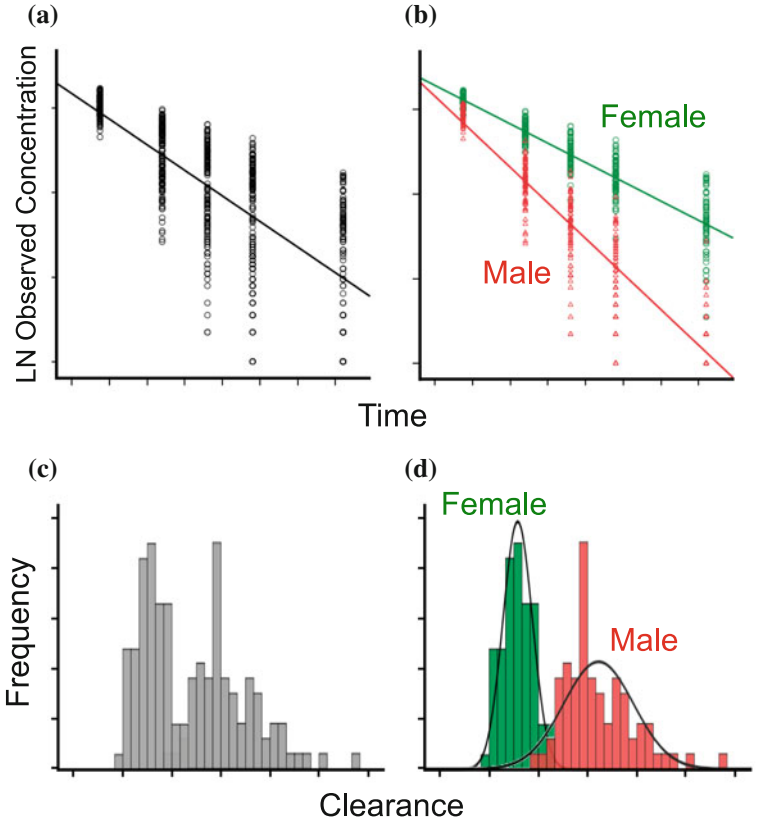

Fig. 13.1 **a** Natural log-transformed concentration values after an IV bolus dose following single compartment kinetics in a simulated population. The expected concentration values for the population at a given time point are represented by a *solid line*. **b** The same simulated data, with separate population predictions for males and females after the addition of gender as a covariate to the model. **c** Distribution of observed clearance values in the original population, whereas **d** highlights the identification of the true underlying bimodal distribution after inclusion of gender as a covariate in the model

clearance values in the same sample. After the inclusion of gender as a covariate, two subgroups can be identified, and the population predicted values can be adjusted appropriately (Fig. 13.1b), allowing separate predictions for males and females. Figure 13.1d illustrates this concept from the perspective of the observed clearance values, whereby the addition of the covariate (gender) enables the identification of subgroups and significantly improves the estimation of clearance, shown now as a bimodal distribution. A perfect covariate model would enable the identification of all relevant subgroups of patients in the population, allowing researchers and clinicians to more accurately describe the expected concentration-time (or concentration-effect) profiles for a given individual based on the values of the covariates.

Although the evaluation of PK/PD covariate effects within the context of a given structural model has been well studied (Joerger 2012; Jonsson and Karlsson 1998; Khandelwal et al. 2011; Ribbing 2007; Ribbing et al. 2007; Wählby 2002; Wahlby et al. 2001, 2002), research on the identification of the most appropriate covariates affecting PK/PD structural model parameters from high-dimensional genetic and environmental data is in its infancy. The identification of drug disposition, efficacy, and toxicity-related covariates from high-dimensional pharmacogenomic (or other) datasets presents numerous challenges that must be overcome by the PK/PD and pharmacometrics communities in order to realize the potential and promise of systems pharmacology in individualizing therapy.

13.3 Introduction to Covariates and Interactions

13.3.1 Covariates and Covariate Models

In statistics, a covariate is an independent variable that displays a relationship with a dependent variable(s) of interest (Hair 1995; Tabachnick and Fidell 2001). There are multiple ways to define the effect of a covariate on a phenotype of interest (Nonyane and Foulkes 2008)—covariates can exert effects directly via main effects and via interactions with other covariates. A covariate model is a formal description of the relationship between the value of the covariate and the outcome of interest.

In population PK/PD modeling, covariate models may be built for observed outputs (e.g., maximum concentration or the area under the concentration-time curve) or for PK/PD parameters (e.g., the clearance or the theoretical volume of distribution). The possible covariates for these models can be based on available genetic, environmental, or patient demographic information. Additionally, when genetic variations such as single nucleotide polymorphisms are used as covariates, it is common to require separate fixed-effect parameters for different genotype groups, meaning one covariate may require multiple parameters to be estimated.

13.3.2 Linear Covariate Models

Let an observed outcome, Y, be explained by a set of predictors, $\boldsymbol{X} = \{x_1, \ldots, x_N\}$, with a set of unknown relationships, $\mathrm{B} = \{\beta_0, \beta_1, \ldots, \beta_M\}$, through some function, f, such that, $Y \approx f(\boldsymbol{X}, \mathrm{B})$. The set $\boldsymbol{X}$ could contain covariates as well as primary predictor(s) of interest. For example, if we were interested in finding out whether or not a treatment had an effect on cholesterol concentrations (which would be Y), then $\boldsymbol{X}$ would contain one x_i term for the treatment effect, and additional x_i terms representing factors external from treatment (covariates) that may influence cholesterol concentrations, such as age, gender, dietary intake, genetic factors, etc.

In the simplest case, the relationship of the covariate with the parameter of interest is additive, and we observe a proportional change in f for each value, j, of the ith predictor, x_{ij}. With one predictor we have:

$$f(\boldsymbol{X}, \mathrm{B}) = \beta_0 + \beta_1 x_{1j} + \varepsilon, \tag{13.1}$$

where β_0 is the baseline value, or intercept, of the outcome, β_1 represents the coefficient for proportional effect of the states of predictor x_1 on the outcome, and ε is an additive error term representing random variations in the outcome. The different values, j, of x_i, may represent genotype states, gender, or specific observations of some other categorical/ordinal or continuous variable.

Figure 13.2a, b represents two examples of main effects. Figure 13.2a shows a direct relationship between the measured outcome, Y, and age—the form of this equation would be identical to that of Eq. 13.1, such that $Y = \beta_0 + \beta_1 Age + \varepsilon$. Figure 13.2b shows an example of two predictors, age and gender, which both display additive main effects, where $Y = \beta_0 + \beta_1 Age + \beta_2 Gender + \varepsilon$, and "*Gender*" is a binary indicator variable.

13.3.3 Interactions in Regression

In regression analyses, statistical interactions are implemented via product terms in an appropriate regression equation. Building on the linear regression Eq. 13.1 above, if we add a second predictor, x_2, and an interaction term, our new expression becomes:

$$f(\boldsymbol{X}, \mathrm{B}) = \beta_0 + \beta_1 x_{1j} + \beta_2 x_{2k} + \beta_3 (x_{1j} x_{2k}) + \varepsilon, \tag{13.2}$$

where β_3 represents the coefficient for the deviation from additivity, or interaction, between x_1 and x_2 on the outcome. It is customary to refer to the β_1 and β_2 terms as main effects. In principle, statistically significant interaction terms can result from predictor sets with significant main effects, and also from predictor sets wherein one or more of the predictors does not show main effects.

Figure 13.2c, d shows examples of what statistical interactions look like visually. Figure 13.2c is an example of an interaction *with* main effects; in this case the outcome, Y, is estimated as $Y = \beta_0 + \beta_1 Age + \beta_2 Gender + \beta_3 (Age \times Gender) + \varepsilon$. Figure 13.2d illustrates what an interaction *without* main effects could look like, where $Y = \beta_0 + \beta_1 (Age \times Gender) + \varepsilon$. Although both Fig. 13.2c, d display similar "criss-crossing" graphical relationships, the absence of main effects in Fig. 13.2d can be inferred from both the lack of differences between mean values of the outcome in males and females when age is not considered, and the relatively stable mean of the outcome across age when gender is not considered (highlighted by the symmetric distribution around β_0 across age).

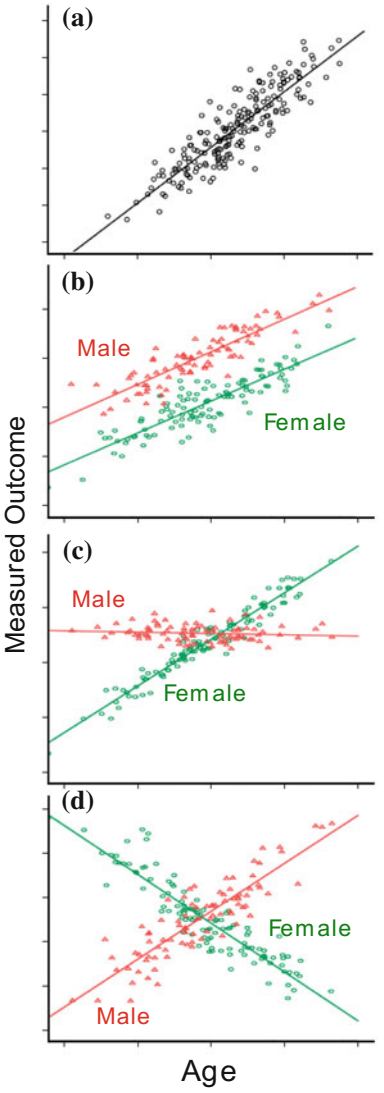

Fig. 13.2 Graphical representation of statistical interactions, where **a** contains only a main effect of age on the measured outcome, **b** contains main effects for both age and gender, **c** displays an interaction between age and gender with main effects, and **d** displays an interaction between age and gender without main effects

One of the main computational complexities with interaction analyses in regression is the rapidity with which the number of parameters (β) to be evaluated increases with the number of parameters (x_i). For a saturated additive regression model, testing all interactions between N predictors (such as in Eq. 13.2), 2^N β terms are required.

Parametric regression approaches are restrictive in that the detection and modeling of interactions is limited by the specific functional form of the product term representing the interaction. The ability to identify statistical interactions in this framework is thus dictated by the magnitude of the effect of the interaction, by the

form of the functional inter-dependence of the predictors, and by the sample size. Further, statistical regression models generally fit the combined model, containing the main effect and the interaction effect, simultaneously to the data, which makes identifying the contribution of the interaction term more difficult.

13.3.4 Biological Versus Statistical Interactions

Several reports have made distinctions between biological and statistical interactions (Cordell 2002, 2009; Moore and Williams 2005; Siemiatycki and Thomas 1981). Biological interactions refer to a physical interaction of molecules (such as protein-protein interactions, protein-small molecule binding, binding of drugs with their receptors) and are generally mediated by an exchange of chemical potential, energy, or information.

Statistical interactions are those interactions that produce observable differences in a measured outcome that can be quantified from the available data. Interactions are ubiquitous in many areas of science—in the pharmaceutical sciences, drug-drug interactions, and drug synergy/antagonism are examples of interactions, whereas in genetics an interaction between genetic variations is referred to as epistasis.

In the past, the definition of a statistical interaction has been used to refer to a non-additive relationship(s) across groups of two or more predictors; however, statistical interactions are defined as outcomes that occur only when two or more variables are observed simultaneously. With this definition, the conceptual framework for interactions becomes functional form independent, and simultaneously more general, effective, and elegant. Ideally, once a model is sufficiently mechanistic, it should be possible for statistical interactions in the model to correspond to biological interactions, but not all biological interactions may manifest in statistical interactions.

Figure 13.3 schematically illustrates biological gene-gene (GGI) and gene-environment (GEI) interactions for case-control data. In the top panel, a gene-gene interaction is depicted wherein different combinations of genotypes correspond to observable differences in a phenotype of interest. The penetrance table for the phenotype for different combinations of the genotypes is also shown. In the lower panel of Fig. 13.3, a GEI is shown schematically using exposure to an environmental agent, such as air pollution (high levels of pollution are depicted by the smoke stack versus low levels depicted by the healthy tree), in conjunction with a certain genotype. An environmental factor can be any observable non-genetic variable: within this definition, environmental factors can include exposure to infectious agents, smoking, diet, and other lifestyle factors. The Fig. 13.3 schematics of GGI/GEI, which for simplicity suggest that there be a direct or causal link between representative genotypes and the phenotype, can be applied to phenotypes that result from more complex interactions in biological networks and pathways.

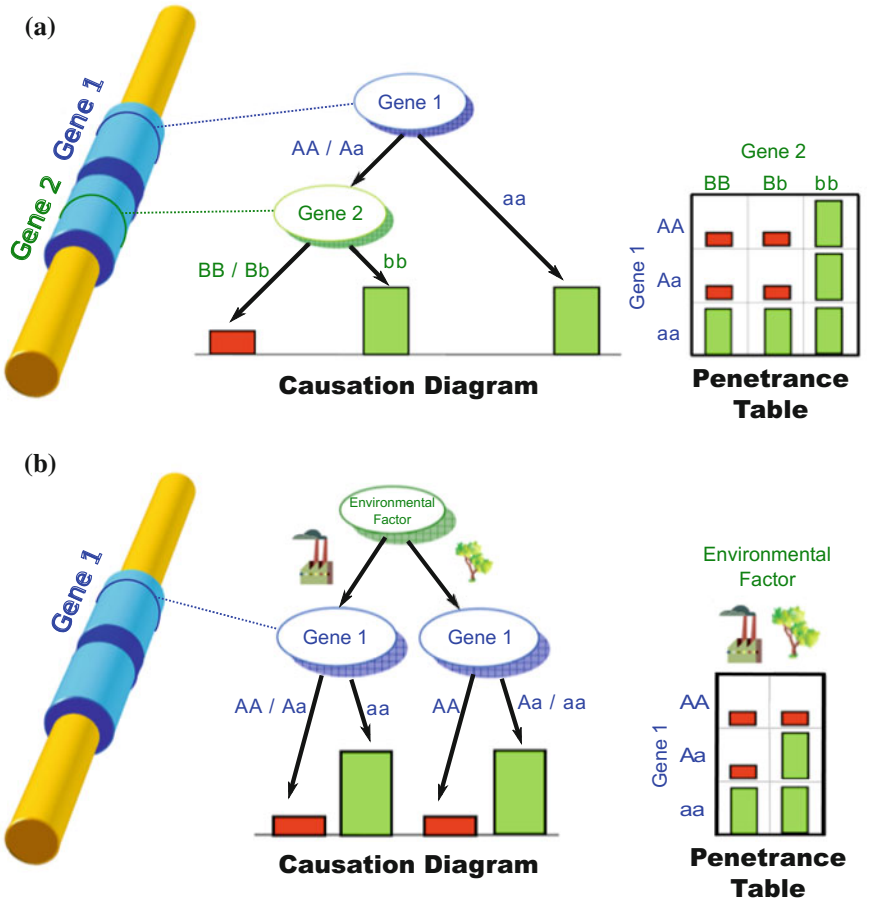

Fig. 13.3 **a** An example of a gene-gene interaction, wherein different combination of genotypes are associated to observable differences in a discrete phenotype. **b** An example of a gene-environmental interaction whereby an environmental factor modifies observations of a phenotype of interest, conditioned on a particular genotype. Although penetrance tables correspond to a frequency of a discrete phenotype such as in case-control studies, the same principle would hold for continuous data and other types of data

13.4 Covariate Modeling Challenges in Systems Pharmacology

In the past, the spectrum of potential covariates in pharmaceutically relevant data sets consisted of a modest, manageable number of candidate genes, along with relevant patient demographic and clinical characteristics. However, systems approaches to PK/PD (e.g., systems biology models and physiologically based PK/PD models) are gaining interest, and acquisition of rich, high-dimensional data

is now readily obtainable during clinical trials from various 'omic' platforms (e.g., pharmacogenomics, proteomics).

Technologies such as microarrays, next generation sequencing, metabolomics, and mass spectrometry are enabling the simultaneous collection of highly multiplexed measurements of genetic variations, mRNA levels, and proteins; however, the addition of extra dimensions exponentially increases the hypervolume in which the data is distributed, resulting in the so-called curse of dimensionality, which increases the computational complexity and degrades the statistical power of algorithms (Bellman 1961).

The primary advantage of massively multiplexed measurement systems is that information is obtained on many genes, gene products, and chemical species, simultaneously—each of which may (or may not be) altered by the disease or drug treatment. Thus, these multiplexed systems contain measurements on both informative and uninformative genes, which can be leveraged to gain insight into the underlying system of interest. As genome-scale sequencing commonly produces data on the order of $10^6 - 5 \times 10^6$ unique genetic markers (and possible two-way interactions on the order of 10^9–10^{11}), which are many orders of magnitude higher than candidate gene approaches and modest clinical datasets, the identification of individual covariates and covariate combinations from these high-dimensional datasets is a far more complex problem than that of covariate identification on a candidate gene or clinical level.

13.5 Current Covariate Model Building Approaches

The purpose of this section is to briefly introduce some available software packages for performing population PK/PD modeling and provide a discussion of the various approaches to covariate model building vis-a-vis a description of current methodologies and practices: The discussion will also enable the reader to appreciate the time-intensive nature of even relatively simple population PK/PD modeling projects; why only modest numbers of covariates are currently considered in the modeling process; and why the ability to screen PK/PD parameters against high-dimensional datasets for possible covariates could increase overall confidence in future models.

Three commonly utilized software packages for population PK/PD analysis are NONMEM (ICON/Globomax, Ellicott, MD), MONOLIX (http://www.lixoft.eu/products/monolix/product-monolix-overview/), S-ADAPT and ADAPT5 (University of Southern California, Biomedical Simulations Resource, Los Angeles, CA), and Phoenix NLME (Pharsight, Mountain View, CA). Although evidence has been documented that differences in the estimation algorithms of some early versions of these software packages meant the choice of which software to use could have been in part driven by the complexity and sparsity of the data (Bauer et al. 2007), current versions of these packages have become similar with respect to their estimation algorithms. Additionally, other differences affecting the potential complexity of models supported

by a particular software package have largely been eliminated, e.g., NONMEM7 now allows up to 50 columns of data as opposed to the 20 columns of NONMEM6. Despite a recent report from Pharsight that the current expectation-maximization algorithm implemented in the Phoenix NLME package has improved accuracy and run time over NONMEM7 with a complex PD problem (Leary et al.), the improvements to the available population PK/PD modeling software packages have done much towards accuracy and run-time convergence, making the choice of what modeling package to use more a matter of economics and preference, as opposed to modeling or data-centric considerations.

Multiple factors must be considered when building both structural and covariate models alike: First, the sample size and number of data points per subject limit the model complexity that can be supported by the data; second, the timing of the concentration measurements may limit the reliability of parameter estimates—for instance, analysis of population datasets that do not contain adequate concentration values immediately following oral doses may not support covariates on an absorption parameter; and third, model evaluation is time-intensive and requires a high-degree of user intervention. For these reasons, covariate models in population PK/PD are usually explored with fewer than twenty predictors.

Figure 13.4 provides a brief representation of the various steps involved in synthesis and verification of a population PK/PD model. Briefly, after exploratory data analysis and base structural model selection, potential covariates for each parameter must be identified from available data. As the selection of possible covariates is often largely driven by (prior) biological knowledge, one's confidence that all appropriate covariates will ultimately be evaluated is directly related to the extent of that knowledge. Following selection, the relationships of the potential covariates with the parameter(s) of interest must be assessed in the context of the overall structural model, the residual error model, and the available data. The principle of parsimony, which limits the complexity of models, also limits the number of covariates that can be incorporated into the final model—only those covariates whose inclusion offsets the penalty from increasing the complexity of the model may be carried forward. The necessary time commitment of the initial steps (exploratory data analysis, structural model selection, and identification of possible covariates) will depend on the richness of the available data and prior knowledge of the underlying system being investigated; however, the iterative demand of subsequent steps is related to the number of covariate terms that must be evaluated and is inherently time-intensive: For instance, in the final evaluation step of Fig. 13.4, the sensitivity of model performance to each covariate in the preliminary model is evaluated by iteratively comparing model performance in the absence of each individual covariate term. It should be noted that covariates may be included as part of the structural model or the residual error model (e.g., study or assay specific random error).

There has also been interest in implementing full covariate models after base structural model selection (Gastonguay 2004), foregoing the initial forward inclusion of covariates. In this approach, the full set of covariates are selected and included based more on physiological rational and plausibility than pure statistical criteria; while this is appealing when the underlying system is well-studied, and

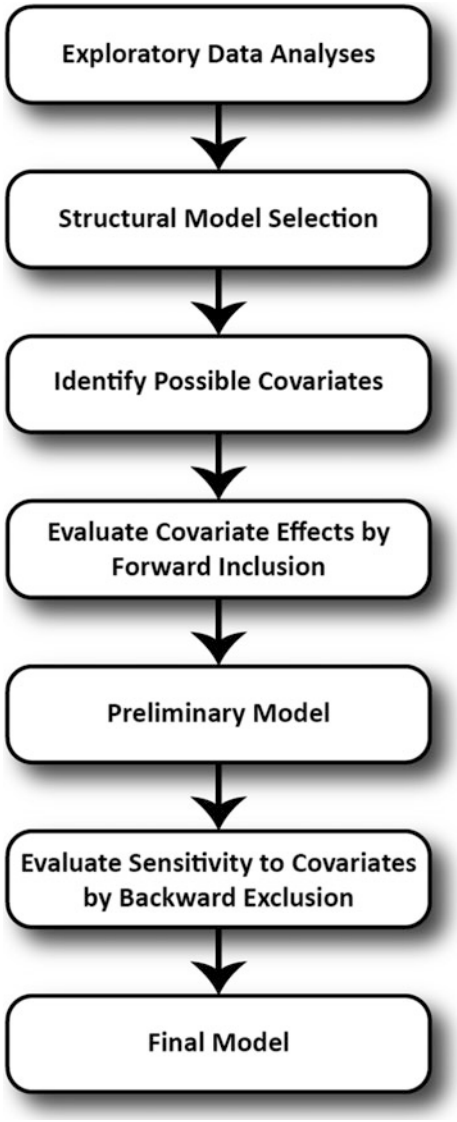

Fig. 13.4 Representation of the steps involved in building a population PK/PD model, starting with the selection of the structural model

potential limitations with respect to availability of data notwithstanding, this approach will also, by definition, deliver a model that is only as informative as the current understanding of the presumed true underlying physiology. Further, a considerable amount of evaluation is still required to ensure that the data supports all parameters.

Regardless of how they enter the model, covariates are included as part of the parameter counts and are included in the calculation of the Akaike Information Criterion, Schwarz Information Criterion, or other criterion used to assess

parsimony (Fisher and Shafer 2007; Ludden et al. 1994); it is these metrics that dictate whether or not improvements in model performance overcome added model complexity and justify inclusion of a covariate in the final model. As discussed above, once a base structural model has been identified, a set of potential covariates must be determined, and individual posterior Bayes' estimates from the base structural model may be used to explore covariate relationships in a stepwise (or full inclusion) fashion. The significance/impact of a particular covariate on the estimation of a model parameter is driven by visual inspection of predicted values, residuals, as well as improvements in the variance associated with that parameter and in the model objective function—which in some cases may be evaluated based on a chi-square distribution with degrees of freedom equal to the number of parameters added to the model which is being compared (Fisher and Shafer 2007).

Generalized additive models (GAM) have been utilized for evaluation of covariate relationships with parameter estimates. Originally proposed by Mandema et al. (1992), this framework is beneficial in that it allows nonlinear covariate relationships to be discovered without independent model runs; however, within this framework, covariate effects are only determined for individual parameters, and detection of covariate interactions are not directly supported. Although it has been shown that forward covariate selection using the GAM framework (in a statistical package such as S-PLUS), followed by backwards elimination in a population PK/PD modeling software package such as NONMEM, performs similar to doing both forward selection and backwards elimination in NONMEM (Wahlby et al. 2002), this process also requires relatively high numbers of model runs and user intervention. Additionally, independently assessing the effects of each covariate on a particular parameter does not allow appropriate evaluation of the subsequent effects between that covariate and another parameter in the structural model, and can cause unnecessarily redundant models being taken into evaluation (Jonsson and Karlsson 1998).

More recently, automated covariate model building algorithms have emerged that evaluate the benefit of adding a covariate to the model on a given parameter with respect to the entire structural model (Jonsson and Karlsson 1998; Ribbing et al. 2007). The appeal of this process lies in its ability to evaluate a covariate in the context of the overall model and reduce the need for user intervention and subjective decision-making. For instance, Jonsson and Karlsson (1998) extended NONMEM's first-order (FO) Taylor series estimation method by including a term for covariate effects within the estimation procedure, allowing the addition of covariates to be evaluated in the context of the given structural model as a whole. This approach is appropriate for additive and proportional models of inter- and intra-individual variability, but caution must be taken with nonlinear relationships: In order to reduce the computation time for evaluating covariate effects in more complex models, Jonsson and Karlsson employ a linearization of the function describing the covariate effects, which requires that function to be centered on zero. The result is a linearization that works well for weak covariate relationships and for covariate values close to the "typical" value, but becomes less accurate with strong (and nonlinear) effects. Additionally, only covariates with bivariate relationships

may be considered under this linearization, and computational burden may increase nonlinearly with both model complexity *and* the size of the dataset being analyzed. These limitations are potentially problematic for complex PK/PD/Disease models or even relatively large datasets.

Ribbing et al. (2007) suggest a method closely related to ridge regression called the "least absolute shrinkage and selection operator" (lasso). This methodology is aimed at constructing a model with the highest *predictive performance* and utilizes cross-validation of a dataset to assess model performance. In essence, the lasso standardizes covariates and limits the total absolute value of the regression coefficients (effects) of these covariates by specifying a "tuning parameter". The lasso is designed only for linear models, but additional surrogate variables can be created to account for nonlinear effects. However, it is not appropriate for power-model covariate relationships, and further subtleties such as breakpoints for piecewise relationships need to be pre-specified.

Although the automated approaches outlined above allow parsimony to be implemented in real-time when evaluating the effects of covariates in NONMEM, this benefit comes with subsequent limitations and a steep computational cost. Similar to the standard GAM approach, these algorithms do not support direct evaluation of covariate interactions, and the computational complexity limits the number of possible covariates that can be included in the analysis. Neither method is generally attempted with more than ten covariates.

As discussed, high-dimensional datasets being generated in the field of pharmacogenomics and systems biology contain of the order of 10^2–10^8 possible predictors, making the problem space of covariate identification many orders of magnitude different than the problem space of covariate model synthesis. With this difference of many orders of magnitude, along with the limitations of covariate model building algorithms specified above, it should become evident why traditional approaches designed for covariate model building from a modest number of possible covariates cannot be implemented on a genome or systems scale. To incorporate the full range of pharmacogenetic and pharmacogenomic data, covariate detection and covariate model synthesis should be considered distinct problems where pre-processing with search metrics and innovative algorithms (with efficient implementations) is needed in the detection phase to obtain a tractable number of possible covariates for more formal model synthesis.

13.6 Search Strategies for Covariate Detection in High-Dimensional Datasets

13.6.1 Regression-Based Methods

Linear regression approaches find their utility in the model-building and evaluation phase, as opposed to covariate identification. Main effects can feasibly be exhaustively searched on high-dimensional datasets using regression methodologies

such as logistic or linear regression; however, these methodologies require model specification a priori, and multiple models are needed to assess different types of main effects (e.g., additive and multiplicative). For any second-order (or higher) interactions, parametric approaches become infeasible on genome-scale datasets and search algorithms must be employed. Regression-based methods also encounter challenges when the interacting predictors exhibit collinearity with each other, which occurs frequently in pharmacogenomic data sets and is often referred to as linkage disequilibrium (LD).

13.6.2 Restricted Partition Method

The restricted partition method (RPM) (Culverhouse et al. 2004) detects interactions from continuous outcomes and has also been extended to case-control data (Culverhouse 2007). RPM is a computational simplification of the combinatorial partition method (CPM) (Nelson et al. 2001): It reduces the computational requirements by eliminating the exhaustive search nature of the CPM. The RPM algorithm seeks to identify the "best" predictor-value partitions that explain the observed variance in the outcome of interest. For each combination of predictors, RPM utilizes Games and Howell's version of Tukey's honest significant difference test (Games and Howell 1976) to determine which groups have statistically different means—if all groups have different means, the algorithm stops for that combination. If there are groups with similar means, the algorithm ranks the non-significant groups and combines the two groups that are the most similar; this process is repeated until either all groups have different means or no other simplifications can be made.

The RPM is capable of producing robust relationships, including higher-order interactions, and has outperformed both the multifactor dimensionality reduction methodology, as well as support vector machines in a report that compared interaction analysis methods on simulated case-control data of modest size (Culverhouse 2012). It is worth noting that the RPM algorithm would not be appropriate for stochastic, or non-normally distributed outcome measures, and to our knowledge, has not been characterized on full genome-wide data in the presence of linkage disequilibrium and population heterogeneity.

13.6.3 Dimensionality Reduction Methods

These are a class of exhaustive search methods used primarily in genetic epidemiology that are applicable to binary outcomes. The multi-factor dimensionality reduction (MDR) method, developed by Ritchie and her colleagues (Hahn et al. 2003; Moore et al. 2006; Ritchie et al. 2001b), is based on non-parametric multi-factor models and allows statistical and cross-validation analysis of

interactions for balanced case-control and discordant sib-pair designs (Bush et al. 2006; Hahn et al. 2003; Ritchie et al. 2001b, 2003); it has also been extended to unbalanced data sets (Velez et al. 2007). MDR uses constructive induction wherein the dimensionality of the multi-locus genotype is systematically reduced by pooling into high and low risk groups (Moore et al. 2006). The similarity of the MDR classifier to the naïve Bayes classifier has been shown (Hahn and Moore 2004).

The generalized multifactor dimensionality reduction (GMDR) (Lou et al. 2007) approach has also been used in the context of genetic epidemiology datasets (Gassó et al. 2010; Grady et al. 2010; Motsinger-Reif 2012; Sabbagh and Darlu 2009). GMDR extends the original case-control MDR method (Ritchie et al. 2001a) to include continuous data by enabling MDR's high/low risk partition of groups to be based on score statistics derived from the generalized linear model instead of observed odds ratios in case-control data. GMDR enables covariate corrections and handles both discrete and continuous phenotypes in population-based study designs. GMDR employs the same risk-pooling (dimensionality reduction) strategy as MDR and yields the original MDR as a special case when covariates are not present and the phenotype is discrete (Lou et al. 2007). Similar to CPM and MDR, GMDR is an exhaustive search methodology and has only been practically applied to candidate gene approaches (Gassó et al. 2010; Li et al. 2008).

GMDR and RPM share many commonalities in their algorithmic approaches and do not require a parametric definition of an interaction. GMDR has an additional computational burden in that it randomly segments the data into a learning set and nine cross-validation sets. It is possible that part of the increased performance of RPM over MDR in the study mentioned above (Culverhouse 2012) could be due to initial sampling variation; however, the RPM consistently outperformed MDR on that simulated set of case-control datasets. Of the two, MDR is the only one with a well-developed user interface.

13.6.4 Information Theoretic Methods

Information theoretic methods can provide powerful non-parametric search and identification algorithms for covariates and covariate interactions. These methods are those based on the concept of entropy, first introduced by Shannon and Weaver (1948), as a way to quantitate the amount of information necessary to send (and receive) a message. However, entropy is a descriptor of distributions, discrete and continuous alike, and has many applications in modeling. The Shannon entropy, $H()$, of a discrete random variable, X, is defined as:

$$H(X) = -\sum_{\forall x \in CX} p(x) \log[p(x)]. \tag{13.3}$$

Entropy is a measure of the uncertainty associated with the observations of a random variable. As can be seen from Eq. 13.3, impossible events ($p(x) = 0$) do not

add uncertainty to the overall term (by convention, $0 \times \log(0) = 0$ in this framework), and random variables that have only one outcome ($p(x) = 1$) do not have any uncertainty. As a corollary, random variables whose outcomes are equiprobable have the maximum amount of uncertainty and the highest entropy.

The application of entropy for interactions analyses is based on the concept of joint entropy. For the general case of a discrete predictor (or set of predictors), X, and a discrete (categorical or ordinal) outcome, Y, the joint entropy is given by the expression:

$$H(X,Y) = -\sum_{\forall (x,y) \in X \times Y} p(x,y) \log[p(x,y)], \tag{13.4}$$

where $X \times Y$ is the Cartesian product of X and Y. In the case of a continuous outcome, Y, it can be shown that

$$H(X,Y) = H(X) + \sum_{\forall x \in X} p(x) H(y|X = x), \tag{13.5}$$

where $H(Y|X = x)$ is the conditional entropy of Y, given that $X = x$, which for the normal distribution is $ln\left(\sigma_{X=x}\sqrt{2\pi e}\right)$, where $\sigma_{X=x}$ is the standard deviation of the outcome distribution given $X = x$. Conditional entropy is the amount of uncertainty in Y, after accounting for X, and is thus a measure of the dependence between random variables. A useful reference describing the theoretical relationship of entropy and higher-order information theoretic metrics (such as the k-way interaction information, described below) to familiar statistical concepts is available (Tritchler et al. 2011).

Entropy serves as the computational framework for many commonly encountered search algorithms, including regression trees and random forests. Additional algorithms employing entropy concepts are, PLATO (Grady et al. 2010), BOOST (Wan et al. 2010), and a host of search algorithms based on the k-way interaction information (KWII) (Chanda et al. 2008, 2009; Knights and Ramanathan 2012; Knights et al. 2013b) including AMBIENCE (Chanda et al. 2008), CHORUS (Chanda et al. 2009), and SYMPHONY (Knights et al. 2013b), which have shown initial promise for detection of informative covariates for gemcitabine and warfarin (Knights et al. 2013a).

13.6.4.1 Plato and Boost

The Platform for the Analysis, Translation, and Organization (PLATO) of large-scale data, is a suite of data filters designed to identify potentially informative interactions in large datasets through the utilization of multiple search strategies: It was created by the developers of the MDR and GMDR algorithms and utilizes conditional entropy in multiple filters such as the normalized mutual information and the uncertainty coefficient. Although PLATO has not been scaled up to

genome-wide datasets, the availability of multiple filters could make it a valuable resource for discrete and continuous variables; however, count data and other mixed distributions common to pharmaceutical datasets have not been evaluated using this platform.

The Boolean Operation-based Screening and Testing (BOOST) algorithm is an efficient search algorithm powered by the Kullback-Leibler (K-L) divergence that has been applied to several genome datasets from the Wellcome-Trust Case-Control Consortium (Wan et al. 2010). The K-L divergence is also known as the relative entropy (Cover and Thomas 1991). BOOST begins with a saturated log-likelihood model of the data, given a particular set of predictors, and builds to a K-L divergence definition of an interaction by removing the likelihood of the homogenous association model (given the data) from the saturated model, theoretically leaving only the quantity associated with the interaction. This methodology highlights the relationship between entropy-based approaches and more familiar log-likelihood approaches, which has been described (Tritchler et al. 2011). However, there is no closed form solution for the likelihood of the homogenous association model, and BOOST employs the Kirkwood Superposition Approximation (KSA), which is related to the KWII (Jakulin 2005), to quantitate this likelihood. Given the assumption of a homogenous interaction in the BOOST algorithm, the power of BOOST will likely suffer in the presence of population heterogeneity (stratification); additionally, as will be discussed later, the KWII accomplishes the same intended task of quantifying only the information gained from accounting for all variables of interest, without the need for approximation statistics.

13.6.4.2 Random Forests

Random forests are an extension of the classification and regression tree (CART) analysis of Breiman (Olshen and Stone 1984) and eliminate some of the sensitivity to data partitioning by randomly bootstrapping the portion of the original data selected as the training set. The random forest algorithm then performs a specified number of CART analyses on randomly selected sets of m predictors from the training data to build each of the 'trees' in the 'forest'. By selecting m random predictors from the data at each node, each tree is grown by identifying the most informative partition of the data at that node using the Gini impurity, which is built on the concept of entropy. Each tree in the forest produces a vote for the most appropriate classification set. After all trees in the forest have been grown, the classification set with the most votes, the "most popular" set, is identified (Breiman 2001). This approach operates under the assumption that a relationship between two or more predictors will exist no matter how the data is partitioned. One of the most appealing features of random forests is the existence of executable versions of the algorithm in the open source statistics language, R. At their essence, random forests seek to identify *the best set* of predictors for a dataset: While it is possible to learn about the relationships that exist in the dataset (Goldstein et al. 2010) from a random forest analysis, this information is not necessarily easily accessible, nor

easily interpretable, making random forests less appealing in situations when the maximum amount of knowledge is desired from the data.

Random forests have been successfully applied to genome-wide data (Garcia-Magarinos et al. 2009; Goldstein et al. 2010; Kim et al. 2009; Sun et al. 2007); however, their results to date have been mixed. For instance, the default settings for the number of trees and the size of the random vector of predictors for each tree are not appropriate for genome-wide data (Goldstein et al. 2010), and there is still more work necessary to test the suggested adjustments of these parameters. Although random forests have also been explored in the pharmaceutical industry for molecular predictors of pharmacokinetic properties in silico (Lombardo et al. 2006; Paine et al. 2010), and for homogenous population candidate gene analysis (Cosgun et al. 2011), their performance in the presence of genetic complexities such as linkage disequilibrium and population stratification has not been systematically evaluated and remains an important question for their utility in detecting PK/PD covariates from these datasets: In fact, it has been shown that random forests may have difficulty detecting predictor effects in the presence of covariates (Nonyane and Foulkes 2008) and have even been outperformed on smaller scale pharmacogenetic datasets by MDR and neural networks (Sabbagh and Darlu 2006).

13.6.4.3 KWII-Based Methods

The KWII is a multivariate extension of mutual information that provides a way to quantify higher-order interactions while removing the confounding effects of factors such as LD. The KWII removes the contributions of lower-order interactions and can be written as an alternating sum over all possible subsets T, of a set Υ. using the difference operator notation of Han (1980):

$$KWII(\upsilon) = -\sum_{\mathrm{T}\subseteq\Upsilon}(-1)^{|\Upsilon|-|\mathrm{T}|}H(\mathrm{T}), \tag{13.6}$$

where the symbols $|\Upsilon|$ and $|T|$ represent the cardinality of the set Υ, and the subset T, respectively. The number of genetic and environmental variables, k (not including the phenotype), in a combination is called the *order* of the interaction.

The KWII of a combination represents the amount of information that can only be gained (or lost) from the inclusion of every variable in the combination: Operationally, positive values indicate a net gain of information or synergistic interactions, negative KWII values indicate the net redundancy of information, and values of zero indicate net absence of interactions. This simple heuristic property enables KWII output to be easily interpreted, and can be visualized as a "KWII spectrum" which plots the KWII values for each combination. The most prominent interactions can be readily identified by visual inspection from such spectra.

As the KWII can be computationally expensive, KWII-based algorithms employ two search metrics: the total correlated information (TCI) (Watanabe 1960) and the phenotype-associated information (PAI) (Chanda et al. 2008). The TCI quantifies the amount of correlated information between a set of variables, and the PAI is designed to provide an efficient search metric for predictors and predictor combinations that carry information about a particular phenotype of interest. For the same set Υ above, let $\Upsilon \backslash P$ be the set minus the phenotype of interest: the PAI is then defined as

$$PAI(\Upsilon) = TCI(\Upsilon) - TCI(\Upsilon \setminus P). \tag{13.7}$$

The PAI is always positive, and when a non-informative predictor is added to a combination (i.e., one SNP in LD with another SNP in the set already), the PAI is unchanged. However, the addition of an informative predictor increases the PAI. This property of the PAI enables the construction of KWII-based search algorithms that identify interesting regions of a combinatorial space where the individual KWIIs can then be computed—for more information on the PAI see (Chanda et al. 2008, 2009).

The significance of information theoretic metrics such as the KWII can be assessed using permutation-based methods. Permutations are a commonly used, robust, and generalizable method for significance assessments in many applications (including the RPM algorithm) because it is an easy implementation strategy for obtaining the null distribution for any statistic of interest. The p value for the statistics can be obtained by comparing the observed value of the statistic to the corresponding null distribution. The p value is easier to interpret for the wider potential audience, which may be unfamiliar with the underlying statistic. Significance assessment is thus an essential but computationally time-intensive element in many algorithms because a large number of permutations have to be conducted when closed form expressions for the distribution of the underlying statistic are not available. Although statistics based on multiple mutual information (such as the KWII) have been shown to approximate a chi-square distribution (Han 1980), large sample sizes necessary for accurate significance testing via this method have restricted the use of this approach.

The most general form of permutation testing involves randomly shuffling the phenotype data in the input and repeatedly computing the KWII (or other statistic) of interest. However, for phenotypes involving discrete or dichotomous binary outcomes, the significance of the statistic can be evaluated using a fast exact permutation test. This fast test is exact (i.e., it yields the same results as a brute force permutation test); however, it derives its efficiency from randomly permuting the contingency table derived from the data. Random permutations of contingency tables properly constrained on the margins can be obtained efficiently using the Patefield algorithm (1981), which eliminates the need for repeated data access and speeds up significance assessments. Improving the computational efficiency of permutations has a considerable impact because a large number of permutations have to be done independently for each combination. More work is needed on

improving the computational efficiency of permutations for PK/PD outcomes that are continuous.

The KWII is one of the few search methodologies that has been studied for covariate detection of PK/PD covariates (Knights et al. 2013a), evaluated at the genome-scale (Knights and Ramanathan 2013), and assessed systematically in the presence of LD (Chanda et al. 2007; Sucheston et al. 2010) and population stratification (Knights et al. 2013b). Additionally, although the AMBIENCE, CHORUS, and SYMPHONY suite of KWII-based algorithms were designed for discrete, continuous, and multivariate datasets, respectively, they are built on the same search strategy that is theoretically versatile for different data distributions. The KWII has also been shown to outperform, or perform comparably, to MDR and regression (Sucheston et al. 2010), including Poisson regression for count/rate data (Knights and Ramanathan 2012).

13.6.5 Improving PK/PD Covariate Detection in High-Dimensional Data

For high-dimensional pharmacogenomic datasets, it has been said that "… the primary goal of analysis is not the genetic association with the phenotype, but rather the effect of genetics on the association between a certain drug and the phenotype" (Peters et al. 2010). For multidimensional datasets there is simply too much information and complexity for traditional approaches to exhaustively search for, and model, relationships. In a drug development setting, analyzing high-dimensional datasets is useful, not only because they enable detection of genetic/environmental influences on the disposition of a compound, but they may also provide evidence for lack of significant genetic/environmental associations, which can also be helpful.

Presumably, if there were a high level of confidence regarding possible covariates, a more focused, and perhaps parametric, candidate gene/predictor approach would be preferred; however, the availability of high-dimensional pharmacogenomic and pharmacogenetic data can enable insights into the molecular mechanism and also facilitate identification of previously unsuspected pathways.

Of the methodologies discussed, the KWII-based algorithms are among the few to combine a search strategy with powerful non-parametric interaction-identification metrics, and enable the easy identification of informative predictors (and predictor combinations), which may be explored further. These predictors and predictor combinations can be further reduced using information theoretic model building methods such as AMBROSIA (Chanda et al. 2011). Additionally, the data set could be concomitantly analyzed using other approaches, (e.g., PLATO, RPM, and random forests), to increase confidence in the robustness of the results. The outputs from these non-parametric search-enhanced methodologies can complement, strengthen, and inform more formal population PK/PD modeling approaches. Implementations of most of these algorithms are available in the public domain.

In contrast to case-control genetic epidemiology studies, PK/PD studies offer a wealth of information on the underlying system, including observed parameters such as C_{max}, derived non-compartmental values such as AUC, and model specific parameter values such as drug clearance from the body and the volume of distribution. Each of these values carries unique information on the underlying system and each could be used with the same high-dimensional dataset to identify potential predictors and predictor combinations (covariates) that are informative about the disposition of that compound—the results of these analyses could then be used for hypothesis generation and model building. For instance, using non-compartmental PK values generated from infusion data of gemcitabine (and active metabolite), along with a candidate gene dataset of 92 SNPs from Japanese cancer patients, the top-five KWII values for each parameter analyzed contained all but one of the final covariates from the final published NONMEM population PK model (Knights et al. 2013a). In a follow up study using the same non-compartmental values, but with genome data instead of candidate gene data, novel relationships with gemcitabine disposition were detected by the KWII (Knights and Ramanathan 2013). This type of naïve, unbiased analysis of high-dimensional datasets offers the greatest potential for improving the detection of relevant PK/PD covariates and can be executed with simple observed values, and sophisticated, calculated values alike; however, it should always be remembered that the results of any analysis of a phenotype are conditioned on the original assumptions of the model creation (i.e., assuming the appropriate base-model has been identified in a population PK/PD model).

13.7 Conclusions

The problem of covariate detection from multidimensional datasets is gaining attention in the PK/PD and pharmacometric communities as high-dimensional pharmacogenetic and pharmacogenomic datasets become more common in clinical trials and drug development. The identification of potential covariates from high-dimensional datasets should be considered a separate problem from modeling covariate relationships. Automated covariate modeling algorithms and iterative model assessments are useful for population modeling when the number of potential covariates are limited (Jonsson and Karlsson 1998; Ribbing et al. 2007), starting with no more than ten covariates. However, the size and complexity of pharmacogenetic and pharmacogenomic approaches requires novel search-based methods. Entropy-based information theoretic search algorithms are among the most promising approaches to improving the detection of PK/PD covariates in high-dimensional datasets—their versatility and non-parametric definition of interactions facilitates detection of both linear and nonlinear types of interactions, as well as higher-order relationships. Because they result in the identification of a manageable number of predictors, the output from these methods can be used as input for subsequent population modeling. Early inclusion of these approaches will increase the ability to detect covariates and covariate combinations in

high-dimensional pharmacogenetic and pharmacogenomic datasets, which could enhance the predictive capacity of population modeling and bring us one step closer to realizing the goal of individualized therapy.

References

Bauer RJ, Guzy S, Ng C (2007) A survey of population analysis methods and software for complex pharmacokinetic and pharmacodynamic models with examples. AAPS J 9:E60–E83

Bellman R (1961) Adaptive control processes: a guided tour. Princeton University Press, Princeton

Breiman L (2001) Random forests. Mach Learn 45:5–32

Bush WS, Dudek SM, Ritchie MD (2006) Parallel multifactor dimensionality reduction: a tool for the large-scale analysis of gene-gene interactions. Bioinformatics 22:2173–2174

Chanda P, Zhang A, Brazeau D, Sucheston L, Freudenheim JL, Ambrosone C, Ramanathan M (2007) Information-theoretic metrics for visualizing gene-environment interactions. Am J Hum Genet 81:939–963

Chanda P, Sucheston L, Zhang A, Brazeau D, Freudenheim JL, Ambrosone C, Ramanathan M (2008) AMBIENCE: a novel approach and efficient algorithm for identifying informative genetic and environmental associations with complex phenotypes. Genetics 180:1191–1210

Chanda P, Sucheston L, Liu S, Zhang A, Ramanathan M (2009) Information-theoretic gene-gene and gene-environment interaction analysis of quantitative traits. BMC Genom 10:509

Chanda P, Zhang A, Ramanathan M (2011) Modeling of environmental and genetic interactions with AMBROSIA, an information-theoretic model synthesis method. Heredity 107:320–327

Cordell HJ (2002) Epistasis: what it means, what it doesn't mean, and statistical methods to detect it in humans. Hum Mol Genet 11:2463–2468

Cordell HJ (2009) Detecting gene–gene interactions that underlie human diseases. Nat Rev Genet 10:392–404

Cosgun E, Limdi NA, Duarte CW (2011) High-dimensional pharmacogenetic prediction of a continuous trait using machine learning techniques with application to warfarin dose prediction in African Americans. Bioinformatics 27:1384–1389

Cover T, Thomas J (1991) Elements of information theory. Wiley, New York

Culverhouse R (2007) The use of the restricted partition method with case-control data. Hum Hered 63:93–100

Culverhouse RC (2012) A comparison of methods sensitive to interactions with small main effects. Genet Epidemiol 36:303–311

Culverhouse R, Klein T, Shannon W (2004) Detecting epistatic interactions contributing to quantitative traits. Genet Epidemiol 27:141–152

Fisher D, Shafer S (2007) Fisher/Shafer NONMEM workshop pharmacokinetic and pharmacodynamic analysis with NONMEM

Games PA, Howell JF (1976) Pairwise multiple comparison procedures with unequal n's and/or variances: a Monte Carlo study. J Educ Behav Stat 1:113–125

Garcia-Magarinos M, Lopez-de-Ullibarri I, Cao R, Salas A (2009) Evaluating the ability of tree-based methods and logistic regression for the detection of SNP–SNP interaction. Ann Hum Genet 73:360–369

Gassó P, Mas S, Álvarez S, Trias G, Bioque M, Oliveira C, Bernardo M, Lafuente A (2010) Xenobiotic metabolizing and transporter genes: gene–gene interactions in schizophrenia and related disorders. Pharmacogenomics 11:1725–1731

Gastonguay MR (2004) A full model estimation approach for covariate effects: inference based on clinical importance and estimation precision. AAPS J 6:W4354

Goldstein B, Hubbard A, Cutler A, Barcellos L (2010) An application of random forests to a genome-wide association dataset: methodological considerations & new findings. BMC Genet 11:49

Grady BJ, Torstenson E, Dudek SM, Giles J, Sexton D, Ritchie MD (2010) Finding unique filter sets in PLATO: a precursor to efficient interaction analysis in GWAS data. In: Pacific Symposium on Biocomputing. World Scientific, pp 315–326

Hahn LW, Moore JH (2004) Ideal discrimination of discrete clinical endpoints using multilocus genotypes. In Silico Biol 4:183–194

Hahn LW, Ritchie MD, Moore JH (2003) Multifactor dimensionality reduction software for detecting gene-gene and gene-environment interactions. Bioinformatics 19:376–382

Hair JF (1995) Multivariate data analysis with readings. Prentice Hall, Englewood Cliffs

Han TS (1980) Multiple mutual informations and multiple interactions in frequency data. Inf Control 46:26–45

Jakulin A (2005) Machine learning based on attribute interactions. Univerza v Ljubljani

Joerger M (2012) Covariate pharmacokinetic model building in oncology and its potential clinical relevance. AAPS J 14:119–132

Jonsson EN, Karlsson MO (1998) Automated covariate model building within NONMEM. Pharm Res 15:1463–1468

Khandelwal A, Harling K, Jonsson EN, Hooker AC, Karlsson MO (2011) A fast method for testing covariates in population PK/PD models. AAPS J 13:464–472

Kim Y, Wojciechowski R, Sung H, Mathias RA, Wang L, Klein AP, Lenroot RK, Malley J, Bailey-Wilson JE (2009) Evaluation of random forests performance for genome-wide association studies in the presence of interaction effects. BMC Proc 3(Suppl 7):S64

Knights J, Ramanathan M (2012) An information theory analysis of gene-environmental interactions in count/rate data. Hum Hered 73:123–138

Knights J, Ramanathan M (2013) Genetic factors associated with gemcitabine pharmacokinetics, disposition, and toxicity. Submitted: Pharmacogenomics

Knights J, Chanda P, Sato Y, Kaniwa N, Saito Y, Ueno H, Zhang A, Ramanathan M (2013a) Vertical integration of pharmacogenetics in population PK/PD modeling: a novel information theoretic method. CPT Pharmacomet Syst Pharmacol 2:e25

Knights J, Yang J, Chanda P, Zhang A, Ramanathan M (2013b) SYMPHONY, an information-theoretic method for gene–gene and gene–environment interaction analysis of disease syndromes. Heredity

Leary B, Dunlavey M, Chittenden J, Matzuka B, Guzy S. QRPEM—a new standard of accuracy, precision, and efficiency in NLME population PK/PD methods

Li MD, Lou X-Y, Chen G, Ma JZ, Elston RC (2008) Gene–gene interactions among CHRNA4, CHRNB2, BDNF, and NTRK2 in nicotine dependence. Biol Psychiatry 64:951–957

Lombardo F, Obach RS, DiCapua FM, Bakken GA, Lu J, Potter DM, Gao F, Miller MD, Zhang Y (2006) A hybrid mixture discriminant analysis-random forest computational model for the prediction of volume of distribution of drugs in human. J Med Chem 49:2262–2267

Lou XY, Chen GB, Yan L, Ma JZ, Zhu J, Elston RC, Li MD (2007) A generalized combinatorial approach for detecting gene-by-gene and gene-by-environment interactions with application to nicotine dependence. Am J Hum Genet 80:1125–1137

Ludden TM, Beal SL, Sheiner LB (1994) Comparison of the akaike information criterion, the Schwarz criterion and the F test as guides to model selection. J Pharmacokinet Biopharm 22:431–445

Mandema JW, Verotta D, Sheiner LB (1992) Building population pharmacokineticpharmacodynamic models. I. Models for covariate effects. J Pharmacokinet Biopharm 20:511–528

Moore JH, Williams SM (2005) Traversing the conceptual divide between biological and statistical epistasis: systems biology and a more modern synthesis. BioEssays 27:637–646

Moore JH, Gilbert JC, Tsai CT, Chiang FT, Holden T, Barney N, White BC (2006) A flexible computational framework for detecting, characterizing, and interpreting statistical patterns of epistasis in genetic studies of human disease susceptibility. J Theor Biol 241:252–261

Motsinger-Reif AA (2012) Developments in analyses in pharmacogenetic datasets. Pharmacogenet Individ Ther, 415–435

Nelson M, Kardia S, Ferrell R, Sing C (2001) A combinatorial partitioning method to identify multilocus genotypic partitions that predict quantitative trait variation. Genome Res 11:458–470

Nonyane BA, Foulkes AS (2008) Application of two machine learning algorithms to genetic association studies in the presence of covariates. BMC Genet 9:71

Olshen LBJFR, Stone CJ (1984) Classification and regression trees. Wadsworth International Group, Belmont

Paine SW, Barton P, Bird J, Denton R, Menochet K, Smith A, Tomkinson NP, Chohan KK (2010) A rapid computational filter for predicting the rate of human renal clearance. J Mol Graph Model 29:529–537

Patefield WM (1981) Algorithm AS 159: an efficient method of generating random R x C tables with given row and column totals. J R Stat Soc Ser C (Appl Stat) 30:91–97

Peters BJ, Rodin AS, De Boer A, Maitland-van der Zee AH (2010) Methodological and statistical issues in pharmacogenomics. J Pharm Pharmacol 62:161–166

Ribbing J (2007) Covariate model building in nonlinear mixed effects models. Uppsala University

Ribbing J, Nyberg J, Caster O, Jonsson EN (2007) The lasso—a novel method for predictive covariate model building in nonlinear mixed effects models. J Pharmacokinet Pharmacodyn 34:485–517

Ritchie MD, Hahn LW, Roodi N, Bailey LR, Dupont WD, Parl FF, Moore JH (2001a) Multifactor-dimensionality reduction reveals high-order interactions among estrogen-metabolism genes in sporadic breast cancer. Am J Hum Genet 69:138

Ritchie MD, Hahn LW, Roodi N, Bailey LR, Dupont WD, Parl FF, Moore JH (2001b) Multifactor-dimensionality reduction reveals high-order interactions among estrogen-metabolism genes in sporadic breast cancer. Am J Hum Genet 69:138–147

Ritchie MD, Hahn LW, Moore JH (2003) Power of multifactor dimensionality reduction for detecting gene-gene interactions in the presence of genotyping error, missing data, phenocopy, and genetic heterogeneity. Genet Epidemiol 24:150–157

Sabbagh A, Darlu P (2006) Data-mining methods as useful tools for predicting individual drug response: application to CYP2D6 data. Hum Hered 62:119–134

Sabbagh A, Darlu P (2009) Data mining methods as tools for predicting individual drug response. Pharm Data Min Approaches Appl Drug Discov 6:379

Shannon CE, Weaver W (1948) A mathematical theory of communication: American Telephone and Telegraph Company

Siemiatycki J, Thomas DC (1981) Biological models and statistical interactions: an example from multistage carcinogenesis. Int J Epidemiol 10:383–387

Sucheston L, Chanda P, Zhang A, Tritchler D, Ramanathan M (2010) Comparison of information-theoretic to statistical methods for gene-gene interactions in the presence of genetic heterogeneity. BMC Genom 11:487

Sun YV, Cai Z, Desai K, Lawrance R, Leff R, Jawaid A, Kardia SL, Yang H (2007) Classification of rheumatoid arthritis status with candidate gene and genome-wide single-nucleotide polymorphisms using random forests. BMC Proc 1(Suppl 1):S62

Tabachnick BG, Fidell LS (2001) Using multivariate statistics. Allyn and Bacon, Boston

Tritchler DL, Sucheston L, Chanda P, Ramanathan M (2011) Information metrics in genetic epidemiology. Stat Appl Genet Mol Biol 10:Article 12

Velez DR, White BC, Motsinger AA, Bush WS, Ritchie MD, Williams SM, Moore JH (2007) A balanced accuracy function for epistasis modeling in imbalanced datasets using multifactor dimensionality reduction. Genet Epidemiol 31:306–315

Wählby U (2002) Methodological studies on covariate model building in population pharmacokinetic–pharmacodynamic analysis. Uppsala University

Wahlby U, Jonsson EN, Karlsson MO (2002) Comparison of stepwise covariate model building strategies in population pharmacokinetic-pharmacodynamic analysis. AAPS PharmSci 4:E27

Wählby U, Jonsson EN, Karlsson MO (2001) Assessment of actual significance levels for covariate effects in NONMEM. J Pharmacokinet Pharmacodyn 28:231–252

Wan X, Yang C, Yang Q, Xue H, Fan X, Tang NL, Yu W (2010) BOOST: a fast approach to detecting gene-gene interactions in genome-wide case-control studies. Am J Hum Genet 87:325

Watanabe S (1960) Information theoretical analysis of multivariate correlation. IBM J Res Dev 4:66–82

Part III
Multi-scale Models of Drug Action

Chapter 14
Multi-scale Modeling of Drug Action in the Nervous System

Hugo Geerts, Patrick Roberts, Athan Spiros and Robert Carr

Abstract Drug discovery and development in CNS diseases has one of the greatest failure rates of all indications. This is due to poor translation ability of preclinical animal models for diseases like schizophrenia, Alzheimer's disease, and depression. In addition, treatment of patients in real-life situations is far from perfect, and polypharmacy is attempted without a rational understanding of the interactions of the various drugs with each other and with the brain circuits. A possible alternative is to develop an in silico model of relevant brain circuits using the existing expertise of computational neurosciences to which very specific neuropharmacology processes are added. This chapter illustrates a multi-scale drug action model for CNS diseases. We show various applications of this platform in actual CNS research and development projects.

Keywords Polypharmacy · In silico model · Alzheimer's disease · MAO-A inhibitors · Tricyclic · Glutamatergic systems · Pharmacogenetics · Gene-gene interaction · Epistasis · Olanzapine metabolism · Trial design · Inputs · Outputs · Calibration · Microcircuit parameters

H. Geerts · P. Roberts · A. Spiros · R. Carr
In Silico Biosciences, Lexington, MA, USA

H. Geerts (✉)
Perelman School of Medicine, University of Pennsylvania, 686 Westwind Dr, Berwin, PA, USA
e-mail: hugo-geerts@in-silico-biosciences.com

P. Roberts
Oregon Health and Science University, Portland, OR, USA

D.E. Mager and H.H.C. Kimko (eds.), *Systems Pharmacology and Pharmacodynamics*, AAPS Advances in the Pharmaceutical Sciences Series 23,
DOI 10.1007/978-3-319-44534-2_14

14.1 Introduction

14.1.1 Why Multi-scale Modeling of Drug Action?

CNS diseases, like depression and Alzheimer's disease, come with a steep societal impact, are difficult to treat, and most therapies are symptomatic rather than disease modifying or preventive. According to the World Health Organization, one in every four humans will develop a form of mental illness at some point, and the number of patients with dementia will rise to 75 million in the next 18 years. This is a huge challenge and likely to cast an enormous burden on developed societies.

While disease-modifying approaches are actively pursued, clinical trial failures in CNS diseases (notably Alzheimer's disease) (Cummings et al. 2014) have significantly delayed this time horizon. Therefore it is likely that symptomatic treatment based upon modulation of neuronal circuits will remain the staple of treatment paradigms and that it is absolutely mandatory to use such available therapies in an optimal way. For instance, the annualized incidence of schizophrenia is 82.9 per 100,000 males and 32.2 per 100,000 females for a young population (Anderson et al. 2012), leading to more than 500,000 new schizophrenia patients diagnosed every year in the developed world, and over 2 % of the adult population in developed countries has been diagnosed with a form of serious mental health issue (Pratt 2012). Furthermore about 30 % of the currently treated 10 million patients are not satisfied with their current medication and therapeutic strategy.

As a consequence of decreased psychotherapy, drug prescriptions for treatment of US mental health have substantially increased, up to $68 billion in 2008, almost 25 % of all drug prescriptions (Olfson et al. 2009). In many cases, physicians resort to polypharmacy as a way to enhance therapeutic response in a trial-and-error approach that is not based upon on a rational interpretation of the pharmacology of the drugs. In addition, it becomes increasingly clear that therapeutic response and sensitivity to side-effects of individual patients has a genetic basis that is being increasingly documented. Currently, physicians in clinical practice tend to combine various medications (polypharmacy) to alleviate symptoms based on trial and error approaches, not on a rational understanding of the interaction of drugs with the human neuronal networks in disease. Such an improper combination of CNS active drugs often leads to increased side-effects without therapeutic benefit, in addition to higher medication costs. Also the individual patient pathology (often defined by the patient's history and genotypes) or specific comedication modulates the response to individual therapies. Current pharmacogenomics approaches, while a good first step to identify factors associated with therapeutic response, rely much more on correlation than on the available scientific understanding of the neurobiology and often do not take into account gene-gene interactions, patient history, comedications, or environmental effects.

Developments in computational neurosciences have made it possible to simulate the complex network dynamics of neuronal brain circuits based upon realistic

representations of spiking neurons. Quantitative Systems Pharmacology has expanded this approach considerably to include the pharmacology of CNS active drugs, the interaction between different brain circuits, the implementation of human pathology and genotypes, and the calibration with clinical data. This 'humanized' platform (currently in schizophrenia, Alzheimer's disease, and Parkinson's and Huntington's disease) has been successfully used in situations relevant to drug discovery. The Institute of Medicine (Washington DC) has identified Quantitative Systems Pharmacology as one of the promising technologies to address the translational disconnect in CNS R&D (http://iom.edu/Activities/Research/NeuroForum/2012-MAR-28.aspx).

14.1.2 CNS Drug Discovery and Development

Developing successful drugs for CNS is extremely difficult; as many animal models are not predictive (Geerts 2009) for clinical trials. In fact in schizophrenia, no major new breakthrough has been observed since the serendipitous discovery of chlorpromazine and haloperidol in the late 1950s. In Alzheimer's disease, according to a recent study (Cummings et al. 2014), only 1 in 244 clinical development projects is ultimately successful, and a number of highly visible trial failures have led to a feeling of despair in the public perception. The last approved medication was memantine in 2004, a compound that does not work at all in the so-called standard animal models of Alzheimer's disease. The situation is similar in major depression; MAO-A inhibitors and tricyclics were discovered serendipitously, before the successful development of serotonin transport inhibitors, based on rational understanding of human neuropathology. Additionally, new targets in the glutamatergic systems were discovered based upon serendipitous discovery of the unanticipated anti-depressant effects of ketamine in humans (Zarate et al. 2006).

14.1.3 The Issue of Polypharmacy in Real-Life Situations

Many well controlled studies fail to identify substantial clinical benefits of polypharmacy, i.e., combination of antipsychotics in real-life situations (Waddington et al. 1998; Kroken et al. 2009; Yu et al. 2009; Gellad et al. 2012; Kroken and Johnsen 2012; Langle et al. 2012), whereas the incidence of both polypharmacy and high-dose antipsychotic combinations in clinical practice increases over time (Roh et al. 2014; Suokas et al. 2013). For example, in a naturalistic study with 56 patients (Elie et al. 2010), polypharmacy was associated with significantly lower BACS scores, suggesting an increased cognitive deficit. Often, combinations of antipsychotics are graded using chlorpromazine equivalents (Davis 1976; Kukreja et al. 2013). Although this grading definition has been used more successfully for typical antipsychotics, the nonlinear interaction of two or

more contemporary atypical antipsychotics with a more complex pharmacology at different receptor systems makes this approach less useful and likely erroneous. Animal models on the other hand are ill-equipped to provide good predictability for polypharmacy questions, because among many other problems (Geerts 2009): comedications of drugs are extremely difficult to test in preclinical conditions owing to very different PK profiles, varying drug affinities among preclinical species and humans, and the frequent presence of unique drug metabolites in humans. Retrospective studies indicate that even in patients with a first episode, polypharmacy is quite common, and clinical practice varies substantially from one treatment center to another (Goren et al. 2013). The current knowledge basis to provide a rational guidance for polypharmacy in psychiatric disorders is insufficient, and a better, more rational approach is desperately needed (Ballon and Stroup 2013; Fujita et al. 2013; Jureidini et al. 2013; Tani et al. 2013). A recent well controlled study suggests that increasing doses or switching to alternate antipsychotics in first-episode patients does not improve the outcome (Agid et al. 2013). Polypharmacy cannot be tested accurately in preclinical animal models, so this suggests the need for a completely new humanized approach. We will show that Quantitative Systems Pharmacology can provide a solution for this problem.

14.1.4 Personalized Treatment in CNS Diseases

With the increasing availability of genomic technology, pharmacogenetics studies have identified individual genetic differences in drug response or side-effect vulnerability in certain indications. However, the situation is much more complex in psychiatric diseases. For instance, a large GWAS study failed to find genetic predictors of clinical response to serotonergic and noradrenergic antidepressants (Tansey et al. 2012); likely because of incomplete genomic coverage with the current technology and the computational burden associated with the study of gene-gene interaction or epistasis. One possible way to get around this problem is to include biological information on pathways that could identify possible gene combinations. However, correlation does not guarantee causation, and it is very difficult to predict the direction of the response associated with a certain combination of genetic markers.

New big-data analytical approaches are currently being explored; as an example a systematic investigation of drug-gene interactions in schizophrenia (Putnam et al. 2011) suggested that haloperidol has a unique drug-gene interaction that might explain some of its clinical effects. However, the correlative nature of this study precludes any conclusion with regard to dosing or drug-drug combinations.

Furthermore, the fraction of active metabolites can be modulated by interaction of concomitant medication at the specific P450 enzymes that metabolize the parent antipsychotic. Anti-epileptic drugs, as well as smoking, can significantly affect serum concentrations of olanzapine and its metabolites (Haslemo et al. 2012). In addition, certain genetic polymorphisms in specific enzymes might affect

olanzapine metabolism; as an example, the FMO1rs7877C>T mutation in flavin-containing mono-oxygenase 1, involved in the metabolism of olanzapine, significantly affects the concentrations of the N-oxide metabolite of olanzapine (Soderberg et al. 2013).

It is therefore clear that a new approach is needed to identify and frame the issue of pharmaceutical treatment so that the best treatment strategy for an individual patient can be selected from the list of available medications. Quantitative Systems Pharmacology has expanded mechanism-based computer modeling of relevant human brain circuits considerably to include the pharmacology of CNS active drugs, the interaction between different brain circuits, the implementation of human pathology and genotypes, and the calibration with clinical data.

14.2 Multi-scale Modeling Approach

Quantitative systems pharmacology (QSP) multi-scale modeling and simulation platforms for addressing R&D challenges in CNS disorders is based on biophysically detailed models of neuronal circuitry, complete with membrane voltages of individual neurons and synaptic currents. This is in contrast to approaches that rely on curve-fitting and statistical optimization methods. In fact, the QSP approach could be considered as physiology-based pharmacodynamic modeling that is complementary to more traditional pharmacokinetic/pharmacodynamic modeling and simulation platforms (Geerts et al. 2012a, 2013c).

The critical insight to make such a biophysical computational platform practical for use in CNS pharmaceutical R&D is to focus model calibration on the parameters that have the greatest uncertainty and are most closely tied to pharmacology. These are the parameters that link the activation of receptors (especially G-protein coupled receptors or GPCRs) and other targets to their effects on electrical currents in neuronal membranes and synapses. This platform implements a method for calibration of key parameters with clinical data by linking pharmacology to neuronal function as a perturbation of circuit dynamics. Receptor activations are linearly coupled to a neuronal circuit simulator through parameters that are calibrated by relating circuit outputs to clinical data. This calibration approach, i.e., calibrating the linear sensitivity of a system around a known state, has been extremely productive in both physics and engineering.

The modeling and simulation platform has three major components at different scales:

Component 1: Models of neuronal modulators acting on receptors in the synaptic cleft.

Component 2: Models of neuronal microcircuits modulated by those receptors. (the linear coupling of Component 1 is a key part of these models)

Component 3: Models of neuronal connectivity between microcircuits (brain nodes).

Disease pathology is introduced into the platform models by changing parameters consistent with known pathologies associated with a disease and derived from human imaging and postmortem data. In assessing a target/indication, compound, or trial design, the **inputs** to the platform are primarily the human receptor affinities of a new compound being assessed (also see section on non-receptor targets). The **outputs** could be defined as "in silico biomarkers", such as network spike train information content (entropy) or some other biometric (e.g., fMRI signals, attractor pattern stability, or working memory analog) that can be correlated with human clinical data; and which can also be used to help confirm systemic hypotheses about the target or compound effect.

Different concepts of implementing CNS-based Quantitative Systems Pharmacology are shown in Fig. 14.1; each step is described below:

Step 1: *Calculate Receptor Activation*. Calculate the activation of each receptor in the presence of drugs using the synaptic cleft model (Component 1). It is illustrated for a dopamine synapse, but there are many other receptor types.

Step 2: *Calculate Local Activation Effects on Neurons*. Calculate the changes in membrane and synaptic currents (using coupling parameters) due to receptor activation, and simulate resultant neuronal activity changes in microcircuits for each drug/dose combination (Component 2). The

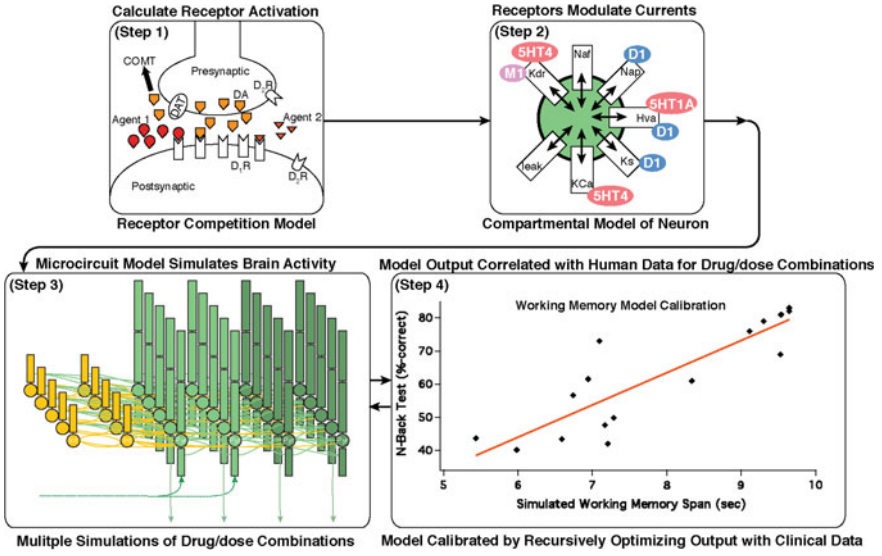

Fig. 14.1 Sequence of steps in a multi-scale modeling and simulation platform for drug action in the nervous system

example here is the soma of a pyramidal cell in a cortical microcircuit model containing membrane currents for sodium (Naf, Nap), potassium (Kdr, KCa, Ks), calcium (Hva), and a nonspecific leak current (leak). The activation level of receptors change the maximum conductance of the labeled currents.

Step 3: *Calculate Network Effects*. Calculate the change in the neuronal network activity (Components 2 and 3) and the altered outputs such as neuronal spike rates, spike train information content (entropy), or some other biometric (e.g., fMRI signals, attractor pattern stability or working memory analog), which result from the changes in synaptic and membrane currents caused by receptor activations.

Step 4: *Calibrate Local Activation Effects on Neurons*. Within biologically realistic constraints, recursively optimize correlation of clinical drug effects (e.g., N-back working memory scores) with measures of Component 3 neuronal systemic output (e.g., network attractor pattern stability) by adjusting the strength (coupling parameters) of the linear coupling between the receptor activation by the drugs and the change in maximum conductances. Coupling parameter calibration also yields a level of correlation with clinical scores as a form of validation of the platform circuit models (i.e., that some of the key circuitry of the disease is being properly captured), and yields a regression curve that can be used to quantitatively estimate human clinical effects of new drugs.

The outputs of Step 3 (simulated physiological measures) and Step 4 (estimated clinical measures) must be weighed and discussed in context, along with standard drug program evaluation inputs, with an awareness of the unique limitations of each type of drug program evaluation input. However, adding the inputs from the platform to drug program data packages can help identify important opportunities and dangers, which would not have otherwise been known, for further investigation (e.g., experiments, literature searches, further discussion, and simulation). This is especially true when differences between animal and human biology result in important differences in animal versus computational circuit outputs.

Such model-guided investigation can potentially yield subsequent program improvements, program cost savings, course changes in indication and compound selection, as well as trial design. As an example, we were able to blindly predict a Phase II clinical trial outcome for a novel dopaminergic drug (Geerts et al. 2012b) in schizophrenia, the Phase II outcome for another new non-dopaminergic stand-alone drug in schizophrenia (Liu et al. 2014), and a Phase I clinical Proof-of-Concept human scopolamine trial for a novel non-cholinergic Alzheimer drug (Nicholas 2013).

14.2.1 Major Platform Dimensions

14.2.1.1 Models of Neuronal Receptor Modulation Based on Pharmacology

This component simulates the activation of receptors based on chemical and physical characteristics of the competition for binding sites on each specific receptor type. The parameters of this receptor competition model are primarily based on the human receptor affinities of the specific pharmaceutical compounds under study. These compound human receptor affinities are the primary input into the platform when running simulations of neuronal systemic effects of actual or desired compounds. This module has been described in detail (Spiros et al. 2010, 2012).

The calculation in the synaptic cleft of diffusion and removal of neuromodulators, competition for binding to the receptors of multiple agents, and receptor activation is done with differential equations that are numerically integrated (Fig. 14.1—example for dopamine). In contrast to simple equations, such as the steady-state calculation of receptor occupancy as a function of drug dose, this approach allows for the competition with the endogenous neurotransmitter to be simulated in many disease states or with certain genotypes, where the neurotransmitter dynamics are significantly changed (Fig. 14.2).

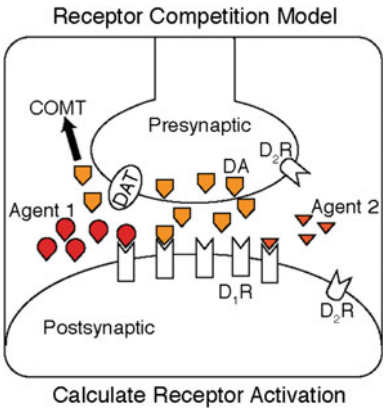

Fig. 14.2 The activation of each receptor for neuromodulators is calculated in the presence of drugs using QSP's unique receptor competition model—here illustrated for a dopamine synapse. Included are the effect of presynaptic D_2 autoreceptor activation on subsequent neurotransmitter release; variable presynaptic firing patterns for neuro-transmitter release; facilitation and depression of synaptic release; the competition between five agents (neurotransmitter, and up to four drugs or two active moieties of a parent drug and its major metabolite) and the dynamics of k_{on}/k_{off} binding of each of these agents

14.2.1.2 Models of the Neuronal Microcircuits Modulated by Receptors Affected by the Compound

The input to the microcircuit models is receptor activation due to the compound (the output from Component 1). The coupling of this output from Component 1 to the effects on electrical currents in neuronal membranes and synapses is a key part of the Component 2 microcircuit models. The outputs of Component 2 microcircuits are neuronal spike rates, spike train information content (entropy), or some other biometric (e.g., fMRI signals, attractor pattern stability or working memory analog) that can be correlated with human clinical data. These outputs can also be used to help confirm systemic hypotheses about a compound's effect.

14.2.2 Four Categories of Microcircuit Parameters

Parameters of the neuronal microcircuit component are constrained by public data found in peer-reviewed literature and can be divided into four categories:

(1) *Channel kinetics*
(2) *Structure*
(3) *Conductance*
(4) *Receptor effects (coupling the activation of receptors to effects on membrane and synaptic currents is a cornerstone of the QSP platform)*
(1) *Channel kinetic parameters are obtained from* in vitro *data*

The *channel kinetic* parameters determine the time-course and voltage sensitivity of membrane and synaptic currents. These parameters are well characterized by physiological experimentation in vitro (N.B. we focus on human receptors).

(2) *Structure of neurons and microcircuits constrained by functionality and anatomy*

Structural parameters define the dimensions of compartments that represent neurons and are determined by the minimal number of compartments that are necessary to simulate the physiological activity of the microcircuit. Structural parameters also define the connectivity between neurons in the microcircuit and are constrained by anatomical data.

(3) *Membrane conductances constrained by experimental data*

Maximum *conductances* of membranes and synapses are adjusted for the initial tuning of each neuronal circuit model to accurately simulate neuronal activity on a systems level. The conductance parameters are determined by accurately simulating electrophysiological recordings of spiking activity in animals and humans as well as data from human EEG and fMRI.

The parameters are constrained by electrophysiological studies of membrane current densities and synaptic currents, but are also dependent on the specific implementation of the compartmental models to represent biophysical microcircuits. A major issue is the difference in inhibitory tone in cortical networks. In fact, experimental studies have suggested that rodent GABA channel kinetics is different from primate GABA tone (Povysheva et al. 2007, 2008; Zaitsev et al. 2009; Volk and Lewis 2010).

(4) *Receptor effects—neuronal network coupling*

The *receptor effect* parameters are the key to including pharmacology in the models and to calibrating the models with human clinical data. The effects of neuronal modulators such as dopamine and serotonin are introduced by coupling the activation of receptors to changes in membrane and synaptic currents.

The localization of all currents in the model is shown in Fig. 14.3 on the left, and the receptor effects of modulators [dopamine (D1), serotonin (5-HT1A, 5-HT4), and acetylcholine (M1)] on currents in the soma compartment are shown on the right. The four categories of parameters are labeled with arrows showing their implementation in the model. The membrane voltage, V, is computed in each compartment by integrating differential equations, and the contribution of each current is calculated by its voltage-dependent kinetics. The receptor effects linearly modify the currents through a coupling parameter, P^{K}_{5HT4}, for the activation, *act5HT4*, calculated using platform component 1.

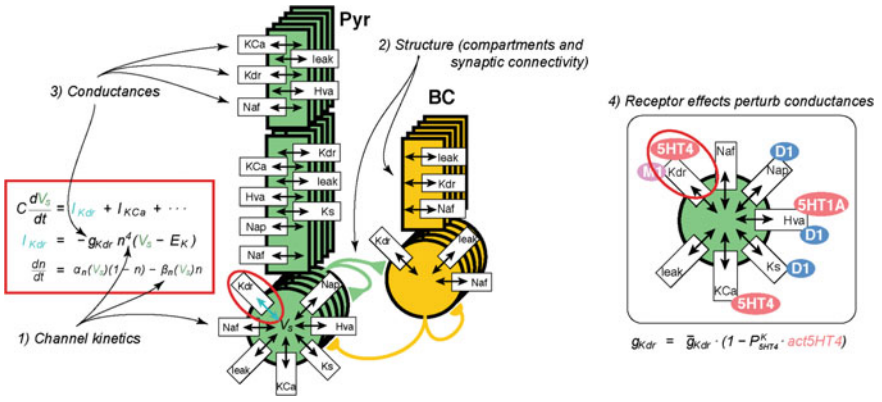

Fig. 14.3 Schematic diagram for a cortical microcircuit model consisting of 3-compartment pyramidal cells (*Pyr-Green*) and 2-compartment inhibitory interneurons with basket cell properties (*BC-yellow*). Changes in membrane potential are calculated from Hodgkin-Huxley equations (1) using time-dependent currents through voltage-gated ion channels, located in specific cell compartments (2). Conductance properties (3), both effect size and dynamics, are implemented. The effect of a GPCR (4), such as 5-HT4, can be implemented through transfer functions with the appropriate ion channels

14.2.2.1 Receptor Coupling Parameters not Directly Accessible from Patients

Although one can often measure receptor activation and their effects on channels via intracellular signaling pathways in vitro, it remains impossible to actually measure the strength of those effects in the clinical situation for humans. Therefore, receptor effect parameters are the largest source of uncertainty in predicting effects caused by pharmacology on clinical measures. However, these effects tend to modulate, rather than drive, the overall activity of the network. Reasonably small changes in receptor activation will not cause drastic change to the overall systems level behavior. In fact, large changes caused by neuromodulators are typically toxic, and would be avoided in clinical treatments. In the clinical situation, compounds typically make small changes to the activation levels of the receptors and the overall dynamics of the neuronal system. Therefore, a linear approximation for the sensitivity of the neuronal circuit to receptor activation is both practical and realistic given the present uncertainties in preclinical and clinical data.

14.2.2.2 Receptor Effects Are Described as First-Order (Linear) Changes to the System

The modulation of receptors by pharmacological agents is assumed to be a small perturbation of a known state of the system, regardless of whether that state is normal or pathological. Because the changes are small, a first-order (linear) approximation of the changes caused by pharmacology to alter the effects of receptor activation can be used.

Receptor coupling parameters are calibrated to maximally correlate the simulated physiological changes (neuronal circuit model readouts) with known clinical outcomes of specific drugs. Higher order, nonlinear approximations can in principle be explored, but such elaborations rarely improve the correlation between the model readout and clinical data.

14.2.2.3 Receptor Coupling Starting Values from Preclinical Electrophysiology

Electrophysiological data from preclinical studies are used to determine the starting values for calibration. For instance, if a 30 % change in a current is observed following a saturating infusion of a modulator in a slice preparation from an animal model, the coupling parameter is initialized at 0.30. Because the clinical situation involves human receptors and an entirely different biochemical environment for the modulated neurons, it is expected that following calibration, these parameters will shift from the preclinical value and be more representative of human receptor coupling.

14.2.2.4 Optimization Method Is not as Important as Biological Basis

The optimization method of calibrating the coupling parameters with clinical data is not as critical as the correct localization of receptor effects on the neuronal circuitry. We have used several methods of optimization including grid searches, gradient ascents, and iterative application of design of experiments to simulation results. The choice of optimization method depends on computational efficiency and whether the method can reliably converge on a maximal correlation. Experience shows convergence to a strong correlation with clinical data depends more on getting the neurobiology as accurate as possible, and less on the specific optimization method.

14.2.2.5 Strong Receptor Activation Changes Can Be Limited by Saturation Limits

The linear approximation of the coupling between receptor activation and the neuronal system is applied with the caveat that large changes in receptor activation could push out of the range of confidence in the validity of a linear approximation. In practice, such large changes are obvious in a breakdown of the system level dynamics or abrupt changes in the readouts. In the few cases where strong changes in activation have been explored, we have applied saturation limits on the receptor coupling as best approximated from physiological data.

14.2.3 Models of Neuronal Connectivity Between Microcircuits (Brain Nodes)

Extensive literature can help to define large-scale connectivity (connections between brain nodes). We usually derive neuronal connectivity properties from imaging studies such as Diffusion Tract Imaging and functional connectomics. Integrating separate models of various brain regions through synaptic connections (Fig. 14.4) reflect disease dynamics among regions and also enable the use of imaging data and predictions to help further refine the platform models.

Imaging data can be used for additional calibration of the models. Moreover links can be identified between model prediction of clinical scales and changes in imaging data caused by novel compounds. The results can help reveal how the biological mechanisms of non-invasive biomarkers, such as fMRI and EEG, correlate with changes in clinical scales. As an example, consider the problem of negative symptoms in schizophrenia. Imaging studies reveal that the strength of interaction between orbitofrontal cortex and ventral striatum is proportional to the subjective reporting on the Physical Anhedonia Scale (Juckel et al. 2006; Harvey et al. 2010), which is very specific and different from the imaging pattern that correlates with positive symptoms (Pinkham et al. 2011a, b) or in subjects with

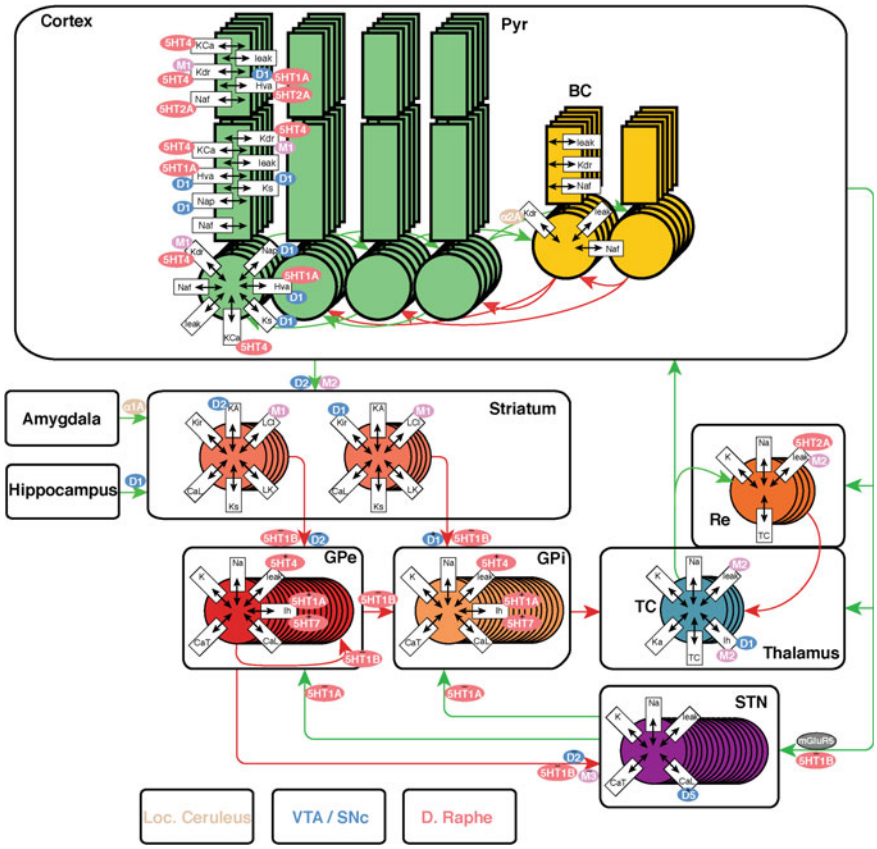

Fig. 14.4 Example of multiple brain nodes (prefrontal cortex, thalamus, and basal ganglia) connected in a large-scale model to simulate how pharmacology changes neuronal activity in the cortical-striatal-thalamic loop. Such larger-scale models leverage calibration of the separate microcircuits and enable further calibration with fMRI and EEG

major depression. This allows focusing on the afferent projections from the cortical region into the ventral striatum medium spiny neurons to develop a computational model of Bold fMRI changes that are correlated with the clinical PANSS negative scale.

14.2.3.1 Application to Non-receptor Targets and Novel Receptor Targets

When the platform is optimally calibrated to predict the effects on neuronal dynamics of clinically tested compounds (many of which hit multiple targets in multiple circuits), the platform is then also capable of estimating the effects of other

perturbations to the circuitry, as the models simulate many biophysical mechanisms of the neuronal circuitry. The QSP modeling platform can thus estimate the effects of novel compounds that modulate intracellular pathways, such as phosphordiesterase-10, because these intracellular pathways are represented in the models with the coupling between receptor activation and changes in membrane and synaptic currents. Modulations of the intercellular pathways are introduced into the models by a multiplicative factor, based on preclinical data, which perturbs the strength of the receptor coupling.

Moreover, any novel receptor target that changes the release of dopamine, such as TAAR1 modulators (Sotnikova et al. 2009), will cause known changes to dopamine receptor activation in a more complex neuronal circuit that has already been calibrated with clinical data. Another example is the action of a modulator of NMDA receptors, such as glycine, that can be modulated by a GlyT1 modulator. The perturbation of NMDA currents caused by changes in background levels of glycine are calculated using preclinical data, then applied to the clinically calibrated model to predict the changes in the human situation.

14.2.3.2 Introducing Pathology into the Circuits

Disease pathology is introduced into the platform models by changing parameters consistent with known pathologies associated with a disease. For example, in the case of schizophrenia, NMDA and GABA currents are modified, along with background noise levels consistent with known human data, along with changes in dopamine concentrations as derived from human imaging studies in specific brain regions such as the cortex or striatum.

The degree to which these parameters are changed is the degree that enables matching of the clinical difference in predictions from platform readouts with the healthy and diseased states. In the schizophrenia example, we often use a PANSS (Positive and Negative Symptoms Scale) scale for models of striatal neurons, and then these parameters are adjusted to correspond to a level of PANSS that represents the predicted clinical deficit that is in the schizophrenic range.

14.2.4 Calibration of the Model with Clinical Outcome

In order to calibrate the in silico platform, we introduced the pharmacology of all antipsychotic drugs (24) that have been tested in the clinic, at the appropriate dose at all receptors in the model for which a clinical outcome has been reported, and correlated the model outcome with the respective outcome on the clinical PANSS total scale (76 drug-dose combinations from 44,117 patients reported in 149 peer-reviewed publications starting in 1988 onwards). Note that these values refer to group averages and not individual patients. Correlation between model outcome and clinical outcome for the 43 drug-dose combinations in PANSS Total is 0.56

(Spiros and Edelstein-Keshet 1998), much larger than with simple D2R occupancy (0.18) or multi-dimensional receptor occupancy variance analysis (0.30), as it takes into account the known neurophysiological interaction between many different receptor subtypes.

The Extra-Pyramidal Symptoms module achieves a much better correlation ($r^2 = 0.66$) with clinical measures of Parkinsonian side-effects (i.e., the number of patients being given anticholinergic medication in the trial) than the single dopamine receptor (D_2R) occupancy ($r^2 = 0.08$). This type of 'calibration' is very different from the traditional animal model validation, where usually only clozapine and haloperidol at a random dose is required to 'qualitatively change the phenotype'.

Additional validation comes from a meta-analysis (Davis et al. 2003) covering 8 antipsychotics at different doses, where the QSP model gives a correlation of 0.56 with the clinical PANSS scales, compared to 0.08 for the simple D_2R occupancy. The QSP platform also outperforms the D_2R occupancy rule at 5 out of 8 'real-life' readouts in the CATIE trial (Lieberman 2007; Spiros et al. 2012). Similarly for our cognitive model, we achieve a correlation of 0.76 between the outcome of 17 different clinical interventions on the N-Back working memory test and the outcome in the computer model for the same interventions (Geerts et al. 2013a).

While retrospective calibration is a good approach to constrain the model outcomes to predict an actual clinical outcome, we have also applied this platform to predict the outcomes of meta-analyses (Geddes et al. 2000; Davis and Chen 2004) and the CATIE trial (Lieberman 2007). In all cases, the platform outperforms the current standard (the D2R occupancy as measured by PET imaging of a dopamine tracer). Furthermore, as a prospective prediction, the platform was able to blindly and correctly predict an unexpected clinical outcome in two schizophrenia and one Alzheimer case (see below), underscoring the superior predictive power of the platform as compared to animal models.

14.2.5 Differentiation from Statistical Data Analysis

The QSP platform is very different from statistical data-analysis or pattern recognition. Whereas a simple multivariate regression analysis based on large datasets can give some idea of expected outcomes, we recently compared this approach to the QSP analysis for the same set of clinical data and drug-receptor affinities (Spiros et al. 2012) for a blind prospective prediction of a clinical outcome. The QSP mechanism-based systemic platform is superior in predicting theses clinical outcomes, likely due to the fact that the multivariate analysis assumes independent processes rather than systemic interactions involving redundancy and feedback.

Actual physiological systems modeling can account for nonlinear processes such as the threshold for action potential generation or the complex interaction between different receptor systems (for instance one neurotransmitter regulating the release of another neurotransmitter) that modulate the membrane potential.

While multivariate regression analysis can identify a possible target that drives the clinical outcome, the computer-based mechanistic modeling approach adds quantitative understanding of the neurobiology (e.g., clarifying the link from receptor modulation to membrane excitability through effect of specific ion channels in specific parts of the neuronal network).

14.3 Summary and Discussion

The QSP modeling and simulation platform has three major components:

(*Component 1*) Models of neuronal modulators acting on receptors in the synaptic cleft.
(*Component 2*) Models of neuronal microcircuits that those receptors modulate.
(*Component 3*) Models of neuronal connectivity between microcircuits (brain nodes).

Integrating these components and utilizing clinical data to calibrate linear receptor effects on targets, by optimizing correlations of simulated circuit outputs with regression equations, enables predictions about the key neuronal circuit effects of new compounds in human patients. In addition, the resultant regression equations enable preclinical predictions of quantitative clinical outcomes based solely on drug pharmacology.

Following calibration of the crucial receptor coupling parameters, the platform models are able to estimate, in a very early stage of drug discovery and development, both neuronal circuit outcomes and clinical outcomes of novel compounds, given knowledge of a compound's effects on receptors or other targets.

Examples of the successful implementation of this platform in CNS R&D include a blinded prediction of the Phase II outcome of a novel dopaminergic drug in schizophrenia (Geerts et al. 2012b), the Phase I human scopolamine proof-of-concept for a novel non-cholinergic drug in Alzheimer's disease (Nicholas 2013), and the quantitative prediction of Phase II outcome for a novel non-dopaminergic drug in schizophrenia (Liu et al. 2014). Additional examples include the identification of the biology of the clinical responders of iloperidone that corresponds with one SNP identified in a traditional pharmacogenomics analysis (Geerts et al. 2015) and the biological explanation of the inverse U-shape dose-response of a Glycine T1 inhibitor for negative symptoms in schizophrenia, based upon the differential affinity of glycine for the excitatory-excitatory NMDA-NR2B subunit versus the excitatory-inhibitory NMDA-NR2C subunit (Spiros et al. 2014).

Furthermore, the QSP platform allows for a biological explanation of the differential effect of memantine and APOE in moderate versus mild AD patients (Roberts et al. 2012) and the negative pharmacodynamic interference of risperidone added to clozapine for cognitive outcome in schizophrenia patients

(Geerts et al. 2013a). The QSP platform can be used in principle for setting up a rational drug discovery program for neuropsychiatric dysfunction in Alzheimer's disease as measured using the Neuropsychiatric Index (Geerts et al. 2013b). This is based upon a combination of genetic rodent (rat, mice) data with the humanized QSP platform, where elements of psychiatric readouts are introduced.

In a drug discovery and development project, such outcomes are important data to be weighed and considered alongside animal physiological and behavioral models. The platform physiological predictions and the clinical predictions become an important new set of data highly complementary to animal results. Examination of the neuronal systemic implications of key differences in animal versus human physiology is enabled. Furthermore, when compounds hit multiple targets or when augmentation trials are considered, which is often the case with CNS drugs, the platform is uniquely useful.

In general, when large differences between animal and QSP platform results occur, the QSP platform can guide further investigations into animal and human differences and how this might affect outcomes before investing in expensive human clinical trials. The platform thus leverages expensive animal data in a most effective way. Furthermore, the platform can illuminate and identify key additional data needed from the literature or additional experimentation. Such investigations can help in better rank ordering compounds and projects, and in improved decisions about target and indication selection, compound selection, and trial design.

The QSP modeling and simulation platform contains realistic biophysical and systemic physiological representations of drug action, and thus it is also a framework for discussion of the details of how targets affect the human central nervous system. Such models provide a quantitative basis for quantitative hypothesis testing and refinement across many projects and stages encompassing the same pathology. This leverages the utilization of expensive data and scientific personnel in the most effective way.

References

Agid O, Siu CO, Pappadopulos E, Vanderburg D, Remington G (2013). Early prediction of clinical and functional outcome in schizophrenia. Eur Neuropsychopharmacol 23(8):842–851

Anderson KK, Fuhrer R, Abrahamowicz M, Malla AK (2012) The incidence of first-episode schizophrenia-spectrum psychosis in adolescents and young adults in Montreal: an estimate from an administrative claims database. Can J Psychiatry 57:626–633

Ballon J, Stroup TS (2013) Polypharmacy for schizophrenia. Curr Opin Psychiatry 26:208–213

Cummings JL, Morstorf T, Zhong K (2014) Alzheimer's disease drug-development pipeline: few candidates, frequent failures. Alzheimers Res Ther 6:37

Davis JM (1976) Comparative doses and costs of antipsychotic medication. Arch Gen Psychiatry 33:858–861

Davis JM, Chen N (2004) Dose response and dose equivalence of antipsychotics. J Clin Psychopharmacol 24:192–208

Davis JM, Chen N, Glick ID (2003) A meta-analysis of the efficacy of second-generation antipsychotics. Arch Gen Psychiatry 60:553–564

Elie D, Poirier M, Chianetta J, Durand M, Gregoire C, Grignon S (2010) Cognitive effects of antipsychotic dosage and polypharmacy: a study with the BACS in patients with schizophrenia and schizoaffective disorder. J Psychopharmacol 24:1037–1044

Fujita J, Nishida A, Sakata M, Noda T, Ito H (2013) Excessive dosing and polypharmacy of antipsychotics caused by pro re nata in agitated patients with schizophrenia. Psychiatry Clin Neurosci 67(5):345–351

Geddes J, Freemantle N, Harrison P, Bebbington P (2000) Atypical antipsychotics in the treatment of schizophrenia: systematic overview and meta-regression analysis. BMJ 321:1371–1376

Geerts H (2009) Of mice and men: bridging the translational disconnect in CNS drug discovery. CNS Drugs 23:915–926

Geerts H, Spiros A, Roberts P, Carr R (2012a) Has the time come for predictive computer modeling in CNS drug discovery and development? CPT Pharmacomet Syst Pharmacol 1:e16

Geerts H, Spiros A, Roberts P, Twyman R, Alphs L, Grace AA (2012b) Blinded prospective evaluation of computer-based mechanistic schizophrenia disease model for predicting drug response. PLoS One 7:e49732

Geerts H, Roberts P, Spiros A (2013a) A quantitative system pharmacology computer model for cognitive deficits in schizophrenia. CPT Pharmacometrics Syst Pharmacol 2:e36

Geerts H, Roberts P, Spiros A, Carr R (2013b) A strategy for developing new treatment paradigms for neuropsychiatric and neurocognitive symptoms in Alzheimer's disease. Front Pharmacol 4:47

Geerts H, Spiros A, Roberts P, Carr R (2013c) Quantitative systems pharmacology as an extension of PK/PD modeling in CNS research and development. J Pharmacokinet Pharmacodyn 40:257–265

Geerts H, Roberts P, Spiros A, Potkin S (2015) Understanding responder neurobiology in schizophrenia using a quantitative systems pharmacology model: application to iloperidone. J Psychopharmacol 29:372–382

Gellad WF, Aspinall SL, Handler SM, Stone RA, Castle N, Semla TP, Good CB, Fine MJ, Dysken M, Hanlon JT (2012) Use of antipsychotics among older residents in VA nursing homes. Med Care 50:954–960

Goren JL, Meterko M, Williams S, Young GJ, Baker E, Chou CH, Kilbourne AM, Bauer MS (2013) Antipsychotic prescribing pathways, polypharmacy, and clozapine use in treatment of schizophrenia. Psychiatr Serv 64:527–533

Harvey PO, Armony J, Malla A, Lepage M (2010) Functional neural substrates of self-reported physical anhedonia in non-clinical individuals and in patients with schizophrenia. J Psychiatr Res 44:707–716

Haslemo T, Olsen K, Lunde H, Molden E (2012) Valproic Acid significantly lowers serum concentrations of olanzapine—an interaction effect comparable with smoking. Ther Drug Monit 34:512–517

Juckel G, Schlagenhauf F, Koslowski M, Filonov D, Wustenberg T, Villringer A, Knutson B, Kienast T, Gallinat J, Wrase J, Heinz A (2006) Dysfunction of ventral striatal reward prediction in schizophrenic patients treated with typical, not atypical, neuroleptics. Psychopharmacology 187:222–228

Jureidini J, Tonkin A, Jureidini E (2013) Combination pharmacotherapy for psychiatric disorders inchildren and adolescents: prevalence, efficacy, risks and research needs. Paediatr Drugs 15 (5):377–391

Kroken RA, Johnsen E (2012) Is rational antipsychotic polytherapy feasible? A selective review. Curr Psychiatry Rep 14:244–251

Kroken RA, Johnsen E, Ruud T, Wentzel-Larsen T, Jorgensen HA (2009) Treatment of schizophrenia with antipsychotics in Norwegian emergency wards, a cross-sectional national study. BMC Psychiatry 9:24

Kukreja S, Kalra G, Shah N, Shrivastava A (2013) Polypharmacy in psychiatry: a review. Mens Sana Monogr 11:82–99

Langle G, Steinert T, Weiser P, Schepp W, Jaeger S, Pfiffner C, Frasch K, Eschweiler GW, Messer T, Croissant D, Becker T, Kilian R (2012) Effects of polypharmacy on outcome in patients with schizophrenia in routine psychiatric treatment. Acta Psychiatr Scand 125:372–381

Lieberman JA (2007) Effectiveness of antipsychotic drugs in patients with chronic schizophrenia: efficacy, safety and cost outcomes of CATIE and other trials. J Clin Psychiatry 68:e04

Liu J, Ogden A, Comery TA, Spiros A, Roberts P, Geerts H (2014) Prediction of efficacy of vabicaserin, a 5-HT2C agonist, for the treatment of schizophrenia using a quantitative systems pharmacology model. CPT Pharmacomet Syst Pharmacols 3:e111

Nicholas AP (2013) Dual immunofluorescence study of citrullinated proteins in Alzheimer diseased frontal cortex. Neurosci Lett 545:107–111

Olfson M, Mojtabai R, Sampson NA, Hwang I, Druss B, Wang PS, Wells KB, Pincus HA, Kessler RC (2009) Dropout from outpatient mental health care in the United States. Psychiatr Serv 60:898–907

Pinkham A, Loughead J, Ruparel K, Wu WC, Overton E, Gur R (2011a) Resting quantitative cerebral blood flow in schizophrenia measured by pulsed arterial spin labeling perfusion MRI. Psychiatry Res 194:64–72

Pinkham AE, Loughead J, Ruparel K, Overton E, Gur RE, Gur RC (2011b) Abnormal modulation of amygdala activity in schizophrenia in response to direct- and averted-gaze threat-related facial expressions. Am J Psychiatry 168:293–301

Povysheva NV, Zaitsev AV, Kroner S, Krimer OA, Rotaru DC, Gonzalez-Burgos G, Lewis DA, Krimer LS (2007) Electrophysiological differences between neurogliaform cells from monkey and rat prefrontal cortex. J Neurophysiol 97:1030–1039

Povysheva NV, Zaitsev AV, Rotaru DC, Gonzalez-Burgos G, Lewis DA, Krimer LS (2008) Parvalbumin-positive basket interneurons in monkey and rat prefrontal cortex. J Neurophysiol 100:2348–2360

Pratt LA (2012) Characteristics of adults with serious mental illness in the United States household population in 2007. Psychiatr Serv 63:1042–1046

Putnam DK, Sun J, Zhao Z (2011) Exploring schizophrenia drug-gene interactions through molecular network and pathway modeling. AMIA Annu Symp Proc 2011:1127–1133

Roberts PD, Spiros A, Geerts H (2012) Simulations of symptomatic treatments for Alzheimer's disease: computational analysis of pathology and mechanisms of drug action. Alzheimers Res Ther 4:50

Roh D, Chang JG, Kim CH, Cho HS, An SK, Jung YC (2014) Antipsychotic polypharmacy and high-doseprescription in schizophrenia: a 5-year comparison. Aust N Z J Psychiatry 48(1):52–60

Soderberg MM, Haslemo T, Molden E, Dahl ML (2013). Influence of FMO1 and 3 polymorphisms onserum olanzapine and its N-oxide metabolite in psychiatric patients. Pharmacogenomics J 13(6):544–550

Sotnikova TD, Caron MG, Gainetdinov RR (2009) Trace amine-associated receptors as emerging therapeutic targets. Mol Pharmacol 76:229–235

Spiros A, Edelstein-Keshet L (1998) Testing a model for the dynamics of actin structures with biological parameter values. Bull Math Biol 60:275–305

Spiros A, Carr R, Geerts H (2010) Not all partial dopamine D(2) receptor agonists are the same in treating schizophrenia. Exploring the effects of bifeprunox and aripiprazole using a computer model of a primate striatal dopaminergic synapse. Neuropsychiatr Dis Treat 6:589–603

Spiros A, Roberts P, Geerts H (2012) A quantitative systems pharmacology computer model for schizophrenia efficacy and extrapyramidal side effects. Drug Dev Res 73:196–213

Spiros A, Roberts P, Geerts H (2014) A computer-based quantitative systems pharmacology model of negative symptoms in schizophrenia: exploring glycine modulation of excitation-inhibition balance. Front Pharmacol 5:229

Suokas JT, Suvisaari JM, Haukka J, Korhonen P, Tiihonen J (2013) Description of long-term polypharmacy among schizophrenia outpatients. Soc Psychiatry Psychiatr Epidemiol 48:631–638

Tani H, Uchida H, Suzuki T, Fujii Y, Mimura M (2013) Interventions to reduce antipsychotic polypharmacy: a systematic review. Schizophr Res 143:215–220

Tansey KE, Guipponi M, Perroud N, Bondolfi G, Domenici E, Evans D, Hall SK, Hauser J, Henigsberg N, Hu X, Jerman B, Maier W, Mors O, O'Donovan M, Peters TJ, Placentino A, Rietschel M, Souery D, Aitchison KJ, Craig I, Farmer A, Wendland JR, Malafosse A, Holmans P, Lewis G, Lewis CM, Stensbol TB, Kapur S, McGuffin P, Uher R (2012) Genetic predictors of response to serotonergic and noradrenergic antidepressants in major depressive disorder: a genome-wide analysis of individual-level data and a meta-analysis. PLoS Med 9: e1001326

Volk DW, Lewis DA (2010) Prefrontal cortical circuits in schizophrenia. Curr Top Behav Neurosci 4:485–508

Waddington JL, Youssef HA, Kinsella A (1998) Mortality in schizophrenia. Antipsychotic polypharmacy and absence of adjunctive anticholinergics over the course of a 10-year prospective study. Br J Psychiatry 173:325–329

Yu AP, Ben-Hamadi R, Birnbaum HG, Atanasov P, Stensland MD, Philips G (2009) Comparing the treatment patterns of patients with schizophrenia treated with olanzapine and quetiapine in the Pennsylvania Medicaid population. Curr Med Res Opin 25:755–764

Zaitsev AV, Povysheva NV, Gonzalez-Burgos G, Rotaru D, Fish KN, Krimer LS, Lewis DA (2009) Interneuron diversity in layers 2–3 of monkey prefrontal cortex. Cereb Cortex 19:1597–1615

Zarate CA Jr, Singh JB, Carlson PJ, Brutsche NE, Ameli R, Luckenbaugh DA, Charney DS, Manji HK (2006) A randomized trial of an N-methyl-D-aspartate antagonist in treatment-resistant major depression. Arch Gen Psychiatry 63:856–864

Chapter 15
Mechanistic Modeling of Inflammation

Jeremy D. Scheff, Kubra Kamisoglu and Ioannis P. Androulakis

Abstract In this chapter we explore the characteristics underlying the development of mechanistic-based models of inflammation. The discussion covers the three basic arms of developing mechanistic models. We begin by exploring the likely experimental analogues producing critical information, we then review modeling alternatives for representing the biological system under study, and finally we review the key methods for executing the model and performing the required calculation. The discussion concludes with a brief overview of the challenges and opportunities in the context of bridging the gap between (mechanistic) disease and pharmacology models as we move towards more integrated systems pharmacology approaches with the ultimate goal of designing relevant in silico clinical trials enabling rational extrapolation of bench observations.

Keywords Bioinformatics · Disease progression · Stochasticity · Immunomodulatory signals · Homeostasis · In vitro models · Cross-system interactions · Lumped · Phenomenological · Statistical · Quasi-mechanistic · In silico · Clinical trials

15.1 Inflammation: "the Good, the Bad, and the Ugly"

The inflammatory response is a key component of the host's reaction to acute stress, acting as a major contributor to the recovery from trauma and injury (Lowry 2009a). Furthermore, low-grade, chronic inflammation has been shown to play a critical role in a wide variety of pathophysiological conditions such as obesity,

J.D. Scheff · I.P. Androulakis (✉)
Biomedical Engineering Department, Rutgers University,
New Brunswick, NJ, USA
e-mail: yannis@rci.rutgers.edu

K. Kamisoglu · I.P. Androulakis
Chemical and Biochemical Engineering Department,
Rutgers University, New Brunswick, NJ, USA

D.E. Mager and H.H.C. Kimko (eds.), *Systems Pharmacology and Pharmacodynamics*,
AAPS Advances in the Pharmaceutical Sciences Series 23,
DOI 10.1007/978-3-319-44534-2_15

diabetes, and cancer (Coussens and Werb 2002; Southerland et al. 2006; Haffner 2006; Luft et al. 2013). Managing, modulating, and eventually controlling the progression of the inflammatory response, be it either acute or chronic, has faced numerous obstacles. At the heart of this conundrum is the fact that the inflammatory response, under normal circumstances, engages an intricate web of interacting protective mechanisms aiming at restoring homeostasis following a stressful challenge. However, when the response does not resolve appropriately, or is initiated inappropriately, it can lead to detrimental results (Laroux 2004). The delicate balance of the forces that induce and maintain a proper response is critical in re-establishing homeostasis under conditions of stress (Bone 1996) as well as performing the balancing act of maintaining homeostasis (Chrousos 2009). Challenges in understanding how to modulate inflammation ultimately stem from the underlying complexity of the inflammatory response itself, a homeostatic mechanism which has served as a major component during our evolutionary development (Lowry and Calvano 2008). Cytokines, hormones, and autonomic signaling all convey immunomodulatory signals that are typically redundant and pleiotropic, making it difficult to infer how perturbing individual components will impact the overall systemic response in a specific context.

The intrinsic complexity of the immune response to stress (Segel and Cohen 2001) naturally triggered interest in systems-based approaches to rationalize the evolution of the dynamic interactions of the constitutive components (Vodovotz and An 2010, 2013; Vodovotz et al. 2013a). Model-based approaches attempt to quantify the causal relationships between the components manifesting and driving the onset, maintenance, and resolution of the inflammatory response. These representations can vary from statistical and correlational (Clermont et al. 2004b) to mechanistic (Foteinou et al. 2009c); from deterministic and continuous (Scheff et al. 2011b) to discrete and stochastic (An et al. 2009; Dong et al. 2010; Nguyen et al. 2013). As we increasingly begin to understand and appreciate the systems characteristics of the inflammatory response and the inflammation-related pathophysiological conditions (Vodovotz et al. 2013a; Carre and Singer 2008), the need for establishing appropriate mathematical and computational frameworks becomes more apparent (Zenker et al. 2007a, b).

15.2 Mathematical Modeling in Health and Disease—A Few Preliminaries

Although this chapter focuses on (approaches towards) mechanistic models of inflammation, it is instructive to put these modeling efforts in a broader context. Building a quantitative model is not simply the process of using an existing, available, and applicable tool in any setting. It is rather a challenging research question requiring a deep understanding of the question to be addressed, the type of answer that is pursued, the access to the physical/biological systems (i.e., data) and,

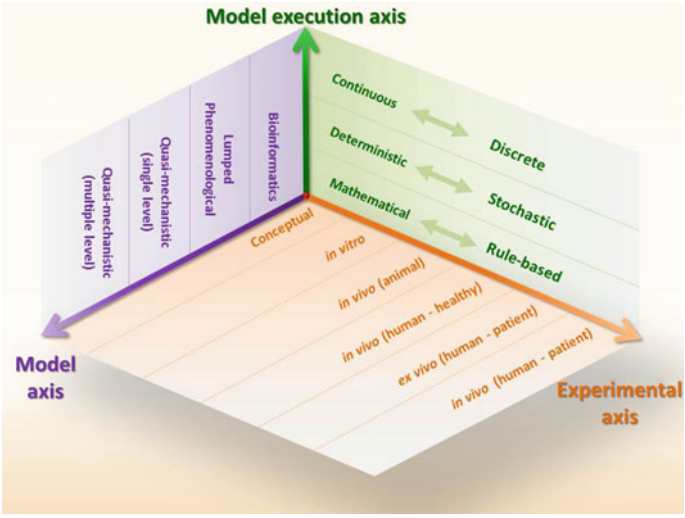

Fig. 15.1 Model development space

of course, the development of the appropriate mathematical and computational representations which synthesize a coherent picture of the physical reality of interest. Therefore, moving towards the development appropriate models, a number of prototypical questions first need to be well articulated, understood, and addressed. A model is a particular representation of reality whose granularity (complexity) depends on the scope and goals of the analysis. Broadly, we will assume that models are developed in the context of a 3-dimensional space whose axes define the level of detail with regards to various decisions, as shown in Fig. 15.1 and described below.

15.2.1 Experimental Axis: Which System Is Modeled?

The first level of classification in mathematical modeling relates to the physical reality, for which an experimental analogue is used as a proxy to explain the biological or biomedical systems of interest being described and analyzed. In that respect, existing systems can be classified according to how they represent biological reality:

(i) Conceptual: The quantitative models do not describe precise biological or physiological phenomena and do not attempt to replicate a physical reality. Rather, the quantitative models aim at developing conceptual relationships and broad(er) analogies between putative components involved in the inflammatory response (Kumar et al. 2004; Lauffenburger and Kennedy

1983, 1981). These models aim at deriving fundamental underlying relationships that should hold between the actual elements of a real system.

(ii) In vitro: The quantitative representations describe relations at the most fundamental physical level such as the cell. These models have the potential of being the most mechanistic, likely capturing a well-defined range of responses in the proper context. The key limitation of in vitro models is that they focus on subsystems, isolated from their functional environment, lacking proper cross-system interactions and interactions with key systemic characteristics such as rhythmic variability (circadian, ultradian, etc.) that play a significant role, as will be discussed later (Jayaraman et al. 2005).

(iii) In vivo–ex vivo (animals): This is the most widely used vehicle for producing an adequate body of experimental observations (Webb 2014). Their advantages and disadvantages are clear and well-articulated: While offering the opportunity to probe the biological system of interest in relatively integrated manner, the cross-species extrapolation remains elusive (Seok et al. 2013; Ovacik and Androulakis 2013; Kamisoglu et al. 2015b).

(iv) In vivo (humans-controlled studies): In a limited number of cases, healthy human volunteers are subjected to appropriate challenges for the purpose of replicating a pathophysiological condition of interest. The advantages and limitations are clear: This provides relevant (human) data albeit limited in terms of elicited responses and cohort composition (usually young and healthy subjects) (Calvano et al. 2005; Kamisoglu et al. 2014, 2015a; Haimovich et al. 2010a, b).

(v) Ex vivo (humans): This appears to be a reasonable compromise. Cells extracted from humans already in a condition of actual interest are analyzed ex vivo. The advantages relate to the appropriateness of the source of the sample (disease or treated human), but the analysis is conducted outside the physical environment of the human (Crome et al. 2010).

(vi) In vivo (patient): This is the most informative source of actual data, yet not necessarily the most appropriate for analysis purposes. A number of confounding factors make such analysis horrendously difficult—i.e., limited data availability with samples that capture a convolution of disturbances and pre-existing conditions, making the dissection of cause-effect relationships difficult (Xiao et al. 2011; Tsalik et al. 2014; Langley et al. 2013, 2014).

15.2.2 Model Axis: How Is the Physical System Modeled?

Once the representation of the biological system has been defined, the next question is the methodological approach used to model this rendition of reality, in other words, the nature and characteristics of mathematical model. Several approaches can be undertaken (as discussed below) and each approach is characterized by its own merits and flaws. The saying "all models are wrong, but some are useful" should be

carefully taken into consideration not so much in order to disqualify the model, but rather to make sure that the proper model is used in its appropriate context. As Segel nicely puts in the preface of his book (Segel 1984) "[…] a good mathematical model —though distorted and hence wrong like any simplified representation of reality— will reveal some essential component of a complex phenomenon".

Broadly speaking, we can characterize the models as one of the following categories:

(i) Statistical: This aims at deciphering correlational relationships based on experimental observations. Albeit simple, these models allow us to extract critical information regarding the constituents of the response.
(ii) Lumped and phenomenological: These models aim at describing broad and coarse characteristic responses as proxies in lieu of precisely defined state variables which are quantities with exact physiological interpretation. Such models tend to be less complex, or at least their complexity can be controlled by design, thus enabling a more detailed analysis (Kumar et al. 2004).
(iii) [quasi] mechanistic (single level): The term mechanistic in biological and biomedical research needs to be used in the proper context. It usually implies increased level of details; however, exact mechanisms, in the context of first principles, are rarely known if ever available. Lumped systems tend to be more phenomenological, whereas the [quasi] mechanistic approach tends to introduce more tangible cause-effect relationships.
(iv) [quasi] mechanistic (multiple levels): This refers to models which aim at engaging multiple cell types, tissues, organs, and eventually integrated host systems interacting with their environment. The physiologically-based pharmacokinetic models (Rowland 2013) can be considered as the typical example of such an approach. The advantages are obvious, i.e., phenomena of interest are placed in the proper context, but the complexity of such models can easily escalate such that critical assumptions and simplifications are often required.

15.2.3 Model Execution Axis: How Is the Model Evaluated?

The choices in terms of the execution of the model do not simply reflect the way the model equations are solved but rather reflect specific characteristics of the way we hypothesize biological processes take place.

(i) Mathematical versus rule-based: The physical reality of a biological system can be described either through mathematical equations (closed form) or through logical statements and execution rules. The underlying hypotheses are the same, but the expression of the outcome of an interaction differs. Often times rule-based descriptions aim at addressing issues related to the discrete nature of the dynamics of the underlying processes (see iii).

(ii) Stochastic versus deterministic: It has been argued that nothing in the physical world is deterministic, in the sense that variability exists in biological and physiological systems (Ullah and Wolkenhauer 2010). Modeling stochastic events increases not only the complexity of the representations but also the complexity of the responses. However, it remains to be evaluated whether this increased complexity necessarily translates to improved insight.

(iii) Discrete versus continuous: The continuum approximation simplifies many of the representations, yet it can be argued that reaction and signaling events take place in a discrete manner. This constitutes a design decision endowing the modeling approach with specific characteristics depending on whether the modeler wishes to emphasize events which evolve continuously or in discrete fashion (Bortolussi and Policriti 2008). A classic example would be the modeling of gene expression as either a discrete or continuous process (Klipp 2005) depending on whether one wishes to adopt a discrete representation of the transcriptional events or assume that the events take place in a continuum.

In the sections that follow, we will attempt to provide an ensemble of approaches spanning a wide range of methodologies exploring various combinations of the three major categories just described. As will become apparent from the discussion which follows, there is not necessarily a clear logical progression in terms of moving from less to more complex models as different approaches are used to address different questions, while the three axes just described can be mixed and matched accordingly. Models are placed in the model space of Fig. 15.1 and therefore a particular approach reflects combinations along the three primary axes. However, for presentation purposes, models have been ordered along the model axes of our classification matrix.

15.3 Model Axis: Towards the Development of Mechanistic Models of Inflammation

Although methods and approaches are presented individually, it needs to be made clear that the process of developing a mechanistic model is iterative in nature and results from multiple refinements based on the interaction and integration of the components to be described in the sections that follow (Fig. 15.2).

15.3.1 Bioinformatics Models of Disease Progression

The computational analysis of biological data has evolved to an entire discipline in and of itself (Altman and Miller 2011). Large amounts of diverse data sets are now routinely assembled, annotated, and analyzed for the purpose of deciphering

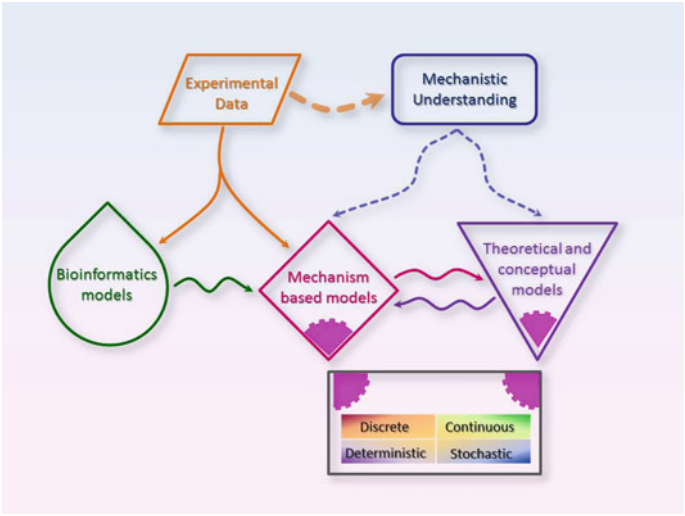

Fig. 15.2 Functional integration and interaction of model development concepts

functional relationships. What is slowly emerging as a promising alternative to the analysis of such diverse data is to perform statistical analyses for the purpose of deriving representation of the dynamic trajectories representing the host's deviation from, and return to, homeostasis. In the work discussed in Polpitiya et al. (2009), McDunn et al. (2008), for example, the transcriptional dynamics of circulating leukocytes are represented in a reduced space in order to map trajectories of critically ill patients as their condition progresses. The implications of such approaches are profound as now we can begin to talk about transcriptional dynamics and place it in the context of a host response to a stressor (Yang et al. 2009). The fundamental idea is that coherent system dynamics are embedded within high-throughput measurements and these, if properly analyzed, could be revealed and used as surrogates of the host response. Although mostly descriptive, these approaches can form the foundation, as will be shown later, for characterizing complex state variables in the context of a complex inflammation model. Interesting preliminary results have emerged demonstrating that the dynamics of a system deviating from its homeostasis can be inferred by proper analysis of systemic markers such as cytokines (Mi et al. 2011). The intriguing opportunity here is that, whereas earlier approaches for building trajectories aimed mostly at characterizing independent components, we are now starting to appreciate that causal relationships can also be inferred; a critical step in moving towards integrated model development. By and large, the application of these models focuses on detecting system dynamics and less so on relating constitutive dynamics elements to each other in the form of an integrated model.

15.3.2 Theoretical and Conceptual Models of Inflammation

In a lumped model, the assumption is made that appropriate biomarkers exist (i.e., masked state variables), which capture basic elemental responses. These are further assumed to be inter-related by appropriate causal dependencies, expressed mostly in the form of phenomenological relationships. These formalisms have been proven extremely powerful (Kumar et al. 2004) since the emphasis is given on analyzing broad systemic characteristics using models readily available for intricate analyses.

Simple mathematical models of inflammation allow efficient exploration of high-level mechanisms, which is typically either much more difficult, or even impossible, to model with increased complexity. An early lumped model of inflammation was proposed to describe the local tissue-level inflammatory response to bacterial invasion (Lauffenburger and Kennedy 1981). This two-variable model considers populations of bacteria and leukocytes with homogeneous distributions within a local region. By modeling the bacterial growth rate, the phagocytosis rate, the leukocyte emigration rate, and the leukocyte death rate, two ordinary differential equations (ODE) were constructed to investigate the dynamical behavior of this type of system. The small size of the model facilitates the derivation of relatively simple closed-form expressions for the steady-states and their associated stability characteristics, allowing high-level mechanistic interpretations of the importance of model parameters in the dynamic responses of the system. Extensions of this work increased the complexity of the model by accounting for the influence of chemotaxis (Fisher and Lauffenburger 1990), allowing the analysis of the relationship between factors, such as cell speed and persistence on bacterial elimination dynamics, at the expense of increased complexity.

While the focus of models such as the aforementioned is on events at the cellular level, models at a higher level of abstraction would allow the assessment of changes at the host level. As such, compact phenomenological model of acute inflammation were proposed in Kumar et al. (2004), incorporating abstractions in the form of: biomarkers describing events at the level a pathogen to instigate inflammation, an early inflammatory marker to induce the inflammatory response, and a later anti-inflammatory biomarker to enable return of the system to homeostasis, assuming a graceful resolution of the response (via dampening and regulating the inflammatory response). This conceptual model aimed at describing the minimum number of required components of an inflammatory response, namely an initiating event, a mechanism for setting the inflammatory response in motion, and finally a negative-feedback-like regulatory control mechanism. Albeit conceptual, the model captures the key macroscopic system dynamics at a high level.

The tractability of such mathematical representations makes it possible to identify steady-states and perform stability analysis, thus resulting in intuitive interpretation of the expected responses leading to mechanistic insight, despite the coarseness of the representation. As such, parameterizations of the model were identified, which correspond to observed phenotypes: (i) a healthy response in which the pathogen is eliminated and inflammation resolves; (ii) a recurrent

infection scenario where both the pathogen and inflammatory response oscillate in a predator-prey-like relationship; (iii) a persistent non-infectious inflammatory state where the pathogen is cleared but inflammation persists due to positive feedback; (iv) a persistent infectious inflammation state where the acute inflammatory response is not sufficient to restore homeostasis; and (v) severe immune-deficiency where even high levels of pathogen do not elicit a robust inflammatory response. The richness of these responses shows that even small, simplified models can lead to the emergence of complex results shedding light on possible functional inter-relationships among structural components.

The model complexity can be increased to account for the inflammatory response including: the initiating event (pathogen or injury); a pro-inflammatory response; an anti-inflammatory response; and tissue damage (Day et al. 2006; Reynolds et al. 2006). Such conceptual models begin to elucidate more complex questions. As such, it was hypothesized that exogenous treatment aiming at simulating the anti-inflammatory response does not always result in reduced inflammation, depending on the dose and the timing; if a sufficient pro-inflammatory response is suppressed, it can result in a persistent infectious state. Therefore, even such a simple model illustrates generalizable characteristics of interventions that are aimed at modulating inflammation-driven diseases: Targeting components of the inflammatory response can produce unintuitive results, which may contribute to controversies about the effectiveness of immunomodulatory treatments such as glucocorticoids or anti-cytokine therapies, which have proven successful in some cases but ineffective in others. If even a simple model can exhibit these complex results, the situation is far more challenging for a real physiological system.

Therefore, conceptual and lumped models can provide critical insight into the inflammatory response, but at a fairly high level of abstraction. A critical limitation of such models is that it is difficult to translate the meaning of a lumped variable capturing broader characteristics (such as “pro-inflammatory activity”) and phenomenological relations, such as the complicated, nonlinear forms used in these models, to specific measureable quantities and tangible interventions. However, such models are powerful (in theory) to provide insightful characterization of an idealized response.

The role of theoretical models cannot, and should not, be either undermined or underestimated. Theoretical models aim at identifying, what appear to be, simpler structures with the ability to generate macroscopic observables and dynamic characteristics of the more complex biological reality whose mechanistic description remains elusive (Segel 1998; Segel and Bar-Or 1999). Therefore, a theoretical model of the inflammatory response will begin to outline and characterize either properties of the host response to an inflammatory stimulus or properties that the host response needs to adopt in order to enhance its ability to control the inflammatory response. In other words, theoretical models are the rational source of generating testable hypothesis for elucidating mechanistic underpinnings.

15.3.3 Putting Data in the Context of [Semi]Mechanistic Formalisms

After obtaining an understanding of the intrinsic dynamics (using correlational models) of the data and a basic framework of the functional relationships among the state variables (using theoretical models), we can then proceed to developing a mechanistic framework, based on the theoretical model, that would rationalize the experimental dynamics.

As an example of this type of model, Chow et al. developed a model incorporating individual cytokines, different types of immune cells, and other key physiological parameters to investigate inflammation more intricately (Chow et al. 2005). A significant amount of experimental data is required to estimate the numerous parameters for a model of this size. However, the end result is a model that is potentially much closer to a real physiological system. Data from multiple mouse experiments were used to evaluate the model's ability to capture responses to a variety of inflammatory states induced by different injuries (endotoxemia, hemorrhage, and surgical trauma). They found that they were able to model these different scenarios simply by altering the initial conditions of the core inflammation model, providing some evidence towards the hypothesis that these diverse inflammatory shock states have similarities in their underlying mechanisms, even when cytokine-concentration data may look quite heterogeneous. One key potential application of this type of model is in understanding how the internal dynamics of the inflammatory response lead to specific types of responses to therapies in an individual (Clermont et al. 2004a).

The complexity of such models can increase (Prince et al. 2006; Torres et al. 2009; Daun et al. 2008; Lagoa et al. 2006) eventually reaching the level of description of the host response (Nieman et al. 2012). A much higher level of detail and a broader scope can be defined and explored. In addition to breaking down general "inflammatory signaling" variables into individual variables for different cytokines, integrated models incorporate more physiologically-based influences on inflammation, including lung function, gas exchange, and oxygen transport. Similar to the results of the previously discussed works, they found that heterogeneity between genetically distinct swine with different responses to injuries could be encoded in the initial conditions of the model. Additionally, insight can be gained into the relationship between oxygen transport and endotoxemia-induced damage. From a modeling perspective, one of the key aspects of such models is that individual components are selected in a data-driven fashion, using statistical techniques, thus moving a step closer to the closing of the theory-modeling-experiment group. This is important as many studies make a priori assumptions about which components are important enough to be included in a model, although those assumptions may not always be true. A conceptually parallel approach integrating rigorous statistical analysis of data, formalisms translating prior biological knowledge, and further development of putative mechanistic links were pursued (Yang et al. 2011a). The ultimate result was an integrated model describing tissue specific (i.e., liver) response to acute stress

following burn injury. The approach further demonstrated how signaling events can begin to emerge in such semi-mechanistic formalisms.

The latter became clearly apparent in a series of publications aiming at modeling human endotoxemia. Using high-throughput microarray mRNA measurements from peripheral blood cells (Foteinou et al. 2009a, b; Nguyen et al. 2011) it was possible to develop semi-mechanistic, tissue specific dynamic models linking the ligand (lipopolysaccharide, LPS) recognition by appropriate (TLR4) receptors, eventually activating inflammation-specific signaling cascades (NF-κB) driving the peripheral release of pro- and anti-inflammatory cytokines. The underlying hypothesis was that critical pathways activated in endotoxemia will result in the emergence of coherent transcriptional dynamics representing the key signals to be included in a dynamical model of endotoxemia (Yang et al. 2009). Analysis of the human microarray data enabled the definition of three key transcriptional responses: (1) an early pro-inflammatory response, including genes in the Toll-like receptor and NF-κB pathways that are closely linked to LPS signal transduction; (2) a late inflammatory response, including components of the anti-inflammatory IL-10 signaling pathway; and (3) an early down-regulated cohort of genes related to cellular bio-energetic processes. The proposed ODE-based physicochemical model aimed at linking cellular recognition of LPS with the production and downstream effects of the aforementioned transcriptional responses. In a subsequent work it was demonstrated how further the network with appropriate signaling cascades, extensions of this model would begin to shed light on complex phenomena such as endotoxin tolerance (Yang et al. 2011b).

The inflammatory response induces the involvement of the neuroendocrine system modulating the release of anti-inflammatory hormones and neurotransmitters. As such, cortisol and epinephrine lead to anti-inflammatory downstream effects, cortisol through glucocorticoid receptor-mediated signaling and epinephrine through the stimulation of adrenergic receptors, leading to elevated intracellular cAMP concentrations (van der Poll et al. 1996b; van der Poll 2000). These immunomodulatory hormones have been experimentally studied in human endotoxemia by giving exogenous hormone infusion before, during, or after LPS administration (Alvarez et al. 2007; van der Poll et al. 1996a, b; Jan et al. 2009). Leveraging established models of hormone activity (Ramakrishnan et al. 2002) to account for the effects of cortisol and epinephrine, the investigation of how cellular-level transcriptional responses to inflammation are modulated by hormonal cues (Foteinou et al. 2009a, 2010) was further explored, such as how hormone levels can influence whether the system exhibits a healthy self-limited inflammatory response or whether it will instead move to a persistent chronic inflammatory state.

15.3.4 Accounting for Stochasticity and Discrete Events

Stochasticity and heterogeneity have profound effects on the function of biological systems (Bahcall 2005; Blake et al. 2003; Rosenfeld et al. 2005), and an alternative,

more intuitive, approach—agent-based modeling (ABM) has been explored (An 2008; Chavali et al. 2008). An ABM consists of simulations of discrete interactions between discrete agents, based on the concept that relatively simple local interactions can model complex global phenomena. Each agent represents a component of a system (such as an individual cell), and at discrete time points, each agent stochastically moves and interacts with its surroundings based on previously defined probability distributions. ABMs are fundamentally different than ODE models because of the key roles played by spatial heterogeneity and stochasticity. In the context of inflammation, ABMs have been widely used to study a variety of conditions (An et al. 2009), particularly in cases where incorporating a spatial component or stochasticity is important. The usefulness and applicability of ABMs vary, but applications to immunological problems and findings derived from these models generated a lot of insights into the interactions and dynamics at the cellular level in immune responses. Jenkins and colleagues (Catron et al. 2004) investigated B-T cell interactions in the absence of directed cell chemotaxis during the first 50 h of a primary immune response to an antigen. Gary An and coworkers have pioneered the application of ABMs in the context of evaluating the dynamics of the innate immune response, the efficacy of proposed interventions for SIRS/multiple organ failure (MOF) (An 2004, 2001), and the dynamics of the TLR4 signal transduction cascade with LPS preconditioning and dose-dependent effects (An 2009; An and Faeder 2009). A result of this effort was the development of a basic immune simulator (BIS) to qualitatively examine the interactions between innate and adaptive interactions of the immune responses to a viral infection (Folcik et al. 2007). Furthermore, a variety of successful agent-based simulators have been constructed as frameworks for immunology/disease understanding and exploration, such as IMMSIM (Baldazzi et al. 2006; Celada and Seiden 1992), SIMMUNE (Meier-Schellersheim et al. 2006), and CyCells (Warrender et al. 2006). Challenges and limitations of agent-based modeling include fitting large numbers of parameters, interpreting "emergent" model output from basic agent interactions, and slow performance with large numbers of agents. Below, several insightful ABMs as examples are discussed to highlight how ABMs of diverse origins can be used to gain insight into the inflammatory response.

Mi et al. implemented an ABM that considers the activities of inflammatory cells and cytokines in the wounded tissue, as well as the surrounding blood and tissue, to study diabetic foot ulcers (Mi et al. 2007). First they constructed a general model to capture known behaviors related to skin wound healing. Then, they evaluated two alternative hypotheses about which inflammatory mediators drive the development of diabetic foot ulcer (DFU). Finally, they evaluated a variety of simulated therapies to compare their performances. Therefore, this ABM contributed both towards the understanding of the mechanisms driving DFU and towards the evaluation of treatment options. Through these avenues, this type of ABM can influence both the development and testing of therapies for DFU.

Bailey et al. combined a model of blood flow with an ABM of the microvasculature to investigate leukocyte trafficking (Bailey et al. 2007). In this model, agents are individual cells in the microvasculature. The hemodynamic model

provided an added modulatory function on top of the cells as they experienced changing mechanical force in addition to biochemical cues from other cells. Through this, they investigated the relationship between adhesion molecules, chemokine/cytokine secretion, and monocyte trafficking. The fundamental mechanical/spatial aspects of this model made it well-suited for an ABM approach that can naturally consider interactions between adjacent cells and the position of cells relative to the endothelium.

Possibly the most comprehensive ABM used to study inflammation was proposed by An (2008). This work presented a multi-level model, starting with the typical cell-as-agent paradigm but then scaling up to tissues and organs with their own agent-based rules, with the ultimate goal of better understanding complex, systemic diseases like multiple organ failure that cannot be explained purely by a single local model. A key hypothesis of this integrated model is that epithelial barrier dysfunction plays an important role in organ dysfunction. Damage markers from compromised epithelial and endothelial cells move into a blood compartment where they can influence other parts of the system, simulating inter-organ communication. This general model structure was validated by reproducing a variety of conditions including pneumonia, pulmonary edema, and ischemia. The vast scope of this model is indicative of the potential for complex, multiscale interactions to be encoded in ABMs. Dong et al. (2010) discussed an ABM in the context of human endotoxemia, aiming at analyzing the inflammatory dynamics at the level of both immune cells and inflammatory mediators such as cytokines and LPS. In Nguyen et al. (2013), an ABM was developed to investigate the cellular variability through the interactions and dynamics of inflammatory cytokines in acute inflammatory responses following endotoxin administration. Whereas in previous studies (Foteinou et al. 2009a, b; Scheff et al. 2010) the focus was on the possibility of modeling the transcriptional dynamics of cellular responses, the attempt here was to capture stochastic variation in the transcriptional process, one of the key factors leading to phenotypic variation besides the genetic and environmental variability (Kaern et al. 2005; Kilfoil et al. 2009; Niepel et al. 2009; Raser and O'Shea 2005). Because stochasticity is an inherent property of agent interactions, non-genetic cell-to-cell variability originating from stochastic variance is captured by our proposed model. Therefore, elucidating the relationship between the behaviors measured at the single-cell level and those measured in a population of cells is among the aims of the study, in order to provide an insight into the host inflammatory response under different external stimuli.

15.3.5 Inflammation Models Accounting for Physiological Rhythms

Clearly all living systems are open systems in the sense that they exist in an environment constantly exposed to challenges and perturbations. Therefore, any

realistic representation of a disease, in general, and inflammation in particular, needs to eventually possess the ability to allow for interactions between the host and its environment. Of all possible interactions, we choose to focus here on external signals which impose on host internal variability strongly suspected to endow the host with increased adaptability to stresses critically affecting the response to inflammatory challenges. Among those signals, the ones driving daily (circadian) rhythms are particularly important. Although the nature of the source of circadian biological rhythms will not be discussed here (Albert 2010), the relevance for the discussion stems from the fact that intrinsic biological rhythms are known to be related to the overall ability of the host to adapt and respond (Lehrer and Eddie 2013), whereas the loss of rhythmic variability is a confounding factor in the context of the inflammatory response (Lowry 2009b).

Circadian rhythms are of importance in the context of the inflammatory response proximally because they impose patterns on a wide range of inflammatory mediators (Coogan and Wyse 2008). The hypothalamic-pituitary-adrenal (HPA) axis and the sympathetic nervous system (SNS) produces stress hormones (Sternberg 2006) whose pattern of release follow broad circadian rhythmicity and play critical roles in immune responses (Coogan and Wyse 2008; Levi and Schibler 2007; Sukumaran et al. 2010; Cutolo et al. 2003). This rhythmicity is regulated by the 24 h light/dark cycle exerting diurnal effects on numerous inflammatory cytokines (Lissoni et al. 1998; Petrovsky et al. 1998). Furthermore, clock genes responsible for circadian timekeeping are also linked to cytokine production and their expression patterns significantly change in human endotoxemia (Haimovich et al. 2010a). In addition to disruptions in circadian rhythms due to the activation of inflammatory machinery, circadian rhythms can be diminished in a critical care setting where there is constant activity and clinicians often aim at imposing constancy on physiological signals (Lowry 2009b).

To account for these circadian-immune linkages within a model of human endotoxemia, Scheff et al. (2010) explored the relationship between the central circadian clock in the suprachiasmatic nucleus and its putative regulation of peripheral immune function via centrally-released systemic hormones, such as cortisol and melatonin, and exploring established circadian pharmacokinetic/pharmacodynamic models (Chakraborty et al. 1999) related to these central circadian hormones. The propagation of these signals through the inflammatory network produced patterns in cytokine and hormone responses that corresponded with observed experimental data (Petrovsky et al. 1998), suggesting that this is a plausible mechanism for coupling between circadian rhythms and the inflammatory response. Interestingly, despite its phenomenological nature, the model predicted a circadian (time-of-day dependent) pattern in inflammatory responsiveness beginning to shed light on the cross-talk between the circadian clock and the immune system (Keller et al. 2009).

In addition to the aforementioned circadian patterns with 24 h periods, there are also important physiological rhythms at other frequencies. The circadian rhythm of the immunomodulatory hormone cortisol is fundamentally produced by circadian patterns in the amplitude of a faster pattern called an ultradian rhythm. Cortisol is

secreted in roughly hourly bursts that have garnered much interest in recent years towards unraveling their physiological implications (Lightman and Conway-Campbell 2010). Due to the rapid binding between activated glucocorticoid receptor (GR) and DNA (McNally et al. 2000), pulsatile patterns in transcriptional activity tracking glucocorticoid concentrations can be observed (Stavreva et al. 2009). This is likely to contribute to the broad transcriptional differences that were observed when comparing constant and oscillatory exposure of cells to glucocorticoids (McMaster et al. 2011). Based on these underlying biological principles, Scheff et al. (2011a) sought to understand how nonlinear ligand-receptor kinetics can lead to differential responses to ultradian and constant cortisol exposure. Furthermore, we investigated how altering key parameters of the model leads to perturbed ultradian patterns in homeostasis, illustrating how analysis of biological rhythms can give insight into underlying mechanisms (Scheff et al. 2012a). The stress responsiveness of the HPA axis was further tested by quantifying the peak levels of glucocorticoid-responsive genes in response to an acute inflammatory stimulus. Peak stress responsiveness was found to be proportional to the amplitude of ultradian rhythms, even when controlling for the mean values in homeostasis. This again illustrates how studying biological rhythms can lead to informative insights about the state and behavior of a physiological system.

Whereas circulating molecules like cytokines and hormones are important markers of inflammation, they do not reveal the entire inflammatory state of the host and they require invasive procedures for measurement, which complicates the high frequency sampling needed to quantify biological rhythms. This has motivated interest in noninvasive metrics that can correlate with disease severity in inflammation-linked disorders, most prominently heart rate variability (HRV) (Schmidt et al. 2001), roughly speaking the quantification of the variability of the time interval between successive heart beats.

Decreased HRV is a commonly-observed response in critically ill patients and thus has been studied with the goal of providing clinically actionable information about a patient through noninvasive means. However, there is still significant uncertainty in ascribing specific underlying mechanistic causes to observed patterns in HRV, and most clinical applications of HRV in this context are phenomenological. Human endotoxemia provides a controlled experimental setting to study the relationship between inflammation and the loss of HRV (Gholami et al. 2012; Godin et al. 1996; Rassias et al. 2005, 2011; Sayk et al. 2008; Alvarez et al. 2007; Jan et al. 2009, 2010; Kox et al. 2011). Based on this, we sought to formalize and extend these experimental observations through semi-mechanistic modeling of the effects of endotoxemia on the heart.

The sympathetic and parasympathetic branches of the autonomic nervous system converge at the sinoatrial (SA) node of the heart, and oscillations in the release of their corresponding autonomic neurotransmitters produce oscillatory patterns in the firing of action potentials at the SA node and thus the beating of the heart. Circadian rhythms exert a clear pattern on HR and HRV mediated by the autonomic nervous system. Much higher-frequency rhythms in HR can be categorized into two frequency bands (Akselrod et al. 1981; Task 1996): high frequency (HF) rhythms

ranging from 0.15 to 0.4 Hz driven largely by the respiratory sinus arrhythmia and transduced to the heart via the vagus nerve (Berntson et al. 1997); and low frequency (LF) rhythms ranging from 0.04 to 0.15 Hz driven in part by baroreflex-mediated fluctuations in blood pressure which respond to both sympathetic and parasympathetic modulation. While the power in each frequency band (LF and HF) gives some indication of the sympathetic and parasympathetic activities, their ratio is commonly used to quantify sympathovagal balance. These metrics are at best indirect and imprecise measures of autonomic activity (Karemaker 1999).

Driven by the desire to evaluate systems-level properties of biological oscillators through quantitative modeling (Novak and Tyson 2008), a heart rate and HRV regulation model of human endotoxemia based on multiple rhythmic signals driving the pattern of heart beats through a model of autonomic influence on the heart was proposed by Scheff et al. (2011b). The translation from a continuous oscillatory (activity of the ANS) system to a noisy discrete output (heartbeats) is an essential step in modeling a physiological process like the beating of the heart, which is fundamentally discrete. The resulting heartbeats were then analyzed to characterize time domain, frequency domain, and nonlinear metrics, all aimed at either gaining some specific physiological insight or optimizing the correlation of the HRV metric with a clinical outcome. Thus, based on the discrete output of our model, we highlighted discrepancies in responsiveness of different HRV metrics to endotoxemia. Such models lay the foundation of integrated models which merge the multiple scales involved in the inflammatory response and begin to relate cellular events with systemic host responses (Scheff et al. 2013b). Through increasingly detailed mechanistic modeling of HR and HRV in human endotoxemia, we continue to work towards understanding the biological processes linking inflammation and biological rhythms (Dick et al. 2012). Semi-mechanistic models were further explored to rationalize the likely permissive-suppressive inflammatory effects of cortisol as manifestations of the balance between pro- and anti-inflammatory characteristics induced by circadian rhythms (Mavroudis et al. 2012, 2013, 2014, 2015; Scheff et al. 2012b, 2013b). Figure 15.3 provides a broad overview of the continuum of model development, accounting for variety of the elements just described, with emphasis on inflammation.

15.3.6 Mechanistic Models of Inflammation Meet Systems Pharmacology

The preceding sections have placed major emphasis on modeling aspect of inflammation (or any disease for that matter). Therefore, we discussed approaches which aim at developing dynamic models characterizing the onset and evolution of the inflammatory response. From an intervention point of view, numerous studies

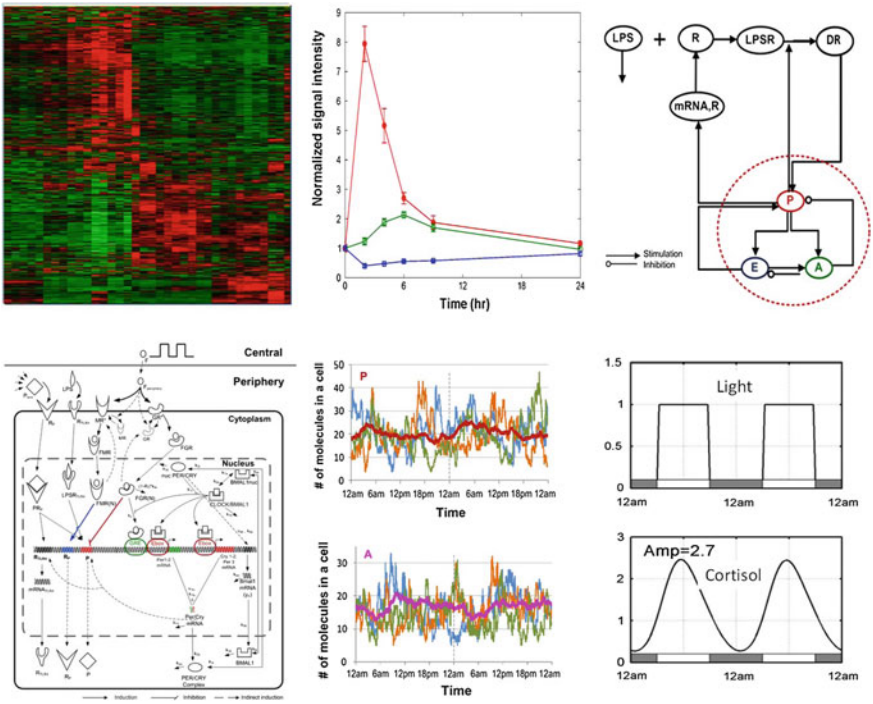

Fig. 15.3 Developing mathematical models of inflammation—from high-throughput data to (semi)mechanistic models: (*top row—left*) genomics data capturing the dynamics of numerous transcripts are clustered and annotated (Nguyen et al. 2011). (*Top row—middle and right*) Clustered profiles define emerging dynamics of coherent responses which can be used as surrogate variables for the development of simple and theoretical models (Foteinou et al. 2009b). (*Bottom row—left*) Detailed mechanistic information—including putative receptors and regulators—is embedded within broader structures resulting in detailed (semi)-mechanistic models in the form of ordinary differential equations (Scheff et al. 2011a, 2012a; Mavroudis et al. 2012, 2014, 2015; Foteinou et al. 2009a, 2010). (*Bottom row—middle*) Discrete and stochastic events in aforementioned networks can be captured and analyzed using agent based models (Dong et al. 2010; Nguyen et al. 2013). (*Bottom row—right*) Biological rhythms (circadian) can account for capturing underlying dynamics of inflammatory mediators (Scheff et al. 2010)

have attempted to delineate the mode of action of various drug, or other modulating agents (Iorio et al. 2010; Felmlee et al. 2012). Systems pharmacology (Bai et al. 2013) takes the systems view in order to further elucidate the systemic effects of a drug's efficacy and effects beyond the local site of action leading to the development of more comprehensive approach towards systems level PK/PD models aiming at understanding the relationship between drugs and physiology through mathematical modeling (Jusko 2013).

It is only natural then to appreciate the importance of early attempts to bridge the gap between disease progression and systems pharmacology models. Furthermore, a disease state is not a stable condition but rather one which intimately and closely

interacts with the therapeutic intervention. In that respect, linking disease progression and pharmacology is of paramount importance (Gao and Jusko 2012; Gao et al. 2011).

Earp et al. followed this paradigm to study the relationship between glucocorticoids and inflammation in a rat model of arthritis, based on their previous work on more traditional PK/PD modeling of glucocorticoids (Earp et al. 2008a, b). They used PK/PD modeling principles such as indirect response modeling and transit compartments to link key individual inflammatory mediators with changes in bone density and edema. Evaluating scenarios where different combinations of cytokines were inhibited or pharmacologically modulated shed some light on the redundancy in inflammatory signaling pathways and the complexity inherent in developing effective therapies. Additionally, they evaluated how different cytokines contribute to different aspects of disease. Along similar line Lon et al. (2012) further examined

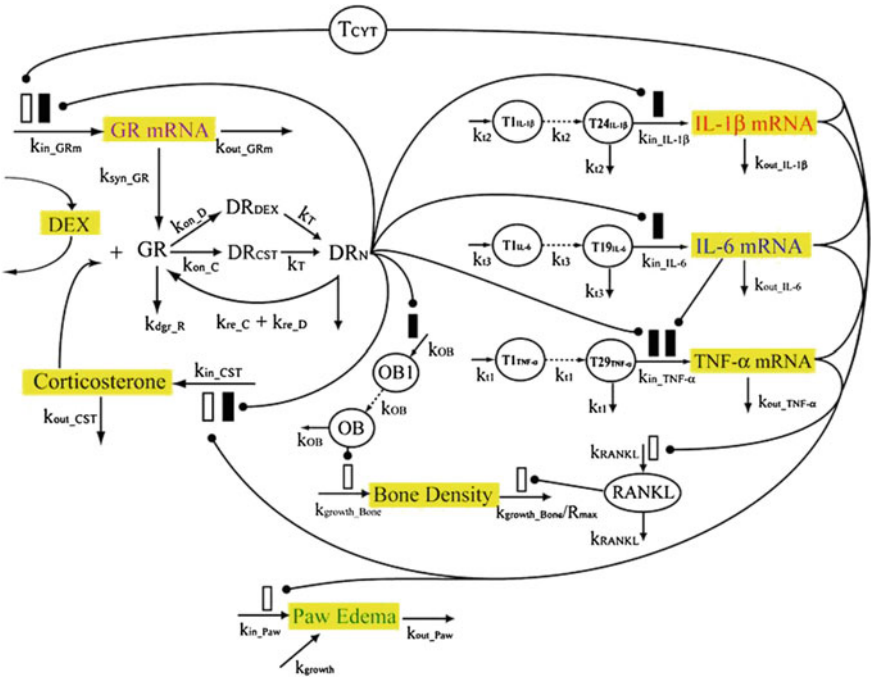

Fig. 15.4 Integrated Pharmacokinetic–Pharmacodynamic–Disease progression (arthritis) model: advanced models will incorporate a drug's PK/PD, the dynamics of disease mediators (cytokines such as IL-1, IL-6 and TNF), the regulation of the disease mediators by the drug, and the dynamics of disease markers (paw edema and bone density) as well as their regulation post drug administration (Earp et al. 2008a; Earp et al. 2008b) (© William J. Jusko, April 29, 2008, Modeling Corticosteroid Effects in a Rat Model of Rheumatoid Arthritis II: Mechanistic Pharmacodynamic Model for Dexamethasone Effects in Lewis Rats with Collagen-Induced Arthritis, The Journal of Pharmacology and Experimental Therapeutics Online, http://www.jpet.aspetjournals.org/)

the role of anti-inflammatory agents in the context of an inflammatory disease progression models. The basic elements of such a mathematical model are depicted in Fig. 15.4. Finally, of particular importance is the work presented in Meyer-Hermann et al. (2009) which evaluated the interplay between disease progression, pharmacologic treatment and biological rhythms.

15.4 Concluding Remarks: Challenges and Opportunities

A diverse set of models of inflammation are discussed above, varying in scope, complexity, mathematical foundations, and ultimate goals. From a broad perspective, the purpose of mathematical models fall into the same two categories that all experiments can be divided into: Basic and applied science. From a basic science perspective, we seek to identify the fundamental principles underlying a physiological system. Mathematical modeling clearly plays a role here, as any well understood system is supported by a well-studied model. In terms of more direct applications, systems biology of inflammation has the potential to ultimately improve clinical practice, not just through greater understanding of the basic science of inflammation, but also through advances in the context of model-based personalized medicine (Hood 2013) and in silico clinical trials (Foteinou et al. 2009c; Vodovotz 2010; Vodovotz et al. 2008). Continual feedback between theoretical and practical models of inflammation will continue to push the field forward in an attempt to develop integrated frameworks which couple cellular, physiological, pharmacologic, disease, and environmental models advancing the state of the art in clinical trials, Fig. 15.5. Particularly promising in that respect are results illustrating, in principle, how imminent transitions during the progression of a disease could be predicted using appropriate theoretical, modeling, and computational approaches (Scheff et al. 2013a). This work advocates the idea that it may not

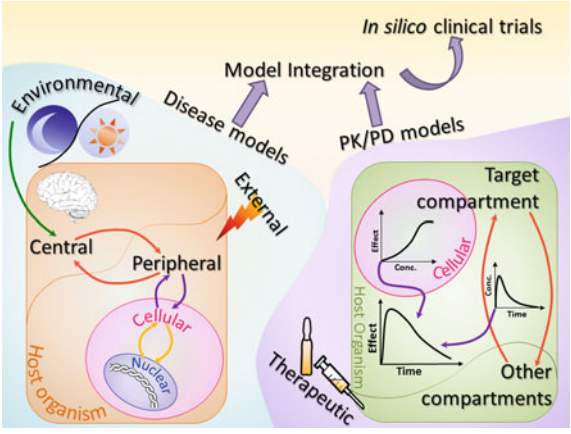

Fig. 15.5 From cellular mechanisms to in-silico clinical trials

be necessarily critical to estimate the exact state of the host during the evolution of the disease, and by extension following treatment, but rather assess whether improvement or deterioration is imminent.

Finally, a point of critical importance relates to long-term effects of either inflammatory diseases or the effects of anti-inflammatory treatments. The challenge, of course, is how to decipher the mechanistic causes of long term effects of persistent, albeit possibly low grade, perturbations of a biological system, which may open a possibility for alternative mechanisms activated as a result of long-term stress (Yang et al. 2011b; Paterson et al. 2003). Ultimately, disease and drug action models will need to be integrated with models accounting for not only the host (patient) and the drug, but also the environment (including social) the patient resides in, thus leading to more "holistic" approaches (Androulakis 2015; Vodovotz et al. 2013b; Androulakis 2014).

Acknowledgments The authors acknowledge financial support from NIH GM082974.

References

Akselrod S, Gordon D, Ubel FA, Shannon DC, Berger AC, Cohen RJ (1981) Power spectrum analysis of heart rate fluctuation: a quantitative probe of beat-to-beat cardiovascular control. Science 213(4504):220–222. doi:10.1126/science.6166045

Albert U (2010) The circadian clock. Springer, Berlin

Altman RB, Miller KS (2011) 2010 translational bioinformatics year in review. J Am Med Inform Assoc JAMIA 18(4):358–366. doi:10.1136/amiajnl-2011-000328

Alvarez SM, Katsamanis Karavidas M, Coyle SM, Lu SE, Macor M, Oikawa LO, Lehrer PM, Calvano SE, Lowry SF (2007) Low-dose steroid alters in vivo endotoxin-induced systemic inflammation but does not influence autonomic dysfunction. J Endotoxin Res 13(6):358–368

An G (2001) Agent-based computer simulation and sirs: building a bridge between basic science and clinical trials. Shock 16(4):266–273

An G (2004) In silico experiments of existing and hypothetical cytokine-directed clinical trials using agent-based modeling. Crit Care Med 32(10):2050–2060

An G (2008) Introduction of an agent-based multi-scale modular architecture for dynamic knowledge representation of acute inflammation. Theor Biol Med Model 5:11

An G (2009) A model of TLR4 signaling and tolerance using a qualitative, particle-event-based method: introduction of spatially configured stochastic reaction chambers (SCSRC). Math Biosci 217(1):43–52

An GC, Faeder JR (2009) Detailed qualitative dynamic knowledge representation using a BioNetGen model of TLR-4 signaling and preconditioning. Math Biosci 217(1):53–63

An G, Mi Q, Dutta-Moscato J, Vodovotz Y (2009) Agent-based models in translational systems biology. Wiley Interdiscip Rev Syst Biol Med 1(2):159–171

Androulakis IP (2014) A chemical engineer's perspective on health and disease. Comput Chem Eng 71:665–671. doi:10.1016/j.compchemeng.2014.09.007

Androulakis IP (2015) Systems engineering meets quantitative systems pharmacology: from low-level targets to engaging the host defenses. Wiley Interdiscip Rev Syst Biol Med 7(3):101–112. doi:10.1002/wsbm.1294

Bahcall OG (2005) Single cell resolution in regulation of gene expression. Mol Syst Biol 1:0015

Bai JPF, Fontana RJ, Price ND, Sangar V (2013) Systems pharmacology modeling: an approach to improving drug safety. Biopharm Drug Dispos. doi:10.1002/bdd.1871

Bailey AM, Thorne BC, Peirce SM (2007) Multi-cell agent-based simulation of the microvasculature to study the dynamics of circulating inflammatory cell trafficking. Ann Biomed Eng 35 (6):916–936

Baldazzi V, Castiglione F, Bernaschi M (2006) An enhanced agent based model of the immune system response. Cell Immunol 244(2):77–79

Berntson GG, Bigger JT Jr, Eckberg DL, Grossman P, Kaufmann PG, Malik M, Nagaraja HN, Porges SW, Saul JP, Stone PH, van der Molen MW (1997) Heart rate variability: origins, methods, and interpretive caveats. Psychophysiology 34(6):623–648

Blake WJ, Kaern M, Cantor CR, Collins JJ (2003) Noise in eukaryotic gene expression. Nature 422(6932):633–637

Bone RC (1996) Immunologic dissonance: a continuing evolution in our understanding of the systemic inflammatory response syndrome (SIRS) and the multiple organ dysfunction syndrome (MODS). Ann Intern Med 125(8):680–687

Bortolussi L, Policriti A (2008) Hybrid systems and biology. In: Bernardo M, Degano P, Zavattaro G (eds) Formal methods for computational systems biology, vol 5016., Lecture notes in computer science. Springer, Berlin, pp 424–448

Calvano SE, Xiao W, Richards DR, Felciano RM, Baker HV, Cho RJ, Chen RO, Brownstein BH, Cobb JP, Tschoeke SK, Miller-Graziano C, Moldawer LL, Mindrinos MN, Davis RW, Tompkins RG, Lowry SF, Inflamm and Host Response to Injury Large Scale Collab. Res. Program (2005) A network-based analysis of systemic inflammation in humans. Nature 437 (7061):1032–1037. doi:10.1038/nature03985

Carre JE, Singer M (2008) Cellular energetic metabolism in sepsis: the need for a systems approach. Biochim Biophys Acta 1777(7–8):763–771. doi:10.1016/j.bbabio.2008.04.024

Catron DM, Itano AA, Pape KA, Mueller DL, Jenkins MK (2004) Visualizing the first 50 hr of the primary immune response to a soluble antigen. Immunity 21(3):341–347

Celada F, Seiden PE (1992) A computer model of cellular interactions in the immune system. Immunol Today 13(2):56–62

Chakraborty A, Krzyzanski W, Jusko WJ (1999) Mathematical modeling of circadian cortisol concentrations using indirect response models: comparison of several methods. J Pharmacokinet Biopharm 27(1):23–43

Chavali AK, Gianchandani EP, Tung KS, Lawrence MB, Peirce SM, Papin JA (2008) Characterizing emergent properties of immunological systems with multi-cellular rule-based computational modeling. Trends Immunol 29(12):589–599

Chow CC, Clermont G, Kumar R, Lagoa C, Tawadrous Z, Gallo D, Betten B, Bartels J, Constantine G, Fink MP, Billiar TR, Vodovotz Y (2005) The acute inflammatory response in diverse shock states. Shock 24(1):74–84

Chrousos GP (2009) Stress and disorders of the stress system. Nat Rev Endocrinol 5(7):374–381. doi:10.1038/nrendo.2009.106

Clermont G, Bartels J, Kumar R, Constantine G, Vodovotz Y, Chow C (2004a) In silico design of clinical trials: a method coming of age. Crit Care Med 32(10):2061–2070

Clermont G, Chow C, Constantine G, Vodovotz Y, Bartels J (2004b) Mathematical and statistical modeling of acute inflammation. In: Banks D, McMorris F, Arabie P, Gaul W (eds) Classification, clustering, and data mining applications. Studies in classification, data analysis, and knowledge organisation. Springer, Berlin, pp 457–467

Coogan AN, Wyse CA (2008) Neuroimmunology of the circadian clock. Brain Res 1232:104–112

Coussens LM, Werb Z (2002) Inflammation and cancer. Nature 420(6917):860–867

Crome SQ, Clive B, Wang AY, Kang CY, Chow V, Yu J, Lai A, Ghahary A, Broady R, Levings MK (2010) Inflammatory effects of ex vivo human Th17 cells are suppressed by regulatory T cells. J Immunol 185(6):3199–3208. doi:10.4049/jimmunol.1000557

Cutolo M, Seriolo B, Craviotto C, Pizzorni C, Sulli A (2003) Circadian rhythms in RA. Ann Rheum Dis 62(7):593–596

Daun S, Rubin J, Vodovotz Y, Roy A, Parker R, Clermont G (2008) An ensemble of models of the acute inflammatory response to bacterial lipopolysaccharide in rats: results from parameter space reduction. J Theor Biol 253(4):843–853

Day J, Rubin J, Vodovotz Y, Chow CC, Reynolds A, Clermont G (2006) A reduced mathematical model of the acute inflammatory response II. Capturing scenarios of repeated endotoxin administration. J Theor Biol 242(1):237–256

Dick TE, Molkov YI, Nieman G, Hsieh YH, Jacono FJ, Doyle J, Scheff JD, Calvano SE, Androulakis IP, An G, Vodovotz Y (2012) Linking inflammation, cardiorespiratory variability, and neural control in acute inflammation via computational modeling. Front Physiol 3:222. doi:10.3389/fphys.2012.00222

Dong X, Foteinou PT, Calvano SE, Lowry SF, Androulakis IP (2010) Agent-based modeling of endotoxin-induced acute inflammatory response in human blood leukocytes. PLoS One 5(2): e9249

Earp JC, Dubois DC, Molano DS, Pyszczynski NA, Almon RR, Jusko WJ (2008a) Modeling corticosteroid effects in a rat model of rheumatoid arthritis II: Mechanistic pharmacodynamic model for dexamethasone effects in Lewis rats with collagen-induced arthritis. J Pharmacol Exp Ther 326(2):546–554. doi:10.1124/jpet.108.137414

Earp JC, Dubois DC, Molano DS, Pyszczynski NA, Keller CE, Almon RR, Jusko WJ (2008b) Modeling corticosteroid effects in a rat model of rheumatoid arthritis I: Mechanistic disease progression model for the time course of collagen-induced arthritis in Lewis rats. J Pharmacol Exp Ther 326(2):532–545. doi:10.1124/jpet.108.137372

Felmlee MA, Morris ME, Mager DE (2012) Mechanism-based pharmacodynamic modeling. Methods Mol Biol 929:583–600. doi:10.1007/978-1-62703-050-2_21

Fisher ES, Lauffenburger DA (1990) Analysis of the effects of immune cell motility and chemotaxis on target elimination dynamics. Math Biosci 98(1):73–102

Folcik VA, An GC, Orosz CG (2007) The basic immune simulator: an agent-based model to study the interactions between innate and adaptive immunity. Theor Biol Med Model 4:39

Foteinou PT, Calvano SE, Lowry SF, Androulakis IP (2009a) In silico simulation of corticosteroids effect on an NFkB- dependent physicochemical model of systemic inflammation. PLoS One 4(3):e4706

Foteinou PT, Calvano SE, Lowry SF, Androulakis IP (2009b) Modeling endotoxin-induced systemic inflammation using an indirect response approach. Math Biosci 217(1):27–42

Foteinou PT, Calvano SE, Lowry SF, Androulakis IP (2009c) Translational potential of systems-based models of inflammation. Clin Transl Sci 2(1):85–89

Foteinou PT, Calvano SE, Lowry SF, Androulakis IP (2010) Multiscale model for the assessment of autonomic dysfunction in human endotoxemia. Physiol Genomics 42(1):5–19

Gao W, Jusko WJ (2012) Modeling disease progression and rosiglitazone intervention in type 2 diabetic Goto-Kakizaki rats. J Pharmacol Exp Ther 341(3):617–625. doi:10.1124/jpet.112.192419

Gao W, Bihorel S, DuBois DC, Almon RR, Jusko WJ (2011) Mechanism-based disease progression modeling of type 2 diabetes in Goto-Kakizaki rats. J Pharmacokinet Pharmacodyn 38(1):143–162. doi:10.1007/s10928-010-9182-0

Gholami M, Mazaheri P, Mohamadi A, Dehpour T, Safari F, Hajizadeh S, Moore KP, Mani AR (2012) Endotoxemia is associated with partial uncoupling of cardiac pacemaker from cholinergic neural control in rats. Shock 37(2):219–227

Godin PJ, Fleisher LA, Eidsath A, Vandivier RW, Preas HL, Banks SM, Buchman TG, Suffredini AF (1996) Experimental human endotoxemia increases cardiac regularity: results from a prospective, randomized, crossover trial. Crit Care Med 24(7):1117–1124

Haffner SM (2006) The metabolic syndrome: inflammation, diabetes mellitus, and cardiovascular disease. Am J Cardiol 97(2A):3A–11A

Haimovich B, Calvano J, Haimovich AD, Calvano SE, Coyle SM, Lowry SF (2010a) In vivo endotoxin synchronizes and suppresses clock gene expression in human peripheral blood leukocytes. Crit Care Med 38(3):751–758. doi:10.1097/CCM.0b013e3181cd131c

Haimovich B, Reddell MT, Calvano JE, Calvano SE, Macor MA, Coyle SM, Lowry SF (2010b) A novel model of common Toll-like receptor 4- and injury-induced transcriptional themes in human leukocytes. Crit Care 14(5):R177. doi:10.1186/cc9283

Hood L (2013) Systems biology and p4 medicine: past, present, and future. Rambam Maimonides Med J 4(2):e0012. doi:10.5041/RMMJ.10112

Iorio F, Bosotti R, Scacheri E, Belcastro V, Mithbaokar P, Ferriero R, Murino L, Tagliaferri R, Brunetti-Pierri N, Isacchi A, di Bernardo D (2010) Discovery of drug mode of action and drug repositioning from transcriptional responses. Proc Natl Acad Sci USA 107(33):14621–14626. doi:10.1073/pnas.1000138107

Jan BU, Coyle SM, Oikawa LO, Lu SE, Calvano SE, Lehrer PM, Lowry SF (2009) Influence of acute epinephrine infusion on endotoxin-induced parameters of heart rate variability: a randomized controlled trial. Ann Surg 249(5):750–756

Jan BU, Coyle SM, Macor MA, Reddell M, Calvano SE, Lowry SF (2010) Relationship of basal heart rate variability to in vivo cytokine responses after endotoxin exposure. Shock 33(4):363–368

Jayaraman A, Yarmush ML, Roth CM (2005) Evaluation of an in vitro model of hepatic inflammatory response by gene expression profiling. Tissue Eng 11(1–2):50–63. doi:10.1089/ten.2005.11.50

Jusko WJ (2013) Moving from basic toward systems pharmacodynamic models. J Pharm Sci 102 (9):2930–2940

Kaern M, Elston TC, Blake WJ, Collins JJ (2005) Stochasticity in gene expression: from theories to phenotypes. Nat Rev Genet 6(6):451–464

Kamisoglu K, Calvano SE, Coyle SM, Corbett SA, Androulakis IP (2014) Integrated transcriptional and metabolic profiling in human endotoxemia. Shock 42(6):499–508. doi:10.1097/SHK.0000000000000248

Kamisoglu K, Haimovich B, Calvano SE, Coyle SM, Corbett SA, Langley RJ, Kingsmore SF, Androulakis IP (2015a) Human metabolic response to systemic inflammation: assessment of the concordance between experimental endotoxemia and clinical cases of sepsis/SIRS. Crit Care 19:71. doi:10.1186/s13054-015-0783-2

Kamisoglu K, Sukumaran S, Nouri-Nigjeh E, Tu C, Li J, Shen X, Duan X, Qu J, Almon RR, DuBois DC, Jusko WJ, Androulakis IP (2015b) Tandem analysis of transcriptome and proteome changes after a single dose of corticosteroid: a systems approach to liver function in pharmacogenomics. OMICS 19(2):80–91. doi:10.1089/omi.2014.0130

Karemaker JM (1999) Autonomic integration: the physiological basis of cardiovascular variability. J Physiol 517(Pt 2):316

Keller M, Mazuch J, Abraham U, Eom GD, Herzog ED, Volk HD, Kramer A, Maier B (2009) A circadian clock in macrophages controls inflammatory immune responses. Proc Natl Acad Sci USA 106(50):21407–21412. doi:10.1073/pnas.0906361106

Kilfoil ML, Lasko P, Abouheif E (2009) Stochastic variation: from single cells to superorganisms. HFSP J 3(6):379–385

Klipp E (2005) Systems biology in practice: concepts, implementation and application. Wiley-VCH, Weinheim

Kox M, Ramakers BP, Pompe JC, van der Hoeven JG, Hoedemaekers CW, Pickkers P (2011) Interplay between the acute inflammatory response and heart rate variability in healthy human volunteers. Shock 36(2):115–120

Kumar R, Clermont G, Vodovotz Y, Chow CC (2004) The dynamics of acute inflammation. J Theor Biol 230(2):145–155

Lagoa CE, Bartels J, Baratt A, Tseng G, Clermont G, Fink MP, Billiar TR, Vodovotz Y (2006) The role of initial trauma in the host's response to injury and hemorrhage: insights from a correlation of mathematical simulations and hepatic transcriptomic analysis. Shock 26(6):592–600

Langley RJ, Tsalik EL, van Velkinburgh JC, Glickman SW, Rice BJ, Wang C, Chen B, Carin L, Suarez A, Mohney RP, Freeman DH, Wang M, You J, Wulff J, Thompson JW, Moseley MA, Reisinger S, Edmonds BT, Grinnell B, Nelson DR, Dinwiddie DL, Miller NA, Saunders CJ, Soden SS, Rogers AJ, Gazourian L, Fredenburgh LE, Massaro AF, Baron RM, Choi AM, Corey GR, Ginsburg GS, Cairns CB, Otero RM, Fowler VG Jr, Rivers EP, Woods CW,

Kingsmore SF (2013) An integrated clinico-metabolomic model improves prediction of death in sepsis. Sci Transl Med 5(195):195ra195. doi:10.1126/scitranslmed.3005893

Langley RJ, Tipper JL, Bruse S, Baron RM, Tsalik EL, Huntley J, Rogers AJ, Jaramillo RJ, O'Donnell D, Mega WM, Keaton M, Kensicki E, Gazourian L, Fredenburgh LE, Massaro AF, Otero RM, Fowler VG Jr, Rivers EP, Woods CW, Kingsmore SF, Sopori ML, Perrella MA, Choi AM, Harrod KS (2014) Integrative "omic" analysis of experimental bacteremia identifies a metabolic signature that distinguishes human sepsis from systemic inflammatory response syndromes. Am J Respir Crit Care Med 190(4):445–455. doi:10.1164/rccm.201404-0624OC

Laroux FS (2004) Mechanisms of inflammation: the good, the bad and the ugly. Front Biosci J Virtual Libr 9:3156–3162

Lauffenburger DA, Kennedy CR (1981) Analysis of a lumped model for tissue inflammation dynamics. Math Biosci 53(3–4):189–221. doi:10.1016/0025-5564(81)90018-3

Lauffenburger DA, Kennedy CR (1983) Localized bacterial infection in a distributed model for tissue inflammation. J Math Biol 16(2):141–163

Lehrer P, Eddie D (2013) Dynamic processes in regulation and some implications for biofeedback and biobehavioral interventions. Appl Psychophysiol Biofeedback 38(2):143–155. doi:10.1007/s10484-013-9217-6

Levi F, Schibler U (2007) Circadian rhythms: mechanisms and therapeutic implications. Annu Rev Pharmacol Toxicol 47:593–628. doi:10.1146/annurev.pharmtox.47.120505.105208

Lightman SL, Conway-Campbell BL (2010) The crucial role of pulsatile activity of the HPA axis for continuous dynamic equilibration. Nat Rev Neurosci 11(10):710–718

Lissoni P, Rovelli F, Brivio F, Brivio O, Fumagalli L (1998) Circadian secretions of IL-2, IL-12, IL-6 and IL-10 in relation to the light/dark rhythm of the pineal hormone melatonin in healthy humans. Nat Immun 16(1):1–5

Lon HK, Liu D, Jusko WJ (2012) Pharmacokinetic/pharmacodynamic modeling in inflammation. Crit Rev Biomed Eng 40(4):295–312

Lowry SF (2009a) The evolution of an inflammatory response. Surg Infect 10(5):419–425. doi:10.1089/sur.2009.018

Lowry SF (2009b) The stressed host response to infection: the disruptive signals and rhythms of systemic inflammation. Surg Clin N Am 89(2):311–326, vii

Lowry SF, Calvano SE (2008) Challenges for modeling and interpreting the complex biology of severe injury and inflammation. J Leukoc Biol 83(3):553–557. doi:10.1189/jlb.0607377

Luft VC, Schmidt MI, Pankow JS, Couper D, Ballantyne CM, Young JH, Duncan BB (2013) Chronic inflammation role in the obesity-diabetes association: a case-cohort study. Diabetol metab Syndr 5(1):31. doi:10.1186/1758-5996-5-31

Mavroudis PD, Scheff JD, Calvano SE, Lowry SF, Androulakis IP (2012) Entrainment of peripheral clock genes by cortisol. Physiol Genomics 44(11):607–621. doi:10.1152/physiolgenomics.00001.2012

Mavroudis PD, Scheff JD, Calvano SE, Androulakis IP (2013) Systems biology of circadian-immune interactions. J Innate Immun 5(2):153–162. doi:10.1159/000342427

Mavroudis PD, Corbett SA, Calvano SE, Androulakis IP (2014) Mathematical modeling of light-mediated HPA axis activity and downstream implications on the entrainment of peripheral clock genes. Physiol Genomics 46(20):766–778. doi:10.1152/physiolgenomics.00026.2014

Mavroudis PD, Corbett SA, Calvano SE, Androulakis IP (2015) Circadian characteristics of permissive and suppressive effects of cortisol and their role in homeostasis and the acute inflammatory response. Math Biosci 260:54–64. doi:10.1016/j.mbs.2014.10.006

McDunn JE, Husain KD, Polpitiya AD, Burykin A, Ruan J, Li Q, Schierding W, Lin N, Dixon D, Zhang W, Coopersmith CM, Dunne WM, Colonna M, Ghosh BK, Cobb JP (2008) Plasticity of the systemic inflammatory response to acute infection during critical illness: development of the riboleukogram. PLoS One 3(2):e1564. doi:10.1371/journal.pone.0001564

McMaster A, Jangani M, Sommer P, Han N, Brass A, Beesley S, Lu W, Berry A, Loudon A, Donn R, Ray DW (2011) Ultradian cortisol pulsatility encodes a distinct, biologically important signal. PLoS One 6(1):e15766

McNally JG, Muller WG, Walker D, Wolford R, Hager GL (2000) The glucocorticoid receptor: rapid exchange with regulatory sites in living cells. Science 287(5456):1262–1265

Meier-Schellersheim M, Xu X, Angermann B, Kunkel EJ, Jin T, Germain RN (2006) Key role of local regulation in chemosensing revealed by a new molecular interaction-based modeling method. PLoS Comput Biol 2(7):e82

Meyer-Hermann M, Figge MT, Straub RH (2009) Mathematical modeling of the circadian rhythm of key neuroendocrine-immune system players in rheumatoid arthritis: a systems biology approach. Arthritis Rheum 60(9):2585–2594. doi:10.1002/art.24797

Mi Q, Riviere B, Clermont G, Steed DL, Vodovotz Y (2007) Agent-based model of inflammation and wound healing: insights into diabetic foot ulcer pathology and the role of transforming growth factor-beta1. Wound Repair Regen 15(5):671–682

Mi Q, Constantine G, Ziraldo C, Solovyev A, Torres A, Namas R, Bentley T, Billiar TR, Zamora R, Puyana JC, Vodovotz Y (2011) A dynamic view of trauma/hemorrhage-induced inflammation in mice: principal drivers and networks. PLoS One 6(5):e19424. doi:10.1371/journal.pone.0019424

Nguyen TT, Foteinou PT, Calvano SE, Lowry SF, Androulakis IP (2011) Computational identification of transcriptional regulators in human endotoxemia. PLoS One 6(5):e18889. doi:10.1371/journal.pone.0018889

Nguyen TT, Calvano SE, Lowry SF, Androulakis IP (2013) An agent-based model of cellular dynamics and circadian variability in human endotoxemia. PLoS One 8(1):e55550. doi:10.1371/journal.pone.0055550

Nieman G, Brown D, Sarkar J, Kubiak B, Ziraldo C, Dutta-Moscato J, Vieau C, Barclay D, Gatto L, Maier K, Constantine G, Billiar TR, Zamora R, Mi Q, Chang S, Vodovotz Y (2012) A two-compartment mathematical model of endotoxin-induced inflammatory and physiologic alterations in swine. Crit Care Med 40(4):1052–1063

Niepel M, Spencer SL, Sorger PK (2009) Non-genetic cell-to-cell variability and the consequences for pharmacology. Curr Opin Chem Biol 13(5–6):556–561

Novak B, Tyson JJ (2008) Design principles of biochemical oscillators. Nat Rev Mol Cell Biol 9 (12):981–991

Ovacik MA, Androulakis IP (2013) Enzyme sequence similarity improves the reaction alignment method for cross-species pathway comparison. Toxicol Appl Pharmacol 271(3):363–371. doi:10.1016/j.taap.2010.09.009

Paterson HM, Murphy TJ, Purcell EJ, Shelley O, Kriynovich SJ, Lien E, Mannick JA, Lederer JA (2003) Injury primes the innate immune system for enhanced Toll-like receptor reactivity. J Immunol 171(3):1473–1483

Petrovsky N, McNair P, Harrison LC (1998) Diurnal rhythms of pro-inflammatory cytokines: regulation by plasma cortisol and therapeutic implications. Cytokine 10(4):307–312

Polpitiya AD, McDunn JE, Burykin A, Ghosh BK, Cobb JP (2009) Using systems biology to simplify complex disease: immune cartography. Crit Care Med 37(1 Suppl):S16–S21. doi:10.1097/CCM.0b013e3181920cb0

Prince JM, Levy RM, Bartels J, Baratt A, Kane JM 3rd, Lagoa C, Rubin J, Day J, Wei J, Fink MP, Goyert SM, Clermont G, Billiar TR, Vodovotz Y (2006) In silico and in vivo approach to elucidate the inflammatory complexity of CD14-deficient mice. Mol Med 12(4–6):88–96

Ramakrishnan R, DuBois DC, Almon RR, Pyszczynski NA, Jusko WJ (2002) Fifth-generation model for corticosteroid pharmacodynamics: application to steady-state receptor down-regulation and enzyme induction patterns during seven-day continuous infusion of methylprednisolone in rats. J Pharmacokinet Pharmacodyn 29(1):1–24

Raser JM, O'Shea EK (2005) Noise in gene expression: origins, consequences, and control. Science 309(5743):2010–2013

Rassias AJ, Holzberger PT, Givan AL, Fahrner SL, Yeager MP (2005) Decreased physiologic variability as a generalized response to human endotoxemia. Crit Care Med 33(3):512–519

Rassias AJ, Guyre PM, Yeager MP (2011) Hydrocortisone at stress-associated concentrations helps maintain human heart rate variability during subsequent endotoxin challenge. J Crit Care

Reynolds A, Rubin J, Clermont G, Day J, Vodovotz Y, Bard Ermentrout G (2006) A reduced mathematical model of the acute inflammatory response: I. Derivation of model and analysis of anti-inflammation. J Theor Biol 242(1):220–236

Rosenfeld N, Young JW, Alon U, Swain PS, Elowitz MB (2005) Gene regulation at the single-cell level. Science 307(5717):1962–1965

Rowland M (2013) Physiologically-based pharmacokinetic (PBPK) modeling and simulations principles, methods, and applications in the pharmaceutical industry. CPT Pharmacomet Syst Pharmacol 2:e55. doi:10.1038/psp.2013.29

Sayk F, Vietheer A, Schaaf B, Wellhoener P, Weitz G, Lehnert H, Dodt C (2008) Endotoxemia causes central downregulation of sympathetic vasomotor tone in healthy humans. Am J Physiol Regul Integr Comp Physiol 295(3):R891–R898

Scheff JD, Calvano SE, Lowry SF, Androulakis IP (2010) Modeling the influence of circadian rhythms on the acute inflammatory response. J Theor Biol 264(3):1068–1076

Scheff JD, Kosmides AK, Calvano SE, Lowry SF, Androulakis IP (2011a) Pulsatile glucocorticoid secretion: origins and downstream effects. IEEE Tran Bio-med Eng 58(12):3504–3507. doi:10.1109/TBME.2011.2162236

Scheff JD, Mavroudis PD, Calvano SE, Lowry SF, Androulakis IP (2011b) Modeling autonomic regulation of cardiac function and heart rate variability in human endotoxemia. Physiol Genomics 43(16):951–964

Scheff JD, Calvano SE, Lowry SF, Androulakis IP (2012a) Transcriptional implications of ultradian glucocorticoid secretion in homeostasis and in the acute stress response. Physiol Genomics 44(2):121–129. doi:10.1152/physiolgenomics.00128.2011

Scheff JD, Mavroudis PD, Foteinou PT, Calvano SE, Androulakis IP (2012b) Modeling physiologic variability in human endotoxemia. Crit Rev Biomed Eng 40(4):313–322

Scheff JD, Calvano SE, Androulakis IP (2013a) Predicting critical transitions in a model of systemic inflammation. J Theor Biol 338C:9–15. doi:10.1016/j.jtbi.2013.08.011

Scheff JD, Mavroudis PD, Calvano SE, Androulakis IP (2013b) Translational applications of evaluating physiologic variability in human endotoxemia. J Clin Monit Comput 27(4):405–415. doi:10.1007/s10877-012-9418-1

Schmidt HB, Werdan K, Muller-Werdan U (2001) Autonomic dysfunction in the ICU patient. Curr Opin Crit Care 7(5):314–322

Segel L (1984) Modeling dynamic phenomena in cellular and molecualr biology. Camrbidge University Press, Cambridge, MA

Segel LA (1998) Multiple attractors in immunology: theory and experiment. Biophys Chem 72(1–2):223–230

Segel LA, Bar-Or RL (1999) On the role of feedback in promoting conflicting goals of the adaptive immune system. J Immunol 163(3):1342–1349

Segel LA, Cohen IR (eds) (2001) Design principles for the immune system and other distributed autonomous systems. Oxford University Press, Oxford

Seok J, Warren HS, Cuenca AG, Mindrinos MN, Baker HV, Xu W, Richards DR, McDonald-Smith GP, Gao H, Hennessy L, Finnerty CC, Lopez CM, Honari S, Moore EE, Minei JP, Cuschieri J, Bankey PE, Johnson JL, Sperry J, Nathens AB, Billiar TR, West MA, Jeschke MG, Klein MB, Gamelli RL, Gibran NS, Brownstein BH, Miller-Graziano C, Calvano SE, Mason PH, Cobb JP, Rahme LG, Lowry SF, Maier RV, Moldawer LL, Herndon DN, Davis RW, Xiao W, Tompkins RG, Inflammation, Host Response to Injury, L.S.C.R.P. (2013) Genomic responses in mouse models poorly mimic human inflammatory diseases. Proc Natl Acad Sci USA 110(9):3507–3512. doi:10.1073/pnas.1222878110

Southerland JH, Taylor GW, Moss K, Beck JD, Offenbacher S (2006) Commonality in chronic inflammatory diseases: periodontitis, diabetes, and coronary artery disease. Periodontology 40(1):130–143. doi:10.1111/j.1600-0757.2005.00138.x

Stavreva DA, Wiench M, John S, Conway-Campbell BL, McKenna MA, Pooley JR, Johnson TA, Voss TC, Lightman SL, Hager GL (2009) Ultradian hormone stimulation induces glucocorticoid receptor-mediated pulses of gene transcription. Nat Cell Biol 11(9):1093–1102

Sternberg EM (2006) Neural regulation of innate immunity: a coordinated nonspecific host response to pathogens. Nat Rev Immunol 6(4):318–328

Sukumaran S, Almon RR, DuBois DC, Jusko WJ (2010) Circadian rhythms in gene expression: relationship to physiology, disease, drug disposition and drug action. Adv Drug Deliv Rev 62 (9–10):904–917

Task Force of the European Society of Cardiology and the North American Society of Pacing and Electrophysiology (1996) Task: heart rate variability: standards of measurement, physiological interpretation and clinical use. Circulation 93(5):1043–1065

Torres A, Bentley T, Bartels J, Sarkar J, Barclay D, Namas R, Constantine G, Zamora R, Puyana JC, Vodovotz Y (2009) Mathematical modeling of posthemorrhage inflammation in mice: studies using a novel, computer-controlled, closed-loop hemorrhage apparatus. Shock 32 (2):172–178

Tsalik EL, Langley RJ, Dinwiddie DL, Miller NA, Yoo B, van Velkinburgh JC, Smith LD, Thiffault I, Jaehne AK, Valente AM, Henao R, Yuan X, Glickman SW, Rice BJ, McClain MT, Carin L, Corey GR, Ginsburg GS, Cairns CB, Otero RM, Fowler VG Jr, Rivers EP, Woods CW, Kingsmore SF (2014) An integrated transcriptome and expressed variant analysis of sepsis survival and death. Genome Med 6(11):111. doi:10.1186/s13073-014-0111-5

Ullah M, Wolkenhauer O (2010) Stochastic approaches in systems biology. Wiley Interdiscip Rev Syst Biol Med 2(4):385–397. doi:10.1002/wsbm.78

van der Poll T (2000) Effects of catecholamines on the inflammatory response. Sepsis 4:159–167

van der Poll T, Barber AE, Coyle SM, Lowry SF (1996a) Hypercortisolemia increases plasma interleukin-10 concentrations during human endotoxemia–a clinical research center study. J Clin Endocrinol Metab 81(10):3604–3606

van der Poll T, Coyle SM, Barbosa K, Braxton CC, Lowry SF (1996b) Epinephrine inhibits tumor necrosis factor-alpha and potentiates interleukin 10 production during human endotoxemia. J Clin Invest 97(3):713–719

Vodovotz Y (2010) Translational systems biology of inflammation and healing. Wound Repair Regen 18(1):3–7

Vodovotz Y, An G (2010) Systems biology and inflammation. Methods Mol Biol 662:181–201

Vodovotz Y, An G (eds) (2013) Complex systems and computational biology approaches to acute inflammation. Springer, Berlin

Vodovotz Y, Csete M, Bartels J, Chang S, An G (2008) Translational systems biology of inflammation. PLoS Comput Biol 4(4):e1000014

Vodovotz Y, An G, Androulakis IP (2013a) A systems engineering perspective on homeostasis and disease. Front Bioeng Biotechnol. doi:10.3389/fbioe.2013.00006

Vodovotz Y, An G, Androulakis IP (2013b) A systems engineering perspective on homeostasis and disease. Front Bioeng Biotechnol. doi:10.3389/fbioe.2013.00006

Warrender C, Forrest S, Koster F (2006) Modeling intercellular interactions in early Mycobacterium infection. Bull Math Biol 68(8):2233–2261

Webb DR (2014) Animal models of human disease: inflammation. Biochem Pharmacol 87 (1):121–130. doi:10.1016/j.bcp.2013.06.014

Xiao W, Mindrinos MN, Seok J, Cuschieri J, Cuenca AG, Gao H, Hayden DL, Hennessy L, Moore EE, Minei JP, Bankey PE, Johnson JL, Sperry J, Nathens AB, Billiar TR, West MA, Brownstein BH, Mason PH, Baker HV, Finnerty CC, Jeschke MG, Lopez MC, Klein MB, Gamelli RL, Gibran NS, Arnoldo B, Xu W, Zhang Y, Calvano SE, McDonald-Smith GP, Schoenfeld DA, Storey JD, Cobb JP, Warren HS, Moldawer LL, Herndon DN, Lowry SF, Maier RV, Davis RW, Tompkins RG, Inflammation, Host Response to Injury Large-Scale Collaborative Research, P. (2011) A genomic storm in critically injured humans. J Exp Med 208(13):2581–2590. doi:10.1084/jem.20111354

Yang EH, Almon RR, Dubois DC, Jusko WJ, Androulakis IP (2009) Identification of global transcriptional dynamics. PLoS One 4(7):e5992

Yang Q, Berthiaume F, Androulakis IP (2011a) A quantitative model of thermal injury-induced acute inflammation. Math Biosci 229(2):135–148. doi:10.1016/j.mbs.2010.08.003

Yang Q, Calvano SE, Lowry SF, Androulakis IP (2011b) A dual negative regulation model of Toll-like receptor 4 signaling for endotoxin preconditioning in human endotoxemia. Math Biosci 232(2):151–163. doi:10.1016/j.mbs.2011.05.005

Zenker S, Clermont G, Pinsky MR (2007a) Using mathematical models to improve the utility of quantitative ICU data. In: Vincent J-L (ed) Intensive care medicine. Springer, New York, pp 479–492

Zenker S, Rubin J, Clermont G (2007b) From inverse problems in mathematical physiology to quantitative differential diagnoses. PLoS Comput Biol 3(11):e204. doi:10.1371/journal.pcbi.0030204

Chapter 16
Systems Pharmacology of Tyrosine Kinase Inhibitor-Associated Toxicities

Yoshiaki Kariya, Masashi Honma and Hiroshi Suzuki

Abstract Tyrosine kinase inhibitors (TKIs) are designed to exhibit marked efficacy against cancer progression, based on accumulated molecular knowledge. The administration of TKIs is associated with much lower general toxicities (such as pancytopenia and gastrointestinal tract disturbance) than the administration of classical cytotoxic anti-tumor agents. However, TKIs provoke certain adverse reactions, which cannot be explained by the molecular mechanisms known at the time of drug development. Unfortunately, these unfavorable events often force the discontinuation of TKI treatment, with a typical worsening of therapeutic outcomes. Therefore, elucidating the molecular mechanisms behind TKI-related adverse reactions is a critical task in current and future chemotherapeutic drug management. Here, we provide a concrete mechanistic investigation of the adverse reactions of erlotinib, a TKI prototype, using a systems pharmacology-based approach. The molecular mechanism of erlotinib remains largely unknown, probably because there has been no unbiased drug analysis or account taken of the information available in numerous archives. In this study, we separated the mechanism of skin inflammation, a prominent erlotinib-mediated adverse reaction, into multiple pharmacokinetic/pharmacodynamic layers constituting drug responses. Importantly, an examination of the candidate mechanisms associated with each layer effectively extracted mechanisms from a myriad of contenders, enabling the design of polished "wet" experiments for further confirmation. This strategy is conceptually applicable to drugs other than erlotinib, and might facilitate the mechanistic exploration of the adverse reactions of cancer drugs in general.

Y. Kariya · M. Honma · H. Suzuki (✉)
Department of Pharmacy, The University of Tokyo Hospital,
7-3-1, Hongo, Bunkyo-Ku, Tokyo 113-8655, Japan
e-mail: suzukihi-tky@umin.ac.jp

Y. Kariya · M. Honma · H. Suzuki (✉)
Department of Pharmacy, The University of Tokyo Hospital,
7-3-1, Hongo, Bunkyo-Ku, Tokyo 113-8655, Japan
e-mail: suzukihi-tky@umin.ac.jp

M. Honma
Laboratory of Pharmacology and Pharmacokinetics, Faculty of Medicine,
The University of Tokyo Hospital, 7-3-1, Hongo, Bunkyo-Ku, Tokyo 113-8655, Japan

D.E. Mager and H.H.C. Kimko (eds.), *Systems Pharmacology and Pharmacodynamics*,
AAPS Advances in the Pharmaceutical Sciences Series 23,
DOI 10.1007/978-3-319-44534-2_16

Keywords Oncogene · Erlotinib · Skin inflammation · Protein linkage network

16.1 Development of Molecularly Targeted Drugs

Since the 1990s, many genes involved in the initiation of oncogenic events and the promotion of tumor growth have been identified (Hornberg et al. 2006; Futreal et al. 2004; Vogelstein and Kinzler 2004), which has led to the development of molecularly targeted drugs against these genes (Khuri and Cohen 2004; Kim and Murren 2002; Herbst and Bunn 2003). Among such drugs, several low molecular weight compounds targeting receptor tyrosine kinases and non-receptor tyrosine kinases are now clinically employed, and exhibit the great advantage of oral bioavailability coupled with good clinical outcomes (Herbst and Bunn 2003; Sridhar et al. 2003). For example, gefitinib, erlotinib, and lapatinib, which all belong to the epidermal growth factor receptor (EGFR) family of tyrosine kinase inhibitors (TKIs), are often used for the treatment of non-small cell lung cancer (Sridhar et al. 2003). In addition, assorted monoclonal antibodies against protein products derived from these genes are also utilized as drugs (e.g., cetuximab and panitumumab) to treat many kinds of cancer (Sridhar et al. 2003; Heymach et al. 2006). These treatment-related achievements strongly indicate the efficacy of molecularly targeted drugs.

Because TKIs were originally developed as molecularly targeted drugs, investigators expected that these agents would show high specificity against primary target molecules. However, TKIs often inhibit several other off-target kinases. For instance, imatinib was developed to inhibit the breakpoint cluster region-Abelson murine leukemia viral oncogene homolog Bcr-Abl, which causes chronic myelocytic leukemia; however, imatinib also inhibits c-kit and is thus used also to constrain the growth of c-kit-positive gastrointestinal stromal tumors (Tuveson et al. 2001). Furthermore, sunitinib, a drug used for the treatment of renal cell carcinoma, blocks the actions of multiple kinases such as vascular endothelial growth factor receptor-2, platelet-derived growth factor receptor-β (PDGFR-β), and c-kit, and exhibits its anti-cancer potential through the integrative suppression of tumor growth and angiogenesis (Mendel et al. 2003; Motzer et al. 2006). These observations suggest that these drugs inhibit not one, but several kinases at the same time.

On the other hand, adverse reactions that are unlikely to occur as an extension of beneficial anti-tumor effects are suspected to be caused by the blockade of off-target kinases, which are not the intended pharmacological targets of TKIs. In this regard, more than 50 % of patients receiving imatinib were found to exhibit decreases in serum phosphate and calcium levels in a recent study (Berman et al. 2006). These results may be explained by observations showing that imatinib inhibits c-fms, c-kit, carbonic anhydrase II, and PDGFR in osteoclasts and osteoblasts, resulting in reduced bone resorption and the obstruction of the release of mineral components from bone into blood (Vandyke et al. 2010). Moreover, approximately 69 % of the patients receiving the EGFR inhibitor, erlotinib, suffered severe skin rashes (over grade 2, classified according to Common Terminology Criteria for Adverse Events

v3.0) (Tarceva®, Japanese package insert, 2010; Chugai Pharmaceutical Corp, Tokyo, Japan), which was considerably higher than the percentage of suffering patients (35 %) receiving gefitinib (Iressa®, Japanese package insert, 2010; AstraZeneca, Osaka, Japan). Given that erlotinib and gefitinib both inhibit EGFR to a similar extent, the difference between the occurrence rates is probably associated with the inhibition of kinases other than EGFR.

In anti-cancer therapy with TKIs, certain adverse reactions (e.g., the severe skin rashes described above) are a major cause of therapy discontinuation and/or dose reduction. This in turn results in a concomitant degeneration of clinical efficacy, because the cytotoxic actions of EGFR inhibitors against cancer cells are concentration-dependent (Ono et al. 2004). Indeed, the dose intensity of sunitinib correlates with its anti-tumor capacity (Houk et al. 2010). Therefore, elucidation of the mechanisms of the side effects of TKIs will probably improve the clinical profile of these agents. Nevertheless, in contrast to the molecularly targeted mechanism of the main therapeutic drug action, adverse TKI reactions occur via unintended mechanisms. In addition, even in those cases where the mechanisms behind adverse reactions seem to involve some off-target kinases, the detailed action pathways have not yet been clarified for most TKIs.

To shed light on such mechanisms, a comprehensive analysis of all possible mechanisms is mandatory. For this reason, we propose that systems pharmacology is ideal for the mechanistic scrutiny of TKI-stimulated adverse reactions. Systems pharmacology is an area of pharmacology that recognizes drug action as an outcome of comprehensive biological systems. In this chapter, we describe a systems pharmacology-based approach to the mechanistic analysis of adverse events associated with erlotinib as a prototypical analysis.

16.2 Approaches to Reveal the Mechanisms of Adverse Reactions to TKIs by Focusing on the Drug-Target Molecule Layer

As noted above, the mechanisms of adverse reactions to TKIs are, at present, largely unknown. Therefore, it is essential to formulate plausible working hypotheses regarding the prospective mechanisms by using non-biased methodologies, such as systems pharmacology-based analyses. Concrete protocols for systems pharmacology-based approaches are now being established, as we reviewed previously (Kariya et al. 2013). The procedure can be summarized as follows (Kariya et al. 2013). Generally, drug actions can be separated into a pharmacokinetic layer and several pharmacodynamic layers (Fig. 16.1). Once a drug is administered, the agent is distributed and gains access to various sites in the body, after which it is eliminated by metabolism or excretion. These pharmacokinetic properties determine the degree of exposure of all organs and cells to the drug (Fig. 16.1) and are responsible for determining the magnitude of both main effects and adverse reactions.

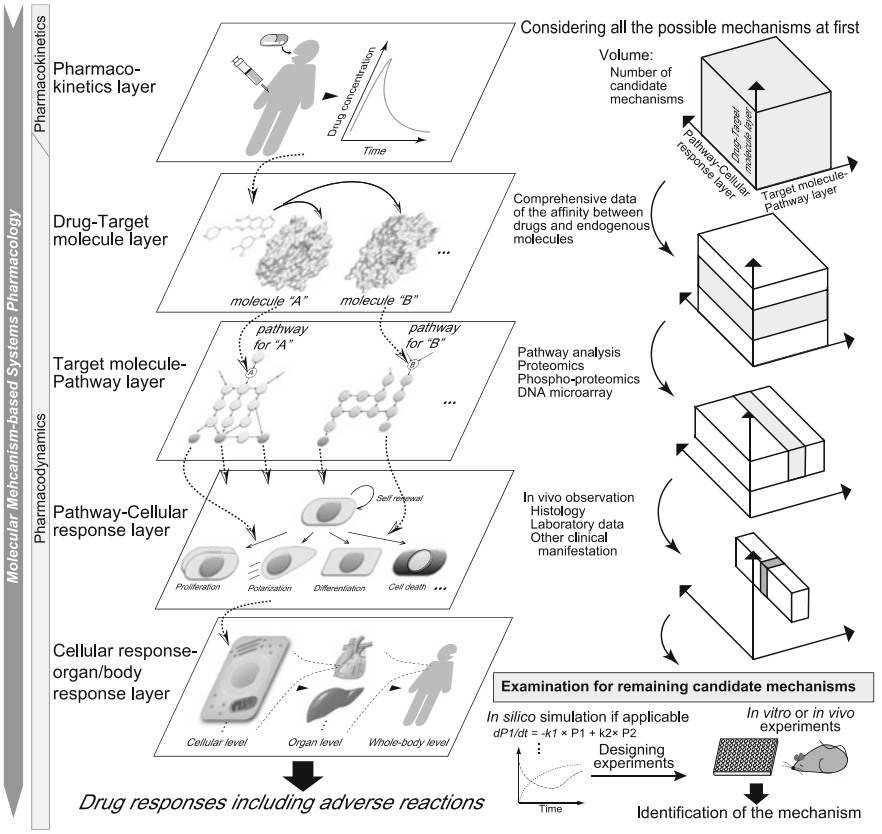

Fig. 16.1 Systems pharmacology-based approach for the elucidation of adverse drug reaction mechanisms

Cellular responses can be subdivided into multiple pharmacodynamic layers, comprising the drug-target molecule layer, the target molecule-pathway layer, and the pathway-cellular response layer (Fig. 16.1). The first layer provides the information regarding direct interactions between drugs and biological target molecules in the cell (e.g., proteins and endogenous small molecules). The second layer describes the manner in which target molecules affect cellular signaling or metabolic pathways. The third layer corresponds to a conversion of intracellular events into cellular output by integrating the upshots of multiple signaling or metabolic pathways. The concerted information emanating from all three layers specifies the detailed mechanism of the drug's action on cells. If omics data are available, we can superimpose these data on the respective layer(s), making comprehensive analyses possible (Abu-Asab et al. 2011; Gehlenborg et al. 2010). In addition, ideally speaking, to understand the drug response of the whole body, an additional pharmacodynamic layer is required for the integration of cellular responses with the

whole-organ response, or the whole-body response, in cases of adverse reactions resulting from inter-organ communication. However, the analysis of such a process is very difficult because of its complexity.

16.3 A Quest for Kinases Involved in Erlotinib-Associated Skin Inflammation

Skin inflammation is an undesirable reaction linked to the EGFR TKIs, gefitinib and erlotinib. The primary target of both of these TKIs is EGFR, but, as noted above, the frequency of skin inflammation is much higher in patients receiving erlotinib than in those receiving gefitinib. We previously explored the mechanism of skin inflammation exacerbation after erlotinib administration (Yamamoto et al. 2011). Firstly, we approached the adverse drug mechanism at the drug-target molecule layer. For TKIs, the targets comprise the ATP-binding regions of tyrosine kinases, whose structures are similar among all tyrosine kinases. Thus, it was previously assumed that TKIs would target many other kinases in addition to their primary targets, and the association of the drug of interest with all tyrosine kinases must therefore be considered in order not to lose comprehensiveness.

Karaman et al. (2008) contributed greatly in this regard by establishing the methodology to measure the value of the dissociation constant (K_d) between a compound of interest and 317 kinases. They reported the values for staurosporine, 21 TKIs, 15 serine-threonine kinase inhibitors, and one lipid kinase inhibitor (Karaman et al. 2008). These data can be utilized as comprehensive information for the drug-target molecule layer. According to the data, erlotinib inhibits many kinases with a K_d of <300 nM: Abelson murine leukemia viral oncogene homolog 2 (ABL2), K_d = 160 nM; B lymphocyte kinase (BLK), K_d = 190 nM; EGFR (primary target), K_d = 0.67 nM; erythroblastic leukemia viral oncogene homolog 4 (ERBB4), K_d = 230 nM; cyclin G-associated kinase (GAK), K_d = 3.1 nM; serine/threonine protein kinase (STK) 10, K_d = 19 nM; and STE20-like STK (SLK), K_d = 26 nM.

The ratio of the K_d value of the primary target (EGFR) to that of the K_d value of each kinase reflects the selectivity of the drug for the primary target. The ratio becomes smaller when the primary target is selective for a kinase of interest. For example, the K_d ratios for GAK and STK10 are $\sim$0.22 and 0.035, indicating that EGFR is highly selective over GAK and STK10 (Fig. 16.2a). However, whether the kinases are actually inhibited clinically depends not only on drug-target affinities, but also on the drug concentration at inflammatory sites. In general, if a drug is sufficiently lipophilic, the protein-unbound concentration of the drug in the plasma reaches equilibrium with that in the tissue. Therefore, given the plasma-unbound concentration (C_u) and the K_d values for kinases, occupancies of kinases by drugs of interest can be calculated under clinical situations. Drug

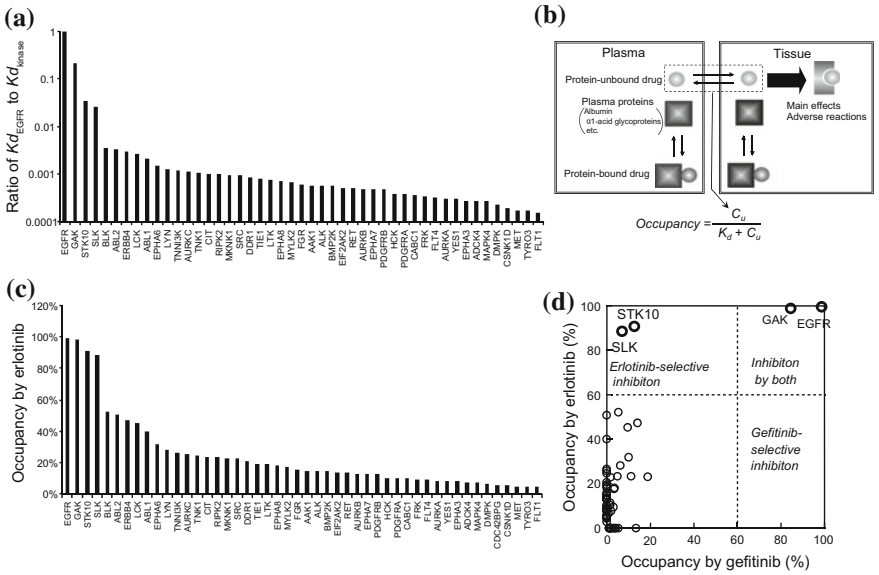

Fig. 16.2 Drug occupancy against kinases at clinical concentrations. **a** Selectivity of erlotinib against EGFR. Ratios of EGFR K_d to the K_d of each kinase are shown. **b** Drug concentration equilibrium between blood and tissues. **c** Occupancy by erlotinib. **d** Comparison of the occupancy profile of erlotinib with that of gefitinib

occupancy is then calculated according to the reaction kinetics between a protein and a drug, as follows:

$$[Kinase] + [Drug] \rightleftarrows [Kinase{:}Drug]$$

$$K_d = [Kinase][Drug]/[Kinase{:}Drug],\ C_u = [Drug]$$

$$\begin{aligned} Occupancy\ (\%) &= \frac{[Kinase{:}Drug]}{[Kinase{:}Drug] + [Kinase]} \\ &= \frac{1}{1 + [Kinase]/[Kinase{:}Drug]} \\ &= \frac{[Drug]}{[Drug] + \frac{[Kinase][Drug]}{[Knase{:}Drug]}} = \frac{C_u}{C_u + K_d} \end{aligned}$$

Based on this equation, we calculated the occupancies for each kinase examined in Karaman's comprehensive assay, as shown in Fig. 16.2c. Consequently, only four kinases, namely EGFR, GAK, STK10 and SLK, showed occupancies of >80 % when the average plasma concentration at steady-state was assigned to C_u, indicating that clinically significant targets are limited to these four kinases. Moreover, as shown in Fig. 16.2d, the comparison with the profile of occupancy by

gefitinib yielded an even greater restriction, in that STK10 and SLK are not inhibited by this drug at clinical concentrations. Because an extraordinarily high frequency of skin inflammation is observed with erlotinib but not with gefitinib, candidate kinases involved in the exacerbation of skin inflammation can be narrowed down to STK10 and SLK (Fig. 16.2d). Thus, by combining information from clinical drug concentrations (which can be estimated through pharmacokinetic analysis) with comprehensive data concerning the affinity between a drug and assorted kinases (which can be obtained from the drug-target kinase layer), the numerous candidate kinases involved in the adverse reaction mechanism were reduced to only two.

16.4 Building a Protein-Protein Linkage Network for the Analysis of Drug Responses

Even if candidate kinases are successfully identified, the definitive elucidation of the mechanisms behind erlotinib-associated skin inflammation requires further analysis, because we still do not know which molecular pathways and downstream events are perturbed by the inhibition of off-target kinases. Relevant information could be forthcoming from in-depth analysis of the target molecule-pathway layer and the pathway-physiological response layer. For this analysis, information available on the web database is frequently used, as introduced previously (Kariya et al. 2013).

In the case of erlotinib, the analysis of the pharmacokinetics and drug-target molecule layers indicates that two kinases, STK10 and SLK, are likely responsible for erlotinib-induced skin inflammation. Unfortunately, the signaling pathways involving these two kinases are not sufficiently described in the databases introduced above. Therefore, we manually constructed a protein linkage network around these two kinases using the iHOP (information Hyperlinked Over Proteins) web service to uncover protein linkages for STK10 and SLK. With the iHOP program, we can find proteins that appear along with STK10 and SLK in single sentences in the abstract of original articles available from PubMed (Hoffmann and Valencia 2004). When “STK10” was input as a query, the service returned seven proteins as molecules simultaneously appearing with STK10 in single sentences, including mitogen-activated protein kinase kinase kinase 1 (MAP3K1), STK25, Misshapen kinase (MSN), SLK, and interleukin 2 (IL2).

To expand this network for comprehensiveness, the seven selected proteins were then input as iHOP queries to obtain further protein linkages. In the case of STK10 and SLK, one-time iteration generated the protein linkage map shown in Fig. 16.3, which exhibits substantial complexity. Consequently, additional assessments were performed on the basis of this map.

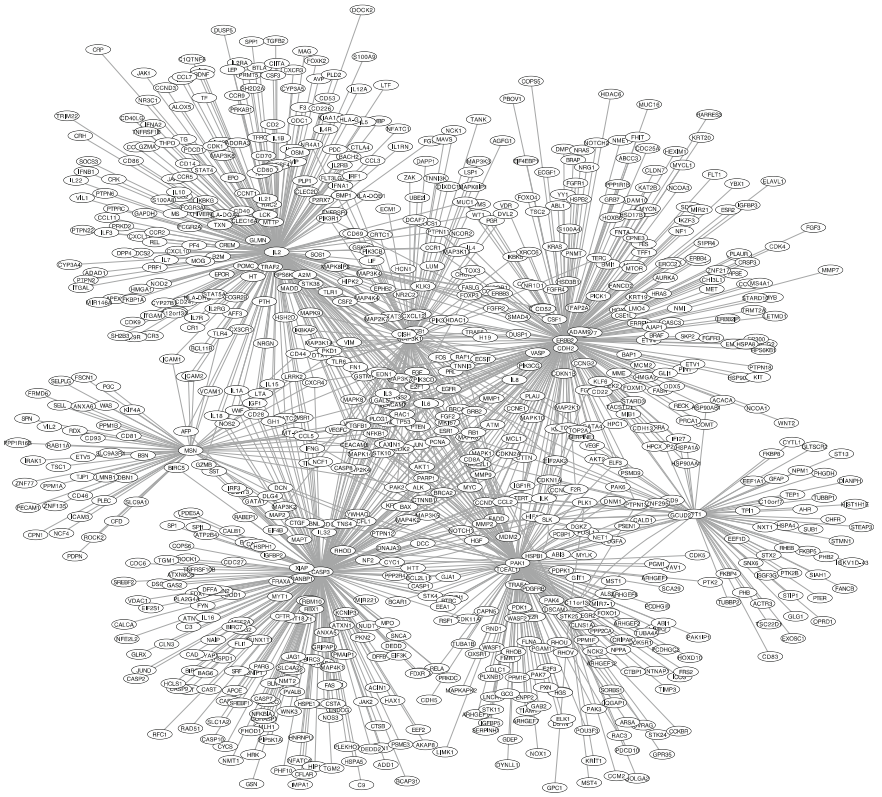

Fig. 16.3 iHOP-based protein linkage network for STK10 and SLK

16.5 Analysis Based on a Protein Linkage Network and Graph Theory

Once the protein linkage network is prepared, the next step is to focus on which molecules or events need to be assessed. The network for STK10 and SLK contains 896 molecules and appears comprehensive (Fig. 16.3), but the large number of molecules makes it difficult to define which molecules or events should be the focus of further investigation. This kind of network is accessible to mathematical graph theory. Mathematical graph theory provides information on the qualitative properties of key components in target networks, including the importance of each component for maintaining the network structure. In this type of analysis, information obtained from networks is introduced with the aid of simple hypothetical networks (Fig. 16.4a). Figure 16.4a assumes that the network was prepared to analyze events surrounding molecule "A".

According to the mathematical graph theory, the following characteristics can be obtained: (1) the distance of the shortest path to any molecule, showing how many

(a)

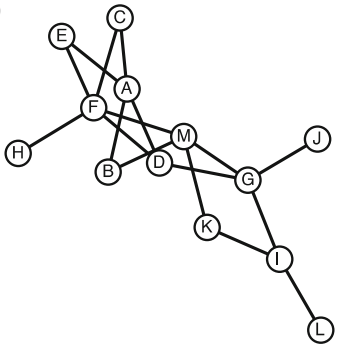

(b) Characteristics of nodes

node	Stress	Betweenness
A	28	0.10353535
B	4	0.03030303
C	4	0.01010101
D	60	0.19191919
E	4	0.01010101
F	96	0.34848485
G	98	0.36111111
H	0	0
I	52	0.18686869
J	0	0
K	24	0.06565657
L	0	0
M	84	0.32828283

(c)
Characteristics of molecule linkages from "A" to hub-like molecuels

Linkage pathway	Number of paths	Sum of betweenness
A – F	1	0.45202020
A – G	1	0.46464646
A – F – M	2	0.78030303
A – G – M	2	0.79292929

(d)
Criteria for high impact linkages

Primary criteria
Higher impact when a linkage has smaller number of paths
Secondary criteria
If the node is a specific and selective goal on the map, the impacts on other nodes should be as low as possible, therefore, the sum of the betweeness of nodes on a linkage shoul be smaller.
If there are goal events other than focusing node globally on the map, the impacts on other nodes should be as high as possible, therefore, the sum of the betweeness of nodes on a linkage should be larger.

Fig. 16.4 Graph theory-based ordering of molecule linkages

steps are required to advance from one node to another; (2) the number of shortest paths between any two molecules; and (3) the number of paths leading into and out of each molecule, defined as $degree_{in}$ and $degree_{out}$. In addition to these basic characteristics, the importance of each molecule can be calculated according to "*stress*" and "*betweenness*".

Stress is calculated by counting the number of shortest paths between any two given molecules that pass through a particular molecule. Mathematically, the stress of node v is given by the following equation:

$$Stress(v) = \sum_{s \neq v \in V} \sum_{t \neq v \in V} \sigma_{st}(v)$$

where V is a class of all nodes, and $\sigma_{st}(v)$ is the number of shortest paths between nodes s and t that pass through node v. The stress value reflects how deeply a particular molecular node is involved in the system, but does not necessarily reflect the regulatory ability of the molecule within the entire map, since the stress value is not influenced by whether a particular molecular node is on a unique pathway or on a pathway with alternative conduits between nodes s and t. The regulatory ability of node v is higher if the node is on a unique pathway; therefore, in a calculation of the betweenness centrality of node v, $\sigma_{st}(v)$ is normalized by σ_{st}, the total number of

shortest paths between nodes s and t, which takes the regulatory effect into consideration. The mathematical description is as follows:

$$Betweenness(v) = \sum_{s \neq v \in V} \sum_{t \neq v \in V} \frac{\sigma_{st}(v)}{\sigma_{st}}$$

The higher the betweenness value of a molecule, the more hub-like and more important the function of the molecule is for controlling the network. Thus, molecules "F", "G", and "M" are predicted to be focus points in the network (Fig. 16.4a). Once hub molecules are found, the distances to "A" can be focused on to analyze the effect of external perturbation on "A", given that "A" will have a more direct effect when the distance is smaller. The distances from "A" to "F", "G" and "M" are 1, 1 and 2, respectively, and therefore, "F" and "G" are primary targets for further analyses. In addition, the betweenness centralities of "F" and "G" are 0.348 and 0.361, respectively, indicating that "G" has a higher impact on the entire network. Therefore, the order of analytical focus is determined as "G", "F", and finally "M". In addition to this order, a consideration of the observed physiological outputs upon perturbation on "A" provides us with a plausible molecular mechanism.

16.6 Identification of Key Events and Pathways Related to Drug Responses

In the erlotinib network, molecules corresponding to "A" are identified as STK10 and SLK. In accordance with the ordering rule proposed above, we first sought to establish hub molecules by elucidating molecules with high betweenness centrality. For this purpose, Cytoscape, an open source platform for complex network analysis and visualization, is useful because the platform automatically calculates scores based on graph theory and visualizes all scores in the network (Smoot et al. 2011). With this platform, the betweenness centrality of the erlotinib network can not only be calculated, but also graphically superimposed onto the network structure, where the size of each circle reflects the degree of betweenness centrality (Fig. 16.5a). Figure 16.5a indicates that STK10 and SLK are surrounded by seven hub networks whose centers are ERBB2, MSN, translationally controlled tumor protein 1 (TPT1), STK25, P21-activated kinase 1 (PAK1), caspase 3 (CASP3), and IL2, and the distances from STK10 or SLK to these central molecules all have a value of one. In other words, the signaling pathways or cellular events linked to these proteins are likely to be strongly influenced by erlotinib administration when they function in signaling pathways downstream of STK10 and SLK, although we cannot eliminate the possibility that signaling pathways or cellular events will be affected upstream of these kinases.

(a)

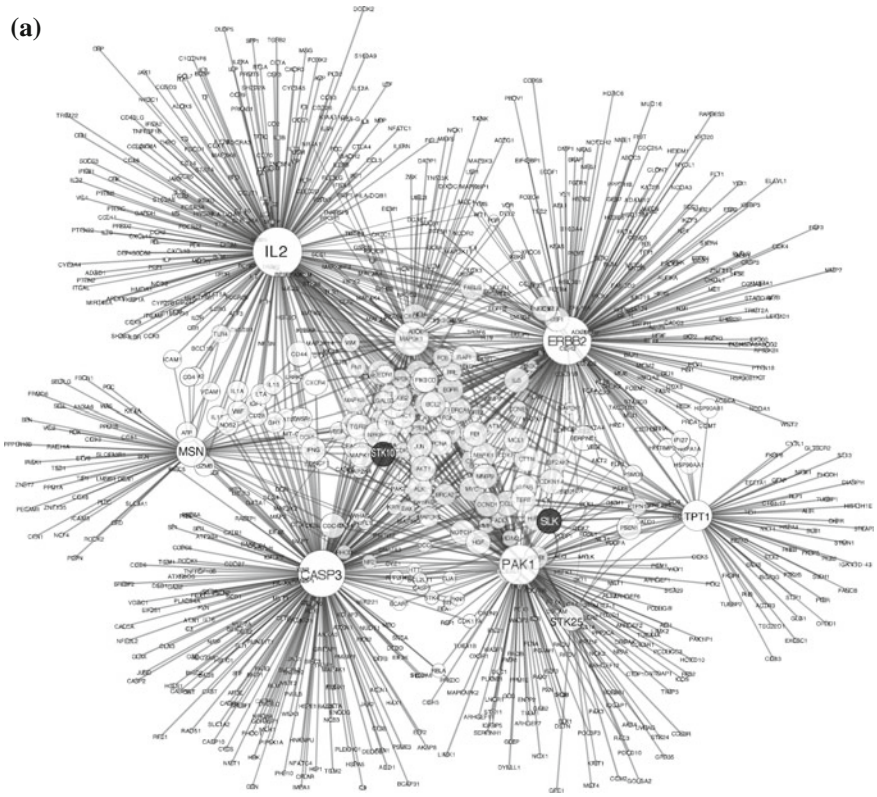

(b)

Protein	Related pathway/ Physiological responses
ERBB2	Protein sysnthesis, Cell growth
TPT1	Microtubule stabilization
STK25	Protein transport, Cell adhesion, Polarity formation
PAK1	Cytoskeltal dynamics
CASP3	Apoptosis
MSN	Scaffolding of membrane
IL2	Immune response (T cell activation)

Fig. 16.5 Graph theory-based network analysis of erlotinib protein linkage network. **a** The size of each circle indicates the betweenness centrality value. *Black circles* denote the "start" molecules, STK10 and SLK. **b** Related pathways and downstream physiological responses for the central hub network nodes

By using the Uniprot protein database, the pathways and cellular events linked to the above seven proteins were ascertained and summarized in Fig. 16.5b. Because these pathways/cellular events correspond to physiological responses, we were able to compare clinical and pathological observations according to the pertinent signaling cascades/cellular events. In pathological studies, cells committed to a T cell

fate accumulate at sites of skin inflammation after erlotinib administration (Busam et al. 2001), which is consistent with the signaling pathway and downstream physiological responses of the IL2 hub. Therefore, we combined the above network analysis with this pathological observation, and concluded that the putative cause for skin inflammation was the perturbation of IL2-related immune responses by STK10 or SLK inhibition. In the protein linkage network analysis, the linkages with the minimal number of paths from STK10 and SLK to IL2 are STK10–IL2 and SLK–STK10–IL2. The distance to IL2 is shorter for STK10 than for SLK, indicating that STK10 is more likely to be responsible for the IL2-faciliated immune response. Thus, the results of pharmacokinetic analysis together with information about the drug-target molecule layer, the target molecule-pathway layer, and the pathway-physiological response layer indicate that the most plausible mechanism underlying erlotinib-associated skin inflammation involves STK10–IL2 linkage-mediated T cell activation. Hence, this linkage was used as the basis for additional in vitro and in vivo wet analyses, as discussed below.

16.7 "Wet" Experiments to Verify the Molecular Mechanism Behind Erlotinib-Associated Skin Inflammation

As mentioned earlier, the protein linkage network analysis does not contain a dedicated mode of drug-target interactions (e.g., inhibition and enhancement) and therefore, the relationship between IL2 and STK10 requires a more detailed review of the original literature. STK10 is responsible for the suppression of IL2 secretion from T cells (Tao et al. 2002). In addition, T cells are the predominant secretors of IL2 (Lenschow et al. 1996). Moreover, STK10 is highly expressed in rapidly proliferating tissues and cells, such as the spleen, placenta, and peripheral blood leukocytes (Walter et al. 2003). Thus, the first point to be confirmed by "wet" experiments was whether or not either inhibition of STK10 by erlotinib increases IL2 secretion from T cells.

IL2 secretion was first measured in Jurkat E6-1 cells, a cell line derived from primary leukemia cells. After testing several clinical, protein-unbound concentrations of erlotinib or gefitinib (a negative control), we found that cell treatment with erlotinib (200 nM), but not with gefitinib (70 nM), resulted in an increase in IL2 secretion (Fig. 16.6a). The effect of STK10 or SLK knockdown was assessed by using Jurkat E6-1 cells transfected with a small interfering RNA (siRNA) against STK10 (siSTK10) or SLK (siSLK). Suppression of STK10 expression, but not SLK expression, increased IL2 secretion; moreover, treatment of the cells with erlotinib diminished the enhanced IL2 secretion observed after STK10 knockdown (Fig. 16.6b). These in vitro data suggest that the increase in IL2 secretion from T cells following erlotinib exposure occurred at least in part via an STK10-facilitated mechanism. Given that IL2 mediates inflammation and provokes T cell activation,

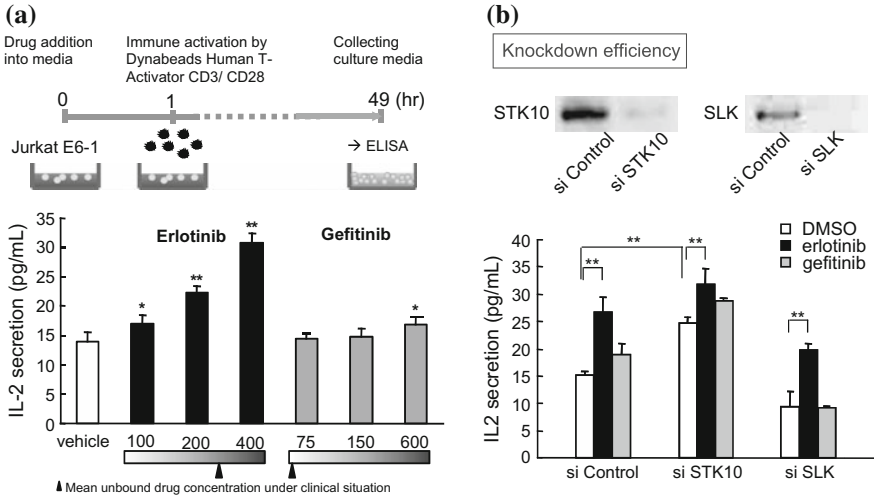

Fig. 16.6 Suppression of STK10-enhanced IL2 secretion in vitro. **a** The effect of erlotinib or gefitinib treatment on IL2 secretion is shown in Jurkat E6-1 cells. A clinical concentration of erlotinib (200 nM) significantly enhanced IL2 secretion, whereas that of gefitinib (70 nM) did not. **b** The effect of siRNA-mediated STK10 or SLK suppression on IL2 secretion is illustrated in Jurkat E6-1 cells. Treatment with siSTK10 enhanced IL2 secretion under erlotinib-free conditions, whereas such enhancement was weakened by erlotinib exposure. Values are given as the mean ± the standard deviation (SD); $*P < 0.05$; $**P < 0.01$. These data are taken from Yamamoto et al. (2011), with permission of the publisher

the secretion of IL2 and the inhibition of STK10 inhibition apparently aggravate inflammation.

Furthermore, we determined whether in vivo inflammatory responses associated with erlotinib are mediated by IL2. Before performing in vivo experiments in mice, we determined the IC_{50} values of erlotinib and gefitinib against mouse STK10 by performing in vitro kinase assays using the recombinant catalytic regions of each protein (Yamamoto et al. 2011). In addition, pharmacokinetic profiles in mice were obtained after the administration of a single dose of erlotinib or gefitinib, and the pharmacokinetic parameters for an oral one-compartment model for each drug were established (Fig. 16.7a). With these data, we finally determined the conditions under which each drug suppressed STK10 activity in a murine croton oil-induced skin inflammation model, in order to mimic clinical situations (Fig. 16.7b).

Following the administration of the first dose of the drugs to the mice, the earflaps were exposed to croton oil to induce inflammation. The thickness of each earflap was then measured after a period of time. As a result, erlotinib strongly enhanced the tumentia of the earflaps, whereas gefitinib did not (Fig. 16.8a). In addition, because in silico network analyses and in vitro analyses suggest that IL2 is a mediator of skin inflammation, we anticipated that neutralizing IL2 would suppress erlotinib-associated inflammation. Indeed, when an anti-IL2 antibody was administered immediately before the application of croton oil, the thickness of the

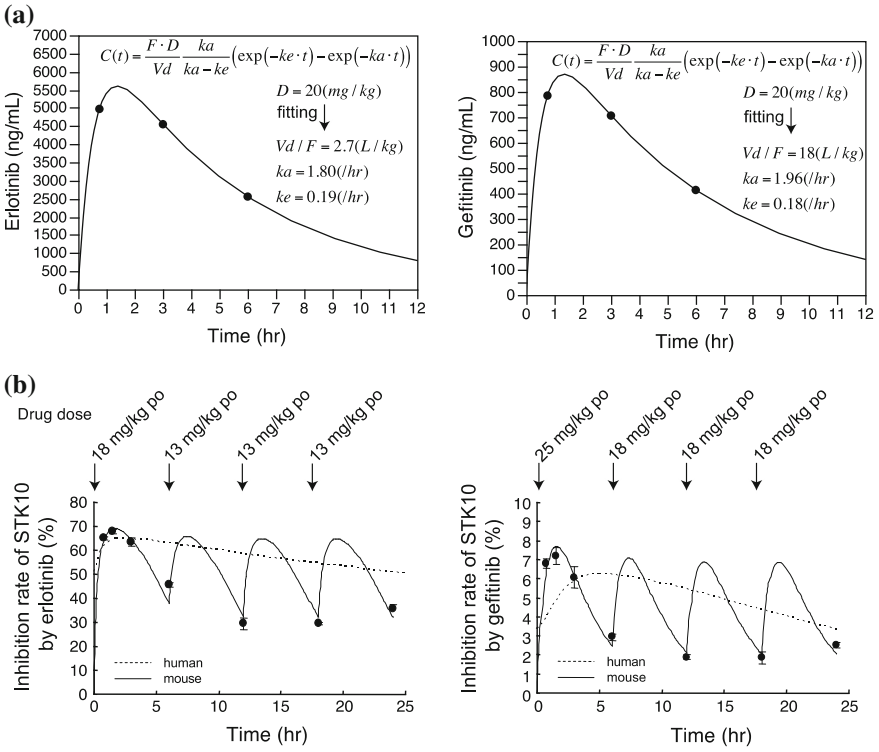

Fig. 16.7 Determination of conditions for animal model. **a** Pharmacokinetic profiles after a single dose of erlotinib or gefitinib in mice. Based on these profiles, pharmacokinetic parameters for oral one-compartment models were determined. $C(t)$, concentration at time t; D, dose; F, bioavailability; V_d, distribution volume; ka, rate constant for absorption; k_e, rate constant for elimination. *Black circle*, experimental data point; *solid line*, fitted curve. **b** Designing the dosage of each drug in mice. Based on the pharmacokinetic data obtained in (**a**), the dosages were designed to give a comparable inhibition profile for STK10 as that obtained in human clinical situations. *Black circle*, inhibition rate calculated from measured serum concentration of each drug (mean ± SD); *solid line*, inhibition rate curve calculated from pharmacokinetic parameters obtained in (**a**); *dotted line*, inhibition rate curve predicted under human clinical conditions. These data are taken from Yamamoto et al. (2011), with permission of the publisher

earflaps recovered (Fig. 16.8b). These results confirm that an in in vivo model skin inflammation stems from enhanced erlotinib-facilitated IL2 secretion. Additional biological experiments to support the present systems pharmacology-based network analysis of multiple layered pharmacological responses would greatly contribute to the clarification of adverse drug reaction mechanisms and provide clues for overcoming such reactions.

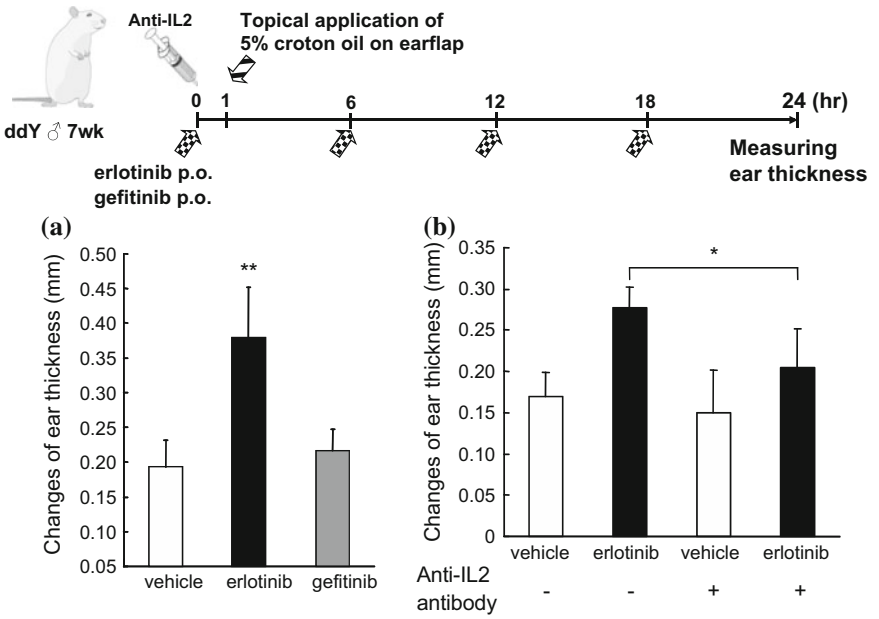

Fig. 16.8 Erlotinib-associated skin inflammation is mediated by IL2 in vivo. **a** Croton oil-treated mouse earflaps were challenged by the administration of erlotinib or gefitinib. The aggravation of the tumentia was selectively observed in erlotinib-administered mice, but not in gefitinib-administered mice. **b** Anti-IL2 antibody alleviated the aggravation of tumentia induced by erlotinib administration. Values are given as the mean ± SD; $*P < 0.05$; $**P < 0.01$. These data are taken from Yamamoto et al. (2011), with permission of the publisher

16.8 Conclusions

Conventional anti-tumor agents provoke numerous adverse reactions, including damage to the gastrointestinal epithelium, hair loss, and myelosuppression via their cytotoxic actions on normal cells, in which the mechanism of each adverse event is the same as that of the main therapeutic event. Conversely, the adverse reactions of other agents, such as TKIs, cannot be explained as merely an extension of the main therapeutic event (Gainor and Shaw 2013; Ku and Ilson 2013). Adverse TKI reactions often limit drug dosing, and it is expected that exploring the molecular mechanisms of these adverse events will potentially improve therapeutic outcomes. Nonetheless, little information is available concerning the precise mechanisms of adverse TKI reactions. Thus, a more comprehensive, systems-based mechanistic analysis and an examination of a wealth of candidate mechanisms will be required.

To accelerate this process, the present chapter proposes a multi-layer focusing strategy. Physiological responses following drug administration can be separated into multiple pharmacodynamic layers, including the drug-target molecular layer, the target molecule-pathway layer, and the pathway-physiological response layer.

Multi-dimensional focusing based on a consideration of these layers can provide an order of plausibility for the candidate mechanisms. Designing further "wet" experiments to examine the candidate mechanisms suggested by this approach is regarded as an efficient way to identify the actual mechanism, while identification of the mechanisms of already occurring adverse events might suggest a means of prevention and/or counteraction. In addition, we suggest that the approach described herein can be used to predict adverse reactions in advance of clinical drug use by anticipating plausible drug responses, such as cell death, immune reactions/inflammation, and oxidative stress. Moreover, identification of the precipitating factors for adverse events during the early stages of drug development will likely contribute to the discovery of new compounds that avoid such pitfalls.

Prediction of adverse events of anti-cancer drugs is very important during novel drug development and for the safe and efficient pharmacotherapy of cancer. Therefore, a systems-based analysis of adverse drug events conducted by applying the present methodology will hypothetically improve both current anti-cancer drug therapy and future drug development.

Acknowledgments This work was supported in part by a Grant-in-Aid for Scientific Research on Innovative Areas "HD-physiology" 22136015, by a Grant-in-Aid for Scientific Research (A) 24249034, and by a Grant-in-Aid for challenging Exploratory Research 26670265 from the Ministry of Education, Culture, Sports, Science, and Technology in Japan.

References

Abu-Asab MS, Chaouchi M, Alesci S, Galli S, Laassri M, Cheema AK, Atouf F, VanMeter J, Amri H (2011) Biomarkers in the age of omics: time for a systems biology approach. OMICS 15(3):105–112. doi:10.1089/omi.2010.0023

Berman E, Nicolaides M, Maki RG, Fleisher M, Chanel S, Scheu K, Wilson BA, Heller G, Sauter NP (2006) Altered bone and mineral metabolism in patients receiving imatinib mesylate. N Engl J Med 354(19):2006–2013. doi:10.1056/NEJMoa051140

Busam KJ, Capodieci P, Motzer R, Kiehn T, Phelan D, Halpern AC (2001) Cutaneous side-effects in cancer patients treated with the antiepidermal growth factor receptor antibody C225. Br J Dermatol 144(6):1169–1176

Futreal PA, Coin L, Marshall M, Down T, Hubbard T, Wooster R, Rahman N, Stratton MR (2004) A census of human cancer genes. Nat Rev Cancer 4(3):177–183. doi:10.1038/nrc1299

Gainor JF, Shaw AT (2013) Emerging paradigms in the development of resistance to tyrosine kinase inhibitors in lung cancer. J Clin Oncol 31(31):3987–3996. doi:10.1200/JCO.2012.45.2029

Gehlenborg N, O'Donoghue SI, Baliga NS, Goesmann A, Hibbs MA, Kitano H, Kohlbacher O, Neuweger H, Schneider R, Tenenbaum D, Gavin AC (2010) Visualization of omics data for systems biology. Nat Methods 7(3 Suppl):S56–S68. doi:10.1038/nmeth.1436

Herbst RS, Bunn PA Jr (2003) Targeting the epidermal growth factor receptor in non-small cell lung cancer. Clin Cancer Res 9(16 Pt 1):5813–5824

Heymach JV, Nilsson M, Blumenschein G, Papadimitrakopoulou V, Herbst R (2006) Epidermal growth factor receptor inhibitors in development for the treatment of non-small cell lung cancer. Clin Cancer Res 12(14 Pt 2):4441s–4445s. doi:10.1158/1078-0432.CCR-06-0286

Hoffmann R, Valencia A (2004) A gene network for navigating the literature. Nat Genet 36 (7):664. doi:10.1038/ng0704-664

Hornberg JJ, Bruggeman FJ, Westerhoff HV, Lankelma J (2006) Cancer: a systems biology disease. Bio Syst 83(2–3):81–90. doi:10.1016/j.biosystems.2005.05.014

Houk BE, Bello CL, Poland B, Rosen LS, Demetri GD, Motzer RJ (2010) Relationship between exposure to sunitinib and efficacy and tolerability endpoints in patients with cancer: results of a pharmacokinetic/pharmacodynamic meta-analysis. Cancer Chemother Pharmacol 66(2):357–371. doi:10.1007/s00280-009-1170-y

Karaman MW, Herrgard S, Treiber DK, Gallant P, Atteridge CE, Campbell BT, Chan KW, Ciceri P, Davis MI, Edeen PT, Faraoni R, Floyd M, Hunt JP, Lockhart DJ, Milanov ZV, Morrison MJ, Pallares G, Patel HK, Pritchard S, Wodicka LM, Zarrinkar PP (2008) A quantitative analysis of kinase inhibitor selectivity. Nat Biotechnol 26(1):127–132. doi:10.1038/nbt1358

Kariya Y, Honma M, Suzuki H (2013) Systems-based understanding of pharmacological responses with combinations of multidisciplinary methodologies. Biopharm Drug Dispos 34 (9):489–507. doi:10.1002/bdd.1865

Khuri FR, Cohen V (2004) Molecularly targeted approaches to the chemoprevention of lung cancer. Clin Cancer Res 10(12 Pt 2):4249s–4253s. doi:10.1158/1078-0432.CCR-040019

Kim TE, Murren JR (2002) Angiogenesis in non-small cell lung cancer. A new target for therapy. Am J Respir Med Drugs Devices Other Interv 1(5):325–338

Ku GY, Ilson DH (2013) Emerging tyrosine kinase inhibitors for esophageal cancer. Expert Opin Emerg Drugs 18(2):219–230. doi:10.1517/14728214.2013.805203

Lenschow DJ, Walunas TL, Bluestone JA (1996) CD28/B7 system of T cell costimulation. Annu Rev Immunol 14:233–258. doi:10.1146/annurev.immunol.14.1.233

Mendel DB, Laird AD, Xin X, Louie SG, Christensen JG, Li G, Schreck RE, Abrams TJ, Ngai TJ, Lee LB, Murray LJ, Carver J, Chan E, Moss KG, Haznedar JO, Sukbuntherng J, Blake RA, Sun L, Tang C, Miller T, Shirazian S, McMahon G, Cherrington JM (2003) In vivo antitumor activity of SU11248, a novel tyrosine kinase inhibitor targeting vascular endothelial growth factor and platelet-derived growth factor receptors: determination of a pharmacokinetic/pharmacodynamic relationship. Clinical Cancer Res 9(1):327–337

Motzer RJ, Michaelson MD, Redman BG, Hudes GR, Wilding G, Figlin RA, Ginsberg MS, Kim ST, Baum CM, DePrimo SE, Li JZ, Bello CL, Theuer CP, George DJ, Rini BI (2006) Activity of SU11248, a multitargeted inhibitor of vascular endothelial growth factor receptor and platelet-derived growth factor receptor, in patients with metastatic renal cell carcinoma. J Clin Oncol 24(1):16–24. doi:10.1200/JCO.2005.02.2574

Ono M, Hirata A, Kometani T, Miyagawa M, S-i U, Kinoshita H, Fujii T, Kuwano M (2004) Sensitivity to gefitinib (Iressa, ZD1839) in non-small cell lung cancer cell lines correlates with dependence on the epidermal growth factor (EGF) receptor/extracellular signal-regulated kinase 1/2 and EGF receptor/Akt pathway for proliferation. Mol Cancer Ther 3(4):465–472

Smoot ME, Ono K, Ruscheinski J, Wang PL, Ideker T (2011) Cytoscape 2.8s: new features for data integration and network visualization. Bioinformatics 27(3):431–432. doi:10.1093/bioinformatics/btq675

Sridhar SS, Seymour L, Shepherd FA (2003) Inhibitors of epidermal-growth-factor receptors: a review of clinical research with a focus on non-small-cell lung cancer. Lancet Oncol 4(7):397–406

Tao L, Wadsworth S, Mercer J, Mueller C, Lynn K, Siekierka J, August A (2002) Opposing roles of serine/threonine kinases MEKK1 and LOK in regulating the CD28 responsive element in T-cells. Biochem J 363(Pt 1):175–182

Tuveson DA, Willis NA, Jacks T, Griffin JD, Singer S, Fletcher CD, Fletcher JA, Demetri GD (2001) STI571 inactivation of the gastrointestinal stromal tumor c-KIT oncoprotein: biological and clinical implications. Oncogene 20(36):5054–5058. doi:10.1038/sj.onc.1204704

Vandyke K, Fitter S, Dewar AL, Hughes TP, Zannettino AC (2010) Dysregulation of bone remodeling by imatinib mesylate. Blood 115(4):766–774. doi:10.1182/blood-2009-08-237404

Vogelstein B, Kinzler KW (2004) Cancer genes and the pathways they control. Nat Med 10 (8):789–799. doi:10.1038/nm1087

Walter SA, Cutler RE Jr, Martinez R, Gishizky M, Hill RJ (2003) Stk10, a new member of the polo-like kinase kinase family highly expressed in hematopoietic tissue. J Biol Chem 278 (20):18221–18228. doi:10.1074/jbc.M212556200

Yamamoto N, Honma M, Suzuki H (2011) Off-target serine/threonine kinase 10 inhibition by erlotinib enhances lymphocytic activity leading to severe skin disorders. Mol Pharmacol 80 (3):466–475. doi:10.1124/mol.110.070862

Chapter 17
Translational Modeling of Antibacterial Agents

Gauri G. Rao, Neang S. Ly, Brian T. Tsuji, Jürgen B. Bulitta and Alan Forrest

Abstract The golden era of antibiotic discovery almost 60 years ago seems to be an interlude in the eternal battle against bacteria; the spread of resistant bacteria has led to the emergence of highly resistant pathogens and hard-to-treat infections. In vitro infection models have made it possible to gather time-course data regarding antibiotic and bacteria interaction. The main drawback of these in vitro systems is that they do not take into account the host immune system, drug-protein binding, and characteristics of the infection site. Hence, animal studies are important to gain insights into the host response and the progression of infection. Modeling antimicrobials has

Gauri G. Rao and Neang S. Ly are joint first authors.

G.G. Rao (✉) · N.S. Ly (✉) · B.T. Tsuji
School of Pharmacy and Pharmaceutical Sciences, University at Buffalo, SUNY,
K317 Kapoor Hall, Buffalo, NY 14051, USA
e-mail: gaurirao@buffalo.edu

N.S. Ly
e-mail: neangly@gmail.com

G.G. Rao (✉) · N.S. Ly (✉) · B.T. Tsuji
School of Pharmacy and Pharmaceutical Sciences, University at Buffalo, SUNY,
K317 Kapoor Hall, Buffalo, NY 14051, USA
e-mail: gaurirao@buffalo.edu

N.S. Ly
e-mail: neangly@gmail.com

J.B. Bulitta
Department of Pharmaceutics, College of Pharmacy, University of Florida,
6550 Sanger Road, Office 475, Orlando 32827, FL, USA

Present Address:
N.S. Ly
Clinical Pharmacology and DMPK, MedImmune LLC, 319 N. Bernardo Ave,
Mountain View, CA, USA

A. Forrest
Eshelman School of Pharmacy, University of North Carolina,
2317 Kerr Hall, 301 Pharmacy Lane, Chapel Hill, NC 27599, USA

D.E. Mager and H.H.C. Kimko (eds.), *Systems Pharmacology and Pharmacodynamics*,
AAPS Advances in the Pharmaceutical Sciences Series 23,
DOI 10.1007/978-3-319-44534-2_17

the distinct advantage wherein the target is readily accessible since the bacterial load can be quantified in both in vitro and in vivo experimental conditions. The increasing knowledge base about molecular mechanisms of interactions between antibiotics and antibiotic targets, coupled with advanced experimental techniques and computational capability, makes the development of mechanism-based PK/PD models incorporating receptor binding and bacterial physiology possible. This new generation of mechanism-based PK/PD models will enable the exploration and increased understanding of the underlying complex mechanisms of the infectious process. The transition toward systems-based approaches requires the ability to integrate diverse data types and experimental platforms. Most approaches for translating preclinical antimicrobial research focus only on antibiotic activity and interactions between the drug and bacteria. Mathematical modeling can assist in this process by integrating the behavior of multiple components into a comprehensive network-based model, and by addressing questions that are not yet accessible to experimental analysis.

Keywords Network-based model · Minimum inhibitory concentration (MIC) · Target values · Optimal sequencing · Combination regimens · In vitro models · Static time-kills · Open system dynamic models · In vivo · Polymorphonuclear lymphocytes (PMNs) · Bacterial growth model · Systems modeling

17.1 Introduction

The term antibiotic refers to substances produced by microorganisms that have the ability to kill bacteria, a term first coined by Waksman (Bush 2010). Antibiotics were considered to be natural products that produced both bacteriostatic and bactericidal effects. Antibiotics are a class of "anti-infectives," a larger group that also includes anti-viral, anti-fungal, and anti-parasitic drugs. In 1946, at the Section of Biology of the New York Academy of Sciences meeting, penicillin was termed as the "wonder drug". The 60 or so years after penicillin came to the market appears to be an interlude in the eternal battle against bacteria, as we are now being confronted with the emergence of bacterial strains resistant to almost all current approved antibacterial agents.

Despite our decreased reliance on natural products and increased sophisticated structure-based drug design, we continue to be plagued by pathogens resistant to current approved agents. The World Health Organization (WHO) and Infectious Diseases Society of America (IDSA) have identified antimicrobial resistance as one of the three greatest threats to human health (Boucher et al. 2013a). IDSA has highlighted the current state of antibiotics, '*as antibiotic research and discovery stagnates, a public health crisis brews*', needing urgent attention of the global medical community (Boucher et al. 2009, 2013b).

Employing quantitative systems pharmacology (QSP) principles and an interdisciplinary approach are necessary to aid in understanding the underlying disease mechanisms and effects of therapeutic agents on processes spanning several biological scales (consisting of cell, animal-based experiments, and clinical studies in infected patients). A framework that incorporates in vivo biology should facilitate the development of new approaches for optimization of current agents, increase the probability of therapeutic effectiveness of newly discovered compounds, and increase the rate of success of clinical trials. Mathematical modeling and sophisticated computation are critical for the vertical and horizontal integration of data that span multiple spatial and temporal scales (Sorger et al. 2011). The primary focus of this chapter is to highlight modeling trends for antibacterials and the transition towards a system-based modeling approach.

Systems pharmacology involves, "*the quantitative analysis of the dynamic interactions between drug(s) and a biological system… [that] aims to understand the behavior of the system as a whole, as opposed to the behavior of its individual constituents*" (Sorger et al. 2011). This is in contrast with traditional pharmacokinetic (PK) and pharmacodynamic (PD) modeling, which involves simplification of complex physiological processes involved in the distribution and action of drugs as a series of interconnected "black boxes" or "compartments". Although these models are not mechanistic at a molecular level, the PK/PD modeling approach provides information about the interactions between bacteria, disease processes, and the drug within individual patients and patient populations. PK/PD models are widely employed in clinical trials and are critical to drug development (Sorger et al. 2011; Lee et al. 2011; Gobburu and Sekar 2002; Bhattaram et al. 2007).

In this chapter, we provide relevant background and concepts that are commonly used in the development of mathematical PK/PD models based on in vitro and animal infection models and/or human data. We describe the process of selecting relevant candidate models for both empirical and mechanism-based model development and review the merits and limitations of each of these models.

17.2 Minimum Inhibitory Concentration (MIC)

The MIC is defined as the visual quantification of the lowest selected antimicrobial concentration that inhibits the visible growth of a microorganism, at an initial inoculum of 5×10^5 CFU (colony forming units) per mL and incubated for 18–22 h at 37 °C (Clinical Laboratory Standards Institute Guideline 2007). The MIC is considered as a measure of susceptibility, and when combined with antibiotic exposure measures (e.g., the time free drug concentration remains above the MIC, $fT > \text{MIC}$, or the area under the free drug concentration-time curve ratio, $f\text{AUC/MIC}$), the result is a measure of activity that may be related to specific and general outcomes (such as time to clinical resolution, bacterial eradication, emergence of resistance, and probability of clinical success or bacterial eradication), and may be used as a target to optimize outcomes in patients (Craig 1998).

Although the MIC is commonly used as a measure of bacterial susceptibility to antibiotics and a guide for dosing antibiotics in the clinical setting, it is seriously flawed in these applications. The reported MIC is dependent on the time frame of measurement (usually 18–22 h post incubation), the initial inoculum (usually 5×10^5 CFU/mL), and the visual assessment of turbidity (inter-strain variance in bacterial density associated with turbidity) (Stevens et al. 1993; Simard and Bergeron 1982). For example, in Fig. 17.1, we conducted a simulation of an MIC determination (using Berkeley Madonna 8.3.18), assuming the preexistence of three bacterial subpopulations. The more sensitive population has an EC_{50} of 5.30 mg/L and an initial inoculum of $10^{5.5}$ CFU/mL, and the less sensitive subpopulations have an EC_{50} of $\sim$31.8 mg/L and an initial inoculum of $\sim 10^2$ CFU/mL. The resistant subpopulation is usually less fit, which explains the small percent of the initial inoculum. The bacterial load curves show an initial decrease and hit a nadir, which is followed by regrowth after drug treatment. This initial net kill is due to the drug affecting the sensitive population, reducing competition for the resistant subpopulation, which can then propagate and take over the inoculum. The vertical limit lines denote the 18–22 h window within which the MIC could be determined. The horizontal limit lines represent the bacterial concentration threshold counts required for visual assessment of turbidity. If, for example, the MIC is determined at 18 h instead of 22 h, the MIC value reported will be 2 mg/L compared to 4 mg/L that would be reported at 22 h. The bacterial burden at 18–22 h in this experiment (or at any other single point of time) is not particularly representative or reflective of the overall bacterial response to a drug concentration (compare the $\log_{10}$CFU at 4–8, 18–22, and 48 h in Fig. 17.1). Characterizing the temporal profile of bacterial kill and growth will provide better insights into drug efficacy, as compared to the MIC as a predictor of outcome.

The initial bacterial inoculum is usually a heterogeneous population consisting of bacterial sub-populations with differing susceptibilities. The dominant subpopulation, which usually determines the MIC, is often the most susceptible subpopulation, but may not be the one responsible for treatment failures. The MIC value might be used to adequately describe bacterial isolates that are a mixture of populations with various susceptibilities. However, if only one MIC value is allowed to represent the mixture, the MIC of the less susceptible subpopulation should be reported. Detection of the resistant subpopulation would be favored by determination of the bacterial count at a later sample point (e.g., 48 h) or characterizing the MIC based on a higher initial inoculum (such as 10^7 CFU/mL). Despite its deficiencies, the MIC is sometimes used as a covariate for describing concentration-effect relationships of antibacterials.

The MIC is not an intrinsic property of a microorganism. Instead, it is the net difference between the growth rate of the bacteria and rate of kill due to the fixed antibacterial concentration (Boucher et al. 2009, 2013b). MICs are determined at a fixed concentration after a fixed amount of time, as compared to in vivo conditions, in which the concentrations of the antibiotic are dynamic in nature (changing as a function of time). In addition, pre-selected drug concentrations in MIC experiments usually follow two-fold increments. This can result in significant uncertainty in the

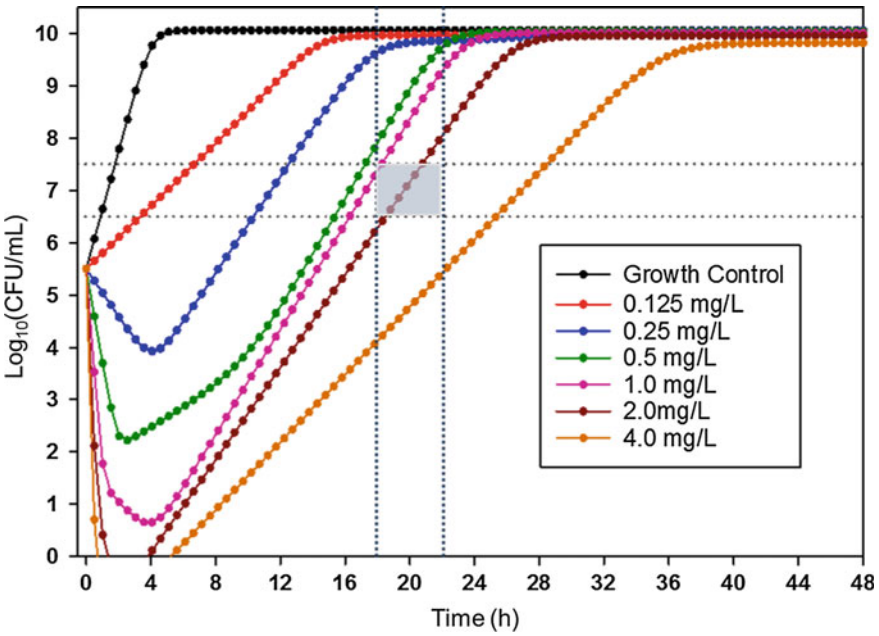

Fig. 17.1 Simulations of an example *Staphylococcus aureus* strain following treatment with a fluoroquinolone assuming three bacterial subpopulations: a sensitive, less sensitive, and a resistant subpopulation. The *dashed vertical limit lines* denote the 18–22 h window within which the MIC should be determined. The *dashed horizontal limit lines* represent the bacterial concentration threshold counts required for visual assessment of turbidity. If, for example, the MIC is determined at 18 h instead of 22 h, the MIC value reported will be 2 mg/L as compared to 4 mg/L at 22 h. The bacterial burden at 18–22 h in this experiment (or at any other single point of time) is not particularly reflective of the overall bacterial response to a drug concentration. These simulations illustrate the problems associated with determining the MIC

MIC, which might be reduced by using a denser grid of drug concentrations. Quantification of the bacterial count, as opposed to just visual assessment of the turbidity (dichotomous output), would help alleviate the ambiguity in determination of the MIC.

17.3 Determining the PK/PD Driver, Target Values, and Target Attainment

A common practice in modern antibiotic drug development is the grouping of drugs by their predominant PK/PD driver and the determination of which target is a good predictor of antimicrobial activity in patients. The drivers considered are usually the area under the free (unbound) concentration-time profile to MIC (*f*AUC/MIC, the percentage time that the unbound drug concentration exceeds the MIC of the

organism (%*f*T > MIC), and the peak free drug plasma concentration to MIC ratio (*f*Cmax/MIC) (Craig 1998; Andes and Craig 2002; Mouton et al. 2005). A major, early objective in infectious disease drug development is the determination of the PK/PD index and the magnitude of this PK/PD index necessary for targeted degrees of effect (e.g., net stasis, 1-, 2- or 3-logs of net kill). These objectives are accomplished by conducting dose-ranging studies, followed by dose fractionation studies, with selected strains of bacteria. The design of these studies typically include a range of 3 or 4 daily doses, each fractionated (e.g., entire daily dose given once a day dosed as q24 h, one-half the daily dose given twice a day as q12 h, one-quarter the daily dose given four times a day as q6 h, and one-eighth the daily dose given eight times a day dosed as q3 h). This design enables decoupling the autocorrelation between Cmax, AUC, and time above a threshold, which would occur in a simple dose-ranging study (i.e., for the same AUC, a range of Cmax and T > MIC values are achieved). Three plots are typically constructed relating drug effect to each of the three indices, and the index that fits the data the best is selected as the PK/PD driver for the tested antibiotic. The fitted PK/PD model is also used to determine the index values necessary to achieve targeted drug effects (e.g., net stasis, 1-, 2-, 3-logs of net kill). These index values then become 'targets' for developing dosing guidelines, by calculating target attainment using Monte Carlo simulation.

Dose fractionation and target attainment studies are common and serve a useful, but limited purpose. These studies provide insights into proper maintenance regimens (daily dose and dosing intervals), but they do not provide the necessary knowledge for predicting optimal initial therapy, the expected time-course of drug effects, and the duration of therapy. The main shortcoming of the PK/PD index driver approach is that the time-course of antimicrobial pharmacokinetics and pharmacodynamics is not taken into consideration. Modeling the time-course of the relationship between drug concentration and the pharmacodynamic effect should aid in (a) the development of novel regimens, such as those with front-loading (Tsuji et al. 2012; Rao et al. 2013, 2016) and optimal sequencing of combination regimens, or (b) the determination of optimal duration of therapy.

17.4 Experimental Models for Infectious Disease

In vitro experimental models of infection are important tools that aid in the PK/PD characterization of antibacterial agents in conjunction with in vivo systems (Wootton et al. 2001). The in vitro experimental model provides a quick and cost effective method to assess the pharmacodynamic activity of an antibacterial against a bacterial population of interest, which can serve as preliminary data for further evaluation of proposed hypotheses. These experimental models provide flexibility over in vivo animal models given the ease of working with different inocula that will be exposed to the drug regimen of interest, the range of effective drug concentrations, and frequency of sampling necessary for full characterization of the PK/PD relationship. The results from in vitro studies may significantly differ from

that obtained in vivo as the only interaction possible in vitro is between the drug and the bacteria, whereas the in vivo system also includes interactions with the host immune system. In vitro experiments can be broadly classified into two categories, namely static and dynamic systems, based on the nature of the drug concentration profiles imposed for the duration of the experiment.

17.4.1 Static in Vitro Experimental Models

The time-kill experimental setup is the simplest in vitro experimental system consisting of a single culture tube that contains the growth media, bacteria of interest, and the antibacterial agent. The time-kill culture tubes are incubated in a water bath at 35–37 °C, with constant shaking to maintain a homogenous environment. The main assumption is that the bacteria are exposed to a static environment in which the drug concentration is constant for the duration of the experiment. It is also assumed that bacterial growth is not limited by the supply of the nutrients as long as bacterial regrowth does not exceed the initial inoculum (Keil and Wiedemann 1995). The environment within each time-kill system is continually changing as the growth media is being depleted of nutrients while toxins released from the bacteria are accumulating. The duration of time-kill studies range from as short as 8 h to as long as 72 h. This model can be used for dose-ranging studies to provide insight into the killing dynamics of the drug and approximating the behavior of a continuous infusion in vivo. The limitation of this static experimental setup is the inability to simulate human pharmacokinetic dosing regimens.

17.4.2 Dynamic in Vitro Experimental Models

One-compartment and hollow fiber in vitro infection models (HFIM) are dynamic systems as the antibiotic concentration can be altered over the duration of the experiment, hence allowing for the assessment of the pharmacodynamics under experimentally simulated human dosing conditions. Dynamic in vitro experimental models are classified as open or closed systems depending on the loss of bacteria based on the in vitro experimental setup.

17.4.3 Open Systems (Models Without Filters)

The apparatus for a one-compartment system consists of a reservoir connected by airtight silicon tubing to an Erlenmeyer flask equipped with magnetic stirrers to ensure homogenous mixing maintained at 35–37 °C. Fresh media is pumped at a constant rate by a peristaltic pump from the reservoir into the Erlenmeyer flask

(central compartment) containing the antibiotic and bacteria of interest, which causes an equal amount of volume to be displaced as it is pumped out so as to maintain a constant working volume (Grasso et al. 1978). The addition of fresh growth media at a constant rate allows dilution of the antibiotic and bacteria, resulting in "washout" of the bacteria in addition to the antibiotic. The antibiotic of interest can be added to the central compartment at regular intervals to simulate human pharmacokinetics, or it can be added to the reservoir containing the growth media to simulate a continuous infusion. Peristaltic pumps are used to control the flow of fresh media into and the isovolumetrical removal of media from the central reservoir at rates programmed to simulate the half-life of the drug in humans. The main disadvantage of this in vitro experimental system is the continuous loss of bacteria from the central reservoir by dilution. This interferes with the ability to determine the reduction in the initial bacterial inoculum as a result of the antibacterial agent alone. The loss of bacteria due to flow can be neglected as long as the concentration-time curve is not affected or when the antibacterial effect results in reductions of the initial bacterial load below the limit of detection rapidly with no visible regrowth. Correction for bacterial loss as a result of dilution is necessary for comparisons of antibiotics with different elimination half-lives or different killing dynamics (Murakawa et al. 1980; Keil and Wiedemann 1995). Equation 17.1 enables the necessary correction for the bacterial loss from the system:

$$\frac{\mathrm{dCFU}}{\mathrm{dt}} = \mathrm{k_g} \cdot \left(1 + \frac{\mathrm{CFU}}{\mathrm{CFU_{max}}}\right) \cdot \mathrm{CFU} - \frac{\mathrm{FR}}{\mathrm{V}} \cdot \mathrm{CFU}, \quad \mathrm{IC:\ CFUo} \tag{17.1}$$

with CFU as the total bacteria in the reservoir (CFU/mL), $\mathrm{CFU_{max}}$ is the maximal growth rate of the bacteria (CFU/mL), CFUo is the initial inoculation (CFU/mL), $\mathrm{k_g}$ is the net first-order growth rate constant (units of $\mathrm{time^{-1}}$), FR is the flow rate of media (mL/units of time), and V, is the volume of the central reservoir (mL).

17.4.4 Closed Systems (Models with Filters)

Several systems with filter membranes to prevent the loss of bacteria due to washout have been proposed (Lowdin et al. 1996). The membrane based systems face the possibility of the membrane pores becoming blocked, especially with high flow rates necessary for drugs with relatively short half-lives. Hence, the two-compartment diffusion or dialysis-based systems were proposed to overcome the shortcomings of filter membrane systems (Navashin et al. 1989; Reeves 1985; Schneider and Lewis 1982; Gloede et al. 2010). In this system, the bacteria are contained in a peripheral compartment, separated from the central compartment by a membrane, in order to avoid dilution of the bacterial inoculum at the same rate as the antibiotic. Similar to the experimental systems in Sect. 17.4.3, the drug and fresh media are added to the same central compartment to dilute the drug. The drug and the necessary nutrients diffuse (via the membrane) into the peripheral space

containing the bacteria. The main limitation of these single membrane systems is that the equilibration between the two compartments is slow as it depends on passive diffusion across the membrane.

Therefore, an increase in the surface area of the dialysis membrane will allow for rapid equilibration resulting in the kinetics of the peripheral compartment resembling the kinetics in the central compartment (Zinner et al. 1981). The hollow fiber system consists of a collection of dialysis capillaries of hollow fibers (Blaser 1985; Blaser et al. 1985). The capillaries have a fixed central compartment working volume and are connected to a pump that pumps fresh media, with a flow rate determined by the elimination rate of the drug. Similar to previous systems, the peripheral compartment consists of the extracapillary space that contains the bacteria. The concentration gradient across the capillaries is the driving force for the diffusion of drug and nutrients from the central compartment into the peripheral space. The semipermeable nature of the capillaries allows for only waste from the peripheral space to diffuse into the central space. The commercial hollow fiber systems allow for sampling of the central and the peripheral space and dosing via computer controlled syringe systems that can simulate the desired dosing regimens for the drug(s) of interest. Since these systems are less prone to contamination related issues, they can be used to conduct studies over a prolonged duration of time (e.g., up to 28 days) necessary to study the emergence of drug resistance (Drusano et al. 2010b; Srivastava et al. 2011).

17.4.5 Limitations of in Vitro Experimental Systems

The main drawback of these in vitro experimental systems is that they do not take into account the host immune system, drug-protein binding, and characteristics of the infection site. Other limitations include: the high surface area to volume ratio of the hollow fiber system, the facilitation of bacterial growth by nutrient rich environments, static antibiotic concentrations in time-kill experiments, the lack of infection site-specific pharmacokinetics, and the lack of concentration-time profile measurements in most in vitro studies. These limitations may necessitate the evaluation of promising treatment regimens in an in vivo infection model.

17.4.6 In Vivo Infection Experimental System

Animal studies are important to gain insights into the host response and the progression of infection. Animal infection experimental systems play an important role in bridging the gap between characterization of the antimicrobial agent using in vitro concentration-effect experiments and evaluation of clinical efficacy. Specifically, carefully defined animal models of infection not only provide insight into the efficacy of newer antimicrobial agents, but they can also be used to assess

the pharmacokinetics and toxicities of these compounds. Furthermore, important information can be obtained regarding unique or unusual infections that may serve as an example or precursor for clinical trials in humans. In vivo systems capable of mimicking the time-course and pathophysiology of infections in patients are useful for preclinical assessments of new antibiotics, as well as optimization of existing antibiotic regimens using approved antibiotics. There are a number of animal infection systems, based on the site of infection under investigation, immune status, and the renal function of the animal. The use of appropriate pharmacodynamic analyses can account for these differences and allow for comparison of data between different studies by determining the magnitude of the PK/PD index necessary for antimicrobial efficacy across animal species and humans. Differences in pharmacokinetic profiles, drug metabolism/excretion, and anatomical differences between the animal species and humans can result in incorrect predictions of toxicity in humans based on animal toxicity data (Zak and O'Reilly 1990). Despite these challenges and limitations, toxicity evaluation of antimicrobial agents in animals has been and will continue to be an essential part of drug development as they have shown to be predictive of maximum tolerable doses, a prerequisite for clinical trials.

17.5 Bacterial Quantification

17.5.1 Total Bacterial Population

The determination of bacterial counts is performed by obtaining serial samples from any of the previously described in vitro systems at pre-determined times that will best characterize the pharmacodynamics of the antibacterial agent(s) being evaluated. The samples for the experimental system are immediately serially diluted in cold 0.09 % sodium chloride. Viable bacterial counts are determined by plating aliquots of each diluted sample, generally 50 μL, on agar plates either manually or by using an automated spiral dispenser. The plated samples are incubated at 37 °C for 24 h, and colony counts are determined in $\log_{10}$ CFU/mL either manually or by using an automated bacterial colony counter.

17.5.2 Resistance Quantification

Population Analysis Profile (PAP) is an experimental method that allows for characterization of different resistant subpopulations and determination of the emergence of resistance during therapy for both in vitro and in vivo studies (Jumbe et al. 2003; Li et al. 2006; Wootton et al. 2001). Incorporating these data into the pharmacodynamic mathematical model will aid in predicting emergence of resistance due to treatment, as well as the optimization of antibiotic treatment to prevent the emergence of resistance.

17.6 Experimental Design

17.6.1 In Vitro Experiment

The design of in vitro experimental studies involves the selection of the appropriate conditions based on the nature of analysis and the duration of the study. The initial bacterial inoculum can affect the rate and extent of kill that can be attained by antibacterials and the probability of observing the emergence of resistant subpopulations under drug pressure. The nature of the inoculum (heterogeneous log phase or homogenous late-log phase), the range of doses studied (clinically achievable or a wide dose range), susceptibilities of the strain, and analytical methods used to quantify the antibacterial pharmacodynamic effect are just some of the other relevant factors that need to be considered in experimental designs.

17.6.2 In Vivo Experiment

The design of animal studies is critical for the translation of promising interventions to the clinic. The lack of correlation between results from clinical trials and pre-clinical animal studies are multifactorial and could stem from inadequacies of animal studies. The first of the more common flaws is the lack of sufficient statistical power of animal studies to detect the true benefit or effect of a given treatment. The second error, compounding the first, is over-optimistic interpretation of the results from a poorly powered animal study. The third error is the inability of the animal model to emulate the full course of disease pathophysiology in humans. The lack of external validity can be a rate-limiting step in the translation of pre-clinical animal results to the clinic. Lastly, in some cases, the in vivo experimental design and results may be valid, but errors in calibration between pre-clinical species and humans could result in incorrect translation of the results.

Selection of an appropriate in vivo system is guided by multiple considerations, including: specific disease states being studied, the nature of sampling (e.g., destructive), the amount per sample (e.g., volume of blood that can be obtained from the animal per sample), the number of samples intended during the duration of the study, the route of drug administration, the ability to dose the drug, and the nature of the toxicodynamics of the drug. For example, the murine model does not lend itself well for sampling at multiple time points to track the time-course of individual disease progression, given the limited total amount of blood that can be obtained. This often results in destructive sampling at each of the intended time points. Ideally, the pharmacokinetics and pharmacodynamics should be evaluated in the same animals to reduce the variability in resulting concentration-effect relationships. Current animal infection models are not convenient to study disease progression using a systems biology approach (Drusano et al. 2010a, 2011a, b) in which multiple biomarkers of interest are monitored to associate disease

progression and the severity of the infection with the host immune response to the bacterial infection. Ideally, the efficacy of a proposed treatment regimen should be evaluated using an intact host immune system as opposed to an immunity deficient system (many current animal infection models are immune compromised in nature).

17.7 Current Practice of Antibacterial Modeling

The modeling philosophy of antibacterial data has evolved over the past 50 years, resulting in a few generations of different model structures describing the growth kinetics of bacteria and the evolution of the bacterial population under drug pressure. Modeling antimicrobials has the distinct advantage wherein the target is readily accessible since the bacterial load can be quantified in both in vitro and in vivo experimental conditions. In this section, we describe some of the representative key models.

17.7.1 Bacterial Growth Model in Absence of Drug

The typical bacterial growth curve exhibits an initial lag phase, during which time the bacteria are acclimatizing to the new environment, and is followed by an exponential growth phase when the bacteria start dividing by binary fission processes. The different models proposed to characterize bacterial growth are exponential (Mouton et al. 1997; Nielsen et al. 2007; Zhi et al. 1988; Garrett et al. 1970; Garrett and Wright 1967), logistic (Jumbe et al. 2003; Mouton et al. 1997), capacity limited (Bulitta et al. 2010; Harigaya et al. 2009; Meagher et al. 2004), and the life-cycle model (Bulitta et al. 2009; Landersdorfer et al. 2013; Tsuji et al. 2012). The exponential growth model was commonly used in the 1970s and 1980s, as these models describe the exponential growth phase well, given that the bacteria never attained maximum growth capacity within the relatively short duration or limited conditions of the experimental setup at the time (Zhi et al. 1988; Garrett et al. 1970; Garrett and Wright 1967). The logistic growth model is commonly used when the experimental data is obtained over a prolonged period of time comprising of all phases of bacterial growth. The equations for the different growth models are as follows:

(A) **Exponential growth model**:

$$\frac{d(CFU)}{dt} = \left(k_g - k_d\right) \cdot CFU, \quad IC: CFU_o \tag{17.2}$$

Equation 17.2 represents a common model describing bacterial growth (Fig. 17.2a). CFU is the bacterial population, k_g is a first-order rate constant

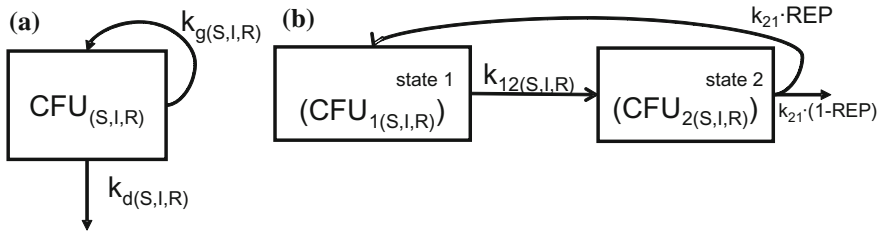

Fig. 17.2 Simple models of bacterial growth. **a** An exponential bacterial growth model with a first-order rate constant describing bacterial growth (k_g) and a first-order rate constant controlling bacterial death (k_d). **b** The life-cycle growth model in which bacteria are assumed to exist in two-states: a vegetation state (state 1) and a replicative state (state 2)

describing bacterial growth, and k_d is a first-order rate constant describing bacterial death. Based on in vitro data, it is difficult to determine both rate constants, k_g and k_d, and only the net growth rate constant (the difference between k_g and $k_{d,}$) is estimable.

(B) **Logistic growth model**:

$$\frac{d(CFU)}{dt} = k_g \cdot \left(1 - \frac{CFU}{CFU_{MAX}}\right) \cdot CFU - k_d \cdot CFU, \quad IC: \ CFU_o \tag{17.3}$$

Equation (17.3) describes bacterial growth for a system constrained by a maximal population (Fig. 17.2a). CFU_{MAX} is the maximum bacterial population attainable within the study system. When the bacterial population approaches CFU_{MAX}, the net growth rate approaches zero.

(C) **Capacity Limited Growth Model**

$$\frac{d(CFU)}{dt} = \left(\frac{VG_{max}}{CFU_m + CFU} - kd\right) \cdot CFU, \quad IC: \ CFU_o \tag{17.4}$$

Equation (17.4) describes the total bacterial growth using a Michaelis-Menten type function. The rate of bacterial replication is parameterized by the maximal velocity of bacterial growth, VG_{max} (CFU/mL/h), and CFU_m is the CFU at which the rate of replication is half the maximal velocity of bacterial growth. VG_{max} could be reparametrized in terms of k_d, CFU_m, and CFU_{max} as:

$$\text{At the plateau, } \left(\frac{VG_{max}}{CFU_m + CFU_{max}} - kd\right) \cdot CFU_{max} = 0 \tag{17.5}$$

$$VG_{max} = kd \cdot (CFU_m + CFU_{max}) \tag{17.6}$$

(D) **Life cycle model**

$$\frac{d(CFU_1)}{dt} = Rep \cdot k_{21} \cdot CFU_2 - k_{12} \cdot CFU_1, \quad IC: \ CFU_o \tag{17.7}$$

$$\frac{d(CFU_2)}{dt} = \quad -k_{21} \cdot CFU_2 + k_{12} \cdot CFU_1, \quad IC: 0 \tag{17.8}$$

$$CFU_{all} = CFU_1 + CFU_2 \tag{17.9}$$

$$Rep = 2 \cdot \left(1 - \frac{CFUall}{CFUmax + CFUall}\right) \tag{17.10}$$

The life-cycle model (Fig. 17.2b) is based on physiological processes of bacterial replication, and the flexibility of this model allows for easy incorporation of antibiotic mechanisms of action against bacteria (Bulitta et al. 2009; Tsuji et al. 2012; Landersdorfer et al. 2013). In this growth model, the replication process is simplified to two states, a vegetative state (CFU_1, preparing for replication) and replicative state (CFU_2, a state prior to dividing or binary fission) as described by Eqs. (17.7) and (17.8). The total bacteria in the two states is represented by Eq. (17.9). The conversion rate constant (k_{12}) between the two states, CFU_1 to CFU_2, is assumed to be rate-limited while conversion rate constant (k_{21}) from CFU_2 to CFU_1 is assumed to be rapid. The replication factor (REP) shown in Eq. (17.10) provides the doubling factor for each cycle, and CFUmax is representative of the carrying capacity of the system.

The effect of antibiotics can be incorporated in the model either by stimulating k_d or inhibiting bacterial replication (i.e., k_{12}, k_g, and VG_{max}). Additionally, first-order or second-order killing kinetics of the antibiotic could be incorporated into these models. The logistic, capacity-limited, and life cycle models describe the experimentally observed plateau well and are frequently used to describe the growth kinetics of bacteria.

17.7.2 Modeling Bacterial Populations

There are a number of pharmacodynamic models that assume different characteristics of the bacterial population. The nature of the experiment often dictates the nature of the bacterial population (heterogeneous or homogenous).

Single population Prior to the 1990s, models describing bacteria growth and killing dynamics assumed a single homogeneous bacterial population (Zhi et al. 1988; Garrett et al. 1970; Garrett and Wright 1967), and the initial killing was

reasonably explained by these models. In vitro and in vivo experimental studies were conducted over a relatively short period of time, typically up to 300 min (Zhi et al. 1988; Garrett et al. 1970; Garrett and Wright 1967), and selected doses were much higher or lower relative to the MIC of the bacteria of interest, resulting in complete suppression or uninhibited growth (Meagher et al. 2004). The assumption of a homogenous bacterial population seemed reasonable. However, advanced experimental methods and increased knowledge of bacterial physiology have led to a consensus that the bacterial population is heterogeneous in nature arising from differences in fitness, which led to the development of pharmacodynamic models that could explain this heterogeneity.

Mixture model bacteria population The bacterial population consists of a mixture of subpopulations with varying degrees of susceptibilities, which becomes apparent during the course of dose ranging in vitro studies conducted over an extended period of time. The signature profile for heterogeneous subpopulations is regrowth after initial decline in the bacterial inoculum or continued persistent bacterial populations without further growth or decline in the bacterial population when exposed to antibiotic drug pressure (Bulitta et al. 2009, 2010; Jumbe et al. 2003; Landersdorfer et al. 2013; Meagher et al. 2004). We described the heterogeneity in the initial inoculum by assuming two or more pre-existing genotypic bacterial subpopulations with differing susceptibility to antibiotics. Meagher et al. observed attenuation of killing upon repeated dosing, and they assumed two pre-existing subpopulations to account for this behavior (Meagher et al. 2004). Campion et al. developed a similar model with unique growth and killing rate constants for the susceptible and resistant bacterial subpopulations to describe the activity of ciprofloxacin against *Staphylococcus aureus* when exposed to different pharmacokinetic profiles (Campion et al. 2005). The authors assumed pre-existing subpopulations, enrichment of resistant subpopulations in the presence of ciprofloxacin, and allowed for the conversion of the susceptible subpopulation to a resistant phenotype. Multiple investigators have provided evidence of adaptive resistance when bacteria are exposed to environmental or antibiotic pressures (Macfarlane et al. 1999; McPhee et al. 2003; Fernandez et al. 2010). This results in a shift in subpopulations (inter-conversion between existing sub-populations) and the emergence of new subpopulations, and mathematical models have been implemented with this inter-conversion between existing subpopulations (Nielsen et al. 2007; Yano et al. 1998). Jumbe et al. (2003) proposed two pre-existing subpopulations similar to the models of Meagher et al. (2004) and Campion et al. (2005), with the exception that Jumbe et al. (2003) incorporated PAP experimental data enabling the quantification of the total and resistant subpopulations. This model allows for the quantification of the time-course of emergence of resistant subpopulations during the course of therapy and can aid in dose selection for suppression of the emergence of resistance.

17.7.3 Mechanism-Based Models

The increasing knowledge base about molecular mechanisms of interactions between antibiotics and antibiotic targets, coupled with advanced experimental techniques and computational capability, makes the development of mechanism-based PK/PD models incorporating receptor binding and bacterial physiology feasible. This new generation of mechanism-based PK/PD models will enable the exploration and increased understanding of the underlying complex mechanisms of the infectious process.

Bulitta et al. developed a mechanism-based mathematical model incorporating the current knowledge about bacterial physiology, receptor binding, and antibiotic mechanism of action that could describe and predict the time-course of bacterial growth and killing (Bulitta et al. 2009, 2010). The pharmacodynamic model for ceftazidime against *P. aeruginosa* incorporated bacterial physiology in terms of the lag time of bacterial killing as a result of the turnover of cell wall constituents, and the lag time was dependent on the antibiotic concentration. Additionally, the mechanism of action of ceftazidime was incorporated and accounted for the delay observed in the binding of the antibiotic to its target, penicillin-binding protein (i.e., PBP3). The authors observed an attenuation of ceftazidime activity with increasing initial inocula. This led to the hypothesis that bacteria produce and release signal molecules at high bacterial densities that may result in the modulation of certain pathways resulting in antibiotic tolerance. The final model that included this mechanism allowed for the characterization of the attenuated bacterial killing at high bacterial inoculum.

Monte Carlo simulations, using a ceftazidime population pharmacokinetic model and the final mechanism-based pharmacodynamic model, were used to predict the time-course of effect in response to two different infusion durations (i.e., 5 h vs. 30 min) against two different initial bacterial inocula. The model predicted that prolonged infusion of ceftazidime provided a better pharmacodynamic profile, and the high inoculum resulted in attenuated killing by ceftazidime (Bergen et al. 2011), which is in agreement with the clinical PK/PD target (i.e., time above MIC). This mechanism-based model was developed based on known bacterial physiology and mechanism of action of ceftazidime and enabled the enhanced characterization and prediction of bacterial response with increased precision and under new experimental conditions.

17.7.4 Quantification of Combination Therapy

The rapid rise in antibiotic resistance has led to the emergence of so-called ‘super bugs’ and, coupled with the lack of viable treatment options, it has forced clinicians to increasingly prescribe antibiotic combinations. Combination therapy can provide broad-spectrum empirical coverage, resulting in the increased likelihood of clinical

success by maximizing the decrease in bacterial load while minimizing the emergence of resistance as well as adverse drug effects. The benefit of synergy is an increased rate of killing; one drug may potentiate or enhance the activity of the other drug in the combination, resulting in significant improvement of outcomes against resistant and hard to treat bacteria. The ability to quantify drug interactions is one of the major challenges when assessing antibiotic combinations. Qualitative terms like synergy, additivity, or antagonism are used to describe the pharmacodynamic drug interaction of antimicrobials. Based on the traditional definition of synergy, the interaction between two drugs is classified as synergistic (or antagonistic) when the observed effect of the combination is more (or less) than what would be predicted based on the knowledge of the effects of each drug acting independently (Greco et al. 1996). The two main metrics used to quantify the interactions between drugs are Loewe additivity and Bliss Independence. The main difference between the different metrics for evaluating pharmacodynamic interactions is based on the definition of additivity, "no interaction" between the two agents used in combination.

Loewe additivity defines a drug as non-interacting with itself. For example, if drugs A and B are the same drugs or very close structural analogues, then the combination of drug A and B at equal concentrations should produce the same effect if either A or B were used at twice the dose (Greco et al. 1995; Yeh et al. 2009). Loewe additivity is presented in Eq. (17.11), in which the concentrations of drug A and B contained in the combination is indicated by C_A and C_B, and the concentrations required to produce the given effect (e.g., 50 % inhibition of maximum, IC_{50}) are D_A and D_B:

$$1 = \frac{C_A}{D_A} + \frac{C_B}{D_B} \tag{17.11}$$

Synergy, additivity, or antagonism is indicated by the required concentrations C_A and C_B. For example, the combination of drug A and drug B is additive if 2.5 mg/L of drug A combined with 2.5 mg/L of drug B produces 50 % inhibition of bacterial growth equivalent to 1 mg/L of drug A or drug B used alone. The combination is synergistic in nature if the drug required to achieve the same amount of inhibition is less as compared to when either drug is used independently. However, the combination is antagonistic if the drug required to achieve the same effect as a part of a combination is more compared to when either drug is used independently.

Bliss independence, on the other hand is defined as fractional response due to the combination of two agents at specific concentrations (Greco et al. 1995; Yeh et al. 2009). Bliss independence assumes that both agents used in combination have distinct mechanisms and that each agent in the combination produces an effect independent of the presence of the other agent. Hence, it is the product of the fractional responses of each agent applied alone at the specific concentrations (Eq. 17.12), where E_{AB} is the effect of drug A and B in combination, E_A and E_B are the effect of drug A and B alone:

$$E_{AB} = E_A \cdot E_B \tag{17.12}$$

The fraction of effect when drug A and drug B are used in combination (F_{AB}) based on the definition of Bliss Independence can be calculated using Eq. (17.13):

$$F_{AB} = F_A + F_B - F_A \cdot F_B \tag{17.13}$$

where F_A is fraction of the effect due to drug A alone, and F_B is fraction of the effect due to drug B alone. Therefore based on Bliss Independence, the combination is additive when the joint activity is equal to that predicted by Eq. (17.13). When the joint activity is greater than that predicted, the combination is considered to be synergistic. For example, if drug A produces 50 % of inhibition, and drug B produces 25 % of inhibition when evaluated independently then together, the interaction is quantified as synergistic when the joint activity of A and B is greater than the activity of each acting independently, i.e., decrease in growth due to the combination based on Eq. (17.13) is greater than 62.5 % ($F_{AB} = 0.5 + 0.25 - (0.5) \cdot (0.25) = 0.625$). Bliss Independence in the logarithmic domain will be additive. The drawback of these metrics is that the classification labels do not appropriately describe the nature of the interactions. A label of synergy may not always mean that the outcome will be favorable, and similarly a combination labeled antagonistic may not mean that the outcome is less than favorable. The following examples will help illustrate the drawbacks of these classification methods.

The first example involves an additivity classification with linezolid, a synthetic antibacterial agent, a member of the oxazolidinone class that prevents protein synthesis by targeting the 50s ribosomal site (Shinabarger et al. 1997). Nisin is a peptide antibiotic that induces pore formation in bacterial membranes and inhibits the synthesis of peptidoglycan (Gao et al. 1991). The pharmacodynamic activity of linezolid and nisin, when dosed simultaneously as a combination against a high inoculum of a MRSA strain, was suggestive of limited promising joint activity (Landersdorfer et al. 2013). By definition of Bliss Independence, this combination is classified as simply additive, but despite this classification, the interaction has meaningful clinical benefits.

The second example is for a synergistic classification with colistin, also known as polymyxin E, which belongs to the polymyxin class of antibiotics. Colistin exerts its bactericidal effect by competitively displacing Mg^{2+} and Ca^{2+} ions (divalent cations) necessary to form cross-linkages between the adjacent negatively charged phosphate groups of the lipopolysaccharides (LPS) in the outer cell membrane of Gram-negative bacteria (Lim et al. 2010). This results in disruption of the outer cell membrane, leakage of intracellular contents, and eventually bacterial death. Doripenem is a carbapenem that displays bactericidal activity by inhibiting cell wall synthesis via inactivation of penicillin-binding proteins (Davies et al. 2008). Based on the definition of Bliss Independence, the simultaneous dosing of colistin and doripenem resulted in greater combined activity compared to when either drug was used as monotherapy (Landersdorfer et al. 2013).

An excellent example to illustrate antagonism is the combination of rifampicin and vancomycin. Rifampicin is a semisynthetic derivative of the rifamycins class of antibiotics. It is bactericidal in nature as it inhibits bacterial RNA polymerase responsible for DNA transcription (Drusano et al. 2010b; Wehrli 1983). Vancomycin, a glycopeptide that primarily inhibits cell-wall biosynthesis, binds with high affinity to the D-Ala-D-Ala C-terminus of the pentapeptide, thus preventing the incorporation of *N*-acetylmuramic acid (NAM) and *N*-acetylglucosamine (NAG)-peptide subunits into the peptidoglycan matrix (Hammes and Neuhaus 1974). In vitro studies suggest that this combination is antagonistic in nature based on the definition of Bliss Independence. Despite this categorization, rifampicin and vancomycin represents a highly beneficial combination against acute clinical staphylococcal infections, as it prevents the emergence of resistance and helps reduce the virulence of the pathogen.

The classification of in vitro synergy is not necessarily associated with clinical success, as two drugs could be synergistic but do not exhibit sufficient activity when dosed together resulting in a good clinical outcome. Labels like antagonism, synergy, or additivity that are typically used to group the joint activity of antibiotics may misrepresent the outcome of the interaction of these antibiotic combinations. The label is not indicative of the clinical outcome, as it is the overall activity based on the interaction that determines the outcome. In part, this failure may be due to the lack of mechanistic information about the interaction of the drugs when used in combination. The gap in knowledge about the "mechanisms of interaction" of drug combinations can be addressed by quantitative systems modeling incorporating information about the drugs and the biological target and host physiology.

17.7.5 Modeling Antimicrobial Combinations

Quantifying antibiotic interactions is generally achieved by performing measurement at pre-determined end points. However, the limitation of all such methods is that they are point-based estimates, which do not take the time-course of interaction into consideration. More importantly, none of these approaches recognize or account for the presence of multiple bacterial subpopulations with differing susceptibilities (Bulitta 2009). Earp et al. (2004) proposed a framework for quantifying drug-drug interactions based on the principle of indirect response models as the measured response for basic turnover processes. Drugs can perturb the production or elimination of a biomarker or the turnover process of the bio-signal in a competitive or noncompetitive fashion. Additionally, both drugs could act on the same process in a competitive or noncompetitive manner. The net response of a combination is not only dependent on the intrinsic pharmacological properties of the single agents but also on their pharmacokinetics, the nature of the antibiotic target, and the mechanism of interaction between the two agents. Hence, two agents with similar pharmacodynamic and pharmacokinetic properties may elicit different responses depending on whether both agents affect the same target in a competitive

or non-competitive manner. Such a framework could be applied to quantify drug interactions of an antimicrobial combination.

For chemotherapeutic combinations, agents could perturb replication or elimination process of bacteria, which is illustrated in Fig. 17.3. The first example is for a case in which both drug A and B act on the same process, i.e., bacterial replication (Fig. 17.3a). The two antibiotics ceftolozane and ceftazidime act on inhibiting the replication of *P. aeruginosa* by inhibiting the cell wall synthesis through binding to the penicillin binding protein (PBP) (Hayes and Orr 1983; Hong et al. 2013). The second example is for one in which drug A inhibits replication and drug B stimulates elimination of the bacteria (Fig. 17.3b). The combination of vancomycin and tobramycin provides such an interaction. Vancomycin inhibits bacterial growth (Hammes and Neuhaus 1974), and tobramycin binds to bacterial 30S and 50S ribosome, resulting in protein synthesis inhibition and enhanced bacterial killing

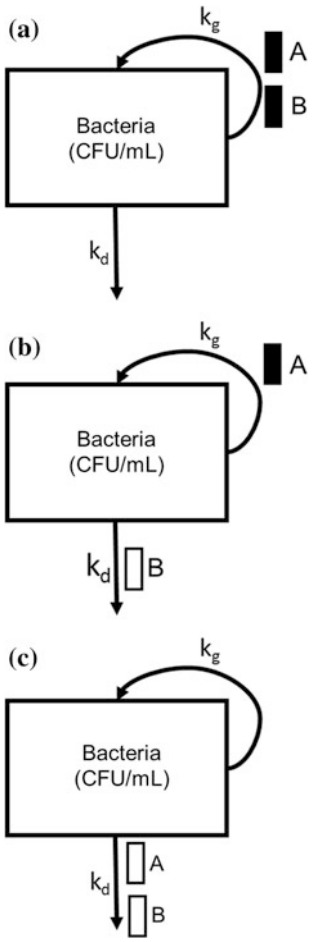

Fig. 17.3 Approaches for drug-drug interaction models for **a** both Drug *A* and *B* inhibiting the bacterial growth rate, **b** Drug *A* inhibiting the growth rate and Drug *B* stimulating bacterial cell killing, and **c** both Drug *A* and *B* stimulate cell killing

(Le Goffic et al. 1979). The last example is when both antibiotics, such as tobramycin and daptomycin, stimulate the bacterial killing process (Fig. 17.3c). Tobramycin inhibits protein synthesis (Le Goffic et al. 1979), whereas daptomycin intercalates into the bacterial membrane in a phosphatidyl glycerol dependent manner causing the disruption of the bacterial cell wall resulting in bacterial cell death (Baltz 2009).

17.8 Translation Using Monte Carlo Simulations

Monte Carlo simulation (MCS) allows for the integration of prior knowledge and drug-target interactions to predict the clinical performance of a drug at the dose(s) selected for clinical trials. Once the goal of therapy is established (bacterial kill necessary for the eradication of the organism and/or suppression of resistance), the sources of variability that will affect the achievement of the therapeutic goal (e.g., variability in pharmacokinetics, MIC values, and protein binding) can be accounted for using MCS in determining the probability of target attainment. Models derived from animal and/or in vitro experiments can be coupled with MCS to predict the probability of patients likely to achieve a specific target (target attainment) and for determining an initial antimicrobial dose (Drusano 2004; Drusano et al. 2001). This approach is commonly used and has been successful in the translation of pre-clinical studies to humans, and MCS is the method of choice for the optimization of antibiotic treatment regimens. The main drawback of the current approach is that it fails to account for the variability in pharmacodynamic activity (i.e., variability in initial inoculum, between strain variability, and bacterial heterogeneity) and host-bacteria interactions (Bergen et al. 2011; Soon et al. 2013).

One of the main reasons for clinical antibacterial failure is the emergence of resistance during the course of therapy. Translational PK/PD approaches derived from relatively short-term studies that are only 24 to 48 h in duration cannot be used to determine the target required for the suppression of the emergence of resistance. The in vitro hollow fiber system offers an advantage compared to animal experiments for testing the target necessary for suppressing bacterial resistance given the long duration of experiments possible with this in vitro experimental setup. Experiments monitoring the emergence of resistance are not routine for antibiotic development and optimization, and accounting for the time-course and variability in pharmacodynamics is essential for the effective translation of promising antibacterial compounds to the clinical setting.

17.9 Proposed Systems Modeling for Antibacterials

A major limitation of pharmacodynamic models developed based on in vitro data is that they do not take the immune system or the underlying biology that influences the time-course of in vivo infection into consideration. Figure 17.4 shows a theoretical approach for incorporating the immune system; its influence on the infecting bacteria superimposed with the drug pharmacological effect. For simplicity, the initial inoculum is assumed to consist of a single bacterial population. Bacterial growth is described by a growth model and bacteria are lost by a first-order natural death rate constant. As the infection progresses, the bacteria could undergo an adaptive process that results in the secretion of virulence factors causing the degradation of tissue and activation of the immune system, resulting in the release of cytokines and the onset or increase in symptoms. Therapeutic agents could target multiple system components, such as stimulating bacterial killing, inhibiting the production of virulence factors, and/or inhibiting the replication of bacteria.

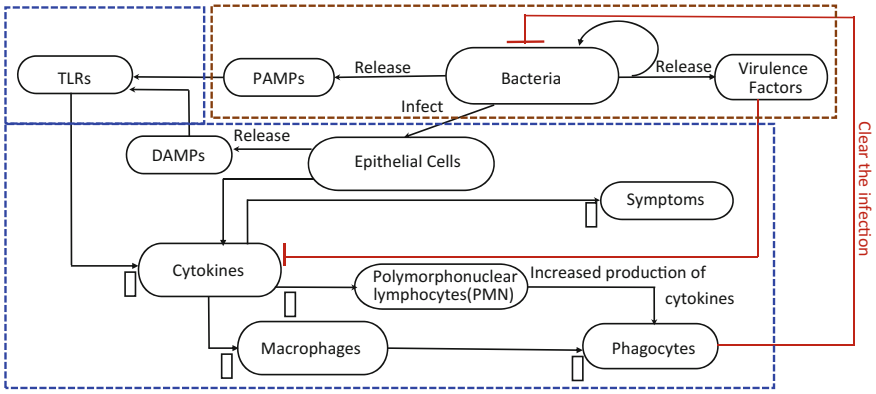

Fig. 17.4 A network of systems level regulation of host immune responses, including several interactions between the host immune system and bacteria. Host immune components are outlined (*blue box*) along with bacterial components (*brown box*). The bacteria infect the host (epithelial cells are used as an example of an infection site), and PAMPs (pathogen-associated molecular patterns) and virulence factors are released by the bacteria that influence cytokine production. DAMPs (danger-associated molecular patterns) released by damaged tissue are recognized by neutrophils, which stimulate the production of cytokines. PMNs, released by activation of the host immune system, result in increased production of cytokines and up-regulation of host symptoms through the release of cytokines. *Black* indicate stimulation processes while the *red lines* indicate inhibition processes

17.10 Considerations for Moving Toward Systems Based Approaches

17.10.1 Bacterial Physiology

Bacterial physiology and gene regulatory systems are complex and resilient. Over the past million years, both host and bacteria have co-evolved, with pathogenic bacteria adapting to host defense systems by modifying their virulence in order to change their pathogenicity. These virulence mechanisms enable the bacteria to overcome host defense mechanisms, and develop resistance under drug pressure, allowing them to adapt and survive in competitive new niches. The inability to measure these processes occurring at a molecular level precludes the development of detailed and quantitatively accurate mathematical models describing the time-course of infection. However, experimental methods like quantitative PCR, transcriptomics, proteomics, and metabolomics have enabled the quantification of molecular markers of bacterial resistance like β-lactamases, efflux pumps, and related protein activity (e.g., elastase and antibiotic target receptors).

Bacteria have a network of regulatory systems interacting with each other to promote antibiotic tolerance, drug resistance, and their adaptation and survival when exposed to hostile environments (Friedberg and Friedberg 2006). The role of the mismatch repair (MMR) system is to correct mismatched base pairs to maintain genome stability. MMR has the ability to turn on and off during different phases of bacterial growth. During the stationary phase or chronic infection, MMR genes are transiently shut down to promote mutation rates (Li et al. 2003). The SOS response system, a regulatory system that is up-regulated upon detecting DNA damage (e.g., exposure to UV light or β-lactam antibiotics), can arrest the replication process and operate in a repair mode (Friedberg and Friedberg 2006; Janion 2008). The SOS and MMR systems are examples of genetic regulators that have been associated with clinical antibacterial failure.

Another genetic regulatory system is the two-component regulatory system that consists of a sensor, a membrane spanning histidine kinase, and a regulator (cognate response regulator). The sensor allows bacteria to sense the extracellular and intracellular environments, and the response regulator then controls the downstream effect, resulting in the development of antibiotic resistance or the production of virulence factors. For example, in *P. aeruginosa*, the two-component system consists of 10 % of all genes that allow for bacteria to adapt and survive in diverse environmental conditions (Stover et al. 2000; Laub and Goulian 2007; Gooderham and Hancock 2009). Examples of a well-studied two-component regulatory systems responsible for adaptive resistance among polypeptide and cationic peptides (Macfarlane et al. 1999; McPhee et al. 2003; Fernandez et al. 2010) are PhoP-phoQ (Macfarlane et al. 1999), pmrA-pmrB (McPhee et al. 2003), and ParR-ParS (Fernandez et al. 2010). These systems have been proposed to regulate adaptive resistance in polymyxins and aminoglycosides.

Quorum sensing is another well-studied regulatory system in bacteria representing an alternative approach for bacterial resistance. Quorum sensing is a cell-to-cell communication mechanism used by bacteria as a means to regulate cell population and a diverse range of physiological processes, such as secretion of virulence factors, invasion host defences, and up-regulation of genes that may be involved in regulating antibiotic tolerance (Driscoll et al. 2007; Pesci et al. 1997; Pesci and Iglewski 1997; Pearson et al. 1995). None of the proposed PK/PD models of antibiotics incorporate virulence factors or bacterial signalling that influence the pathogenicity of bacteria.

The intrinsic or acquired resistance in response to antimicrobial treatment, coupled with limited antibiotics in the drug development pipeline, is of great concern. Pathogens can develop resistance to antibiotics during the course of therapy, especially when exposed to sub-optimal antibiotic concentrations. The common known mechanisms of antibiotic resistance are: induction of β-lactamase production (e.g., treatment with cefepime and ceftazidime), up-regulation of efflux pumps, and mutations of the target binding site that alter drug-target affinity (e.g., fluoroquinolones and aminoglycosides) (Buynak 2013; Guan et al. 2013). Although many efforts have been made to evaluate inhibitors for β-lactamases or efflux pumps (Buynak 2013), the high mutation rate of bacteria, compounded with their constantly evolving mechanisms of mutation and the lack of complete, in-depth knowledge of bacterial resistance mechanisms, has precluded the inclusion of such critical components into PK/PD models.

Molecular mechanisms of bacterial responses to external pressures have been proposed and well characterized in the literature (Blair et al. 2015). However, the temporal profiles of such regulatory factors have not been integrated into quantitative PK/PD models. Incorporation of quantitative measurements of factors controlling antibiotic resistance and bacterial virulence into mechanistic translational models will provide opportunities to link with population-based models, a powerful tool for the optimization of clinical dosage regimens. Additionally, such models could be used to guide the study of underlying mechanisms of bacterial and host responses to new treatments. An increased knowledge of bacterial regulatory pathways will aid in uncovering new targets for therapeutic intervention leading to altered production of aggressive bacteria.

17.10.2 Host Immune Response

Bacterial regulatory systems can allow for adaptation and persistence within the host by subverting phagocytosis by immune cells or by countering the host immune system by producing immunosuppressive effects. The dynamic interaction between the host and the invading pathogen can result in complete recovery of the host, due to eradication of the infecting pathogen, the emergence of a resistant hard-to-treat pathogen, or death of the host system due to complete failure of the immune response. Interactions of the host immune system and bacteria are complex in

nature and are dependent on both the bacteria and the status of the host immune system. A homogenous initial bacterial population may give rise to a heterogeneous bacterial population during the course of treatment owing to genomic and proteomic variability. A number of bacterial species are capable of manipulating and altering signaling pathways responsible for the generation of host immune responses that could result in hyper-activation (e.g., symptoms observed during infections) or immune system avoidance. Circumventing the host immune system is vital for bacterial survival and persistence within the host (Gyles 2010). Hence, alterations to the host immune system (e.g., increase or decrease in the number of white blood cells) or changes in bacterial regulatory pathways will influence the dynamics of an infection.

Neutrophils or polymorphonuclear lymphocytes (PMNs) are essential innate immune components that determine host response to bacterial infections. Neutrophils are the first immune components to arrive at the site of an infection that act to produce antimicrobial products and pro-inflammatory factors to help contain the infection. Additionally they cause the activation of other innate immune cells, such as epithelial cells, mast cells, macrophages, and endothelial cells (among others). PMNs and macrophages recruit phagocytes that are responsible for the phagocytosis of the invading pathogen (Silva 2010).

Neutrophils express toll-like receptors (TLRs) that play a key role in early innate immune responses by sensing endogenous signals that might prevent the progression of infection (Kawai and Akira 2011; Medzhitov et al. 1997). TLRs have the ability to recognize pathogen-associated microbial patterns (PAMPs), exclusively expressed by bacteria, or danger-associated molecular patterns (DAMPs) that are endogenous molecules released by infected or dying cells in the damaged tissue. After the molecular recognition of PAMPs, TLRs activate signaling pathways that provide specific immunological responses tailored to the particular pathogen expressing that PAMP (Akira et al. 2006). Examples of PAMPs include bacterial cell wall components, such as lipopolysaccharide, peptidoglycan, and lipopeptides present in Gram-negative bacteria. In contrast, DAMPs are typically intracellular proteins, such as high-mobility group proteins (e.g., HMGB1) and heat shock proteins. The potential to recruit and direct the innate immune system in combination with drugs targeting TLRs to prevent the inflammatory process associated with infection holds great therapeutic potential. Figure 17.4 contains a network or framework of a systems level regulation of host immune responses, with several interactions between the host immune system and bacteria, which is adapted from the Consensus Network of Immunological Steps and Processes Activated upon invasion by Bordetellae species (Thakar et al. 2007). The ability to detect and quantify a number of these immune components, and integrate them into mathematical models, should enhance understanding of the underlying infectious process and improve the translation of preclinical research to humans.

Pharmacokinetic parameters have been successfully scaled from pre-clinical species to humans for both small and large molecule drugs, especially renally cleared drugs, using either allometric scaling or physiologically based pharmacokinetic models (Mager et al. 2009). The drug concentration in the plasma is

frequently used as the main driving function of pharmacological activity; however it is not indicative of the concentration at the site of infection (e.g., epithelial lining fluid or bone). Some agents have significantly greater distribution to certain tissues, whereas some other compounds may remain confined in the plasma space (Burian et al. 2012; Rodvold et al. 2006). Tigecycline is an example of an agent resulting in low plasma concentrations but significantly greater tissue concentrations. Hence, the recommended tigecycline dose does not result in sufficiently high drug concentrations in the plasma to treat blood stream infections (Rodvold et al. 2006).

In addition, disease states (e.g., cancer or cystic fibrosis) can alter the available albumin resulting in altered protein binding within the host. In the case of highly protein bound drugs, the concentration of free drug will be considerably greater in cases of hypoalbuminemia observed in critically ill patients (Joynt et al. 2001; Briscoe et al. 2012; Ulldemolins et al. 2010; Wong et al. 2013). Close drug monitoring in the case of polymyxins or aminoglycosides may be critical to avert adverse events.

17.11 Prospectus on Antimicrobial Translation with a Systems Approach

Systems biology seeks a quantitative understanding of biological systems and control processes (Kitano 2002), whereas systems pharmacology focuses on the responses of biological systems upon perturbation by drugs. As noted by Sorger and colleagues, "Quantitative system pharmacology will create understanding of disease mechanisms and therapeutic effects that span biochemistry and structural studies, cell and animal-based experiments and clinical studies in human patients" (Sorger et al. 2011). The goal of adopting a systems-based approach in the area of infectious disease is to accommodate the multifactorial components of the immune system, host immune system-bacteria interactions, bacterial physiology, and mechanisms of drug action. The transition toward systems-based approaches requires the ability to integrate diverse data types and experimental platforms. Most approaches for translating preclinical antimicrobial research focus only on antibiotic activity and interactions between the drug and bacteria. Mathematical modeling can assist in this process by integrating the behavior of multiple components into a comprehensive network-based model, and by addressing questions that are not yet accessible to experimental analysis. In addition, combining systems models and adaptive feedback control, in which pharmacokinetic and biomarker measurements of immune status and pharmacological response, could be used to personalize antibacterial pharmacotherapy and improve clinical outcomes in individual patients.

Our PK/PD modeling philosophy is to use microbiology, biochemistry, pharmacology, and -omics data to inform our mechanism-based models. A systems approach will foster the development of more complete models that incorporate the pharmacology of the therapeutic agents, molecular signaling and factors released by

the bacteria, and components of immune response (e.g., TNF-α, pro-inflammatory and anti-inflammatory cytokines, and tissue damage signals). This approach will improve the ability to predict the progression of the infectious process under treatment conditions and provide a framework for the translation of preclinical antimicrobial research.

References

Akira S, Uematsu S, Takeuchi O (2006) Pathogen recognition and innate immunity. Cell 124 (4):783–801. doi:10.1016/j.cell.2006.02.015

Andes D, Craig WA (2002) Animal model pharmacokinetics and pharmacodynamics: a critical review. Int J Antimicrob Agents 19(4):261–268

Baltz RH (2009) Daptomycin: mechanisms of action and resistance, and biosynthetic engineering. Curr Opin Chem Biol 13(2):144–151. doi:10.1016/j.cbpa.2009.02.031

Bergen PJ, Forrest A, Bulitta JB, Tsuji BT, Sidjabat HE, Paterson DL, Li J, Nation RL (2011) Clinically relevant plasma concentrations of colistin in combination with imipenem enhance pharmacodynamic activity against multidrug-resistant *Pseudomonas aeruginosa* at multiple inocula. Antimicrob Agents Chemother 55(11):5134–5142. doi:10.1128/AAC.05028-11

Bhattaram VA, Bonapace C, Chilukuri DM, Duan JZ, Garnett C, Gobburu JV, Jang SH, Kenna L, Lesko LJ, Madabushi R, Men Y, Powell JR, Qiu W, Ramchandani RP, Tornoe CW, Wang Y, Zheng JJ (2007) Impact of pharmacometric reviews on new drug approval and labeling decisions—a survey of 31 new drug applications submitted between 2005 and 2006. Clin Pharmacol Ther 81(2):213–221. doi:10.1038/sj.clpt.6100051

Blair JMA, Webber MA, Baylay AJ, Ogbolu DO, Piddock LJV (2015) Molecular mechanisms of antibiotic resistance. Nat Rev Micro 13(1):42–51. doi:10.1038/nrmicro3380

Blaser J (1985) In-vitro model for simultaneous simulation of the serum kinetics of two drugs with different half-lives. J Antimicrob Chemother 15(Suppl A):125–130

Blaser J, Stone BB, Zinner SH (1985) Two compartment kinetic model with multiple artificial capillary units. J Antimicrob Chemother 15(Suppl A):131–137

Boucher HW, Talbot GH, Bradley JS, Edwards JE, Gilbert D, Rice LB, Scheld M, Spellberg B, Bartlett J (2009) Bad bugs, no drugs: no ESKAPE! An update from the infectious diseases society of America. Clin Infect Dis 48(1):1–12. doi:10.1086/595011

Boucher HW, Talbot GH, Benjamin DK, Bradley J, Guidos RJ, Jones RN, Murray BE, Bonomo RA, Gilbert D, Infectious Diseases Society of America (2013a) 10 × ′20 Progress—development of new drugs active against gram-negative bacilli: an update from the infectious diseases society of America. Clin Infect Dis 56(12):1685–1694. doi:10.1093/cid/cit152

Boucher HW, Talbot GH, Benjamin DK, Jr., Bradley J, Guidos RJ, Jones RN, Murray BE, Bonomo RA, Gilbert D, Infectious Diseases Society of A (2013b) 10 x ‘20 Progress—development of new drugs active against gram-negative bacilli: an update from the infectious diseases society of America. Clin Infect Dis 56(12):1685–1694. doi:10.1093/cid/cit152

Briscoe SE, McWhinney BC, Lipman J, Roberts JA, Ungerer JP (2012) A method for determining the free (unbound) concentration of ten β-lactam antibiotics in human plasma using high performance liquid chromatography with ultraviolet detection. J Chromatogr B Anal Technol Biomed Life Sci 907:178–184. doi:10.1016/j.jchromb.2012.09.016

Bulitta JB LJ, Poudyal A, Yu HH, Owen RJ, Tsuji BT, Nation RL (2009) Forrest A quantifying synergy of colistin (C) combinations against MDR gram negatives by mechanism-based models (MBM). In: Abstract: 49th Interscience conference on antimicrobial agents and chemotherapy, San Francisco, CA, USA, Sept 12–15, 2009

Bulitta JB, Ly NS, Yang JC, Forrest A, Jusko WJ, Tsuji BT (2009) Development and qualification of a pharmacodynamic model for the pronounced inoculum effect of ceftazidime against

Pseudomonas aeruginosa. Antimicrob Agents Chemother 53(1):46–56. doi:10.1128/aac.00489-08

Bulitta JB, Yang JC, Yohonn L, Ly NS, Brown SV, D'Hondt RE, Jusko WJ, Forrest A, Tsuji BT (2010) Attenuation of colistin bactericidal activity by high inoculum of *Pseudomonas aeruginosa* characterized by a new mechanism-based population pharmacodynamic model. Antimicrob Agents Chemother 54(5):2051–2062. doi:10.1128/AAC.00881-09

Burian B, Zeitlinger M, Donath O, Reznicek G, Sauermann R (2012) Penetration of doripenem into skeletal muscle and subcutaneous adipose tissue in healthy volunteers. Antimicrob Agents Chemother 56(1):532–535. doi:10.1128/AAC.05506-11

Bush K. 2010. The coming of age of antibiotics: discovery and therapeutic value. Ann N Y Acad Sci 1213:1–4

Buynak JD (2013) β-Lactamase inhibitors: a review of the patent literature (2010–2013). Expert Opin Ther Pat 23(11):1469–1481. doi:10.1517/13543776.2013.831071

Campion JJ, McNamara PJ, Evans ME (2005) Pharmacodynamic modeling of ciprofloxacin resistance in *Staphylococcus aureus*. Antimicrob Agents Chemother 49(1):209–219. doi:10.1128/AAC.49.1.209-219.2005

Clinical Laboratory Standards Institute Guideline C (2007) Performance standards for antimicrobial susceptibility testing. In: 17th informational supplement, vol 27

Craig WA (1998) Pharmacokinetic/pharmacodynamic parameters: rationale for antibacterial dosing of mice and men. Clin Infect Dis 26(1):1–10 (quiz 11–12)

Davies TA, Shang W, Bush K, Flamm RK (2008) Affinity of doripenem and comparators to penicillin-binding proteins in *Escherichia coli* and *Pseudomonas aeruginosa*. Antimicrob Agents Chemother 52(4):1510–1512. doi:10.1128/aac.01529-07

Driscoll JA, Brody SL, Kollef MH (2007) The epidemiology, pathogenesis and treatment of *Pseudomonas aeruginosa* infections. Drugs 67(3):351–368

Drusano GL (2004) Antimicrobial pharmacodynamics: critical interactions of 'bug and drug'. Nat Rev Microbiol 2(4):289–300. doi:10.1038/nrmicro862

Drusano GL, Preston SL, Hardalo C, Hare R, Banfield C, Andes D, Vesga O, Craig WA (2001) Use of preclinical data for selection of a phase II/III dose for evernimicin and identification of a preclinical MIC breakpoint. Antimicrob Agents Chemother 45(1):13–22. doi:10.1128/AAC.45.1.13-22.2001

Drusano GL, Fregeau C, Liu W, Brown DL, Louie A (2010a) Impact of burden on granulocyte clearance of bacteria in a mouse thigh infection model. Antimicrob Agents Chemother 54(10):4368–4372. doi:10.1128/AAC.00133-10

Drusano GL, Sgambati N, Eichas A, Brown DL, Kulawy R, Louie A (2010b) The combination of rifampin plus moxifloxacin is synergistic for suppression of resistance but antagonistic for cell kill of *Mycobacterium tuberculosis*. mBio. doi:10.1128/mBio.00139-10

Drusano GL, Liu W, Kulawy R, Louie A (2011a) Impact of granulocytes on the antimicrobial effect of tedizolid in a mouse thigh infection model. Antimicrob Agents Chemother 55(11):5300–5305. doi:10.1128/AAC.00502-11

Drusano GL, Vanscoy B, Liu W, Fikes S, Brown D, Louie A (2011b) Saturability of granulocyte kill of *Pseudomonas aeruginosa* in a murine model of pneumonia. Antimicrob Agents Chemother 55(6):2693–2695. doi:10.1128/AAC.01687-10

Earp J, Krzyzanski W, Chakraborty A, Zamacona MK, Jusko WJ (2004) Assessment of drug interactions relevant to pharmacodynamic indirect response models. J Pharmacokinet Pharmacodyn 31(5):345–380

Fernandez L, Gooderham WJ, Bains M, McPhee JB, Wiegand I, Hancock RE (2010) Adaptive resistance to the "last hope" antibiotics polymyxin B and colistin in *Pseudomonas aeruginosa* is mediated by the novel two-component regulatory system ParR-ParS. Antimicrob Agents Chemother 54(8):3372–3382. doi:10.1128/AAC.00242-10

Friedberg EC, Friedberg EC (2006) DNA repair and mutagenesis, 2nd edn. ASM Press, Washington

Gao FH, Abee T, Konings WN (1991) Mechanism of action of the peptide antibiotic nisin in liposomes and cytochrome *c* oxidase-containing proteoliposomes. Appl Environ Microbiol 57 (8):2164–2170

Garrett ER, Wright OK (1967) Kinetics and mechanisms of action of drugs on microorganisms. VII. Quantitative adherence of sulfonamide action on microbial growth to a receptor-site model. J Pharm Sci 56(12):1576–1585

Garrett ER, Heman-Ackah SM, Perry GL (1970) Kinetics and mechanisms of action of drugs on microorganisms. XI. Effect of erythromycin and its supposed antagonism with lincomycin on the microbial growth of *Escherichia coli*. J Pharm Sci 59(10):1448–1456

Gloede J, Scheerans C, Derendorf H, Kloft C (2010) In vitro pharmacodynamic models to determine the effect of antibacterial drugs. J Antimicrob Chemother 65(2):186–201. doi:10.1093/jac/dkp434

Gobburu JV, Sekar VJ (2002) Application of modeling and simulation to integrate clinical pharmacology knowledge across a new drug application. Int J Clin Pharmacol Ther 40(7):281–288

Gooderham WJ, Hancock RE (2009) Regulation of virulence and antibiotic resistance by two-component regulatory systems in *Pseudomonas aeruginosa*. FEMS Microbiol Rev 33 (2):279–294. doi:10.1111/j.1574-6976.2008.00135.x

Grasso S, Meinardi G, de Carneri I, Tamassia V (1978) New in vitro model to study the effect of antibiotic concentration and rate of elimination on antibacterial activity. Antimicrob Agents Chemother 13(4):570–576

Greco WR, Bravo G, Parsons JC (1995) The search for synergy: a critical review from a response surface perspective. Pharmacol Rev 47(2):331–385

Greco WR, Faessel H, Levasseur L (1996) The search for cytotoxic synergy between anticancer agents: a case of Dorothy and the ruby slippers? J Natl Cancer Inst 88(11):699–700

Guan X, Xue X, Liu Y, Wang J, Wang Y, Wang J, Wang K, Jiang H, Zhang L, Yang B, Wang N, Pan L (2013) Plasmid-mediated quinolone resistance–current knowledge and future perspectives. J Int Med Res 41(1):20–30. doi:10.1177/0300060513475965

Gyles CL (2010) Pathogenesis of bacterial infections in animals, 4th edn. Wiley-Blackwell, Ames, Iowa

Hammes WP, Neuhaus FC (1974) On the mechanism of action of vancomycin: inhibition of peptidoglycan synthesis in *Gaffkya homari*. Antimicrob Agents Chemother 6(6):722–728

Harigaya Y, Bulitta JB, Forrest A, Sakoulas G, Lesse AJ, Mylotte JM, Tsuji BT (2009) Pharmacodynamics of vancomycin at simulated epithelial lining fluid concentrations against methicillin-resistant *Staphylococcus aureus* (MRSA): implications for dosing in MRSA pneumonia. Antimicrob Agents Chemother 53(9):3894–3901. doi:10.1128/AAC.01585-08

Hayes MV, Orr DC (1983) Mode of action of ceftazidime: affinity for the penicillin-binding proteins of Escherichia coli K12, *Pseudomonas aeruginosa* and *Staphylococcus aureus*. J Antimicrob Chemother 12(2):119–126

Hong MC, Hsu DI, Bounthavong M (2013) Ceftolozane/tazobactam: a novel antipseudomonal cephalosporin and β-lactamase-inhibitor combination. Infect Drug Resist 6:215–223. doi:10.2147/IDR.S36140

Janion C (2008) Inducible SOS response system of DNA repair and mutagenesis in *Escherichia coli*. Int J Biol Sci 4(6):338–344

Joynt GM, Lipman J, Gomersall CD, Young RJ, Wong EL, Gin T (2001) The pharmacokinetics of once-daily dosing of ceftriaxone in critically ill patients. J Antimicrob Chemother 47(4):421–429

Jumbe N, Louie A, Leary R, Liu W, Deziel MR, Tam VH, Bachhawat R, Freeman C, Kahn JB, Bush K, Dudley MN, Miller MH, Drusano GL (2003) Application of a mathematical model to prevent in vivo amplification of antibiotic-resistant bacterial populations during therapy. J Clin Investig 112(2):275–285. doi:10.1172/JCI16814

Kawai T, Akira S (2011) Toll-like receptors and their crosstalk with other innate receptors in infection and immunity. Immunity 34(5):637–650. doi:10.1016/j.immuni.2011.05.006

Keil S, Wiedemann B (1995) Mathematical corrections for bacterial loss in pharmacodynamic in vitro dilution models. Antimicrob Agents Chemother 39(5):1054–1058

Kitano H (2002) Systems biology: a brief overview. Science 295(5560):1662–1664. doi:10.1126/science.1069492

Landersdorfer CB, Ly NS, Xu H, Tsuji BT, Bulitta JB (2013) Quantifying subpopulation synergy for antibiotic combinations via mechanism-based modeling and a sequential dosing design. Antimicrob Agents Chemother 57(5):2343–2351. doi:10.1128/aac.00092-13

Laub MT, Goulian M (2007) Specificity in two-component signal transduction pathways. Annu Rev Genet 41:121–145. doi:10.1146/annurev.genet.41.042007.170548

Le Goffic F, Capmau ML, Tangy F, Baillarge M (1979) Mechanism of action of aminoglycoside antibiotics. Binding studies of tobramycin and its 6′-*N*-acetyl derivative to the bacterial ribosome and its subunits. Eur J Biochem/FEBS 102(1):73–81

Lee JY, Garnett CE, Gobburu JV, Bhattaram VA, Brar S, Earp JC, Jadhav PR, Krudys K, Lesko LJ, Li F, Liu J, Madabushi R, Marathe A, Mehrotra N, Tornoe C, Wang Y, Zhu H (2011) Impact of pharmacometric analyses on new drug approval and labelling decisions: a review of 198 submissions between 2000 and 2008. Clin Pharmacokinet 50(10):627–635. doi:10.2165/11593210-000000000-00000

Li B, Tsui HC, LeClerc JE, Dey M, Winkler ME, Cebula TA (2003) Molecular analysis of mutS expression and mutation in natural isolates of pathogenic *Escherichia coli*. Microbiology 149 (Pt 5):1323–1331

Li J, Rayner CR, Nation RL, Owen RJ, Spelman D, Tan KE, Liolios L (2006) Heteroresistance to colistin in multidrug-resistant *Acinetobacter baumannii*. Antimicrob Agents Chemother 50 (9):2946–2950

Lim LM, Ly N, Anderson D, Yang JC, Macander L, Jarkowski A 3rd, Forrest A, Bulitta JB, Tsuji BT (2010) Resurgence of colistin: a review of resistance, toxicity, pharmacodynamics, and dosing. Pharmacotherapy 30(12):1279–1291. doi:10.1592/phco.30.12.1279

Lowdin E, Odenholt I, Bengtsson S, Cars O (1996) Pharmacodynamic effects of sub-MICs of benzylpenicillin against *Streptococcus pyogenes* in a newly developed in vitro kinetic model. Antimicrob Agents Chemother 40(11):2478–2482

Macfarlane EL, Kwasnicka A, Ochs MM, Hancock RE (1999) PhoP-PhoQ homologues in *Pseudomonas aeruginosa* regulate expression of the outer-membrane protein OprH and polymyxin B resistance. Mol Microbiol 34(2):305–316

Mager DE, Woo S, Jusko WJ (2009) Scaling pharmacodynamics from in vitro and preclinical animal studies to humans. Drug Metab Pharmacokinet 24(1):16–24

McPhee JB, Lewenza S, Hancock RE (2003) Cationic antimicrobial peptides activate a two-component regulatory system, PmrA-PmrB, that regulates resistance to polymyxin B and cationic antimicrobial peptides in *Pseudomonas aeruginosa*. Mol Microbiol 50(1):205–217 doi:3673 [pii]

Meagher AK, Forrest A, Dalhoff A, Stass H, Schentag JJ (2004) Novel pharmacokinetic-pharmacodynamic model for prediction of outcomes with an extended-release formulation of ciprofloxacin. Antimicrob Agents Chemother 48(6):2061–2068. doi:10.1128/AAC.48.6.2061-2068.2004

Medzhitov R, Preston-Hurlburt P, Janeway CA Jr (1997) A human homologue of the Drosophila Toll protein signals activation of adaptive immunity. Nature 388(6640):394–397. doi:10.1038/41131

Mouton JW, Vinks AA, Punt NC (1997) Pharmacokinetic-pharmacodynamic modeling of activity of ceftazidime during continuous and intermittent infusion. Antimicrob Agents Chemother 41 (4):733–738

Mouton JW, Dudley MN, Cars O, Derendorf H, Drusano GL (2005) Standardization of pharmacokinetic/pharmacodynamic (PK/PD) terminology for anti-infective drugs: an update. J Antimicrob Chemother 55(5):601–607. doi:10.1093/jac/dki079

Murakawa T, Sakamoto H, Hirose T, Nishida M (1980) New in vitro kinetic model for evaluating bactericidal efficacy of antibiotics. Antimicrob Agents Chemother 18(3):377–381

Navashin SM, Fomina IP, Firsov AA, Chernykh VM, Kuznetsova SM (1989) A dynamic model for in-vitro evaluation of antimicrobial action by simulation of the pharmacokinetic profiles of antibiotics. J Antimicrob Chemother 23(3):389–399

Nielsen EI, Viberg A, Lowdin E, Cars O, Karlsson MO, Sandstrom M (2007) Semimechanistic pharmacokinetic/pharmacodynamic model for assessment of activity of antibacterial agents from time-kill curve experiments. Antimicrob Agents Chemother 51(1):128–136. doi:10.1128/AAC.00604-06

Pearson JP, Passador L, Iglewski BH, Greenberg EP (1995) A second *N*-acylhomoserine lactone signal produced by *Pseudomonas aeruginosa*. Proc Natl Acad Sci USA 92(5):1490–1494

Pesci EC, Iglewski BH (1997) The chain of command in *Pseudomonas quorum* sensing. Trends Microbiol 5(4):132–134. doi:10.1016/S0966-842X(97)01008-1 (discussion 134–135)

Pesci EC, Pearson JP, Seed PC, Iglewski BH (1997) Regulation of las and rhl quorum sensing in *Pseudomonas aeruginosa*. J Bacteriol 179(10):3127–3132

Rao GG, Ly NS, Haas CE, Garonzik S, Forrest A, Bulitta JB, Kelchlin PA, Holden PN, Nation RL, Li J, Tsuji BT (2013) New dosing strategies for an 'old' antibiotic: pharmacodynamics of front-loaded regimens of colistin at simulated pharmacokinetics of patients with kidney or liver disease. Antimicrob Agents Chemother 16:16

Rao GG, Ly NS, Bulitta JB, Soon RL, San Roman MD, Holden PN, Landersdorfer CB, Nation RL, Li J, Forrest A, Tsuji BT (2016) Polymyxin B in combination with doripenem against heteroresistant Acinetobacter baumannii: pharmacodynamics of new dosing strategies. J Antimicrob Chemother doi:10.1093/jac/dkw293

Reeves DS (1985) Advantages and disadvantages of an in-vitro model with two compartments connected by a dialyser: results of experiments with ciprofloxacin. J Antimicrob Chemother 15:159–167

Rodvold KA, Gotfried MH, Cwik M, Korth-Bradley JM, Dukart G, Ellis-Grosse EJ (2006) Serum, tissue and body fluid concentrations of tigecycline after a single 100 mg dose. J Antimicrob Chemother 58(6):1221–1229. doi:10.1093/jac/dkl403

Schneider EL, Lewis J (1982) Comparison of in vivo and in vitro SCE induction. Mutat Res 106 (1):85–90

Shinabarger DL, Marotti KR, Murray RW, Lin AH, Melchior EP, Swaney SM, Dunyak DS, Demyan WF, Buysse JM (1997) Mechanism of action of oxazolidinones: effects of linezolid and eperezolid on translation reactions. Antimicrob Agents Chemother 41(10):2132–2136

Silva MT (2010) Neutrophils and macrophages work in concert as inducers and effectors of adaptive immunity against extracellular and intracellular microbial pathogens. J Leukoc Biol 87(5):805–813. doi:10.1189/jlb.1109767

Simard P, Bergeron MG (1982) Inoculum size effect on the MIC of cefoperazone, moxalactam, cefotaxime, cefoxitin and cephalothin for 118 strains of Haemophilus influenzae including 'tolerant' micro-organisms. J Antimicrob Chemother 10(5):397–402

Soon RL, Ly NS, Rao G, Wollenberg L, Yang K, Tsuji B, Forrest A (2013) Pharmacodynamic variability beyond that explained by MICs. Antimicrob Agents Chemother 57(4):1730–1735. doi:10.1128/AAC.01224-12

Sorger PK, Allerheiligen SRB, Abernethy DR, Altman RB, Brouwer KLR, Califano A, D'Argenio DZ, Iyengar R, Jusko WJ, Lalonde R, Lauffenburger DA, Shoichet B, Stevens JL, Subramaniam S, Van der Graaf P, Vicini P (2011) Quantitative and systems pharmacology in the post-genomic era: new approaches to discovering drugs and understanding therapeutic mechanisms. An NIH white paper

Srivastava S, Sherman C, Meek C, Leff R, Gumbo T (2011) Pharmacokinetic mismatch does not lead to emergence of isoniazid- or rifampin-resistant *Mycobacterium tuberculosis* but to better antimicrobial effect: a new paradigm for antituberculosis drug scheduling. Antimicrob Agents Chemother 55(11):5085–5089. doi:10.1128/AAC.00269-11

Stevens DL, Yan S, Bryant AE (1993) Penicillin-binding protein expression at different growth stages determines penicillin efficacy in vitro and in vivo: an explanation for the inoculum effect. J Infect Dis 167(6):1401–1405

Stover CK, Pham XQ, Erwin AL, Mizoguchi SD, Warrener P, Hickey MJ, Brinkman FS, Hufnagle WO, Kowalik DJ, Lagrou M, Garber RL, Goltry L, Tolentino E, Westbrock-Wadman S, Yuan Y, Brody LL, Coulter SN, Folger KR, Kas A, Larbig K, Lim R, Smith K, Spencer D, Wong GK, Wu Z, Paulsen IT, Reizer J, Saier MH, Hancock RE, Lory S, Olson MV (2000) Complete genome sequence of *Pseudomonas aeruginosa* PAO1, an opportunistic pathogen. Nature 406(6799):959–964. doi:10.1038/35023079

Thakar J, Pilione M, Kirimanjeswara G, Harvill ET, Albert R (2007) Modeling systems-level regulation of host immune responses. PLoS Comput Biol 3(6):e109. doi:10.1371/journal.pcbi.0030109

Tsuji BT, Brown T, Parasrampuria R, Brazeau DA, Forrest A, Kelchlin PA, Holden PN, Peloquin CA, Hanna D, Bulitta JB (2012) Front-loaded linezolid regimens result in increased killing and suppression of the accessory gene regulator system of *Staphylococcus aureus*. Antimicrob Agents Chemother 56(7):3712–3719. doi:10.1128/AAC.05453-11

Ulldemolins M, Roberts JA, Wallis SC, Rello J, Lipman J (2010) Flucloxacillin dosing in critically ill patients with hypoalbuminaemia: special emphasis on unbound pharmacokinetics. J Antimicrob Chemother 65(8):1771–1778. doi:10.1093/jac/dkq184

Wehrli W (1983) Rifampin: mechanisms of action and resistance. Rev Infect Dis 5(Suppl 3):S407–S411

Wong G, Briscoe S, Adnan S, McWhinney B, Ungerer J, Lipman J, Roberts JA (2013) Protein binding of β-lactam antibiotics in critically ill patients: can we successfully predict unbound concentrations? Antimicrob Agents Chemother 57(12):6165–6170. doi:10.1128/aac.00951-13

Wootton M, Howe RA, Hillman R, Walsh TR, Bennett PM, MacGowan AP (2001) A modified population analysis profile (PAP) method to detect hetero-resistance to vancomycin in *Staphylococcus aureus* in a UK hospital. J Antimicrob Chemother 47(4):399–403

Yano Y, Oguma T, Nagata H, Sasaki S (1998) Application of logistic growth model to pharmacodynamic analysis of in vitro bactericidal kinetics. J Pharm Sci 87(10):1177–1183. doi:10.1021/js9801337

Yeh PJ, Hegreness MJ, Aiden AP, Kishony R (2009) Drug interactions and the evolution of antibiotic resistance. Nat Rev Microbiol 7(6):460–466. doi:10.1038/nrmicro2133

Zak O, O'Reilly T (1990) Animal models as predictors of the safety and efficacy of antibiotics. Eur J Clin Microbiol Infect Dis 9(7):472–478

Zhi JG, Nightingale CH, Quintiliani R (1988) Microbial pharmacodynamics of piperacillin in neutropenic mice of systematic infection due to *Pseudomonas aeruginosa*. J Pharmacokinet Biopharm 16(4):355–375

Zinner SH, Husson M, Klastersky J (1981) An artificial capillary in vitro kinetic model of antibiotic bactericidal activity. J Infect Dis 144(6):583–587

Chapter 18
Viral Dynamic Modeling of Hepatitis C Virus Infection: Past Successes and Future Challenges

Eric L. Haseltine and Holly H.C. Kimko

Abstract Viral dynamic modeling has had a long history of providing insight into the dynamics of hepatitis C virus infection. This chapter reviews a model used to predict treatment outcomes for regimens including the direct-acting antiviral telaprevir. Challenges for modeling existing and upcoming regimens are also discussed.

Keywords Interferon · Direct-acting antiviral (DAA) · Telaprevir · Multi-variant model · Parameterization · Sequencing methods · Interferon-free regimens · Nonlinear mixed-effect (NLME) · Limit of detection (LOD) · Sustained virologic response (SVR)

18.1 Introduction

Viral dynamic modeling has had a long history of providing insight into the dynamics of hepatitis C virus (HCV) infection. For example, the seminal work of Neumann et al. provided a rational explanation for the two slopes of decline commonly observed in the viral load (i.e., HCV RNA levels) of patients treated with interferon (Neumann et al. 1998). The first, typically rapid decline observed with interferon therapy was attributed to inhibition of viral replication, whereas the second, prolonged decline was attributed to clearance of infected hepatocytes. Guedj et al. constructed a model incorporating both the intracellular and extracellular infection dynamics to explain how different mechanisms of action account for the apparent difference in the virus decay rate of different antiviral regimens (Guedj et al. 2013a). Many of these seminal works have been reviewed elsewhere (see, for

E.L. Haseltine (✉)
Vertex Pharmaceuticals Incorporated, Boston, MA, USA
e-mail: Eric_Haseltine@vrtx.com

H.H.C. Kimko
Johnson & Johnson Pharmaceutical Research & Development, LLC, Raritan, NJ, USA

D.E. Mager and H.H.C. Kimko (eds.), *Systems Pharmacology and Pharmacodynamics*, AAPS Advances in the Pharmaceutical Sciences Series 23,
DOI 10.1007/978-3-319-44534-2_18

example, Chatterjee et al. 2012, 2013). Most viral dynamic models were developed to characterize the HCV viral load after treatment with antiviral regimens in small studies. This chapter reviews the use of viral dynamic modeling to predict both the HCV viral load and the clinical outcome as measured by sustained virologic response (SVR) for larger HCV clinical studies.

The dynamics of the HCV viral load, both on- and post-treatment, provide useful information that can help predict whether patients will achieve SVR with antiviral therapy. In patients treated with only interferon and ribavirin, these dynamics provide important information about how these drugs work since a wide range of viral loads above the limit of detection (LOD) are observed. Based on these dynamics, interferon-regimen responses are typically characterized into the four main categories shown in Fig. 18.1a: (1) achievement of SVR, (2) viral relapse (undetectable viral load at the end of treatment but subsequent detectable viral load), (3) partial response (detectable viral load at the end of treatment), and (4) null response (<2 log drop in viral load after 12 weeks of treatment). Treatment with an interferon regimen generally results in one or two phases of viral decline on the log scale. Also, the viral infection can persist below the LOD as inferred from the dynamics of viral relapse (Fig. 18.1a).

The viral dynamics are significantly different when a direct-acting antiviral (DAA) is added to an interferon regimen. With these triple regimens, patients usually exhibit a rapid first phase of viral decline, followed by a second phase decline that is steeper than that observed when the DAA is excluded (compare Fig. 18.1b to 18.1a). Even when patients exhibit similar viral dynamics above the LOD followed by viral dynamics below the LOD for the remaining on-treatment period, some of these patients achieve SVR, whereas others relapse. These viral dynamics occurring below the LOD cannot be directly measured, but they can be inferred with the use of viral dynamic modeling. If one can accurately account for the dynamics of the infection systems that are, in turn, integrated into the viral

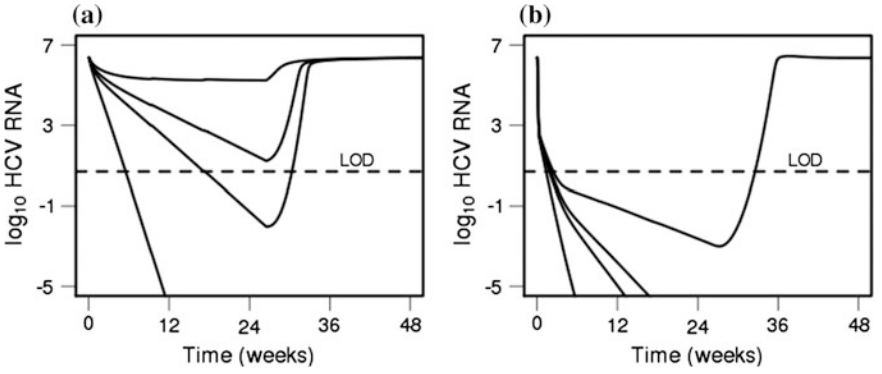

Fig. 18.1 Categories of responses to **a** interferon and **b** the corresponding HCV viral dynamics when a direct-acting antiviral (DAA) is added to the interferon regimen. In both cases the treatment duration is 24 weeks

dynamics, then it is possible to predict the efficacy of antiviral regimens. In this light, viral dynamic modeling is truly an exercise in systems pharmacology.

Numerous studies have sought to explain the viral dynamics observed in patients during the initial treatment response before the viral load becomes undetectable (Chatterjee et al. 2012, 2013). However, these studies have limited utility in predicting SVR. For example, a model developed by Guedj et al. integrated the intracellular and extracellular infection cycles of HCV (Guedj et al. 2013a) to describe the viral dynamics before they initially drop below the LOD. When the authors fit this model to these early viral dynamics, the parameter representing the inhibition of virion assembly and secretion by telaprevir was significantly weaker than that estimated for daclatasvir ($P < 10^{-6}$) (Guedj et al. 2013a). Although telaprevir and daclatasvir have not been directly compared in a controlled clinical study, they have both been independently evaluated in combination with pegylated interferon (Peg-IFN) and ribavirin (PR). From these studies, it appears that the patient populations (treatment-naïve patients with genotype 1 HCV infection) and treatment durations (24 or 48 weeks, depending on early viral response) were comparable. Telaprevir-based treatment resulted in a 79 % SVR rate (N = 363) versus PR alone in Phase 3 studies (INCIVEK (telaprevir) [US Prescribing Information] 2013), whereas daclatasvir resulted in a 65 % SVR rate (N = 147) versus PR alone in Phase 2 studies (Hezode et al. 2012). The apparent disconnect between early viral dynamics and SVR outcome (although subject to the uncertainty arising from a cross-trial comparison) suggests that other antiviral factors, in particular those that might exert influence on the viral dynamics below the LOD, are critical to understanding and predicting viral eradication.

To the best of our knowledge, only three models have successfully been used to predict treatment outcomes in HCV clinical studies:

1. A model developed for PR regimens (Snoeck et al. 2010)
2. A model developed for alisporivir and ribavirin regimens (Guedj et al. 2013b), and
3. A model developed for telaprevir and PR (T/PR) regimens (Adiwijaya et al. 2012).

This chapter reviews the third model in depth and discusses the challenges that will need to be addressed for viral dynamic modeling to be useful for modeling of existing and upcoming regimens.

18.2 Modeling Telaprevir-Based Regimens

Adiwijaya et al. developed a multi-variant viral dynamic model to understand and predict the effects of treating genotype 1 HCV-infected patients with T/PR (Adiwijaya et al. 2012). This model helped inform design of clinical studies, playing a pivotal role in determining the telaprevir treatment duration used to design Phase 3 clinical studies. These Phase 3 studies ultimately validated the model predictions.

The model integrates the pharmacokinetics (PK) of each drug with the pharmacodynamics of the viral dynamics. To better understand this integrative model, we first discuss the viral dynamic portion of the model, then how the PK is integrated into the model to drive the viral dynamics. Next we consider how this model was parameterized and how predictions were made using the model. Finally, we review the model predictions and their potential utility in helping guide the design of clinical studies.

18.2.1 HCV Viral Dynamics

The multi-variant model used by Adiwijaya et al. is conceptually similar to the single variant models originally developed to understand dynamics with interferon-based treatment (Neumann et al. 1998). Namely, the model considers a population of target cells that can be infected by the virus. The infected cells produce additional virus, leading to an exponential replication cycle of virus that is ultimately limited by how quickly new target cells can be regenerated. This limited regeneration leads to a chronically infected state, where virus production is balanced by degradation of the virus and infection of additional target cells.

The model was developed to capture the different types of patient responses observed in clinical data, including on-treatment viral breakthrough, relapse after the end of treatment, and achievement of SVR at different times. Each of these treatment outcomes can be attributed to the types of viral quasi-species (i.e., the mix of viral variants present at any given time) and the effectiveness of the antiviral regimen on these quasi-species. Viral variants exhibit a broad range of sensitivity to telaprevir, from extremely sensitive (e.g., wild-type and R155K variants) to largely insensitive (e.g., R155K/V36M and A156T variants). Telaprevir is dosed to effectively inhibit the sensitive variants, but not the insensitive variants (Sarrazin et al. 2007). Although these telaprevir-insensitive variants remain sensitive to PR (Kieffer et al. 2007), PR inhibition of viral replication can vary widely from patient to patient and is generally not as profound as telaprevir inhibition of telaprevir-sensitive variants. Typically the telaprevir-sensitive wild-type (WT) variant is the most fit (i.e., replicates the fastest) and dominates the quasi-species. Therefore, the rationale behind the T/PR regimen is that telaprevir swiftly and strongly inhibits the predominant, drug-sensitive variants, while PR inhibits to a more moderate degree the telaprevir-resistant variants. When all agents are effective and the treatment duration is sufficiently long, SVR is achieved. If the regimen is not dosed long enough, the patient relapses after the end of treatment. When PR has little antiviral effect, the outcome is viral breakthrough.

To explain these key features of the clinical data, the single variant model must be made more complex by adding multiple viral variants. For comparison, the governing model equations for both the single variant and multi-variant dynamic models are presented in Fig. 18.2. Overall, the two models are quite similar. However, in contrast to the single variant model, the multi-variant model tracks

Table 18.1 HCV viral dynamic model symbol definitions

Symbol name	Description
c	Plasma virion clearance rate constant
d	Healthy hepatocyte death rate constant
f_i	Fitness of virus variant i relative to WT (p_i/p)
I_i	Concentration of cells infected with viral variant i
$m_{j,i}$	Mutation rate from variant j to variant i
p	WT virion production rate constant
s	Synthesis rate of healthy hepatocytes
T	Concentration of healthy hepatocytes
V_i	Plasma concentration of viral variant i
V_{SVR}	Eradication limit for the virus
β	Healthy hepatocyte infection rate constant
δ_i	Clearance rate constant for hepatocytes infected with virus variant i
δ_{nodrug}	Clearance rate constant for infected hepatocytes in the absence of drug
$\delta_{d,i}$	Effect of drug d on the clearance of hepatocytes infected with virus variant i
$\varepsilon_{d,i}$	Production blockage factor of drug d on virus variant i
ε_i	Total blockage factor on virus variant i
η	Peg-IFN effect of blocking infection

(a)

$$\frac{dT}{dt} = s - dT - (1-\eta)\beta TV$$
$$\frac{dI}{dt} = (1-\eta)\beta TV - \delta I$$
$$\frac{dV}{dt} = (1-\varepsilon)pI - cV$$

(b)

$$\frac{dT}{dt} = s - dT - \sum_i (1-\eta)\beta TV_i$$
$$\frac{dI_i}{dt} = (1-\eta)\beta TV_i - \delta_i I_i \text{ if } V_i \geq V_{\text{SVR}}, 0 \text{ otherwise}$$
$$\frac{dV_i}{dt} = \sum_j (1-\varepsilon_j) m_{j,i} f_j p I_j - cV \text{ if } V_i \geq V_{\text{SVR}}, 0 \text{ otherwise}$$

Fig. 18.2 Equations for the **a** single variant and **b** multi-variant HCV viral dynamic models. Definitions for model parameters are presented in Table 18.1

multiple numbers of infected cells and viral variants, with the primary differences being that, in the multi-variant model, (1) target cells are lost due to infection by multiple viral variants and (2) viral variants are generated within cells infected with that variant and within cells infected with other variants via mutation.

Conceptually, the different outcomes attainable by the multi-variant model can be understood by using the mathematical construct of the reproductive number, R_0

(Nowak and May 2000). In the absence of antiviral therapy, R_0 is defined as follows for each variant (j):

$$R_{0,j} = \frac{sf_j p\beta}{dc\delta_j} \tag{18.1}$$

Similarly, R_0 can also be defined in the presence of antiviral therapy:

$$R_{0,j,\text{treat}} = (1-\varepsilon_i)(1-\eta)\frac{sf_j p\beta}{dc\delta_j} \tag{18.2}$$

R_0 corresponds to the number of viruses that are produced during a single infection cycle. This definition allows for an intuitive understanding of the parameters governing R_0 from Eq. 18.1. For example, increasing the viral production rate (p) or the infection rate (β) increases the number of viruses produced during an infection cycle, and correspondingly R_0 increases. In contrast, increasing the viral (c) or infected cell (δ) clearance rates decreases the number of viruses produced during an infection cycle, so R_0 decreases. If R_0 is greater than or equal to 1, then the infection propagates until it becomes chronic. Otherwise, the infection does not persist and will be cleared. For a multi-variant model, if R_0 is known for the WT variant, then R_0 for each variant in the absence of antiviral therapy can be calculated by specifying the relative fitness for each variant. Typically the WT variant has the highest relative fitness (i.e., $f_{\text{WT}} = 1$), whereas the relative fitness of all other variants is lower (i.e., $f_j < 1$). These variants are included in the model only if they are fit enough to replicate, that is their R_0 values in the absence of antiviral treatment are greater than or equal to 1. In the presence of antiviral therapy, the R_0 for each variant is multiplied by the efficacy of each antiviral treatment (telaprevir, Peg-IFN, and ribavirin in this case) as shown in Eq. 18.2 to yield $R_{0,\text{treat}}$. To achieve SVR in a patient, $R_{0,\text{treat}}$ values of all variants must be less than 1. For viral relapse, generally all variants' $R_{0,\text{treat}}$ values are less than 1 during treatment, but the treatment duration is not long enough for each variant to be cleared. In some cases, viral relapse can occur with $R_{0,\text{treat}}$ values slightly greater than 1 during treatment. For viral breakthrough, at least one variant's $R_{0,\text{treat}}$ is larger than 1, thereby allowing the variant to cause an observable, persistent infection during antiviral treatment.

Another feature of this multi-variant model is that the variant with the highest fitness (i.e., the largest R_0) outcompetes all other variants. Thus, though theoretically each variant can infect target cells and replicate, in practice the variant with the highest fitness dominates. All other variants are primarily generated from the variant with the highest fitness via mutation. Which variant has the highest fitness is typically determined by the selective pressure: antiviral therapy selects drug-resistant variants, whereas the absence of antivirals selects the WT variant.

One practical consideration that must be taken into account is the number of mutants to include in the model and their genetic barrier (i.e., the number of mutations that make the drug-resistant variants different from the dominant drug-sensitive variant). The genetic barrier along with the mutation rate determines whether a given variant pre-exists at the beginning of treatment and how much of that variant exists. Theoretical arguments suggest that all single and double mutants pre-exist as part of the viral quasi-species before the start of antiviral treatment (Rong et al. 2010). However, to avoid generating an unnecessarily complicated viral dynamic model, only those mutants that are relatively fit in the presence of antiviral treatment are modeled. For the T/PR model, many key mutants were identified first using in vitro data (Lin et al. 2006; Zhou et al. 2007, 2008) and then confirmed clinically by sequencing virus from patients treated with telaprevir-based regimens in Phase 1 studies (Adiwijaya et al. 2010). Although data from Phase 2 and 3 clinical studies were used to identify additional mutations (Kieffer et al. 2012) not considered by the T/PR model (Adiwijaya et al. 2012), these mutations were similar to those included in this model in terms of genetic barrier and telaprevir resistance. That is, mutants could be classified into three groups: (1) high fitness, low resistance mutants that varied from the WT virus by one mutation; (2) high fitness, high resistance mutants that varied from the WT virus by two mutations; and (3) low fitness, high resistance mutants that varied from the WT virus by one mutation. By accounting for these three main groups of mutants, the model generically accounts for the broad range of mutants observed in clinical studies.

18.2.2 Integrating Drug Pharmacokinetics with the HCV Viral Dynamics

The parameters ε, δ, and η are used to model the effect of antivirals on the viral dynamics. Telaprevir and ribavirin affect ε, the inhibition of viral production, whereas Peg-IFN affects both ε and η, the blockage of viral infection. The model parameter δ, which primarily affects the steepness of the second phase of viral decline, is assumed to be correlated with ε. Because potent DAAs such as telaprevir inhibit viral replication to a much greater degree than PR, modeling ε and δ in this way results in the first and the second phase viral declines for telaprevir being much faster than those observed for PR.

Hill functions are used to map drug concentrations onto the actual values of ε, δ, and η, along with a factor (κ) that nominally accounts for drug exposure differences in the plasma and liver. These mappings are presented in Eq. 18.3, where [drug] denotes the drug concentration in plasma. The coefficients for the Hill functions were fixed in the viral dynamic model to values estimated from in vitro experiments in the HCV replicon system (Lin et al. 2006; Zhou et al. 2007, 2008).

$$
\begin{aligned}
(1-\varepsilon_i) &= \prod_d \left(1-\varepsilon_{d,i}\right) \\
\varepsilon_{\text{drug},i} &= \frac{\left(\kappa_{\text{drug}}[\text{drug}]\right)^{h_{\text{drug},i}}}{IC_{50,\text{drug},i}^{h_{\text{drug},i}} + \left(\kappa_{\text{drug}}[\text{drug}]\right)^{h_{\text{drug},i}}} \\
\eta &= \frac{\left(\kappa_{\eta}[\text{Peg-IFN}]\right)^{h_{\text{Peg}-\text{IFN}}}}{IC_{50,\text{Peg-IFN}}^{h_{\text{Peg}-\text{IFN}}} + \left(\kappa_{\eta}[\text{Peg-IFN}]\right)^{h_{\text{Peg}-\text{IFN}}}} \\
\delta_i &= \delta_{nodrug} - \sum_{\text{drug}} \delta_{\text{drug},i} \log_{10}\left(1-\varepsilon_{\text{drug},i}\right)
\end{aligned}
\tag{18.3}
$$

Approximations are used to account for the dynamics of the drug exposure. Each drug is administered on a regimented schedule: orally every 8 h for telaprevir, orally twice a day for ribavirin, and weekly injections for Peg-IFN. Rather than accounting for the discrete dynamics of this schedule, the exponential approximations presented in Eq. 18.4 are used to roughly capture the dynamics of the initial drug administration:

$$
\begin{aligned}
&\text{Telaprevir}: \quad [\text{TVR}] = \frac{F_{1T}D_T}{\tau_T Cl_T}\left(1-\exp\left(-\frac{Cl_T t}{V_T}\right)\right) \\
&\text{Peg-IFN}: \quad [\text{Peg-IFN}] = \frac{D_{\text{P}}}{\tau_{\text{P}} Cl_{\text{P}}}\left(1-\exp\left(-\frac{t}{\frac{V_{\text{P}}}{Cl_{\text{P}}}+\frac{1}{K_{\text{aP}}}}\right)\right) \\
&\text{Ribavirin}: \quad [\text{RBV}] = \frac{F_{1\text{R}}D_{\text{R}}}{\tau_{\text{R}} Cl_{\text{R}}}\left(1-\exp\left(-\frac{t}{\frac{V2_{\text{R}}}{Cl_{\text{R}}}+\frac{V2_{\text{R}}}{Q3_{\text{R}}}+\frac{V3_{\text{R}}}{Q3_{\text{R}}}+\frac{V4_{\text{R}}}{Q4_{\text{R}}}+\frac{1}{F_{1\text{R}}K_{\text{aR}}}}\right)\right)
\end{aligned}
\tag{18.4}
$$

Here, D_j is the dose for drug j, τ_j is the dosing interval for drug j, F_1 values are the bioavailabilities, Cl values are the drug clearances, V values are the volumes, Q values are the inter-compartmental clearances, and K_a values are the absorption rate constants. As shown in Fig. 18.3, this approximation roughly captures the average drug concentration and neglects the fluctuations due to discrete dosing. Drug parameters for each patient treated with T/PR are obtained from population PK models. The primary benefit of this approximation is that it reduces the computational expense required to integrate the model. Simulation of discrete dosing introduces numerous discontinuities into the model (e.g., every 8 h for the duration of q8h telaprevir dosing as shown in Fig. 18.3). These discontinuities substantially slow down model simulation when using an adaptive time-step integrator such as LSODE (Hindmarsh 1980) or DASSL (Petzold 1982) because they force the integrator to take small time steps to resolve the PK dynamics (hours), whereas the SVR dynamics occur on a longer time scale (weeks). Consequently, parameter estimation, which requires numerous model-based predictions for calculations of residuals from the observed values, can become prohibitively time consuming when dosing is discretely simulated.

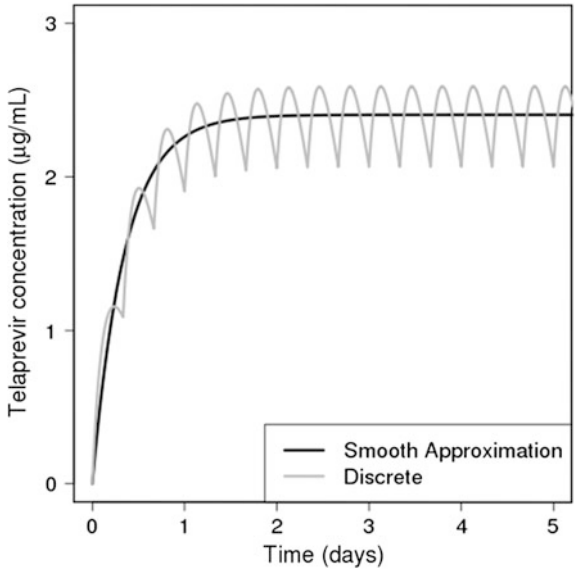

Fig. 18.3 Comparison of discrete telaprevir PK with the smooth approximation

18.2.3 Model Parameterization

The model contains a large number of parameters that govern the dynamics of the target cells, infected cells, and viral variants. However, because only total viral load data (i.e., the sum of all viral variants) were used to fit the model, many parameters are correlated and cannot be uniquely determined. Therefore, some parameters were fixed to reasonable values prior to estimation. These parameters include those listed in Table 18.2 as well as the drug-related parameters $IC_{50,d,i}$ and $h_{d,i}$ which were obtained from published literature (Lin et al. 2006; Zhou et al. 2007, 2008) as discussed in the previous section.

The remaining parameters were estimated using all the available patient data. The telaprevir-resistant variants are HCV genotype dependent. Table 18.3 lists the variants analyzed for HCV genotypes 1a and 1b in this model. The parameters estimated for the different treatment groups (control [PR], T/PR in genotype 1a patients, and T/PR in genotype 1b patients) are listed in Table 18.4.

Nonlinear optimization was used to determine these parameters by minimizing the squared residuals between the model predictions and the observed HCV RNA

Table 18.2 Parameters fixed in the multi-variant HCV viral dynamic model

Parameter	Value
$T_{\max}$	10 cells (normalized)
s	0.084 h^{-1}
$R_{0,WT}$	55.24
δ_{nodrug}	5.2 (10^{-3}) h^{-1}
β	0.05 h^{-1} $virion^{-1}$

Table 18.3 Telaprevir-resistant variants for each HCV genotype

HCV genotype	Resistant variants
1a	R155K, A156T, V36M/R155K
1b	V36A, A156T

Table 18.4 Estimated parameters for each treatment group

Study arm	Estimated parameters
Control (PR only)	c, $\delta_{\text{Peg-IFN}}$, $\kappa_{\text{Peg-IFN}}$, κ_{RBV}, κ_{η}
Genotype 1a (T/PR)	c, $\delta_{\text{Peg-IFN}}$, δ_{TVR}, κ_{TVR}, $\kappa_{\text{Peg-IFN}}$, κ_{RBV}, κ_{η}, f_{R155K}, f_{A156T}, $f_{\text{V36M/R155K}}$
Genotype 1b (T/PR)	c, $\delta_{\text{Peg-IFN}}$, δ_{TVR}, κ_{TVR}, $\kappa_{\text{Peg-IFN}}$, κ_{RBV}, κ_{η}, η, f_{V36A}, f_{A156T}

levels on-treatment. Both the viral load data and the model predictions were converted to $\log_{10}$ change from the baseline viral load before determining the residuals. Viral load data at the limit of quantification (LOQ) or LOD are problematic because they do not provide precise quantitative information with which to fit model parameters. Consequently, only the first LOQ or LOD data point was fitted with the assumption that the viral load was the LOQ or LOD value at that time. Multi-start nonlinear optimization, where the optimizer starts from different initial guesses of the parameters, was used to determine optimal parameters as this parameter estimation problem is prone to local or poorly-defined optima. During the multi-start optimization, starting the parameter estimation from differing η values (the Peg-IFN blockage parameter) is particularly helpful as the primary variation in treatment outcome results from variability in the interferon response.

18.2.4 Model Predictions and Validation

Originally this model was developed using data from Phase 2 clinical studies of telaprevir (Hézode et al. 2009). As shown in Fig. 18.4, the model was fit to data from these studies (PROVE1 and PROVE2) which evaluated 12 weeks of telaprevir in combination with 12–48 weeks of PR in HCV treatment-naïve patients (i.e., never been previously treated for HCV). Subsequently, the model was used to computationally explore the treatment outcomes expected from different patient populations (e.g., patients who did not achieve SVR with prior PR treatment) and different durations of telaprevir treatment. Model predictions were made by selecting patients with similar characteristics (e.g., genotype, prior response to PR, cirrhosis status, etc.) to the analysis of interest. Because patients who did not achieve SVR with prior PR treatment were not included in the training data set, response to PR for treatment-naïve patients given T/PR was simulated by setting the telaprevir dose to zero. Data from treatment-naïve patients with the appropriate PR

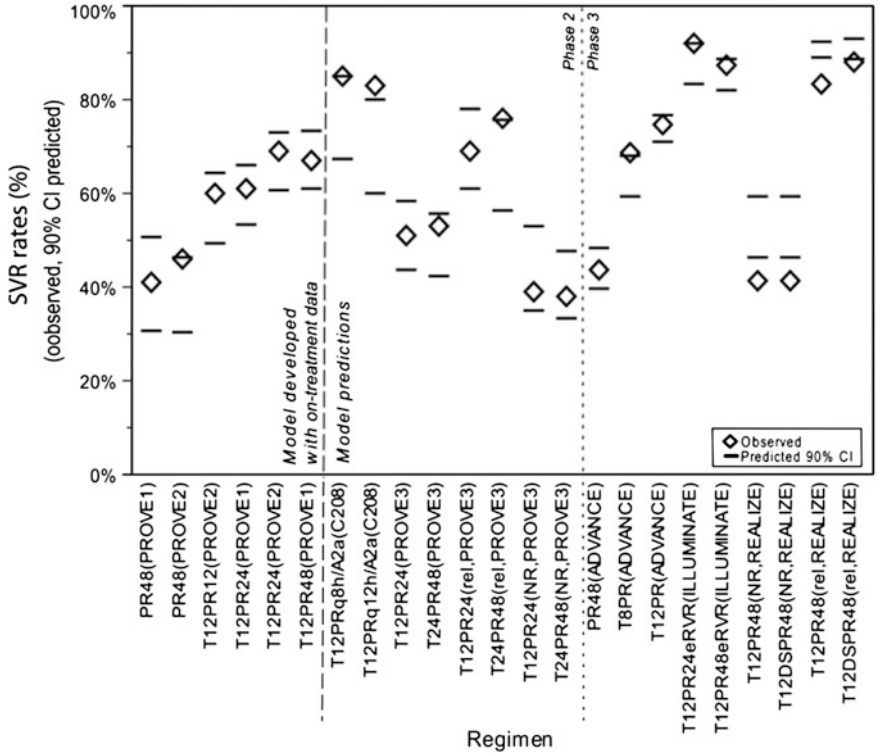

Fig. 18.4 Model verification: comparison between observed and predicted SVR rates (Adiwijaya et al. 2012)

responses (e.g., null response) were used in lieu of data from patients who did not achieve SVR with prior PR treatment.

As shown in Fig. 18.4, the SVR rates for the vast majority of subsequent Phase 2 and Phase 3 studies were within the 90 % confidence intervals of the model predictions. The model was also used to explore and eliminate study designs that were predicted to yield low SVR rates. Another critical contribution of the model concerned the determination of the telaprevir treatment duration. The design of the Phase 3 clinical studies was based on this prediction, with the results of the studies ultimately validating the model predictions.

Data are from the clinical studies PROVE1 (Hézode et al. 2009), PROVE2 (Hézode et al. 2009), PROVE3 (McHutchison et al. 2010), C206, ADVANCE (Jacobson et al. 2011), ILLUMINATE (Sherman et al. 2011), and REALIZE (Zeuzem et al. 2011). The notation "TxPRy" indicates that telaprevir and PR were dosed for x and y weeks, respectively. "DS" indicates that PR was dosed for 4 weeks prior to the start of telaprevir dosing. "rel" indicates that patients relapsed in previous PR48 treatment. "NR" indicates that patients never had undetectable HCV RNA during previous PR48 treatment (null and partial responders).

18.3 Future Challenges

While viral dynamic modeling was successfully used to guide the clinical development of telaprevir, there are many challenges that need to be overcome in future modeling efforts. In this section, those challenges are reviewed as they pertain to both interferon-based and interferon-free regimens.

18.3.1 Incorporation of Sequencing Data

Resistance to DAAs is a key factor that contributes to the failure of these regimens to suppress an HCV infection. Viral sequencing is routinely performed in clinical studies to understand the dynamics of this viral resistance in individual patients. The three most common types of sequencing methods used for this purpose are population sequencing, clonal sequencing, and deep sequencing (DS), all of which require sequencing of RT-PCR products amplified from patient plasma. These sequencing methods differ in their sensitivity to detect the frequency of resistant variants. Population sequencing provides only qualitative information about the frequency of the variant and has a relatively insensitive LOD of 20 % for minority variants. Clonal sequencing is more sensitive than population sequencing ($\sim$5 % LOD versus 20 %) and provides a quantitative estimate of the frequency of resistant variants. Like clonal sequencing, DS is also quantitative but has a lower LOD ($\sim$1 %) (Thomas et al. 2012).

The multi-variant viral dynamic model was originally developed using clonal sequencing data to inform key model parameters governing the dynamics of the viral variants (Adiwijaya et al. 2010). However, the subsequent modeling effort (Adiwijaya et al. 2012) did not include any sequencing data. Rather, the parameters estimated from the prior modeling effort (Adiwijaya et al. 2010) were used for the initial parameter estimates.

The viral dynamic model was developed using efficacy data from primarily one telaprevir dosing regimen (750 mg q8h). Therefore, it is reasonable to question whether or not the model is correctly sensitive to the telaprevir concentration. To answer this question clinically, the data from population sequencing analysis of patients who did not achieve SVR with a telaprevir-based regimen were evaluated (Kieffer et al. 2012). It was found that the majority of patients experiencing viral breakthrough during telaprevir treatment had variants that were highly resistant to telaprevir, implying that telaprevir was dosed sufficiently to suppress variants with lower levels of resistance to telaprevir. It is expected that sequencing data can be also used to construct viral dynamic models that are sensitive to the varying time-course of antiviral concentrations, even if the majority of the data are from studies evaluating only one dosing regimen for the antiviral. The sensitivity of

different viral variants to the antiviral, combined with the inherent variability of exposures in a population of patients, can be used to understand such effects from both the on-treatment and post-treatment dynamics of viral variants observed from the sequencing data.

The model of Adiwijaya et al. (2012) was developed by fitting solely on-treatment data. Accordingly, the PK approximations given by Eq. 18.4 account only for the dynamics resulting from the initial drug administration period. These approximations should be revised to account for the dynamics of time-varying doses and the post-dosing period. Additionally, the constraints used to enforce SVR (whereby individual viral species are eradicated once their HCV RNA levels fall below a pre-defined threshold; see the equation for the viral species in Fig. 18.2b) will likely hinder the post-treatment reversion back to drug-sensitive virus over time at the end of treatment (Sullivan et al. 2012). Consider the scenario shown in Fig. 18.5a, where WT virus and the V36A variant are eradicated by the SVR constraints in the Adiwijaya et al. model. These constraints prevent WT and the V36A variant from re-emerging after treatment, and consequently the model makes the unlikely prediction that the unfit A156T variant takes over the viral population. One way to overcome this problem is to implement the viral eradication boundary used by Snoeck et al. (Snoeck et al. 2010). In this framework, the number of infected cells must be greater than 1 in order for those cells to produce virus. As shown in Fig. 18.5b, this method allows the drug-sensitive virus and infected cells to be eradicated during treatment, then re-emerge after treatment. The mechanism for this re-emergence is as follows: first mutation from a drug-resistant variant repopulates the drug-sensitive infected cells, and then the drug-sensitive infected cells repopulate the drug-sensitive virus. Thus, this framework elegantly allows for scenarios which the Adiwijaya et al. approach cannot account.

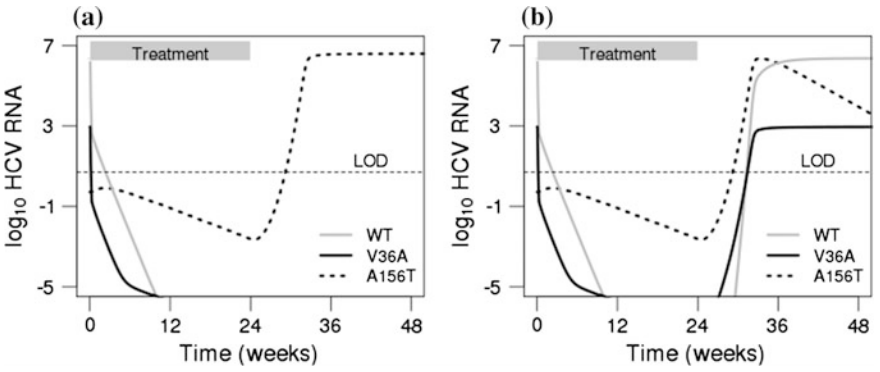

Fig. 18.5 Comparison of the variant dynamics for a hypothetical patient with HCV genotype 1b infection using the eradication criteria of **a** Adiwijaya et al. (2012) and **b** Snoeck et al. (2010). Note that the latter criterion permits eradication and re-emergence of drug-sensitive variants after the end of treatment whereas the former boundary criterion does not. The treatment phase is depicted by the *gray bar*

One further complication results from the fact that large-scale studies of resistance currently utilize the population sequencing method due to its relatively low cost. As previously noted, population sequencing data provides only qualitative information about the resistance variant's presence. To incorporate these data, new modeling techniques such as those pioneered by Sullivan et al. (2012) will need to be adapted to viral dynamic models to account for the lack of precise, quantitative information. In their work, Sullivan et al. constrained quantitative models of resistance dynamics using the qualitative data provided by population sequencing (Sullivan et al. 2012). In the future, it is anticipated that large-scale resistance studies will be performed using DS as the cost of next-generation sequencing technologies rapidly decreases.

18.3.2 Modeling Interferon-Free Regimens

Several interferon-free HCV regimens have moved into clinical development and are likely to be approved. Many of these regimens have demonstrated high SVR rates even in difficult-to-treat patients. Additionally, the majority of these regimens quickly bring the viral loads below the LOD. For these regimens, since there are only a few measurable viral loads during the rapid initial decline, if any, most of the useful information for the modeling exercise is contained in the viral dynamic data from both on-treatment breakthrough and post-treatment relapse. Therefore, variants identified by sequencing provide important information on how to model the effect of the exposure of each drug in the combination therapy.

For regimens containing the potent nucleotide inhibitor (nuc) sofosbuvir, no virologic breakthrough has been observed (Lawitz et al. 2013). In four Phase 3 trials with sofosbuvir and ribavirin with or without pegylated interferon, no resistance to sofosbuvir was detected (Svarovskaia et al. 2013). In addition, different patient populations such as treatment-naïve and prior PR null responders can exhibit dramatic differences in SVR rates even when the on-treatment viral dynamics are indistinguishable. Here, the majority of the viral dynamics fall below the LOD. For example, when sofosbuvir was dosed for 12 weeks in combination with ribavirin in the ELECTRON study, SVR rates of 84 versus 10 % were observed for the treatment-naïve and prior PR null responder populations, respectively (Gane et al. 2013a, b). When another potent DAA such as ledipasvir is added to the regimen, then SVR rates of 100 % were observed in both of these populations (Gane et al. 2013a, b). One possible explanation consistent with these observations is that resistance to a potent nucleotide inhibitor results in a relatively unfit mutant that replicates below the LOD. Such dynamics are graphically illustrated in Fig. 18.6a, where the gray lines below the LOD (the third phase of viral decline) denote the mutant dynamics in different patients. Attainment of SVR depends on whether or not an individual patient can clear this unfit mutant during treatment. When another potent DAA is added to the original regimen, this unfit mutant must be resistant to both the nuc and the DAA, and therefore the genetic barrier (i.e., the number of

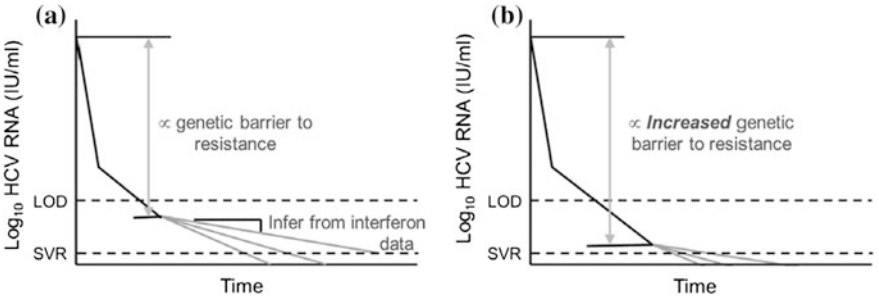

Fig. 18.6 Hypothesized response for interferon-free regimens: **a** a potent nucleotide inhibitor (nuc) and **b** a nuc combined with another DAA (nuc + DAA). The variability in these regimens is consistent with a resistant virus that replicates to at differing degrees below the LOD (*gray lines*). The initial drop decrease in the viral load for the first two phases of viral decline is proportional to (denoted by the $\propto$ *symbol*) the genetic barrier of resistance for the regimen

mutations from WT to this resistant mutant) is increased. Consequently, the variability of the third phase of viral decline occurs farther below the LOD for a regimen containing both a nuc and another DAA (nuc + DAA; see Fig. 18.6b) than with the nuc alone (see Fig. 18.6a). As a result, the chances of SVR are increased in the nuc + DAA regimen. Because the mutant dynamics occur exclusively below the LOD and are thus unobservable, assumptions must be made to parameterize the mutant for viral dynamic modeling. The fact that prior PR response results in different SVR rates suggests these parameters may be related to those obtained by fitting PR data.

When the viral dynamics above the LOD contain rich dynamic information, nonlinear mixed-effect (NLME) modeling is a useful tool to quantify the variability in parameters. For example, Snoeck et al. (2010) and Guedj et al. (2013c) used MONOLIX to model viral dynamics in patients treated with PR and alisporivir, respectively. For interferon-free regimens, NLME modeling is expected to have more limited utility because the most important dynamics occur below the LOD. That is, patients who exhibit similar on-treatment viral dynamics and achieve SVR are expected to have differing dynamics below the LOD (see, for example, Figs. 18.1b and 18.6). In order to accurately predict viral dynamics in these patients, particularly when reducing the efficacy of the regimen (e.g., shortening the treatment duration), assumptions will need to be made concerning the variability below the LOD.

18.4 Conclusions

Viral dynamic modeling is a powerful tool for interpreting and predicting the efficacy of HCV regimens. The Adiwijaya et al. model of telaprevir-based regimens (Adiwijaya et al. 2012) demonstrates the utility of these models for helping guide

the design of clinical studies. As the HCV treatment landscape continues to change, challenges for viral dynamic modeling include incorporating viral sequencing data to better inform model predictions and modeling regimens in which most of the viral dynamics occur below the LOD. These challenges will require development of novel methods and clever assumptions that are derived from better understanding of viral infection systems pharmacology. These investments will facilitate the use of viral dynamic modeling for designing clinical studies and analyzing their results.

References

Adiwijaya BS, Herrmann E, Hare B, Kieffer T, Lin C, Kwong AD, Garg V, Randle JCR, Sarrazin C, Zeuzem S, Caron PR (2010) A multi-variant, viral dynamic model of genotype 1 HCV to assess the in vivo evolution of protease-inhibitor resistant variants. PLoS Comput Biol 6:e1000745

Adiwijaya BS, Kieffer TL, Henshaw J, Eisenhauer K, Kimko H, Alam JJ, Kauffman RS, Garg V (2012) A viral dynamic model for treatment regimens with direct-acting antivirals for chronic hepatitis C infection. PLoS Comput Biol 8:e1002339

Chatterjee A, Guedj J, Perelson AS (2012) Mathematical modelling of HCV infection: what can it teach us in the era of direct-acting antiviral agents? Antivir Ther 17:1171–1182

Chatterjee A, Smith PF, Perelson AS (2013) Hepatitis C viral kinetics: the past, present, and future. Clin Liver Dis 17:13–26

Gane EJ, Stedman CA, Hyland RH, Ding X, Svarovskaia ES, Pang PS, Symonds WT (2013a) Once daily sofosbuvir/ledipasvir fixed dose combination with or without ribavirin: the ELECTRON trial. Hepatology 58:243A

Gane EJ, Stedman CA, Hyland RH, Pang PS, Ding X, Symonds WT, McHutchison JG (2013b) All-oral sofosbuvir-based 12-week regimens for the treatment of chronic HCV infection: the ELECTRON Study. J Hepatol 58(Supplement 1):S6–S7

Guedj J, Dahari H, Rong L, Sansone ND, Nettles RE, Cotler SJ, Layden TJ, Uprichard SL, Perelson AS (2013a) Modeling shows that the NS5A inhibitor daclatasvir has two modes of action and yields a shorter estimate of the hepatitis C virus half-life. PNAS 110:3991–3996

Guedj J, Yu J, Levi M, Li B, Kern S, Naoumov NV, Perelson AS (2013b) Modeling viral kinetics and treatment outcome during alisporivir interferon-free treatment in HCV genotype 2/3 patients. Hepatology 59:1706–1714

Guedj J, Yu J, Levi M, Li B, Kern S, Naoumov NV, Perelson AS (2013c) Modeling early viral kinetics with alisporivir: interferon-free treatment and SVR predictions in HCV G2/3 patients. PAGE 22 Abstr. 2944[http://www.page-meeting.org/?abstract=2944]

Hézode C, Forestier N, Dusheiko G, Ferenci P, Pol S, Goeser T, Bronowicki J-P, Bourlière M, Gharakhanian S, Bengtsson L, McNair L, George S, Kieffer T, Kwong A, Kauffman RS, Alam J, Pawlotsky J-M, Zeuzem S (2009) Telaprevir and peginterferon with or without ribavirin for chronic HCV infection. N Engl J Med 360:1839–1850

Hezode C, Hirschfield GM, Ghesquiere W, Sievert W, Rodriguez-Torres M, Shafran S, Thuluvath PJ, Tatum HA, Waked I, Esmat G, Lawitz EJ, Rustgi VK, Pol S, Weis N, Pockros P, Bourliere M, Serfaty L, Vierling JM, Fried MW, Weiland O, Brunetto MR, Everson GT, Zeuzem S, Kwo PY, Sulkowski M, Brau N, Wind-Rotolo M, Liu Z, Hughes EA, Yin PD, Schnittman S (2012) Daclatasvir, an NS5A replication complex inhibitor, combined with peginterferon Alfa-2a and ribavirin in treatment-naïve HCV-genotype 1 or 4 patients: phase 2b COMMAND-1 SVR12 results. Hepatology 56:553A

Hindmarsh AC (1980) LSODE and LSODI, two new initial value ordinary differential equation solvers. SIGNUM Newsl 15:10–11

INCIVEK (telaprevir) [US Prescribing Information, http://pi.vrtx.com/files/uspi_telaprevir.pdf] (2013)

Jacobson IM, McHutchison JG, Dusheiko G, Di Bisceglie AM, Reddy KR, Bzowej NH, Marcellin P, Muir AJ, Ferenci P, Flisiak R, George J, Rizzetto M, Shouval D, Sola R, Terg RA, Yoshida EM, Adda N, Bengtsson L, Sankoh AJ, Kieffer TL, George S, Kauffman RS, Zeuzem S (2011) Telaprevir for previously untreated chronic hepatitis C virus infection. N Engl J Med 364:2405–2416

Kieffer TL, De Meyer S, Bartels DJ, Sullivan JC, Zhang EZ, Tigges A, Dierynck I, Spanks J, Dorrian J, Jiang M, Adiwijaya B, Ghys A, Beumont M, Kauffman RS, Adda N, Jacobson IM, Sherman KE, Zeuzem S, Kwong AD, Picchio G (2012) Hepatitis C viral evolution in genotype 1 treatment-naïve and treatment-experienced patients receiving telaprevir-based therapy in clinical trials. PLoS ONE 7:e34372

Kieffer TL, Sarrazin C, Miller JS, Welker MW, Forestier N, Reesink HW, Kwong AD, Zeuzem S (2007) Telaprevir and pegylated interferon–alpha-2a inhibit wild-type and resistant genotype 1 hepatitis C virus replication in patients. Hepatology 46:631–639

Lawitz E, Mangia A, Wyles D, Rodriguez-Torres M, Hassanein T, Gordon SC, Schultz M, Davis MN, Kayali Z, Reddy KR, Jacobson IM, Kowdley KV, Nyberg L, Subramanian GM, Hyland RH, Arterburn S, Jiang D, McNally J, Brainard D, Symonds WT, McHutchison JG, Sheikh AM, Younossi Z, Gane EJ (2013) Sofosbuvir for previously untreated chronic hepatitis C infection. N Engl J Med 368:1878–1887

Lin K, Perni RB, Kwong AD, Lin C (2006) VX-950, a novel hepatitis C virus (HCV) NS3-4A protease inhibitor, exhibits potent antiviral activities in HCV replicon cells. Antimicrob Agents Chemother 50:1813–1822

McHutchison JG, Manns MP, Muir AJ, Terrault NA, Jacobson IM, Afdhal NH, Heathcote EJ, Zeuzem S, Reesink HW, Garg J, Bsharat M, George S, Kauffman RS, Adda N, Di Bisceglie AM (2010) Telaprevir for previously treated chronic HCV infection. N Engl J Med 362:1292–1303

Neumann AU, Lam NP, Dahari H, Gretch DR, Wiley TE, Layden TJ, Perelson AS (1998) Hepatitis C viral dynamics in vivo and the antiviral efficacy of interferon-α therapy. Science 282:103–107

Nowak MA, May RM (2000) Virus dynamics: mathematical principles of immunology and virology. Oxford University Press, New York

Petzold LR (1982) Description of Dassl: a differential/algebraic system solver (No. SAND-82-8637; CONF-820810-21). Sandia National Labs, Livermore

Rong L, Dahari H, Ribeiro RM, Perelson AS (2010) Rapid emergence of protease inhibitor resistance in hepatitis C virus. Sci Transl Med 2:30ra32

Sarrazin C, Kieffer TL, Bartels D, Hanzelka B, Müh U, Welker M, Wincheringer D, Zhou Y, Chu H, Lin C, Weegink C, Reesink H, Zeuzem S, Kwong AD (2007) Dynamic hepatitis C virus genotypic and phenotypic changes in patients treated with the protease inhibitor telaprevir. Gastroenterology 132:1767–1777

Sherman KE, Flamm SL, Afdhal NH, Nelson DR, Sulkowski MS, Everson GT, Fried MW, Adler M, Reesink HW, Martin M, Sankoh AJ, Adda N, Kauffman RS, George S, Wright CI, Poordad F (2011) Response-guided telaprevir combination treatment for hepatitis C virus infection. N Engl J Med 365:1014–1024

Snoeck E, Chanu P, Lavielle M, Jacqmin P, Jonsson EN, Jorga K, Goggin T, Grippo J, Jumbe NL, Frey N (2010) A comprehensive hepatitis C viral kinetic model explaining cure. Clin Pharmacol Ther 87:706–713

Sullivan J, De Meyer S, Haseltine E, Dierynck I, Bartels DJ, Ghys A, Zhang EZ, Spanks J, Tigges A, Davis A, Martin EC, Picchio G, Kieffer TL (2012) Rate of disappearance of telaprevir resistant variants using clonal and population sequence data from phase 3 studies. 63rd Annual Meeting of the American Association for the Study of Liver Diseases, Poster 756

Svarovskaia ES, Dvory HS, Hebner C, Doehle B, Gontcharova V, Martin R, Gane EJ, Jacobson IM, Nelson DR, Lawitz E, Bekele BN, Brainard DM, Symonds WT, McHutchison JG, Miller MD (2013) No resistance detected in four phase 3 clinical studies

in HCV genotype 1-6 of sofosbuvir + ribavirin with or without peginterferon. Hepatology 58:1091A

Thomas XV, de Bruijne J, Sullivan JC, Kieffer TL, Ho CKY, Rebers SP, de Vries M, Reesink HW, Weegink CJ, Molenkamp R, Schinkel J (2012) Evaluation of persistence of resistant variants with ultra-deep pyrosequencing in chronic hepatitis C patients treated with telaprevir. PLoS One 7:e41191

Zeuzem S, Andreone P, Pol S, Lawitz E, Diago M, Roberts S, Focaccia R, Younossi Z, Foster GR, Horban A, Ferenci P, Nevens F, Müllhaupt B, Pockros P, Terg R, Shouval D, van Hoek B, Weiland O, Van Heeswijk R, De Meyer S, Luo D, Boogaerts G, Polo R, Picchio G, Beumont M (2011) Telaprevir for Retreatment of HCV Infection. N Engl J Med 364:2417–2428

Zhou Y, Bartels DJ, Hanzelka BL, Müh U, Wei Y, Chu H-M, Tigges AM, Brennan DL, Rao BG, Swenson L, Kwong AD, Lin C (2008) Phenotypic characterization of resistant Val36 variants of hepatitis C virus NS3-4A serine protease. Antimicrob Agents Chemother 52:110–120

Zhou Y, Müh U, Hanzelka BL, Bartels DJ, Wei Y, Rao BG, Brennan DL, Tigges AM, Swenson L, Kwong AD, Lin C (2007) Phenotypic and structural analyses of hepatitis C virus NS3 protease Arg155 variants sensitivity to telaprevir (VX-950) and interferon α. J Biol Chem 282:22619–22628

Chapter 19
Using Systems Pharmacology to Advance Oncology Drug Development

Daniel C. Kirouac

Abstract Cytotoxic chemotherapies have been the foundation of oncology for the last 50 years. The emergence of molecularly targeted anti-cancer drugs promises to deliver inherently safer and more effective treatments by attacking the unique biochemical vulnerabilities of tumor cells. However, the promise of these agents is fundamentally limited by the heterogeneity of cancer genomes and the robustness of protein signaling networks which control tumor cell growth. By quantifying these cellular and molecular properties, computational systems biology has the potential to accelerate progress and increase success rates of anti-cancer drug development programs. Mechanism-based computational models which integrate molecular cell biology and drug pharmacology may thus enhance the predictive power of pre-clinical research, the utility of clinical data, and ultimately inform critical drug development decisions. Examples are provided through which orthogonal computational modeling approaches, from data-driven statistical models to physicochemical-based differential equations, have been used to address challenges arising at different stages of such programs. These include drug target selection, therapeutic design, identification of biomarkers for patient stratification, dose selection, and the design of combination regimens.

Keywords Orthogonal computational modeling approaches · Statistical models · Drug target selection · Therapeutic design · Biomarkers · Patient stratification · Dose selection · Combination regimen · Mechanism-based computational models · Cytotoxic chemotherapies · Oncogenic signaling networks · Physicochemical - based models · Model-based liposome design · Antibody engineering · Network redundancy · Vertical integration · Horizontal integration

D.C. Kirouac (✉)
Merrimack Pharmaceuticals Inc., One Kendall Square, Cambridge, MA, USA
e-mail: kirouac.daniel@gene.com

Present Address:
D.C. Kirouac
Genentech Research & Early Development, 1 DNA Way, South San Francisco, CA, USA

D.E. Mager and H.H.C. Kimko (eds.), *Systems Pharmacology and Pharmacodynamics*,
AAPS Advances in the Pharmaceutical Sciences Series 23,
DOI 10.1007/978-3-319-44534-2_19

19.1 Introduction

19.1.1 A Brief History of Oncology Drug Development

Military rhetoric is often used to describe the human experience of cancer—Richard Nixon declared war on cancer, patients battle the disease, and oncologists employ arsenals of drugs. The war metaphor is perhaps appropriate, as the first effective chemotherapy agents, nitrogen mustards, were derivatives of the chemical warfare agent mustard gas. Characteristic injuries stemming from mustard gas exposure include bone marrow hypocellularity and cytopenia, the inverse symptoms of blood cancers, characterized by the excess production of white blood cells. Following the Second World War their use was audaciously re-purposed in last ditch attempts to treat childhood leukemias and lymphomas. These attempts produced unprecedented symptomatic remissions, in what was then an untreatable death sentence. Thus were born the first class of anti-cancer chemotherapies, Alkylating agents, which function by attaching alkyl groups to DNA and impeding its proper replication and transcription (DeVita and Chu 2008).

These were followed by other anti-proliferative chemotherapies, including anti-metabolites (5-flourouracil, methotrexate, capecitabine, gemcitabine), anthracyclines (doxorubicin, epirubicin, mitomycin), platinum-based agents (cicplatin, carboplatin, oxaliplatin), topoisomerase inhibitors (campotecan, irinotecan), and anti-microtubule agents (paclitaxel, docetaxel). All of these drugs function by directly damaging and/or inhibiting the replication of DNA. A degree of selectivity for cancerous vs. healthy tissue arises from two distinctive properties of cancer cells—an enhanced rate of proliferation (perhaps *the* quintessential hallmark of cancer), and impaired DNA damage repair machinery (required to accommodate the mutational processes underlying neoplastic transformation). Given the razor thin and highly variable therapeutic index of these drugs, serious toxicities associated with their use are an expected part of therapy, biased to tissues with higher rates of cellular turnover such as the gastrointestinal tract and hair follicles.

As a result of the narrow therapeutic index, clinical dosing regimens for anti-cancer drugs have been based around toxicity. That is, establishing a maximum tolerated dose (MTD) beyond which toxicities are unbearable, and pushing as close as possible to this bar. Chemotherapies are rarely effective as single agents, and are thus typically administered as multi-drug combination regimens. While such combination regimens are the mainstay of clinical oncology, and in some cases curative, they have largely been established via trial and error rather than rational design. Very few have been evaluated pre-clinically to optimize doses or schedules, fewer still are considered to display synergistic efficacy, and no regimens in current use are selected based on biomarkers predictive of individual patient responses (Dancey and Chen 2006). The practice of developing drug regimens by empirical clinical testing is not only slow and inefficient, but borne out of the misery of patients and their families.

19.1.2 Molecularly Targeted Agents

Oncology drug development has been transformed over the last decade, from a focus on deriving broadly cytotoxic agents toward molecularly targeted drugs, designed to attack the molecular underpinnings of cancerous growth rather than the characteristic phenotypes. This movement began with development of anti-estrogens and anti-androgens, used to treat hormone-dependent breast and prostate cancers, respectively. Imatinib, the first marketed tyrosine kinase inhibitor (TKI) was a trail-blazer. A selective inhibitor of the protein Ableson kinase (ABL) which is constitutively activated in the majority of chronic myeloid leukemias (CML) through a chromosomal translocation (BCR-ABL), the drug produces durable clinical remissions in the majority of patients (Druker et al. 2001; Kesselheim and Avorn 2013). In addition to transforming the management of the disease, these results also validated the concept that molecular defined cancers could be cured using relatively non-toxic agents, a discovery which set a goal post for a flurry of successive TKIs. Examples include gefitinib and erlotininb (Epidermal Growth Factor Receptor [EGFR] inhibitors used in lung cancer), crizotinib (an Anaplastic Lymphoma Kinase [ALK] inhibitor also used in lung cancer), vemurafinib (a B-Raf inhibitor used in melanoma), and lapatinib (a Human Epidermal Growth Factor Receptor-2 [HER2, or ERBB2] inhibitor used in breast cancer). While these drugs have been transformative, the degree of success of imitainib for the treatment CML has not been repeated —likely due to the unique monogenetic origin of the disease in contrast with the bewildering mutational diversity of most cancers (Ciriello et al. 2013).

Oncology drug development has similarly been transformed by new therapeutic modalities capable of achieving highly selective and potent target engagement. Monoclonal antibodies (mAbs) in particular have proven highly effective, as they are able to both inhibit signaling through oncogenic cell surface receptors, and engage anti-tumor immunity through the induction of antibody-dependent cell mediated cytotoxicity (ADCC). Trastuzumab (Herceptin®) was the first mAb approved for the treatment of cancer. It binds to the receptor tyrosine kinase (RTK) HER2, an ErbB-family receptor expressed on approximately 25 % of breast cancers and associated with aggressive disease. Clinical studies showed the agent to be effective only in patients with elevated expression of the protein in their tumors (HER2+), necessitating development of a companion molecular diagnostic (HerceptTest™) along with the drug, becoming the first example of a molecularly-stratified cancer therapy (Slamon et al. 2001). Following Herceptin, as of 2013, thirteen mAbs approved by the FDA for the treatment of cancer (Sliwkowski and Mellman 2013). The target specificity achievable with these molecules has more recently been employed for directing traditional cytotoxic payloads to cancerous tissue, either through chemical coupling as antibody-drug conjugates (ADC), or embedded in immuno-liposomes (Sliwkowski and Mellman 2013). Small interfering RNA (siRNA) represents another emerging therapeutic modality, holding great promise for blocking the synthesis oncogenic proteins if delivery problems can be adequately addressed (Whitehead et al. 2009).

19.1.3 Challenges to Developing Effective Targeted Agents in Oncology

The poor and declining efficiency of modern pharmaceutical research has been widely reported and opined upon. It currently costs over two billion dollars on average to bring a new medicine to market (Scannell et al. 2012), the main driver being the capitalized cost of clinical failures, particularly in Phase 2 proof of concept studies (Paul et al. 2010). This is where pre-clinical hypotheses, developed and honed over years of research, are first evaluated in actual patients. Attrition rates at this stage of development are estimated at 50–70 % across the industry (DiMasi et al. 2010), where failures are most often due to lack of efficacy (Arrowsmith and Miller 2013). These failures imply that the fundamental assumptions on which multimillion dollar and decade-long drug development programs rest, are frequently incorrect.

Focusing on oncology, the probability that an agent entering clinical testing will eventually attain regulatory approval is currently estimated at 13 % (DiMasi et al. 2013), poorer than all other major disease indications (Hay et al. 2014). Changes to in clinical strategy could help alleviate expensive late stage clinical failures. In particular, the use of surrogate measures of drug activity such as pharmacodynamic readouts or changes in tumor growth kinetics (Ferté et al. 2013) would help in establishing clinical proof of concept as early as possible (preferably in Phase I). Prioritizing candidates for larger Phase II and III trials using even such imperfect metrics of clinical responses could improve the likelihood of success (Paul et al. 2010). This will also require a shift away from fixed 2-arm comparative trials, towards biomarker-based, multi-agent, adaptive designs (Yap et al. 2010). So-called multi-arm "bucket trials" may be an effective and increasingly common strategy. These types of trials are designed to prospectively evaluate multiple biomarkers and multiple experimental agents simultaneously, with adaptive randomization protocols such that arms can be added or purged as information is gleaned during the course of an ongoing study (Kaplan et al. 2013).

Prior to the initiation of clinical testing, the success of a drug development program ultimately depends upon a variety of factors, including the appropriate selection of drug targets and agents capable of achieving pharmacologically-relevant target modulation, the selection of appropriate patient populations, the use of biologically active doses and dosing schedules, and the design of effective combination regimens. The unique biological properties of cancer cells pose fundamental challenges to each of these decisions and cumulatively hinder the success of drug development programs.

19.2 Oncogenic Signaling Networks and Drug Development

Knowledge of the molecular underpinnings of cancer has grown at an unprecedented rate over the last decade, fueled by advances in high-throughput measurement technologies such as next generation DNA sequencing, gene expression arrays, quantitative proteomics, and robotic platforms for high-throughput screening (Watson et al. 2013). The number of molecular targeted drugs approved or developed for the treatment of cancer has also greatly expanded. As of 2012, there were almost 1000 new cancer medicines in clinical testing from American pharmaceutical companies alone (PhRMA 2012). While this offers tremendous hope for patients, there remain significant scientific and technical obstacles to fully realize the potential of these resources. As such, we have yet to witness commensurate advances in curative therapies, particularly for metastatic disease. When used in molecularly-defined populations, targeted therapies can demonstrate profound efficacy, reducing tumor burden, and extending lives. However, a substantial fraction of patients, even within prospectively selected populations, fail to respond, and those that do almost universally relapse within a year. The challenge of producing durable remissions with current targeted drugs can be interpreted through the fundamental properties of cancer cell biology.

19.2.1 Molecular Heterogeneity

Oncologists have long recognized that each patient is unique with respect to their clinical presentation, disease progression, and response to drug therapy. Genome sequencing projects have revealed that at the molecular level as well, no two cancers are identical. Even within individual patients, clonal diversity is often evident between lesions and within different areas of the same tumor (Gerlinger et al. 2012). Despite the well documented heterogeneity, a paucity of molecular biomarkers exists that can reliably identify patients most likely to respond to treatment, or rapidly predict whether an effective dose has been attained (Schilsky 2010). Molecular biomarkers used in current clinical practice are limited to genetic mutations or amplified expression of the drug target. Prototypic examples include sequencing the BRAF gene for V600E mutations to guide vemurafinib therapy in melanoma, and immunohistochemistry measurements of HER2 gene amplification for trastuzumab treatment in breast cancer (Majewski and Bernards 2011). However, single gene/protein measurements have limited clinical utility, as objective response rates to targeted inhibitors within pre-selected (biomarker+) patient populations are most less than 20 % (Sharma et al. 2010). The complexities of molecular biology simply outwit efforts to characterize disease using a single measurement.

Genome sequencing projects have revealed that mutations are incredibly disparate even within histologically similar tumors. However, when mutations are mapped onto protein interaction networks, a limited number of cell regulatory pathways and functional modules are found to be recurrently altered (Yaffe 2013). Most notable are the Phosphatidylinositide 3-kinase (PI3K) and Mitogen Activated Protein Kinase (MAPK) cascades, and the receptor tyrosine kinases (RTKs) which regulate their activities. Others include the TP53 and cell cycle control modules, the apoptotic caspase machinery, as well as a handful of other more indication- and tissue-specific pathways such as Wnt, Hedgehog, and Transforming Growth Factor (TGF)-beta (The Cancer Genome Atlas 2008; Hammerman et al. 2012; Stephens et al. 2012; Ciriello et al. 2013). Mutations within these network modules are generally found to be mutually exclusive, prototypic examples being *PI3KCA*-activating mutations versus *PTEN* deletions and *KRAS* versus *BRAF*-activating mutations (Ciriello et al. 2012). This indicates that what "matters" to the cell is the activation state of network modules rather than individual genes or proteins per se (Vogelstein and Kinzler 2004). Following this, metrics of network activity could be

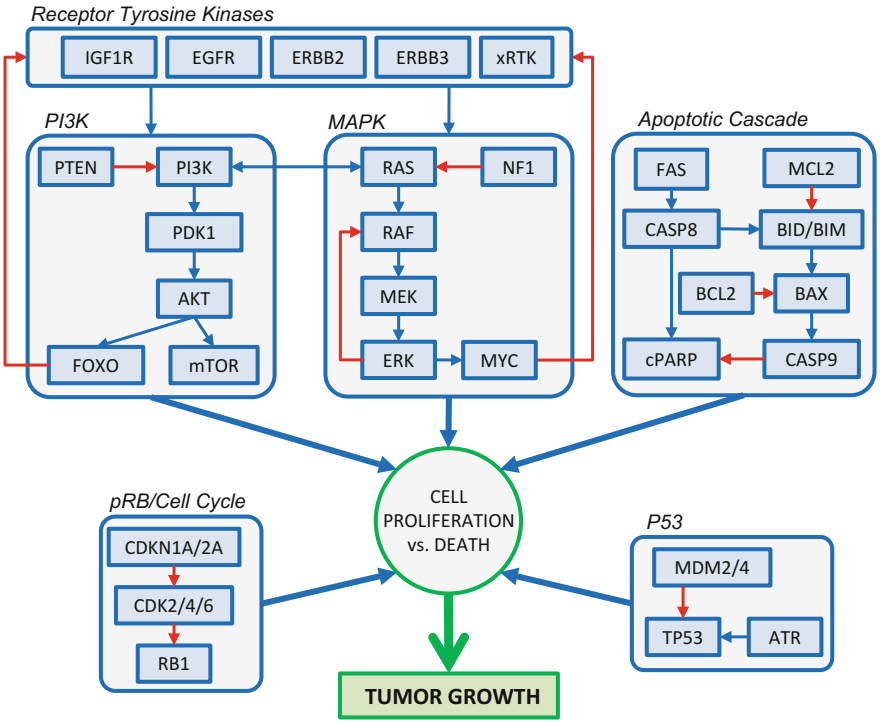

Fig. 19.1 Cell signaling and regulatory network modules recurrently mutated in cancer. Cancer genes are indicated in *boxes*, and organized into canonical pathways. Much of the molecular details (genes and interactions) have been omitted for simplicity, and there exist many cross module interactions. The activity of signaling modules combine to regulate cell proliferation and death, the balance of which determines bulk tumor growth

more informative predictors of functional pathway dependence and drug sensitivity than single gene or protein measurements (Fig. 19.1).

19.2.2 Network Redundancy

Redundancy is observed at multiple levels within biochemical networks. As mentioned, mutations within a network module often display functionally equivalent (or at least highly similar) effects. This is a consequence of biochemical information flow- disrupting a signal at different points along the transmission route will have similar effects ("vertical" redundancy). An alternative form of "horizontal" redundancy arises from cellular capacity for alternative biochemical wiring. A consequence of evolutionary recycling of protein binding domains, network modules, and their constitutive proteins are capable of combining in alternate configurations. Consider the signal "input" level to the cell: while at least 58 receptor tyrosine kinases exist (Blume-Jensen and Hunter 2001), through the recurrent use of adaptor proteins they activate a relatively conserved set of signaling cascades. This topological feature has been referred to as "bow tie" architecture, wherein signals emanating from diverse extracellular ligands converge on a limited set of intracellular "hub" proteins such as AKT, ERK (extracellular signal-related kinase), and TP53 (Kirouac et al. 2012). The clinical consequences are becoming increasingly appreciated in oncology through the phenomena of "oncogenic shift." Tumors displaying "addiction" to a single oncogenic kinase are often capable of switching dependency to an alternate, but functionally equivalent node following inhibitor treatment (Wilson et al. 2012). RTKs have even been found to be functionally exchangeable within individual tumors (Snuderl et al. 2011). A consequence of such molecular redundancies is that the number of potential resistance pathways is staggering. For example, activation of at least 20 alternate kinases have been reported to mediate resistance to EGFR inhibitors in lung cancer (Chong and Jänne 2013) and a similar number to BRAF inhibitors in melanoma (Lito et al. 2013). These patterns of dependency switching are however difficult to predict, and are not necessarily apparent from genetic changes if arising from subtle shifts in protein expression patterns (Niederst and Engelman 2013). The core cytosolic signaling cascades themselves also display a degree of horizontal redundancy. For example, the PI3K and MAPK cascades coverage on an overlapping set of effectors (Sos et al. 2009; She et al. 2010).

19.2.3 Network Adaptation

A distinguishing feature of living versus non-living matter is the ability to maintain internal stasis in the face of a continually shifting environment. Homeostatic regulation typically involves feedback control circuits, and many such biochemical

feedback circuits have been characterized in cancer cells. Feedback controls within signal transduction cascades buffer the effect of targeted inhibitors and other perturbations, an example being active (phosphorylated) ERK inhibiting the activation of its upstream kinases RAF and RAS (Cirit et al. 2010; Fritsche-Guenther et al. 2011). The activities of intracellular signaling cascades are also fine-tuned through the regulated expression of cell surface receptors (Chandarlapaty et al. 2011; Duncan et al. 2012). Pathway inhibition can thus result in the compensatory activation of parallel, redundant pathways through the relief of antagonistic feedback circuits. Expression of a range of RTKs are elevated in response to both PI3K/AKT (Chandarlapaty et al. 2011) and MAPK/ERK pathway inhibition (Duncan et al. 2012). This phenomenon is particularly well documented for the ErbB3 receptor, where EGFR and HER2 inhibitors such as lapatinib and gefitinib increase compensatory ErbB3-mediated PI3K/AKT signaling (Chakrabarty et al. 2012; Chandarlapaty et al. 2011; Garrett et al. 2011; Amin et al. 2010; Sergina et al. 2007). These receptor-coupled feedback circuits underlie the so called "*Whac-a-Mole*®" effect, named after the popular arcade game, wherein suppression of a single RTK or pathway induces compensatory activation of a parallel, functionally redundant pathway.

19.2.4 Combating Network Robustness Using Biomarker-Based Drug Combinations

The rational application of combination therapies has been widely touted as a strategy for battling these mechanisms of network resilience (Creixell et al. 2012; Robin et al. 2013). By simultaneously blocking functionally redundant pathways or co-targeting an adaptive feedback circuit along with the primary oncogenic driver, one could in theory substantially enhance therapeutic efficacy, delay the onset of resistance, and provide durable disease remissions (Fitzgerald et al. 2006). Indeed, evolutionary dynamic models predict that therapy with two drugs, if appropriately chosen to target distinct oncogenic driver pathways, could produce curative treatments (Bozic et al. 2013). However, given the number of molecularly targeted agents currently available for testing combined with the diversity of human cancers, the number of possible drug-drug and drug-genome combinations is rapidly exceeding what is feasible through empirical screening. Strategies for prioritizing the most promising combination regimens and predictive biomarkers could therefore greatly advance clinical practice (Dancey and Chen 2006). In silico screening offers a possible solution if predictive computational models of cancer biology and pharmacology can be developed.

Model-based drug development (MBDD) was advocated by the FDA Critical Path Initiative as a potentially powerful but underutilized approach to improving pharmaceutical industry efficiency (Lalonde et al. 2007). Implementation to date has largely focused on clinical pharmacometrics, and evidence suggests this

investment has improved clinical decision making across the industry (Lee et al. 2011). However, by the time a compound is tested in humans, the risk/benefit properties are largely pre-determined and many critical decisions underlying the success or failure of the program are irrevocably locked in (Milligan et al. 2013). Computational modeling at this stage can be used to extract efficacy and safety signals from noise, but little can be done to correct fundamental problems buried in the program's history. Developing computational models at the earliest stages of a drug development, based around the biology of the disease rather than a specific compound, could help bridge the gap between discovery-stage research, pre-clinical development, and clinical testing. Importantly, many of the described properties of cancer cell regulatory networks which make them robust to targeted therapies (molecular heterogeneity, redundancies, and adaptation) can be represented mathematically, and thus formulated as computational models. By contextualizing drug targets within the networks they are embedded, and linking network responses to tumor growth, mechanism-based models could prove pivotal in improving rates of Phase 2 success and realizing the promise of precision medicine (Pe'er and Hacohen 2011).

19.2.5 Approaches to Model Cancer Signaling Networks

There are a wide variety of computational modeling tools available to draw from, each with specific limitations, biases, and data requirements. Because no modeling framework is intrinsically superior, the choice between alternatives depends largely on the data available for model calibration and the specific questions to be addressed. Methods can be roughly mapped onto a continuum based on their degree of mechanistic abstraction, from data-driven statistical models at one end, to mass action kinetic-based chemical reaction networks at the other (Kholodenko et al. 2012). While statistical modeling approaches have the advantage of being relatively free of predefined hypotheses, ignoring prior knowledge about the function of biomolecules and their relationships is also a limitation. Incorporating established mechanisms enables one to focus on the most relevant questions, rather than using statistical power to re-discover what is already known. There are a multitude of resources available to draw from, in which pathways and regulatory relationships are commonly represented as interaction networks (Bauer-Mehren et al. 2009). Pathguide (www.pathguide.org) currently links to over 500 databases covering metabolic pathways, signaling pathways, transcription factor targets, gene regulatory networks, genetic interactions, protein-compound interactions, and protein-protein interactions (Bader et al. 2006). Pathway Commons (www.pathwaycommons.org) is a web-based portal, enabling researchers to browse information and download source data from 9 of the most commonly used pathway and molecular interaction databases such as Reactome, MINT, and NCI-PID (Cerami et al. 2011).

These resources are typically used as platforms to functionally interpret genomic and other molecular profiling data (Carter et al. 2013). While the derivative graphs

have limited predictive power, they can serve as a starting point towards developing causal models. Boolean or Fuzzy Logic-based networks for example start with a defined network topology and describe the activities of components connected using logical operators, as found in electronic circuits (Morris et al. 2010). While these model formalisms are causal in that they describe information flow through networks, they are gross abstractions of the underlying biochemical processes. Physicochemical-based models aspire to describe biochemical networks from the "bottom-up", based on fundamental biochemical processes. Such models are generally implemented as sets of ordinary or partial differential equations, which can be derived from lists of reactions using the principles of mass action kinetics. As the level of molecular detail increases, the number of free parameters expands accordingly. Parameterization then becomes the main challenge, necessitating as substantial amount of training data and fast optimization algorithms to estimate unknown rate constants and initial conditions. As such, mass action kinetic-based ODEs are likely best-suited to describing the dynamics of networks with well-defined mechanisms and richly-sampled time-course data (Aldridge et al. 2006).

Hybrid modeling approaches are possible, which may overcome limitations associated with alternate forms, or capture different levels of biological detail (Karr et al. 2012). For example, one can imagine using a detailed mass action kinetic-based model to describe interactions between a drug and receptors at the cell surface, and then a statistical or logic-based model to link receptor engagement to intracellular signaling and phenotypic responses. As mathematical models are often problem-specific, multiple orthogonal models could be developed to describe different aspects of the same biological process. By focusing on successive stages of drug development, the next sections will provide examples of how different computational approaches (statistical, causal, and physicochemical models) can be applied to specific problems along the path from discovery to clinical testing (Fig. 19.2).

19.3 Modeling Signaling Networks for Drug Target Identification

Appropriate target selection is perhaps the most important decision underlying a drug development program. However, it is quite challenging as the effects of target inhibition or antagonism are often context dependent. Genetics and epigenetics, the choice of animal or cell culture model, and experimental details all affect biological responses. Due to these multiple confounding factors, the majority of landmark cancer target discovery publications have been reported to be irreproducible in industry laboratories (Begley and Ellis 2012; Prinz et al. 2011). Even under highly controlled experimental conditions, relationships between target modulation and biological responses are often nonlinear and multivariate, and thus difficult to deduce from intuition alone (Janes and Lauffenburger 2013). Mathematical models can serve as a framework for integrating information learned about key system

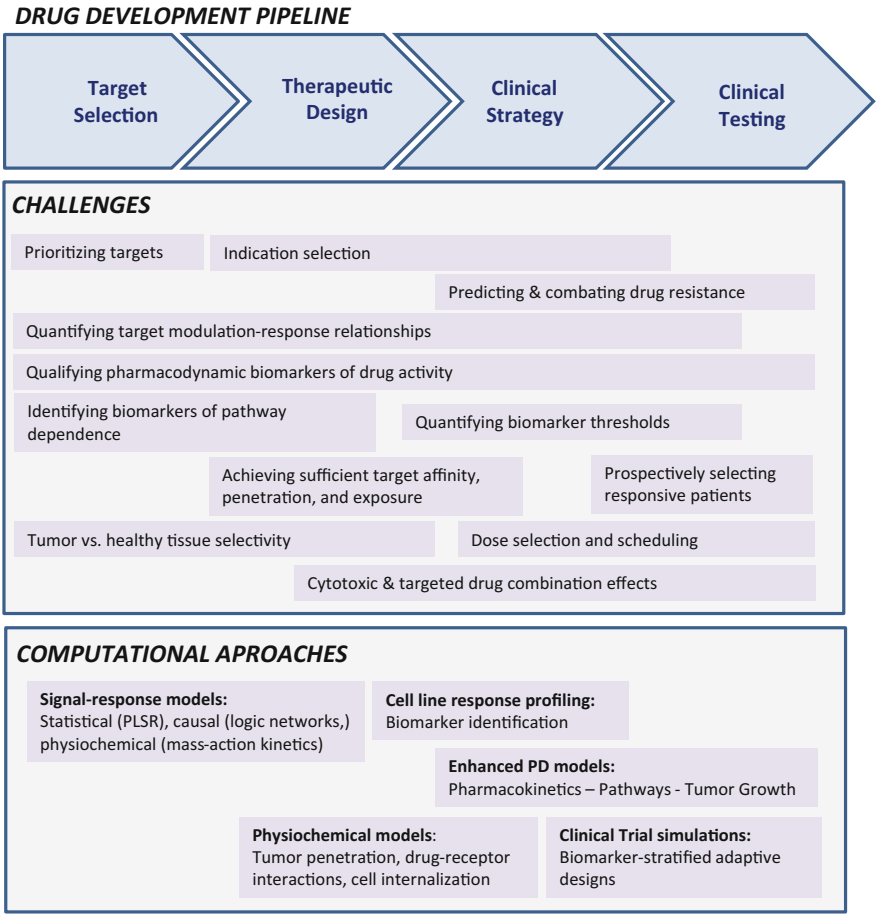

Fig. 19.2 Challenges and computational approaches to address such challenges during oncology drug development

variables and their quantitative relationships, and subsequently exploring these system behaviors computationally. Simulations can then be used to evaluate potential therapeutics in silico, and establish design specifications for effective drug candidates (Hendriks 2010).

19.3.1 Physicochemical-Based Models of Signaling Pathways

The PI3K and MAPK signaling cascades are two of the most frequently deregulated pathways in human cancers (Kan et al. 2010; Zack et al. 2013). Currently, there are

at least 33 inhibitors targeting components in these pathways in clinical development, not including cell surface receptors which normally regulate their activity (Saini et al. 2013). The cascades can be hyper-activated by multiple mechanisms, including gene amplifications, point mutations, and micro-deletions in cell surface receptors such as EGFR or HER2 and cytosolic kinases such as RAS, RAF, or PI3KCA, deletions of inhibitory phosphatases such as PTEN and NF1, and excess autocrine or paracrine growth factor secretion (Tamborero et al. 2013; Kan et al. 2010; Zack et al. 2013). The dynamic properties of these pathways have been extensively explored through the use of mass action kinetic-based ODE models, demonstrating that known behaviors can be reconstructed "bottom up" from physicochemical mechanisms. For example, a foundational mass-action kinetic-based model of the three tier enzymatic cascade connecting RAF, MEK, and ERK was shown to produce switch like-behavior, consistent with its functional role in converting variable external stimuli into discrete cell fate decisions such as proliferation (Huang and Ferrell 1996). The complexity in such models have expanded over time with the incorporation of negative feedback circuits within the cascades (Asthagiri and Lauffenburger 2001), the inclusion of receptor activation, internalization and recycling in response to ligand binding (Schoeberl et al. 2002), and combinatorial patterns of ligand-receptor interactions linked to both MAPK and PI3K cascade activation (Chen et al. 2009). However, the building blocks remain the same, as the principles of mass action allow one to convert any set of reactions, regardless of size or complexity, into ordinary differential equations.

The precise molecular mechanisms connecting intracellular signals to cellular responses such as proliferation and survival remain obscure (Courcelles et al. 2013). Using physicochemical models for target identification thus relies on surrogate readouts of efficacy, such as downstream pathway effectors phospho-AKT or ERK. Parameter sensitivity analysis can then be applied to identify critical network components, which may serve as optimal points of therapeutic intervention. Sensitivity analyses can be performed under different conditions (i.e., stimulation by alternate growth factors) and cellular contexts (i.e., mutations and protein expression levels) to assess robustness of the potential target to biological variation, and identify mechanistic biomarkers which may influence cellular responses to target modulation. Using this approach, the ErbB3 receptor was identified as a novel target in ErbB signaling network-driven cancers. This was surprising at the time, as ErbB3 lacks intrinsic kinase activity found in ErbB1 (EGFR) and ErbB2 (HER2), and was not known to be mutated or amplified in cancers (Schoeberl et al. 2009). Ligand–driven tumor growth via the ErbB3-binding growth factor Heregulin has since been identified as an alternate mechanism of oncogenic growth in a variety of cancers (Campbell et al. 2010), and mutations in the *ERBB3* gene have been identified as recurrent in colon and gastric cancers (Jaiswal et al. 2013). This model-guided insight motivated three clinical programs at Merrimack based around ErbB3 inhibition, MM-111, M-121, and MM-141.

19.3.2 Modeling Network Robustness: Feedback Circuits and Redundancy

Extensive redundancy between alternate RTKs underlie resistance to their targeted inhibitors (Wagner et al. 2013). For example, activation of ErbB3, cMET, and FGFR family members by their respective ligands can attenuate the effect of inhibitors targeting ErbB2 (lapatinib), EGFR (erlotinib), cMET (crizotinib), and PDGFR (sunitinib) and FGFR (PD173074) (Wilson et al. 2012). Models incorporating more than a single activating receptor are thus critical for understanding patterns of RTK inhibitor sensitivity and resistance. For example, incorporating both Insulin Receptor (IR) and EGFR-mediated activation of the PI3K and MAPK cascades into a single model was necessary to quantify signal amplification and compensation between these pro-metabolic and mitogenic growth factors (Borisov et al. 2009). Similarly, a model integrating Insulin-like Growth Factor-1 Receptor (IGF1R) and ErbB3 receptor signaling pathways served as a basis for design of MM-141, an tetravalent antibody targeting the two receptors and thus disabling this compensatory signaling axis (Harms et al. 2014; Fitzgerald et al. 2014).

The PI3K and MAPK cascades both regulate transcription and subsequent cell surface expression of their upstream driving RTKs, forming complex feedback regulatory circuits. Characterizing these feedback circuits is thus important for predicting cellular responses to pathway inhibitors. For example, negative feedback regulation of EGFR expression by phospho-ERK was included in a model of EGFR and IGF1R-mediated signaling. Co-targeting of EGFR (erlotininb) and MEK (GDC-0973) was identified as an optimal means of inhibiting tumor growth in silico and validated across a genetically diverse panel of colon cancer cell lines (Klinger et al. 2013). The strategy of targeting intracellular kinases in tandem with their activating receptors has proven successful in other pre-clinical systems and is currently being pursued in clinical trials. Resistance to the BRAF inhibitor vemurafenib for example has been found to be mediated by compensatory up-regulation of ERBB3 (Abel et al. 2013), IGF1R (Villanueva et al. 2010), and EGFR (Prahallad et al. 2012), such that co-treatment with respective inhibitors re-sensitized tumors to drug treatment. Similarly, KRAS-mutant colorectal cancer models have been found to be insensitive to MEK inhibition via feedback-mediation activation of IGFR and subsequent PI3K signaling. Co-treatment with a MEK and IGF1R inhibitor blocked the adaptive response, resulting in robust apoptosis and regression in xenograft models (Ebi et al. 2011).

Intracellular feedback circuits embedded within the MAPK and PI3K cytosolic cascades can also modulate responses to signal inhibitors. Physicochemical models of MAPK signaling revealed the negative feedback from ERK to RAS functions to stabilize pathway output under both extrinsic noise and pharmacological perturbations. This provides a mechanistic explanation for the poor clinical efficacy observed with MEK inhibitor monotherapies (Fritsche-Guenther et al. 2011; Sturm et al. 2010; Cirit et al. 2010). As previously mentioned, cellular robustness to MEK inhibition is also mediated by partial functional redundancy between the MAPK

and PI3K cascades. The pathways converge on downstream effectors of cell cycle progression such as CyclinD and P27, as well as apoptotic regulators such as BIM and BAD (She et al. 2010). Predicting cellular responses to targeted inhibitors thus necessitates the consideration of both canonical cascades (Kirouac et al. 2013). As an additional complexity, the MAPK and PI3K cascades are not insulated but "cross-talk"; signaling through one pathway may affect activity of the other. The precise mechanisms and dynamics mediating these interactions are still incomplete and context-dependent, modulated by exogenous growth factor stimulation and genetic heterogeneity (Aksamitiene et al. 2012; Wang et al. 2009a).

19.3.3 Using Perturbation-Response Experiments to Develop Causal Network Models

While mathematical models of cellular signaling networks can be used in drug discovery, targeted inhibitors themselves also serve as tools for building and parameterizing models. Implemented as chemical probes, the topology and dynamics of cellular networks can be inferred by measuring molecular and phenotypic responses to combinations of growth factor stimulation and/or drug treatments (Nelander et al. 2008; Mitsos et al. 2009). Logic-based modeling formalisms such as Boolean Logic (Saez-Rodriguez et al. 2009), Quantitative/Fuzzy Logic (Morris et al. 2011), or logic-based ODEs (Nelander et al. 2008), have been developed for semi-automating the process of network inference and parameterization from systematic perturbation-response data. Such causal models, which describe signal flow through networks but omit mechanistic details, can be powerful tools for developing comprehensive yet granular descriptions of cellular information processing. For example, data from perturbation-response experiments utilizing 14 TKIs against the PI3K, MAPK, and JAK/STAT cascades was recently used to develop a model connecting cell signaling to growth regulation in liposarcoma cells. Simulations identified that inhibition of the cell cycle regulator CDK4 in combination with blockade of the PI3K pathway (either via PI3K inhibitors directly, or the upstream RTK activator IGF1R) as a potent synergistic combination, motivating design of a multi-drug clinical trial (Miller et al. 2013). This demonstrates that model simulations can rapidly transform into clinical strategy, given buy-in at an exploratory clinical center.

19.3.4 Molecular Heterogeneity and Single Cell Modeling

Models are fundamentally limited by the data available, and the data used to build biochemical network models is typically derived from cell populations. Such measurements represent averages across pools of many thousands of cells,

smoothing out cell-to-cell variability. However, this variability can contain relevant information, analogous to population-based pharmacometric models. Cell population-based models can similarly be developed to account for the mechanistic basis of cell-cell variation by using quantitative single cell-based measurements, such as multi-color flow cytometry or light-centered microscopy (Bendall and Nolan 2012). Heterogeneous cell populations can then be simulated by Monte Carlo sampling across the observed distributions of biochemical measurements. This approach has been applied to interrogate cell-cell variability in response to TRAIL-induced apoptosis. Natural variation in protein concentrations was found to account for cell-cell variability in treatment sensitivity (Spencer et al. 2009), and co-variation in the distribution of protein abundances was found to change the relative importance of signaling nodes as determined by parameter sensitivity analysis (Gaudet et al. 2012). Biochemical cell-cell variability can also affect the shape of dose-response curves, with heterogeneity producing in lower apparent Hill coefficients (Fallahi-Sichani et al. 2013). These findings have important implications in drug target and biomarker identification, which rely on such analyses.

In summary, causal models of cellular signaling networks can be valuable tools for quantitatively interrogating potential drug targets. By building a quantitative understanding of how molecular network structure and dynamics underlie cellular pathologies, mechanistic models can help prioritize drug targets, explore alternative modes of intervention, and define quantitative relationships between the degree and duration of target modulation and biological responses. These criteria then set design specifications for drug candidates, enabling *in silico* evaluation of potential therapeutics (Hendriks 2010).

19.4 Using Physicochemical Models to Guide Therapeutic Design

19.4.1 Model-Guided Antibody Engineering

Monoclonal antibodies have become an important therapeutic modality, and their clinical usage is expected to continue to grow relative to synthetic small molecules (Sliwkowski and Mellman 2013). The modular format of these proteins enables their combinatorial assembly through genetic engineering to produce designs not seen in nature. However, it is often not intuitively apparent what an optimal design or format should be to achieve therapeutic objectives. Physicochemical-based models describing protein-protein interactions on the cell surface and/or in solution can be a useful tool for understanding the properties of these molecules, and prospectively specifying design constraints. Given target expression levels and turnover rates, antibody-target binding affinity, tissue partition coefficients, and clearance rates, fairly simple mathematical models can be used to evaluate relationship between such properties target engagement/inhibition.

Optimizing antibody potency provides a unique challenge as compared to small molecules, as target binding is driven by two forces. The first is the intrinsic affinity of the monovalent fragment antigen-binding (Fab) arms for the target, and the second arises from the multivalency of antibodies. Following the binding of the first Fab arm to an antigen on the cell surface, the second free Fab arm becomes spatially restricted to a shell around the target, increasing the local concentration and thereby binding kinetics. The increased affinity due to multi-valency is referred to as the avidity effect, and can be quantified by a cross-linking factor (χ), an epitope and format-dependent biophysical property. While cross-linking can be an important determinant of potency, it cannot be measured directly. However, it can be computationally inferred given monovalent Fab binding affinities and dose-binding curves for a panel of cell lines with different receptor densities (Harms et al. 2012).

Molecules with high χ values can have significant potency advantages. For targets with low surface expression ($<10^5$ mol/cell), high avidity can improve the apparent binding affinity of mAbs by up to 10-fold. Furthermore, for such low abundance targets, bi-specific antibodies (targeting two antigens) can be designed to leverage the avidity effect and increase potency by selecting a highly expressed ($>10^6$ mol/cell) tumor antigen to serve as a cell surface "anchor". Performance of bi-specific mAbs depends on the ratio of anchor-to-target expression level, as well as the cross-linking factor. Using this approach, target inhibition can be improved up to 100-fold, a feat not easily achievable via affinity maturation. Mass action kinetic-based models of antibody-receptor interactions can be used in design and analysis of this novel drug class, as was used in the development of MM-111, a bi-specific antibody directed against ErbB2 and ErbB3. The targeting of ErbB2 (a highly expressed antigen) is exploited to enhance the potency of ErbB3 inhibition (a relatively low expressed drug target) in ERBB2-amplified tumors (McDonagh et al. 2012). Similarly, avidity can be utilized to increase the potency of bi-specifics targeting two oncogenic receptors over what could be achievable with two independent antibodies (Harms et al. 2014). This strategy motivated design of MM-141, a tetravalent bi-specific antibody targeting two compensatory signaling growth factor receptors, IGF1R and ErbB3, with 10-fold improved potency over the single IgG combinations (Xu et al. 2013).

19.4.2 Model-Based Liposome Design

Liposomes function as nanoparticle drug carriers, capable of preferentially accumulating in tumors and slowly releasing their drug depot into the diseased tissue. In comparison to free drug, liposomal encapsulation can extend pharmacokinetics, increase local exposure, and decrease systemic toxicities. The leaky vasculature and impaired lymphatic clearance characteristic of solid tumors give rise to the Enhanced Permeability and Retention (EPR) effect, wherein large molecules such as liposomes (on the order of 100 nm) are preferentially retained (Noble et al. 2004). This principle is the basis for the design of MM-398, a nanoliposomal

formulation of irinotecan currently being evaluated for the treatment of patients with metastatic pancreatic cancer (Ko et al. 2013). It is not however readily apparent how liposome design parameters and tumor characteristics interact to affect tumor drug exposure. To enable such insight, a multi-scale kinetic model of liposomal doxorubicin was developed, accounting for drug pharmacokinetics, tumor deposition, cell binding, and liposomal uptake. Parameter sensitivity analyses were used to identify critical features affecting drug potency, identifying liposome clearance and tumor permeability (a function of liposome and vascular pore size) as the two most sensitive parameters. Prospective identification of patients with high liposomal tumor deposition could thus increase the successful use of this therapeutic class (Hendriks et al. 2012).

Tumor selectivity can be improved by the inclusion of monoclonal antibodies against tumor-selective antigens into the lipid bi-layers (Kirpotin et al. 2012). The choice of tumor cell antigen and the density of liposomal antibody then become two additional therapeutic design parameters. To quantify the relationship between antigen expression and performance characteristics of targeted nanoparticles, a computational model was developed for MM-302, a HER2-targeted liposomal formulation of doxorubicin. Parameter sensitivity analysis was again applied to rank the relative importance of key drug and cellular variables. Target expression on tumor cell surfaces was identified as the most sensitive parameter. Due to the high multi-valency of antibodies on the liposome surface and resultant binding cooperativity, a threshold effect occurs such that cells expressing receptor densities below a threshold density will not uptake significant amounts of the active drug (Hendriks et al. 2013). Appropriate choice of target antigen and disease indication is thus critical for designing specificity into this class of drugs.

These examples demonstrate how a quantitative understanding of the relationships between target expression, binding affinities, and avidity can be used to optimize the design of antibodies and liposomes for increasing the therapeutic window between target and non-target tissues. A next step in the development path is to assess the activity of prospective drugs in pre-clinical disease models.

19.5 Cancer Cell Line Selection and Biomarker Identification

Drug development relies on the use of model systems to predict drug efficacy and safety. Anti-cancer drugs are typically evaluated by quantifying their effects on the growth kinetics of immortalized cancer cell lines in vitro and in vivo. While these are derived from primary tumor resections, the process of passaging cells in tissue culture likely selects for additional mutations which enable in vitro propagation. For cell line models to maintain their biological relevance, it is essential that the genetic and epigenetic history of the derivative cancer is maintained. Currently, the degree to which this assumption holds true is unclear.

The most widely used group of cell lines in the NCI-60 panel, established in the 1980 s by the Developmental Therapeutics Program (DTP) of the National Cancer Institute, representing 9 solid tumor types. These 60 lines are capable of growing both in tissue culture and as orthotopic grafts in immunodeficient mice, and thousands of anti-cancer compounds have been evaluated for growth inhibition across the panel (Shoemaker 2006). Given the extensive genetic diversity of human neoplasms, larger cell line collections have since been established to more thoroughly cover this heterogeneity, such as the Center for Molecular Therapeutics CMT1000 (Sharma et al. 2010), and the Cancer Cell Line Encyclopedia (CCLE) (Caponigro and Sellers 2011) collections of over 1000 cell lines each.

19.5.1 Molecular Characterization of Cancer Cell Lines

Given the availability of cancer cell line collections, a new challenge arises in rationally selecting among hundreds of cell line models for use in pre-clinical studies. Furthermore, patterns of drug sensitivity and resistance across cell lines can be used to develop predictive biomarkers which may translate into clinical practice. The availability of comprehensive molecular profiling data for both cell lines and primary tumor tissue now provides a means of systematically assessing relationships between genomic and proteomic profiles, pathway dependencies, and pharmacological sensitivities. Due to its extensive history, the NCI-60 panel is the most comprehensively characterized set of cell lines. Whole exome sequences are now available (Abaan et al. 2013), complementing mRNA expression profiles and proliferative responses to hundreds of FDA-approved anti-cancer agents (Reinhold et al. 2012). Comprehensive pharmacogenomic databases consisting of both gene mutation and mRNA expression profiling linked to drug responses are now available for larger collections of cell lines, such as the Welcome Trust Sanger Center COSMIC database (Garnett et al. 2012), the Cancer Cell Line Encyclopedia (CCLE) (Barretina et al. 2012), and the Cancer Therapeutics Response Portal (Basu et al. 2013).

19.5.2 Identifying Disease-Representative Cell Line Models for Study

Immortalized cell lines have adapted over many generations for survival in highly non-physiological environments. As a result of this sustained selective pressure, the molecular characteristics of these cells may have diverged substantially from the tissues from which they were derived (Horrobin 2003). In addition to genetic changes, anatomical constraints (heterotypic cell-cell and cell-ECM interactions), micro-environmental conditions (nutrients, oxygen supply), and exogenous stimuli (endocrine and paracrine hormones and growth factors) will substantially differ

between culture dishes and in vivo environments. The importance of such elements is revealed by the fact that culture conditions, such as media components and stromal cell co-culture, affect drug responses (Straussman et al. 2012). Alternatives to immortalized cell lines are becoming more common, such as primary tissue-derived xenografts (Williams et al. 2013) and genetically engineered mouse models (Sharpless and Depinho 2006), which recapitulate primary tumor structure and physiology more accurately. However, it is still too early to determine whether these alternative experimental models offer clear predictive advantages over traditional immortalized cell line modes. Due to their ease of use and extensive history, immortalized cell lines and xenograft assays are likely to remain the dominant platform for the immediate future, and available comprehensive molecular databases should enhance their predictive utility.

As part of The Cancer Genome Atlas (TCGA), tens of thousands of primary tumors have now been characterized by exome and whole genome sequencing, copy number variations, and mRNA expression profiling (Chin et al. 2011). By comparing molecular features of experimental cell lines to these resources, it is now possible to quantify how representative immortalized cell line models are of their derivative diseases. For example, by comparing somatic mutations, CNVs, and mRNA expression data from ovarian cell lines in the CCLE database to primary ovarian cancers in TCGA, cell line models were classified by similarity to ovarian tumor resections (Domcke et al. 2013). Cell lines were identified which appeared to neatly recapitulate the molecular profiles of underlying disease, as well as some that appeared to be egregious outliers, and thus likely to be poor predictors of clinical responses.

19.5.3 Predictive Biomarker Identification from Genomic Databases

Extracting predictive molecular biomarkers from these databases presents formidable statistical and computational challenges. The strongest statistical relationships pulled from analyses of these resources are generally the most obvious drug-target correlations. The acid test of their utility rests on their ability to produce non-intuitive, but clinically meaningful relationships. Epigenetic context appears to affect even the most ostensive relationships, as genomic features can correlate with drug sensitivity only within specific tissue lineages. For example, effectiveness of the EGFR inhibitor neratinib appears restricted to non-small cell lung cancer (NSCLC) cells, consistent with clinical development of the drug. However, it is not obvious why this would be so, given that EGFR signaling dependence occurs in many indications. Along the same lines, Wnt/β-catenin signaling was found to predict sensitivity to the Bcl-2 inhibitor navitoclax (Basu et al. 2013). Though this finding needs further validation, there is no immediately obvious connection between the Wnt/β-catenin signaling pathway and sensitivity to apoptotic

induction. These resources can also be used as a means to evaluate mechanism-based hypotheses. For example, sensitivity to the EGFR inhibitors gefitinib and erlotinib were found to be negatively correlated with elevated expression of the RTKs MET (Wagner et al. 2013) and AXL (Meyer et al. 2013), validating predictions emanating from focused experiments.

19.5.4 Limitations of Genomic Biomarkers

Mutant genes and their expression patterns do not directly control cancer cell growth. Rather it is the proteins they encode, and their subsequent assembly into signaling and regulatory networks. The utility of genomic resources may therefore be fundamentally limited, as the relationship between genetic changes and alternated protein signaling networks is often nonlinear (Brennan et al. 2013). Basal protein or gene expression measurements represent a homeostatic, quasi-equilibrium state, from which it may not be possible to infer the activity of multi-layered feedback circuits. The activity of such nested cellular feedback loops thus obscures the relationship between such biochemical measurements and pathway dependencies. However, molecular measurements following gross cellular perturbations of key pathways by growth factor stimulation and selective inhibitors can reveal the conduits by which information flows through cellular regulatory circuits, and may be a more accurate prediction of functional responses to drug treatment (Bendall and Nolan 2012). As a proof of principle, this approach was used to predict responsiveness to 23 targeted therapeutics across a panel of 43 breast cancer cell lines. Both basal and growth factor stimulated responses of a subset of key signaling proteins (ERK, AKT, STAT, and RTKs) were used to train partial-least squared regression models (Niepel et al. 2013). Growth factor-induced signaling profiles were found to be better predictors of drug response than basal biochemical profiles, which in turn were better than mutational status or clinical subtype alone. Several non-obvious predictors were also identified in this approach. For example, sensitivity to PI3K inhibitors was effectively predicted by phospho-ERK responses to stimulation by the ErbB3 ligand heregulin, while the abundance of phospho-AKT or mutational status of the pathway components did not. The intuitive connection between basal phospho-AKT abundance and PI3K inhibitor sensitivity was also found to be absent in models of leukemia (Casado et al. 2013), as was the connection between phospho-ERK and MEK inhibitor sensitivity in melanoma and colorectal cancers cells (Pratilas et al. 2009). These results highlight the challenge of translating basal biochemical measurements into predictive biomarkers, as well as the potential pitfalls of using intuition alone to guide biomarker strategies.

19.5.5 Clinical Translation of Biomarker Strategies

The resources described in Sect. 19.5.2–19.5.4 are still in their infancy, hence their long-term utility remains to be seen. Statistical challenges emanate from the "*Large p Small n*" problem—the number of predictor variables to test (i.e., genes) vastly exceeds the number of samples cell lines. In addition, the multivariate and nonlinear nature of cellular information processing means that single gene predictors of drug sensitivity are likely to be the exception rather than the norm. Going forward, methods to extract multiple biomarkers and combine them in nonlinear models will likely be essential to better represent the underlying biology and improve predictive accuracy.

How to best translate pre-clinical biomarkers into clinical strategy remains an open problem. The traditional approach would be to run an "all-comers" (unselected) phase 2 clinical trial and collect patient biopsies for subsequent profiling and retrospective analyses. Biomarker-response correlations could then be used to define thresholds for prospectively stratifying patients in subsequent trials to assess clinical benefit. However, if biomarker-positive patient populations are rare, such designs may be statistically under-powered to specify such relationships. An alternative approach is to use cutoffs estimated from preclinical research and run early clinical studies in prospectively enriched biomarker-positive patients (Freidlin and Korn 2013; Freidlin et al. 2012). Given initial signals of efficacy, such as pharmacodynamic readouts or tumor size changes (Hansson et al. 2013), the study could subsequently be expanded to evaluate benefit in wider patient populations and validate the predictive value of the biomarker. This strategy has been applied in cases where biomarker expression is limited to small patient populations with compelling pre-clinical evidence supporting the biomarker hypothesis, as in the approval of crizotinib (Kwak et al. 2010) and vemurafenib (Chapman et al. 2011) for *EML4-ALK* and $BRAF^{V600E}$ cancers, respectively. When biomarker positivity is limited to rare patient segments (i.e., less than 25 % of a population), such designs would ideally be implemented as "bucket trials", simultaneously evaluating multiple drugs and corresponding biomarkers in parallel arms. Such designs leverage the limited availability of patient biopsies and increase a patient's chance of getting placed on a study (Kaplan et al. 2013). While this may not be a universal or ideal solution, changes to the standard paradigm of clinical trial designs are necessary if the practice of oncology is to keep up with the pace of research. Statistical models (beyond the scope of this text) can be used to test the sensitivity of a particular trial design to assumptions about the prevalence and clinical benefit of particular biomarkers (Freidlin et al. 2012; Kaplan et al. 2013).

Without an appropriate dosing schedule, a program based around a valid target and selective inhibitor can still fail. Methods for rationally optimizing drug dosing schedules are thus highly valuable. In the next section, modeling strategies for predicting optimal dosing regimens from preclinical data will be discussed.

19.6 Tumor Growth Models for Translational Pharmacology

The defining characteristic of cancer is uncontrolled cellular growth, and the goal of cancer therapy is largely to deplete tumor mass. Growth in tumor size is thus a logical endpoint for translational models, both due to clinical relevance and the relative ease of measurement clinically (via X-ray, CT, or MRI scans) and experimentally (by counting cells or measuring tumor volume). Empirical, population-based models of tumor growth kinetics have been found to be predictive of patient survival from multiple clinical trials in lung, colorectal, and breast cancers (Wang et al. 2009c; Claret et al. 2009, 2012, 2013; Cameron et al. 2000). Results to date suggest that changes in tumor growth kinetics may serve as an indication-specific, but treatment-agnostic early metric of clinical efficacy (Ferté et al. 2013).

19.6.1 Dynamic Models of Tumor Growth

Bulk tissue growth is the result of cell replication, which is a discrete and partially stochastic process at the level of individual cells. However, considering that a 1 mm^3 tissue may contain 200,000 cells, cell-level stochasticity will average out at the macroscopic level. Changes in cell numbers or tumor size over time are thus amenable to approximation by differential equations. Many ODE-based models of tumor cell growth have been developed, using simple linear or exponential growth kinetics, Gompertz, and Logistic equations which account for limited carrying capacity of the host, and the modified-Gompertz or Simeoni model, describing initial exponential and later linear phases of tumor growth kinetics (Simeoni et al. 2004). In all forms, variations change in tumor size (V) over time is expressed as a function of the current size, and nonlinear system parameters [P]:

$$\frac{dV}{dt} = g(V, [P]) \tag{19.1}$$

In any population of cells there will be continuous turnover of cell birth (μ) and death (δ), the net balance of which determines the *apparent* rate of cell growth (α):

$$\alpha = (\mu - \delta) \tag{19.2}$$

The ratio of cell birth to death thus determines whether the tumor mass is growing ($\mu/\delta > 1$), regressing ($\mu/\delta < 1$), or in stasis ($\mu/\delta = 1$). Exposure-response effects on cell proliferation and death can be quantified using Hill-type equations and combined within a tumor growth model:

$$\frac{dV}{dt} = g(V) \cdot \mu_{MAX} \cdot \left(1 - \frac{C^{K1}}{EC1_{50} + C^{K1}}\right) - \delta_{MAX} \cdot \left(\frac{C^{K2}}{EC2_{50} + C^{K2}}\right) \cdot V \quad (19.3)$$

In this generalized equation, *g(V)* is the tumor growth kinetic model, μ_{MAX} the maximal rate of proliferation, and δ_{MAX} the maximal rate of cell death, modulated by drug concentration (C) and response parameters ($K1$, $K2$, $EC1_{50}$, $EC2_{50}$). Implementing the commonly used Logistic growth model for example, wherein constraints limit tumor size to V_{MAX}, produces:

$$\frac{dV}{dt} = V \cdot \left[\left(1 - \frac{V}{V_{MAX}}\right) \cdot \mu_{MAX} \cdot \left(1 - \frac{C^{K1}}{EC1_{50} + C^{K1}}\right) - \delta_{MAX} \cdot \left(\frac{C^{K2}}{EC2_{50} + C^{K2}}\right)\right] \quad (19.4)$$

The effects of cytotoxic chemotherapeutics are typically described as inducing cell death, and kinase inhibitors as reducing cell proliferation, thus eliminating either the respective first or second Hill function. Given the functional pleitropy of most proteins and the distributed nature of cell regulatory networks, it is highly unlikely that anti-cancer drugs will specifically affect only one of these cellular processes. However, without direct measures of proliferation and cell turnover rates, these parameters cannot be parsed from bulk tumor size measurements alone. Transit compartments are also commonly included to account for the delay between drug exposure and cell growth responses (Yang et al. 2010; Sun and Jusko 1998). In addition to the obvious utility in simulating the activity of alternate dosing regimens, the drug-specific parameters in these equations allow for the quantitative comparison of agents independent of dose or schedule effects (Rocchetti et al. 2007).

19.6.2 Mechanism-Based Pharmacodynamic Models of Tumor Growth

The tumor growth models described thus far have been empirical, in that rates of cellular proliferation or death are described as direct functions of drug exposure. Of course, drugs do not directly affect these cellular processes, but act on regulatory proteins and pathways. Mechanism-based pathway models thus pose to link drug exposure to efficacy via the intermediating biochemical networks. This may enable the prediction of novel drug combination effects and biomarker-response relationships, not feasible with empirical exposure-response models which are inexorably bound to the model system on which they were parameterized. Clinically, mechanism-based pharmacodynamic models may be crucial in shifting the current paradigm of dose optimization in oncology from toxicity, toward on biologically-based endpoints such as pharmacodynamics measures of pathway inhibition (Marshall 2012).

19.6.3 Semi-mechanistic Models of Signal Transduction Inhibitors

Given the centrality of MAPK and PI3K signaling pathways in human cancers (Kan et al. 2010; Zack et al. 2013), a variety of pharmacological strategies have been implemented to attenuate the activity of these cascades. These include biologics which block signaling and down-regulate expression of the cell surface RTKs (EGFR, ErbB2, ErbB3, IGF1R, MET, FGFR), and ATP-competitive tyrosine kinase inhibitors (TKI) directed against these receptors as well as the intracellular pathway components RAF, MEK, ERK, PI3K, AKT, and MTOR. Phosphorylation status of canonical pathway outputs AKT and ERK are commonly quantified as molecular readouts of drug activity (pS), and changes from baseline levels (pS_0) can be linked to drug concentrations using direct response models:

$$pS = pS_0 \cdot \left(1 - I_{MAX} \frac{C^{k1}}{IC_{50}^{k1} + C^{k1}}\right) \tag{19.5}$$

Signal attenuation can then be linked to tumor growth using a second equation, either describing the induction of cell death or inhibition of proliferation:

$$\frac{dV}{dt} = g(V)\left(\mu_{MAX} \cdot \frac{pS^{k2}}{GI1_{50}^{k2} + pS^{k2}}\right) - \delta_{\max}\left(1 - \frac{pS^{k3}}{GI3_{50}^{k3} + pS^{k3}}\right) \tag{19.6}$$

Again, substituting in the logistic growth equation for exemplary purposes:

$$\frac{dV}{dt} = V \cdot \left[\left(1 - \frac{V}{V_{MAX}}\right)\left(\mu_{MAX} \cdot \frac{pS^{k2}}{GI1_{50}^{k2} + pS^{k2}}\right) - \delta_{\max}\left(1 - \frac{pS^{k3}}{GI3_{50}^{k3} + pS^{k3}}\right)\right] \tag{19.7}$$

Models are typically parameterized using data from xenograft experiments: mice are treated with various doses of an inhibitor, and tumors are extracted for signal measurement shortly after treatment to parameterize the first equation [I_{MAX}, IC_{50}, k1]. Tumor growth kinetics of the xenograft are quantified following similar treatment regimens to establish an appropriate kinetic model [g(V)] and parameterize the second equation [δ_{MAX}, μ_{MAX}, GI_{50}, K_2, and K_3]. After parameterizing drug-signal-response models from experimental data, human pharmacokinetics and tumor growth rates can be substituted to simulate clinical responses to alternate dosing regimens. Such approaches were used in the development of the MEK inhibitor GDC-0973 (Cobimetinib) for $BRAF^{V600D}$ mutant melanoma (Wong et al. 2012), and the PI3K inhibitor GDC-0941 in breast cancer (Salphati et al. 2010) using phospho-ERK and-AKT as the respective pharmacodynamic signals.

As the level of receptor expression on the cell surface is a dynamic balance of turnover and production, indirect response models may be more appropriate for the description of RTK inhibitors:

$$\frac{dpR}{dt} = k_{in}\left(pR_0 - I_{MAX}\frac{C^{k1}}{IC_{50}^{k1} + C^{k1}}\right) - k_{\circ} \cdot pR \tag{19.8}$$

Tumor growth kinetics may then either modeled as direct functions of phospho-Receptor activity (pR), or mediated by downstream intracellular signals (pS) such as phospho-AKT or -ERK, coupled by an indirect response model:

$$\frac{dpS}{dt} = k_{on} \cdot pR \cdot (S_T - pS) - k_{off} \cdot pS \tag{19.9}$$

Additional transit compartments can be incorporated to account for downstream signaling processes and temporal delays between receptor inhibition and cellular responses. That is, considering a cascade of N successive signals (Si):

$$\frac{dS_i}{dt} = k_i(S_{i-1} - S_i) \quad for\, i = 1 : N \tag{19.10}$$

Semi-mechanistic PK/PD models of the form above have for example been developed for the EGFR inhibitor gefitinib in EGFR mutant and wild-type glioblastoma, using phospho-EGFR as the target receptor and pERK as the effector signal (Wang et al. 2008, 2009b). For the multi-TKI inhibitor crizotinib, two separate PD models were developed to quantify PD and efficacy relationships of the drug in different clinical settings; MET and ALK-oncogene driven cancers using phosphor-MET and -ALK as direct tumor growth effectors (Yamazaki 2013; Yamazaki et al. 2008).

19.6.4 Multi-pathway Pharmacodynamic Models of Tumor Growth

The pharmacodynamic tumor growth models discussed thus far have been limited to the study of single agents. This contrasts with the way in which many oncology drugs are used in clinical practice, as part of combination regimens. The non-additive effects of drug combinations on tumor growth can be captured using empirical "interaction parameters" (φ), specifying the EC_{50} of one agent as a dependent upon the concentration of another (Pawaskar et al. 2013; Choo et al. 2013):

$$\frac{dV}{dt} = V\left[\left(1 - \frac{V}{V_{MAX}}\right) \cdot \mu_{MAX}\left(1 - \frac{I1_{MAX} \cdot C_1^{N1}}{\varphi \cdot EC1_{50}^{N1} + C_1^{N1}}\right) \cdot \left(1 - \frac{I2_{MAX} \cdot C_2^{N2}}{EC2_{50}^{N2} + C_2^{N2}}\right) - \delta_{MAX}\right] \tag{19.11}$$

Here, φ <1 implies synergy, φ >1 antagonism, and φ = 1 independence. The equation is highly similar to the Bliss independence model, wherein drug synergy or antagonism is quantified by comparison of measured responses (ΔV) as compared to that expected with φ = 1 (Fitzgerald et al. 2006).

While these empirical models may be useful tools for quantitative analyses, they are inherently incapable of predicting the effects of novel combinations, or even combination effects emanating from alternate dosing schedules. To do so necessitates the incorporation of mechanisms by which drug treatments affect regulatory pathways, and how respective pathways interact to control tumor cell growth. Developing more biochemically detailed multi-pathway models is thus a logical step forward in improving their translational relevance.

Another critical limitation of the tumor growth models described so far is that the PD parameters are estimated using a single, or at best, limited number of xenograft models, and thus "locked" to the experimental model. Translating predictions from such models to clinical strategy then depends on an assumption that the parameters are invariant from model systems to human patients. There are a number of examples of predictions from xenograft studies translating faithfully to clinical responses (Haddish-Berhane et al. 2013; Shah et al. 2012). However, growth inhibition in xenograft models is often a poor predictor clinical activity, as evidenced by the high clinical failure rates of oncology drug programs, all of which have been vetted in these assays. The PK/PD-efficacy relationships encoded in by 4-parameter Hill equations often represent complex, multistep reaction sequences. These lumped parameters summate the concentration and kinetics of multiple components (including receptors, adaptor proteins, enzymes, transcription factors) which are likely to vary between cell lines and among patients. By incorporating some of the underlying biological complexity learned from pre-clinical research, mechanistically detailed models may be able to retrospectively explain and prospectively simulate both drug combination effects and response heterogeneity, based on the structure and dynamical properties of cellular regulatory networks. Enhanced PD (ePD) models are beginning to bridge the divide between discovery research-focused systems biology and PK/PD models used in translational pharmacology (Iyengar et al. 2012).

The properties of signaling networks which foster robustness to therapeutic intervention, signal redundancy and adaptation, can be described mathematically. Multi-pathway integration can be modelled using quantitative logic gates, which are simply multi-input derivatives of Hill Equations. For logical OR-gates, the output signal output (Y) is a function of two weighted inputs (X_1, X_2) of the form:

$$Y = Y_{MIN} + (Y_{MAX} - Y_{MIN}) \cdot \left(\frac{(w_1 \cdot X_1 + w_2 \cdot X_2)^k}{\tau^k + (w_1 \cdot X_1 + w_2 \cdot X_2)^{k1}} \right) \tag{19.12}$$

Logical AND-Gates can be defined by multiplying individual Hill Equations:

$$Y = Y_{MIN} + (Y_{MAX} - Y_{MIN}) \cdot \left(\frac{X_1^{k1}}{\tau_1^{k1} + X_1^{k1}} \right) \cdot \left(\frac{X_2^{k2}}{\tau_2^{k2} + X_2^{k2}} \right) \tag{19.13}$$

Using this formalism one can, for example, describe convergence of alternate RTK inputs (X_i) on single pathway output (Y) such as phospho-AKT. In cases where the output requires both input signals must be active, Eq. 19.13 is more fitting. For example, proliferation in some cancer cells requires activity of both PI3K/pAKT and MAPK/pERK signals (Kirouac and Onsum 2013).

Feedback regulation of upstream signals (such as RTKs) via downstream effectors (such as pAKT or pERK) can be described using control theory-based equations:

$$\frac{dX}{dt} = r_x \cdot \left(X_{basal} \left(1 + G_X \cdot \left(1 - \frac{Y^k}{\tau^k + Y^k} \right) \right) - X \right) \tag{19.14}$$

Where X represents receptor expression, X_{basal} the steady-state "set point" when downstream signaling is fully activated, G_X the "gain", or fold-induction in response to the output Y suppression, and r_R the symmetric rate of X (receptor) turnover and synthesis.

The preceding equations describe cell signal transmission, interaction, feedback-mediated adaptation, and regulation of cell growth. These can be combined, altered, and integrated with mass action kinetics-based equations as desired to capture the structure and dynamics of a wide variety of cell signaling networks. The size and complexity of such models is no longer limited by mathematics or computational power, but rather by the availability of data required for parameterization. Establishing an optimal degree of model complexity involves striking a nuanced balance between detailing the molecular mechanisms, and allowing for sufficient granularity such that model parameters can be estimated using the data available. Reviews on experimental methods and strategies for generating such multivariate proteomic data (Albeck et al. 2006) and global optimization algorithms required for making use of it can be found elsewhere (Moles et al. 2003; Cvijovic et al. 2014; Kreutz and Timmer 2009).

Two recent studies used multi-pathway models of tumor growth to computationally explore the combination effects between targeted drugs, and mechanistic biomarkers predictive of drug combination efficacy. While exploring very different diseases (HER2+ breast cancer (Kirouac et al. 2013) and non-Hodgkin lymphoma (Harrold et al. 2012)) with different cell surface receptors (HER2 and HER3 vs. CD20 and death receptors DR4/DR5) and associated intracellular signaling pathways (PI3K/AKT and MAPK/ERK cascades vs. extrinsic apoptosis (Bcl-xL) and NF-kB),

in both cases a similar balance was struck between the mechanistic complexity typical systems biology models versus parametric identifiability and predictive power typical of pharmacometric models. Synergistic anti-tumor effects of clinically relevant drug combinations were predicted for both models and subsequently validated in vivo using xenograft experiments. While model parameterization and testing in both cases were based around single cell line models, the inclusion of molecular mechanisms enables one to vary putative biomarkers (protein expression, mutations, and receptor feedback circuits) and create panels of synthetic tumors for assessing the effects of such biomarkers on treatment responses in silico (Kirouac et al. 2013; Iyengar et al. 2012).

19.6.5 Modeling Molecular Targeted and Cytotoxic Drug Combinations

While combinations of targeted therapies are becoming an increasingly critical element of clinical practice, the vast majority are currently being combined with standard of care cytotoxic chemotherapy regimens. A key question then, is how do signaling networks regulating cell proliferation and apoptosis interface with cellular responses to DNA damage and cytotoxic stress? Given limitations in our knowledge about the underlying molecular biology, coupled with the broad spectrum effects of cytotoxic agents on cellular processes, mechanistically detailed models are likely to be unfeasible at present. Data-driven statistical models however can be implemented to overcome these limitations and elucidate the molecular relationships underlying drug combination effects. By quantifying a wide panel of molecular readouts in parallel with cellular responses to drug treatments, input-output relationships can be specified using statistical models, and critical proteins or pathways mediating the responses identified. As a recent example, interactions between DNA-damaging chemotherapies and targeted kinase inhibitors in breast cancer cells were investigated (Lee et al. 2012). Multiple proteomic technologies were used to quantify the activation of pathways regulating cell survival (PI3K/AKT), proliferation (MAPK/ERK, cyclins), apoptosis (caspase), stress response (MAPK/p38), and genetic integrity (p53, HDAX) in response to multiple kinase inhibitor-genotoxic drug combinations. Sequence-dependent effects were identified, where suppression of ErbB receptor signaling 24 h to prior to doxorubicin treatment potentiated the chemotherapy's activity. A partial least squared regression (PLSR) model was developed, predicting cell viability as a function of multivariate signaling dynamics. Through analysis of the model parameters, apoptotic potentiation via caspase 8 was identified as the convergence point between DNA damage and signaling pathways. As this example illustrates, multivariate statistical models can be useful tools for interrogating the mechanisms by which cytotoxic drugs and targeted inhibitors interact, and ultimately optimizing combination dosing regimens.

19.6.6 Limitations of Tumor Growth Models: Clonal Heterogeneity, Stem Cells, and Metastasis

In the process of building and parameterizing tumor growth models, it is often noted that reliance on a specific signal or pathway will depreciate over time (i.e., the EC_{50} parameter will increase over an extended course of treatment). This is consistent with clinical observations, as tumors initially dependent on an oncogenic driver will often develop resistance. The phenomena can be empirically described by setting the EC_{50} as a time-dependent variable (Kay et al. 2012). However, it would be much more informative to account for the mechanistic basis of drug resistance, such as through the activation of redundant survival pathways or clonal competition. Mechanism-based dynamic models could then be used to optimize dosing or combination strategies which pre-emptively combat its development (Al-Lazikani et al. 2012). Cell compartment-based models are a possible approach, wherein tumor mass is described as consisting of two or more cell sub-populations of drug sensitive and resistant cells. Key parameters are the net growth rates of the cell sub-populations as functions of drug concentration, and the compartment transition rates (i.e. the acquisition of genetic mutations which confer drug resistance). The relative contribution of each to bulk tumor mass is then a dynamic function of drug concentration.

Consider the simplest scenario wherein a tumor is composed of two clonal sub-populations, sensitive vs. drug resistant as defined by proliferation rates in the absence versus presence of drug. This is not an entirely unrealistic simplification. During treatment with the EGFR TKI gefitinib, resistance most often develops through the acquisition of a single T790M "gatekeeper" mutation, which affects drug binding to the ATP pocket (Engelman and Jänne 2008). A two compartment model was developed to desicrbe the phenomoenon, quantifying differential proliferation rates of the two genetically defined sub-popultaions (resistant (R) versus sensitive (S)) as functions of gefitinb concentration (C), and parameterized using in vitro cell culture of an EGFR-dependent lung cancer cell line:

$$\frac{dV_S}{dt} = \alpha_S(C, V_S) \tag{19.15}$$

$$\frac{dV_R}{dt} = \alpha_R(C, V_R) \tag{19.16}$$

$$V = \sum V_S + V_R \tag{19.17}$$

Model simulations were then used to optimize dosing schedules so as to limit the development of resistance, defined as dominance of the resistant clone ($V_R/V_S > 1$). A pulsatile dosing schedule (high weekly doses, followed by lower daily maintenance doses) was predicted to significantly delay the onset of resistance.

This finding was subsequently validated in vivo using a xenograft model, and has been followed up with clinical trials (Chmielecki et al. 2011).

In addition to genetic heterogeneity, tumor cells with identical genomes can display extensive phenotypic diversity. This highlights a flaw in the commonly employed simplifying assumption of modeling tumors as a homogenous mass of clonogenic cells. This may be a reasonable approximation for bacterial cultures or perhaps clonally-derived cell lines. However, only a minority of cells (termed cancer stem cells; CSCs) are capable of initiating tumor formation and recurrence (Dick 2008). The existence of cancer stem cells is however still controversial. While broadly accepted in hematological malignancies, it is still debatable whether they fuel growth of all solid cancers or a subset, and the cellular frequency of CSCs in human tumors remains highly contested (Meacham and Morrison 2013). It is also still debated as to whether CSC represent a stable cell type at the base of a fixed developmental hierarchy (as in normal tissue), vs. a transitory cellular phenotype (Meacham and Morrison 2013). The implications for basic drug discovery are profound, as tumorigenic stem cells and their non-tumorigenic progeny may depend on distinct signaling pathways (Tam et al. 2013). Agents designed to kill bulk tumor cells may be ineffective in CSCs, and thus incapable of achieving sustained remissions or cures. Understanding the population structure of tumors and mechanisms of drug efficacy (what parameters are affected and in which populations) has implications for the interpretation of tumor growth responses to drug treatment, as has been documented for responses to imatinib in chronic myeloid leukemia (Roeder et al. 2006; Tang et al. 2011; Michor et al. 2005), and radiation therapy in glioblastoma (Leder et al. 2014).

It is important to highlight another crucial discrepancy between the mathematical models of tumor growth described and clinical reality. Cancer mortality is most often attributed to metastases rather than growth of the primary tumor. Quantitative models with functional outputs of cancer cell migration, tissue invasion, systemic dissemination, and colonization would therefore be highly complementary to models of tumor growth, and provide a more complete description of disease progression. However, tumor size is fundamentally easier to quantify than the complex, multistep process leading to metastasis. As such, cancer research and drug discovery, and by extension the derivative computational models, have primarily focused on cell proliferation and survival. In fact, there are no drugs currently available that specifically target the metastatic process. Advances in biomaterials, 3D cell culture, and microscopy are however increasing our ability to quantify cancer cell invasiveness in vitro and in vivo (Zaman 2013), and such data should be leveraged to build more comprehensive models of metastatic disease. A more quantitative understanding of the networks underlying these processes could enable metastasis-oriented drug development programs to target signaling pathways driving the process, such as TGF-β, Wnt, and PDGF- β (Lu et al. 2013; Tam and Weinberg 2013; Wan et al. 2013).

Regardless of the underlying pathways involved, the metastatic potential of a carcinoma appears to depend on phenotypic plasticity of the cells. That is, the capacity for de-differentiating via epithelial-mesenchymal transition (EMT) for

dissemination, and then re-differentiation (MET) for metastatic site colonization and re-growth (Brabletz et al. 2013). Notably, the molecular and morphological characteristics of cancer stems cells are highly overlapping with post-EMT cells, suggesting the terms may refer to similar or perhaps the same sub-populations, in at least some tumor types. Integrating the emerging science of genetic heterogeneity, phenotypic plasticity, and cancer stem cells into mathematical models would add significant breadth to current models of tumor growth and improve their translational relevance.

19.7 Next Generation Translational PD Models

Tumor growth models used in translational research have been evolving from highly empirical formulations which describe the effects of cytotoxic drugs, towards mechanism-based descriptions for interpreting the pharmacology of molecularly-targeted therapies. This has been driven by both supply and demand. On the demand side, the critical challenges in oncology drug development—including target identification, therapeutic design, dose selection, combination regimen design and biomarker stratification strategies—necessitate a mechanistic understanding of how drugs interact with oncogenic regulatory networks. On the supply side, the availability of potent and selective inhibitors combined with multiplex and high-throughput profiling technologies mean that the data necessary to parameterize such models is increasingly attainable. A particular area of focus is the expansion beyond single pathway-focused models (vertical integration), towards quantitative descriptions of multi-pathway interactions and cellular dependencies (horizontal integration). Particularly notable are the interfaces between PI3K and MAPK signaling, apoptotic and cell cycle regulatory controls, and DNA damage repair pathways.

19.7.1 Leveraging Available Data

Much of the data necessary to develop mechanism-based translational models are either available or at least readily attainable. Discovery and translational researchers now regularly explore the effects of combining inhibitors of key regulatory pathways, and quantify dynamic molecular readouts in tandem with in vitro or in vivo phenotypic responses. Studies can be conducted across panels of genomic-characterized cell lines, enabling cell regulatory networks to be interpreted within tissue and genetic-context. For example, the effect of PI3K/AKT and MEK inhibitor combinations on cell signaling and survival have been profiled in vitro using cell line models of breast cancer (Hoeflich et al. 2009), non-small cell lung cancer (Meng et al. 2010), thyroid cancer (Jin et al. 2011), colorectal cancer (Ebi et al. 2011), KRAS-mutant but indication-diverse panels (Wee et al. 2009; She et al. 2010), as

well as in genetically engineered mouse models (Roberts et al. 2012). The interplay of apoptosis and pro-survival signaling pathways have also been studied using combinations of Bcl-2 inhibitors with MEK and PI3K inhibitors in in panels of cell lines (Tan et al. 2013; Corcoran et al. 2013). An important facet often unexplored in vitro is the impact of signal inhibition dynamics on cellular responses, and the reversibility of signal-response relationships (i.e., how long does a critical survival signal need to be suppressed to inhibit proliferation or induce cell death, and what is the cellular recovery time?). This is a particularly critical consideration for molecules with short serum half-lives. A number of published in vivo xenograft studies have explored the effects of both kinase inhibitor dose and timing on anti-tumor efficacy, including measurements of key signaling nodes (kinases) and effectors of apoptosis and cell cycle regulation. These include studies of the ErbB2 inhibitor lapatininb in breast cancer (Amin et al. 2010), the BCR-ABL inhibitors dasatinib and imatinib in CML (Shah et al. 2010), the EGFR inhibitor gefitinib in breast cancer (Solit et al. 2005), and MEK and PI3K inhibitor combinations in various indications (Hoeflich et al. 2012).

There is no technical reason that mathematical modeling could not play an essential component of such studies. One of the challenges of applying systems-modeling in industry is the time sensitive nature of decisions. When critical decisions related to clinical development arise, there often is not sufficient time or resources available to develop biologically-based models of drug activity from scratch. However, by building drug-agnostic but disease-specific models as a key element of discovery research, one could leverage such resources repeatedly across different programs and continually fold in new information as it accumulates. A cultural push is required for modeling and simulation to play a more prominent role in early discovery and translational research, following what has begun to occur over the last decade in clinical pharmacometrics.

19.7.2 Remaining Challenges to Modeling Cancer Cell Biology for Drug Development

19.7.2.1 Toxicity

Mechanism-based PD models have focused extensively on the single endpoint of drug efficacy—largely tumor growth inhibition or molecular surrogates of proliferation and survival. This contrasts sharply with standard clinical practice of dose selection based around toxicity. Ultimately, clinical dosing regimens should be designed around a therapeutic window—the region between minimally accepted efficacy and maximally tolerable toxicity. Toxicity for oncology drugs is often due to on-target effects at non-target (healthy) tissues (Muller and Milton 2012). On-target toxicity mechanisms imply that it should be possible to include toxicity endpoints in mechanism-based models. Predictive models of drug safety have been

advocated by the FDA (Abernethy et al. 2011) and would be a highly valuable tool to complement contemporary empirical approaches (Lesko et al. 2013). At minimum, hybrid models incorporating empirically-defined toxicity thresholds could be integrated within mechanism-based efficacy models for translational regimen designs.

19.7.2.2 Tumor Architecture

It has long been recognized and explicitly described in physiologically-based PK models that drug concentrations in tumors may be different from that in the serum or other body tissues. This is a particularly important consideration in oncology, given the abnormal vasculature of tumors and resulting poor perfusion. Drug penetration into tumor tissue, particularly for large molecules such as biologics and liposomal formulations, can be a critical determinant of efficacy. Models incorporating spatial information and tissue architecture, including vascular and tissue permeability of drugs, may thus be essential in certain situations (Thurber and Weissleder 2011).

19.7.2.3 Non-cell Autonomous Pharmacology

Tumors are not simply collections of autonomous replicating cells, but complex multi-cellular tissues, wherein communication with local vasculature, stromal tissue (such as fibroblasts), extra-cellular matrix, and infiltrating immune cells govern disease progression and response to pharmacological intervention (Hanahan and Weinberg 2011). Vascular disrupting agents such as VEGF inhibitors (Ribba et al. 2011), or immune checkpoint antagonists against PD1 or CTLA4 (Mullard 2013) could not be studied though the cell signaling models described thus far. A more thorough understanding of the heterotypic cell-cell interactions involved in tumor development and progression are necessary to build out more realistic models of cancer cell behavior as integrated tissue responses. Unfortunately, our basic scientific understanding of these relationships remains primitive. Further research in this area would not only improve our ability to interpret the pharmacology of drugs currently in development, but may open up entirely new drug targets and pharmacological strategies against the supporting niche rather than cancer cells themselves.

19.7.2.4 Interfacing Signaling, Gene Expression and Metabolism Networks

Protein signal transduction networks do not function as isolated entities, but rather interface with extracellular stimuli, transcriptional regulation, and metabolism. Oncogenic pathways such as PI3K/AKT signaling are key regulators of cellular

metabolism, and the concept of metabolic re-wiring is opening up new targets in cancer drug discovery (Galluzzi et al. 2013). More comprehensive models of cancer cell biology will require consideration of signal transduction, gene expression, and metabolic networks, though mathematical methods to integrate these biological processes are in their infancy (Gonçalves et al. 2013).

19.7.2.5 The Dark Matter of Cancer Biology

The majority of cancer genes identified to date through The Cancer Genome Atlas (TCGA) sequencing projects map onto a relatively limited number of known oncogenic pathways (Vogelstein et al. 2013; Tamborero et al. 2013; Ciriello et al. 2013). However, there have been some surprises. Chromatin regulators and mRNA splicing factors are two novel classes of cancer genes which do not fit neatly into established knowledge. Given the wide ranging effects that such mutations would have on gene expression patterns, it has yet to be seen how (or if) such processes can be consolidated with our current understanding of cancer cell biology. Another finding from the cancer genome sequencing projects is that mutational frequencies display "long-tail" distributions. While established oncogenes and tumor suppressors such as TP53, PI3KCA, as RAS are highly recurrent across many tumors, a comprehensive understanding of how such drivers interact with less frequent, and likely less potent mutations has yet to be established (Davoli et al. 2013). Outside of cancer research, recent genetic studies have revealed deeper complexities in the molecular regulation of cell biology than was ever assumed. The ENCODE (Encyclopedia of DNA Elements) project has reported a mere 5.5 % of expressed RNAs consist of protein coding exons (Bernstein et al. 2012), overturning previously held protein-centric view of genetic material. It is humbling to consider that the precise function of the majority of transcribed DNA elements remain mysterious.

19.8 Summary

Biological systems are unnervingly complex. Given the incessant pace of paradigm shifting discoveries in molecular biology, current conceptual and computational models are likely to contain yawning gaps and mistakes. Incorporating a strong dose of humility and skepticism in the predictions emanating from our models is thus critically important to realizing their promise. As the boundaries of knowledge about cancer biology progressively advance, computational modeling has a vital role to play in navigating the unknown, and forging the next generation of medicines to better serve the needs of patients.

Acknowledgments I would like to thank Brigit Schoeberl, Ulrik Nielsen, Matthew Onsum, Charlotte McDonagh, Johanna Lahdenranta, Jinyan Du, Yamsin Hashamboy-Ramsey, Bart

Hendricks, Petra Loesch, and Debbie Tseng providing helpful feedback on the manuscript, and many other colleagues at Merrimack Pharmaceuticals who have contributed ideas and supported this work over the years.

References

Abaan OD et al (2013) The Exomes of the NCI-60 panel: a genomic resource for cancer biology and systems pharmacology. Cancer Res 73(14):4372–4382

Abel EV et al (2013) Melanoma adapts to RAF/MEK inhibitors through FOXD3-mediated upregulation of ERBB3. J Clin Investig 123(5):2155–2168

Abernethy DR, Woodcock J, Lesko LJ (2011) Pharmacological mechanism-based drug safety assessment and prediction. Clin Pharmacol Ther 89(6):793–797. doi:10.1038/clpt.2011.55/nature06264

Aksamitiene E, Kiyatkin A, Kholodenko BN (2012) Cross-talk between mitogenic Ras/MAPK and survival PI3K/Akt pathways: a fine balance. Biochem Soc Trans 40(1):139–146

Albeck JG et al (2006) Collecting and organizing systematic sets of protein data. Nat Rev Mol Cell Biol 7(11):803–812

Aldridge BB et al (2006) Physicochemical modelling of cell signalling pathways. Nat Cell Biol 8 (11):1195–1203

Moles CG et al (2003) Parameter estimation in biochemical pathways: a comparison of global optimization methods. Genome Res 13:2467–2474

Al-Lazikani B, Banerji U, Workman P (2012) Combinatorial drug therapy for cancer in the post-genomic era. Nat Biotechnol 30(7):679–692

Amin DN et al (2010) Resiliency and vulnerability in the HER2-HER3 tumorigenic driver. Sci Transl Med 2(16):16ra7

Arrowsmith J, Miller P (2013) Trial watch: phase II and phase III attrition rates 2011–2012. Nat Rev Drug Discov 12(8):569

Asthagiri aR, Lauffenburger Da (2001) A computational study of feedback effects on signal dynamics in a mitogen-activated protein kinase (MAPK) pathway model. Biotechnol Prog 17 (2):227–239

Bader GD, Cary MP, Sander C (2006) Pathguide: a pathway resource list. Nucleic Acids Res 34 (Database issue):D504–D506

Barretina J et al (2012) The cancer cell line encyclopedia enables predictive modelling of anticancer drug sensitivity. Nature 483(7391):603–307

Basu A et al (2013) An interactive resource to identify cancer genetic and lineage dependencies targeted by small molecules. Cell 154(5):1151–1161

Bauer-Mehren A, Furlong LI, Sanz F (2009) Pathway databases and tools for their exploitation: benefits, current limitations and challenges. Mol Syst Biol 5:290. doi:10.1038/msb.2009.47

Begley CG, Ellis LM (2012) Drug development: raise standards for preclinical cancer research. Nature 483(7391):531–533

Bendall SC, Nolan GP (2012) From single cells to deep phenotypes in cancer. Nature Biotechnol 30(7):639–647. doi:10.1038/nbt.2283

Bernstein BE et al (2012) An integrated encyclopedia of DNA elements in the human genome. Nature 489(7414):57–74

Blume-Jensen P, Hunter T (2001) Oncogenic kinase signalling. Nature 411(6835):355–365

Borisov N et al (2009) Systems-level interactions between insulin-EGF networks amplify mitogenic signaling. Mol Syst Biol 5(256):256

Bozic I et al (2013) Evolutionary dynamics of cancer in response to targeted combination therapy. eLife 2:e00747-e00747

Brabletz T et al (2013) Roadblocks to translational advances on metastasis research. Nature Med 19(9):1104–1109

Brennan CW et al (2013) The somatic genomic landscape of glioblastoma. Cell 155(2):462–477
Cameron Da et al (2000) Identification of long-term survivors in primary breast cancer by dynamic modelling of tumour response. Br J Cancer 83(1):98–103
Campbell MR, Amin D, Moasser MM (2010) HER3 comes of age: new insights into its functions and role in signaling, tumor biology, and cancer therapy. Clin Cancer Res 16(5):1373–1383
Caponigro G, Sellers WR (2011) Advances in the preclinical testing of cancer therapeutic hypotheses. Nat Rev Drug Discovery 10(3):179–187
Carter H, Hofree M, Ideker T (2013) Genotype to phenotype via network analysis. Curr Opin Genet Dev 23(6):611–621
Casado P et al. (2013) Phosphoproteomics data classify hematological cancer cell lines according to tumor type and sensitivity to kinase inhibitors. Genome Biol 14(4):R37
Chandarlapaty S et al (2011) AKT inhibition relieves feedback suppression of receptor tyrosine kinase expression and activity. Cancer Cell 19(1);58–71. doi:10.1016/j.ccr.2010.10.031
Cerami EG et al (2011) Pathway Commons, a web resource for biological pathway data. Nucleic Acids Res 39(SUPPL. 1):685–690
Chakrabarty A et al (2012) Feedback upregulation of HER3 (ErbB3) expression and activity attenuates antitumor effect of PI3K inhibitors. Proc Natl Acad Sci USA 109(8):2718–2723
Chapman PB et al (2011) Improved survival with vemurafenib in melanoma with BRAF V600E mutation. N Engl J Med 364(26):2507–2516
Chen WW et al (2009) Input-output behavior of ErbB signaling pathways as revealed by a mass action model trained against dynamic data. Mol Syst Biol 5:239
Chin L et al (2011) Making sense of cancer genomic data. Genes Dev 25(6):534–555
Chmielecki J et al (2011) Optimization of dosing for EGFR-mutant non-small cell lung cancer with evolutionary cancer modeling. Sci Transl Med 3(90):90ra59
Chong CR, Jänne PA (2013) The quest to overcome resistance to EGFR-targeted therapies in cancer. Nature Med 19(11):1389–1400
Choo EF et al (2013) PK-PD modeling of combination efficacy effect from administration of the MEK inhibitor GDC-0973 and PI3K inhibitor GDC-0941 in A2058 xenografts. Cancer Chemother Pharmacol 71(1):133–143
Ciriello G et al (2012) Mutual exclusivity analysis identifies oncogenic network modules. Genome Res 22(2):398–406
Ciriello G et al (2013) Emerging landscape of oncogenic signatures across human cancers. Nature Genet 45(10):1127–1133
Cirit M, Wang C-C, Haugh JM (2010) Systematic quantification of negative feedback mechanisms in the extracellular signal-regulated kinase (ERK) signaling network. J Biol Chem 285 (47):36736–36744
Claret L et al (2009) Model-based prediction of phase III overall survival in colorectal cancer on the basis of phase II tumor dynamics. J Clin Oncol 27(25):4103–4108
Claret L et al (2012) Simulations using a drug-disease modeling framework and phase II data predict phase III survival outcome in first-line non-small-cell lung cancer. Clin Pharmacol Ther 92(5):631–634
Claret L et al (2013) Evaluation of tumor-size response metrics to predict overall survival in Western and Chinese patients with first-line metastatic colorectal cancer. J Clin Oncol Off J Am Soc Clin Oncol 31(17):2110–2114
Corcoran RB et al. (2013) Synthetic lethal interaction of combined BCL-XL and MEK inhibition promotes tumor regressions in KRAS mutant cancer models. Cancer Cell 23(1):121–128. doi:10.1016/j.ccr.2012.11.007
Courcelles M et al (2013) Phosphoproteome dynamics reveal novel ERK1/2 MAP kinase substrates with broad spectrum of functions. Mol Syst Biol 9(669):669
Creixell P et al (2012) Navigating cancer network attractors for tumor-specific therapy. Nat Biotechnol 30(9):842–848
Cvijovic M et al. (2014) Bridging the gaps in systems biology. Mol Genet Genomics 289:727–734
Davoli T et al (2013) Cumulative haploinsufficiency and triplosensitivity drive aneuploidy patterns and shape the cancer genome. Cell 155:1–15

Dancey JE, Chen HX (2006) Strategies for optimizing combinations of molecularly targeted anticancer agents. Nat Rev Drug Discovery 5(8):649–659
DeVita VT, Chu E (2008) A history of cancer chemotherapy. Cancer Res 68(21):8643–8653
Dick JE (2008) Stem cell concepts renew cancer research. Blood 112(13):4793–4807
DiMasi JA et al. (2013) Clinical approval success rates for investigational cancer drugs. Clin Pharmacol Ther 94(3):329–35
DiMasi Ja et al (2010) Trends in risks associated with new drug development: success rates for investigational drugs. Clin Pharmacol Ther 87(3):272–277
Domcke S et al. (2013) Evaluating cell lines as tumour models by comparison of genomic profiles. Nature Commun 4:2126
Druker BJ et al (2001) Efficacy and safety of a specific inhibitor of the BCR-ABL tyrosine kinase in chronic myeloid leukemia. N Engl J Med 344(14):1031–1037
Duncan JS et al (2012) Dynamic reprogramming of the kinome in response to targeted MEK inhibition in triple-negative breast cancer. Cell 149(2):307–321
Ebi H et al (2011) Receptor tyrosine kinases exert dominant control over PI3K signaling in human KRAS mutant colorectal cancers. J Clin Investig 121(11):4311–4321
Engelman Ja, Jänne Pa (2008) Mechanisms of acquired resistance to epidermal growth factor receptor tyrosine kinase inhibitors in non-small cell lung cancer. Clin Cancer Res 14(10):2895–2899
Fallahi-Sichani M et al (2013) Metrics other than potency reveal systematic variation in responses to cancer drugs. Nat Chem Biol 9(11):708–714
Ferté C et al (2013) Tumor growth rate is an early indicator of antitumor drug activity in phase I clinical trials. Clin Cancer Res Off J Am Assoc Cancer Res 20(1):246–252
Fitzgerald JB et al (2006) Systems biology and combination therapy in the quest for clinical efficacy. Nat Chem Biol 2(9):458–466
Fitzgerald JB et al (2014) MM-141, an IGF-IR- and ErbB3-directed bispecific antibody, overcomes network adaptations that limit activity of IGF-IR inhibitors. Mol Cancer Ther 13 (2):410–425
Freidlin B, Korn EL (2013) Biomarker enrichment strategies: matching trial design to biomarker credentials. Nature Rev Clin Oncol 11(2):81–90
Freidlin B et al (2012) Randomized phase II trial designs with biomarkers. J Clin Oncol 30 (26):3304–3309
Fritsche-Guenther R et al (2011) Strong negative feedback from Erk to Raf confers robustness to MAPK signalling. Mol Syst Biol 7(489):489
Galluzzi L et al (2013) Metabolic targets for cancer therapy. Nat Rev Drug Discovery 12(11):829–846
Garnett MJ et al (2012) Systematic identification of genomic markers of drug sensitivity in cancer cells. Nature 483(7391):570–575
Garrett JT et al (2011) Transcriptional and posttranslational up-regulation of HER3 (ErbB3) compensates for inhibition of the HER2 tyrosine kinase. Proc Natl Acad Sci USA 108 (12):5021–5026
Gaudet S et al. (2012) Exploring the contextual sensitivity of factors that determine cell-to-cell variability in receptor-mediated apoptosis. PLoS Comput Biol 8(4):e1002482
Gerlinger M et al (2012) Intratumor heterogeneity and branched evolution revealed by multiregion sequencing. N Engl J Med 366(10):883–892
Gonçalves E et al (2013) Bridging the layers: towards integration of signal transduction, regulation and metabolism into mathematical models. Mol BioSyst 9(7):1576–1583
Haddish-Berhane N et al (2013) On translation of antibody drug conjugates efficacy from mouse experimental tumors to the clinic: a PK/PD approach. J Pharmacokinet Pharmacodyn 40 (5):557–571
Hammerman PS et al (2012) Comprehensive genomic characterization of squamous cell lung cancers. Nature 489(7417):519–525
Hanahan D, Weinberg Ra (2011) Hallmarks of cancer: the next generation. Cell 144(5):646–674

Hansson EK et al. (2013) PKPD modeling of VEGF, sVEGFR-2, sVEGFR-3, and sKIT as predictors of tumor dynamics and overall survival following sunitinib treatment in GIST. CPT Pharmacometrics Syst Pharmacol, 2, e84

Harms BD et al (2012) Optimizing properties of antireceptor antibodies using kinetic computational models and experiments. Methods Enzymol 502:67–87

Harms BD et al. (2014) Understanding the role of cross-arm binding efficiency in the activity of monoclonal and multispecific therapeutic antibodies. Methods 65:95–104

Harrold JM, Straubinger RM, Mager DE (2012) Combinatorial chemotherapeutic efficacy in non-Hodgkin lymphoma can be predicted by a signaling model of CD20 pharmacodynamics. Cancer Res 72(7):1632–1641

Hay M et al (2014) Clinical development success rates for investigational drugs. Nat Biotechnol 32 (1):40–51

Hendriks BS (2010) Functional pathway pharmacology: Chemical tools, pathway knowledge and mechanistic model-based interpretation of experimental data. Curr Opin Chem Biol 14(4):489–497

Hendriks BS et al (2012) Multiscale kinetic modeling of liposomal doxorubicin delivery quantifies the role of tumor and drug-specific parameters in local delivery to tumors. CPT Pharmacometr Syst Pharmacol 1(11):e15

Hendriks BS et al (2013) Impact of tumor HER2/ERBB2 expression level on HER2-targeted liposomal doxorubicin-mediated drug delivery: multiple low-affinity interactions lead to a threshold effect. Mol Cancer Ther 12(9):816–828

Hoeflich KP et al (2009) In vivo antitumor activity of MEK and phosphatidylinositol 3-kinase inhibitors in basal-like breast cancer models. Clin Cancer Res 15(14):4649–4664

Hoeflich KP et al (2012) Intermittent administration of MEK inhibitor GDC-0973 plus PI3K inhibitor GDC-0941 triggers robust apoptosis and tumor growth inhibition. Cancer Res 72 (1):210–219

Horrobin DF (2003) Modern biomedical research: an internally self-consistent universe with little contact with medical reality? Nat Rev Drug Discovery 2(2):151–154

Huang CY, Ferrell JE (1996) Ultrasensitivity in the mitogen-activated protein kinase cascade. Proc Natl Acad Sci USA 93(19):10078–10083

Iyengar R et al (2012) Merging systems biology with pharmacodynamics. Sci Transl Med 4 (126):126ps7

Jaiswal B et al. (2013) Oncogenic ERBB3 mutations in human cancers. Cancer Cell 23(5):603–617. doi: 10.1016/j.ccr.2013.04.012

Janes Ka, Lauffenburger Da (2013) Models of signalling networks—what cell biologists can gain from them and give to them. J Cell Sci 126(9):1913–1921

Jin N et al (2011) Synergistic action of a RAF inhibitor and a dual PI3K/mTOR inhibitor in thyroid cancer. Clin Cancer Res 17(20):6482–6489

Kan Z et al (2010) Diverse somatic mutation patterns and pathway alterations in human cancers. Nature 466(7308):869–873

Kaplan R et al (2013) Evaluating many treatments and biomarkers in oncology: a new design. J Clin Oncol 31(36):4562–4568

Karr J et al. (2012) A whole-cell computational model predicts phenotype from genotype. Cell 150 (2):389–401. doi:10.1016/j.cell.2012.05.044

Kay BP et al (2012) Intracellular-signaling tumor-regression modeling of the pro-apoptotic receptor agonists dulanermin and conatumumab. J Pharmacokinet Pharmacodyn 39(5):577–590

Kesselheim AS, Avorn J (2013) The most transformative drugs of the past 25 years: a survey of physicians. Nat Rev Drug Discovery 12(6):425–431

Kholodenko B, Yaffe MB, Kolch W (2012) Computational approaches for analyzing information flow in biological networks. Sci Signal 5(220):re1

Kirouac DC, Onsum MD (2013) Using network biology to bridge pharmacokinetics and pharmacodynamics in oncology. CPT Pharmacometr Syst Pharmacol 2:e71

Kirouac DC et al (2012) Creating and analyzing pathway and protein interaction compendia for modelling signal transduction networks. BMC Syst Biol 6:29
Kirouac DC et al (2013) Computational modeling of ERBB2-amplified breast cancer identifies combined ErbB2/3 blockade as superior to the combination of MEK and AKT inhibitors. Sci Signal 6(288):ra68
Kirpotin DB et al (2012) Building and characterizing antibody-targeted lipidic nanotherapeutics. Methods Enzymol 502:139–166
Klinger B et al (2013) Network quantification of EGFR signaling unveils potential for targeted combination therapy. Mol Syst Biol 9:673
Ko AH et al. (2013) A multinational phase 2 study of nanoliposomal irinotecan sucrosofate (PEP02, MM-398) for patients with gemcitabine-refractory metastatic pancreatic cancer. Br J Cancer 109:920–925
Kreutz C, Timmer J (2009) Systems biology: experimental design. FEBS J 276(4):923–942
Kwak EL et al (2010) Anaplastic lymphoma kinase inhibition in non-small-cell lung cancer. N Engl J Med 363(18):1693–1703
Lalonde RL et al (2007) Model-based drug development. Clin Pharmacol Ther 82(1):21–32
Leder K et al. (2014) Mathematical modeling of PDGF-driven glioblastoma reveals optimized radiation dosing schedules. Cell 156(3):603–616. doi: 10.1016/j.cell.2013.12.029
Lee JY et al (2011) Impact of pharmacometric analyses on new drug approval and labelling decisions: a review of 198 submissions between 2000 and 2008. Clin Pharmacokinet 50 (10):627–635
Lee MJ et al (2012) Sequential application of anticancer drugs enhances cell death by rewiring apoptotic signaling networks. Cell 149(4):780–794
Lesko LJ, Zheng S, Schmidt S (2013) Systems approaches in risk assessment. Clin Pharmacol Ther 93(5):413–424
Lito P, Rosen N, Solit DB (2013) Tumor adaptation and resistance to RAF inhibitors. Nature Med 19(11):1401–1409
Lu M et al (2013) MicroRNA-based regulation of epithelial-hybrid-mesenchymal fate determination. Proc Natl Acad Sci USA 110(45):18144–18149
Majewski IJ, Bernards R (2011) Taming the dragon: genomic biomarkers to individualize the treatment of cancer. Nature Med 17(3):304–312. doi:10.1038/nm.2311
Marshall JL (2012) Maximum-tolerated dose, optimum biologic dose, or optimum clinical value: dosing determination of cancer therapies. J Clin Oncol Off J Am Soc Clin Oncol 30(23): 2815–2816
McDonagh CF et al (2012) Antitumor activity of a novel bispecific antibody that targets the ErbB2/ErbB3 oncogenic unit and inhibits heregulin-induced activation of ErbB3. Mol Cancer Ther 11(3):582–593
Meacham CE, Morrison SJ (2013) Tumour heterogeneity and cancer cell plasticity. Nature 501 (7467):328–337
Meng J et al (2010) Combination treatment with MEK and AKT inhibitors is more effective than each drug alone in human non-small cell lung cancer in vitro and in vivo. PLoS ONE 5(11): e14124
Meyer AS et al (2013) The receptor AXL diversifies EGFR signaling and limits the response to EGFR-targeted inhibitors in triple-negative breast cancer cells. Sci Signal 6(287):ra66
Michor F et al (2005) Dynamics of chronic myeloid leukaemia. Nature 435(7046):1267–1270
Miller ML et al (2013) Drug synergy screen and network modeling in dedifferentiated liposarcoma identifies CDK4 and IGF1R as synergistic drug targets. Sci Signal 6(294):ra85-ra85
Milligan PA et al (2013) Model based drug development: a rational approach to efficiently accelerate drug development. Clin Pharmacol Ther 93(6):502–514
Mitsos A et al. (2009) Identifying drug effects via pathway alterations using an integer linear programming optimization formulation on phosphoproteomic data. PLoS Comput Biol 5(12): e1000591
Morris MK et al (2010) Logic-based models for the analysis of cell signaling networks. Biochemistry 49(15):3216–3224

Morris MK et al (2011) Training signaling pathway maps to biochemical data with constrained fuzzy logic: quantitative analysis of liver cell responses to inflammatory stimuli. PLoS Comput Biol 7(3):e1001099
Mullard A (2013) New checkpoint inhibitors ride the immunotherapy tsunami. Nature Rev Drug Discovery 12(7):489–492
Muller PY, Milton MN (2012) The determination and interpretation of the therapeutic index in drug development. Nat Rev Drug Discovery 11(10):751–761
Nelander S et al (2008) Models from experiments: combinatorial drug perturbations of cancer cells. Mol Syst Biol 4:216
Niederst MJ, Engelman Ja (2013) Bypass mechanisms of resistance to receptor tyrosine kinase inhibition in lung cancer. Sci Signal 6(294):re6–re6
Niepel M et al (2013) Profiles of Basal and stimulated receptor signaling networks predict drug response in breast cancer lines. Sci Signal 6(294):84
Noble CO et al (2004) Development of ligand-targeted liposomes for cancer therapy. Expert Opin Ther Targets 8(4):335–353
Paul SM et al (2010) How to improve R&D productivity: the pharmaceutical industry's grand challenge. Nat Rev Drug Discovery 9(3):203–214
Pawaskar DK et al (2013) Synergistic interactions between sorafenib and everolimus in pancreatic cancer xenografts in mice. Cancer Chemother Pharmacol 71(5):1231–1240
Pe'er D, Hacohen N (2011) Principles and strategies for developing network models in cancer. Cell 144(6):864–873
Prahallad A et al (2012) Unresponsiveness of colon cancer to BRAF(V600E) inhibition through feedback activation of EGFR. Nature 483(7387):100–103
Pratilas CA et al (2009) (V600E)BRAF is associated with disabled feedback inhibition of RAF-MEK signaling and elevated transcriptional output of the pathway. Proc Natl Acad Sci USA 106(11):4519–4524
Prinz F, Schlange T, Asadullah K (2011) Believe it or not: how much can we rely on published data on potential drug targets? Nature Rev Drug Discovery 10(9):712. doi:10.1038/nrd3439-c1
Reinhold WC et al (2012) Cell miner: a web-based suite of genomic and pharmacologic tools to explore transcript and drug patterns in the NCI-60 cell line set. Cancer Res 72(14):3499–3511
Ribba B et al (2011) A model of vascular tumour growth in mice combining longitudinal tumour size data with histological biomarkers. Eur J Cancer 47(3):479–490
Roberts PJ et al (2012) Combined PI3K/mTOR and MEK inhibition provides broad antitumor activity in faithful murine cancer models. Clin Cancer Res 18(19):5290–5303
Robin X et al. (2013) Personalized network-based treatments in oncology. Clin Pharmacol Ther 94:646–650
Rocchetti M et al (2007) Predicting the active doses in humans from animal studies: a novel approach in oncology. Eur J Cancer 43(12):1862–1868
Roeder I et al (2006) Dynamic modeling of imatinib-treated chronic myeloid leukemia: functional insights and clinical implications. Nat Med 12(10):1181–1184
Saez-Rodriguez J et al (2009) Discrete logic modelling as a means to link protein signalling networks with functional analysis of mammalian signal transduction. Mol Syst Biol 5(331):331
Saini KS et al (2013) Targeting the PI3K/AKT/mTOR and Raf/MEK/ERK pathways in the treatment of breast cancer. Cancer Treatment Rev 39(8):935–946. doi:10.1016/j.ctrv.2013.03.009
Salphati L et al. (2010) Pharmacokinetic-pharmacodynamic modeling of tumor growth inhibition and biomarker modulation by the novel phosphatidylinositol 3-kinase inhibitor GDC-0941 Abstract 38(9):1436–1442
Scannell JW et al (2012) Diagnosing the decline in pharmaceutical R&D efficiency. Nat Rev Drug Discovery 11(3):191–200
Schilsky RL (2010) Personalized medicine in oncology: the future is now. Nat Rev Drug Discovery 9(5):363–366
Schoeberl B et al (2002) Computational modeling of the dynamics of the MAP kinase cascade activated by surface and internalized EGF receptors. Nat Biotechnol 20(4):370–375

Schoeberl B et al (2009) Therapeutically targeting ErbB3: a key node in ligand-induced activation of the ErbB receptor-PI3K axis. Science signaling 2(77):ra31
Sergina NV et al (2007) Escape from HER-family tyrosine kinase inhibitor therapy by the kinase-inactive HER3. Nature 445(7126):437–441
Shah NP et al (2010) Potent, transient inhibition of BCR-ABL with dasatinib 100 mg daily achieves rapid and durable cytogenetic responses and high transformation-free survival rates in chronic phase chronic myeloid leukemia patients with resistance, suboptimal response or int. Haematologica 95(2):232–240
Shah DK, Haddish-Berhane N, Betts A (2012) Bench to bedside translation of antibody drug conjugates using a multiscale mechanistic PK/PD model: a case study with brentuximab-vedotin. J Pharmacokinet Pharmacodyn 39(6):643–659
Sharma SV, Haber DA, Settleman J (2010) Cell line-based platforms to evaluate the therapeutic efficacy of candidate anticancer agents. Nat Rev Cancer 10(4):241–253
Sharpless NE, Depinho Ra (2006) The mighty mouse: genetically engineered mouse models in cancer drug development. Nat Rev Drug Discovery 5(9):741–754
She QB et al (2010) 4E-BP1 is a key effector of the oncogenic activation of the AKT and ERK signaling pathways that integrates their function in tumors. Cancer Cell 18(1):39–51. doi:10.1016/j.ccr.2010.05.023
Shoemaker RH (2006) The NCI60 human tumour cell line anticancer drug screen. Nat Rev Cancer 6(10):813–823
Simeoni M et al (2004) Predictive pharmacokinetic-pharmacodynamic modeling of tumor growth kinetics in xenograft models after administration of anticancer agents. Cancer Res 64(3): 1094–1101
Slamon DJ et al (2001) Use of chemotherapy plus a monoclonal antibody against HER2 for metastatic breast cancer that overexpresses HER2. N Engl J Med 344(11):783–792
Sliwkowski MX, Mellman I (2013) Antibody Therapeutics in cancer. Science 341:1192–1198 September
Snuderl M et al (2011) Mosaic amplification of multiple receptor tyrosine kinase genes in glioblastoma. Cancer Cell 20(6):810–817. doi:10.1016/j.ccr.2011.11.005
Solit DB et al (2005) Pulsatile administration of the epidermal growth factor receptor inhibitor gefitinib is significantly more effective than continuous dosing for sensitizing tumors to paclitaxel. Clin Cancer Res 11(5):1983–1989
Sos ML et al (2009) Identifying genotype-dependent efficacy of single and combined PI3K- and MAPK-pathway inhibition in cancer. Proc Natl Acad Sci USA 106(43):18351–18356
Spencer SL et al (2009) Non-genetic origins of cell-to-cell variability in TRAIL-induced apoptosis. Nature 459(7245):428–432
Stephens PJ et al (2012) The landscape of cancer genes and mutational processes in breast cancer. Nature 486(7403):400–404
Straussman R et al (2012) Tumour micro-environment elicits innate resistance to RAF inhibitors through HGF secretion. Nature 487(7408):500–504
Sturm OE et al (2010) The mammalian MAPK/ERK pathway exhibits properties of a negative feedback amplifier. Science signaling 3(153):ra90
Sun YN, Jusko WJ (1998) Transit compartments versus gamma distribution function to model signal transduction processes in pharmacodynamics. J Pharm Sci 87(6):732–737
Tam WL, Weinberg RA (2013) The epigenetics of epithelial-mesenchymal plasticity in cancer. Nature Med 19(11):1438–1449
Tam WL et al (2013) Protein kinase C α is a central signaling node and therapeutic target for breast cancer stem cells. Cancer Cell 24(3):347–364
Tamborero D et al (2013) Comprehensive identification of mutational cancer driver genes across 12 tumor types. Sci Rep 3:2650
Tan N et al (2013) Bcl-2/Bcl-xL inhibition increases the efficacy of MEK inhibition alone and in combination with PI3Kinase inhibition in lung and pancreatic tumor models. Mol Cancer Ther 12(6):853–864

Tang M et al (2011) Dynamics of chronic myeloid leukemia response to long-term targeted therapy reveal treatment effects on leukemic stem cells. Blood 118(6):1622–1631
PhRMA (2012) Medicines in development cancer 2012. Report from the Pharmacetuical and Manufaturers of America
The Cancer Genome Atlas (2008) Comprehensive genomic characterization defines human glioblastoma genes and core pathways. Nature 455(7216):1061–1068
Thurber GM, Weissleder R (2011) A systems approach for tumor pharmacokinetics. PLoS ONE 6 (9):e24696
Villanueva J et al (2010) Acquired resistance to BRAF inhibitors mediated by a RAF kinase switch in melanoma can be overcome by cotargeting MEK and IGF-1R/PI3K. Cancer Cell 18(6):683–695. doi:10.1016/j.ccr.2010.11.023
Vogelstein B, Kinzler KW (2004) Cancer genes and the pathways they control. Nat Med 10 (8):789–799
Vogelstein B et al (2013) Cancer genome landscapes. Science (New York, N.Y.) 339(6127):1546–1558
Wagner JP et al (2013) Receptor tyrosine kinases fall into distinct classes based on their inferred signaling networks. Sci Signal 6(284):58
Wan L, Pantel K, Kang Y (2013) Tumor metastasis: moving new biological insights into the clinic. Nature Med 19(11):1450–1464
Wang S et al (2008) Preclinical pharmacokinetic/pharmacodynamic models of gefitinib and the design of equivalent dosing regimens in EGFR wild-type and mutant tumor models. Mol Cancer Ther 7(2):407–417
Wang C-C, Cirit M, Haugh JM (2009a) PI3K-dependent cross-talk interactions converge with Ras as quantifiable inputs integrated by Erk. Mol Syst Biol 5(246):246
Wang S, Zhou Q, Gallo JM (2009b) Demonstration of the equivalent pharmacokinetic/pharmacodynamic dosing strategy in a multiple-dose study of gefitinib. Mol Cancer Ther 8 (6):1438–1447
Wang Y et al (2009c) Elucidation of relationship between tumor size and survival in non-small-cell lung cancer patients can aid early decision making in clinical drug development. Clin Pharmacol Ther 86(2):167–174
Watson IR et al (2013) Emerging patterns of somatic mutations in cancer. Nature Rev Genet 14 (10):703–718
Wee S et al (2009) PI3K pathway activation mediates resistance to MEK inhibitors in KRAS mutant cancers. Cancer Res 69(10):4286–4293
Whitehead Ka, Langer R, Anderson DG (2009) Knocking down barriers: advances in siRNA delivery. Nat Rev Drug Discovery 8(2):129–138
Williams SA et al (2013) Patient-derived xenografts, the cancer stem cell paradigm, and cancer pathobiology in the 21st century. Lab Invest J Tech Methods Pathol 93(9):970–982
Wilson TR et al (2012) Widespread potential for growth-factor-driven resistance to anticancer kinase inhibitors. Nature 487(7408):505–509
Wong H et al (2012) Bridging the gap between preclinical and clinical studies using pharmacokinetic-pharmacodynamic modeling: An analysis of GDC-0973, a MEK inhibitor. Clin Cancer Res 18(11):3090–3099
Xu L et al (2013) Rapid optimization and prototyping for therapeutic antibody-like molecules. mAbs 5(2):237–254
Yaffe MB (2013) The scientific drunk and the lamppost: massive sequencing efforts in cancer discovery and treatment. Sci Signal 6(269):13
Yamazaki S (2013) Translational pharmacokinetic-pharmacodynamic modeling from nonclinical to clinical development: a case study of anticancer drug, crizotinib. AAPS J 15(2):354–366
Yamazaki S et al (2008) Pharmacokinetic-pharmacodynamic modeling of biomarker response and tumor growth inhibition to an orally available cmet kinase inhibitor in human tumor xenograft mouse models ABSTRACT. Drug Metab Dispos 36(7):1267–1274
Yang J, Mager DE, Straubinger RM (2010) Comparison of two pharmacodynamic transduction models for the analysis of tumor therapeutic responses in model systems. AAPS J 12(1):1–10

Yap TA et al (2010) Envisioning the future of early anticancer drug development. Nature Rev Cancer 10(7):514–523. doi:10.1038/nrc2870

Zack TI et al (2013) Pan-cancer patterns of somatic copy number alteration. Nature Genet 45 (10):1134–1140

Zaman MH (2013) The role of engineering approaches in analysing cancer invasion and metastasis. Nature Rev Cancer 13(8):596–603

Chapter 20
Systems Pharmacology Modeling in Type 2 Diabetes Mellitus

James R. Bosley, Tristan S. Maurer and Cynthia J. Musante

Abstract This chapter provides an introduction to quantitative systems pharmacology (QSP) modeling of type 2 diabetes mellitus (T2DM). For practical reasons, biological scope is limited to those factors which determine glucose homeostasis as is commonly determined in 12-week, Phase 2 intervention trials via measurements of glycated hemoglobin (HbA1c). A review of information essential to a QSP effort in T2DM is provided. This includes a biological overview of the physiology and pathophysiology of glucose regulation along with the pharmacology of therapeutically relevant mechanisms of intervention. Literature references of use in quantifying key physiological and therapeutic effects are provided in this context. Although an explicit QSP model of T2DM is not provided, diagrams representing key pathways and organs are included along with an outline of the requisite steps in constructing such a model. Finally, two illustrative case examples of QSP model application in both preclinical and clinical pharmaceutical research are provided.

Keywords Gluconeogenesis · Frayn's text · Anti-diabetic drugs · Insulin analogs · Oral glucose tolerance test (OGTT) · Hyperglycemic clamp · Intravenous glucose tolerance test (IVGTT) · Hyperinsulinemic · Euglycemic clamp · Metabolic fluxes · Area-under-the-curve (AUC) · Hormone synthesis · Dalla Man model · Model qualification

J.R. Bosley
Clermont Bosley, LLC, 108 Soule Lane, Kennett Square, PA 19348, USA
e-mail: jbosley@clerbos.com

T.S. Maurer · C.J. Musante (✉)
Pfizer Inc., 610 Main Street, Cambridge, MA 02139, USA
e-mail: cynthia.j.musante@pfizer.com

T.S. Maurer
e-mail: tristan.s.maurer@pfizer.com

D.E. Mager and H.H.C. Kimko (eds.), *Systems Pharmacology and Pharmacodynamics*,
AAPS Advances in the Pharmaceutical Sciences Series 23,
DOI 10.1007/978-3-319-44534-2_20

20.1 Introduction

Diabetes Mellitus, a disease clinically characterized by hyperglycemia, has been estimated to affect as much as 9.5 % of the adult population, or about 347 million people worldwide (Danaei et al. 2011). The disease exists in two forms: type 1, characterized by insulin-deficiency resulting from pancreatic β-cell loss; and type 2, characterized by insulin resistance and compensation/decompensation of pancreatic β-cell function. Both forms are associated with serious micro- and macro-vascular sequelae which impose significant morbidity and mortality for patients. Debilitating complications include neuropathy, nephropathy, and retinopathy, with diabetes being a leading cause of renal failure, new blindness, and non-trauma amputations. These complications, in turn, impose a significant economic burden to society, with indirect and direct costs estimated at $245 billion for the U.S. alone in 2012 (American Diabetes Association 2013). Even more alarming, diabetes is a rapidly growing global epidemic for which the Centers for Disease Control estimate will affect 1 in 3 adults in the U.S. by 2050 if current trends continue (Boyle et al. 2010). This is despite the fact that diabetes is an ancient disease; the term being coined by Demetrius of Apameia in the 1st or 2nd century BC and symptoms being recorded in Indian texts dating as far back as the 5th century BC (Eknoyan and Nagy 2005). Enormous research investments have generated a substantial body of information related to diabetes etiology, manifestation, progression, and response to treatment. Although great strides have been made in the last century with the discovery of insulin and oral anti-diabetic agents, there is currently no well-functioning pharmaceutical intervention for diabetes. Furthermore, like many therapeutic areas, pharmaceutical research in diabetes is costly and associated with an unacceptably low probability of clinical success (Paul et al. 2010).

In order to address the unmet needs of diabetic patients, improvements in decision-making within the pharmaceutical industry are required with regard to both: (1) the selection of viable molecular targets and novel therapeutic molecules and (2) the design of cost effective clinical trials. With regard to the former, classical reductionist approaches have provided insight into specific molecular mechanisms related to diabetes metabolism and disease pathophysiology, but the associated therapeutic implications for relevant clinical trial outcomes (e.g., HbA1c) are not clear, as the etiology, manifestation, and progression of diabetes occurs across multiple metabolic and signaling pathways, organs, and cell types. Descriptive pharmacostatisical models are effective tools in analyzing clinical data to design optimal subsequent studies. However, they are of more limited value when used to predict clinical outcomes where there is no direct prior clinical experience as with novel therapies, new combinations, or untested patient populations. These challenges and limitations to decision-making have motivated physiologically-based systems modeling approaches. In fact, diabetes represents one of the more tractable diseases for a quantitative systems pharmacology (QSP) approach due to an abundance of available biochemical biomarker information, which have defined some of the key metabolic pathways of importance in

conditions of normal and impaired glucose homeostasis. The need for the type of quantitative framework provided by QSP modeling is also clear due to the complex network of interacting diabetes mechanisms. For example, the system has multiple, interacting feedback loops (e.g., insulin effect on glucose storage, release, and disposal), multiple parallel pathways (e.g., the effects of glucose, incretins, and glucagon on insulin secretion), nonlinear responses (saturation effects of drugs, endogenous hormones, and metabolites), time-dependent responses (e.g., plasma glucose can be higher, the same, or lower than baseline in response to a meal or glucose challenge, depending upon relative sampling time), and state-dependent responses (e.g., the net flux of some pathways can change sign depending upon fed or fasted condition and differs by disease state). Other complexities common to disease modeling are also present, such as inter-subject variability (e.g., disease state, genetic and phenotypic differences in metabolism, disease etiology, diet, and therapeutic intervention history) and intra-subject variability (e.g., assay variability, day-to-day compliance with treatment(s), food intake, and exercise). As described by Cedersund and Strälfors (2009), such models must represent the physiological knowledge of glucose homeostasis at multiple levels including the whole-body, organ, and cellular level to allow clinical predictions for decision support. This QSP approach (also called multiscale, hierarchical, or mechanistic modeling) is required for the aforementioned pharmaceutical applications as it allows linkage of drug mechanisms and disease pathology occurring at the cellular level to clinical whole-body manifestations. Such an approach also allows for some practical modularity at the organ level where evolving details of cellular metabolism and signaling within an organ can be incorporated and evaluated with respect to the arteriovenous balance of key metabolites (e.g., glucose, insulin, GLP-1, glucagon, and FFA) within an organ as it functions in the context of the whole-body model. Although many isolated and incomplete components of such a modeling approach exist at the whole-body, organ, and cellular metabolism/signaling levels, there are few examples where these components have been functionally integrated in this manner (Ajmera et al. 2013).

The first and perhaps most complex published example of such a systems pharmacology model of glucose homeostasis is that by Kim et al. (2007), which describes hormonal control over relevant cellular metabolic processes in response to 60 min of moderate intensity exercise in fasting healthy subjects. This particular model captures the dynamics of carbohydrate and lipid metabolism within key organs (e.g., brain, heart, liver, gastrointestinal (GI) tract, muscle, and adipose tissue) and interaction at the whole-body level with respect to blood/tissue transport of numerous circulating metabolites (e.g., glucose, insulin, pyruvate, lactate, glycerol, alanine, fatty acids, triglyceride, oxygen, and carbon dioxide). A short duration of moderate exercise is assumed to affect epinephrine concentrations as a function of time and work rate, which in turn, modulates glucagon and insulin secretion through a controller that maintains a constant blood glucose concentration. Metabolic fluxes upon exercise are modulated in a number of ways including: as direct step change to ATP hydrolysis (due to neural activation in heart and muscle); as a function of glucagon/insulin ratio (in the liver); as a nonlinear function

of epinephrine (in tissues not expressing glucagon); and as a combined nonlinear function of epinephrine and insulin (lipolysis in GI and adipose). The model is parameterized from literature information at several levels including: tissue flow and size; O_2 and CO_2 consumption; steady-state arterial and tissue concentrations of metabolites; and steady-state uptake and release rate of metabolites in tissues. These data are used to determine the 25 intracellular metabolic fluxes across 6 organs at rest via flux-based analysis. Finally, twenty-seven parameters related to hormonal control and dynamic responses of epinephrine, glucagon, and insulin to a change in work rate are either estimated by "adjustment" or a nonlinear optimization algorithm matching whole-body glucose appearance/disappearance rates and arterial metabolite concentrations. Another notable model of this nature is that of Chew and colleagues (2009a, b), which includes cellular level detail regarding insulin signaling. In this work, two independent publications of insulin signaling (Sedaghat et al. 2002) and whole-body glucose homeostasis (Cobelli and Mari 1983) are combined in a manner that maintains fidelity with the underlying data in response to a glucose challenge at both levels. Interstitial insulin from the whole-body model is used as input to the insulin signaling model, and glucose uptake rate from the insulin signaling model is fed back to the whole-body model via a Michaelis–Menten function (with Vmax as a function of the fraction of GLUT4 receptors at the cell surface as output from the insulin signaling model). Two parameters are estimated, namely a theoretical upper limit to Vmax for the entire body (assuming all GLUT4 are at the cell surface) and a Km for GLUT4 transport. Although this model seems to imply that insulin signaling can be scaled in this manner, it is not highly constrained by the whole-body model and generates parameters that are either inconsistent with independent estimates (Km) or which cannot be independently verified (Vmax). Perhaps the most ideal approach published to date is that from Nyman et al. (2011) which links insulin signaling in adipocytes to whole-body glucose homeostasis. At the top physiological level, several key organs (gastrointestinal tract, liver, pancreas, muscle and adipose tissue) interact via glucose and insulin to govern glucose homeostasis at the whole-body level. Each organ is highly constrained by insulin and glucose input/outputs in keeping with that modeled from triple-tracer studies performed following a meal challenge in healthy subjects (Dalla Man et al. 2007). A model of insulin control of glucose determined in primary adipocytes was then modified by constraints imposed by glucose uptake in adipose tissue according to the whole-body glucose homeostasis model. Finally, this approach was further used to incorporate more detailed models of insulin signaling. The result is a mathematical model that could feasibly be used to scale new in vitro data obtained in adipocytes (e.g., novel therapeutic interventions) to an expectation in whole-body glucose homeostasis. This approach is attractive in that the modularity provides a means for codifying and constraining increasing levels of detail, both at the top and subcellular level, necessary to support drug discovery efforts. This aspect is particularly important as the currently published models lack the degree of detail necessary to support drug discovery efforts. More specifically, the models mentioned focus largely on the healthy state; lack one or more key hormonal controls of relevance to drug action (e.g., glucagon, GLP-1, and/or FFA); do

not include the ability to simulate glucose control in daily life, and; lack linkage to clinically relevant endpoints (e.g., HbA1c). Other more comprehensive models, such as those described in the case examples later in this chapter, exist but are proprietary and therefore not freely available to the scientific community. For this reason, while the number of mathematical models being developed in support of diabetes research has been steadily increasing over the past 50 years (Ajmera et al. 2013; Landersdorfer and Jusko 2008; Li et al. 2010), there are no publications that describe the application of such a human systems diabetes model to support pharmaceutical research. With this application in mind, we define fit-for-purpose quantitative systems pharmacology models as those having a structure based upon physiological knowledge, with adequate mechanistic detail to represent pathophysiological dysregulation and drug action.

This chapter provides information to those seeking to develop such a QSP model of diabetes. Although an explicit model is neither published nor described in detail herein, case examples are provided to illustrate how critical development decisions can be supported by the prediction of changes in glycated hemoglobin (HbA1c) in response to novel therapeutic interventions as typically observed in a 12-week Phase 2b trial. Until there are widely available, detailed, and comprehensive diabetes models, the information here is offered as a starting point and guide to creating and using such models, with brief accounts to show how this is already being done within the industry.

20.2 Diabetes Biology Overview

Glucose homeostasis—the balance between the pancreatic hormones, insulin and glucagon, to maintain healthy blood glucose concentrations—is a tightly regulated process involving multiple organs and pathways. Diabetes is a complex disease characterized by chronically elevated blood glucose concentrations in the fasted state (overnight fasted or postabsorptive plasma glucose), the fed state (postprandial glucose), or both. The American Diabetes Association (ADA) (2014) has defined four criteria for diabetes diagnosis:

- HbA1c $\geq$ 6.5 %

  OR

- Fasting plasma glucose (FPG) $\geq$ 126 mg/dL (7.0 mmol/L)

  OR

- 2-h plasma glucose $\geq$ 200 mg/dL (11.1 mmol/L) during an oral glucose tolerance test (OGTT)

  OR

- A random plasma glucose $\geq$200 mg/dL (11.1 mmol/L), in patients with classic symptoms of hyperglycemia or hyperglycemic crisis.

In addition, the ADA has classified individuals at increased risk for developing diabetes (i.e., pre-diabetes) as having impaired fasting glucose (IFG) or impaired glucose tolerance (IGT):

- IFG: fasting plasma glucose (FPG) concentrations of 100–125 mg/dL (5.6–6.9 mmol/L)
- IGT: 2-h plasma glucose (2-h PG) in the 75-g oral glucose tolerance test (OGTT) of 140–199 mg/dL (7.8–11.0 mmol/L).

20.2.1 Glucose Homeostasis in Non-diabetic Subjects

Normal glucose tolerant individuals are capable of maintaining blood glucose concentrations in a healthy range under a variety of conditions. The primary mechanisms responsible for glucose homeostasis differ under fed and fasted conditions. In response to food intake, carbohydrates and other nutrients in the stomach are released into the lumen of the proximal small intestine at a gastric emptying rate that varies depending on a number of factors, including the volume of food in the stomach and the composition of the meal (energy content, nutrient composition, etc.). Nutrients are digested and absorbed as they travel through the intestinal tract, while a small amount remain unabsorbed and are excreted in the feces. Blood glucose concentrations rise and the incretin hormones, glucagon-like peptide 1 (GLP-1) and gastric inhibitory peptide (GIP), are produced from intestinal L and K cells, respectively. GLP-1 and GIP released into the circulation signal pancreatic beta cells to produce and secrete insulin. The first-phase of insulin secretion, from pre-formed insulin stored in vesicles in the beta cells, begins just minutes after meal ingestion and is followed by a second phase of insulin production and secretion that continues until glucose concentrations return to baseline.

In this postprandial state, glucose concentrations are controlled largely through the action of insulin (Fig. 20.1). Glucose-stimulated insulin secretion (GSIS) from the pancreas suppresses glucagon production and signals the body to preferentially utilize glucose and store excess energy as glycogen or fat. In the liver, hepatic glucose production is suppressed, hepatic glucose uptake through the enzyme glucokinase is increased, and glucose that is not oxidized is stored in the form of glycogen primarily under the action of glycogen synthase. In adipose tissue, lipolysis is inhibited by insulin action, free fatty acid (FFA) uptake is increased, and excess fat is stored in the form of triglycerides. Skeletal muscle is responsible for taking up the majority of glucose after a meal through the action of GLUT4 transporters; glucose is oxidized to meet the energy needs of the tissue and excess is stored in the form of glycogen to meet future energy demands. In this way,

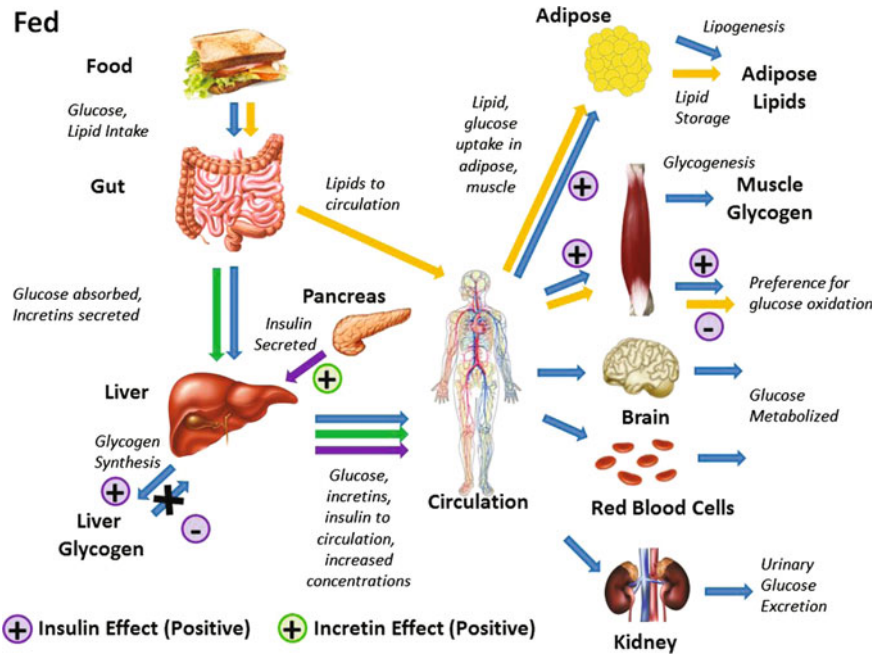

Fig. 20.1 Metabolic fluxes in the fed state, with glucose (*blue*), incretins (*green*), insulin (*purple*), and lipids (*yellow*). Major fluxes are shown as *arrows*, with the effects of insulin and incretins highlighted

postprandial glucose excursions are controlled until all nutrients have been absorbed and pre-meal glucose concentrations are restored.

In the overnight fasted state (Fig. 20.2), blood glucose concentrations are maintained primarily through hepatic glycogenolysis and gluconeogenesis, each contributing approximately 50 % to hepatic glucose output. Gluconeogenesis is the process by which the body converts non-sugar substrates (mainly lactate, alanine, and glutamine) to glucose. An increase in adipose tissue lipolysis supplies fatty acids for fuel to peripheral tissues, sparing glucose for use by the brain. The brain has limited capacity to store nutrients to meet its energy demands and, therefore, a continuous supply of fuel in the form of glucose or ketone bodies is necessary for survival. During a prolonged fast lasting a day or more, glucagon concentrations increase in response to hypoglycemia, hepatic fatty acid (FA) uptake and metabolism are increased along with ketone production, providing an alternate fuel source to maintain brain function. Under these conditions, when muscle and liver glycogen stores are low, hepatic and renal gluconeogenesis are the primary sources of glucose to the circulation. The reader is referred to Frayn's text (2010) on human metabolism for more information.

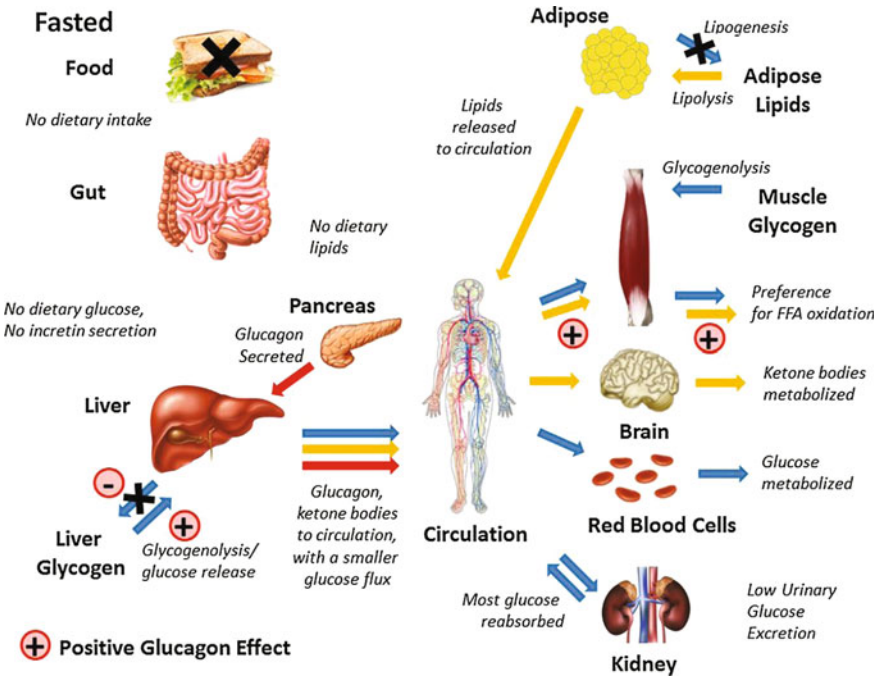

Fig. 20.2 Metabolic fluxes in the fasted state, with glucose (*blue*), glucagon (*red*), and lipids (*yellow*). Major fluxes are shown as *arrows*, with the effects of glucagon highlighted

20.2.2 Impaired Glucose Regulation in Individuals with Type 2 Diabetes

The pathogenesis of type 2 diabetes includes pancreatic beta cell insufficiency (the inability to secrete sufficient insulin to meet glucose demands) and insulin resistance (impairment of signaling of insulin at various tissues). Although the sequence of events leading to the diabetic state are unclear, early in the disease the beta cells increase insulin production to compensate for peripheral insulin resistance. As the disease progresses, beta cell function gradually declines and may result in beta cell failure, requiring exogenous insulin delivery to maintain adequate glucose control.

Diabetes may result from a combination of environmental (e.g., diet and exercise) and genetic predispositions (Leahy 2005; Nolan et al. 2011; Ostenson 2001). Current treatment options (Table 20.1) may slow or delay the progression of the disease; however, as evidenced in the UKPDS trial (UK Prospective Diabetes Study (UKPDS) Group 1998a, b), treatment effects are not durable. Persistently elevated glucose and lipid concentrations, characteristic of the diabetic phenotype, lead to further progression of the disease and have been attributed to gluco-, lipo-, or glucolipotoxicity, at the pancreatic beta cells and cells of other organs (Ostenson 2001).

Table 20.1 Anti-diabetic drugs and insulin analogs

Main pathway	Function	Type/target	Subclass and *examples*	
Insulin	Sensitizers	Biguanides	Metformin[a], Buformin[b], Phenformin[b]	
		TZDs/ "glitazones" (PPAR)	Pioglitazone, Rivoglitazone[c], Rosiglitazone, Troglitazone[b]	
		Dual PPAR agonists	Aleglitazar[c], Muraglitazar[d], Saroglitazar, Tesaglitazar[d]	
	Secretagogues	K + ATP	Sulfonylureas—1st Generation	Acetohexamide/Carbutamide, Chlorpropamide, Metahexamide, Tolbutamide, Tolazamide
			Sulfonylureas—2nd Generation	Glibenclamide (Glyburide)[a], Glibornuride, Glipizide. Gliquidone, Glisoxepide, Glyclopyramide, Glimepiride, Gliclazide
			Meglitinides/`glinides"	Nateglinide, Repaglinide, Mitiglinide
		GLP-1 agonists	Exenatide, Liraglutide, Taspoglutide[c], Albiglutide[c], Lixisenatide	
		DPP-IV inhibitors	Alogliptin, Anagliptin, Gemigliptin, Linagliptin, Saxagliptin, Sitagliptin, Teneligliptin, Vildagliptin	
		GPR40 Free fatty acid receptor 1	Fasiglifam[c]	
	Analogs/other insulins	Insulin or insulin receptor ligand	Fast acting	Insulin, lispro, Insulin aspart, Insulin glulisine
			Short-acting	Regular insulin
			Long-acting	Insulin glargine, Insulin detemir, NPH insulin
			Ultra-long acting	Insulin degludec[e]
Other	Alpha-glucosidase inhibitors		Acarbose, Miglitol, Voglibose	
	Amylin analog		Pramlintide	
	SGLT2 inhibitors		Canaglifozin, Dapaglifozin, Empaglifiozin[c], Remoglifozin[d], Sergliflozln[d], Tofogliflozin[c], Ertuglifozin[c]	
	Other		Bromocriptine, Benfluorex[b], Tolrestat[b]	

Adapted from Wikipedia contributors (2015)

[a]Therapy is a WHO essential medicine, [b]Withdrawn from market, [c]Phase 3 clinical trials, [d]Did not progress to Phase 3, [e]Approved in Europe and Japan, FDA has declined to approve and requested more information, trial underway

A hallmark characteristic in the development of type 2 diabetes is impairment of first-phase insulin release in response to a glucose challenge (Del Prato et al. 2002; Bunt et al. 2007). Several studies have demonstrated the importance of early insulin secretion in the control of postprandial hyperglycemia, although insufficient suppression of glucagon secretion and endogenous glucose production may also contribute to this effect (Bruce et al. 1988; Luzi and DeFronzo 1989; Markovic et al. 1995). Deficiency in insulin secretion and impairment of insulin signaling result in an imbalance in the rate of glucose appearance and disappearance in the postprandial state, leading to hyperglycemia (Aronoff et al. 2004). In the overnight fasted state, elevated glucagon secretion and hepatic glucose production contribute to fasting hyperglycemia, although the contribution of hepatic glucose production likely is less than originally reported (Beck-Nielsen et al. 2002).

Several clinical protocols have been developed for diabetes diagnosis or assessment (Table 20.2). Although we primarily have focused on differences between glucose, insulin, and glucagon concentrations and signaling between the non-diabetic and diabetic conditions, many other metabolic changes occur with progression from the healthy to disease state. Some of these differences have been referenced in Table 20.3. The data contained in the sample references from Tables 20.2 and 20.3 may serve as calibration or validation data for a diabetes systems pharmacology model, as discussed in the next section.

20.3 Quantitative Systems Pharmacology Modeling Approach

The first step in diabetes QSP modeling is to define the research question or decision that the modeling will support or change. A written model plan should include: modeling program goals, model scope, data to be used, criteria that define testing and stopping points, and specific predictions that will be needed to support the research goals.

Scoping and planning

1. Define the research question in a way that supports program goals and timelines
2. Define the data required to build and test the model
3. Define and graphically formalize the necessary scope and level of model detail required

Develop the model

4. Mathematically formalize a parsimonious model of glucose regulation
5. Enhance the model by adding function and detail as required for the research question

Table 20.2 Clinical protocols in diabetes diagnosis or assessment

Test	Protocol	Direct or indirect measures	Sample references
Oral glucose tolerance test (OGTT)	Ingestion of 50-, 75-, or 100-g glucose solution	Overnight fasted and 2-h glucose and insulin measurements frequently utilized as diagnostic test; beta-cell sensitivity to glucose; tissue sensitivity to insulin	Færch et al. (2008), Ceriello et al. (2011), De Gaetano et al. (2013), Møller et al. (2014), Meyer et al. (2004)
Intravenous glucose tolerance test (IVGTT); frequently sampled IVGTT (FSIVGTT)	Glucose injected into vein at 300 mg/kg for 1 min	First-phase insulin response; beta-cell sensitivity to glucose; tissue sensitivity to insulin	Bergman et al. (1981), Quddusi et al. (2003)
Hyperglycemic clamp	Plasma glucose levels are acutely raised to 125 mg/dL above basal and maintained at this level by variable glucose infusion	Beta-cell sensitivity to glucose; tissue sensitivity to insulin	DeFronzo et al. (1979), Rave et al. (2010)
Hyperinsulinemic, euglycemic clamp	Plasma insulin levels are acutely raised to 100 μU/mL and maintained at this level by continuous insulin infusion. Plasma glucose levels are held constant at basal (euglycemic) levels by a variable glucose infusion	Tissue sensitivity to insulin; considered "gold standard" for assessment of whole-body insulin sensitivity; endogenous glucose production	DeFronzo et al. (1979, 1985)
Two-step hyperinsulinemic, euglycemic clamp	Hyperinsulinemic, euglycemic clamp protocol at low and high insulin infusion rates (protocols vary)	Hepatic and peripheral insulin sensitivity	Johannsen et al. (2014), Perriello et al. (1994)
Short-term fast	Calorie deprivation for 2–3 days	Plasma glucose, insulin, free-fatty acids, ketone bodies, and other biomarker concentrations	Horowitz et al. (2001), Beer et al. (1989), Browning et al. (2012), Watts and Digirolamo (1990)
Multiple mixed meal tests	Protocols vary; typically consist of three standardized meals over the course of one day	Plasma glucose and insulin time-course measurements	Polonsky et al. (1988a, b), Peter et al. (2010)

Table 20.3 Sample references illustrative of those that may be used in the calibration and validation of select metabolic parameters, pool sizes, or pathways in a diabetes systems pharmacology model

Parameter, pool, or pathway	Types of protocols	Sample references
Plasma C-peptide concentrations	Single nutrient or mixed meal challenges; incretin infusions	Meier et al. (2007), Christensen et al. (2014)
Plasma incretin concentrations	Single nutrient or mixed meal challenges; incretin infusions	Bagger et al. (2011), Vilsbøll et al. (2003), Christensen et al. (2014)
Plasma glucagon concentrations	Single nutrient meals or mixed meal challenges; incretin infusions	Lund et al. (2011), Christensen et al. (2014)
Gastric emptying rate	Imaging following liquid and solid meals, paracetamol absorption	Seimon et al. (2013), Horowitz et al. (1991), Bagger et al. (2011), Samsom et al. (2009)
Endogenous glucose output	Euglycemic, hyperinsulinemic clamp; tracer techniques	Ferrannini et al. (2014), Merovci et al. (2014), Toffolo et al. (2006)
Liver glycogen content	In vivo analytical imaging techniques (e.g., nuclear magnetic resonance (NMR) spectroscopy)	Stephenson et al. (2013), Tomiyasu et al. (2010), Petersen et al. (2001)
Muscle glycogen content	In vivo analytical imaging techniques (e.g., NMR)	Stephenson et al. (2013), Roden (2001)
Glomerular filtration rates (GFR, eGFR)	Inulin, ^{51}Cr-EDTA, or ^{99}mTc-DTPA plasma clearances (GFR); or estimated from serum creatinine levels (eGFR)	Mussap et al. (2002), Premaratne et al. (2005), Zhang et al. (2010)
24-h urine glucose excretion	Urine collection over a 24-h period	Zhang et al. (2010), Kapur et al. (2013)
Insulin response to GLP-1 infusion	IVGTT + GLP-1 infusion; graded glucose infusion + GLP-1; meal + GLP-1 infusion	Ahrén et al. (2003), Kjems et al. (2003), Brandt et al. (2001), Quddusi et al. (2003)

6. Augment model to allow simulation of required protocols
7. Evaluate sensitivity of model outcomes to parametric and structural changes
8. Create sets of parameters representing inter-subject variability
9. Evaluate and document model performance

Apply the model

10. Exploit the model to support research goals

20.3.1 Scoping and Planning

20.3.1.1 Define the Research Question in a Way that Supports Program Goals and Timelines

QSP models can support a range of research questions relevant to pharmaceutical research and development, including predictions of: (1) efficacy relative to standards of care, (2) efficacy in combination, (3) efficacy in diabetic subpopulations, (4) durability of efficacy with respect to disease progression (5) safety risk (e.g., hypoglycemia), (6) different dose regimens to determine an optimum for efficacy and safety, and (7) identification of biomarkers related to efficacy or safety. The research question of interest strongly influences model scope. For example, if co-morbidities of diabetes are of interest, the macro- and micro-vascular pathophysiologies that occur secondary to impaired glucose homeostasis must be included. The discussion here is focused on efficacy of glucose regulation in response to a novel compound. The HbA1c endpoint is the clinical standard for this and must be included in a way supporting predictive simulations for a representative trial duration (chosen here as 12 weeks). The model must allow replication of data for the intended trial population, for example, in moderate to severe diabetic subjects ranging from normal weight to obese. The model scope should include a list of physiological components necessary to give accurate response to target modulation of the drug of interest in the population of interest. Exclusions to scope should be explicitly stated. In this chapter, disease progression and beta cell health are excluded, but these can be (and have been) represented in other models.

20.3.1.2 Define the Data Required to Build and Test the Model

A key advantage of QSP modeling is the ability to exploit a wide range of data directly by providing physiological context to integrate disparate data sets to predict human outcomes. This allows building and testing model components individually (e.g., specific rate equations) or as an integrated system (whole-body tests). There are nearly half a million diabetes references in PubMed, leading to a strong recommendation that the modeler work closely with a diabetes domain expert(s) familiar with the pathophysiology of the disease. Such an expert can efficiently find, evaluate, curate, disqualify, and select data needed to build a model.

Each individual reaction or flux in the model requires data to establish the appropriate kinetics. Fitting individual reactions with small data sets is a well-developed skill in pharma R&D and is not covered here. The model components are integrated using pathway analysis, known physiology, and mass conservation laws. The list of required data must be sufficient to build and test the integrated disease model. This is best done using data from a variety of different experiments.

As the QSP model is created and improved, whole-body testing using standard diabetes clinical protocols may guide development and provide tests for the model.

The data set should support this for normal and diabetic physiology. The data set includes the types of clinical study data listed in Table 20.2. Clamp studies are useful in modeling for the same reason that they are useful in the clinic: they eliminate confounding changes. For example, fixing glucose concentrations with infusions allows assessment of beta cell sensitivity to glucose or hepatic/peripheral insulin sensitivity. Acute nutrient challenges, such as intravenous or oral glucose, meals of mixed macronutrient composition, or caloric restriction, are also useful. Many of the protocols listed in Table 20.2 include references to relevant data, collected in both the healthy and diabetic state.

The model must not only match steady-state (e.g., clamps, fasting) data, but also must reproduce the size and timing of various challenges and therapeutic interventions. These data include dynamic responses of other endogenous compounds (e.g., incretins, glucagon); physiological processes (e.g., gastric emptying, glomerular filtration rate (GFR), renal glucose excretion, and endogenous glucose output); and physiological pools (e.g., liver and muscle glycogen, plasma c-peptide, incretin, and glucagon). Table 20.3 provides illustrative examples of these types of data with reference to both the healthy and diabetic conditions.

QSP models can use clinical data from studies of existing therapies for building and testing of the model. Especially useful are data for existing drugs that have pathways that overlap with that of a novel study drug. For example, GPR119 agonists affect the release of GLP-1; therefore, a base QSP model for GPR119 should account for therapeutic responses to DPP-IV inhibitors and GLP-1 agonists. Likewise, the SGLT2 model described in the case examples was built in part from publically available data, such as glucose clamp data (which characterize the renal glucose threshold) and emerging clinical pharmacology data on the effect of SGLT2 inhibition on renal glucose threshold. Table 20.1 provides an overview of the range of therapeutic mechanisms available for the construction of a fit-for-purpose diabetes QSP model.

20.3.1.3 Define and Graphically Formalize the Necessary Scope and Level of Model Detail Required

Once the research question is defined and relevant data cataloged, a graphical representation of the relevant biology is indispensable in defining the scope of a model. Biological diagrams are ubiquitous; however, schematics used for modeling require a stricter formalism. A useful discussion of modeling diagrams, as well as examples of process diagrams for biology are available (Kitano et al. 2005). The simple "process diagram with reduced notation" approach from Kitano et al. is used here.

Figures 20.3, 20.4, and 20.5 are schematic diagrams (available in the supplemental material) representing important components of diabetes physiology, pathophysiology, and treatments for a model consistent with the research goal in this chapter. They are implemented in freely available software called Pathway Designer (formerly JDesigner, available at pathwaydesigner.org) (Bergmann et al. 2006; Bergmann and Sauro 2006; Hucka et al. 2002). The diagrams are based upon

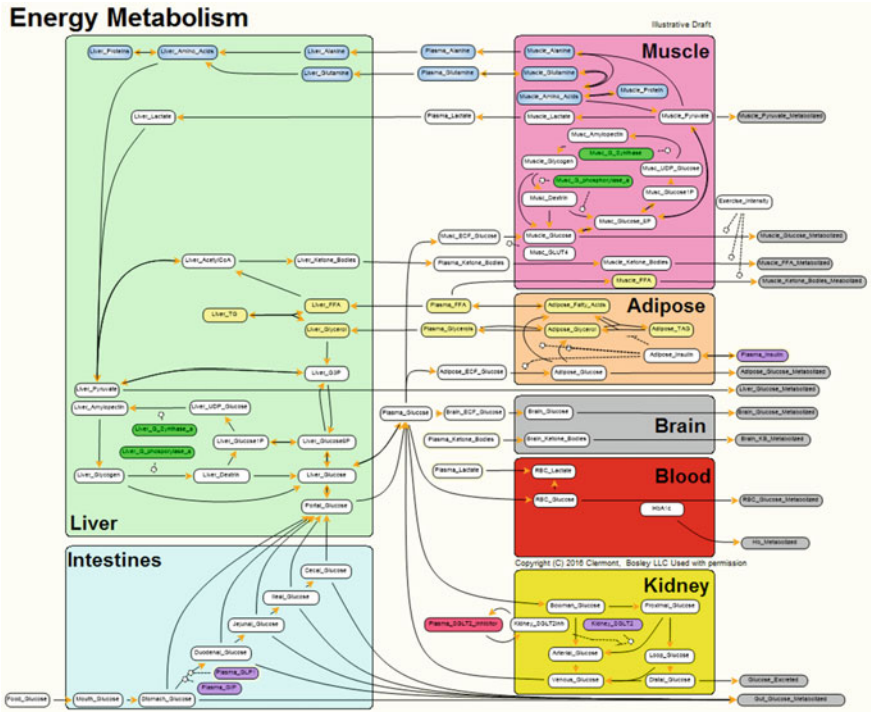

Fig. 20.3 Important aspects of the physiology of energy metabolism in diabetes

many literature sources, including those cited in the biology subsection. A comprehensive collection of detailed metabolism-related diagrams relevant to diabetes is also available (Salway 2004). The figures are similar to several models the authors have built and applied, including those models described in the case study section, which contain a level of detail intended to define a model that can predict HbA1c over a range of experimental conditions. These diagrams are illustrative, and are meant as a starting point for experienced modelers.

Each graphical component in Pathway Designer has a formal mathematical meaning. These are exemplary of many software packages and are illustrative. A "bubble" or node represents a quantity. Some nodes represent a balance equation for a specific biological entity, in a specific state, in a specific location. These are called state or floating nodes. Arrows represent fluxes, which can be reaction rates or fluxes between state nodes. Another type, a boundary node, represents values that are either set by the user as a fixed parameter or calculated by the model based upon algebraic calculations. The influences of states and fixed and calculated values on the various fluxes between state nodes are shown graphically as modifiers (dashed lines ending with crossbars or open circles to designate inhibition or induction). Concrete examples of what state nodes represent include both small molecules (e.g., amount of glucose in plasma) and larger molecular structures (such as GLUT4 transporters

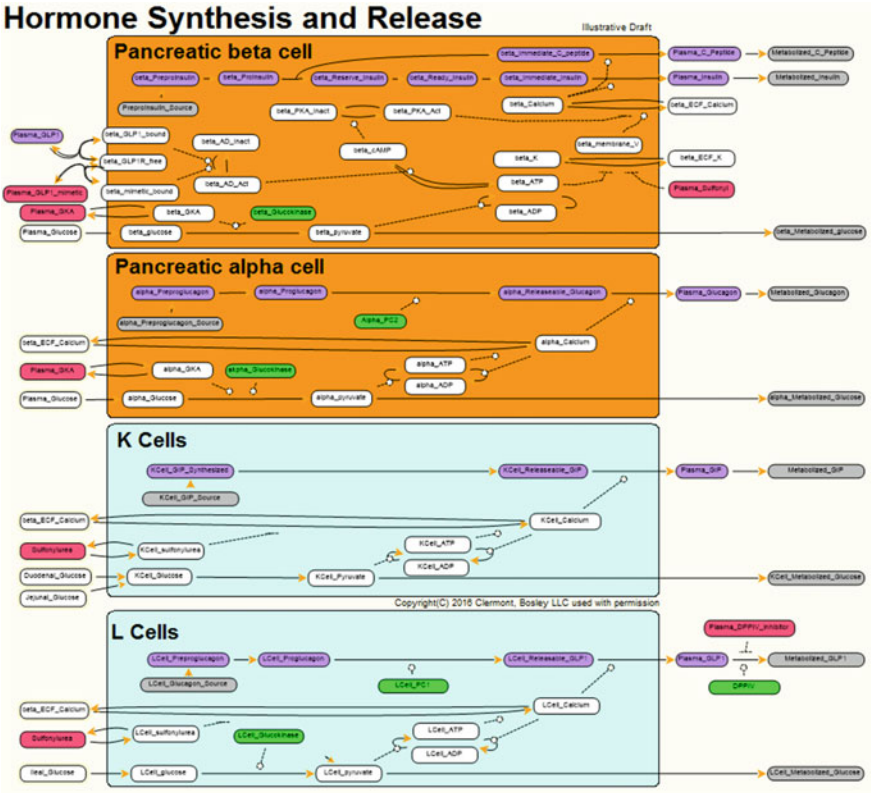

Fig. 20.4 Details of hormone synthesis and release

internal to vesicles in the muscle cells and the mass of glycogen in the liver). Fluxes can represent reactions (e.g., phosphorylation of glucose in the liver) or translocation (e.g., GLUT4 moving from vesicles in the cytosol to muscle cell surface due to the effect of insulin). The main metabolic fluxes are shown in Fig. 20.3, where the most important fluxes relate to trafficking of carbohydrates (mostly as glucose) in the intestines, liver, plasma, muscle, red blood cells, adipose, and brain tissues. Based on the research question that was defined earlier, lipid metabolism is represented in limited form in order to simply account for macronutrient intake, oxidation, and storage. Hormonal signals are shown originating in the pancreatic alpha and beta cells, and in the intestinal L and K cells, in Fig. 20.4. Figure 20.5 illustrates details involved in enzyme activation, hormone production, and release by specific cells, and again, alias nodes provide links.

QSP models should be written to allow simulation of a variety of protocols to facilitate the use of a broad range of data, including different clinical studies. In addition to what is shown in the supplemental diagrams, the model should include structure and parameters to allow such things as daily dosing and meals, various

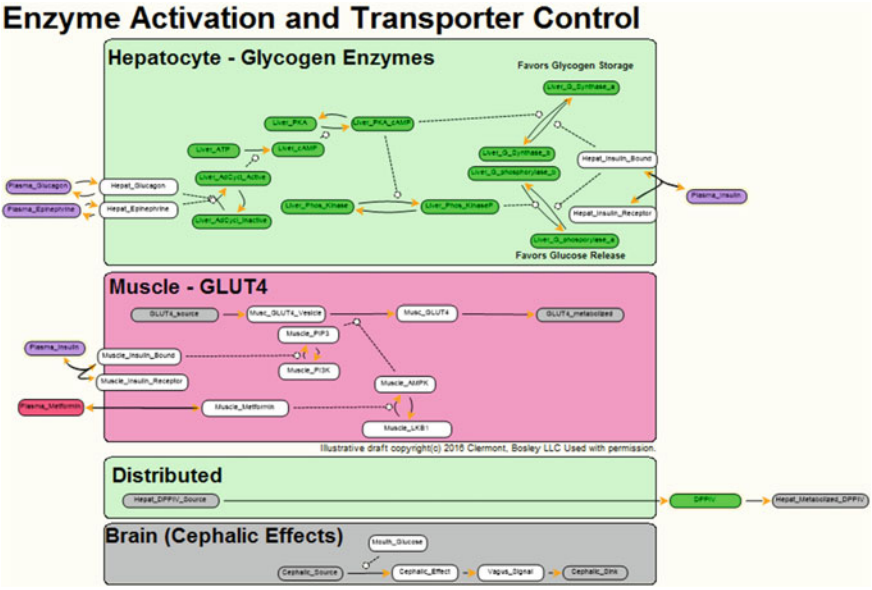

Fig. 20.5 Hormone and metabolites interact to influence both hormone balance and energy metabolism, connect to other diagrams via plasma glucagon and insulin, or by synthase/phosphorylase balance

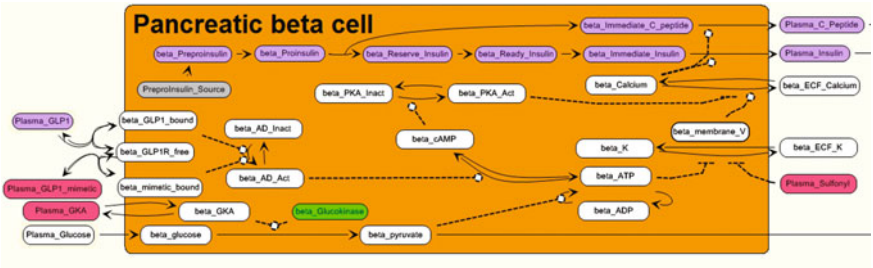

Fig. 20.6 A representative section of a physiological schematic. The specificity of the diagram supports efficient modeling and communication

useful metrics such as the area-under-the-curve (AUC) of glucose, and pharmacometric models for both the investigational drug and any other relevant therapy for which data are available.

Figure 20.6 is an expanded portion of Fig. 20.4. Bound and unbound receptors, and active and inactive enzymes, are represented as different nodes. Movements (e.g., insulin migrating from reserve- to ready- to immediately-releasable pools) or change of state (e.g., inactive to active adenylate cyclase) are represented explicitly as fluxes between nodes. This emphasizes the clear differences between mass flux (beta_immediate_insulin being released to the Plasma_Insulin) and influence on flux (in this case, of cytosolic beta_Calcium). Modeling assumptions and

simplifications are also clear, as is shown by the beta cell calcium node where an exclusively external source is shown (i.e., with endoplasmic reticulum calcium ignored).

20.3.2 Develop the Model

20.3.2.1 Mathematically Formalize a Parsimonious Model of Glucose Regulation

Experience suggests an efficient model-building process starts with a model that is simpler than that shown in Figs. 20.3, 20.4, and 20.5. The model should capture the gross features of physiology—glucose and insulin systems at a minimum—and should replicate to some degree the behavior contained in a selected subset of data. Several models of this nature have been described in the literature and can provide a reasonable starting place (Cobelli and Mari 1983; Dalla Man et al. 2007; Silber et al. 2010). The model by Dalla Man et al. (2007) is used here as an example. Figure 20.7 shows key components of metabolic physiology and their interactions at a high level.

The Dalla Man model has features that make it a useful starting point. Tritiated glucose is accounted for separately, allowing the use of a triple tracer database to determine rates and to understand physiological behavior at the level of key tissues (e.g., liver, kidney, muscle, adipose tissue, pancreas, and GI tract). The modular approach facilitates subsequent model enhancement, allowing the use of a wide

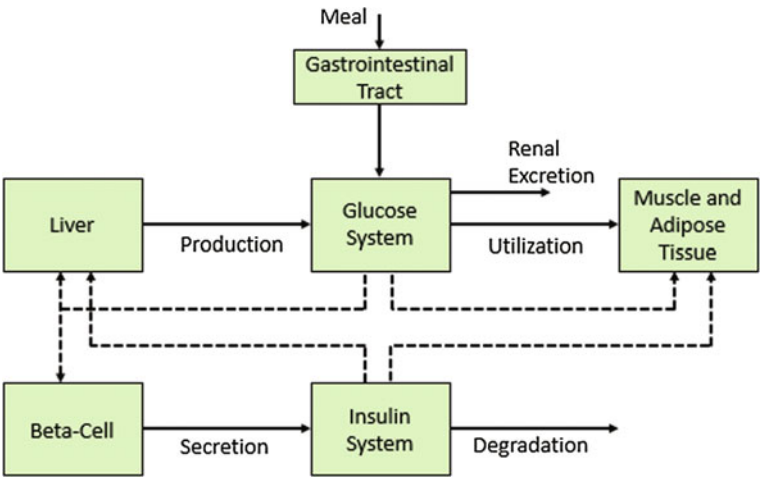

Fig. 20.7 A conceptual starting point with a modular structure, after Dalla Man et al. (2007). Each of the modules must be populated by states, rates, and mechanisms

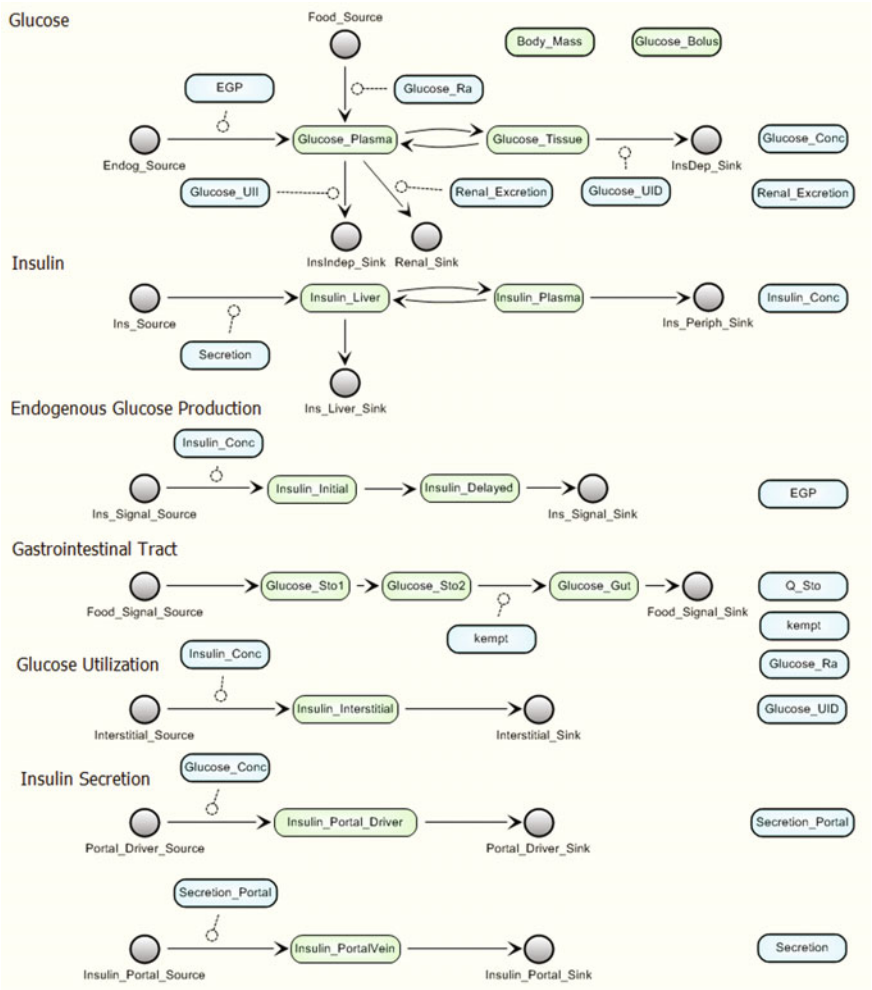

Fig. 20.8 The model of Dalla Man et al. (2007) expressed in the same schematic format as Figs. 20.3, 20.4, and 20.5 as implemented in Pathway Designer

variety of relevant datasets for glucose homeostasis such as fasting, various glucose challenges, and clamp-type studies. The influence of hormones, drugs, and metabolite pool sizes on the mechanism of action can be studied, and various data can be used to augment mechanistic detail. Different disease states should be modeled. It is most useful to start modeling with healthy subjects, modifying the model to account for aspects of disease (e.g., insulin resistance and impaired secretion of insulin). Dalla Man et al. (2007) provide two sets of parameters to represent normal and diabetic behavior (Fig. 20.8).

The modular structure allows the use of data specific and relevant to each module, which were integrated and tested with standard input-output data (e.g.,

glucose and insulin). The authors note that these data were insufficient to capture system behavior, and therefore they obtained data containing several intermediate measurements such as fluxes, rate of appearance, and production. This illustrates how QSP modeling can identify data gaps and focus lab and clinical work on obtaining data that informs not only model development but understanding of disease. The model predictions match not only the magnitude of changes of inputs and outputs, and of intermediate values, but also replicate the rates of rise and decay, times for maximum values, and other temporal trajectories. Taken together, extensive strict testing ensures that the model is suitable for purpose and builds confidence in predictive simulations.

In almost all cases, a simple model must be expanded before it can meet research needs. The prior scoping work will have defined the data to be used, and these data sources provide a checklist of experiments that the model must be able to replicate. Diagrams such as Figs. 20.3, 20.4, and 20.5 include the physiological detail to match the data and the components necessary to make predictive simulations to meet research needs. Moving from the simple model to the fit-for-purpose model involves three driving forces: protocol, mechanistic detail, and subject variability. These enhancements are covered sequentially in following sections and often proceed simultaneously.

20.3.2.2 Enhance the Model by Adding Function and Detail as Required for the Research Question

A prediction of the response of HbA1c over a representative trial duration is often desirable. This requires additions to an initial parsimonious model. For example, there are several possible approaches to relating glucose to glycated hemoglobin. There is a good correlation, albeit with wide confidence limits, between long-term average plasma glucose and HbA1c. Rohlfing et al. (2002) derived an algebraic correlation between average plasma glucose (PG) and HbA1c, which can be written as:

$$\mathrm{HbA1c}(\%) = 0.505 \times \mathrm{PG(mM)} + 2.17 \tag{20.1}$$

This equation reflects a steady-state relationship, ignores the time-dependency that is needed, and is reflected in Fig. 20.9a. Figure 20.9b shows a more realistic representation of glucose and hemoglobin binding. A simplification, which assumes that the plasma glucose pool is not significantly depleted by the glycation reaction, is shown in Fig. 20.9c. The latter approach has been found satisfactory in many cases. However, when erythropoesis or reticuloendothelial clearance is altered, the production or clearance of red blood cells may change the time-course of the effect of glucose on hemoglobin in the blood. For this case, Hamrén et al. (2008) have proposed a model that includes the blood cell life cycle (Fig. 20.9d). The authors used this approach to account for the hemodilution effect of tesaglitazar.

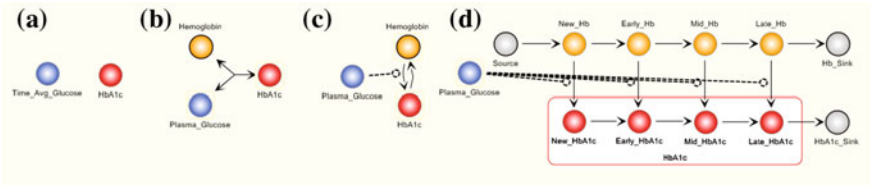

Fig. 20.9 Alternative methods of representing hemoglobin glycosylation to support HbA1c assay prediction

The manner in which insulin clearance is codified provides another example where a researcher may add varying degrees of mechanistic detail. A naïve first-order model of insulin release does not match data for an oral glucose challenge (Seino et al. 2011). Intravenous (i.v.) glucose challenge data have an insulin response that is closer to a first-order lagged model (i.e., an indirect response model with linear kinetics) (Zimei 2013). In an oral challenge, the insulin response is both larger initially and more sustained than can be represented by a simple model (Perley and Kipnis 1967). Physiology gives insight into additional model structure needed at this point. Cephalic effects help stimulate an early response (Taylor and Feldman 1982). Beta cells have a significant pool of readily releasable insulin that facilitates an initial release, which leads to adding a "readily releasable pool" of insulin to the beta cell model (Bratanova-Tochkova et al. 2002). Candidate sub-models for glucose-stimulated insulin secretion can be formulated in isolation and tested using stimulation of time-course data of glucose tests from the literature. Proinsulin is produced and cleaves to form insulin and C-peptide. C-peptide has a different clearance rate, and so may be used to quantify insulin secretion rates and determine transient secretion and clearance parameters.

Considering only insulin clearance, Fig. 20.10 illustrates four possible levels of detail and approaches. One level is represented as a simple flux from plasma to "Cleared_Insulin", using an appropriate rate law. Early development of the insulin receptor model was provided by Quon and Campfield (1991). Hovorka et al. (1993) added hepatocyte and peripheral tissue binding, and receptor-mediated clearance and recycling. Koschorreck and Gilles (2008), and others (notably Cedersund et al.; Brännmark et al. 2013; Cedersund et al. 2008; Nyman et al. 2011, 2012; Palmér et al. 2014), have proposed more complex binding, phosphorylation, clearance, and receptor recycle schemes. Shown in the figure is the scheme of Koschorreck and Gilles for insulin binding, clearance, and receptor recycling in adipose tissues (Fig. 20.10). Cedersund et al. (2008) also describe a useful methodology for deciding which structure is appropriate for matching data. The level of detail actually included in the model should reflect the research context.

A first step is to determine the rate of insulin secretion using both insulin concentration and C-peptide concentration data (Cauter et al. 1992). Using datasets for healthy individuals that provide glucose and insulin data, as well as the source documents that describe the more complex models, the several alternatives shown in Fig. 20.10 can be parameterized and compared with data. As can be seen in the

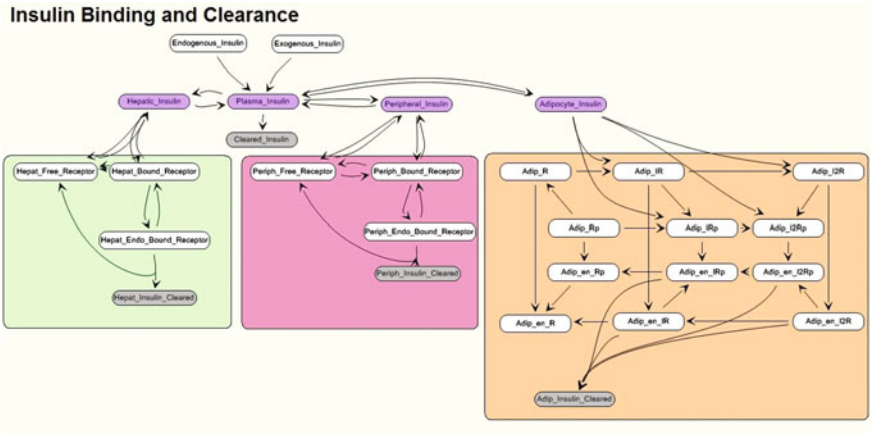

Fig. 20.10 Clearance of insulin by different pathways, showing examples of the different levels of physiological detail that may be chosen

GPR119 case, a simple first-order insulin clearance from a small number of compartments can be adequate in some cases. A more detailed and fundamental understanding, as provided for example by Nyman et al. (2011, 2012) and Brännmark et al. (2013), may be needed in other cases to provide a broader range over which the model is quantitative or to provide mechanistic sites of action for some therapies.

20.3.2.3 Augment Model to Allow Simulation of Required Protocols

The model needs to be able to simulate the protocols in the data list developed in scoping, and the protocols needed to support the research goal. At a minimum, non-physiological constructs are required, such as a 24-h clock to allow for meals, dosing, and testing at specific times. Other non-physiological protocol additions involve assays, which will have been identified in the data sources used to build the model. These may be simple mathematical constructs using existing model elements, such as an integrator of plasma glucose, to get an AUC. Other tests may require some logical programming, as for sampling the fasting glucose and insulin for HOMA test results, so that models of insulin resistance (Matthews et al. 1985; Levy et al. 1998) and beta cell function can be easily compared with data. Published data often describe glucose or meal challenges, administered at different times in the trial, and conditions for simulating these experiments. Protocol flexibility must be sufficient to match published protocols. For example, we may wish to predict the outcome of a 12-week trial where three mixed meals are given every day, with specific interest in oral glucose tolerance test results given on the first and last day of the trial. Conditions for implementing glycemic and insulinemic clamps are also necessary. Also required are pharmacokinetic and pharmacodynamic models of any

therapies to be used in building, testing, or using the model. It is very useful to have components in the model that allow isolation of specific modules for simulation and testing. This requires considerable effort. Sets of parameters that specify the length of simulation, the type of clinical protocol, the assays used, and how the results will be stored or displayed, are called virtual protocols and facilitate easy and repeatable setup of simulations. Protocols used to isolate systems of interest from confounding influences, for example glycemic or insulinemic clamps (Table 20.2), are also very useful for modeling. They allow for the direct assessment of physiological mechanisms in isolation, removing the confounding effect of changing glucose or insulin concentrations.

20.3.2.4 Evaluate Sensitivity of Model Outcomes to Parametric and Structural Changes

Model sensitivity analysis is a well-developed field in statistically-based modeling (Saltelli et al. 1999, 2004). Here, we focus on model outcome parametric sensitivity. Sensitivity analysis methods for systems biology models have been described (Marino et al. 2008; Sumner 2010), and at least one treatise focusing on glucose homeostasis (Sumner 2010). In large causal models, some of the underlying global statistical and analytical sensitivity treatments are not tractable. Whereas rigorous analytical approaches have appeal, a more practical approach may be to simply vary each model parameter in a "reasonable" or "physiological" range and observe the effect on outputs of interest. QSP model parameters often have physical meaning, and there may be lists of representative values published that may suggest this range. For example, finding a range of hepatic extraction of insulin is preferred over setting a range for an arbitrary parameter with no physiological meaning. A diabetes model will have nonlinearities and state-dependencies, and so the sensitivity analysis may need to be performed using different model states (e.g., normal and diabetic) or experimental conditions (e.g., fed or fasted) to be useful.

Several key outcomes may result from a sensitivity analysis. First, we may identify "potent" parameters to which the model is very sensitive. A large confidence interval for a potent parameter identifies a gap and suggests the need for additional data. This focuses lab and clinical work toward obtaining the most useful data. Parameters that do not affect model outcome strongly, or for which we have a very good estimate, do not require additional data. Parameter sensitivities should be reviewed with domain experts, and a subset of variables can be selected as useful in creating representative patients or patient-types. In a model with several hundred parameters, there are not sufficient experimental data that allow for classical simultaneous fitting of all parameters. Sensitivity analysis is used to select a subset of perhaps 5 to 20 parameters for use in differentiating between, for example, normal and diabetic subjects, or patients with impaired insulin resistance and secretion. Outcome sensitivity is a computation based upon mechanism, in the context of a specific clinical protocol. Therefore, the sensitivity in a complete model may indicate improvements in a protocol useful to the clinician. In addition, the

sensitivity analysis may highlight areas of improvement in drug design useful to the medicinal chemist (e.g., pharmacology, binding kinetics, specificity, fat solubility, and pKa).

20.3.2.5 Create Additional Sets of Parameters Representing Inter-subject Variability

For our example, a model representative of a healthy subject is adjusted parametrically to represent diabetic subjects. The parameters used to create diseased conditions are based upon physiology and inferred from the results of the sensitivity analysis. A cohort of "Virtual Patients" (or VPs) can be created to meet research needs. Each VP is a set of parameters that fit a given subject or patient type. They are generated from proprietary and published clinical data (we emphasize the usefulness of placebo patient data here), and from databases such as UKPDS (1998b) and NHANES (2015).

Manual approaches are available to create hundreds of VPs with a diabetes model by experts using the most influential and physiologically sound parameters (Han et al. 2008). The subset of influential parameters identified by the sensitivity analysis is used, and direct adjustment is made for parameters like weight, sex, body mass index, and age. The domain expert may suggest changes to some specific parameters based upon desired virtual patient characteristics. An example would be to set values to realize a specific level of insulin resistance, with adjustments made to ensure that fasting plasma glucose and insulin (and other hormones) are as desired. Other tests (e.g., oral glucose and meal tolerance) will require additional adjustments. This process continues until the VP reflects the disease characteristics desired, and responds as expected to different challenges and therapies. VP creation represents significant effort, and brief treatment is meant to emphasize that VP creation involves a sequential use of many different tests and protocols. The approach can be automated, one example being the creation of 5000 VPs with a rheumatoid arthritis model (Chang 2014).

A useful strategy is to create a representative VP for each of several categories, including elevated fasting glucose, pre-diabetic conditions, mild-diabetes (impaired secretion or insulin resistant), and also moderate and severe diabetes with varying degrees of impaired secretion or insulin resistance. Additional variations include normal weight, overweight, and obese subjects. A cohort of VPs can be used to help build and develop the model and for simulations investigating research goals, such as predicting the efficacy of a novel compound. One early example of this approach included accounting for the physiological parameters, by sampling (with replacement) a population of several hundred VPs, and pharmacokinetic parameters, by sampling parameter distributions (Han et al. 2008). The cases described in this chapter also made use of VP cohorts. A diverse VP cohort was implemented in the Entelos model used for the SGLT2 case, and a focused subset of VPs was created in the GPR119 example and used for trial simulation. However, not all of these categories need to be considered for every research question.

20.3.2.6 Evaluate and Document the Model Performance

Model qualification (National Research Council 2012) is the process of ensuring that a model is suited for its intended purpose. It is recognized, however, that qualification of QSP models (Friedrich 2016) is fundamentally different than that of traditional PK/PD models (Agoram 2014). For a model consisting of hundreds of compartments, and perhaps thousands of parameters, standard statistical methods may not be appropriate.

Qualification starts with tests of modules (e.g., specific reaction pathways comprising the insulin secretion module) using relevant data sets. Tests of the integrated model exploit a variety of clinical trial data, especially including placebo data, for glucose challenge and meal tests. Trial data for a variety of therapies are especially useful at both the component and whole-body level. The diversity of the data used to build and test a model, the veracity of the physiological relationships expressed in the mathematics, and the diversity of protocols and experimental conditions used to generate the data all combine to provide confidence in the predictive power of a model.

Most QSP model variables and parameters have physiological meaning. This allows values from literature to be used in bounding and fixing such values. Throughout model creation, testing ensures that model components remain within physiologically reasonable bounds for each VP in protocols, and builds confidence in model performance. For example, 24-h fasting, IVGTT, OGTT, and mixed-meal tests are simulated with each VP, and key variables such as glucose, insulin and other hormones, and stored liver glycogen are checked to ensure that the model is stable (e.g., liver glycogen is not building up or completely depleting) and that all variables remain within physiological bounds for each VP. This is relatively easy: assays in the models invoke no cost, so simulated values are available for and can be compared with experimental data of any type. When the best value of a model parameter differs significantly from reported values, it may reflect an error in the modeling that must be addressed. It also may indicate a gap or error in the best current knowledge, which can be an opportunity for improved understanding or insight.

The model structure is determined by physiological relationships and physical laws such as mass conservation, and the entire model and model subsections are tested using multiple protocols (including different therapies) and datasets using a range of virtual patients. In modeling systems of this complexity with this level of data support, a comprehensive written documentation of testing is critical if the modeling work is to have appropriate influence. In the GPR119 case, such annotation resulted in a proprietary document with several dozen experiments and trial data, citing nearly 700 sources. This provided decision-makers with the confidence needed to support critical decisions.

20.3.3 Apply the Model

Research questions are frequently addressed in the process of building and testing a model. In other cases, an extensive set of simulations, such as simulated clinical trials with a variety of virtual patients, may be needed. These simulations may be useful for decisions ranging from selection of high-confidence targets to optimized clinical trial design. Outcomes can include efficacy, safety, and indirect benefits such as cardiovascular or renal health, if these aspects have been included in the model scope. In cases where clinical results are ambiguous, or modeling suggests a candidate is "borderline," QSP models can be (and have been) used to identify "de-risking" biomarkers in early-stage trials that can support and/or confirm decisions. In cases where high-risk decisions must be made, such as acquisition of external assets, extensive interactions, and what-if scenarios may be required. Although much of the potential area for QSP application in diabetes research remains to be realized, examples are beginning to emerge.

The following case examples highlight two successful projects in which QSP models delivered significant value. In the first, a systems pharmacology model was used to determine the non-viability of a therapeutic target in the preclinical phases of R&D. In the second, a systems model was used to significantly accelerate clinical development by obviating the need for a dose finding study in diabetic patients prior to a 12-week clinical trial measuring HbA1c.

20.3.3.1 Case Example of Systems Modeling to Support Therapeutic Viability of G Protein Coupled Receptor 119 (GPR119) Agonism for the Treatment of Type 2 Diabetes Mellitus (T2DM)

GPR119 is a member of family-A, rhodopsin-like G-protein coupled receptors (Fredriksson et al. 2003). The major sites of GPR119 expression include pancreatic islets (e.g., insulin containing β-cells) and gastrointestinal enteroendocrine cells (GLP-1 containing L cells) (Chu et al. 2007). This receptor is activated by a series of phospholipids (e.g., lysophosphatidylcholines) and free-fatty acid metabolites (e.g., oleoylethanolamide, 5-HEPE), which are known to have roles in glucose stimulated insulin secretion, appetite, and energy homeostasis (Overton et al. 2006; Soga et al. 2005). Activated GPR119 couples with Gα proteins to induce adenylate cyclase activity and subsequently increase intracellular cyclic adenosine monophosphate (cAMP). In the pancreas, activation of GPR119 results in stimulation of insulin secretion in a glucose-dependent manner. In the intestine, GPR119 activation also promotes glucose-dependent insulin secretion indirectly through the release of GLP-1. This dual mechanism of action has provided a compelling qualitative rationale for the pursuit of small molecule agonists for the treatment of T2DM (Table 20.4).

In the years between 2008 and 2010, GPR119 was one of the most heavily researched drug targets for the treatment of T2DM, with 58 patents being filed by

Table 20.4 Qualitative rationale for GPR119 as a molecular target for the treatment of type 2 diabetes

Effect	Target rationale	Clinical precedent
GLP-1 release	GLP-1 based efficacy already established	Parenteral GLP-1 agonists (e.g., exenatide, liraglutide, lixenatide) Oral DPP-IV inhibitors (e.g., sitagliptin, saxagliptin, vildaliptin)
Direct glucose-dependent insulin secretion	Glucose-dependent nature of insulin (i.e., limited release below a threshold plasma glucose value) secretion limits hypoglycemic risk commonly attributed to insulinotropic agents	Hypoglycemic risk with glucose independent insulin secretion (e.g., sulfonylureas) Reduced hypoglycemic risk with glucose dependent insulin secretion (e.g., GLP-1 agonists, DPP-IV inhibitors)

11 pharmaceutical companies over this time (Carpino and Goodwin 2010). These efforts have led to the identification of multiple small-molecule GPR119 agonists, of which several have advanced to the clinic where a degree of initial promise has been demonstrated (e.g., JNJ-38431055, GSK-1292263, MBX-2982, and PSN-821).

One key concern in the preclinical stages of research was whether a GPR119 agonist would produce meaningful glycemic efficacy as defined by reductions in HbA1c. Much of the initial work regarding the glucose-dependent insulin secretion of endogenous and synthetic agonists demonstrated no insulin release under normoglycemic conditions, but an increase in insulin secretion is observed in islets at glucose concentrations of approximately 16 mM, well above the aforementioned threshold that defines T2DM clinically (Chu et al. 2007; Soga et al. 2005; Ning et al. 2008; Kogure et al. 2011). Furthermore, data with endogenous and synthetic agonists suggested that the degree of active GLP-1 elevation might be less than that commonly observed with DPP-IV inhibitors (Kogure et al. 2011; Hansen et al. 2011). As such, it was unclear whether the direct and indirect effects of GPR119 agonism, alone or in combination, would provide compelling glycemic efficacy. In order to better evaluate the therapeutic potential of both effects in combination, a systems pharmacology model was developed at the inception of the R&D effort. Feasibility of constructing a credible model was considered high due to the wealth of clinical data for drugs working through increases in GLP-1 (GLP-1 agonists, DPP-IV inhibitors) as well as insulin secretagogues (sulfonylureas). Additional rationale for the effort included the ability to leverage emerging public information for this highly competitive molecular target and the potential ability to reuse the model for other novel targets operating through these common physiological pathways.

The model was constructed with several key physiological components, including: (1) insulin and C-peptide metabolism, (2) glucose metabolism, (3) glucagon metabolism, (4) incretin metabolism, and (5) meal composition/absorption. The major effects of GPR119 agonism are expected to result from indirect and

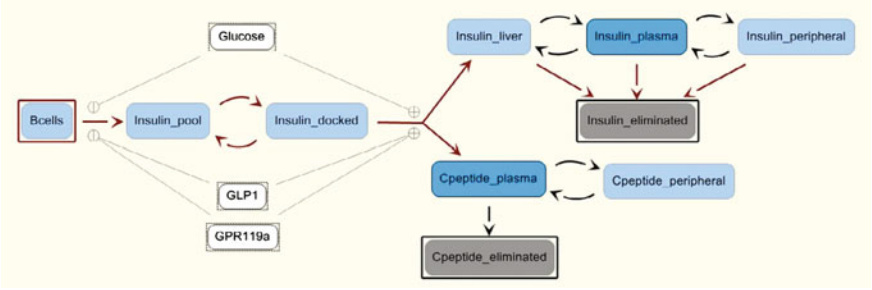

Fig. 20.11 Representation of the insulin component of the GPR119 systems pharmacology model

direct effects on insulin secretion, and a depiction of the insulin and C-peptide metabolism component is provided in Fig. 20.11.

In this component, insulin is produced at a rate proportional to beta cell mass into a storage pool that equilibrates with docked readily releasable insulin. Glucose stimulates insulin secretion in two phases, namely; immediate release of the docked pool followed by prolonged secretion as a function of increased production. In the model, both phases of insulin secretion are potentiated by GLP-1 and GPR119. Finally, secreted insulin and equimolar C-peptide partition between liver, plasma, and peripheral tissues from which they are eliminated. The integration of the 5 components into the systems pharmacology model, composed of 44 state variables and 84 rate constants, is shown in Fig. 20.12.

The model structure and parameter values were implemented in order to be consistent with over 1200 literature reports, where a portion was used for training and another for testing. This process included development and testing of each individual component as well as the integrated model. For example, the insulin component model was tested for its ability to recapitulate data from a number of references, including that from Mari et al. where a quasi-linear relationship between the rate of insulin secretion and glucose concentration was observed in healthy subjects (Mari et al. 2001). The integrated model was also tested for its ability to reproduce the dynamics of whole-body regulation, including changes in glucose, insulin, and GLP-1 during fasting, following IV and oral glucose challenge, and following mixed meal tests (Mari et al. 2001; Dalla Man et al. 2005a, b; Hojlund et al. 2001; Vicini and Cobelli 2001). Virtual patients were constructed by modifying key parameters (e.g., beta cell mass and glucose responsiveness) within the healthy subject model in order to recapitulate key pathophysiological characteristics of representative diabetic patient populations (e.g., fasting plasma glucose, glucose, insulin and incretin excursion upon glucose and meal challenges, mean daily glucose, and HbA1c in NHANES database). The model was further constrained by literature pharmacokinetic and pharmacodynamic data gathered following pharmacological intervention with glyburide, sitagliptin, exenatide, and metformin. In addition to providing some degree of mechanistic overlap with GPR119 agonism (i.e., potentiation of GSIS via GLP-1 elevation with sitagliptin and exenatide),

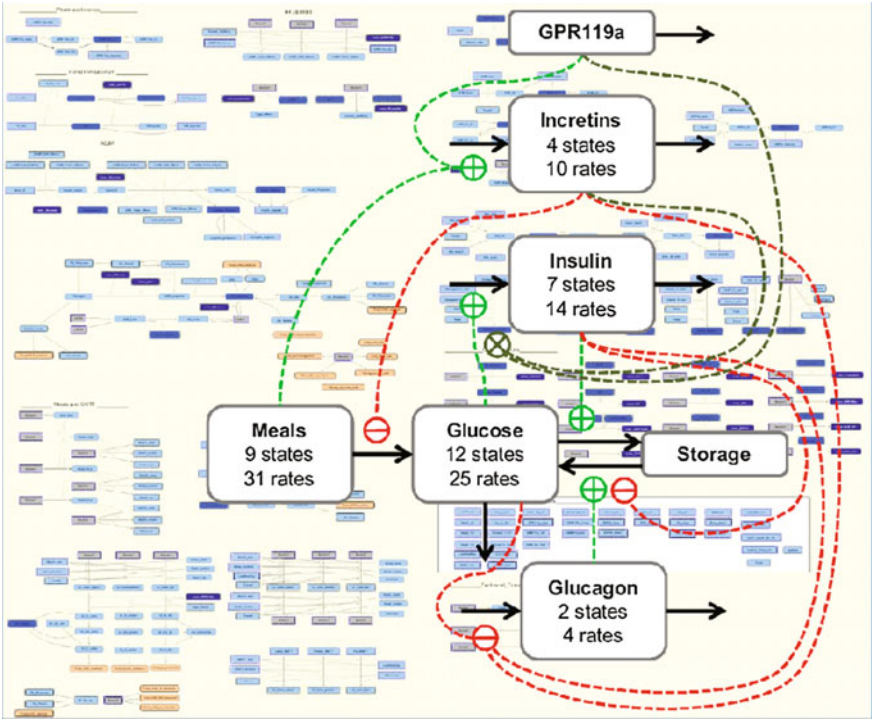

Fig. 20.12 Depiction of the integrated systems pharmacology model for GPR119

inclusion of these standards of care was considered to be important to support future cross-compound comparisons and combination therapy projections. Finally, the primary pharmacological effects of GPR119 on GLP-1 excretion and potentiation of glucose stimulated insulin secretion were codified in the model. This portion of the model was the most speculative initially, with effects being parameterized according to in vitro studies in islets as well as animal studies. For example, in vitro studies in rat islets indicated that GPR119 agonism causes both a concentration dependent left-shift in GSIS as well as an increase in maximal insulin secretion. In addition, animal studies indicated that the maximum increase in GLP-1 would be less than twofold. Even with these assumptions, there remained significant uncertainty regarding the net effect of the combined direct (GPR119 potentiation of GSIS) and indirect (GLP-1 potentiation of GSIS) effects of GPR119 on insulin secretion. It was unclear if the elevations in maximal insulin secretion between the 2 effects would be additive or something less than additive (e.g., in the event that insulin secretion would be nonlinear with increases in intracellular cAMP). Fortunately, the availability of emerging clinical data from competitors in this space allowed for further constraint around these aspects of GPR119 agonism. In particular, reported changes in GLP-1 concentrations (healthy volunteers) and changes in glucose excursions following mixed meal tolerance tests (healthy volunteers,

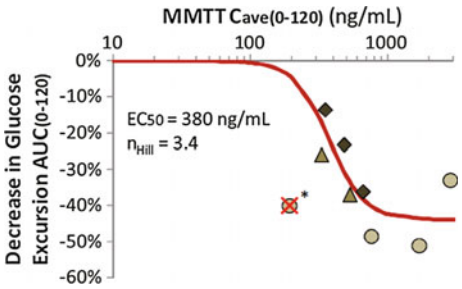

Fig. 20.13 Reported decreases in glucose AUC associated with administration of a MMTT in healthy subjects (*diamonds*), subjects with impaired fasting glucose (*triangles*), and pre-diabetic subjects (*circles*) at different plasma concentrations of a competitor agent. The *red line* represents the calibrated model behavior. The data representing the pre-diabetic group receiving the lowest dose (with overlaid *red* X) was assumed to be an outlier and was eliminated from the calibration

subjects with impaired fasting glucose and pre-diabetic patients) enabled exploration of the appropriate parameterization of the effect on GLP-1 secretion and GSIS (example of model-based characterization of MMTT results shown in Fig. 20.13).

With the final model, 14-day simulations of plasma glucose were performed across the full dose-response for a theoretical full agonist in a diabetic patient population. Anticipated changes in HbA1c associated with simulated changes in mean daily glucose at 14 days were determined according to previously published relationships (Nathan et al. 2007). Results indicated that the maximal potential change in HbA1c would be inferior to sitagliptin (dHbA1c $\sim$ 0.4 %). Based on these results, the program was discontinued in the preclinical stages of R&D despite the availability of a candidate molecule for clinical development. Subsequently, independent 14-day clinical studies in diabetic patients with two GPR119 agonists (JNJ-38431055 and GSK-1292263) failed to show compelling glycemic efficacy and were discontinued (Katz et al. 2012; Nunez et al. 2014). The model-predicted HbA1c reduction for 100 % modulation of the target corresponded to 0.42 %, while the actual clinical outcome for a significant modulation was 0.30 %. Using cost figures for Phase 2 and 3 development alone (Paul et al. 2010), this decision provided approximately $55 million in savings and, perhaps more importantly, allowed deployment of resources to molecular targets with a greater probability of success.

20.3.3.2 Case Example Modeling to Accelerate the SGLT2 Program

Glucose is filtered out of the blood by the kidneys, and under normal conditions, it is almost completely reabsorbed primarily through the action of sodium/glucose co-transporter 2 (SGLT2), a high capacity, low affinity transport protein located in the proximal tubules and responsible for approximately 90 % of renal glucose

reabsorption (Wright et al. 2007). SGLT2 inhibitors (SGLT2i) impair glucose reabsorption by the kidney, allowing for glucose excretion in the urine and thereby lowering plasma glucose. SGLT2 inhibition in type 2 diabetes patients has been shown to reduce HbA1c concentrations with chronic treatment, along with modest reductions in body weight and systolic blood pressure (Cefalu et al. 2013; Nauck et al. 2014). Competition for market share for this class of drugs is high, with several compounds in clinical development or recently approved.

By the time Pfizer entered the first-in-human trial for its lead compound, ertugliflozin, several competitor molecules already were in clinical development. To accelerate the program, a systems pharmacology approach was applied, in addition to other model-based approaches, utilizing published competitor data on the mechanistic biomarker (urine glucose excretion, UGE) and other clinical endpoints (e.g., changes in plasma glucose, plasma insulin, body weight, etc.). Information from the public literature regarding the target (e.g., SGLT2 glucose reabsorption kinetics), relevant human physiology (e.g., glomerular filtration rates, urine glucose excretion under various conditions), disease state (e.g., urinary glucose excretion and glomerular filtration rates in healthy vs. type 2 diabetes subjects), and clinical PK/PD data on a competitor compound (dapagliflozin) were integrated into a proprietary, comprehensive model of human metabolism (Entelos Metabolism PhysioLab®).

The process for updating the existing Entelos QSP model was similar to the method described in the "Modeling Approach" section of this chapter. First, existing cohorts of healthy and type 2 diabetes Virtual Patients were parametrically modified to reflect reported variability in renal glucose threshold (Ruhnau et al. 1997), glucose reabsorption rates (Rahmoune et al. 2005; Wolf et al. 2009; Mogensen 1971), and glomerular filtration rates (Premaratne et al. 2005), resulting in a range of urinary glucose excretion in the Virtual Population consistent with published data (Zhang et al. 2010). Urinary glucose excretion (UGE, in mg/min) in the Metabolism PhysioLab is represented as a function of glomerular filtration rate (GFR, in dL/min), renal glucose threshold (RGT, in mg/dL; the concentration of glucose in plasma at which glucose appears in urine), renal glucose reabsorption rate (RGR, in mg/min), and plasma glucose (in mg/dL) (Wolf et al. 2009):

$$UGE = \begin{cases} 0 & PG \leq RGT \\ GFR * PG - RGR, & PG > RGT. \end{cases} \tag{20.2}$$

Note that this implementation includes an implicit representation of SGLT2 activity. To represent inhibitor PK/PD, a two-compartment, first-order elimination PK model for dapagliflozin was implemented by fitting parameters to published population-based PK data (Komoroski et al. 2009a, b), and an Emax model to represent SGLT2 inhibitor-mediated effects on glucose reabsorption also was included (Fig. 20.14). Parameter values for the E max model were determined by fitting to 24-h urine glucose excretion data from single- and multiple-dose trials for the competitor compound in healthy and type 2 diabetes subjects (Komoroski et al. 2009a, b). Finally, the systems model for SGLT2i was validated by comparing

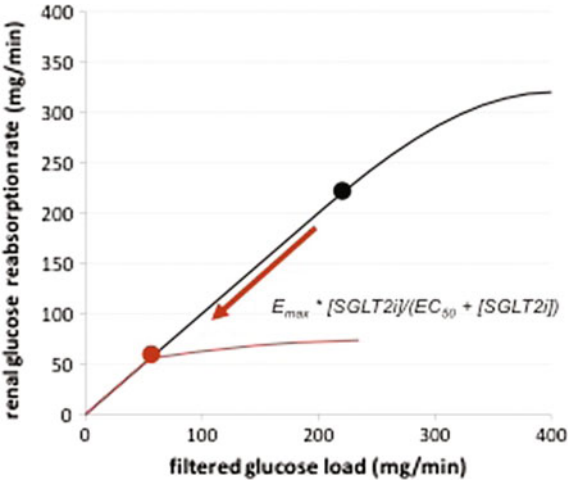

Fig. 20.14 Representation of the renal glucose reabsorption rate for a typical diabetic virtual patient in the Entelos Metabolism PhysioLab platform (*black line*). SGLT2 inhibition is represented as a reduction in the renal glucose reabsorption rate (*red line*), using an Emax model. Filtered glucose load = plasma glucose × glomerular filtration rate. *Black dot* = renal glucose threshold (RGT). *Red dot* = SGLT2i-mediated reduction in renal glucose threshold

simulation results to published data for 12-week dapagliflozin trials in type 2 diabetes subjects (List et al. 2009; Wilding et al. 2009).

Importantly, the validated SGLT2i QSP model was developed prior to the start of Pfizer's Phase 1 trial so that researchers could estimate ertugliflozin-specific PK and Emax model parameters in real-time as clinical data became available. This allowed model predictions of the 12-week, Proof of Concept trial for ertugliflozin to be completed prior to study start, to de-risk key design decisions including dose range, biomarker collection times, and effect of concurrent therapy (e.g., metformin). This process allowed doses for the Phase 2 trial to be set prior to the last subject last visit in the First-In-Human trial, greatly reducing the time between Phase 1 start and Phase 2 end to 14.6 months; moreover, predictions from the in silico investigation of the target and compound, within the context of a model of type 2 diabetes, were a key component in the decision to collapse Phase 2a and 2b into one trial. A post hoc comparison of the 12-week clinical observations to the model predictions showed very good agreement for the HbA1c endpoint, and increased confidence for further investment in QSP modeling efforts within the organization (Fig. 20.15).

In summary, the availability of a type 2 diabetes systems pharmacology model for SGLT2i and the established link between the mechanistic biomarker (UGE) in healthy volunteers and long-term efficacy (HbA1c) in type 2 diabetes subjects provided the project team with confidence to design an aggressive and informative Phase 1 program, providing dose rationale and design for dose ranging for later stage trials and to combine Phase 2a and Phase 2b studies. The model has continued to be applied in support of the ertugliflozin program as the compound has moved into Phase 3 co-development.

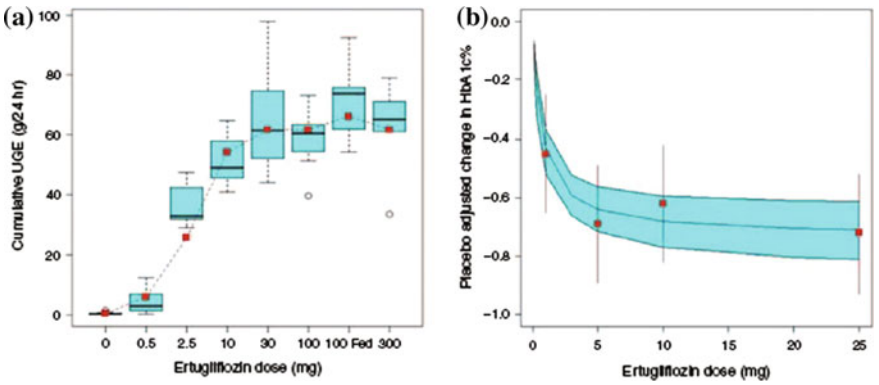

Fig. 20.15 **a** Cumulative urine glucose excretion for ertugliflozin Phase 1 trial in healthy subjects. Model predictions in *red symbols*, *dotted line*; clinical data in *blue box* plots; **b** Placebo-adjusted change in HbA1c in ertugliflozin Phase 2 trial in type 2 diabetes patients. Model predictions with 90 % confidence interval in shaded area; clinical data with 80 % confidence interval in *red symbols* and *bars*. From Milligan et al. (2013)

20.4 Challenges and Future Directions

Developing effective novel therapies for complex diseases like diabetes has become expensive to the point of threatening future investments in the search for more effective agents. The ability to better understand the clinical implications of early data (basic science, in vitro, and preclinical) is a key to improve the efficiency and return of R&D. There are clear cost and time advantages over "brute force" methods in which every target is tested in the clinic (sometimes iteratively). Quantitative outcome predictions for several therapies for novel targets represents a huge opportunity for better decisions, higher yield, and saved costs. With diabetes, where there are hundreds of untested novel targets, the ability to select those with greater likelihood of success has enormous leverage. Denis Noble has emphasized the high leverage of better trial candidate selection, with even slight improvements yielding very large returns (Bertau et al. 2008).

Future QSP efforts must evolve in concert with emerging thinking about what constitutes success in diabetes therapy. While short term HbA1c changes provide a tractable and useful endpoint upon which to define biological scope, future QSP efforts will need to incorporate an even larger scope of biology necessary to address critical issues of therapeutic durability, disease progression, and pathological sequela (neuropathy, nephropathy, and cardiovascular events).

In addition, future QSP efforts must evolve to accommodate and exploit data from emerging technologies (e.g., omics, synthetic biology, 3-D cell/organoid cultures, and CRISPRs) as this will enable a continued evolution of insights and applications. In particular, QSP diabetes models have a role to play in understanding and exploiting the tsunami of 'omics data becoming available. Interpreting the data in the context of the physiological constraints of a QSP model can allow a

more efficient and focused search for causal relationships or "hits." Heinzel et al. (2014) illustrates an integrated 'omics approach for diabetic nephropathy, with a goal of identifying predictive biomarkers. The approach is not limited to diabetes comorbidities and markers. There is no reason not to apply 'omics to modeling outcome predictions for targets, and such data also support better QSP modeling. Wilmes et al. (2013) have integrated transcriptomic, proteomic, and metabolomic data to determine mechanisms for drug-induced cell stress, and Hamon et al. (2014) have created a systems biology model using these data. Lee et al. (2016) have integrated GEnome scale Metabolic (GEM), Transcription Regulatory Network (TRN), and Protein-Protein Interaction Network (PPIN) models into an Integrated Network Model and have used the model to identify mannose as an improved biomarker for insulin resistance. Clearly, the same techniques can be applied in diabetes modeling. Integrating QSP diabetes models and omics databases will result in better correlative searching of the databases and better predictive models of the disease. We expect this to lead to use of QSP models for target identification and evaluation, and for use with patient genotyping to advance precision medicine.

While QSP is increasingly being used to support decision making in search for novel diabetes therapeutics, there are also many cultural and operational challenges that must be overcome in the adoption and continuous improvement of this science. Among the numerous challenges, the dearth of published examples represents one the most significant, which may be within control of the QSP community. Even publications at the case study level provided in this chapter are relatively rare. Currently, there are no whole-disease models of the type and level of detail shown in the figures here for which modeling source code and details have been publicly disclosed. There are many useful papers describing components of diabetes, and there are descriptions of "large-grained" (more in the range of 20 compartments rather than 200) whole-disease models (Magni et al. 2007), but a comprehensive model with enough mechanistic detail to make quantitative predictions sufficient to inform pharma R&D decisions has yet to be published. Most papers with significant modeling detail are academic and focus on only a part of diabetes, and most models of the comprehensive type are proprietary. Commercial considerations aside, publication of QSP models can be difficult. Models with hundreds of reactions and parameters lead to high page- and citation-counts, and even abstracted models violate journal constraints. For example, a proprietary bibliography of the GPR119 model, with about 700 of the 1300 source documents listed, was over 60 pages. The SGLT2 model has over 4500 references. Nevertheless, open source publication of diabetes QSP models should be considered a strategic imperative underwriting the continued evolution and application of this science. Such publically available models would provide a platform from which to leverage ongoing efforts and applications in academia, industry, and regulatory agencies.

In summary, diabetes QSP modeling has been used to improve critical decision making in pharmaceutical R&D. The overwhelming number and diversity of new data create an additional incentive to use QSP models to integrate these data into a scientifically sound predictive tool. As such, although diabetes QSP is in early stages of adoption, it is anticipated to grow.

Acknowledgments We gratefully acknowledge the contributions of G. Nucci (Pfizer), N. Haddish (Pfizer), A. Ghosh (Pfizer) and M. Reed (Entelos) to the SGLT2 modeling; and D. Tess (Pfizer), D. Chen (Pfizer), P. Cornelius (Pfizer), and A. Ghosh, and R. Baillie (Rosa), C. Friedrich (Rosa), and R. Beaver (Rosa) in the collaborative modeling used in the GPR119 work. Paul DaSilva-Jardine (Pfizer) and Tim Rolph (Pfizer) provided critical management support and guidance, and Jeff Trimmer (Pfizer) provided valuable early guidance in writing this chapter.

References

Agoram B (2014) Evaluating systems pharmacology models is different from evaluating standard pharmacokinetic–pharmacodynamic models. CPT Pharmacometrics Syst Pharmacol 3(2). doi:10.1038/psp.2013.77

Ahrén B, Holst JJ, Mari A (2003) Characterization of GLP-1 effects on β-cell function after meal ingestion in humans. Diabetes Care 26(10):2860–2864. doi:10.2337/diacare.26.10.2860

Ajmera I, Swat M, Laibe C, Novere NL, Chelliah V (2013) The impact of mathematical modeling on the understanding of diabetes and related complications. CPT Pharmacometr Syst Pharmacol 2:e54. doi:10.1038/psp.2013.30

American Diabetes Association (2013) Economic costs of diabetes in the U.S. in 2012. Diabetes Care 36(4):1033–1046. doi:10.2337/dc12-2625

American Diabetes Association (2014) Diagnosis and classification of diabetes mellitus. Diabetes Care 37(Suppl 1):S81–S90. doi:10.2337/dc14-S081

Aronoff SL, Berkowitz K, Shreiner B, Want L (2004) Glucose metabolism and regulation: beyond insulin and glucagon. Diabetes Spectrum 17(3):183–190. doi:10.2337/diaspect.17.3.183

Bagger JI, Knop FK, Lund A, Vestergaard H, Holst JJ, Vilsboll T (2011) Impaired regulation of the incretin effect in patients with type 2 diabetes. J Clin Endocrinol Metab 96(3):737–745. doi:10.1210/jc.2010-2435

Beck-Nielsen H, Hother-Nielsen O, Staehr P (2002) Is hepatic glucose production increased in type 2 diabetes mellitus? Curr Diab Rep 2(3):231–236

Beer SF, Bircham PMM, Bloom SR, Clark PM, Hales CN, Hughes CM, Jones CT, Marsh DR, Raggatt PR, Findlay ALR (1989) The effect of a 72-h fast on plasma levels of pituitary, adrenal, thyroid, pancreatic and gastrointestinal hormones in healthy men and women. J Endocrinol 120(2):337–350. doi:10.1677/joe.0.1200337

Bergman RN, Phillips LS, Cobelli C (1981) Physiologic evaluation of factors controlling glucose tolerance in man: measurement of insulin sensitivity and beta-cell glucose sensitivity from the response to intravenous glucose. J Clin Invest 68(6):1456–1467

Bergmann FT, Sauro HM (2006) Computational systems biology: modularity and composition: SBW—a modular framework for systems biology. In: Winter simulation WSC'06, 2006/12/2006. Winter simulations conference, Monterey, pp 1637–1647

Bergmann FT, Vallabhajosyula RR, Sauro HM (2006) Computational tools for modeling protein networks. Curr Proteomics 3(3):181–197. doi:10.2174/157016406779475380

Bertau M, Mosekilde E, Westerhoff HV (2008) Biosimulation in drug development. Wiley-VCH, Weinheim

Boyle JP, Thompson TJ, Gregg EW, Barker LE, Williamson DF (2010) Projection of the year 2050 burden of diabetes in the US adult population: dynamic modeling of incidence, mortality, and prediabetes prevalence. Popul Health Metr 8:29. doi:10.1186/1478-7954-8-29

Brandt A, Katschinski M, Arnold R, Polonsky KS, Göke B, Byrne MM (2001) GLP-1-induced alterations in the glucose-stimulated insulin secretory dose-response curve. Am J Physiol Endocrinol Metab 281(2):E242–E247

Brännmark C, Nyman E, Fagerholm S, Bergenholm L, Ekstrand E-M, Cedersund G, Strålfors P (2013) Insulin signaling in type 2 diabetes: experimental and modeling analyses reveal

mechanisms of insulin resistance in human adipocytes. J Biol Chem 288(14):9867–9880. doi:10.1074/jbc.M112.432062

Bratanova-Tochkova TK, Cheng H, Daniel S, Gunawardana S, Liu Y-J, Mulvaney-Musa J, Schermerhorn T, Straub SG, Yajima H, Sharp GWG (2002) Triggering and augmentation mechanisms, granule pools, and biphasic insulin secretion. Diabetes 51(suppl 1):S83–S90. doi:10.2337/diabetes.51.2007.S83

Browning JD, Baxter J, Satapati S, Burgess SC (2012) The effect of short-term fasting on liver and skeletal muscle lipid, glucose, and energy metabolism in healthy women and men. J Lipid Res 53(3):577–586. doi:10.1194/jlr.P020867

Bruce DG, Chisholm DJ, Storlien LH, Kraegen EW (1988) Physiological importance of deficiency in early prandial insulin secretion in non-insulin-dependent diabetes. Diabetes 37(6):736–744. doi:10.2337/diab.37.6.736

Bunt JC, Krakoff J, Ortega E, Knowler WC, Bogardus C (2007) Acute insulin response is an independent predictor of type 2 diabetes mellitus in individuals with both normal fasting and 2-h plasma glucose concentrations. Diabetes Metab Res Rev 23(4):304–310. doi:10.1002/dmrr.686

Carpino PA, Goodwin B (2010) Diabetes area participation analysis: a review of companies and targets described in the 2008–2010 patent literature. Expert Opin Ther Pat 20(12):1627–1651. doi:10.1517/13543776.2010.533171

Cauter EV, Mestrez F, Sturis J, Polonsky KS (1992) Estimation of insulin secretion rates from C-peptide levels: comparison of individual and standard kinetic parameters for C-peptide clearance. Diabetes 41(3):368–377. doi:10.2337/diab.41.3.368

Cedersund G, Roll J, Ulfhielm E, Danielsson A, Tidefelt H, Stälfors P (2008) Model-based hypothesis testing of key mechanisms in initial phase of insulin signaling. PLoS Comput Biol 4(6):e1000096

Cedersund G, Strälfors P (2009) Putting the pieces together in diabetes research: towards a hierarchical model of whole-body glucose homeostasis. Eur J Pharm Sci 36(1):91–104. doi:10.1016/j.ejps.2008.10.027

Cefalu WT, Leiter LA, Yoon K-H, Arias P, Niskanen L, Xie J, Balis DA, Canovatchel W, Meininger G (2013) Efficacy and safety of canagliflozin versus glimepiride in patients with type 2 diabetes inadequately controlled with metformin (CANTATA-SU): 52 week results from a randomised, double-blind, phase 3 non-inferiority trial. The Lancet 382(9896):941–950. doi:10.1016/S0140-6736(13)60683-2

Ceriello A, Esposito K, Testa R, Bonfigli AR, Marra M, Giugliano D (2011) The possible protective role of glucagon-like peptide 1 on endothelium during the meal and evidence for an "Endothelial Resistance" to glucagon-like peptide 1 in diabetes. Dia Care 34(3):697–702. doi:10.2337/dc10-1949

Chang S (2014) In silico trials. Lessons learned working with Pharma for 9 years (trans: Chang S). In: Presentation at the 2nd Avicenna conference on in silico trial strategies, Rome

Chew YH, Shia YL, Lee CT, Abdul Majid FA, Chua LS, Sarmidi MR, Abdul Aziz R (2009a) Modeling of oscillatory bursting activity of pancreatic beta-cells under regulated glucose stimulation. Mol Cell Endocrinol 307(1–2):57–67. doi:10.1016/j.mce.2009.03.005

Chew YH, Shia YL, Lee CT, Majid FAA, Chua LS, Sarmidi MR, Aziz RA (2009b) Modeling of glucose regulation and insulin-signaling pathways. Mol Cell Endocrinol 303(1–2):13–24. doi:10.1016/j.mce.2009.01.018

Christensen MB, Calanna S, Holst JJ, Vilsboll T, Knop FK (2014) Glucose-dependent insulinotropic polypeptide: blood glucose stabilizing effects in patients with type 2 diabetes. J Clin Endocrinol Metab 99(3):E418–E426. doi:10.1210/jc.2013-3644

Chu Z-L, Jones RM, He H, Carroll C, Gutierrez V, Lucman A, Moloney M, Gao H, Mondala H, Bagnol D, Unett D, Liang Y, Demarest K, Semple G, Behan DP, Leonard J (2007) A role for beta-cell-expressed G protein-coupled receptor 119 in glycemic control by enhancing glucose-dependent insulin release. Endocrinology 148(6):2601–2609

Cobelli C, Mari A (1983) Validation of mathematical models of complex endocrine-metabolic systems. A case study on a model of glucose regulation. Med Biol Eng Comput 21(4):390–399. doi:10.1007/BF02442625

Dalla Man C, Campioni M, Polonsky KS, Basu R, Rizza RA, Toffolo G, Cobelli C (2005a) Two-hour seven-sample oral glucose tolerance test and meal protocol: Minimal model assessment of β-cell responsivity and insulin sensitivity in nondiabetic individuals. Diabetes 54 (11):3265–3273. doi:10.2337/diabetes.54.11.3265

Dalla Man C, Caumo A, Basu R, Rizza R, Toffolo G, Cobelli C (2005b) Measurement of selective effect of insulin on glucose disposal from labeled glucose oral test minimal model. Am J Physiol 289 (5, Pt. 1):E909–E914. doi:10.1152/ajpendo.00299.2004

Dalla Man C, Rizza RA, Cobelli C (2007) Meal simulation model of the glucose-insulin system. IEEE Trans Biomed Eng 54(10):1740–1749

Danaei G, Finucane MM, Lu Y, Singh GM, Cowan MJ, Paciorek CJ, Lin JK, Farzadfar F, Khang Y-H, Stevens GA, Rao M, Ali MK, Riley LM, Robinson CA, Ezzati M, Danaei G, Finucane MM, Lu Y, Singh GM, Cowan MJ, Paciorek CJ, Lin JK, Farzadfar F, Khang Y-H, Stevens GA, Rao M, Ali MK, Riley LM, Robinson CA, Ezzati M, Abdeen Z, Aekplakorn W, Afifi MM, Agabiti-Rosei E, Salinas CAA, Alnsour M, Ambady R, Barbagallo CM, Barcelo A, Barros H, Bautista LE, Benetos A, Bjerregaad P, Bo S, Bovert P, Burszytn M, Cabrera dLA, Castellano M, Castetbon K, Chaouki N, Chen C-J, Chua L, Cifkova R, Corsi AM, Delgado E, Doi Y, Esteghamati A, Fall CHD, Fan J-G, Ferreccio C, Fezeu L, Fuller EL, Giampaoli S, Gomez LF, Carvajal RG, Herman WH, Herrera VM, Ho S, Hussain A, Ikeda N, Jafar TH, Jonas JB, Kadiki OA, Karalis I, Katz J, Khalilzadeh O, Kiechl S, Kurjata P, Lee J, Lee J, Lim S, Lim TO, Lin C-C, Lin X, Lin H-H, Liu X, Lorbeer R, Ma S, Maggi S, Magliano DJ, McFarlane-Anderson N, Miettola J, Miranda JJ, Mohamed MK, Mohan V, Mokdad A, Morales DD, Nabipour I, Nakagami T, Nangia V, Neuhauser H, Noale M, Onat A, Orostegui M, panagiotakos DB, Passos VMA, Perez C, Pichardo R, Phua HP, Plans P, Qiao Q, Ramos LR, Rampal S, Rampal L, Redon J, Revilla L, Rosero-Bixby L, Sanisoglu SY, Scazufca M, Schaan BD, Sekuri C, Shera AS, Shi Z, Silva E, Simons LA, Soederberg S, Solfrizzi V, Soysal A, Stein AD, Stessman J, Vanderpump MP, Viet L, Vollenweider P, Wang N, Wang YX, Waspadji S, Willeit J, Woodward M, Xu L, Yang X, Yoon J-S, Yu Z, Zhang J, Zhang L (2011) National, regional, and global trends in fasting plasma glucose and diabetes prevalence since 1980: systematic analysis of health examination surveys and epidemiological studies with 370 country-years and 2.7 million participants. Lancet 378 (9785):31–40

De Gaetano A, Panunzi S, Matone A, Samson A, Vrbikova J, Bendlova B, Pacini G (2013) Routine OGTT: a robust model including incretin effect for precise identification of insulin sensitivity and secretion in a single individual. PLoS ONE 8(8):e70875. doi:10.1371/journal.pone.0070875

DeFronzo RA, Gunnarsson R, Bjorkman O, Olsson M, Wahren J (1985) Effects of insulin on peripheral and splanchnic glucose metabolism in noninsulin-dependent (type II) diabetes mellitus. J Clin Invest 76(1):149–155. doi:10.1172/jci111938

DeFronzo RA, Tobin JD, Andres R (1979) Glucose clamp technique: a method for quantifying insulin secretion and resistance. Am J Physiol Endocrinol Metab 237(3):E214

Del Prato S, Marchetti P, Bonadonna RC (2002) Phasic insulin release and metabolic regulation in type 2 diabetes. Diabetes 51(suppl 1):S109–S116. doi:10.2337/diabetes.51.2007.S109

Eknoyan G, Nagy J (2005) A history of diabetes mellitus or how a disease of the kidneys evolved into a kidney disease. Adv Chronic Kidney Dis 12(2):223–229

Færch K, Vaag A, Holst JJ, Glümer C, Pedersen O, Borch-Johnsen K (2008) Impaired fasting glycaemia vs impaired glucose tolerance: similar impairment of pancreatic alpha and beta cell function but differential roles of incretin hormones and insulin action. Diabetologia 51(5):853–861. doi:10.1007/s00125-008-0951-x

Ferrannini E, Muscelli E, Frascerra S, Baldi S, Mari A, Heise T, Broedl UC, Woerle H-J (2014) Metabolic response to sodium-glucose cotransporter 2 inhibition in type 2 diabetic patients. J Clin Investig 124(2):499–508. doi:10.1172/JCI72227

Frayn KN (2010) Metabolic regulation: a human perspective, 3rd edn. Wiley, New York
Fredriksson R, Hoglund P, Gloriam DEI, Lagerstrom MC, Schioth HB (2003) Seven evolutionarily conserved human rhodopsin G protein-coupled receptors lacking close relatives. FEBS Lett 554(3):381–388
Friedrich C (2016) A model qualification method for mechanistic physiological QSP models to support model-informed drug development. CPT: Pharmacomet. Syst Pharmacol 5:43–53.
Hamon J, Jennings P, Bois FY (2014) Systems biology modeling of omics data: effect of cyclosporine a on the Nrf2 pathway in human renal cells. BMC Syst Biol 8(1). doi:10.1186/1752-0509-8-76
Hamrén B, Björk E, Sunzel M, Karlsson MO (2008) Models for plasma glucose, HbA1c, and hemoglobin interrelationships in patients with type 2 diabetes following tesaglitazar treatment. Clin Pharmacol Ther 84(2):228–235. doi:10.1038/clpt.2008.2
Han T, Migoya EM, Maganti L, Baillie R, Brazhnik P, Bosley JR (2008) Alteration of glucose and insulin regulatory networks for the treatment of type 2 diabetes mellitus. In: Annual meeting, 2008/06/2008. Marseille, France
Hansen KB, Rosenkilde MM, Knop FK, Wellner N, Diep TA, Rehfeld JF, Andersen UB, Holst JJ, Hansen HS (2011) 2-Oleoyl glycerol is a GPR119 agonist and signals GLP-1 release in humans. J Clin Endocrinol Metab 96(9):E1409–E1417. doi:10.1210/jc.2011-0647
Heinzel A, Perco P, Mayer G, Oberbauer R, Lukas A, Mayer B (2014) From molecular signatures to predictive biomarkers: modeling disease pathophysiology and drug mechanism of action. Front Cell Dev Biol 2. doi:10.3389/fcell.2014.00037
Hojlund K, Wildner-Christensen M, Eshoj O, Skjaerbaek C, Holst JJ, Koldkjaer O, Jensen DM, Beck-Nielsen H (2001) Reference intervals for glucose, β-cell polypeptides, and counterregulatory factors during prolonged fasting. Am J Physiol 280 (1, Pt. 1):E50–E58
Horowitz JF, Coppack SW, Klein S (2001) Whole-body and adipose tissue glucose metabolism in response to short-term fasting in lean and obese women. Am J Clin Nutr 73(3):517–522
Horowitz M, Maddox AF, Wishart JM, Harding PE, Chatterton BE, Shearman DJ (1991) Relationships between oesophageal transit and solid and liquid gastric emptying in diabetes mellitus. Eur J Nucl Med 18(4):229–234
Hovorka R, Powrie JK, Smith GD, Sonksen PH, Carson ER, Jones RH (1993) Five-compartment model of insulin kinetics and its use to investigate action of chloroquine in NIDDM. Am J Physiol Endocrinol Metab 265(1):E162–E175
Hucka M, Finney A, Sauro HM, Bolouri H, Doyle J, Kitano H (2002) The ERATO systems biology workbench: enabling interaction and exchange between software tools for computational biology. In: Pacific symposium on biocomputing pacific symposium on biocomputing, pp 450–461
Johannsen DL, Tchoukalova Y, Tam CS, Covington JD, Xie W, Schwarz J-M, Bajpeyi S, Ravussin E (2014) Effect of eight weeks of overfeeding on ectopic fat deposition and insulin sensitivity: testing the "adipose tissue expandability" hypothesis. Diabetes Care. doi:10.2337/dc14-0761
Kapur A, O'Connor-Semmes R, Hussey EK, Dobbins RL, Tao W, Hompesch M, Smith GA, Polli JW, James CD Jr, Mikoshiba I, Nunez DJ (2013) First human dose-escalation study with remogliflozin etabonate, a selective inhibitor of the sodium-glucose transporter 2 (SGLT2), in healthy subjects and in subjects with type 2 diabetes mellitus. BMC Pharmacol Toxicol 14:26. doi:10.1186/2050-6511-14-26
Katz LB, Gambale JJ, Rothenberg PL, Vanapalli SR, Vaccaro N, Xi L, Sarich TC, Stein PP (2012) Effects of JNJ-38431055, a novel GPR119 receptor agonist, in randomized, double-blind, placebo-controlled studies in subjects with type 2 diabetes. Diabetes Obes Metab 14(8):709–716. doi:10.1111/j.1463-1326.2012.01587.x
Kim J, Saidel GM, Cabrera ME (2007) Multi-scale computational model of fuel homeostasis during exercise: effect of hormonal control. Ann Biomed Eng 35(1):69–90
Kitano H, Funahashi A, Matsuoka Y, Oda K (2005) Using process diagrams for the graphical representation of biological networks. Nat Biotechnol 23(8):961–966. doi:10.1038/nbt1111

Kjems LL, Holst JJ, Vølund A, Madsbad S (2003) The influence of GLP-1 on glucose-stimulated insulin secretion: effects on β-cell sensitivity in type 2 and nondiabetic subjects. Diabetes 52 (2):380–386. doi:10.2337/diabetes.52.2.380

Kogure R, Toyama K, Hiyamuta S, Kojima I, Takeda S (2011) 5-Hydroxy-eicosapentaenoic acid is an endogenous GPR119 agonist and enhances glucose-dependent insulin secretion. Biochem Biophys Res Commun 416(1–2):58–63. doi:10.1016/j.bbrc.2011.10.141

Komoroski B, Vachharajani N, Boulton D, Kornhauser D, Geraldes M, Li L, Pfister M (2009a) Dapagliflozin, a novel SGLT2 inhibitor, induces dose-dependent glucosuria in healthy subjects. Clin Pharmacol Ther 85(5):520–526. doi:10.1038/clpt.2008.251

Komoroski B, Vachharajani N, Feng Y, Li L, Kornhauser D, Pfister M (2009b) Dapagliflozin, a novel, selective SGLT2 inhibitor, improved glycemic control over 2 weeks in patients with type 2 diabetes mellitus. Clin Pharmacol Ther 85(5):513–519. doi:10.1038/clpt.2008.250

Koschorreck M, Gilles ED (2008) Mathematical modeling and analysis of insulin clearance in vivo. BMC Syst Biol 2(1). doi:10.1186/1752-0509-2-43

Landersdorfer CB, Jusko WJ (2008) Pharmacokinetic/pharmacodynamic modelling in diabetes mellitus. Clin Pharmacokinet 47(7):417–448. doi:10.2165/00003088-200847070-00001

Leahy JL (2005) Pathogenesis of type 2 diabetes mellitus. Arch Med Res 36(3):197–209. doi:10.1016/j.arcmed.2005.01.003

Lee S, Zhang C, Kilicarslan M, Piening BD, Bjornson E, Hallström BM, Groen AK, Ferrannini E, Laakso M, et al (2016) Integrated network analysis reveals an association between plasma mannose levels and insulin resistance. Cell Metab 24(1):172–184

Levy JC, Matthews DR, Hermans MP (1998) Correct homeostasis model assessment (HOMA) evaluation uses the computer program. Diabetes Care 21(12):2191–2192. doi:10.2337/diacare.21.12.2191

Li C, Donizelli M, Rodriguez N, Dharuri H, Endler L, Chelliah V, Li L, He E, Henry A, Stefan MI, Snoep JL, Hucka M, Le Novere N, Laibe C (2010) BioModels Database: an enhanced, curated and annotated resource for published quantitative kinetic models. BMC Syst Biol 4:92. doi:10.1186/1752-0509-4-92

List JF, Woo V, Morales E, Tang W, Fiedorek FT (2009) Sodium-glucose cotransport inhibition with dapagliflozin in type 2 diabetes. Diabetes Care 32(4):650–657. doi:10.2337/dc08-1863

Lund A, Vilsboll T, Bagger JI, Holst JJ, Knop FK (2011) The separate and combined impact of the intestinal hormones, GIP, GLP-1, and GLP-2, on glucagon secretion in type 2 diabetes. Am J Physiol Endocrinol Metab 300(6):E1038–E1046. doi:10.1152/ajpendo.00665.2010

Luzi L, DeFronzo RA (1989) Effect of loss of first-phase insulin secretion on hepatic glucose production and tissue glucose disposal in humans. Am J Physiol Endocrinol Metab 257(2): E241–E246

Magni L, Raimondo DM, Bossi L, Dalla Man C, De Nicolao G, Kovatchev B, Cobelli C (2007) Model predictive control of type 1 diabetes: an in silico trial. J Diabetes Sci Technol 1(6):804–812

Mari A, Camastra S, Toschi E, Giancaterini A, Gastaldelli A, Mingrone G, Ferrannini E (2001) A model for glucose control of insulin secretion during 24 h of free living. Diabetes 50(Suppl. 1): S164–S168. doi:10.2337/diabetes.50.2007.S164

Marino S, Hogue IB, Ray CJ, Kirschner DE (2008) A methodology for performing global uncertainty and sensitivity analysis in systems biology. J Theor Biol 254(1):178–196. doi:10.1016/j.jtbi.2008.04.011

Markovic TP, Furler SM, Jenkins AB, Campbell LV, Kraegen EW, Chisholm DJ (1995) Importance of early insulin levels on prandial glycaemic responses and thermogenesis in non-insulin-dependent diabetes mellitus. Diabetes Med 12(6):523–530

Matthews DR, Hosker JP, Rudenski AS, Naylor BA, Treacher DF, Turner RC (1985) Homeostasis model assessment: insulin resistance and β-cell function from fasting plasma glucose and insulin concentrations in man. Diabetologia 28(7):412–419. doi:10.1007/BF00280883

Meier JJ, Holst JJ, Schmidt WE, Nauck MA (2007) Reduction of hepatic insulin clearance after oral glucose ingestion is not mediated by glucagon-like peptide 1 or gastric inhibitory

polypeptide in humans. Am J Physiol Endocrinol Metab 293(3):E849–E856. doi:10.1152/ajpendo.00289.2007

Merovci A, Solis-Herrera C, Daniele G, Eldor R, Fiorentino TV, Tripathy D, Xiong J, Perez Z, Norton L, Abdul-Ghani MA, DeFronzo RA (2014) Dapagliflozin improves muscle insulin sensitivity but enhances endogenous glucose production. J Clin Investig 124(2):509–514. doi:10.1172/JCI70704

Meyer C, Woerle HJ, Dostou JM, Welle SL, Gerich JE (2004) Abnormal renal, hepatic, and muscle glucose metabolism following glucose ingestion in type 2 diabetes. Am J Physiol Endocrinol Metab 287(6):E1049–E1056. doi:10.1152/ajpendo.00041.2004

Milligan PA, Brown MJ, Marchant B, Martin SW, van der Graaf PH, Benson N, Nucci G, Nichols DJ, Boyd RA, Mandema JW, Krishnaswami S, Zwillich S, Gruben D, Anziano RJ, Stock TC, Lalonde RL (2013) Model-based drug development: a rational approach to efficiently accelerate drug development. Clin Pharmacol Ther 93(6):502–514. doi:10.1038/clpt.2013.54

Mogensen CE (1971) Maximum tubular reabsorption capacity for glucose and renal hemodynamics during rapid hypertonic glucose infusion in normal and diabetic subjects. Scand J Clin Lab Invest 28(1):101–109. doi:10.3109/00365517109090668

Møller JB, Man CD, Overgaard RV, Ingwersen SH, Tornøe CW, Pedersen M, Tanaka H, Ohsugi M, Ueki K, Lynge J, Vasconcelos N-M, Pedersen BK, Kadowaki T, Cobelli C (2014) Ethnic differences in insulin sensitivity, beta-cell function, and hepatic extraction between japanese and caucasians: a minimal model analysis. J Clin Endocrinol Metab 99:4273–4280. doi:10.1210/jc.2014-1724

Mussap M, Vestra MD, Fioretto P, Saller A, Varagnolo M, Nosadini R, Plebani M (2002) Cystatin C is a more sensitive marker than creatinine for the estimation of GFR in type 2 diabetic patients. Kidney Int 61(4):1453–1461

Nathan DM, Turgeon H, Regan S (2007) Relationship between glycated haemoglobin levels and mean glucose levels over time. Diabetologia 50(11):2239–2244. doi:10.1007/s00125-007-0803-0

National Research Council (2012) Assessing the reliability of complex models: mathematical and statistical foundations of verification, validation, and uncertainty quantification

Nauck MA, Del Prato S, Durán-García S, Rohwedder K, Langkilde AM, Sugg J, Parikh SJ (2014) Durability of glycaemic efficacy over 2 years with dapagliflozin versus glipizide as add-on therapies in patients whose type 2 diabetes mellitus is inadequately controlled with metformin. Diabetes Obesity Metab n/a–n/a. doi:10.1111/dom.12327

NHANES (2015) National Health and Nutrition Examination Survey Data (NHANES I-III). U.S. Department of Health and Human Services, Centers for Disease Control and Prevention. http://www.cdc.gov/nchs/nhanes/prior_nhanes.htm. 2015

Ning Y, O'Neill K, Lan H, Pang L, Shan LX, Hawes BE, Hedrick JA (2008) Endogenous and synthetic agonists of GPR119 differ in signalling pathways and their effects on insulin secretion in MIN6c4 insulinoma cells. Br J Pharmacol 155(7):1056–1065

Nolan CJ, Damm P, Prentki M (2011) Type 2 diabetes across generations: from pathophysiology to prevention and management. Lancet 378(9786):169–181. doi:10.1016/s0140-6736(11)60614-4

Nunez DJ, Bush MA, Collins DA, McMullen SL, Gillmor D, Feldman PL, Apseloff G, Atiee G, Corsino L, Morrow L (2014) Gut hormone pharmacology of a novel GPR119 agonist (GSK1292263), metformin, and sitagliptin in type 2 diabetes mellitus: results from two randomized studies. PLoS ONE 9(4):e92494

Nyman E, Brännmark C, Palmér R, Brugard J, Nyström FH, Strålfors P, Cedersund G (2011) A hierarchical whole-body modeling approach elucidates the link between in vitro insulin signaling and in vivo glucose homeostasis. J Biol Chem 286(29):26028–26041

Nyman E, Cedersund G, Str\aalfors P (2012) Insulin signaling–mathematical modeling comes of age. Trends Endocrinol Metab 23(3):107–115

Ostenson CG (2001) The pathophysiology of type 2 diabetes mellitus: an overview. Acta Physiol Scand 171(3):241–247. doi:10.1046/j.1365-201x.2001.00826.x

Overton HA, Babbs AJ, Doel SM, Fyfe MCT, Gardner LS, Griffin G, Jackson HC, Procter MJ, Rasamison CM, Tang-Christensen M, Widdowson PS, Williams GM, Reynet C (2006) Deorphanization of a G protein-coupled receptor for oleoylethanolamide and its use in the discovery of small-molecule hypophagic agents. Cell Metab 3(3):167–175

Palmér R, Nyman E, Penney M, Marley A, Cedersund G, Agoram B (2014) Effects of IL-1β–blocking therapies in type 2 diabetes mellitus: a quantitative systems pharmacology modeling approach to explore underlying mechanisms. CPT Pharmacometr Syst Pharmacol 3(6). doi:10.1038/psp.2014.16

Paul SM, Mytelka DS, Dunwiddie CT, Persinger CC, Munos BH, Lindborg SR, Schacht AL (2010) How to improve R&D productivity: the pharmaceutical industry's grand challenge. Nat Rev Drug Discovery 9(3):203–214. doi:10.1038/nrd3078

Perley MJ, Kipnis DM (1967) Plasma insulin responses to oral and intravenous glucose: studies in normal and diabetic subjects. J Clin Invest 46(12):1954–1962

Perriello G, Misericordia P, Volpi E, Santucci A, Santucci C, Ferrannini E, Ventura MM, Santeusanio F, Brunetti P, Bolli GB (1994) Acute antihyperglycemic mechanisms of metformin in NIDDM: evidence for suppression of lipid oxidation and hepatic glucose production. Diabetes 43(7):920–928. doi:10.2337/diab.43.7.920

Peter R, Dunseath G, Luzio SD, Chudleigh R, Roy Choudhury S, Owens DR (2010) Daytime variability of postprandial glucose tolerance and pancreatic B-cell function using 12-h profiles in persons with Type 2 diabetes. Diabet Med 27(3):266–273. doi:10.1111/j.1464-5491.2010.02949.x

Petersen KF, Cline GW, Gerard DP, Magnusson I, Rothman DL, Shulman GI (2001) Contribution of net hepatic glycogen synthesis to disposal of an oral glucose load in humans. Metabolism 50 (5):598–601. doi:10.1053/meta.2001.22561

Polonsky KS, Given BD, Hirsch LJ, Tillil H, Shapiro ET, Beebe C, Frank BH, Galloway JA, Van Cauter E (1988a) Abnormal patterns of insulin secretion in non-insulin-dependent diabetes mellitus. N Engl J Med 318(19):1231–1239. doi:10.1056/nejm198805123181903

Polonsky KS, Given BD, Van Cauter E (1988b) Twenty-four-hour profiles and pulsatile patterns of insulin secretion in normal and obese subjects. J Clin Invest 81(2):442–448. doi:10.1172/jci113339

Premaratne E, MacIsaac RJ, Tsalamandris C, Panagiotopoulos S, Smith T, Jerums G (2005) Renal hyperfiltration in type 2 diabetes: effect of age-related decline in glomerular filtration rate. Diabetologia 48(12):2486–2493. doi:10.1007/s00125-005-0002-9

Quddusi S, Vahl TP, Hanson K, Prigeon RL, D'Alessio DA (2003) Differential effects of acute and extended infusions of glucagon-like peptide-1 on first- and second-phase insulin secretion in diabetic and nondiabetic humans. Diabetes Care 26(3):791–798. doi:10.2337/diacare.26.3.791

Quon MJ, Campfield LA (1991) A mathematical model and computer simulation study of insulin receptor regulation. J Theor Biol 150(1):59–72. doi:10.1016/S0022-5193(05)80475-8

Rahmoune H, Thompson PW, Ward JM, Smith CD, Hong G, Brown J (2005) Glucose transporters in human renal proximal tubular cells isolated from the urine of patients with non-insulin-dependent diabetes. Diabetes 54(12):3427–3434. doi:10.2337/diabetes.54.12.3427

Rave K, Sidharta PN, Dingemanse J, Heinemann L, Roggen K (2010) First-phase insulin secretion has limited impact on postprandial glycemia in subjects with type 2 diabetes: correlations between hyperglycemic glucose clamp and meal test. Diabetes Technol Ther 12(2):117–123. doi:10.1089/dia.2009.0103

Roden M (2001) Non-invasive studies of glycogen metabolism in human skeletal muscle using nuclear magnetic resonance spectroscopy. Curr Opin Clin Nutr Metab Care 4(4):261–266

Rohlfing CL, Wiedmeyer H-M, Little RR, England JD, Tennill A, Goldstein DE (2002) Defining the relationship between plasma glucose and HbA1c analysis of glucose profiles and HbA1c in the diabetes control and complications trial. Dia Care 25(2):275–278. doi:10.2337/diacare.25.2.275

Ruhnau B, Faber OK, Borch-Johnsen K, Thorsteinsson B (1997) Renal threshold for glucose in non-insulin-dependent diabetic patients. Diabetes Res Clin Pract 36(1):27–33. doi:10.1016/S0168-8227(97)01389-2

Saltelli A, Tarantola S, Campolongo F, Ratto M (2004) Sensitivity analysis in practice: a guide to assessing scientific models, 1st edn. Wiley, Hoboken

Saltelli A, Tarantola S, Chan KPS (1999) A quantitative model-independent method for global sensitivity analysis of model output. Technometrics 41(1):39–56. doi:10.1080/00401706.1999.10485594

Salway JG (2004) Metabolism at a glance, 4th edn. Wiley, Oxford

Samsom M, Bharucha A, Gerich JE, Herrmann K, Limmer J, Linke R, Maggs D, Schirra J, Vella A, Worle HJ, Goke B (2009) Diabetes mellitus and gastric emptying: questions and issues in clinical practice. Diabetes Metab Res Rev 25(6):502–514. doi:10.1002/dmrr.974

Sedaghat AR, Sherman A, Quon MJ (2002) A mathematical model of metabolic insulin signaling pathways. Am J Physiol 283 (5 Pt. 1):E1084–E1101

Seimon RV, Brennan IM, Russo A, Little TJ, Jones KL, Standfield S, Wishart JM, Horowitz M, Feinle-Bisset C (2013) Gastric emptying, mouth-to-cecum transit, and glycemic, insulin, incretin, and energy intake responses to a mixed-nutrient liquid in lean, overweight, and obese males. Am J Physiol Endocrinol Metab 304(3):E294–E300. doi:10.1152/ajpendo.00533.2012

Seino S, Shibasaki T, Minami K (2011) Dynamics of insulin secretion and the clinical implications for obesity and diabetes. J Clin Invest 121(6):2118–2125. doi:10.1172/JCI45680

Silber HE, Frey N, Karlsson MO (2010) An integrated glucose-insulin model to describe oral glucose tolerance test data in healthy volunteers. J Clin Pharmacol 50(3):246–256. doi:10.1177/0091270009341185

Soga T, Ohishi T, Matsui T, Saito T, Matsumoto M, Takasaki J, S-i Matsumoto, Kamohara M, Hiyama H, Yoshida S, Momose K, Ueda Y, Matsushime H, Kobori M, Furuichi K (2005) Lysophosphatidylcholine enhances glucose-dependent insulin secretion via an orphan G-protein-coupled receptor. Biochem Biophys Res Commun 326(4):744–751

Stephenson MC, Leverton E, Khoo EYH, Poucher SM, Johansson L, Lockton JA, Eriksson JW, Mansell P, Morris PG, MacDonald IA (2013) Variability in fasting lipid and glycogen contents in hepatic and skeletal muscle tissue in subjects with and without type 2 diabetes: a 1H and 13C MRS study. NMR Biomed 26(11):1518–1526. doi:10.1002/nbm.2985

Sumner T (2010) Sensitivity analysis in systems biology modelling and its application to a multi-scale model of blood glucose homeostasis. UCL (University College London)

Taylor IL, Feldman M (1982) Effect of cephalic-vagal stimulation on insulin, gastric inhibitory polypeptide, and pancreatic polypeptide release in humans. J Clin Endocrinol Metab 55 (6):1114–1117. doi:10.1210/jcem-55-6-1114

Toffolo G, Basu R, Dalla Man C, Rizza R, Cobelli C (2006) Assessment of postprandial glucose metabolism: conventional dual- vs. triple-tracer method. Am J Physiol Endocrinol Metab 291 (4):E800–E806. doi:10.1152/ajpendo.00461.2005

Tomiyasu M, Obata T, Nishi Y, Nakamoto H, Nonaka H, Takayama Y, Autio J, Ikehira H, Kanno I (2010) Monitoring of liver glycogen synthesis in diabetic patients using carbon-13 MR spectroscopy. Eur J Radiol 73(2):300–304. doi:10.1016/j.ejrad.2008.10.019

UK Prospective Diabetes Study (UKPDS) Group (1998a) Effect of intensive blood-glucose control with metformin on complications in overweight patients with type 2 diabetes (UKPDS 34). Lancet 352(9131):854–865

UK Prospective Diabetes Study (UKPDS) Group (1998b) Intensive blood-glucose control with sulphonylureas or insulin compared with conventional treatment and risk of complications in patients with type 2 diabetes (UKPDS 33). Lancet 352(9131):837–853. doi:10.1016/S0140-6736(98)07019-6

Vicini P, Cobelli C (2001) The iterative two-stage population approach to IVGTT minimal modeling: improved precision with reduced sampling. Am J Physiol 280 (1 Pt. 1):E179–E186

Vilsbøll T, Krarup T, Sonne J, Madsbad S, Vølund A, Juul AG, Holst JJ (2003) Incretin secretion in relation to meal size and body weight in healthy subjects and people with type 1 and type 2 diabetes mellitus. J Clin Endocrinol Metab 88(6):2706–2713. doi:10.1210/jc.2002-021873

Watts NBM, Digirolamo MM (1990) Carbohydrate tolerance improves with fasting in obese subjects with noninsulin-dependent (type II) diabetes. Am J Med Sci 299(4):250–256

Wikipedia contributors (2015) Template: oral hypoglycemics and insulin analogs. Wikipedia, the free encyclopedia

Wilding JPH, Norwood P, T'joen C, Bastien A, List JF, Fiedorek FT (2009) A study of dapagliflozin in patients with type 2 diabetes receiving high doses of insulin plus insulin sensitizers: applicability of a novel insulin-independent treatment. Dia Care 32(9):1656–1662. doi:10.2337/dc09-0517

Wilmes A, Limonciel A, Aschauer L, Moenks K, Bielow C, Leonard MO, Hamon J, Carpi D, Ruzek S, Handler A, Schmal O, Herrgen K, Bellwon P, Burek C, Truisi GL, Hewitt P, Di Consiglio E, Testai E, Blaauboer BJ, Guillou C, Huber CG, Lukas A, Pfaller W, Mueller SO, Bois FY, Dekant W, Jennings P (2013) Application of integrated transcriptomic, proteomic and metabolomic profiling for the delineation of mechanisms of drug induced cell stress. J Proteom 79:180–194. doi:10.1016/j.jprot.2012.11.022

Wolf S, Rave K, Heinemann L, Roggen K (2009) Renal glucose excretion and tubular reabsorption rate related to blood glucose in subjects with type 2 diabetes with a critical reappraisal of the "renal glucose threshold" model. Horm Metab Res 41(08):600–604. doi:10.1055/s-0029-1220723

Wright EM, Hirayama BA, Loo DF (2007) Active sugar transport in health and disease. J Intern Med 261(1):32–43. doi:10.1111/j.1365-2796.2006.01746.x

Zhang L, Feng Y, List J, Kasichayanula S, Pfister M (2010) Dapagliflozin treatment in patients with different stages of type 2 diabetes mellitus: effects on glycaemic control and body weight. Diabetes Obes Metab 12(6):510–516. doi:10.1111/j.1463-1326.2010.01216.x

Zimei W (2013) Mathematical models with delays for glucose insulin regulation and applications in artificial pancreas. PhD, National University of Singapore, Singapore

Index

A
Affinity, 163, 167
Agonism, 201
Akaike Information Criterion, 287
Alternative parameterization, 177, 192
Alzheimer's disease, 305, 307, 320, 321
Antibody engineering, 435
Anti-diabetic drugs, 473
Area-under-the-curve (AUC), 481, 486
Ariens equation, 171
Asynchronous, 83, 87–91
Automated, 288, 289, 297
Autoregulation, 229, 231, 242, 243, 246

B
Bacterial growth model, 382
Baroreflex components, 140
Between-subject variability, 257, 258, 261, 264, 266, 269
Bioinformatics, 15, 20, 54, 56, 70, 330
Biological homeostasis, 93
Biomarkers, 278, 421, 422, 424, 425, 428, 432, 438, 439, 441, 447
Biophase model, 184, 186
Biosensor process, 178
Biosignal flux, 178
Bone remodeling, 43
Boolean functions, 86, 87

C
Calibration, 307, 309, 311, 315, 316, 319, 320
Capacity, 162, 165, 167, 170, 172
Cardiotoxicity, 21, 22
Cardiovascular control, 140
Central sleep apnea (CSA), 138, 153, 154
Chemical equilibrium, 212, 214
Cheminformatics, 15, 20, 22
Clinical trials, 325, 343
Closed-loop system, 139–142, 144, 146, 147, 149, 155, 156
Combination regimen, 376, 422, 424, 428, 445, 451
Concentration, 178, 180, 183, 186, 187, 193, 200, 203
Concentration-effect relationship, 214
Controller, 231–233
Covariates, 261, 273
Cross-system interactions, 328
Crosstalk, 106
Cytochrome P450, 56, 59
Cytotoxic chemotherapies, 421

D
Dalla Man model, 482
Deterministic, 87, 88, 90
Direct-acting antiviral (DAA), 404, 414, 416
Direct effect, 177–179, 183, 186
Direct-effect model, 223, 224
Disease progression, 341
Dose selection, 421, 451, 452
Drug-biological interface, 161
Drug-drug interactions (DDI), 17, 19
Druggability, 61, 64, 66
Drug potency, 269
Drug target selection, 421

E
Enhanced pharmacodynamic (ePD) models, 107
Epidermal derived growth factor receptor (Egfr), 81
Epistasis, 308
Erlotinib, 354, 355, 357, 359, 362, 364, 365
Euglycemic clamp, 475

F
Feedback, 106, 113, 120

D.E. Mager and H.H.C. Kimko (eds.), *Systems Pharmacology and Pharmacodynamics*,
AAPS Advances in the Pharmaceutical Sciences Series 23,
DOI 10.1007/978-3-319-44534-2

Feedback Control Indirect Response (FC IDR), 229, 231, 239, 250
Feedback regulation, 229–231, 234, 239, 242, 243, 245, 248, 249, 252
Feedforward, 106
Fick's Laws, 163
Frayn's text, 471

G
Gaddum equation, 171
GenBank, 57
Gene-drug interactions (GDI), 17, 19
Gene-gene interaction, 306, 308
Genomic variation, 59, 63, 65
Gluconeogenesis, 471
Glutamatergic systems, 307
Grodin, 230

H
Hepatotoxicity, 22
High-dimensional data sets, 277
Homeostasis, 138, 168–170, 326, 331–333, 339
Horizontal integration, 451
Hormone synthesis, 480
Hyperglycemic clamp, 475
Hyperinsulinemic, 475, 476
Hypothermia, 264

I
Immunomodulatory signals, 326, 333, 335, 338
Indirect response, 177, 187, 188, 191, 196, 198
Individualized therapy, 298
Informative genes, 285
Inputs, 310, 311
Input signal, 106
In silico, 343
In silico model, 305
Insulin analogs, 473
Interactome, 60
Interferon, 403, 404, 412, 416
Interferon-free regimens, 414, 417
Intravenous Glucose Tolerance Test (IVGTT), 475
In vitro models, 328, 376–378
In vitro studies, 35
In vivo, 374, 376, 377, 379–381, 385
In vivo studies, 34, 36
Irreversible drug action, 220

L
Limit of detection (LOD), 404, 405, 412, 416–418
Linear feedback, 231, 232, 234, 239
Linear model, 257, 258
Link model, 177, 186
Lumped, 329, 332, 333

M
MAO-A inhibitors, 307
MAPK signaling, 97
MAPK/ERK signaling pathway, 231
Mean arterial pressure (MAP), 139–148
Mechanical effect of respiration (MER), 146
Mechanism-based computational models, 421
Mechanism of action, 218, 219, 224, 225
Metabolic control, 151, 156
Metabolic fluxes, 467, 480
Michaelis-Menten equations, 116
Microcircuit parameters, 313
Microdomains, 116
Minimal modeling, 145, 148, 150
Minimum Inhabitory Concentration(MIC), 373, 374, 385, 391
Model-based liposome design, 436
Model qualification, 489
Model qualification method, 46
Monoexponential, 258
Multidimensional, 296, 297
Multimodal distributions, 269
Multi-scale modeling, 7
Multi-state discrete models, 94
Multi-variant model, 406, 408
Myeloperoxidase (MPO), 270

N
Nerve Growth Factor (NGF), 35
Network-based, 55, 62
Network-based model, 372, 396
Network redundancy, 427
Nodes, 53, 65, 69
Nonlinear mixed-effect (NLME), 417
Nonlinear mixed effects models (NMEMs), 255, 256

O
Occam's Razor, 110, 116
Olanzapine metabolism, 309
Oncogene, 354, 357
Oncogenic signaling networks, 425
Ontology, 21
Open-loop system, 139, 141, 142, 149
Open system models, 377
Operational efficacy, 167
Optimal sequencing, 376
Oral Glucose Tolerance Test (OGTT), 469, 475, 486
Ordinary Differential Equation (ODE), 118

Orthogonal computational modeling approaches, 421
Outputs, 309–311, 313, 320
Overparameterization, 261

P
Parameterization, 411
Parameter values, 117, 121, 126–129
Parsimony, 286, 287, 289
Patient stratification, 421
Personalized medicine, 56, 64, 70
Perturbations, 83, 93, 95, 106, 122, 123, 125
Pharmacogenetics, 308
Pharmacogenomics, 56, 59
Pharmacokinetics/Pharmacodynamics, 4
Phenomenological, 329, 332, 333, 338, 339
Physicochemical-based models, 430, 435
Physiological based pharmacokinetic (PBPK) models, 15
Plasma concentration, 234, 246, 248
PNEUMA, 151–155
Polymorphonuclear lymphocytes (PMNs), 392, 395
Polypharmacy, 305–308
Power model, 179, 182
Pre-competitive data, 23
Protein linkage network, 359, 364
Protein–protein interactions(PPI), 53, 60, 61, 64

Q
Quantitative Systems Pharmacology (QSP), 27, 30
Quasi-mechanistic, 329

R
Rasgap state, 97
Reaction rate laws, 116, 119
Receptor occupancy theory, 177, 181
Regression, 281, 282, 289, 292, 296
Rheumatoid Arthritis, 32, 41

S
Schwarz Information Criterion, 287
Sequencing methods, 414
Signal transduction, 177, 200, 201
Skin inflammation, 357, 359, 364, 365
Sleep-wake state, 155, 156
Slow dissociation, 215, 219, 224
State transition, 87, 88, 90, 91
Statistical, 326, 331, 334
Statistical models, 421, 429, 441, 448
Stochasticity, 336
Stoichiometries, 118, 119
Structured modeling, 150, 156
Substrate control, 165
Sustained virologic response (SVR), 404, 405, 408, 410, 412–417
Synchronous, 83, 87, 90, 91
Systems biology, 4, 7
Systems model, 7, 10, 11, 12
Systems pharmacology, 4, 5, 7, 10, 11
Systems physiology, 5

T
Target, 211, 212, 215, 217, 220, 222, 225
Target-binding, 169
Target values, 375
Telaprevir, 405, 406, 408–410, 412, 414
Therapeutic areas, 37
Therapeutic design, 421, 437, 451
Time-kill culture tubes, 377
Total peripheral resistance (TPR), 139–149, 152
Transit compartment model, 201, 202, 205
Trial design, 310, 311, 321
Tricyclic, 307
Turnover, 168–172
Turnover model, 217, 222
Turnover rates, 270, 273

V
Variability, 255–258, 262, 264, 269, 273
Vertical integration, 451

W
Windkessel model, 145, 146